



School of Architecture, Planning and Landscape

**The Impact of Urban Form and Shading on
Microclimate and Indoor Air Temperatures of
Dwellings: A Case Study of Erbil, Kurdistan, Iraq'**

Ali Mohammad Salih

Student Number 130465232.

A Thesis

Submitted to the Graduate School of

Architecture, Planning and Landscape

In Partial Fulfilment of the Requirements for the Degree of

DOCTOR OF PHILOSOPHY

Newcastle University

Newcastle Upon Tyne, UK

March 2021

Acknowledgment

بسم الله الرحمن الرحيم

In the name of Allah the most compassionate and the most Merciful

I am very thankful to *Allah* for giving me health and strength to complete this research. I would thank everybody who has supported and encouraged me during my study.

First and foremost, I'm grateful to my supervisor Dr Steve Dudek, who has supported, helped and show me the way of research step by step throughout of this study. His invaluable guidance and knowledge assisted me to done this thesis. He always support me and my family by his kindness and amazing words.

As well as a high respect and thanks to my second supervisor Prof Tim Townshend for his support and compassion, advice and efforts when I do need it. He was always open doors when I faced close doors. I'm also very appreciative to staff of ministry of Agriculture in Erbil, whom assisted me to collect weather data for Erbil city that were used during the validation process for base model of this study. And thanks to School of Architecture and Mr Mark the IT officer for providing the high speed computers which allow me to run the simulation in short time. Thanks to all stuff of Ministry of municipality and Investment Erbil, and especially to Architect Lana and Architect Aram for providing me with all documents and information about the urban planning of Erbil city.

Special thanks to my friends and PhD students University of Newcastle-UK, for their help and support, and to all Iraqi students at Newcastle University.

This thesis is dedicated to:

My Father

For his love, support and prays all the time

To My Mother

For her uncountable love, sacrifice and kindness

To my lovely wife

For her support and patient during my study

To my brothers and sisters

For their support and efforts

Abstract

The history of the Kurdistan region of northern Iraq is complex, however it was established as an autonomous region (Kurdistan-Iraq) in 1991, since when it has flourished in stark contrast to the remainder of Iraq and Syria. The capital of Kurdistan is the historic city of Erbil one of the most ancient cities in the world (with at least 4000 years of history). In recent times, the city has expanded dramatically after 2003, in a series of concentric rings around the central ancient Citadel, to accommodate Kurds from both Kurdistan-Iraq and the returning diaspora. This rapid urban expansion has turned its back on the traditional design principles of the ancient Citadel which was designed to work in harmony with the hot dry climate; organic designs of narrow, winding streets designed around the needs of the pedestrian. Instead this organic morphology has been replaced by grid-iron planning, with street widths designed to accommodate motor vehicles. The alignment of these grid-iron street patterns has been driven by geometry rather than referencing urban micro climatic needs.

The main aim of this research is to investigate the impact of urban form and shading on the urban micro climate and the indoor air temperature of dwellings in the new (post 2003) developments of Erbil. To achieve these aims two methods were used: The prediction of the urban micro climate used ENVI-met, a numerical climate simulation program. The indoor air temperatures were predicted using the building energy simulation software IES Virtual Environments (IES-VE). The climate modelling compared traditional and grid-iron morphologies and demonstrated that the traditional morphology produced lower external air temperatures. For the modern grid-iron morphologies, higher wind speeds in the urban canyons were achieved when the prevailing wind from the South West flowed through a canyon grid aligned North-South and East-West. Shading by both trees and wire mesh was modelled. Both reduce the external mean radiant temperature, but have little impact on the external air temperature. Moreover, the wire mesh shading did not reduce the urban wind speeds, but the tree shading did reduce urban wind speeds.

When shading buildings, the reduction in indoor air temperature was small; whilst the shading mesh reduced solar gain it also reduced night-time losses to the clear night sky, yielding a small reduction in indoor air temperature. However, when purposeful night-time ventilation was modelled, the reduction in indoor air temperature was significant. By combining building shading (reducing solar gain) and night time purpose ventilation (increasing night-time cooling) allows greater freedom in façade design. This permits modern house design to have a similar thermal performance to the traditional house design. The study has developed a novel method to simulate efficiently wire mesh shading both for urban micro climates and buildings. It has shown how the modern grid-iron urban morphology can be adapted to provide improved micro climates and how individual houses can be designed to benefit from these changed micro climates. For the future, it is recommended that full scale testing of whole housing shading be undertaken and how this shading can be adapted to reflect the local identity of the region.

Table of content Chapter 1: The Introduction

1.0	Introduction.....	2
1.2	Research background.....	3
1.3	Statement of the research problem.....	5
1.4	The importance of Erbil as a case study.....	8
1.5	The gap in knowledge.....	10
1.6	Aim of the research.....	11
1.7	Research methodology.....	13
	Phase 1: Literature and preliminary studies.....	13
	Phase 2: Erbil urban planning development.....	13
	Phase 3: Urban microclimate.....	13
	Phase 4: Individual building modification.....	13
1.8	Scope and limitation.....	14
1.9	Urban microclimate modelling.....	14
1.9.1	Building simulation modelling.....	15
1.10	Research Structure.....	16
	1.10.1 Phase 1: Literature and preliminary studies.....	16
	1.10.2 Phase 2: Erbil urban planning development.....	16
	1.10.3 Phase 3: Urban microclimate.....	17
	1.10.4 Phase 4: Individual building modification.....	17

Chapter 2: Literature review

2.1	Introduction.....	20
2.2	Climate Erbil, Kurdistan-Iraq.....	20
2.3	Erbil History.....	21
	2.3.0 Narratives of historic development.....	21
	2.3.1 Urban development of the Erbil citadel.....	22
	2.3.2 Urban transformation of Erbil city.....	25
2.4	Erbil City Planning.....	28
3.5	Erbil Housing.....	34
2.6	Housing Typology.....	35
	2.6.1 Kurdistan Climate.....	39
	2.6.2 The Climate of Erbil.....	40
	2.6.3 Land use and urbanisation of Erbil.....	44
	2.6.4 Erbil: Land Surface Temperature (LST).....	45
2.7	Urban energy balance.....	49
	2.7.1 Urban microclimate.....	50
2.8	Wind and urban microclimate.....	51
	2.8.1 Wind speed and urban canyon aspect ratio.....	53
2.9	Urban morphology and energy consumption.....	54
2.10	Urban microclimate in hot arid regions compared to other climatic regions.....	56

2.11 Microclimate in Urban Canyons.....	58
2.12 Urban microclimate and urban geometry	61
2.13 Urban Heat Islands (UHI).....	64
2.14 Types of Urban Heat Island UHI.....	65
2.14.1 Urban Surface Heat Island (USHI)	66
2.14.2 Atmospheric UHI	67
2.14.3 Boundary Layer Heat Island (BLHI).....	67
2.14.4 Canopy Layer Heat Island (CLHI).....	68
2.15 Microclimate in Erbil.....	73
2.16 Urban microclimate modelling.....	76
2.17 Building Energy Modelling	82
2.17.1 Integrated Environmental Solutions–Virtual Environment (IES-VE).....	87
2.18 Summary and conclusion of the literature review	88
Chapter 3 The Methodology	91
3.1 Introduction	92
3.2 Over view of the research approach	92
3.3 The rational of using the methodology	94
3.4 Description of process used to collect and analyse data in respect of the qualitative research method utilised in this study.....	95
3.4.1 Samples	95
3.4.2 The contents of semi-structured interview	96
3.4.3 Protocol of the semi-structured interview	97
3.4.4 Analysis the data from the semi-structure interview.....	97
3.5 The urban Housing project case studies	97
3.6 Climate Data for Erbil	100
3.6.1 Weather data stations in Erbil	101
3.6.2 Northern Weather Station.....	102
3.6.3 Airport Weather Station	102
3.6.4 Central Weather Station	102
3.6.5 South weather data station.....	102
3.7 The quality of the weather data	104
3.8 The quantitative method utilised in this study	107

Chapter 4	Urban planning and regulations of Erbil city	116
4.1	Introduction.....	117
4.2	Erbil and Urban Design Process	118
4.2.1	Step one: Master Plan Approval	120
4.2.2	Step two: Land Acquisition.....	121
4.2.3	Step Three: Site Investigation	121
4.2.4	Step Four: Design Proposal.....	121
4.3	Government projects	122
4.5	Private projects.....	125
4.6	Case studies in Erbil Urban Areas	128
4.6.1	Criteria for selecting the case study	129
4.7	Government Project Case Studies.....	132
4.7.1	Baxlwu Manira.....	132
4.7.2	Grad Sor	134
4.7.3	Gadjutiar	137
4.7.4	Rashkin	142
4.8	Private Project Case Studies	145
4.8.1	Italian City 1	145
4.8.2	English Village.....	152
4.8.3	Italian City 2	156
4.8.4	Mass City	162
4.9	Comparison between Government and Private Projects.....	167
4.10	Conclusion	170
Chapter 5	Urban Microclimate Modelling	174
5.1	Introduction.....	175
5.2	Weather data stations in Erbil city.	176
5.2.1	North weather data station	177
5.2.2	Airport Weather Data Station	178
5.2.3	Central weather data station.....	179
5.2.4	South Weather Data Station.....	180
5.2.5	The quality of data and locality in urban context of Erbil	181
5.3	Microclimate Measurement:	183
5.3.1	Air Temperature.....	183
5.3.2	Wind Speed.....	187
5.3.3	Relative Humidity	189
5.4	Summary of weather data for June, July and August 2015.....	190

5.4.1	Air temperature	190
5.4.2	Relative Humidity	191
5.4.3	Wind Speed.....	192
5.5	Climate Simulation	194
5.6	ENVI-met.....	195
5.7	Erbil City Climate Simulation.....	197
5.8	Validation the Microclimate model	198
5.8.1	Case Study1- Tradition Urban Morphology (High density)	201
5.8.2	Microclimate model evaluation of Case Study 1	203
5.8.3	Case Study 2: Modern Urban Morphology (medium urban density).....	207
5.8.4	Microclimate model evaluation for Case Study 2.....	211
5.9	Summary of the validation process.....	215
Chapter 6	Urban Microclimate Modelling	216
6.1	Introduction.....	218
6.2	Compare between Grid-iron and Tradition urban Morphology.....	219
6.2.1	Grid-iron morphology.....	224
6.2.2	Traditional morphology	228
6.3	Comparisons traditional and modern morphologies	231
6.4	Wind direction simulation.....	232
6.4.1	First scenario with 180° wind direction from the North.....	233
6.4.2	Second scenario with 225° wind direction from the north	235
6.4.3	Wind speed for the second scenario.....	236
6.4.4	Third scenario with 270° wind.....	237
6.4.5	Compare between all scenarios for wind directions (180°, 225° and 270°) from the north. 239	
6.4.6	Wind speed for all scenarios	241
6.5	Proposed Design Interventions (Erbil Case Study).....	242
6.5.1	Designed case study scenario.....	245
6.5.2	Adding central open-green areas (first scenario).....	248
6.5.3	Increasing east-west canyons widths (second scenario)	251
6.6	Comparison of Designed case study and all design intervention scenarios.....	256
6.7	Adding trees for green spaces	263
6.7.1	First scenario, Open spaces Without Trees.....	265
	270
6.7.2	Second Scenario (Open Space with trees)	270
6.8	Compare two scenarios	277
6.8.1	Air Temperature (Open Spaces with Tree and Without Trees)	278
6.8.2	Wind Speed (Open Spaces with Tree and Without Trees)	279

6.8.3	Mean Radiant Temperature (Open Spaces with and Without Trees)	280
6.9	Conclusion.....	281
Chapter 7	The Impact of Shading Mesh	283
7.1	Introduction	284
7.2	History of shading	285
7.3	Modern shading devices	291
7.4	Model of shading mesh.....	298
7.5	Adding Shading Mesh	303
7.5.1	Modify (Optimise) the height of the shading mesh from 6, 7, 8, 9, 10, 11 and 12m	307
7.5.2	Shading mesh transparency at 30% and 50%, with shading mesh at two heights (6 and 8 m)	312
7.5.3	Mean Radian Temperature (MRT) and Physiological Equivalent Temperature (PET)	317
7.5.2.1	Shading mesh impact on urban spaces	317
6.5.4	Physiological Equivalent Temperature (PET).....	321
7.6	Discussion and Conclusion.....	324
Chapter 8	Modelling the shade mesh.....	320
8.1	Introduction.....	322
8.2	Numerical modelling and validation (building scale) using IES	323
8.2.1	IES model input and outputs	323
8.2.1	IES and weather data file	324
8.2.1	IES weather dataset with IES references (IES dataset).....	326
8.2.1	IES weather dataset with ENVI-met references (ENVI-met dataset)	328
8.2.1	IES weather dataset with local site measured references (Measured dataset)	330
8.3	Generation of the weather data file for IES	331
8.4	Modelling Shade Mesh using IES.....	333
8.4.1	Plastic shade mesh types	333
8.4.2	The shading mesh model.....	334
8.4.3	Modelling shade meshes	336
8.5	Shading mesh model and validation	339
8.5.1	IES shading mesh model.....	339
8.6	IES shading mesh simplification model (scale, shading coefficient and geometry).....	342
8.6.1	IES shading mesh model with 8 Scale	342
8.6.2	IES shading model with 8 shading coefficient.....	343
8.6.3	IES shading model with 8 shading geometry.....	343
8.6.4	Solar Shading Analysis	343
8.6.5	Thermal analysis simulation	346
8.6.6	IES shading mesh model with 8 shading coefficient	348
8.6.7	Shading mesh coefficient types.....	350

8.6.8	IES shading mesh model with 8 Geometry.....	352
8.6.9	Direct Solar Radiation (Roof of Test Room)	353
8.7	Model Validation	356
8.7.1	HTB 2 Model	357
8.7.2	The IES and HTB2 Model Process	358
8.7.3	Comparison of the IES and HTB2 Models	363
8.8	Building Scale Model.....	363
8.8.1	Typical House With and Without Shade Mesh.....	365
8.8.2	Typical house models with and without openings	367
8.8.3	Typical house with Different Shading Coefficient Ratio 50, and 100%.....	369
8.9	Single and attached typical house models.....	370
8.9.1	Single and attached house	371
8.9.2	Ground and first floor for single and attached typical house	372
8.10	Application of Ventilation Strategies'	375
8.10.1	Window open profile (24 hours opened)	375
8.10.2	Windows open profile (24 hours closed)	376
8.10.3	Window open profile (night time opening).....	379
8.10.4	Comparison of all three scenarios	380
8.11	Conclusion	383
Chapter 9	Discussion	383
9.1	Introduction	384
9.2	Climate Modelling	385
9.2.1	Validation of ENVI-met.....	385
9.2.2	Performance of Grid Iron versus Traditional (Organic) Morphologies	386
9.2.3	The Effect of Wind Direction on the Urban Grid.....	386
9.2.4	Interventions in the Urban Grid.....	387
9.2.5	Natural Shading.....	388
9.2.6	Manmade Shading.....	389
9.3	Building Shading	389
9.4	Mesh Simulation Validation.....	391
9.5	Building Simulation.....	392
Chapter 10	Conclusion	405
10.1	Aim of the research	406
10.2	Conclusion	408
10.2.1	Part one: urban planning, urban design process and regulatory frame work of Erbil.....	408
10.3	Climate modelling and modifying the local urban microclimate.....	409
10.4	Building Simulation modelling.....	412

10.4.1	Modelling shading mesh	413
10.4.2	Design a Base Case Scenario (BCS).....	414
10.4.3	Model a typical house with IES-VE.....	414
10.5	Contributions to knowledge	418
10.6	The study recommendations:	424
10.7	Future work	424

Table of Figures

Figure 1.1: Annual global mean temperature, 1850–2005. Source: berkeleyearth.org (2019)	2
Figure 1.2: Temperature difference of (a) heat island intensity, Aug.13-14, (b) cool island intensity, Aug.11. (Shigeta, Ohashi et al. 2009)	3
Figure 1.3: Temperature distribution. (a) Urban heat island in nighttime, 2300 JST, Aug. 13 , (b) Urban cool island. (Shigeta, Ohashi et al. 2009)	4
Figure 1.4: Iraq map showing Kurdistan Region, Erbil and main cities. Source: http://asorblog.org	5
Figure 1.5 : Kurdistan Regional Government electricity demands by city, and end-use sectors.....	6
Figure 1.6: Erbil Master Plan designed by Dar Alhandasa. The city's development until 2030	7
Figure 1.7: Thesis structure and framework for all four phases	18
Figure 2.1: Kurdistan was divided principally between Turkey, Iran, Iraq and Syria.	22
Figure 2.2: Iraqi Kurdistan.....	23
Figure 2.3: Erbil Citadel (Qala). Source: (Al-Jameel, Al-Yaqoobi et al. 2012).	24
Figure 2.4: Urban development of the Erbil citadel.....	25
Figure 2.5: Erbil urban development from 1200 to 2007.....	26
Figure 2.6: Erbil housing development stages throughout history.....	27
Figure 2.7: The neo-liberal economic city, after 2003	28
Figure 2.8: Erbil Citadel and Buffer Zone A	29
Figure 2.9: The first master plan proposal for Erbil city expansion 1932. Source: Iraqi National Archive, Baghdad, Gort Architects.....	30
Figure 2.10: The second master plan proposal by DOXIADIS for Erbil expansion 1951 Source: Doxiadis,DOX-QA92 (1958p.73).....	31
Figure 2.11: The main Road to connect the city with other Kurdistan cities.....	31
Figure 2.12: Urban development from 1950 to 1980.....	32
Figure 2.13: Master plan of Erbil city 1994.....	33
Figure 2.14: Erbil recent master plan designed by Dar Al-Handasa. Source: KRG (2009)	34
Figure 2.15: Iraq and Kurdistan Koppen climate zones. Source: https://chronicle.fanack.com/iraq/geography	40
Figure 2.16: Average rainfall in Erbil is lowest in June, with an average of 0 mm and highest in January at 112 mm . Source (climate-data.org).	41
Figure 2.17: Erbil's average air temperature is 33.4 °C and July is the hottest month of the year. January has the lowest average temperature of the year at 7.4 °C. Source: climate-data.org.....	42
Figure 2.18: Average annual wind speed in Erbil. Source: www.meteoblue.com	43
Figure 2.19: Wind speed for Erbil (June, July and August).....	44
Figure 2.20: Average annual wind direction for Erbil. Source www.meteoblue.com	44
Figure 2.21: Urban development of Erbil.	45
Figure 2.22: Land surface temperature and thermal infrared radiometer image for Erbil from Landsat TIRS on 19th July 2013. Source of image (Rasul, Balzter, & Smith, 2015)	47
Figure 2.23: Tajeel district is an organic urban area with a surface temperature higher than most grid-iron urban areas with a surface urban temperature.	48
Figure 2.24: Lower surface temperature for S.A part than Erbil International Airport.	49
Figure 2.25: Naz has low density urban areas which recorded higher ST compared to the high density urban areas of Ainkawa. Source of left image (Rasul, Balzter, & Smith, 2015)	49
Figure 2.26: Schematic section (A) and 3D presentation (B) of urban surface energy balance. Sources: (A) Erell et al., (2011), (B) Santamouris (2001b).....	50

Figure 2.27: Urban boundary layer and development of urban canopy layer. Source: Erell, Pearlmutter et al. (2012).	51
Figure 2.28: Urban canopy layer. Source: http://co2montreal.blogspot.com/2010/10/principles-of-urban-meteorology-re.html	52
Figure 2.29: Wind flow pattern over and within urban canyons, and (b), threshold lines	54
Figure 2.30: Secondary wind flow patterns with respect to the primary flow directions above	55
Figure 2.31: Urban canyon and its geometrical descriptors and sky view factor (SVF) as a function of canyon aspect ratio (H/W).	59
Figure 2.32: Schematic view of a rectangular courtyard-type space showing its geometric descriptors and (b) approximated SVFs	60
Figure 2.33: Geometric parameters for calculating the SVF from a point on the ground in plaza-type space (a) at a given distance from one continuous wall and (b) at the centre point of a circular space	60
Figure 2.34: Model layout as viewed from above (plan view) and along a cross-section drawn through the UCL. Source: Mills (1997)	61
Figure 2.35: Urban canyon and its geometrical descriptors and sky view factor (SVF) as a function of canyon aspect ratio (H/W)	61
Figure 2.36: Site maps of some study locations. Source: Shashua-Bar (2004)	62
Figure 2.37: Site maps showing positions and canyons of the study. Source: Bourbia and Boucheriba (2010).	63
Figure 2.38: Map of Iraq, the Kurdistan Region and true colour Landsat of the study area.	74
Figure 2.39: Different air temperatures in all districts in Erbil. Source: Rasul, 2015.	75
Figure 2.40: Samples of selected LULC with true colour Landsat OLI. Source: Rasul, 2015.	76
Figure 2.41: Samples of selected LULC with true colour Landsat OLI. Source: Rasul, 2015	77
Figure 2.42: The urban microclimate model starting from UHI and measurements	78
Figure 2.43: Horizontal dimension and representation of climate modelling scales	79
Figure 2.44: General structure of Building Energy Modelling tools	83
Figure 2.45: Integrated environmental solutions–virtual environment (IES–VE) engine	88
Figure 3.1: Erbil master plan, designed by Dar Al-Handasa	92
Figure 3.2: Thesis Structure – phases 1, 2, 3 and 4.	93
Figure 3.3: The interview structure	95
Figure 3.4: The relationship between the design process and associated problems.	98
Figure 3.5: The Government and Private Case Studies.	99
Figure 3.6: Erbil urban development methodology and the source of information	100
Figure 3.7: location of all weather stations; North, Central, Airport and South.	101
Figure 3.8: Average air temperature for Northern, Central, Airport and Southern stations	105
Figure 3.9: Average wind speed in June, July and August for Northern, Central and Southern stations	106
Figure 3.10: The schematic of the validation process.	108
Figure 3.11: High and Medium urban density of Erbil were used to validate the climate model.	109
Figure 3.12: Organic and grid iron morphologies.	111
Figure 3.13: ENVI-met model showing single walls features.	112
Figure 3.14: Schematic form the methodology of Shading Mesh Modelling process using both IES and HTB2 simulation model.	114
Figure 3.15: The process of prototype dwelling simulation structure using IES-VE model.	115

Figure 4.1: The stages of Erbil's development: HCECR, 2007.....	119
Figure 4.2. Informal housing, Badawa, Erbil	120
Figure 4.3: The six municipalities of Erbil: HCECR, 2007.....	120
Figure 4.4: Similar Steps in Any Urban Design Housing Project Process in Erbil	121
Figure 4.5: Erbil master plan until 2030	121
Figure 4.6: The process of urban design Government and Private projects	123
Figure 4.7: Government urban design projects.....	124
Figure 4.8: The process for government urban design projects.....	125
Figure 4.9: Process for private urban housing projects	126
Figure 4.10: The investment licencing process	128
Figure 4.11: Private urban design projects	129
Figure 4.12: The relationship between the design process and associated problems	130
Figure 4.13: The criteria of selecting case studies and project samples for government and private projects.....	132
Figure 4.14: Baxlwu Manira project located in the south west of Erbil city	133
Figure 4.15: Baxlwu Maira site plan – government-designed case study 1	134
Figure 4.16: Grad Sor site plan – government design case study 2.....	135
Figure 4.17: Part of Grad Sor site plan – commercial area surrounded by green areas.....	136
Figure 4.18: Grad Sor site plan – the residential block is one, repeated shape throughout the site....	137
Figure 4-19: Gadjutiar site plan – the position of the project on Erbil's site plan	138
Figure 4.20: Gadjutiar site plan – government design case study 3, area 16,853,888 m ²	139
Figure 4.21: Gadjutiar site plan – the main axis of project.....	139
Figure 4.22: Gadjutiar site plan – the old main roads crossing the project	140
Figure 4.23: Gadjutiar site plan – the main direction of residential blocks (East-West) in the project	140
Figure 4.24: Gadjutiar site plan – the old main roads crossing the project	141
Figure 4.25: Gadjutiar site plan – the site plan land use.....	141
Figure 4.26: Rashkin site plan – the location of project in the city site plan.....	143
Figure 4.27: Rashkin site plan – the location of the project and City Airport.....	144
Figure 4.28: Rashkin site plan- Government design case study-4.....	144
Figure 4-29: Rashkin site plan – government designed case study 4.....	145
Figure 4.30: Italian City 1 – the location of the project in the city site plan	146
Figure 4.31: Italian City 1 site plan – local and international investment project 1	147
Figure 4.32: Italian City 1 – architectural concept, and the similarity between both site plans	147
Figure 4.33: Italian City 1 – houses have their own gardens, and the large green area.....	148
Figure 4.34: Italian City 1 four types of individual houses A, B, C and D	149
Figure 4.35. Italian City 1: types of individual housing units A, B, and C and D.....	150
Figure 4.36: Italian City 1: ceiling materials (precast concrete).....	151
Figure 4.37: Italian City 1: zonal types of individual housing units A, B, C and D.....	151
Figure 4.38: English Village – the location of the project in the city site plan	153
Figure 4.39: English Village site plan – local and international investment project 2	153
Figure 4.40: (A) The site plan of English Village and one type of individual villa (B, C, D and F) showing there is no fence between the villas. (G, and H) the supermarket at the project site.....	154

Figure 4.41: Expand the title Figure 48. English Village housing unit type	156
Figure 4.42: Italian City 2 – the location of the project in the city site plan	157
Figure 4.43: Italian City 2 site plan – local and international investment project 2	158
Figure 4.44: Site plan of Italian City 2 – housing unit types A, B and C	158
Figure 4.45: House types A, B, and C, Italian City 2	159
Figure 4.46: House types A, B, and C, Italian City 2 – blocks built facing each other	160
Figure 4.47: Italian City 2 – recycled water used for irrigation	161
Figure 4.48: Italian City 2 – the consideration of the site’s topography.....	161
Figure 4.49: Italian City 2 – Power station and water treatment plant on the project	161
Figure 4.50: Mass City – the location of project in the city site plan and citadel.....	163
Figure 4.51: Mass City – local and international investment project 3	164
Figure 4.52: Mass City – prototype housing units.....	165
Figure 4.53: Government housing project in Erbil city, different housing design, height and building materials	168
Figure 4.54: Private housing project in Erbil, with similar housing design, height, and building materials	169
Figure 5.1: Four Weather Data Station locations in Erbil City	176
Figure 5.2: North Weather Data Station in Erbil City	177
Figure 5.3: Airport Weather Data Station in Erbil City	178
Figure 5.4: North Weather Data Station in Erbil City	179
Figure 5.5: North Weather Data Station in Erbil City	180
Figure 5.6: Average air temperature for Northern, Central, Airport and Southern stations	184
Figure 5.7: Average wind speed in June, July and August for Northern, Central and Southern stations	186
Figure 5.8: Average Air temperature, Relative Humidity and Wind speed in June, July and August 2015 for Northern, Central and Southern stations	187
Figure 5.9 Hourly average wind speed in 1st of July 2015 for Northern, Central and Southern stations.	189
Figure 5.10 The maximum and minimum air temperatures for North, Central and South weather stations in June, July and August 2015.	190
Figure 5.11: The maximum and minimum Relative humidity for North, Central and South station in June, July and August 2015.	192
Figure 5.12: The maximum and minimum Wind Speed for North, Central and South station in June, July and August 2015.....	193
Figure 5.13: ENVI-met model validation	198
Figure 5.14: Position of the first case study in Erbil.....	199
Figure 5.15: Case Study 1 urban configuration. Red circle represent Central Weather Station	201
Figure 5.16: Case Study 1 Illustrates the ENVI-met physical model on the left with an aerial view of the area to the right	203
Figure 5.17: Modelled and measured air temperature for Case Study 1	203
Figure 5.18: Correlation and index of agreement for modelled and measured air temperature in 18 hours	204
Figure 5.19: Modelled and measured air temperature for Case Study 1 during daytime hours only..	205
Figure 5.20: Shows the correlation and index of agreement for modelled and measured air temperatures during daytime hours only	205
Figure 5.21: Case study area to the south of the city centre	208
Figure 5.22: Southern Weather Data Station locations in Erbil City	209
Figure 5.23: Real urban plan and configuration model using ENVI-met (left), Zhyan district area on the right.....	210

Figure 5.24: Case Study 2. Modelled and measured air temperatures for Case Study 2	211
Figure 5.25: Correlation and index of agreement for modelled and measured air temperature for 18 hours.....	212
Figure 5.26: Case Study 2. Shows the Modelled and Measured air temperature during daytime (7:00 to 18:00).....	212
Figure 5.27: Explains the correlation and index of agreement for modelled and measured air temperature during daytime (07:00 to 18:00) – Case Study 2	213
Figure 6.1: The residential blocks, 200 m ² plot area and 10m canyon widths.....	220
Figure 6.2: The residential blocks of traditional urban morphology, with different plot areas and canyon widths.....	221
Figure 6.3: The ENVI-met model and samples for all scenarios for both traditional and Modern urban morphologies.....	221
Figure 6.4: Shows the position of Horizontal and Vertical sample positions	224
Figure 6.5: Air temperature for the east-west and north-south samples	225
Figure 6.6: Air temperature using the ENVI-met simulation for the modern morphology at 09:00, 12:00, 15:00 and 21:00.....	226
Figure 6.7: Wind speed using ENVI-met for modern morphology at 09:00, 12:00, 15:00 and 21:00.....	227
Figure 6.8: Illustrates the sample positions of the horizontal and vertical samples for the traditional scenarios.....	228
Figure 6.9: Air temperature for east-west and north-south samples.....	229
Figure 6.10: Air temperatures for the traditional morphology using the ENVI-met morphology at 09:00, 12:00, 15:00 and 21:00	229
Figure 6.11: Shows wind speed for tradition morphology at 9:00, 12:00, 18:00 and 21:00.....	230
Figure 6.12: Shows air temperature for both tradition and modern morphology for horizontal and vertical samples.....	231
Figure 6.13: Case study Scenario modelled using ENVI-met.	232
Figure 6.14: ENVI-met output showing wind speed for the first scenario, wind direction 180° from the north	233
Figure 6.15: Air Temperatures for the first scenario when wind direction is 180° from the North....	233
Figure 6.16: Wind Speed for first scenario when wind direction is 180° from the North	234
Figure 6.17: ENVI-met output for Wind speed for the second scenario when wind direction is 225° from the North.....	235
Figure 6.18: Air Temperature for the second scenario when wind speed is 225° from the north.....	235
Figure 6.19: Wind Speed for second scenario when wind direction is 225° from the North.	236
Figure 6.20: ENVI-met image shows wind speed for main roads and branch roads.....	236
Figure 6.21: ENVI-met output for the third scenario when wind direction is 270° from the north...	237
Figure 6.22: Air temperature for the third scenario when wind direction is 270° from the north	237
Figure 6.23: Wind Speed for third scenario when wind direction is 270° from the North.	238
Figure 6.24: Showing the differences between East-West and North-South canyons.....	238
Figure 6.25: Air temperature for all wind direction scenarios (180°, 225° and 270°) from the north	239
Figure 6.26: Air temperature for all three scenarios (45°, 180°, and 270°).	240
Figure 6.27: Compare Wind Speed (WS) for all scenarios (180°, 225° and 270°) from the North....	241
Figure 6.28: Designed scenario, typical grid-iron urban morphology for low rise residential buildings in Erbil	242
Figure 6.29: Designed case scenario and three proposed design interventions using ENVI-met.....	243
Figure 6.30: Shows the plan of work undertaken to investigate the impact of interventions	244
Figure 6.31: Designed Scenario, showing the location of the samples within the zones.....	245
Figure 6.32: Air Temperature for the Horizontal samples for all zones	246
Figure 6.33: Air temperature for the Designed Case Scenario for Vertical canyon –Zone 1, Zone 2 and Zone 3	246
Figure 6.34: Wind speed for vertical and horizontal canyons (all zones).....	247
Figure 6.35: Scenario 1: adding open green spaces to the Designed case study.....	248

Figure 6.36: Air temperature for second scenario (adding open-green areas) – horizontal samples ..	249
Figure 6.37: Air temperature for the second scenario (adding open-green spaces) – Vertical samples	250
Figure 6.38: Shows Scenario 3, increasing East-West canyons.....	251
Figure 6.39: Air temperature for the second scenario – horizontal samples.....	252
Figure 6.40: Air temperature for the second scenario – vertical samples	253
Figure 6.41: Shows Scenario 3, Adding Individual Open-Green Areas	254
Figure 6.42: Air Temperature for the third scenario- Horizontal samples.....	255
Figure 6.43: Air temperature for the third scenario – vertical samples.....	256
Figure 6.44: Air Temperature for open space in Zone 1 in the Designed case study and all design scenarios.....	259
Figure 6.45: Wind Speed in Zone 1 for open space in the Designed case and all design scenarios (East-West canyons).....	260
Figure 6.46: Wind Speed for the Designed case study and all design scenarios in zone one (open space)	261
Figure 6.47: Wind speed in Zone 1 for the Designed case and design scenarios (north-south canyons)	261
Figure 6.48: ENVI-met Zone 1 model. Three points in east-west canyon samples represented by red stars	263
Figure 6.49: Measurement point in the centre of canyon with different heights	264
Figure 6.50: The horizontal sample position for both types of canyon and open spaces.....	265
Figure 6.51: Vertical sample positions for Open Space 1	266
Figure 6.52: Air Temperature for vertical samples (600mm, 1800 mm, 3000 mm and 6000 mm)....	266
Figure 6.53: Wind speed for horizontal samples (east-west) and (north-south) canyons	267
Figure 6.54: Wind speed for vertical samples in similar positions in the centre of Open Space 1	268
Figure 6.55: Mean Radiant Temperature for Horizontal samples from Open Spaces 1, 2, 3, 4 and 5	269
Figure 6.56: Mean Radiant Temperature for vertical samples.....	270
Figure 6.57: The sample positions Open Space	270
Figure 6.58: Air Temperature for second scenario showing the open spaces air temperature differences at 4:00 am.....	271
Figure 6.59: Air temperature for the second scenario (open spaces)	271
Figure 6.60: Air temperature for vertical samples in three sample positions with four sample heights (Second scenario).....	272
Figure 6.61: Air temperature for the second scenario (with trees).....	272
Figure 6.62: Wind speed for horizontal samples in the centre of all open spaces; second scenario open spaces with trees.	273
Figure 6.63: Wind Speed for the second scenario (with trees), Vertical samples for Open Space 1 ..	273
Figure 6.64: ENVI-met images showing wind speed at different heights for the second scenario (open spaces with trees).	274
Figure 6.65: Mean Radiant Temperature for horizontal samples for the second scenario (open spaces with trees)	275
Figure 6.66: ENVI-met image showing Mean Radiant Temperature for canyons and open spaces (second scenario) at 12:00 noon.....	275
Figure 6.67: Mean Radiant Temperature for vertical samples (second scenario).....	276
Figure 6.68: Mean Radiant Temperature for second scenario (open space with trees) at 16:00 showing the shading effect at different heights	277
Figure 6.69: Compare all five open spaces, air temperatures for both scenarios (open spaces with and without trees)	277
Figure 6.70: Air Temperature for all open spaces for both scenarios at 12:00	278
Figure 6.71: Compare all five open spaces wind speed for both scenarios (open spaces with and without trees).....	278

Figure 6.72: Wind Speed for all scenarios (open spaces with and without trees).....	279
Figure 6.73: Compare all five open spaces Mean Radiant Temperature for both scenarios (open spaces with and without trees).....	280
Figure 6.74: Mean Radiant Temperature for both scenarios at 12:00 showing the impact of tree shading on MRT on open spaces.....	280
Figure 7.1: Traditional urban planning showing the horizontal design elements of an old city in a region with a hot-dry climates. Sources https://thetravelingi.com/2017/10/20/iraq-dining-in-erbil-kurdistan/ , (Khaled 1993), SadikG/123RF.com.....	286
Figure 7.2: Housing unit shows the environmental elements of historical housing in Erbil. Sources (Al Jaff, Al Shabander et al. 2017) (Morad and Ismail 2017)	287
Figure 7.3: Shanasheel in traditional neighbourhoods in Iraqi cities. Source of image https://thereaderwiki.com/en/Mashrabiya , https://www.alamy.com/stock-photo/old-basra.html	289
Figure 7.4: Traditional ally showing the shaded area and SVF through employing the <i>shanasheel</i> ..	290
Figure 7.5: Location of a traditional bazar in Erbil and the inside Qaisaria	291
Figure 7.6: Using Shading devices in modern Erbil city markets.....	292
Figure 7.7: Horizontal shading device across the canyon's width providing shade to pedestrians	293
Figure 7.8: Shading devices for open spaces in individual housing	295
Figure 7.9: A systematic facade element which provides the occupants with maximum daylight and minimum solar radiation	296
Figure 7.10: Vertical shading devices.....	297
Figure 7.11. ENVI-met model showing single walls features	300
Figure 7.12. View of ENVI-met interface showing single walls variables.....	301
Figure 7.13 Adding new materials to the ENVI-met model database	302
Figure 7.14: Shows shading mesh over certain parts of the site plan and sample position of the three zones: Zone 1, Zone 2 and Zone 3.....	303
Figure 7.15 Horizontal single walls model and selected materials	303
Figure 7.16 Sample position of the first simulation set	308
Figure 7.17: Shading mesh at different heights 6-12 metres from ground level.....	309
Figure 7.18: Air Temperature for all zones at different heights (6–12 m).....	309
Figure 7.19: Mean Radiant Temperature for all zones at different heights 6–12 metres.....	311
Figure 7.20 Wind speed for all zones at different heights 6–12 metres.....	312
Figure 7.21: Sample position in Zone 1	313
Figure 7.22: Shading mesh transparencies of 30% and 50%	313
Figure 7.23 Air temperature for Zone 1 with different shading mesh transparencies (30% and 50%) at heights of 6 and 8 metres	314
Figure 7.24: Mean Radiant Temperature for Zone 1 with different shading mesh transparencies (30% and 50%) at heights of 6 and 8 metres	315
Figure 7.25: Sample positions for canyons and open spaces with and without shading mesh in two zones, Zones 2 and 3.....	315
Figure 7.26 Wind speed for Zone 1 with different shading mesh transparencies (30% and 50%) at heights of 6 and 8 metres	315
Figure 7.27: Wind speed for open space in Zones 2 and 3 with and without shading mesh	316
Figure 7.28: Air temperature for canyon and open spaces in Zones 2 and 3 with and without shading mesh	317
Figure 7.30 Mean Radiant Temperature for canyons and open spaces in Zones 1 and 2 with and without shading mesh	319

Figure 7.30 Mean Radiant Temperature for canyons and open spaces in Zones 2 and 3 with and without shading mesh	319
Figure 7.32: Mean Radiant Temperature and WS for open spaces and canyons with and without shading meshN.....	321
Figure 7.32: Mean Radiant Temperature and WS for open spaces and canyons with and without shading mesh.....	321
Figure 7.33: Sample position in Zone 3 with and without shading mesh	323
Figure 7.35: Correlation between PET and MRT	323
Figure 7.35: PET for open space at Zone 3 with and without shading mesh MRT	323
Figure 7.36: PET for open space at Zone 3 with and without shading mesh.....	324
Figure 8.1: Building Energy Modelling structure. From Hao Gao (2019)	323
Figure 8.2: The process of simulating three difference sources of weather data	324
Figure 8.3: IES weather data information published by CIBASE and ASHRAE.....	326
Figure 8.4: IES Design Weather Data Source and Statistics. A: Design of monthly weather data. B: Add unpublished weather data file for locations not included in the IES program database.....	327
Figure 8.5: ENVI-met model and sample position	329
Figure 8.6: Sample of air temperature for sample position in ENVI-met.....	329
Figure 8.7: Four weather data station locations in Erbil	330
Figure 8.8: The process of producing a new weather data file	331
Figure 8.9: IES simulation output using three sources of information	332
Figure 8.10: Sample of air temperature using three sources of data: ENVI-met, IES weather file and Measurement data	332
Figure 8.11: Types of plastic shade mesh.....	333
Figure 8.12: Model the shading mesh using IES-VE.....	338
Figure 8.13: Process of rescaling the shading mesh from a real image to the IES model	339
Figure 8.14: Dry bulb temperature of weather data file.....	340
Figure 8.15: The scale of the shading mesh with different shading coefficient compared to a 5 pence coin.....	340
Figure 8.16: The surfaces most affected by direct solar radiation in buildings	341
Figure 8.17: The test room with shade mesh	342
Figure 8.18: The shade mesh scale in 8 different scenarios. The scale of mesh segments reduced gradually from 500 mm to 1.6 mm	343
Figure 8.19: The top perspective view Showing the shade mesh mode for three scenarios, with solar radiation configuration image that fallen on the roof surfaces. Shape 4, 5 and 6 with similar 50% shading coefficient.....	344
Figure 8.20: The shade mesh mode for three scenarios, with the solar radiation configuration image falling on the roof surfaces. Shapes 4–6 have a similar 50% shading coefficient	345
Figure 8.21: The shade mesh mode for two scenarios, with the solar radiation configuration image falling on the roof surface. Shapes 7 and 8 have a similar 50% shading coefficient.....	345
Figure 8.22: Roof solar radiation for the base case on the left hand side. A high resolution grid was applied on surfaces to accurately match the grid colour and colour chart	346
Figure 8.23: Dry bub temperature for hypothetical test room with and without shading mesh.....	348
Figure 8.24: Test Room with 40%, 50% and 60% shading coefficient	349
Figure 8.25: Comparison of dry bulb temperature for the test room and weather data file	350
Figure 8.26: Dry bulb temperature for the test room with and without shading mesh for 1st and 2nd of July 2017.....	351
Figure 8.27: Dry bulb temperature for the test room with and without shading mesh, 1st July 2017	351
Figure 8.28: Test Room with 50, 60, 70, 80, 90 and 100 % shading coefficient.....	352

Figure 8.29: Eight different shade mesh geometry with similar 50% shading coefficient	353
Figure 8.30: Eight different shade mesh geometries, with 50% shading coefficient. Each image represents single solar roof radiation with and without external shade	354
Figure 8.31: Ambient dry bulb and dry bulb temperature for the test room with three geometry shading meshes and 50% shading coefficient for all, compared with the test room without shading mesh	355
Figure 8.32: Dry bulb air temperature for the test room with three geometries of shading mesh and 50% shading coefficient for all, compared with the test room without shading mesh.....	356
Figure 8.33: Shading mask represented as a sky dome divided into 324 blocks 10 by 10 degrees, the black areas represent obscured, and white areas clear sky.....	357
Figure 8.34: Shading mesh laid over the hypothetical test room in three shapes. Shading coefficient is similar for all shapes	359
Figure 8.35: IES model for the test room with three different shading meshes.....	359
Figure 8.36: Sketch-up model used to run and design mesh objects. Three shapes of shade mesh were applied over a similar hypothetical test room. Input data and shading coefficient were similar for all objects	361
Figure 8.37: Test room and house with and without shade mesh	364
Figure 8.38: IES model for test room, showing DT for the test room with and without shading	365
Figure 8.39: DT for the prototype house with and without shading mesh.....	366
Figure 8.40: Comparison between first floor test houses without shade mesh. Local materials and isolated materials, with and without openings	367
Figure 8.41: Comparison of first floor typical house (Type 3), with and without shade mesh.....	368
Figure 8.42: Comparison of 1st floor typical house with shade mesh and 50% and 100% shading coefficient.	369
Figure 8.43: Single and attached typical houses	370
Figure 8.44: Comparison between the first floor test houses: single and attached typical houses	371
Figure 8.45: Comparison between the attached house on the ground and first floors for the first five days of August	372
Figure 8.46: Compare between attached and single house Ground and first floor with and without shading mesh.....	373
Figure 8.47: Typical house design scenario with and without shading mesh with 24 hour opened profile.....	375
Figure 8.48: Heat transfer through the external walls.....	376
Figure 8.49: DT for the typical house and without shading mesh with 24 hour closed profile	376
Figure 8.50: DT for the typical house with shading mesh 10% to 100% shading coefficient.	377
Figure 8.51: Typical house DT with ten shading coefficients (10% to 100%) with 24 hour closed profile.....	378
Figure 8.52: Typical house DT with and without shading mesh with night time opening profile.....	379
Figure 8.53: Typical house DT with night time opening profile and ten different shading coefficients (10–100%)	380
Figure 8.54: Dry bulb temperature for typical house with three opening profiles and 10 different shading coefficients (10% to 100%).	381
Figure 10.1 Novel methodology to simulate and validate shading mesh using IES and HTB2	415

Table of Tables

Table 1.1: Research phases structure.....	11
Table 1.2: Research aims, objectives and research questions.....	11
Table 2.1 Housing types in Erbil according to their urban planning characteristics Source (www.humanitarianlibrary.org).....	36
Table 2.2: Average air temperature and annual rainfall per month in Erbil. Source: climate-data.org	41
Table 2.3: Annual average wind speed in Erbil. Source: Husami (2007).....	42
Table 2.4 Important factors relating to urban planning indicators.....	54
Table 2.5: Research groups categorised by Ai & Mak, 2015 and Okile (2010).	55
Table 2.6: Climatic strategies in a hot dry climate.....	56
Table 2.7 Urban microclimate studies and findings.....	57
Table 2.8: Factors that affect an urban microclimate.....	65
Table 2.9 : Different factors and methods to measure USHI.....	66
Table 2.10 : Summary of additional papers reviewed creating a wide range of climates including a brief summary of their results	69
Table 2.11: The max and min LST	74
Table 2.12: Different high, low and mean LST for different zones in Erbil. Source: Rasul, 2015	74
Table 2.13: Different LST in different districts in Erbil. Source: Rasul, 2015.....	76
Table 2.14: Microclimate methods ENVI-met simulation program as used by different researchers..	79
Table 2.15: The input and output data of Building Energy Modelling tools	83
Table 2.16: Common microclimate methods used in research	85
Table 3.1: Personnel interviewed, their positions and departments.....	96
Table 3.2: The weather data header package	104
Table 4.1: Government and private projects in Erbil.....	169
Table 5.1: shows the weather data package.....	182
Table 5.2: Maximum and minimum air temperatures in July 2015 for the four stations	184
Table 5.3: Hourly average, maximum and minimum air temperatures for four weather stations 1 July 2015	185
Table 5.4: Average, maximum and minimum relative humidity for four weather stations (Summer 2015).....	191
Table 5.5: Average, maximum and minimum wind speed for four weather stations (Summer 2015)	193
Table 5.6: ENVI-met input data for case study 1.	202
Table 5.7: ENVI-met validation for case study 1 using ENVI-met program (day time and 24 houses)	206
Table 5.8: ENVI-met input data for Case Study 2.....	210
Table 5.9: ENVI-met validation for Case Study 2 using the ENVI-met program (daytime and 24 hours)	214
Table 6.1 : ENVI-met input data for both modern and traditional urban morphology cases	221
Table 6.2: ENVI-met outputs with data from two case studies traditional and grid-iron 1.....	223
Table 6.3: ENVI-met outputs data for Grid-Iron 1.....	223
Table 6.4: ENVI-met outputs for Tradition morphology	227
Table 6.5: Compare between all seniors (180°, 225°, and 270°)	239
Table 6.6: Air temperature and WS in the Designed Case Scenario for a horizontal canyon – Zones 1, 2 and 3.....	245
Table 6.7: Air temperature and WS in the Designed Case Scenario for north-south canyon – Zones 1, 2 and 3.....	247
Table 6.8: Air temperature and WS for the first scenario (adding central open green areas) for east-west	

canyon samples	248
Table 6.9: Air temperature and WS for the first scenario (adding central open-green areas) for vertical canyon samples	249
Table 6.10: Shows Air Temperature and WS for the second scenario (increasing east-west canyons) for horizontal canyon samples	251
Table 6.11: Shows T and WS for the second scenario for vertical canyon samples	252
Table 6.12: Air temperature and WS for the third scenario (adding individual open-green areas) for horizontal canyon samples	254
Table 6.13: Air temperature and wind speed for the third scenario (adding individual open-green areas) for the north-south canyon samples	255
Table 6.14: Air temperature for Zone 1 for the Designed case study and design intervention scenarios in east-west canyons	258
Table 6.15: Air Temperature for case study and design intervention scenarios for the north-south canyons	258
Table 7.1: Air temperature and relative humidity used for simulation input data	303
Table 7.2: Shows ENVI-met input data to generate the simulation configuration file	305
Table 7.3 Ranges of the physiological equivalent temperature	321
Table 8.1: Urban microclimate parameters from the ENVI-met model	328
Table 8.2: Building materials for the hypothetical test room	340
Table 8.3: Shape patterns of shade mesh, showing the number of mesh segments in each scenario	342
Table 8.4: Dry resultant temperature and roof solar radiation for the base case and 8 scenarios. The IES model was used to generate (T) 4 times a day	345
Table 8.5: Comparison of dry resultant temperature for the base case and 8 scenarios. The IES model was used to generate (T) 4 times a day	347
Table 8.6: Eight shapes of solar roof radiation calculated manually in colour charts	353
Table 8.7: IES model outputs showing the effect of shading mesh on annual direct solar radiation on floor surfaces	359
Table 8.8: HTB 2 model outputs showing the effect of the shading mesh on annual DSR on floor surfaces	361
Table 8.9: IES and HTB 2 simulation output for fallen DSR on the roof surfaces	362
Table 8.10: Prototype house scenarios with and without shading mesh	366
Table 10.1: Research phases structure	398
Table 10.2: Research aims, objectives and research questions	399

List of Abbreviations and Nomenclature

ABL	Atmospheric Boundary Layer
AWD	Airport Weather Data station
B	Sample position Beginning of the canyons
BT	Sample position at the Bottom of the canyons
BEM	Building Energy Modelling
BDD	Building Design Department
BLHI	Boundary Layer Heat Island
C	Sample position Centre of the canyons
CWD	Central Weather Data station
CFD	Computational Fluid Dynamics
CLHI	Canopy Layer Heat Island
D	Index of Agreement
DGPP	Directorate General of Physical Planning
DSF	Double Skin Façade
DSR	Direct Solar Radiation
E	Sample position End of the canyons
EBM	Energy Balance Models
ECC	Erbil City Council
EID	Erbil Investment Department
GUDH	Government Urban Housing Design
HME	Head of Municipalities in Erbil
HVAC	Heating Ventilation and Air Conditioning system
H/W	Building's Height to Street's Width aspect ratio
I	Increase East-West canyons scenario
IES-VE	Integrated Environmental Solutions–Virtual Environment
KIB	Kurdistan Investment Board
KRG	Kurdistan Regional Government
LST	Land Surface Temperature
M	Sample position in the Middle of the canyons
MME	Ministry of Municipalities (KRG)
MD	Municipality Department
MRT	Mean Radiant Temperature
MSS	Mesh Segments Scale
NWD	The Northern Weather Data station
O	Adding open spaces scenario
OP	Open spaces
P	Sample position Top of the canyons
PET	Physiological Equivalent Temperature
PSS	Perforated Solar Screens
PUDH	Private Urban Design Housing projects
R	Real case scenario

RH	Relative Humidity
RMSE	Root Mean Square Error
RSR	Roof Solar Radiation
SMG	Shading Mesh Geometry
SRT	Simulation Run Time
SVF	Sky View Factor
SWD	The Southern Weather Data station
SUCI	Surface Urban Cool Islands
SUHI	Surface Urban Heat Island
T	Air Temperature
TIR	Thermal Infrared
TMY	Typical Metrological Year
UHI	Urban Heat Island
HCI	Urban Cool Island
WDF	Weather Data File
WOT	First Scenario Open Spaces without Trees
WS	Wind Speed
UBL	Urban Boundary Layer
UCL	Urban Canopy Layer
UHD	Urban Housing Design
UDH	Urban Design Housing project
UNDP	United Nation Development Program
UNESCO	United Nations Educational Scientific and Cultural Organization
UN-HABITAT	United Nations Human Settlements Programme
V	Adding individual open green spaces scenario
Z1	Zone one
Z2	Zone two
Z3	Zone three

Chapter 1 The Introduction

1.0 Introduction

During the 19th and 20th centuries, there was a systematic migration from rural areas to towns and cities caused by the mechanisation of farming practices and the industrialisation of economies. As towns and cities grew, it became apparent that these urban conurbations were modifying their climates compared to rural areas. This was caused by a decrease in urban wind speeds, good surface drainage (which reduced the water budget close to the surface) and high absorption of solar energy by concrete and asphalt, the so called Urban Heat Island (De Schiller, Bentley et al. 2006). Based on the Intergovernmental Panel on Climate Change (IPCC), the Earth's surface air temperature has increased by 0.74C° in the last 100 years, (Figure 1.1) (Solomon, 2007). The increase in air and surface temperatures in urban areas has had a negative impact on the comfort of individuals and consequently total energy consumption, especially in hot regions (Akbari and Konopacki 2004). To control higher air and surface temperatures, more and more buildings will need to be air conditioned, and the world is moving to a point where the energy needed to cool the inhabitants of buildings will exceed the energy needed to heat them. The current estimate is that this will occur in 2060, but in Iraq and Kurdistan, more than 50% of the summer peak energy is consumed by air conditioning. In summer time, residents use air conditioning everywhere, at home, work, and even in cars. In the EU over the next 15 years, energy used for cooling will rise by 72%, whilst the energy used for heating will fall by 30% (Haywood and Schulz 2007).

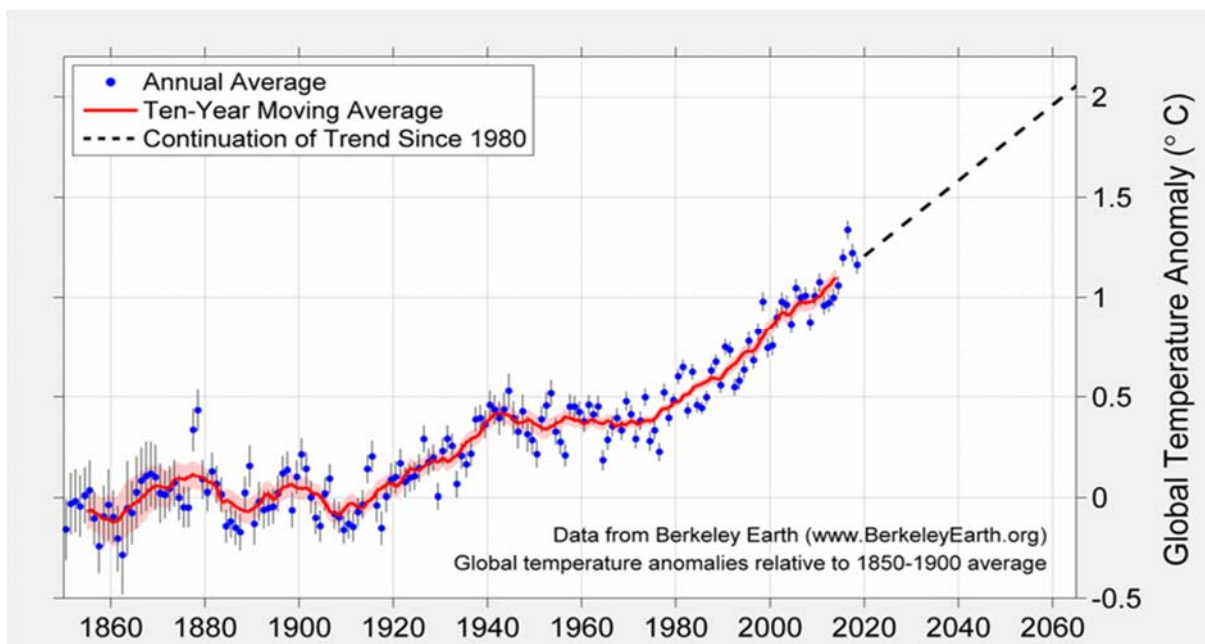


Figure 1.1: Annual global mean temperature, 1850–2005. Source: berkeleyearth.org (2019)

The need for this study arose from my practical design work in Kurdistan, where numerous clients approach me asking for housing designs that were liveable in all year round. What was happening is that during the summer months the upper storey of residential accommodation was abandoned as being too hot, with the ground floor providing the only living space. As many of the houses had multigenerational occupancy, this was a cause of conflict and discord. The provision of mechanical cooling was limited by the lack of electrical energy during the summer months. This lack of electrical energy could be partially rectified by local diesel generators, which are both noisy and polluting. What I felt necessary, but lacked the knowledge was an understanding of how urban development, urban microclimate and building design could work together to mitigate this problem.

To reduce this high demand for energy, we need to rethink current urban design and individual buildings toward sustainability, and propose new building strategies which require less cooling during the summer. In other words, we need to reduce the impact of the urban microclimate on the energy consumption of buildings.

1.2 Research background

The first attempt to study the urban microclimate and urban heat islands (UHI) was by Howard in 1818 (Miles, 2008), who compared the artificial excess of heat in London with other cities in the UK (Oke 1973). However, for cities in hot/dry climate regions, the air temperature in summer, especially in the morning, is lower in urban areas compared with rural areas, and this phenomenon is called an urban cool island (UCI) (Gartland 2012) (Figure 1.2 and Figure 1.3). UHIs and UCIs

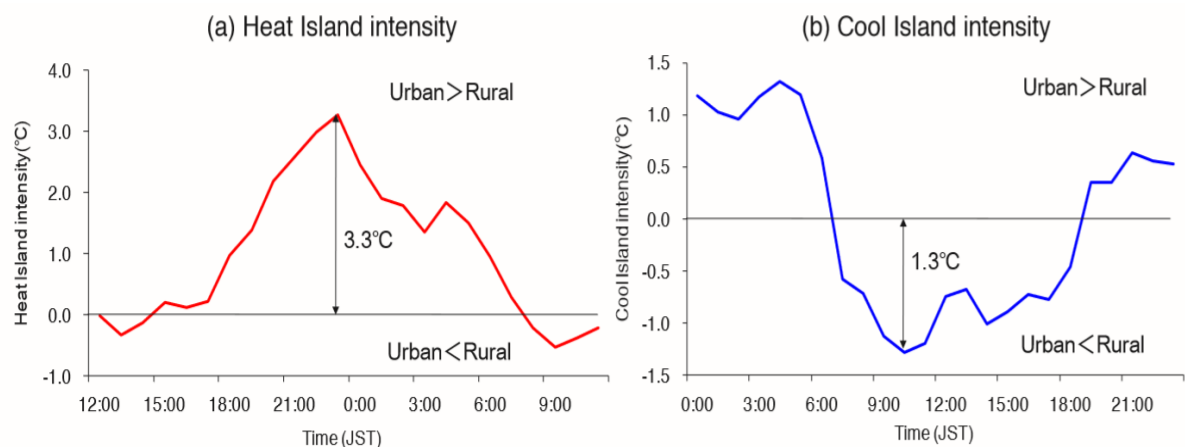


Figure 1.2: Temperature difference of (a) heat island intensity, Aug.13-14, (b) cool island intensity, Aug.11. (Shigeta, Ohashi et al. 2009)

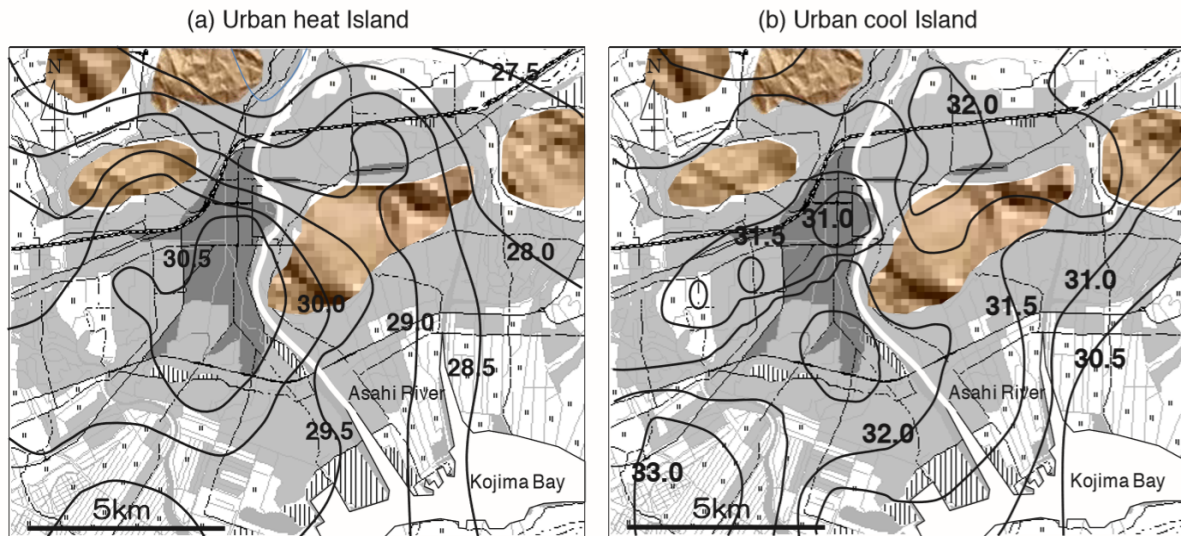


Figure 1.3: Temperature distribution. (a) Urban heat island in nighttime, 2300 JST, Aug. 13, (b) Urban cool island. (Shigeta, Ohashi et al. 2009)

are mainly affected by urban geometry, the thermal properties of the surfaces exposed to sun radiation, and anthropogenic heat outcomes (Oke 2002). Recent research has focused on outdoor thermal comfort by investigating the urban microclimate outdoors, with an emphasis on extending the period of time that individuals can spend outdoors. A consequence of this was that less time was spent indoors, and so less artificial cooling was needed (Thomas 2006). In Thomas's research, based in Isfahan, Iran, two urban areas were considered, the old Jolfa neighbourhood and the new Mardavayj neighbourhood. In the former, comfort levels were within the comfort zone for both the warm and cold seasons, whilst in the latter comfort was only achieved in the cold season. This enabled individuals to spend more time outside buildings in the old, organic, Jolfa neighbourhood. Other researchers have investigated the impact of urbanisation on land surface temperature by means of satellite thermal imaging.

Recent research has investigated the relationships between indoor and outdoor climate, through the evolution of the influence of the external urban microclimate on the indoor building environment. Studies have found that increasing the satisfaction of outdoor thermal comfort will reduce the energy demand for indoor cooling systems (Rijal, Tuohy et al. 2007). Satisfaction with the outdoor urban climate through occupancy encourages people to spend more time in outdoor urban areas, as there is less heat absorption by buildings in urban areas, and residents are less dependent on air conditioning systems, thus lowering energy demands.

The key point is that the research will investigate the thermal performance integration of urban morphology and buildings. However, although many studies have investigated either the

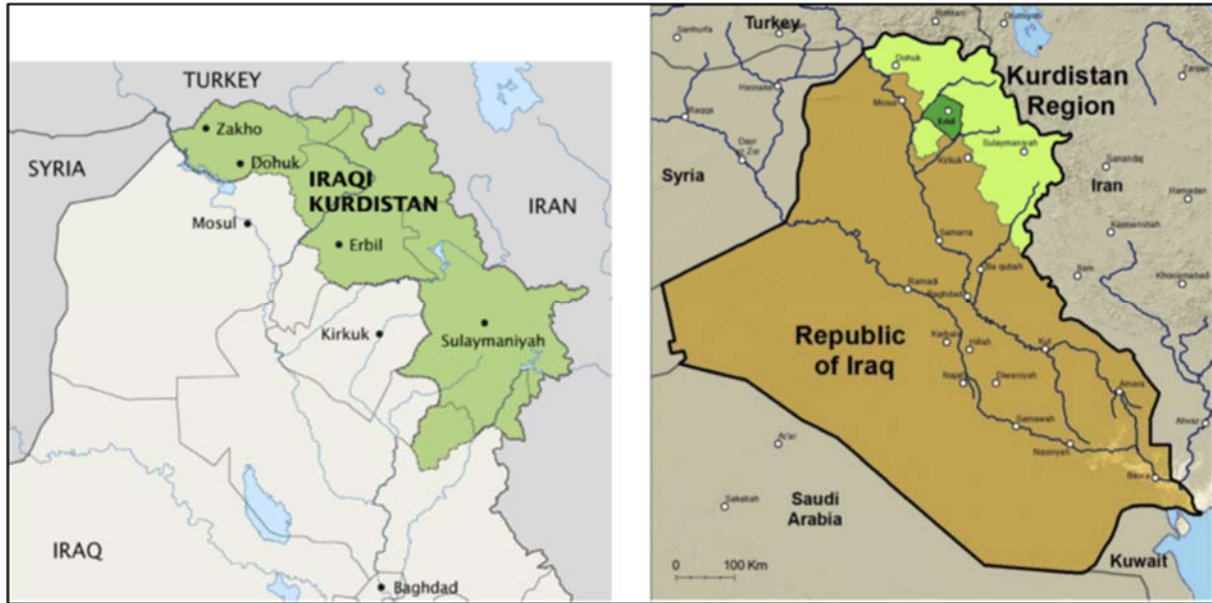


Figure 1.4: Iraq map showing Kurdistan Region, Erbil and main cities. Source: <http://asorblog.org>

impact of urban morphology or building design on energy consumption, very few have taken a holistic approach and studied the interaction of morphology and the built form.

1.3 Statement of the research problem

This study proposes Iraqi Kurdistan as its study area (Figure 1.4). In 1991, Iraqi Kurds formed an autonomous state after Saddam Hussein's regime lost control over the Kurdistan region following the First Gulf War. This autonomy has allowed Iraqi Kurdistan to flourish politically, culturally, and economically (Alkmuhatar 2016). As a historic city, Erbil is now the capital, and it has expanded dramatically since 2003. This expansion has come at a cost, both culturally and environmentally (Ibrahim, Mushatat et al. 2015). Poor planning of infrastructure and architectural design have resulted in the loss of cultural identity in this historic city, with new urban and building designs being heavily influenced by Western thinking (Nooraddin 2012).

One of the issues here is that the principles of urban and building design in the hot/dry climate of Kurdistan Iraq have been ignored. Bornberg (2006) noted that both American and European design style were imported without any knowledge of the thinking that underpins this form of town planning and architecture. The architects and engineers built without any consideration of environment, and used cheap or poor materials such as hollow concrete blocks, which are hot in summer and cool in winter, with high heat transmission (Bornberg, Tayfor et al. 2006). The buildings and housing projects were built with no energy or environmental analysis,

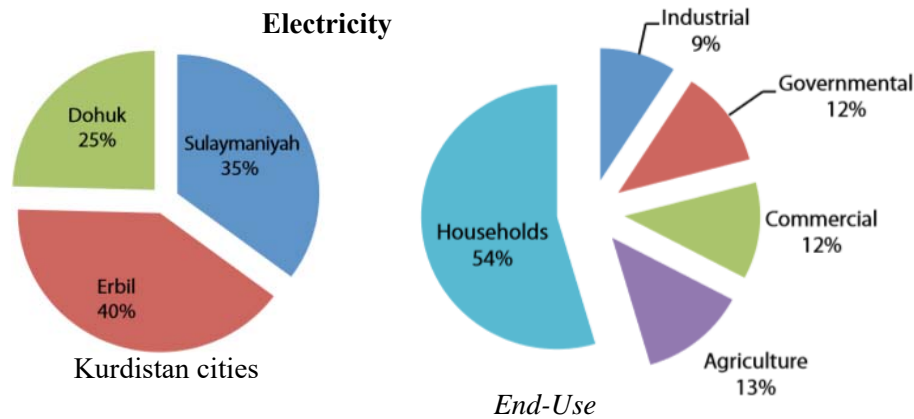


Figure 1.5 : Kurdistan Regional Government electricity demands by city, and end-use sectors

basically because this has not been required by local authorities during the design and construction approval stages (Akram, Ismail et al. 2016).

Figure 1.5 shows that the electricity demand in Erbil City (hereafter referred to as Erbil) is 40% (2,932,615 GWh) of the total demand in the Kurdistan region's cities, compared to Dohuk and Sulaymaniyah (1,793,482 GWh and 2,565,065 GWh, respectfully). The electricity master plan (2009) reported that this demand will grow annually by 7.7% until 2020. In addition, the total demand for electricity has risen gradually from 2,800 MW in 2011, 3,100 MW in 2012, 6,000 MW in 2016, and may reach 10,000 MW by 2020. More importantly, the housing sector now represents 54%, rising to 60% in 2020 of total energy demand compared to other sectors, such as industry, commerce and agriculture (Figure 1.5). This means that the housing sector is the dominant energy consumer in Erbil and any reduction in this sector will be significant.

To achieve comfort in these new housing buildings, imported building services are required, primarily to cool these designs. Operating the air conditioning plant requires electricity, but poor urban planning of infrastructure and the lack of central generating capacity has forced building owners to resort to private, diesel-generated power, and noise and pollution from these generators further degrades the environment.

The main aim of this research is to investigate the impact of the urban form and shading on the urban microclimate and indoor dry bulb temperature.

To prevent the city spiralling out of control, the reintroduction of well-known design principles for a hot/dry climate needs to be achieved. Therefore, the output of this research will demonstrate how a local urban microclimate can be more adaptive environmentally to designs products. The research covers the environmental factors of urban and building scale which play a role in reducing the energy consumption of residential buildings in Erbil. In addition, the study provides a detailed understanding of city climate, a regulatory framework for urban development, urban morphologies, and mitigation strategies for urban areas and buildings.

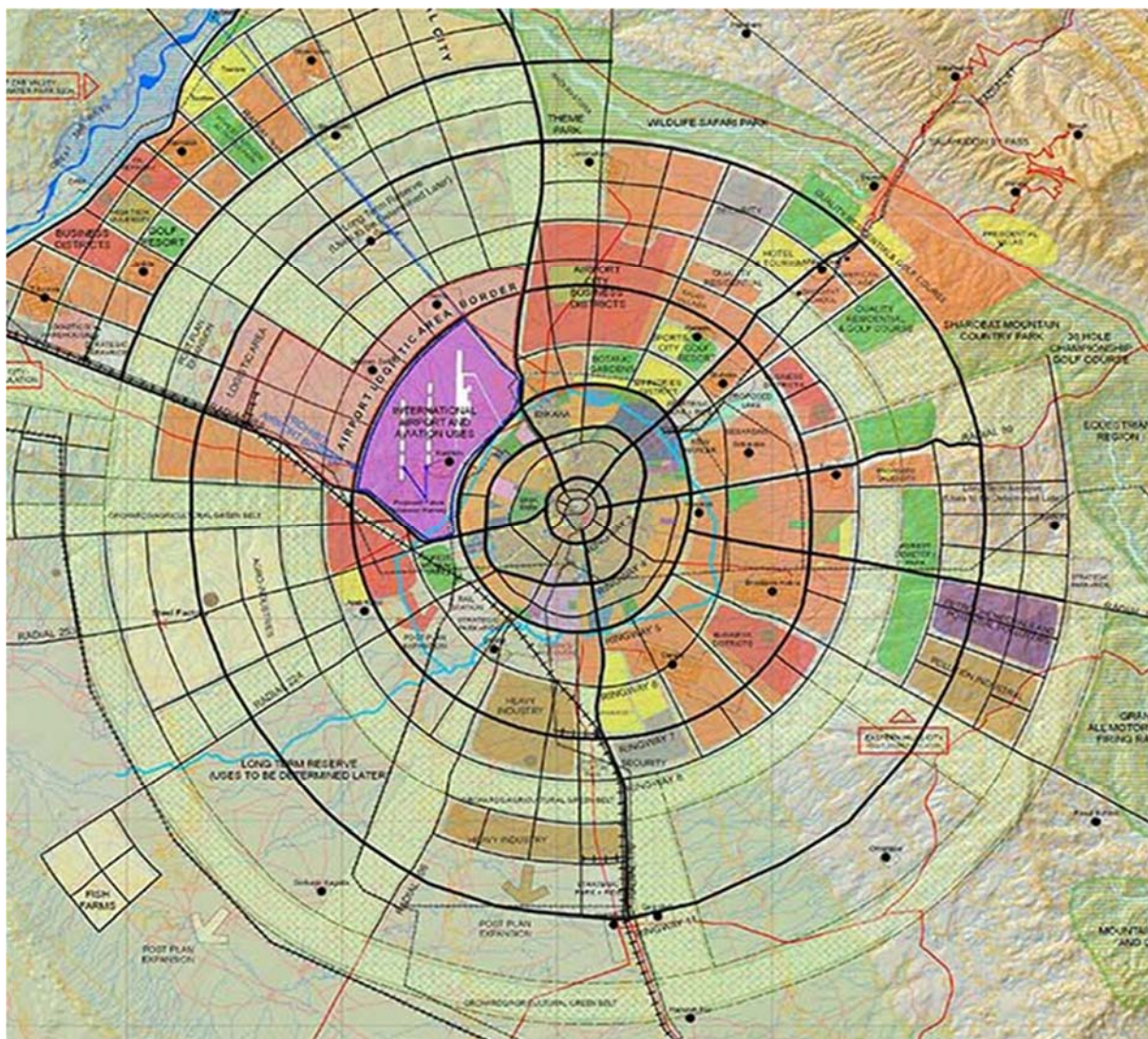


Figure 1.6: Erbil Master Plan designed by Dar Alhandasa. The city's development until 2030

1.4 The importance of Erbil as a case study

The proposed research could be undertaken in any developing city in a hot/dry climate, but Erbil offers a unique opportunity. From 1991 to 2003, there was no development in the city, which meant that it stagnated. Post-2003 Erbil is the only city in the region that has expanding exponentially, and this rate of growth is and has been poorly managed (Alkmuhtar 2016). Despite the existence of a radial master plan (Dar al handasa master plan) giving an overview of the city's future, the plan lacks content (Figure 1.6). Many of the city's residents live in sub-standard housing, in housing developments with poor service provision (Akram, Ismail et al. 2016). The only coordinated developments taking place are aimed at affluent members of Kurdish society and do not represent the needs of the bulk of the population (Rakib 2006). To prevent what is the oldest continuously inhabited city in the world from becoming a development disaster, there is need to design housing development to work with the microclimate and for an improvement in the quality of dwelling design. Here, the phrase quality of design refers to both the visual and performance aspects of these designs.

This study chose Erbil as a case study because of its unique importance historically, architecturally, and climatically. Erbil used to be a sustainable city (Erbil was designed to reduce the impact of climate.) before the new expansion of the last century. As just a citadel, people lived inside it and used the surrounding land for farming. The city has witnessed a rapid expansion of both population and building development, and so its size has become 2,000 times larger compared with 70 years ago (Khayat). Other important values of Erbil are:

1. Historical and cultural value, As the oldest city in the world, the core of Erbil is elevated 30m above ground level over layers and layers of civilisations (UNESCO 2009).
2. Erbil's citadel is located in the centre of the city. The first development happened in the south part of the citadel (Bazar, Arrab, Tajeel, and Khanaqa), in the same organic urban pattern. Remaining developments have followed Western principles of urban design (Akram, Ismail et al. 2016). This caused a split in the urbanisation of the city between its traditional urban fabric and a modern, newly built society. The result of this development was a master plan that quickly spiralled out of control, with no clear vision for the future of the city.
3. The urban structure of the city is binary, combining traditional and modern fabric in different styles of buildings and streets. The majority of the traditional buildings were single storey dwellings built of mud, clay, plaster and timber roofs. In contrast, the new

developments are multi-floored buildings of concrete, steel, aluminium, and glass. Using these non-traditional building materials has resulted in different cooling and heat loads compared to traditional materials.

4. Climatic value: the city is an inland development, removed from any large body of water. Previous research undertaken on the benefits of organic versus grid iron morphologies have all been located close to the sea, in Dubai, Abadan, and Fez (Ali-Toudert and Mayer 2006, Johansson 2006, Charabi and Bakhit 2011, Dalman 2012, Radhi, Fikry et al. 2013, Taleb and Abu-Hijleh 2013). The results of this research cannot therefore be applied to Erbil.
5. Building environment has become the main factor differentiating the traditional and modern parts of city, and it has become increasingly difficult to find an architectural language for the modern construction and renewal process in the recent past. Thus, there is dissatisfaction with the new building process, which has made the city become less sustainable than in the past.
6. One of the main factors that affect urban microclimate is green area, and Erbil has only 4.6% of green spaces in its total area (Naqashbandi 2016).
7. The city is compact, although it has witnessed a rapid expansion, if compared with other European or African cities with a similar sized population.
8. The previous master plans and studies (master plans 1984, and 1994) of the city failed to answer the needs of the local environment, society, commerce, and the new industrial situation as a capital city (Akram, Ismail et al. 2016).
9. There is a lack of a coherent framework or vision, to adapt to the new developments of the city and its expansion needs (Nooraddin 2012). Uncontrolled economic activities coupled with land demands, building, and infrastructure have all challenged the planning authorities.

1.5 The gap in knowledge

1. Old and new morphologies have been compared in terms of modifying local urban microclimate, and a few studies have compared different morphologies to test the UHI effect and its mitigation (Ali-Toudert and Mayer 2006; Johansson 2006; Charabi and Bakhit 2011; Dalman 2012; Radhi, Fikry et al. 2013; Taleb and Abu-Hijleh 2013; (Bakarman and Chang 2015, Bokaie, Zarkesh et al. 2016) (Rasul, Balzter et al. 2015), but have not investigated how interventions in the urban fabric can further modify the microclimate.
2. Recent research has discussed the ‘inter building effect’, or how the urban morphology interacts with the building design, but only considered shading (Pisello, Taylor et al. 2012, Bakarman and Chang 2015) (Pisello, Castaldo et al. 2014). In this research, both shading and building design will be investigated to determine their impact on building microclimate.

1.6 Aim of the research

The main aim of this research is to investigate the impact of the urban form and shading on the urban microclimate and indoor dry bulb temperature. To achieve this aim, the following steps are needed:

1. Establishing the extent of building regulation and control of recent urban developments of Erbil.
2. Understanding Erbil's local climate and investigation of the methodologies that could be employed to alter the urban climate of the grid iron morphology.
3. Modelling the thermal performance of dwelling designs in a hot dry climate in these modified urban climates.

This research is divided into four phases, as shown in Table 1.1.

Table 1-1: Research phases structure

Research Phase	Phase Concept
Phase 1	Literature and preliminary studies
Phase 2	Urban planning and regulations of Erbil Urban design process. Government and private housing projects
Phase 3	Urban microclimate modelling ENVI-met-Validation-Mitigation-Shading mesh
Phase 4	Building Simulation modelling-IES-VE-Shading mesh model-Validation HTB2- Mitigation, shading mesh, interior design, ventilation and façade opening area

Table 1.2 shows each phase's aims, objectives and related research questions

Table 1-2: Research aims, objectives and research questions

Phase 1: Literature and preliminary studies
This phase aims to identify the gap in knowledge in microclimate and building energy studies
Objective
1.1 To understand the climate of Erbil
1.2 To understand the urban development of Erbil
1.3 Review tools to model urban microclimate

1.4 Review tools to model individual building	
Phase 2: Urban planning and regulation of Erbil	
This phase aims to a detailed understanding of the regulatory framework that currently underpins the urban development of Erbil (urban planning and regulations of Erbil).	
Objective	Research question
To understand the urban development process Erbil	2.1 How is urban planning and development in Erbil executed?
To understand the regulatory framework of current urban development of Erbil	
Phase 3: Urban microclimate modelling	
This phase aims to understanding Erbil’s local climate and investigation of the methodologies that could be employed to alter the urban climate of the grid iron morphology	
Objective	Research question
To understand the urban microclimate of Erbil	3.1 How can the urban microclimate be modelled and validated?
To model and validate the urban microclimate of Erbil	
To modify the urban microclimate of the local urban area.	3.2 What is the impact of urban design interventions on urban microclimate (air temperature, wind speed and MRT)?
To understand the impact of shading on urban microclimate	
Phase 4: Building simulation modelling	
Modelling the thermal performance of a typical house in a hot dry climate in these modified urban climates	
Objective	Research question
To understand the impact of shading mesh on typical dwellings performance.	4.1 Does IES-VE simulate shading mesh and how can the proposed model be validated?
To understand the impact of shading mesh, thermal mass and ventilation on air temperature, to allow greater freedom in design	4.2 How does the shading mesh and the dwelling design work together to reduce the indoor air temperature.

1.7 Research methodology

Local urban microclimate studies are characterised by understanding the relationship between urban form and its immediate environment. These studies mainly depend on the location of the studied climatic zone, as well as the well-being of people indoors or outdoors. Ittelson (1978) concluded that a good methodology and data collection must be based on the nature of the research problem. The present study used a multidisciplinary methodology which combines different methods to respond to the research aim. Therefore, the data collection includes local climatic data, a semi-structured interview, and numerical modelling on urban areas, and housing projects case studies. The present study divides the research methodology according to the research phase, as below:

Phase 1: Literature and preliminary studies

1. Previous study
2. Photography (thermal satellite images)

Phase 2: Erbil urban planning development

1. Semi-structured interview
2. Previous studies and government documents
3. Case study analysis (government and private housing projects)

Phase 3: Urban microclimate

1. Analysing climate data (four local weather stations)
2. Validate urban microclimate (two case studies in high and medium urban density areas)
3. Employ climate modelling software (ENVI-met), to mitigate urban microclimate

Phase 4: Individual building modification

1. Simplification approach to model shading
2. Validate the Building simulation, IES-VE model
3. Employ IES-VE to manipulate individual housing units

1.8 Scope and limitation

Erbil urban development

This part of the study took an overview of residential developments between the 2003–2014 in Erbil. This residential development is divided in two parts: government and private housing projects. The data were generated from semi-structured interviews and government documents to redraw the urban design process (UDP) of housing projects. In addition, eight case studies were used to investigate and understand the UDP and environmental considerations during the design and implementation these projects.

The limitation of this part was just covering the urban expansion of the city from an urban design point of view only, such as urban morphology, construction materials, and level of infrastructure in selected housing projects as case studies. The social and economic aspects of the city's expansion are outside the limit of this study, as are other types of developments such as in industry and agriculture, health and tourism projects.

1.9 Urban microclimate modelling

The local urban microclimate is very complicated and difficult to control, so this study investigated factors that had the most influence on the local urban microclimate. The study proposes modification of the urban microclimate for a unique environment specified as a hot/dry climate distant from any water body. Urban and rural areas were climatically analysed to determine the most important factors that can help manipulate the local urban microclimate, for example, air temperature, wind speed, and solar radiation. Any improvement in these factors may lead to improvements in the urban microclimate. This study evaluates the urban microclimate through manipulating the geometry and design strategies without consideration of other factors in the urban microclimate, such as air pollution,¹ noise control, and the anthropogenic heat effect on alerting local urban microclimate.

The study model and validation process of the urban microclimate was carried out in July, because this month represents typical summer in Erbil. Summer months weather data sets were taken from four different urban areas to represent Erbil. The urban microclimate condition of other seasons was not considered because the energy demands in summer are greater, and the cooling load is more than heating loads during the yearly cycle.

¹ Erbil and Kurdistan in general have high demands for energy, and the government can only generate 48% of the total required. Thus, people depend on private diesel generators to fill the shortage of electricity and this causes air pollution.

This study had planned to collect weather data *in situ* to represent the local urban microclimate, but the security condition of the city and Newcastle University policy on safety prevented this. Instead, weather data were obtained from other sources, which were rearranged and analysed systematically to understand the local urban microclimate of city. These weather stations were used to represent high, medium, and low urban densities, and they represent the different microclimate conditions of the city: north (rural), central (traditional morphology), south (grid-iron morphology), and the airport. One of the limitations of using climate modelling (ENVI-met) is that only a discrete part of the city can be modelled. This then requires boundary conditions to be set at the perimeter of the modelled urban area and climate variables predicted close to these boundaries will be very dependent on the conditions set.

1.9.1 Building simulation modelling

Residential housing and individual housing units were selected as a prototype to represent housing in Erbil, and therefore flat and apartments were not considered. The local urban microclimate conditions of Erbil were used as the main boundary conditions of the model. This manipulation modelling addresses housing units during the summer time only, because as stated there is a high energy demand for cooling loads more than other seasons. The modelled strategies were limited to environmental strategies that may help to reduce the indoor air temperature. This includes the environmental aspects of housing design, while the social (local identity) and economic design preferences were not considered.

The prototype house is within the limited neighbourhood scale of ten attached houses in total. In addition, this prototype housing unit follows the building regulations of Erbil in terms of construction materiality (hollow concrete blocks, and reinforcement concrete), setbacks, orientation, and design preferences.

1.10 Research Structure

The present study contains nine chapters, divided into four phases (Figure 1.7). The first chapter is the introduction, research problem, aim and key methods used. Chapter 2 is the literature review. Chapter 3 identifies the thesis methodology and how these models were validated. Chapter 4 outlines the urban regulatory framework of Erbil urban design and planning process. Chapters 5 and 6 are concerned with urban microclimate modelling and manipulation of the local urban microclimate. Chapters 7 and 8 detail the building energy modelling and manipulation of indoor air temperature through appropriate design strategies. The last chapter (9) highlights the key findings of the study, and presents final conclusions and future work.

1.10.1 Phase 1: Literature and preliminary studies

This phase is divided into four sections: Erbil climate, history of Erbil's development, Urban Microclimate Modelling, and Building Energy Modelling. In each section, a comprehensive review of the literature is presented to identify the gap in knowledge regarding: the urban development process in the city, local urban microclimate, and coupling strategies between urban microclimate effects on building thermal performance in hot/dry climate cities. The important feature of this phase is to present the research problem, objectives, and methods in a comparative chronological order to justify the case study position in terms of urban planning, and to select suitable simulation models for urban and building scale.

1.10.2 Phase 2: Erbil urban planning development

This phase aims to identify the current urban planning process in government and private housing projects. Chapter 4 reports on the semi-structured interviews and other sources of data to establish the urban design process in the city. This includes a detailed analysis of housing projects designed by means of case studies. Government and private housing projects are compared in terms of urban design, their construction process, and other related requirements, in order to understand the local environmental process during the design and construction of the housing projects.

1.10.3 Phase 3: Urban microclimate

This phase aims to understand and modify local urban microclimate. This includes: local urban numerical modelling, the validation process, and the manipulating urban microclimate. ENVI-met will be used to simulate the current urban morphologies of traditional and modern Erbil. The validation process compares high and medium urban morphologies using two sources of weather data from the central and southern weather stations. The final section of this phase employs urban design strategies to improve and modify the local urban microclimate of Erbil. These mitigation strategies are an attempt to improve urban microclimate elements such as air temperature, wind speed, and mean radiant temperature.

1.10.4 Phase 4: Individual building modification

This phase attempts to integrate the urban microclimate and the single building scale. The aim is to modify the typical house design's thermal performance and consequently reduce the cooling load during summer time. In Chapter 7 the modelling of the shading mesh is presented and validated. Chapter 8 focuses on shading modelling using Building simulation IES-VE model. This model is employed to explore the effect of shading on indoor air temperature. Chapter 9 discusses the research and presents further building simulations where natural ventilation via window opening was modelled, together with shading for a typical house constructed from local materials. Chapter 10 includes the key findings and important recommendation for future work for designers and urban planners.

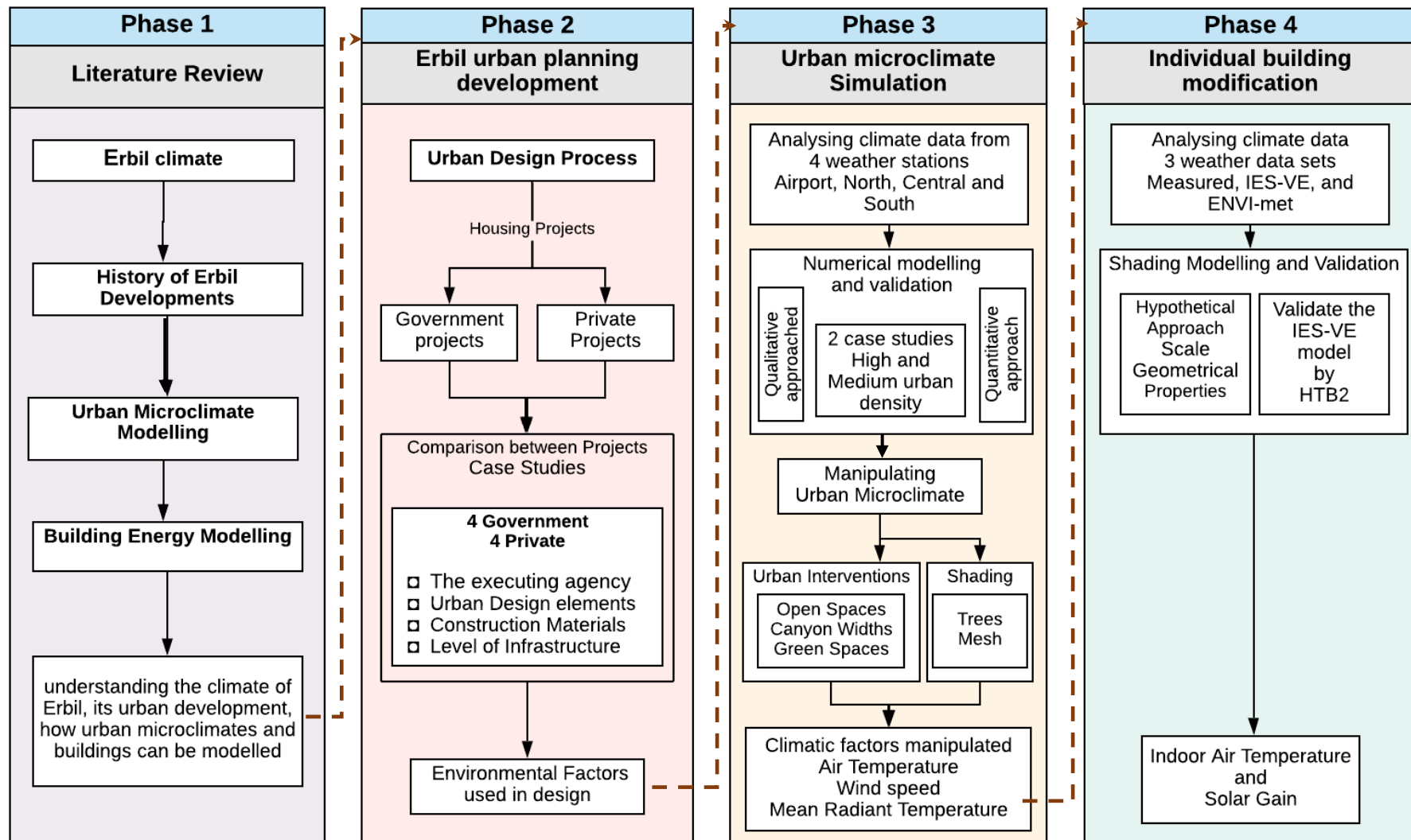


Figure 1.7: Thesis structure and framework for all four phases

Chapter 2 Literature review

2.1 Introduction

This chapter shows the theoretical background of the present study in four phases: Phase 1 is a review of Erbil's climate, Phase 2 is related to urban development in Erbil, Phase 3 investigates urban microclimate modelling, whilst Phase 4 will discuss Building Energy Modelling (BEM). The aim of this chapter is to understand the principles of urban microclimate and identify the gap in knowledge, Erbil's urban design process, and microclimate mitigation for the urban and building scale.

2.2 Climate Erbil, Kurdistan-Iraq

This section presents a general overview of the current climate and environmental condition of Erbil in Kurdistan-Iraq, starting with the geographical location and climatic conditions of Kurdistan generally, and Erbil in particular. The climatic conditions of the city in this study are presented in three main parts; air temperature and wind speed; land use in the city; and satellite measurements of land surface temperature (LST). The latter is used to explain the urban surface temperature distribution pattern of the city, and its relation to the urban microclimate of current urban developments. The outcome of this section will be a general understanding of the urban microclimate and climate conditions of the city, as used to select case studies for validation purposes. In addition, this analysis helps build an understanding of the weather data location used in Chapter 5 for urban microclimate mitigation. This includes climatic input data for computer Fluid Dynamic modelling in ENVI-met, which in turn is used as the output to build a proposed weather data file (WDF) for the local urban microclimate. This file is used as the data source for analysis in Chapters 5–8 with the IES-VE program.

2.3 Erbil History

2.3.1 Narratives of historic development

Kurds are one of the oldest peoples in the Middle East, as descendants of a mixture of Indo-European immigrants who settled in Kurdistan thousands of years ago. In the 20th century, ¹Britain and France abruptly divided the Middle East without regard to ethnicity, and the historical boundaries of where local people dwelt. The affected countries were Palestine (modern day Israel), Syria, Iraq, and Iran. Being on a border, Kurdistan was divided into four main parts totalling 190,000 Square miles split between Turkey (43%), Iran (31%), Iraq (18%) and Syria (6%) (Coban, 2013; Izady, 2015; Meho, 1997) (Figure 2.1 and Figure 2.2).

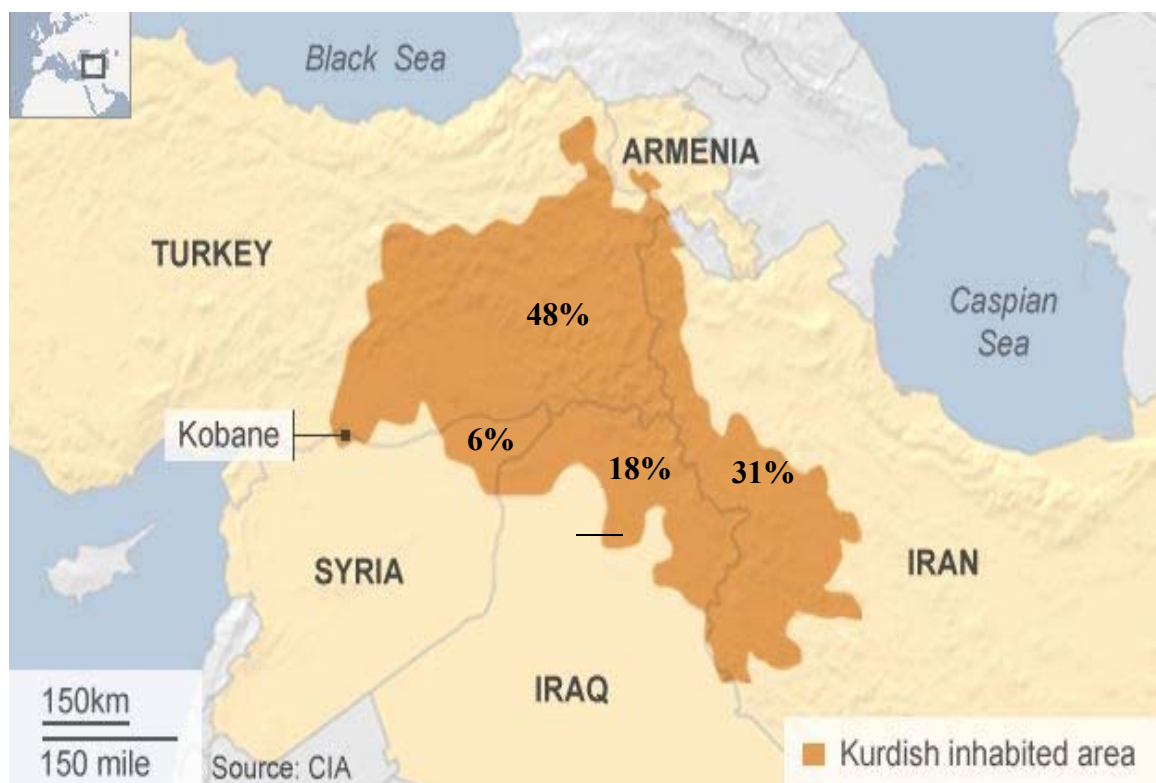


Figure 2.1: Kurdistan was divided principally between Turkey, Iran, Iraq and Syria.

After this division, Kurdistan faced military invasion, attacks, and destruction, which damaged Kurdistan socially, culturally, and economically, as well as by land division. This was the foundation of the political instability that has lasted for almost hundred years. In the last decade of the 20th century, one part of Kurdistan (Iraqi Kurdistan) has started to re-establish Kurdish identity, and Kurdistan has become a distinct, autonomous region once again.

Iraqi Kurdistan is the only part of the original Kurdistan which is an independent region, of which Erbil is the capital (Izady, 2015) (Figure 2.3). Erbil was

¹ Treaty of Sèvres and treaty of Lausanne

founded in the 5th millennium BC, and thus represents one of the earliest examples of urban civilisation in the world. The city had military and administrative functions, and the urban core in the heart of Erbil was a single settlement fortified unit (Akram, Ismail, & Franco, 2016). This unique urban settlement developed over time in an irregular oval shape on many layers of archaeological ruins of historical urbanisation (Figure 2.3).

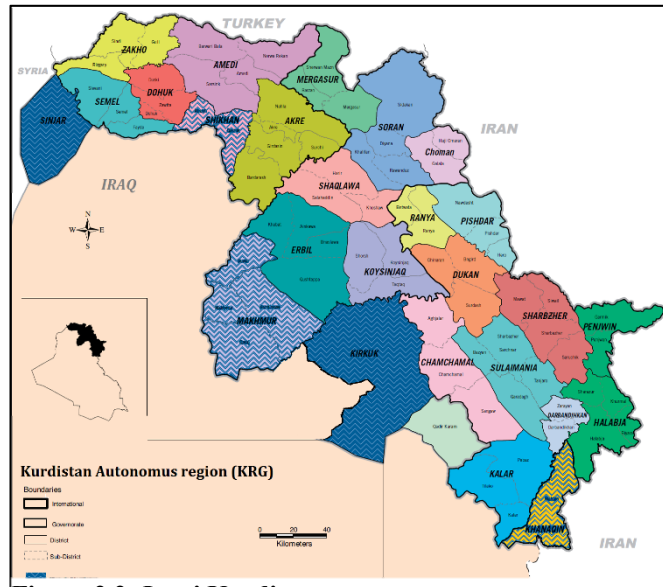


Figure 2.2: Iraqi Kurdistan

The citadel rises layers over layer of civilisations. It now rise 30m over the city level and has an area of c.102,000m² (Abbas, 2017) (Figure 2.3).

2.3.2 Urban development of the Erbil citadel

The citadel of Erbil is considered the core of the city's urban development throughout history. The city had unique architectural features, and strong social and economic forces which helped its gradual population increase. The citadel is considered a unique part of the urban identity of Kurdish people, in terms of representing their lifestyle. As well as being a residential urban area, it is characterised as the main economic and military centre. The urban form and location of the citadel reflect its importance, high above the surrounding urban areas, which are shaped as concentric rings in a radial axis around the citadel (Figure 2.4). As the core of the morphological development of Erbil, the evidence shows that the city had four important stages:

1. Citadel as the city – all the city's population lived inside the Citadel boundary, and so it was the only residential area of the city and all social activity concerned a small community inside its walls (Figure 2.4-Stage one);

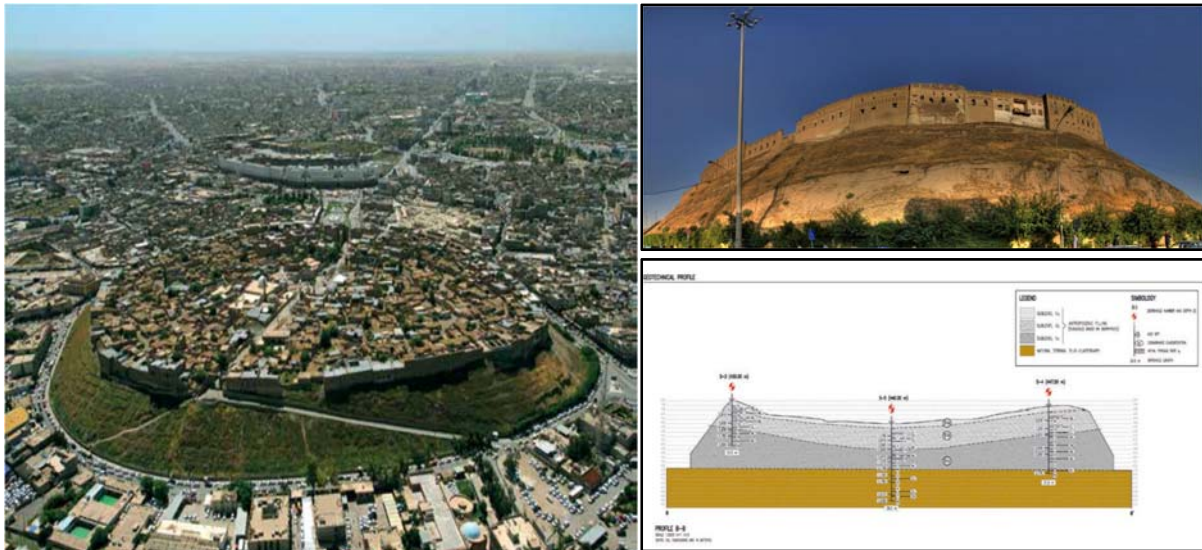


Figure 2.3: Erbil Citadel (Qala). Source: (Al-Jameel, Al-Yaqoobi et al. 2012).

2. Citadel as neighbourhood –which dominate new urban areas surrounding the citadel (Figure 2.4– Stage two). In this stage new organic urban development growth occurred in the south just outside of the Citadel;
3. Citadel as a landmark of urban character – in contrast to the new urban areas outside the citadel, the citadel remained a unique community inside modern grid-iron urban developments (Figure 2.4– Stage three);
4. Citadel as a historic land mark – the KRG² and UNESCO³ announced that the Citadel was a World Heritage Site, and Erbil started to develop outside the citadel as a result of increasing population, deteriorating buildings, and a lack of infrastructure (Bornberg, Tayfor, & Jaimes, 2006). These factors collectively encouraged the local planners to develop and build in new urban areas outside the citadel walls (Figure 2.4– Stage four).

There have been changes to the citadel's urban form, such as opening an axial road between the north and south gates in 1958, and building a new entrance in 1979 (Figure 2.17). For the citadel still consider as a social, associative and identity values for local people in Kurdistan. This is because the Citadel's location within the modern city and its historical role in the city's development over multiple archaeological layers of civilisations (Figure 2.4).

² Kurdistan Government Region, Iraq.

³ The United Nations Educational, Scientific and Cultural Organisation.

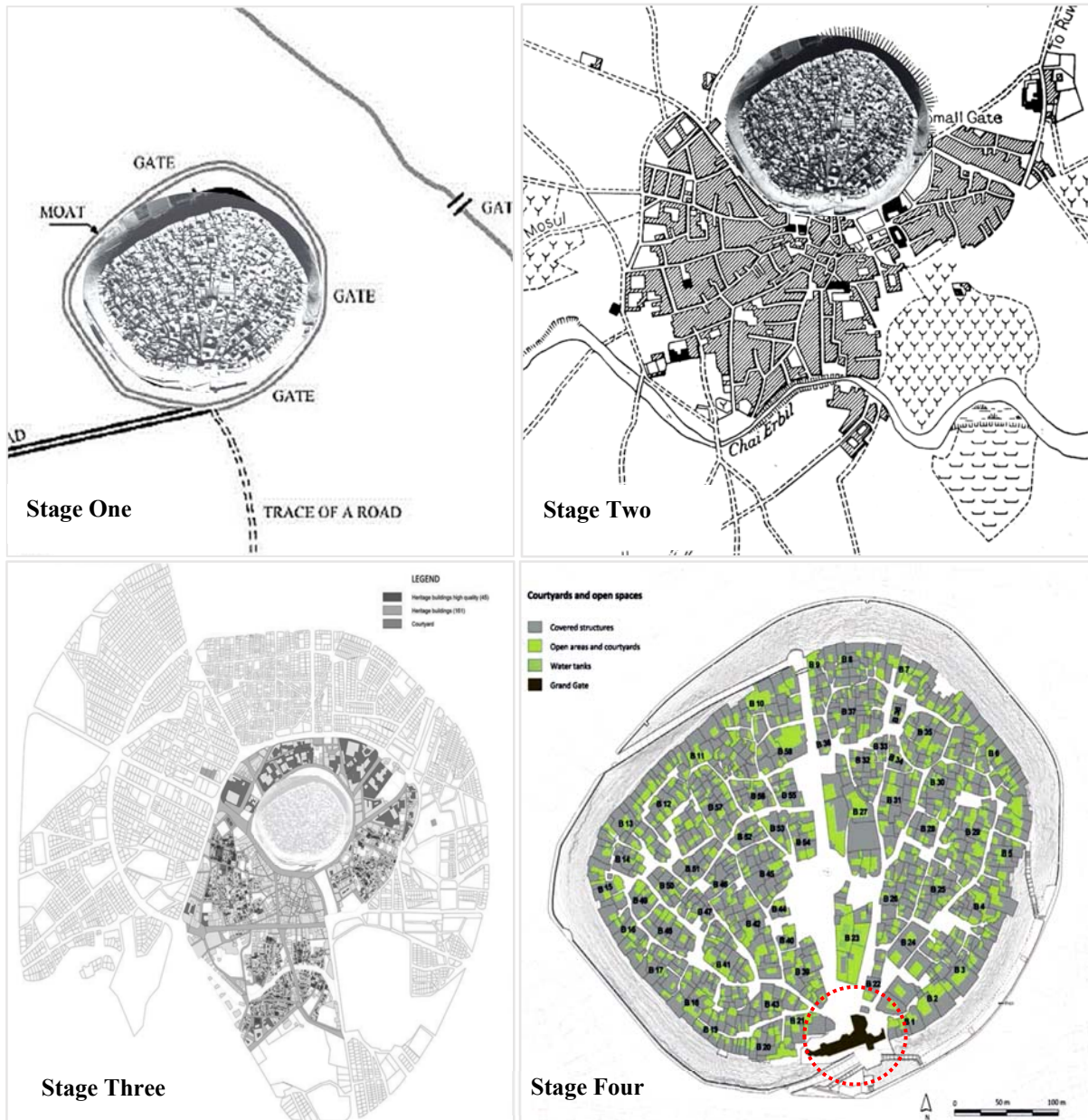


Figure 2.4: Urban development of the Erbil citadel.

2.3.3 Urban transformation of Erbil city

Erbil has witnessed a significant historical and architectural transformation but, even though it has expanded over the past decades, the citadel and most historical urban areas remain well-preserved. This is in contrast to the local building environment and city identity, which have been significantly affected by socio-economics and geo-politics. The flexible master plan (central-radial), following a period of economic and political stability, contributed to a gradual expansion before 2003, and a rapid expansion after 2003 (Bornberg et al., 2006). The urban transformation of city can be divided into five periods (Figure 2.5):

1. The pre-industrial city before 1900 (Ottoman period)

The citadel was surrounded by fortifications to protect the city from attack. The architectural features of this period were fortified walls, including towers and gates, with limited urban areas outside the fortified walls.

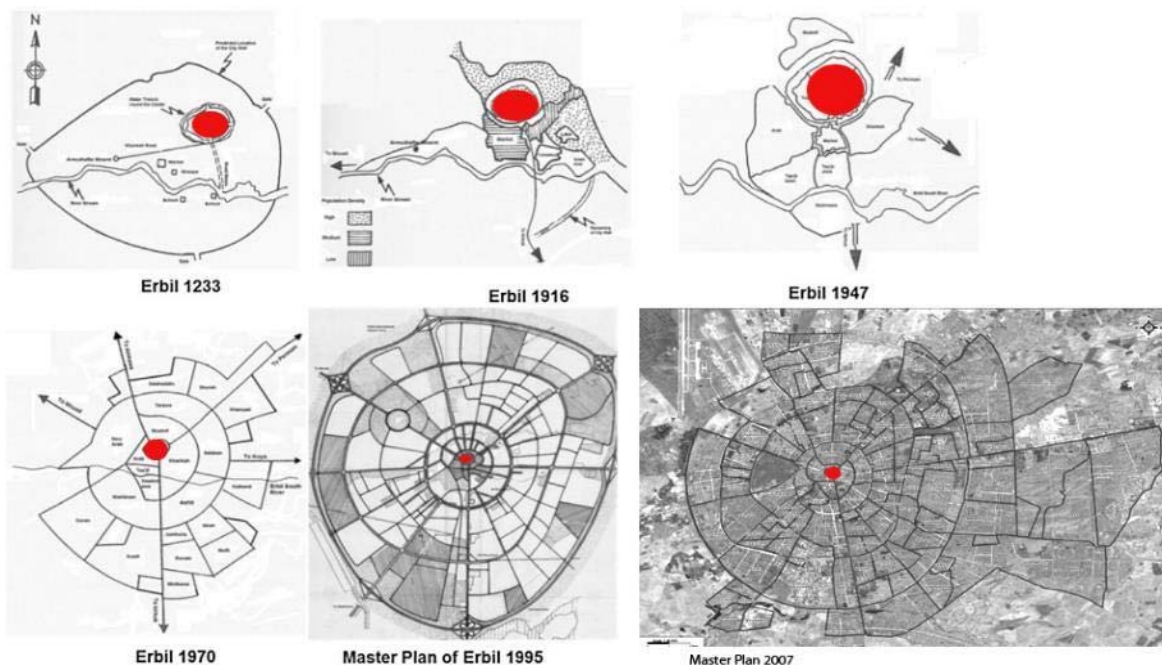


Figure 2.5: Erbil urban development from 1200 to 2007

2. Early modernity 1900–1940 (pre-modern period)

This period of the city is categorised by new architectural and urban aspects. The expansion of the urban areas outside the citadel is comprised of compact blocks of buildings with one or two floors. The streets were narrow and organic, but adapted to modern transport systems. The residential urban areas included compact blocks and courtyards buildings constructed with traditional or modern building materials. The size of openings was small and traditional ways of environmental adaptation were used.

3. Post-modern city and materialism (1940–1980)

In this period, the urban areas expanded as a result of a population increase and social movement from rural areas to the city. The architecture and urban planning of this period was affected by European planning, and the residential blocks around the city centre (the organic fabric) expanded with modern buildings of more than three floors. Modern styles and building materials were used which transformed the building style from traditional (small spaces) to modern house with larger spans using concrete and steel. Courtyards, compactness, and small openings (the traditional style of building) gradually vanished in this period.

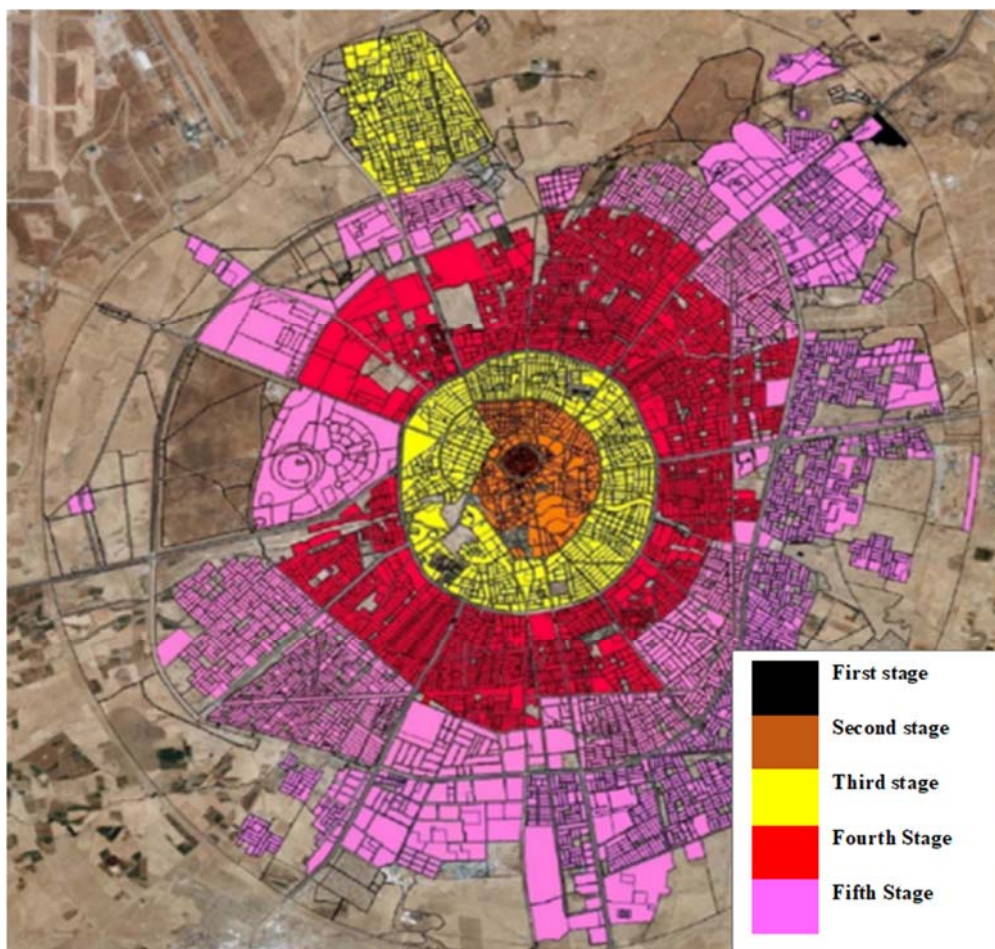


Figure 2.6: Erbil housing development stages throughout history.

4. The autonomous city (1980–2003)

This period was mainly affected by the impact of the First Gulf War and economic sanctions after 1991. These events provoked enormous immigration from rural areas to the city and the rise of informal and suburban settlements. Traditional building techniques and classical builders largely vanished and building relapsed into a post-modern style. The architecture and development was limited and of poor quality. The city showed a confused image of architectural characteristics in urban development that used planning, which started with informal development and infrastructure provided by the local authorities (Figure 2.6).

5. The neo-liberal economic city (since 2003)

After 2003, the Kurdistan region and Erbil city especially witnessed unexpected social and economic movement with large investment in building development and oil extraction (Akram, Franco, & Ismail, 2016). The Western style dominated buildings and residential



Figure 2.7: The neo-liberal economic city, after 2003

blocks, and urban areas became divided between wealthy and middle income districts, with the appearance of exclusive compounds (Figure 2.7).

2.4. Erbil City Planning

The city, dominated by the citadel, represented traditional urban development before the 20th century, beginning with the core of the citadel 30m above the city (Figure 2.8). However, the first developments outside the citadel were not a planned expansion, but a response to high density urban development inside the citadel. The two districts with a vernacular architectural style are called the citadel and buffer zone A. This includes the citadel, Mustawfi, Arab, Bazar, Khanaga, and Tajil (Figure 2.8). These areas have historic urban fabric and heritage buildings that give the area a sense of place.

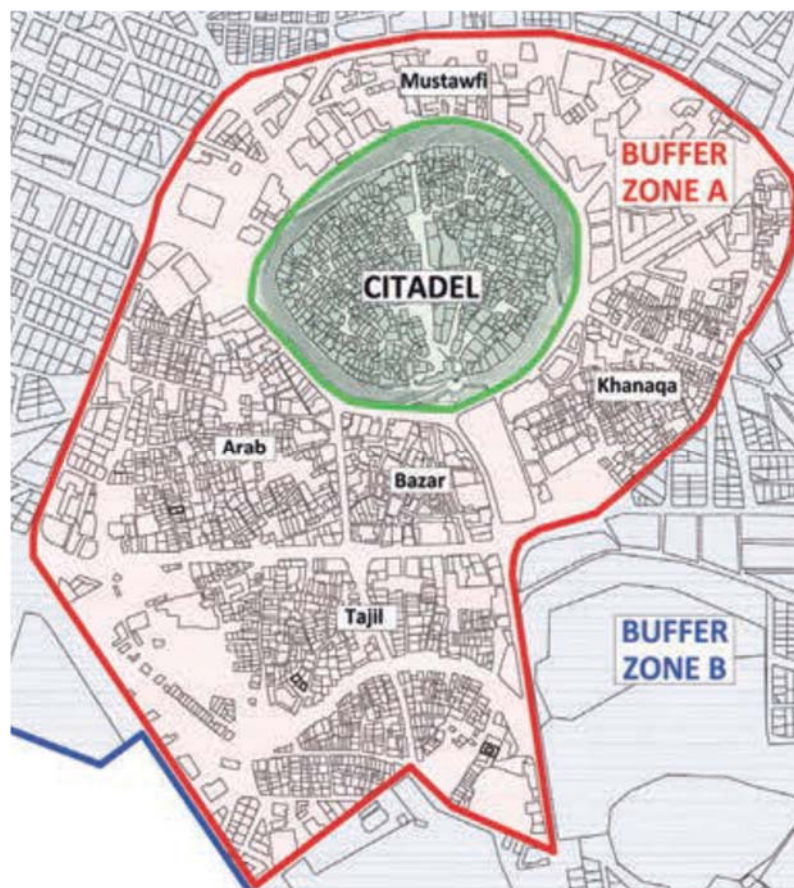


Figure 2.8: Erbil Citadel and Buffer Zone A

These urban areas mostly expanded before 1920, and after this the city further expanded and a new master plan was designed by international companies contracted by the central Iraqi government, without the participation of local city representatives. The city then developed and expanded based on the master plans below.

1. The first Master Plan, proposed and drawn by Grot: Architect P.W.D. – 1932

This proposal master plan include grid-iron roads for the first time and 33,330 house plots in the North West part of the city (Figure 2.9). However, this master plan was not fully implemented and is considered the first attempt to apply grid-iron morphology.



Figure 2.9: The first master plan proposal for Erbil city expansion 1932. Source: Iraqi National Archive, Baghdad, Gort Architects.

2. Second Master Plan by Doxiadis – 1951

Erbil's population increased from 12,000 to 30,400 and Iraq in general witnessed social and technical development. This happened due to large migration from rural areas to cities, and shifting land use around the city. The new development needed a new master plan for the future development of Erbil, and so a new one was proposed by the Doxiadis group and

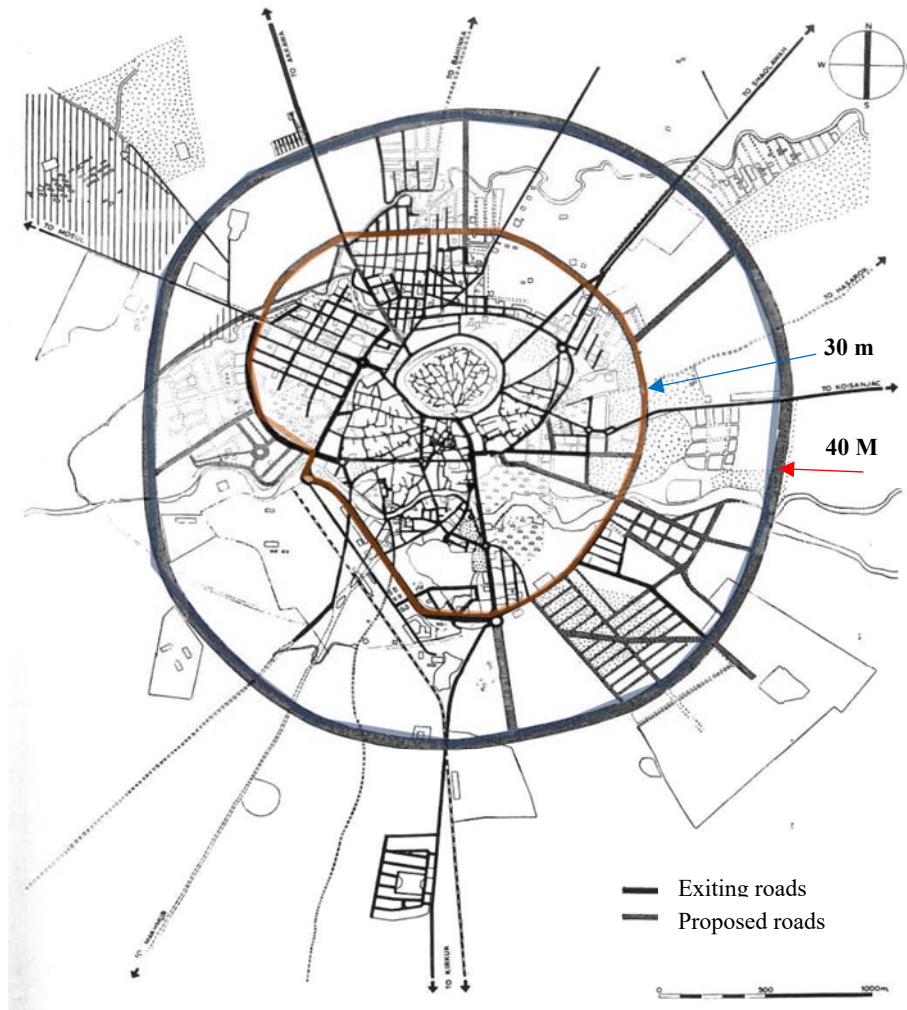


Figure 2.10: The second master plan proposal by DOXIADIS for Erbil expansion 1951 Source: Doxiadis, DOX-QA92 (1958p.73).

approved by the Iraqi government, to be directly implemented (Al-Hashimi, 2016). This master plan was mainly about building roads, and the proposal also included ring roads around the citadel and diagonal roads cutting across the organic fabric of the city (Figure 2.10).

In this proposal, the 30⁴ m and 40⁵ m ring roads were proposed to connect with old roads to assist traffic circulation and connect the bazaar area to other districts. In addition, it proposed new roads to connect the city to

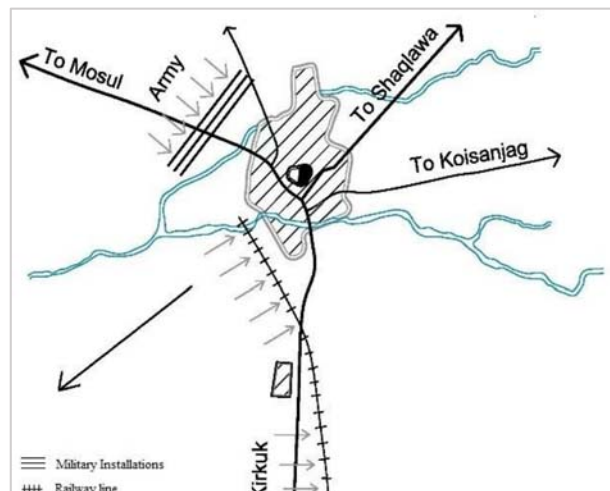


Figure 2.11: The main Road to connect the city with other Kurdistan cities.

⁴ Main Ring roads in Erbil city

⁵ Main Ring roads in Erbil city

other parts of the Kurdistan region, such as Kirkuk, Mosul, Koisanjac, and Duhuk through Shaqlawa (Figure 2.11)

3. The third master plan of the Central Ministry of Planning (Baghdad) – 1977

This proposed master plan of Erbil city was started in 1977 by the centralised Ministry, and finished in 1984 by the Directorate General of Physical Planning in Baghdad. This master plan was not supported by any scientific approach, such as a comprehensive analysis of social participation, and so the resulting plans and road layouts had no relationship to the physical or social needs of the population of Erbil. In addition, the proposed master plan designed by the central government in Baghdad was without any consideration of the local heritage value of the city (Akram, Ismail, & Franco, 2015). Rassam (2009) concluded that this master plan was unsuccessful because it did not involve Erbil local authorities and social desires, and so it failed to meet the real needs of the city. In addition, there was a lack of experienced planners. This initial master plan was still being used until 1994 (Figure 2.12).

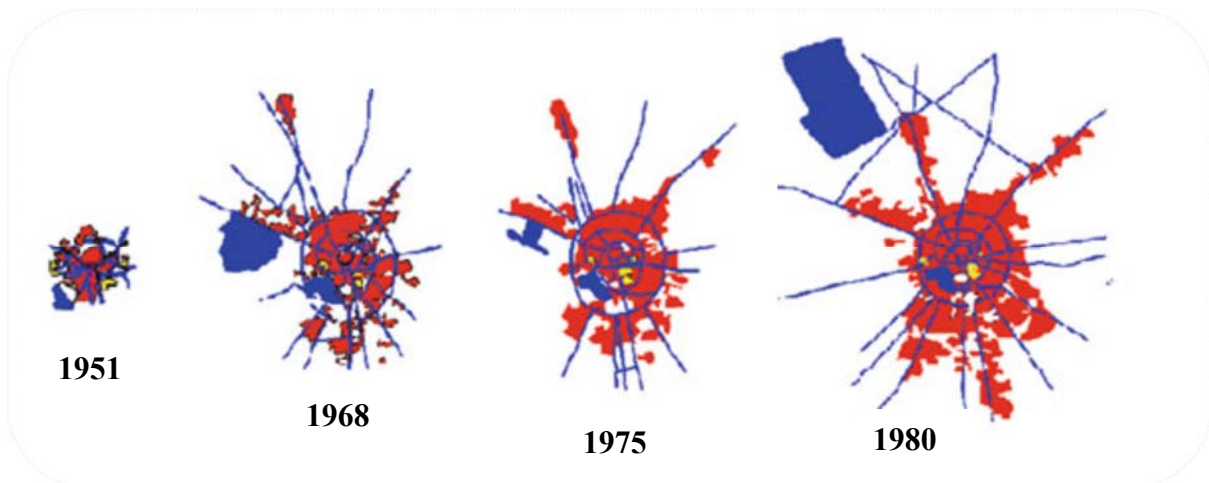


Figure 2.12: Urban development from 1950 to 1980.

The Kurdistan Regional Government was established after the First Gulf War of 1991, and because of freedom and migration from other parts of Kurdistan, the city became the capital city of the Kurdistan region (Sabr, 2016). Due to the lack of appropriate urban planning to meet the increased population requirements, the need for a new master plan had become urgent.

3. The fourth master plan by the Kurdistan Council, Erbil – 1994

The KRG was established in 1991, and the Ministry of Municipality became responsible for urban planning, while the Ministry of Construction and Housing is responsible for the planning

and implementation of the master plan (Akram et al., 2015). The fast growth in the economy, the return of displacement Kurds before 1991, and the increase in land prices led to rapid formal and informal growth in residential, commercial, and industrial development in Erbil (Ammar, 2006). However, the lack of skills and experience in the planning authority resulted in poor implementation of the master plan (Figure 2.13).

This master plan of Erbil was also limited by the lack of consideration of social, economic, and environmental aspects, coupled with limited knowledge of new urban planning trends and management approaches (Ayoob Khaleel & Ibrahim, 2010). The third and fourth master plans (1984 and 1994) lacked a clear vision of the city's development, and had inadequate urban planning policies and frameworks for the upcoming city (Bornberg et al., 2006). In addition, no objectives and priorities were defined in that period, especially for the city centre with its traditional morphology, and this needed to be addressed with an appropriate plan

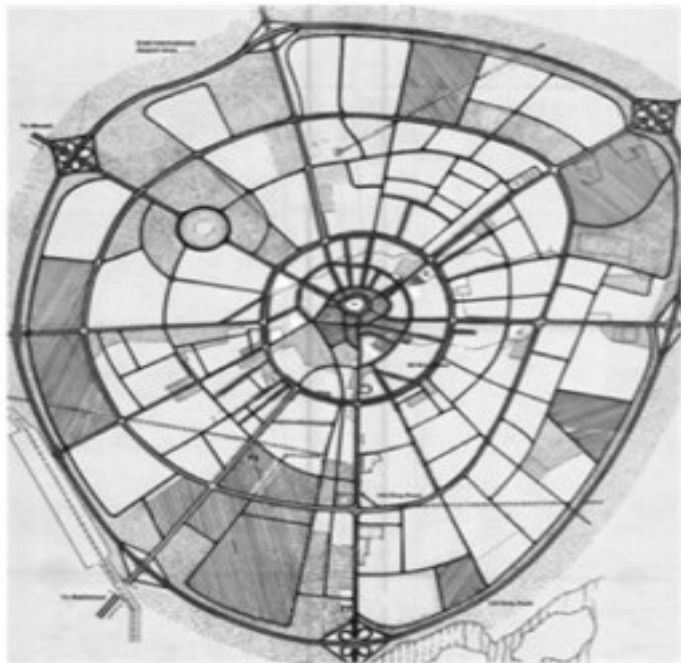


Figure 2.13: Master plan of Erbil city 1994

consistent with the future development of the city (Ammar, 2006). Although the masterplan was envisioned to be active until 2015, the plan did not correspond to the current situation or adapt to the capital city's role (KRG, 2013). As the municipal councils lacked experience, urban management became the responsibility of the community. Moreover, the master plan was unsuccessful because of a number of issues, such as the lack of: housing in poor urban areas, infrastructure, health services, and a poorly maintained physical environment (R. I. Ibrahim, Mushatat, & Abdelmonem, 2015).

4. The fifth master plan by the Jordanian engineering consultancy, Dar Al Handasa – 2006

As a result of the lack of appropriate urban planning, the city had expanded until 2005 without any urban policy framework to allow the new developments to be integrated with the old fabric of Erbil, both environmentally and visually (KRG, 2013).

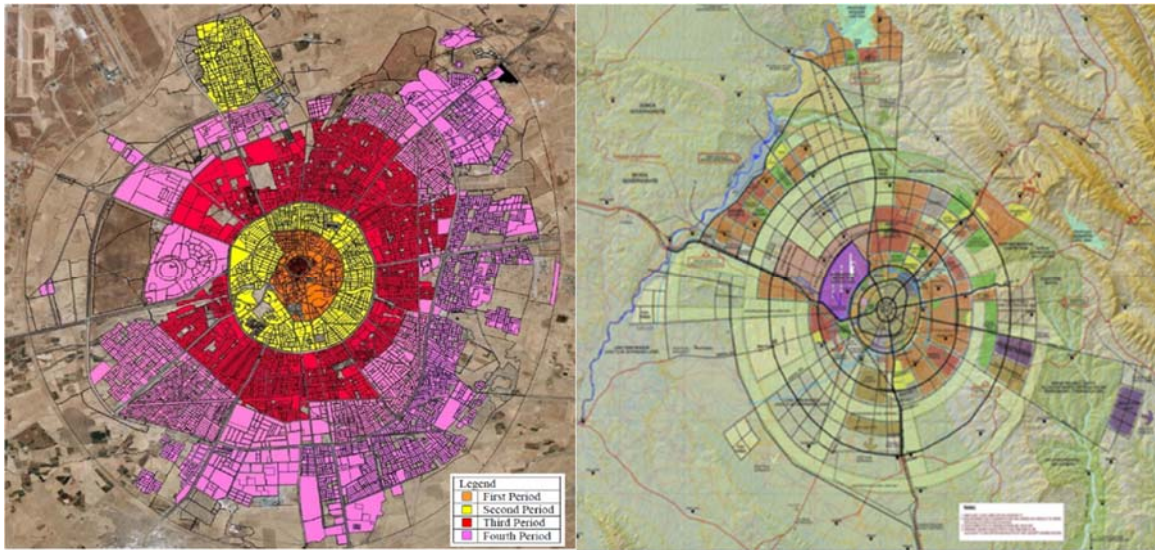


Figure 2.14: Erbil recent master plan designed by Dar Al-Handasa. Source: KRG (2009)

The government was forced to re-design the master plan to control the ongoing expansion required, and so the Erbil master plan was designed by Dar Al Handasa (a Jordanian engineering consultancy); this is the final master plan that will be effective until 2030 (Akram, Ismail et al. 2015). The Jordanian engineering consultancy's plan shows a series of concentric circulation roads. The concept proposed extensions to the city for more than 30 km in all directions (Figure 2.14). The plan was based on idea of the so-called "Bull's eye", with the citadel in the inner circle and the rest the radial growth of the city (Dar, 2016). Dar Al Handasa summarised the seven objectives for Erbil's master plan as follows:

1. Restructuring dilapidated areas;
2. Conserving significant and heritage buildings;
3. Providing a network of urban spaces;
4. Creating quality urban routes;
5. Encouraging new business and development;
6. Developing tourism in the city;
7. Providing adequate infrastructure in the city.

The urban form in Erbil, even with the new proposed plan, still follows a concentric radial layout. This projected future plan starts with the circle of the citadel and the rest of the radial growth is like ripples in water. It is likely that the huge growth of Erbil would have direct consequences on the future of the citadel, which is a factor in the proposed conservation plan which cannot be ignored (Figure 2.14).

This master plan has been proposed without the consideration of social, economic, and environmental aspects. In addition, there is limited knowledge within the planning authorities of information technology and management approaches, and a lack of the multidisciplinary experience required for planning an important city like Erbil.

2.5 Erbil Housing

Erbil city has a rich history of construction and housing design. Housing demands increased as the socio-economic status of the city grew, and with immigration from other parts of Iraq into Kurdistan generally and Erbil specifically. Housing shortages started after 1991 as a result of sanctions. Different housing providers have been instigated in response to growing housing demands. UN-HABITAT (2010) classified housing needs into three types of units: multi-story housing, single storey houses, and single-family housing. This problem of housing and urbanisation is not new, as it started in the last century as a result of city expansion and increasing population. In 1975 Alahami found that Erbil city and urbanisation was suffering from four issues:

1. Population and socio-economic expansion;
2. Rapid expansion;
3. Housing needs;
4. Social problems and public facilities shortage.

In Kurdistan, Iraq, housing needs led to a change in the landscape of major cities. Housing projects reshaped and transformed the layout of the city after 2003 and changed the identity of urban development. On one hand, the housing project in the Kurdistan region represents 42.9% of total investment and 44.51 % of investment lands, which cost more than \$6.5 billion. On the other hand, housing demands are still considered a critical issue in the region because of the rapid expansion and migration from rural areas to the city.

Moreover, the housing sector was ignored by the central government in Baghdad for a long time in terms of regulations and a lack of clear housing strategy (1921–1991). This led to increased demand and a shortage of affordable housing for young families. After oil extraction and global architecture movements in the region, Erbil has witnessed an extraordinarily rapid expansion, represent by the increasing number of neighbourhoods. In 1950, the number of neighbourhoods in the city was just eight, but in 2012 this number had increased dramatically to 82. Such growth in the urban area is ten times that of the last 60 years, and most of this expansion happened after 2003.

Erbil's housing projects are associated with a negative impact on potential users due to the lack of government policies, poor infrastructure, the lack of qualified construction companies, the use of untested construction techniques, and the cost of housing units. Rassam and Dezayi (2006) found that Erbil is suffering from environmental degradation. The poor land management and rapid expansion of the city created major challenges, including informal housing, lack of sufficient roads to health and educational facilities, poor services, and a lack of infrastructure (Chilmeran, Amman et al. 2006).



2.6. Housing Typology


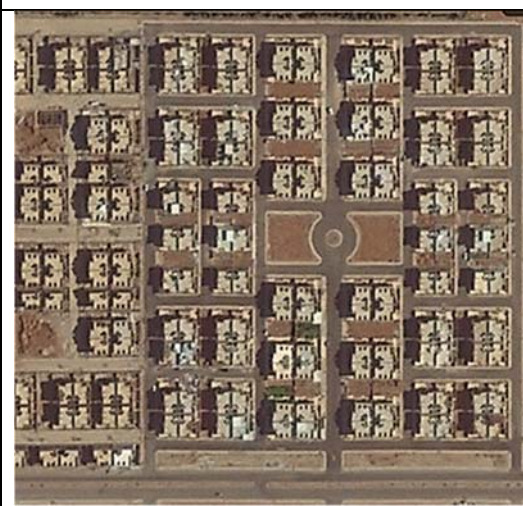

There are eight types of housing in Erbil, classified by the characteristics of residential morphology. Characteristic features are plot size, infrastructure elements, roads, public services and facilities, density of urban area, and built-up area averages. The typology of houses is:




1. Historic core of city (city centre);
2. Courtyard houses (citadel and surrounding areas);
3. Subdivision with small attached housing plots;
4. Subdivision with large housing, attached or detached;
5. Informal settlement;
6. Mixed use houses (commercial and residential);
7. Unfinished peripheral subdivision (> 50% built-up area);
8. Incomplete peripheral subdivision (< 50% built-up area);
9. High rise apartment buildings.



Every housing type refers to a type of residential urban morphology rather than to a specific building type (individual house). Some of these types of houses are difficult to categorise in terms of their housing features, but instead all neighbourhoods can be analysed as a whole. This section explains the housing types in Erbil according to their urban planning characteristic features; the classification of each type includes five characteristics, as below:


Table 2.1 Housing types in Erbil according to their urban planning characteristics Source (www.humanitarianlibrary.org)

Type 1: Historic core of city (city centre)	
	<p><u>Development Process:</u> The city originally developed from the citadel, which represents the social, heritage, and culture of the city. The buffer zone has special planning and urban regulations which is differed with rest of city.</p>
	<p><u>Layout Fabric:</u> The street and road pattern is irregular and organic, similar to most old cities in the Middle East</p>
	<p><u>Housing Units:</u> Compact and attached houses with one to two floors</p>
	<p><u>Urban Density:</u> High dense urban area of around 40 units in one hectare</p>
	<p><u>Level of Infrastructure:</u> Poor infrastructure in the past, and medium or appropriate services more recently</p>
Type 2: Courtyard houses (citadel and surrounding areas)	
	<p><u>Development Process:</u> Roads and streets systematically divided to adapt to new transportation, while plots are informally subdivided and follow the same style as the citadel pattern</p>
	<p><u>Layout:</u> Streets are wide with irregular development within individual blocks</p>
	<p><u>Housing Units:</u> Plots with irregular shape, and houses are a mixture of traditional courtyard houses and modern commercial buildings on the main roads</p>
	<p><u>Urban Density:</u> High density urban area with 30 to 35 units in one hectare</p>
	<p><u>Level of Infrastructure:</u> Roads paved and all houses access the national grid (water, and electricity)</p>
Type 3: Subdivision with small, attached housing	

	<p><u>Development Process:</u> Blocks planned into roads and attached houses by inexperienced planners</p> <p><u>Layout:</u> Housing blocks in a grid-iron pattern</p> <p><u>Housing Units:</u> Plots systematically subdivided into small attached units. Housing units mostly without courtyards</p> <p><u>Urban Density:</u> High density, approximately 35 housing units per hectare</p> <p><u>Level of Infrastructure:</u> Urban area provided and connected with general grids of city infrastructure</p>
Type 4: Subdivision with large housing – semi-detached housing	
	<p><u>Development Process:</u> Blocks planned into roads and attached houses</p> <p><u>Layout:</u> Housing blocks in a grid-iron pattern</p> <p><u>Housing Units:</u> Plots systematically subdivided into small attached units. Housing units without courtyards</p> <p><u>Urban Density:</u> High density, approximately 35 housing units per hectare</p> <p><u>Level of Infrastructure:</u> Urban area provided and connected with general grids of city infrastructure</p>
Type 5: Informal settlement	
	<p><u>Development Process:</u> Blocks not planned by planners and divided into roads and attached houses</p> <p><u>Layout:</u> Housing blocks in an irregular pattern</p> <p><u>Housing Units:</u> Plots not systematically subdivided into small attached units</p> <p><u>Urban Density:</u> High density, approximately 50 housing units per hectare</p> <p><u>Level of Infrastructure:</u> Urban areas lack infrastructure, but after 2003 connected with general infrastructure</p>
Type 6: Mixed use houses (commercial and residential)	

 <p>  Housing blocks  Commercial blocks </p>	<p><u>Development Process:</u> Blocks divided into commercial units on the main roads and housing units at the back</p> <p><u>Layout:</u> Housing blocks in a grid-iron pattern</p> <p><u>Housing Units:</u> Plots systematically subdivided into large plots on the main roads and small attached units</p> <p><u>Urban Density:</u> Medium density, approximately 30 units per hectare</p> <p><u>Level of Infrastructure:</u> Urban areas connected with general infrastructure.</p>
--	--

Type 7: Unfinished peripheral subdivision (> 50% build-up area)	
	<p><u>Development Process:</u> Blocks divided into housing blocks, as either attached or detached houses</p> <p><u>Layout:</u> Grid-iron morphology</p> <p><u>Housing Units:</u> Plots systematically subdivided into large plots on the main roads and small attached units</p> <p><u>Urban Density:</u> Medium density, approximately 20 units per hectare</p> <p><u>Level of Infrastructure:</u> Urban areas connected with general infrastructure and services</p>
Type 8: Incomplete peripheral subdivision (< 50% build- up area)	
	<p><u>Development Process:</u> Planned blocks divided into housing blocks and roads</p> <p><u>Layout:</u> Grid-iron pattern</p> <p><u>Housing Units:</u> Plots systematically subdivided into small attached units</p> <p><u>Urban Density:</u> Low density, approximately 5 to 10 units per hectare</p> <p><u>Level of Infrastructure:</u> Urban areas have unpaved roads and are not connected with government infrastructure</p>

Type 9: High rise apartment buildings	
	<u>Development Process:</u> Built by the government before 1991 or a private company after 2003
	<u>Layout:</u> Housing blocks in a grid-iron or variable pattern
	<u>Housing Units:</u> Plots systematically subdivided into large plots on the main roads and primarily medium or high rise apartment buildings
	<u>Urban Density:</u> High density, approximately 50 units per hectare
	<u>Level of Infrastructure:</u> Urban area connected with general infrastructure

2.6.1 Kurdistan Climate

Kurdistan was divided by France and England after the First World War between four countries. Geographically, Kurdistan has borders with three countries: Syria in the West, Iran in the East, and Turkey in the North. It is now an autonomous part of Iraq. This study focuses

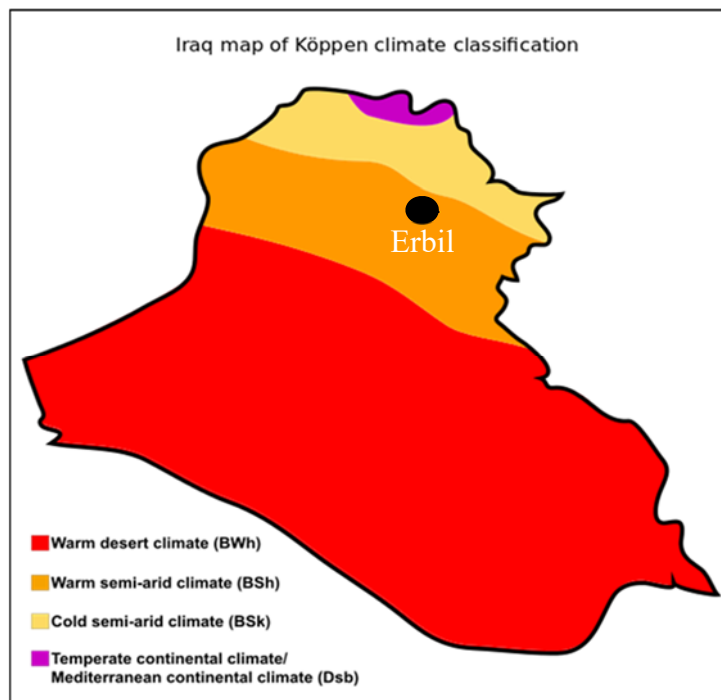


Figure 2.15: Iraq and Kurdistan Köppen climate zones.

Source: <https://chronicle.fanack.com/iraq/geography>.

on the Iraqi-Kurdistan Region, which has three provinces Erbil, Slemani, and Duhok. The area of Kurdistan-Iraq is about 40,000 km² (Husami, 2007a) (Figure 2.2). Kurdistan's mountains are about 2,400 metres high on average, and the highest mountain peak is Halgurd at 3,660 m.

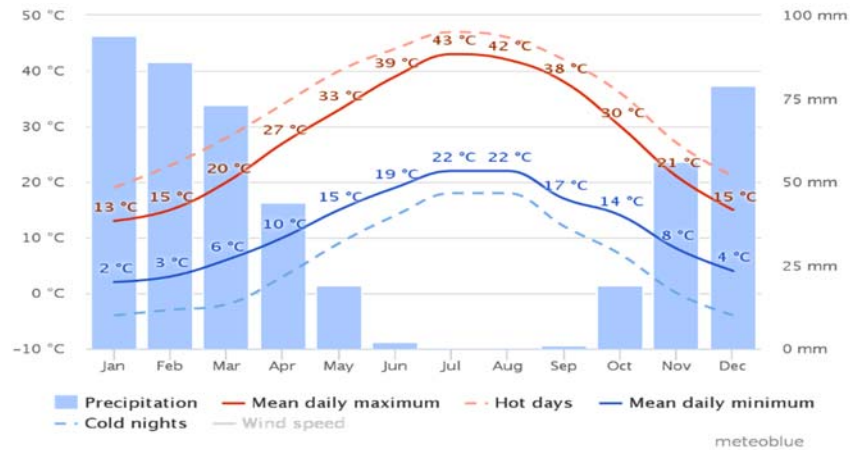


Figure 2.16: Average rainfall in Erbil is lowest in June, with an average of 0 mm and highest in January at 112 mm . Source (climate-data.org).

Average annual rainfall for the region is 375–724 mm. Generally, the climate is semi-arid continental, which is hot and dry in summer, and cold and wet in winter (Figure 2.15).

June–September are considered the summer months, during which the mean air temperatures are 39–43 °C but regularly reach 50 °C and above (Hameed, 2017). Spring is very short and lasts for only one or two months, with a mean air temperature of 25–32 °C. Autumn is also dry and mild and has a mean air temperature of 24–29 °C in October, but is slightly cooler in November. The Kurdistan winter is mild except in the mountains, where the maximum average air temperature is 7–13 °C and the minimum average is 2–7 °C (meteoblue, 2016) (Figure 2.16).

Kurdistan is located between in the sunny belt of 34°42' and 37°22' latitude, and is geographically described as having high solar energy potential. The annual average sunshine is 1,803 kWh/m²/year or 4.94 kWh/m²/day on the horizontal (Al-Jameel, Al-Yaqoobi, & Sulaiman).

2.6.2 The Climate of Erbil

a. Air Temperature

Erbil is located to the north of Iraq and lies between 36°08' to 36°14'N, and 43°57' to 44°03'E. The climate of Erbil according to Köppen's climate classification is a semi-arid (Figure 2.15), which is hot/dry in summer and cool/rainy in winter (Rasul, Balzter, & Smith, 2015). In the driest and wettest months in Erbil, rainfall is 0–112 mm. The average annual temperature of Erbil is 26.0°C with annual rainfall of 386 mm

(Abdulkareem, 2012). The summer months experience hot and dry weather with low relative humidity as a result of no rain in the summer months. June–August are the hottest months and the air temperature usually reaches 49°C. There is normally rain from December to May (Figure 2.16 and Figure 2.17).

Table 2.2: Average air temperature and annual rainfall per month in Erbil. Source: climate-data.org

Month	Jan	Feb	Mar	Apr	May	Jun	Jul	Aug	Sep	Oct	Nov	Dec
Rain (mm)	112	98	90	69	26	0	0	0	0	12	56	80
Average °C	7.4	8.8	12.4	17.5	24.2	29.8	33.4	33.2	29.0	22.5	15.0	9.1
Max °C	12.4	14.1	18.1	24.0	31.5	38.1	42.0	41.9	37.9	30.6	21.2	14.4
Min °C	2.4	3.6	6.7	11.1	16.6	21.5	24.9	24.5	20.1	14.5	8.9	3.9

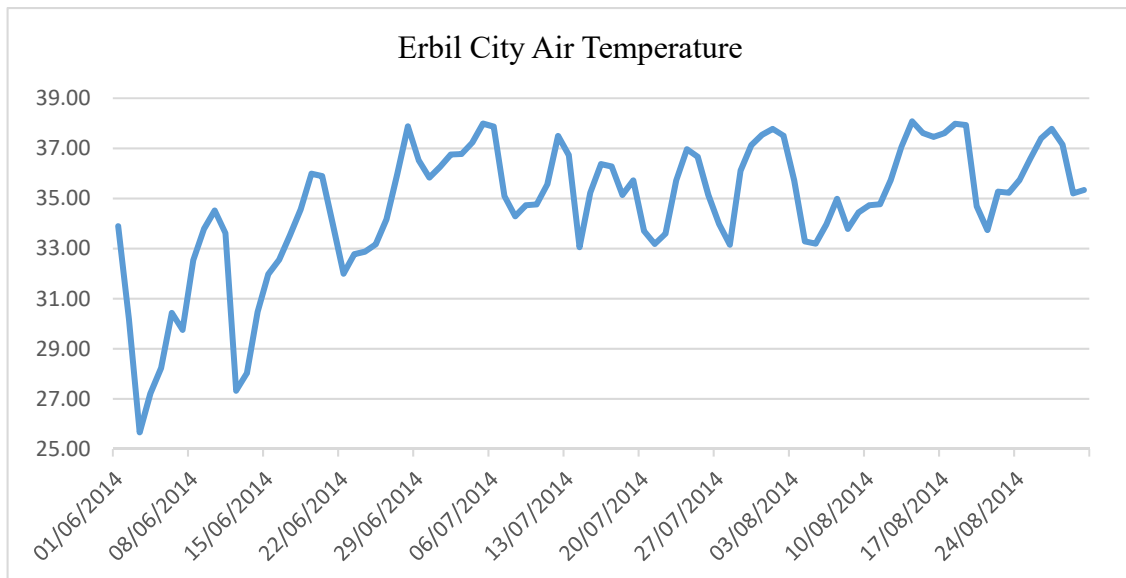


Figure 2.17: Erbil's average air temperature is 33.4 °C and July is the hottest month of the year. January has the lowest average temperature of the year at 7.4 °C. Source: climate-data.org

Table 2.2 shows the climate data for each month. The data presents the rainfall average in millimetres, and maximum and minimum air temperature in Celsius, as sourced from airport data (low urban density). Figure 2.18 shows the air temperature for the weather station located in the central area of the city (high urban density). The maximum average air temperature is 38.0°C and the minimum 25.7°C.

B. Wind speed in Erbil

The Kurdistan climate is under the influence of Mediterranean anticyclones and the subtropical pressure belt. The wind moves from the south west to the north. When the southerly wind blows, it generates dust storms, which also cause the air temperature to rise over 45°C. However, in winter the wind is cold and influenced by Mediterranean cyclones moving from east to north east. The region is also influenced by Arabian Sea cyclones that move northwards. Moreover, the air mass that comes from the polar region down to the Persian Gulf is very cold and can decrease the air temperature in the region significantly.

Average monthly wind speed for Erbil Airport is above two metres per second and varies between 4.34 m/s and 7.8 m/s, but the maximum wind speed is different in winter and summer; the maximum value in May and the minimum in January are shown in Table 2.3 (Husami, 2007) (Figure 2.18).

Table 2.3: Annual average wind speed in Erbil. Source: Husami (2007)

Month	Jan	Feb	Mar	Apr	May	Jun	Jul	Sep	Aug	Oct	Nov	Dec	Ave
m/s	4.34	8.23	5.63	6.28	7.80	6.5	5.63	5.85	6.5	6.06	5.41	5.63	6.34

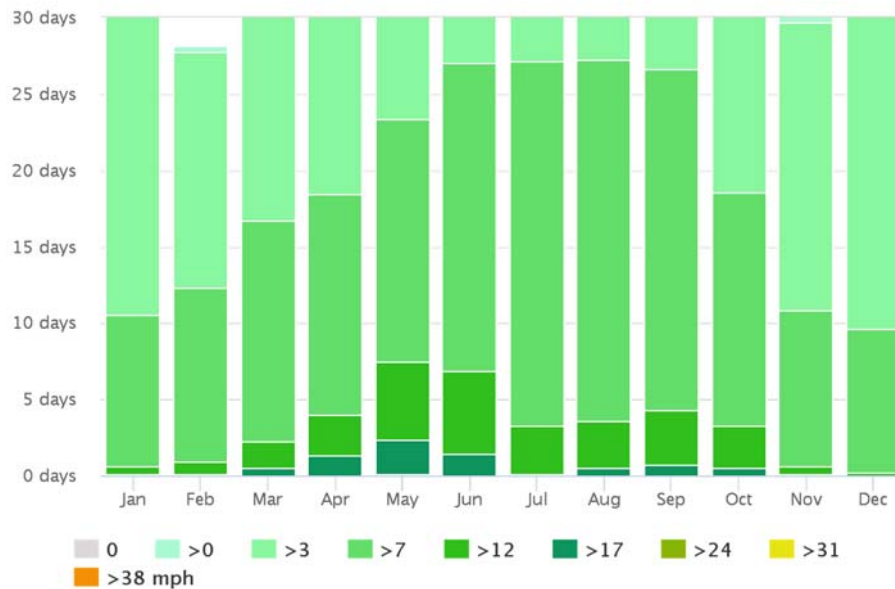


Figure 2.18: Average annual wind speed in Erbil. Source: www.meteoblue.com.

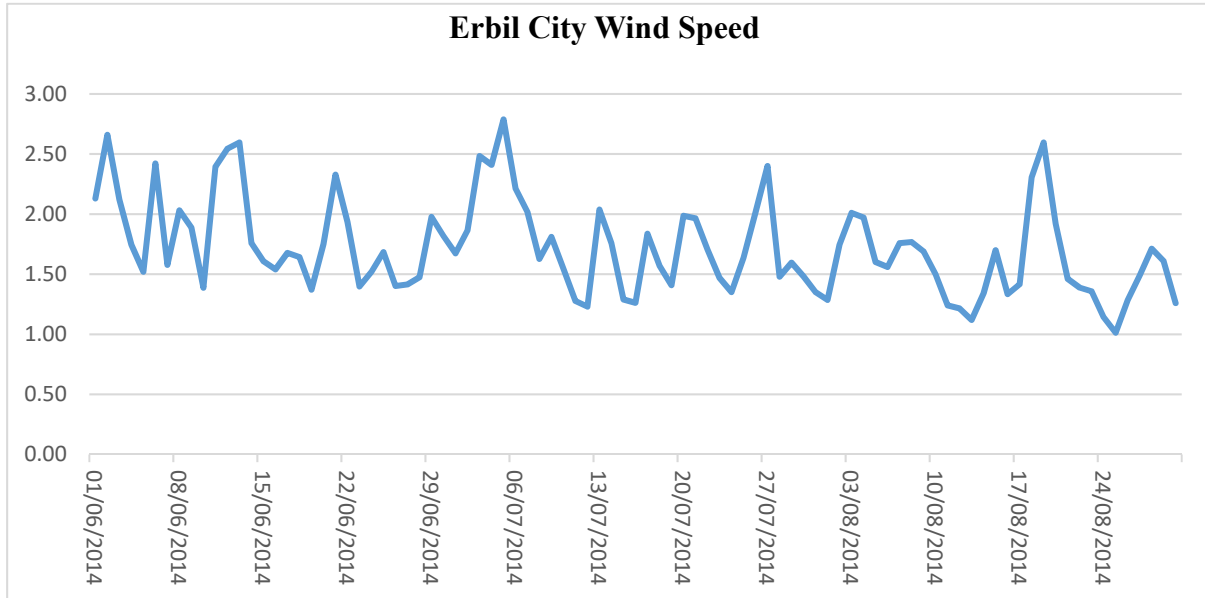


Figure 2.19: Wind speed for Erbil (June, July and August)

Figure 2.19 shows Erbil Airport's monthly wind speeds, which are high from December to April, but calm winds from June to October. Similar to air temperature, the wind speed in urban areas is influenced by urban density.

Figure 2.19 shows the wind speed for the central weather station (high urban density) and the maximum average wind speed is 2.8 m/s and minimum 1 m/s.

This shows the impact of urban density on wind speed, as the buildings in urban areas act as obstacles to wind flow, leading to a drop from 5.0–6.0 m/s to 1–2 m/s, as shown in Figure 2.19. Figure 2.20. This wind rose shows how many hours per year the wind blows from the indicated direction. Generally, the wind blows from the south west to north east (NE) and vice versa (Figure 2.20).

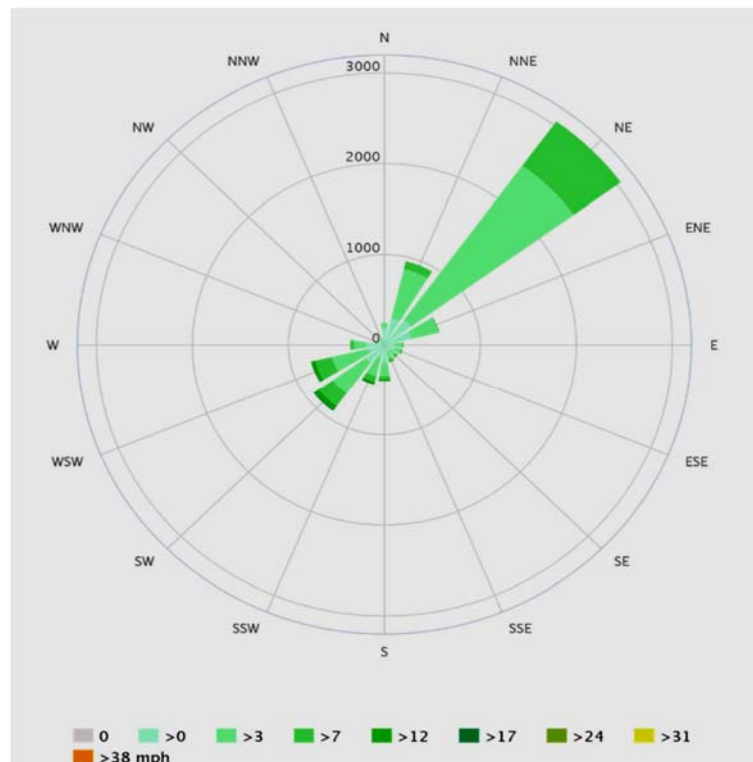


Figure 2.20: Average annual wind direction for Erbil. Source www.meteoblue.com.

2.6.3 Land use and urbanisation of Erbil

In the last decade, several studies have been undertaken on Erbil's urban development, and these have revealed that built-up area in the city represent 39%. Vegetation covers only 8% of the remainder of open land, as the city has a radius of 10 km and encompassed there is a large amount of land yet to be developed (G. R. F. Ibrahim, 2013). The importance of green and blue spaces in urban areas has been recognised for many years as climate modifiers (Gunawardena, Wells, & Kershaw, 2017). Most of these urban areas became residential after 2003. Urbanisation is represented in yellow and it is more concentrated in the city centre (the citadel), expanding in all directions (Figure 2.21). Open areas are mainly located outside the city and are represented in blue, and comprise about 47% of the total land of the studied area.

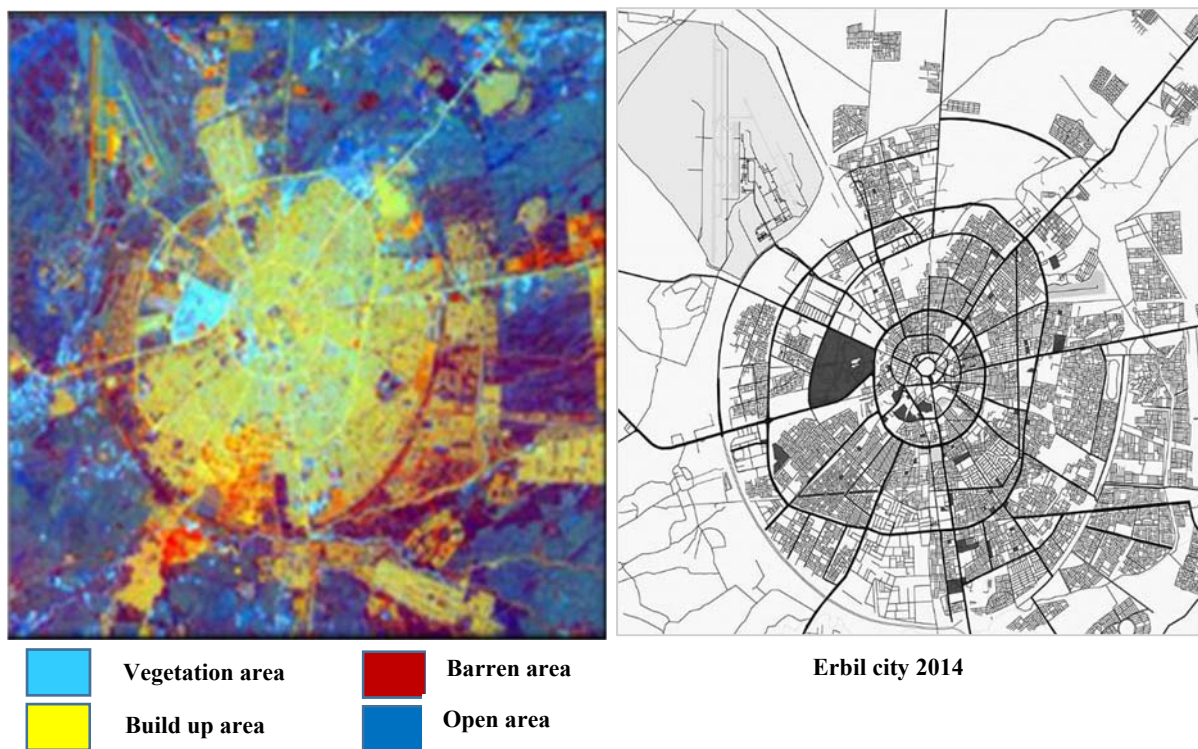


Figure 2.21: Urban development of Erbil.

The urban development of built-up areas is not in balance with vegetation or green areas. This urban development reflects a negative impact on the urban microclimate of the city and outdoor thermal comfort of occupants (R. I. Ibrahim et al., 2015). The city can be divided historically

speaking into two types: the historical urban morphology located in the city centre, and the modern development located outward of the centre as a series of ring roads and radial urban blocks.

The urban features and geographic landscape of Erbil, and the ratio of urbanisation to vegetation (green area), make the city an ideal case study on the impact of urban geometry on the mitigation of the urban microclimate. In doing so, the impact of different urban morphology on the local urban microclimate can be identified, so that we can also consider how energy (cooling load) can be reduced in a hot dry climate city such as Erbil.

2.6.4 Erbil: Land Surface Temperature (LST)

Urbanisation characteristics such as urban geometry, build-up density, surface albedo, vegetation, and building materials impact directly on urban land surface temperature and air temperatures in the local urban microclimate. In temperate and sub-tropical climates, the urbanisation causes a Surface Urban Heat Island (SUHI) as a result of urban expansion (T. R. Oke, 1987). In hot and arid cities, urban expansion can cause Urban Cool Islands (UCL) due to the built-up areas having lower surface temperatures compared with the open areas surrounding the city (Taleb & Abu-Hijleh, 2013). Satellite thermal images can be used to study the surface temperature of urban areas and investigate the impact of solar radiation on the local urban microclimate. From the 1970s, thermal satellite imaging began to be used to study UHI for cities (Carlson, Augustine, & Boland, 1977; Price, 1979; Rao, 1972). In the period 1970–1980, researchers studied UHI using satellite thermal images measurements under clear sky conditions only. This method was applied with small cities to measure the differences between rural and urban areas (Matson, Mcclain, McGinnis Jr, & Pritchard, 1978). Recent studies using satellite thermal images to investigate UHI have had four objectives:

1. To study and analyse building geometry and landscape features impact on UHI (Nichol, 1996);
2. To study thermal comfort and urban planning (Gómez, Tamarit, & Jabaloyes, 2001; Scherer, Fehrenbach, Beha, & Parlow, 1999);
3. To simulate city air temperature and wind speed configurations (Herbert, Johnson, & Arnfield, 1998).
4. To study Surface Urban Cool Islands (SUCI) in hot/dry climate cities (Lazzarini, Marpu, & Ghedira, 2013).

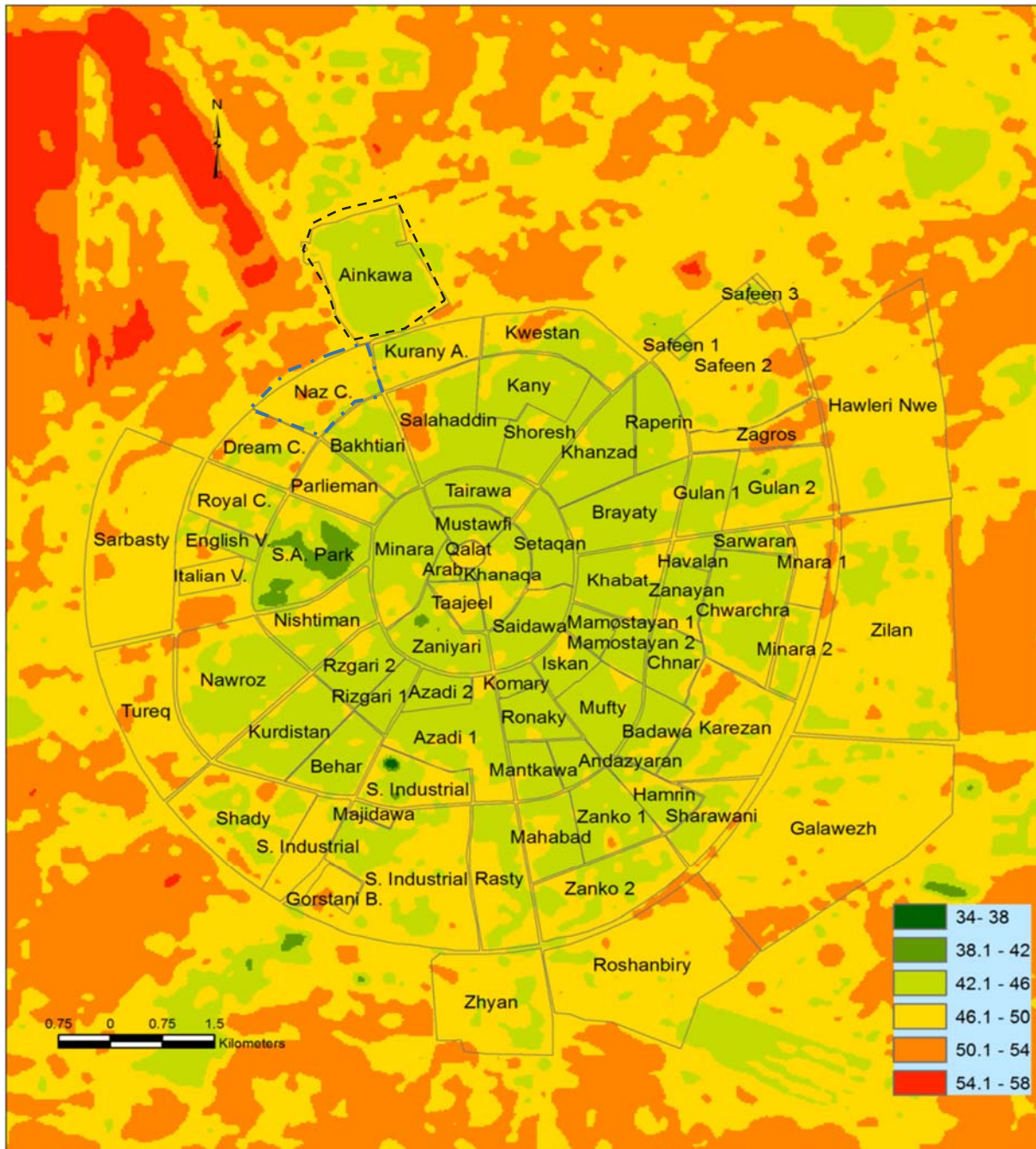


Figure 2.22: Land surface temperature and thermal infrared radiometer image for Erbil from Landsat TIRS on 19th July 2013. Source of image (Rasul, Balzter, & Smith, 2015)

Studies carried out in hot/dry climate cities have concluded that urban areas recorded a lower surface temperature compared to rural areas, because of soil moisture within urban areas (evaporation) and the shading effect of buildings, which reduces solar radiation intensity. In this regard, a study used land surface temperature and a thermal infrared radiometer image for Erbil to investigate the impact of UHI in 2013. The study concluded significant thermal environment differences between urban areas and the surrounding rural areas. The surface temperature 10 km from the centre of Erbil was 50.1–54 °C while at the city centre it was 46.1–

50.0°C (Figure 2.22). This image may be useful to predict and determine the urban microclimate of Erbil, as shown below:

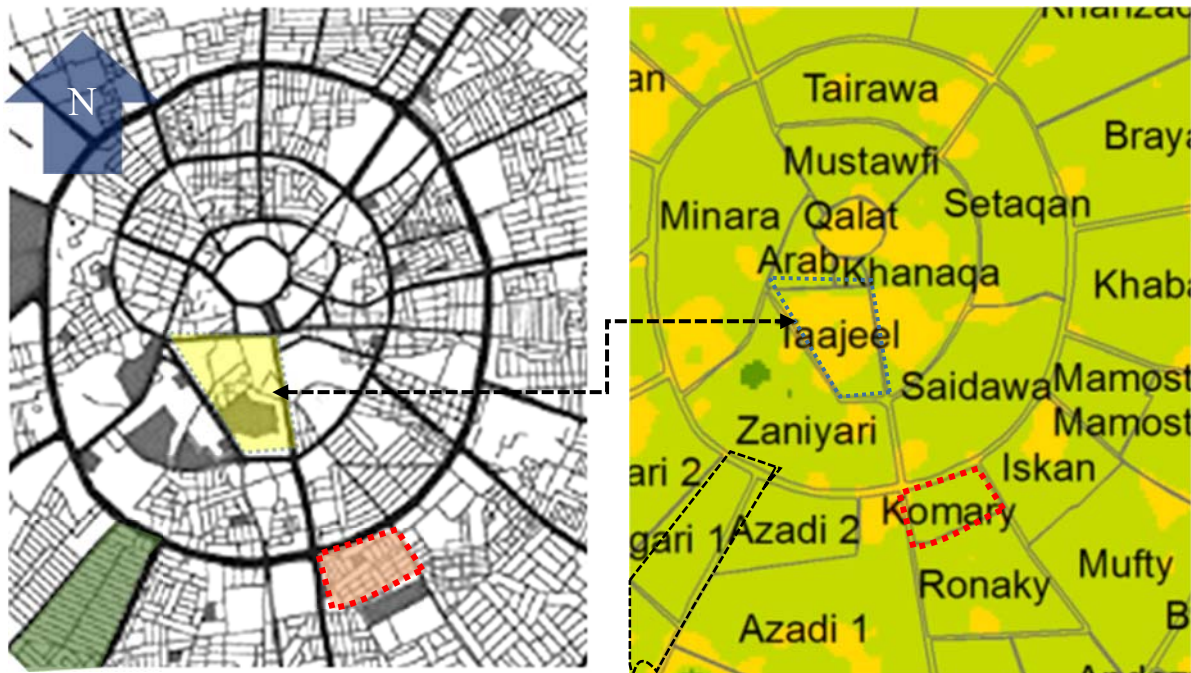


Figure 2.23: Tajeel district is an organic urban area with a surface temperature higher than most grid-iron urban areas with a surface urban temperature.

1. Distance from the city centre: This includes prediction of the organic and grid-iron morphologies Land Surface Temperature (LST) of city, and may be related to wind speed, starting with high values in rural areas and decreasing toward the city centre. Other factors may also be influential, however, as (Alznafer, 2014) has concluded, for example a direct relationship between LST and the population density of the individual urban locations. Alznafer found that the LST of compact urban areas in the core of city (organic morphology) are higher than other, less compact locations with grid-iron morphology. This corresponds with the present study, for example the city centre in Tajeel district has an organic urban morphology with LST 46.2°C, while a grid-iron urban area, such as Komary, had surface urban temperatures of 42.1–46.0°C (Figure 2. 23). This difference in land surface temperature may reflect the high urban density and high population density of the centre as opposed to the more open grid-iron developments.

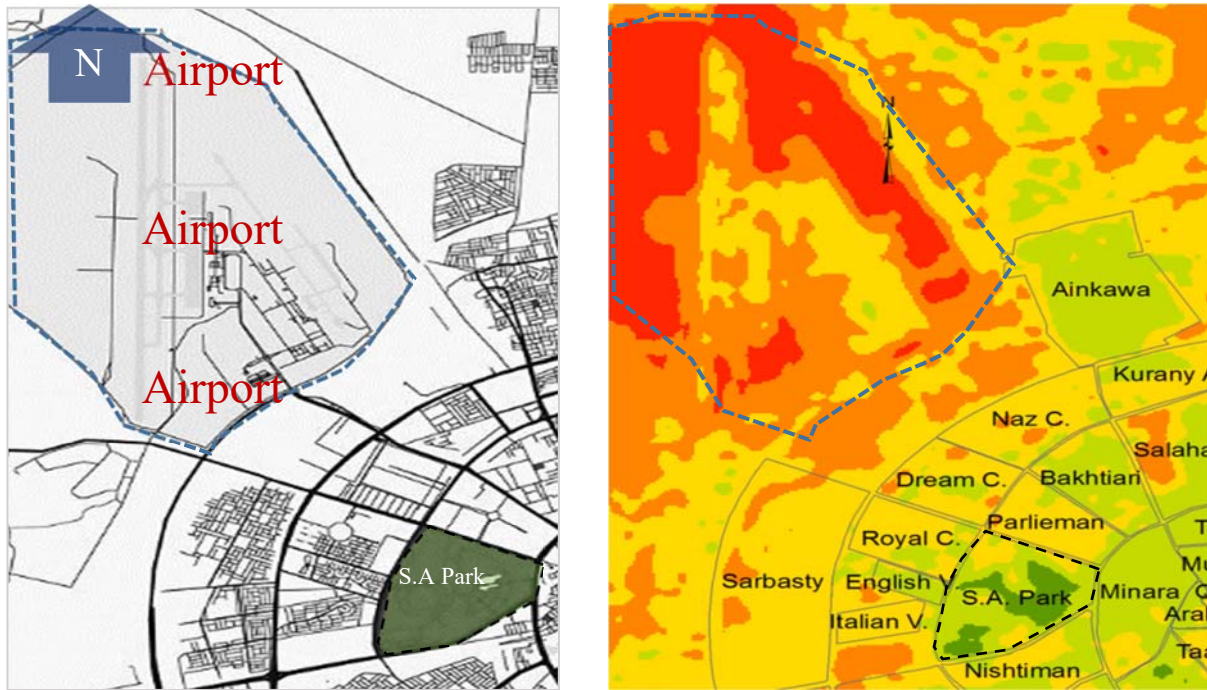


Figure 2.24: Lower surface temperature for S.A part than Erbil International Airport.

2. Land cover and land use characteristics. Surface albedo and the thermal capacity of the surface materials (Kwarteng & Small, 2005). For example, S. A Park⁶, which contains large areas of park land and open water, records lower land surface temperature than the airport areas (Figure 2.24 and 2.25). The ST in S.A Park was between 34–38 °C compared to the airport, which was between 54–58 °C.

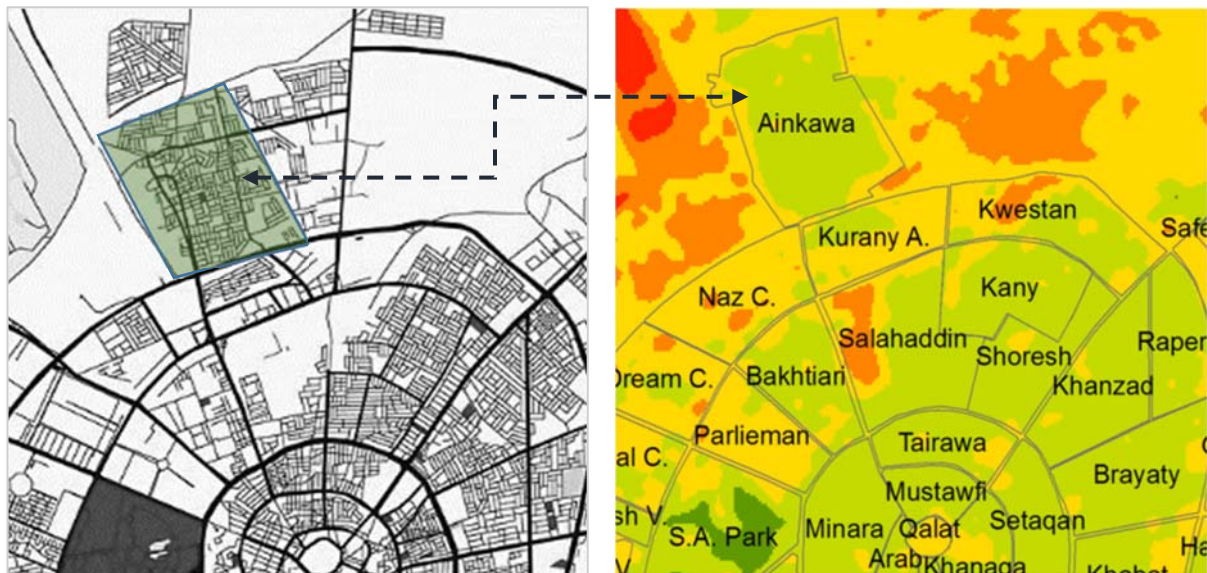


Figure 2.25: Naz has low density urban areas which recorded higher ST compared to the high density urban areas of Ainkawa. Source of left image (Rasul, Balzter, & Smith, 2015)

⁶ S.A. Park: Sami Abdulrahman Park located in western part of Erbil with 200 hectares area. In 2006 constructed on Saddam Hussein's 5th Corps Army military base. The park include two lakes, a rose garden and other activates.

3. Urban Density: Low density urban areas recorded higher LST compared to high density urban areas, regardless of their distance from the city centre. For example, the Ainkawa district recorded a lower ST than Naz C (Figure 2.26). From this study and the analysis of Erbil Satellite images, we can conclude that Erbil, as other cities in hot/dry climate zones, experiences a Surface Urban Cool Island in summer time. The urbanisation areas have lower LST compared to rural areas. In addition, urban land cover and urban characteristics do not necessarily cause urban Land Surface Temperature variation, although there are other factors such as wind speed, direct solar radiation, and shading which might cause variation in LST, and consequently variation in the urban microclimate of specific urban areas.

2.7 Urban energy balance

The main source of the Earth's energy is the sun. The radiation which the sun emits is divided into three components: ultraviolet, visible, and near infrared light. Most of the sun's radiation is absorbed by the Earth's surface, while the rest is reflected by clouds and particles in the air. More than half of the solar radiation which is near infrared is stored on the surface, while the remainder is reflected into the surrounding atmosphere. The stored heat on the Earth's surface,

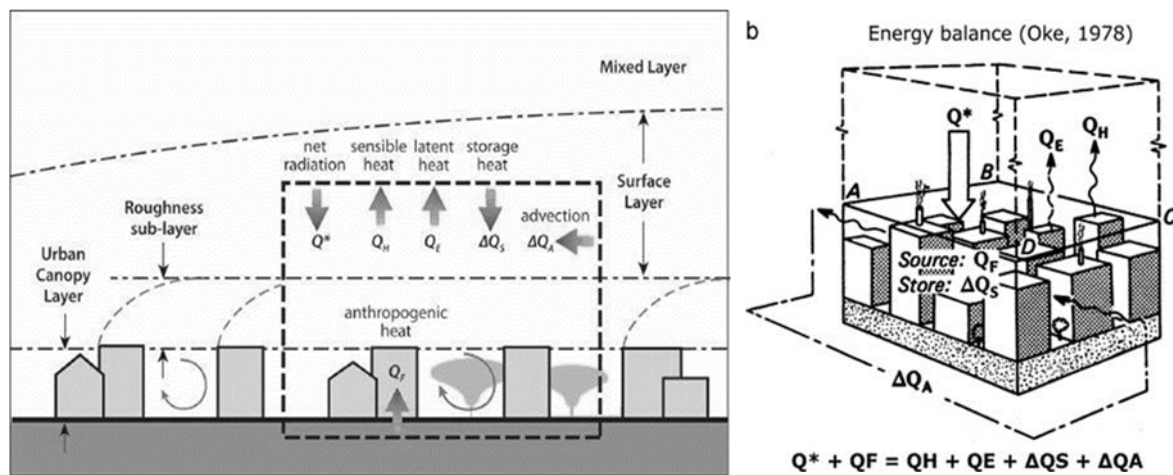


Figure 2.26: Schematic section (A) and 3D presentation (B) of urban surface energy balance. Sources: (A) Erell et al., (2011), (B) Santamouris (2001b)

as well as evaporation, helps to maintain the energy balance of the Earth (Figure 2.26). The concept of energy balance is from the first law of thermodynamics, which states that “Energy can neither be created nor destroyed, only converted from one form to another”.

$$\text{Energy input} = \text{Energy output} + \text{change in stored energy}$$

The energy balance in the urban pattern is more complex because the urban areas have more than one source for heating up the canyons, such as heat radiation and other sources of heat as a result of human activity. The equation below describes the heat balance in urban areas.

$$Q^* + Q_F = Q_H + Q_E + \Delta Q_S + \Delta Q_A$$

Where Q^* is the solar radiation, Q_F anthropogenic heat, $Q_H + Q_E$, sensible and latent heat. Moreover, ΔQ_S the radiation from urban surfaces that is transferred through the air and ΔQ_A

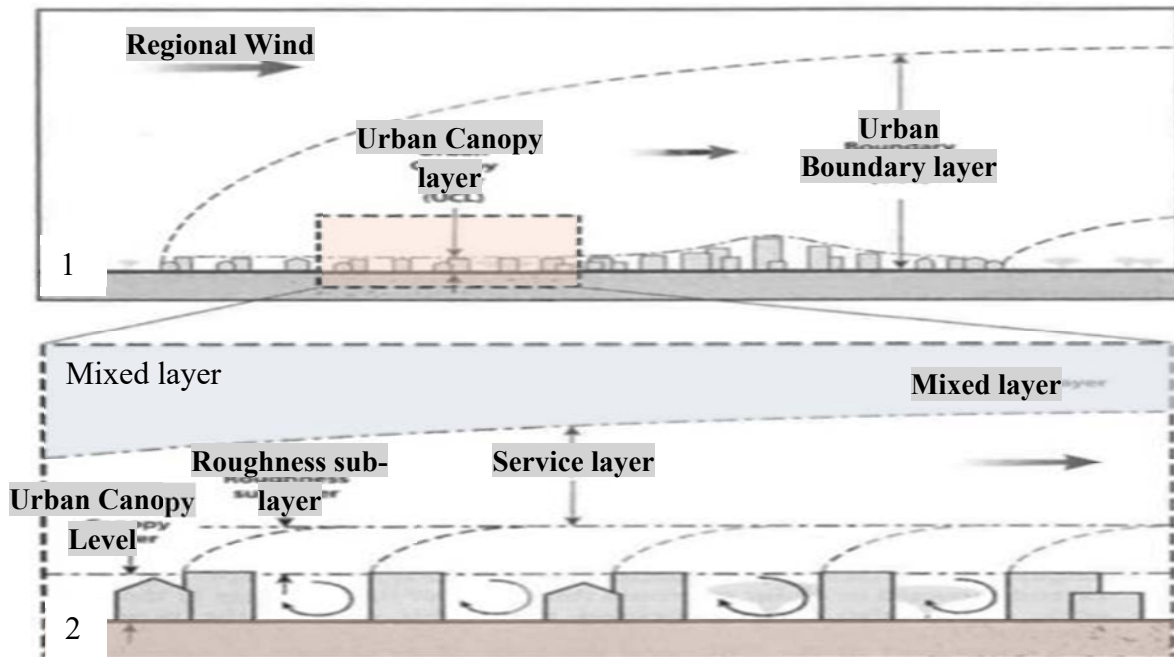


Figure 2.27: Urban boundary layer and development of urban canopy layer. Source: Erell, Pearlmutter et al. (2012).

is the net store heat flux. To understand how this energy balance works and affects an urban microclimate, the following section explains important factors pertaining to the urban microclimate.

2.7.1 Urban microclimate

To study the urban environment and design, it is important to understand the scale and factors as regards an urban microclimate. Microclimate is a part of the urban canopy-layer (UCL), which is the lowest part of the urban atmosphere (Erell, Pearlmutter, & Williamson, 2012) (Figure 2.26 and Figure 2.27). There are different layers that interact to produce an urban microclimate, as described below:

1. Urban boundary layer: defined as the entire amount of air above the city affected by city surfaces and all the activity which happens inside the city (Figure 2.27)

2. Mixed layer: this layer is on the upper part of an urban boundary layer and is not influenced by urban surfaces (Figure 2.27).
3. Surface layer: this layer is located above buildings at four to five times the height of the buildings (Figure 2.28).
4. Roughness sub-layer: this layer, also known as the layer of transition between the very homogeneous layer which is the surface layer, and the layer affected by buildings of different heights, green areas, and open spaces of different dimensions (Figure 2.28).
5. Urban canopy layer: This is defined as the lowest layer of the urban atmosphere, starting from the ground of the urban area to the level of the building's height (Figure 2.28).
6. A microclimate can be defined as "the climate that prevails at the micro-scale level". It is established within any urban space as a result of the high inhomogeneity of the urban canopy layer (Erell et al., 2012).

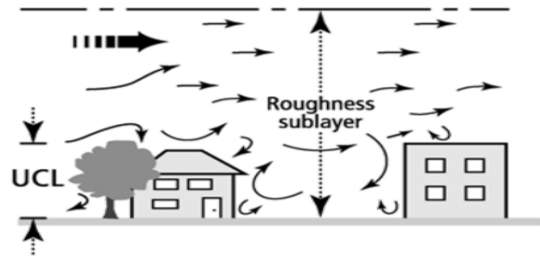


Figure 2.28: Urban canopy layer. Source: <http://co2montreal.blogspot.com/2010/10/principles-of-urban-meteorology-re.html>

The differences in air temperature, wind speed, radiation balance and other climatic indicators create a unique microclimate for any given urban area. Climatic properties are determined by the urban and regional environment and physical nature of the existing surroundings. The design parameters, such as the thermal capacity of building materials, open space dimensions, and landscape and vegetation, all serve to modify the climate at this scale (Jeong et al., 2015). These factors have an effect on outdoor thermal comfort and building's energy loads (Taleb & Abu-Hijleh, 2013).

2.8 Wind and urban microclimate

The wind comprises two factors that mainly affect urban geometry: velocity and pattern of wind flow. In urban areas, wind speed and its patterns are more affected by buildings and land topography (surface roughness). Charabi (2011) studied a UHI in Muscat, Oman, and found that the mountains surrounding Muscat reduce the wind speed and ventilation rate, so the urban areas heat up in the centre of the city where the morphology is compact and organic.

Natural surfaces reduce wind speed. However, rougher surfaces from urban geometry reduce the speed of the wind further. Hence, the ground surfaces in urban areas have a substantial impact on the performance of the wind system above it. The impact of ground texture will change the wind speed and boundary layer of the wind above the ground.

Understanding wind patterns and air movement in urban areas is the primary concern of urban planners and researchers so as to enable them to compare and measure thermal comfort, ventilation, and energy consumption of buildings. Wind speed is considered an important factor that affects outdoor thermal comfort. The second most important factor after shading is wind speed.

Physiological equivalent temperature (PET) is a human biometeorological parameter that describes the thermal perception of an individual. It is defined as the air temperature at which, in a typical indoor setting (without wind and solar radiation), the heat budget of the human body is balanced with the same core and skin temperature as under the complex outdoor conditions to be assessed (Höppe 1999). The typical indoor setting is an indoor room, with windspeed (v)=0.1 , vapour pressure (VP)=12 hPa and mean radiant temperature equal to the air temperature . For calculating the physiological parameters PET makes use of the Munich energy balance model for individuals (MEMI) (Krüger, Rossi et al. 2017).

The Psychological Evaluate Temperature (PET) index decreases by 3.5°C with an increase in wind speed from 1m/s to 2m/s (Andreou, 2013). Wind speed also affects the urban planning of a city. The temperature in a city may change from one specific zone to another as the conformation of the city assists the wind speed and its circulation. Golany (1996) discussed the urban design morphology and thermal performance of a city. These results show that urban morphology in a city directly affects wind speed. The result shows that wind movement on a city scale depends on morphological elements such as morphology designs, orientation, and the shape of roads within a city. Golany (1996) concluded that the urban form of each region or district contributes to making a city cooler or hotter (UHI, UCI).

Finally, traditional organic urban morphology with deep canyons contributes to reducing wind speed, which has a positive impact on urban microclimates in winter. In contrast, the lower wind speed during summer nights will cause discomfort for pedestrians as a result of heat emission from buildings. In summer, the wind speed is low although the canyon has a high aspect ratio (high/width) which reduces the air temperature. In contrast, studies conducted by Taleb (2012) found that in summer the air temperature in urban morphologies is primarily dependent on urban configuration more than wind speed. He argues that wind speed in highly

structured morphologies records higher values in comparison to organic morphologies. The study concluded that wind behaviour is manipulated within urban configurations.

2.8.1 Wind speed and urban canyon aspect ratio

Wind speed is primarily affected by urban canyon geometry. The aspect ratio between height and width (H/W) and sky view factor is the main measurement to identify urban geometry (Figure 2.29). The canyon direction can be with or opposite to the direction of the wind. Oke (1988) divided the aspect ratio for urban canyons into three types and explained its relationship with wind speed as follows:

1. Isolated roughness flow if the aspect ratio is $H/W > 0.05$
2. Weak interference flow if the aspect ratio is $0.5 < H/W < 0.65$
3. Skimming wind flow if the aspect ratio is $H/W > 0.65$.

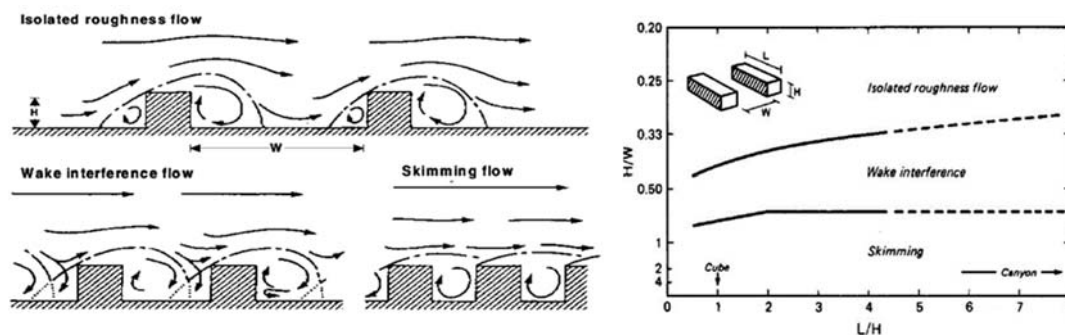


Figure 2.29: Wind flow pattern over and within urban canyons, and (b), threshold lines

While the H/W ratio contributes to the surface roughness of urban areas, the canyon length to width ratio (L/W) contributes to the flow along the canyon and the transition from one specific regime to another when both L/W and H/W interact. Wind flow compared to canyon direction can consist of four separate possibilities, as outlined below (Figure 2.30):

1. Parallel canyons, when both canyons are open to the wind direction
2. Perpendicular canyons with wind direction
3. Angled canyons with wind direction
4. Perpendicular (deep canyons).

Canyon form and direction have an important impact on wind speed and solar radiation in hot dry/dry climates. Thus, it is important for urban planners to consider these factors before urban design. In addition, mitigating an urban microclimate has a direct impact on the thermal performance of a building and consequently energy consumption (Erell et al., 2012).

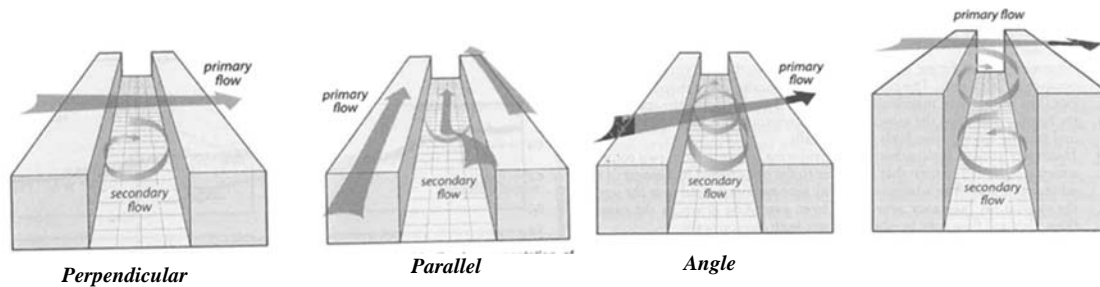


Figure 2.30: Secondary wind flow patterns with respect to the primary flow directions above

2.9 Urban morphology and energy consumption

Urban microclimate is influenced by urban form and geometry. The urban microclimate surrounding the building will affect the performance of the cooling and heating systems of that building. Ratii (2005) explains four factors that directly affect single building energy performance: urban geometry, building design, system efficiency, and occupant behaviour. In hot climate regions, many passive and active design strategies can be used to release heat gain naturally or mechanically (Edussuriya, Chan, & Ye, 2011). Zhao (2011) studied 11 urban morphologies to determine the relationship between urban planning and climate indicators. The research found that green cover ratio in tropical climates is the most influential factor on the urban thermal environment, together with other factors illustrated below (Table 2.4).

Table 2.4 Important factors relating to urban planning indicators

Significant factors relating to urban climate		
1	Urban structure	Dimensions of the buildings and the spaces between them, street widths and spacing
2	Urban cover	Building form, paved, vegetated, bare soil and water
3	Urban fabric	Construction and natural materials of urban areas
4	Urban metabolism	Heat, water and pollutants due to human activity

Urban morphology has a positive and negative impact on human health, thermal comfort, social life, and energy consumption (C. Zhao, Fu, Liu, & Fu, 2011). For example, (Ai & Mak, 2015) and Okile (2010) categorised publications in this field into three main groups, as explained below (Table 2.5).

Table 2.5: Research groups categorised by Ai & Mak, 2015 and Okile (2010).

Groups	Research type	Factors or Variables	Authors (year)
First Group	Human thermal comfort	Application of passive heating, cooling, ventilation and daylighting strategies	(Ali-Toudert & Mayer, 2007; Andreou, 2013; Balslev, Potchter, & Matzarakis, 2015; Brent C Hedquist & Anthony J Brazel, 2014; E. L. Krüger, Minella, & Rasia, 2011; Lin, Matzarakis, & Hwang, 2010; W. Yang, Wong, & Jusuf, 2013)
Second Group	Solar energy	Utilising the sun's radiation to sustain the huge solar resource available within cities	(F. Bourbia & H. B. Awbi, 2004b; Compagnon, 2004; Johansson, 2006; Lin et al., 2010; Martinelli, Lin, & Matzarakis, 2015; Nastaran, 2013; Upreti, Wang, & Yang, 2017; van Esch, Looman, & de Bruin-Hordijk, 2012)
Third group	Urbanisation impact on city microclimate	Application of strategies to minimise UHIs, such as wind flow between buildings, green roofs and the effect of vegetation on microclimate	(Ruksana, 2014; Santamouris, 2014; Shahidan, Jones, Gwilliam, & Salleh, 2012; Sharmin & Steemers, 2019; Taleb & Abu-Hijleh, 2013; van Esch et al., 2012; Wong et al., 2011; C. Zhao et al., 2011; Q. Zhao, Sailor, & Wentz, 2018)

Urban geometry is related to direct solar radiation and solar gain. Givoni studied the structure of a city and how it changes the local microclimate. He established that total regional climate is not solely modified by the exposure of buildings to solar radiation, but that the structure of a city and neighbourhoods of buildings modify the local microclimate. Ratti found after examining six urban patterns that courtyard configuration responds better to environmental variables. The variables that directly affect urban pattern are surface to volume ratio, shadow density, daylight distribution, and sky view factor (Ratti, Baker, & Steemers, 2005).

The critical factors for the urban courtyard are: courtyard layout, thermal mass and surface reflectance. The interior elements of the courtyard interact positively with the urban microclimate, making this type of urban pattern the best form of land use. Ramona (2013) studied thermal comfort in low cost housing units in a hot-dry climate. She found that low cost

housing units used higher amounts of energy in comparison to average housing units because of the characteristics related to design, construction, and occupants' behaviour.

2.10 Urban microclimate in hot arid regions compared to other climatic regions

In cities with a hot dry climate including mid and high latitudes, UHI has a negative impact on human health, comfort, and heat stress. In addition, these negative impacts cause high energy consumption (air conditioning), water use, and air pollution. Therefore, mitigation of an urban microclimate has a positive impact on human health and the economy.

The important features of hot dry climates are: high diurnal air temperature (high solar radiation), low humidity (low moisture availability), low wind speed and a lack of vegetation. This causes significant air temperature fluctuation in some regions, from 50°C during the daytime to 20°C, or possibly lower, during the night. Moreover, in high latitude regions, high seasonal temperature variations happen during summer and winter. In Kurdistan, the air temperature reaches 53°C or 54°C in summer, while in winter it drops to zero and negative values. In hot, dry climate regions, climatic strategies have been implemented to minimise climatic stress (Table 2.6).

Table 2.6: Climatic strategies in a hot dry climate

Climatic issues	Importance	Proposed strategies	Studies
Reduce solar gain	Minimise heat stress to reduce or avoid air conditioning operation time.	Narrow streets Shade devices High-albedo materials Add trees Green roofs	(Akbari, Pomerantz, & Taha, 2001; Baker et al., 2002; Kumar & Kaushik, 2005; Shashua-Bar & Hoffman, 2002; Q. Zhao et al., 2018)
Maximise solar gain in winter	Minimise the indoor air temperature variations	Control the heat storage capacity of building materials	(Brazel & Martin, 1997; Rizwan, Dennis, & Chunho, 2008)
Increase the extent of evaporation	Balance radiation net at the ground surface by increasing the extent of evaporation	Extent of evaporation reducing the non-permeable surfaces Designing irrigated greenbelts	(Bonan, 2000) (Grimmond & Oke, 1995; Kong et al., 2016; Middel et al., 2012; Middel, Chhetri, & Quay, 2015)
Minimise wind exposure	Avoid extreme conditions and reduce thermal stress	Compact geometry and short walking distances. Correct canyons direction	(Andreou & Axarli, 2012; Taleb & Abu-Hijleh, 2013; van Esch et al., 2012)

Studying urban microclimates in hot arid regions is different to some extent compared to other regional climates. Hot and dry climates have specific issues that are unique and considered the most important variables regarding urban microclimates compared to other regional climates, such as tropical and semi-arid regions. Moreover, different methodologies have been employed to examine climate islands in these regions; some researchers have used thermal infrared (TIR) images to analyse thermal urban behaviour by examining LST, and compared the temperature in both urban and rural areas (Rasul, Balzter, & Smith, 2016; Tran, Uchiyama, Ochi, & Yasuoka, 2006), while other researchers used field measurements to examine and determine urban microclimate (Akbari et al., 2001; Chow & Brazel, 2012; Jeong et al., 2015; Eduardo L. Krüger, 2015; Lin et al., 2010).

A further study in a hot and dry climate was conducted by Kwarteng (2005), who compared cities from a hot climatic region with cities in a cold region. Kwarteng used remotely sensed thermal images from Landsat ETM+ to examine the energy fluxes on the urban surfaces. The study connected multispectral imagery and thermal images to determine the thermal patterns of urban surfaces and evaluate the vegetation effect on LST. The study found that vegetation has a strong influence on urban and suburban heat islands. The study also shows that areas surrounding Kuwait City had higher surface land temperatures compared to residential areas, as there was an absence of vegetation in the rural areas. The higher surface temperature in the desert, in contrast to the urban area, is as a result of the lack of vegetation, as well as bare and dry soil compared to overshadowing by manmade elements in city. Additionally, higher surface temperatures were observed in residential and industrial areas in New York compared with rural areas around the city.

Table 2.7 Urban microclimate studies and findings

Authors	Methodology	Case study scale	Factor	Findings
Kwarteng (2005)	Thermal infrared and TIR images	Thermal patterns of urban surfaces	Urbanisation	Area surrounding Kuwait City has a higher surface temperature compared to the residential area
Moohammed Wasim Yahia & Erik Johansson (2012)	Field measurements	Old and new morphology impact on outdoor thermal comfort	Urban density and solar radiation	Traditional morphology is more comfortable than modern urban morphology
Johansson (2006)	Field measurements	Compare between shallow	Urban geometry	6–10k difference between both canyons

		and deep street canyons		
Krüger, Minella et al. (2011)	Field measurements and numerical modelling	Compare between different street canyons	Urban geometry	Urban geometry has an impact on human thermal comfort
Lin, Matzarakis et al. (2010)	Field measurements	Compare between 6 different urban locations	Urban geometry	High SVF causes discomfort in summer and low SVF cause discomfort in winter
Naveed and Brown (2015)	Field measurements and numerical modelling	Two different outdoor spaces. Garden and hard surface courtyard houses	Effect of surface material of landscape on UHI	Solar radiation causes discomfort in hot dry climate urban areas

The urban geometry and landscape materiality (bare soil, vegetation, concrete, etc.) has a great impact on the microclimate of urban areas. In addition, geometry and landscape can vary locally by changing the climate of the regions. This study focuses on urban microclimates in a hot and dry city. The literature so far comprises of only limited studies regarding Erbil's microclimate, so the subsequent section (Section 2.7) extensively describes the research conducted in Erbil by Rasul (2015).

2.11 Microclimate in Urban Canyons

Urban microclimate can be studied through the architectural elements at an urban canyon level. An urban canyon can be defined as a "linear space such as a street which is bounded on both sides by vertical elements such as walls of adjacent buildings"

(Evyatar, 2010). The advantage of modelling the urban canyon is to predict the urban area with

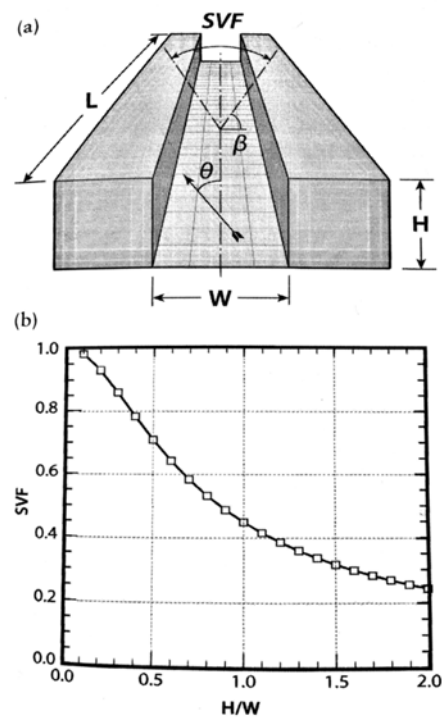


Figure 2.31: Urban canyon and its geometrical descriptors and sky view factor (SVF) as a function of canyon aspect ratio (H/W).

different surface materials (streets and walls) as one unit with a specific environment at ground level. Evyatar (2010) discusses three factors controlling the microclimate of canyons:

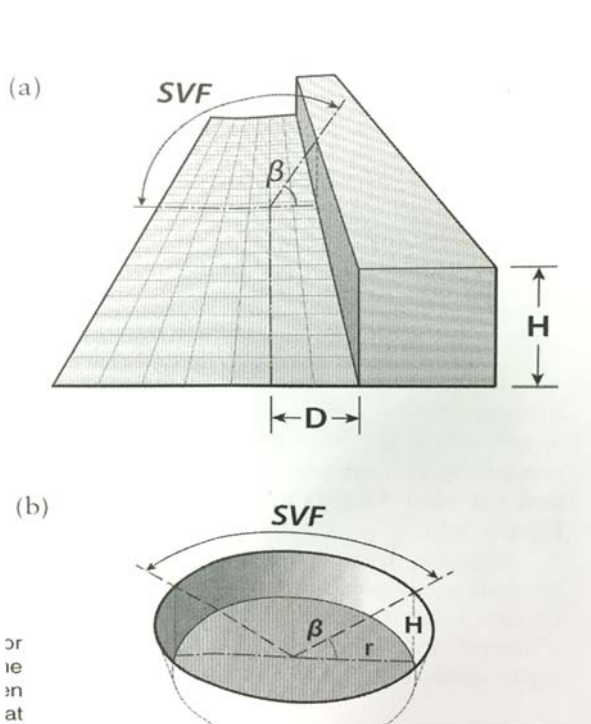


Figure 2.32: Geometric parameters for calculating the SVF from a point on the ground in plaza-type space (a) at a given distance from one continuous wall and (b) at the centre point of a circular space

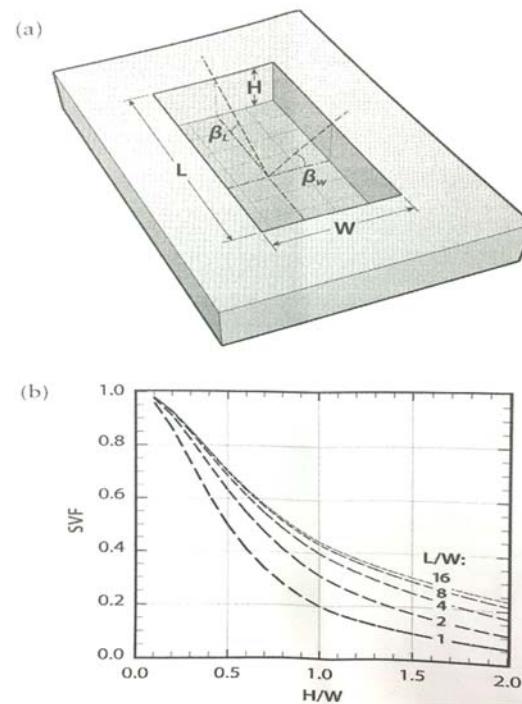


Figure 2.33: Schematic view of a rectangular courtyard-type space showing its geometric descriptors and (b) approximated SVFs

1. **The Height-Width (H/W) ratio** or aspect ratio. This model represents the sectional outline of an urban canyon. It is described as the average of a vertical building surface to the average width of a street (wall to wall distance) (Figure 2.32).
2. **Canyon axis orientation** represents the direction of the canyon to (N-S-E-W) or (NW-SE-NE-SW). It is the angle between a straight line running north-south and the second line running the length of the street (Figure 2.33).
3. The sky view factor (SVF) is the relationship between the H/W ratio. This can be described as the cross-section of a canyon and sky dome that can be seen by any surface from a specific point on the surface (Figure 2.33).

One of the important features of urban microclimate studies is the relationship between SVF and aspect ratio (H/W) on air temperature (Montavez, 2012). Ratti (2003) studied the effect of SVF and H/W aspect ratio on thermal comfort at an urban canyon level. The study concludes that during the day lower sky view factors had a positive impact on pedestrian thermal comfort in high H/W ratios.

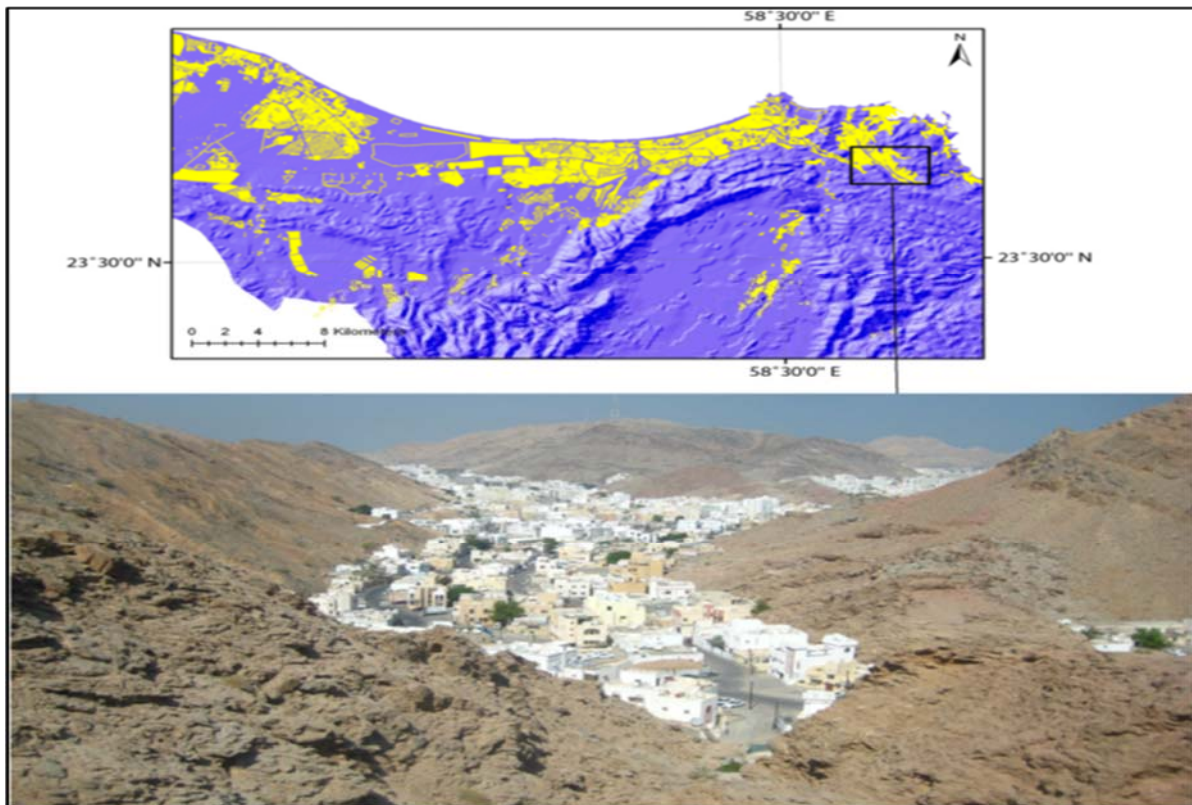


Figure 2.34: Urban canyon and its geometrical descriptors and sky view factor (SVF) as a function of canyon aspect ratio (H/W)

Sky view factor can be used to measure the UHI effect, which is the main indicator of the difference in air temperature between urban and rural areas (Ratti, 2003). However, other researchers have studied the SVF with street geometry factors, such as location and orientation, to examine the environmental aspects of urban canyon and air temperature (Ali, 2004). In a similar way, Bourbia and Boucheriba (2009) considered the effect of street design in semi-arid climates on an urban microclimate. The results of the study confirmed that higher aspect ratio (H/W) generates low air temperatures in semi-arid climates. It is recommended that the SVF of an urban design is decreased because it plays an important role in mitigating the urban microclimate effect.

Other studies have investigated the impact of sky view factor on a UHI (Montávez, Rodríguez, & Jiménez, 2000; Unger, 2004). Mills (1997) simulated the impact of the urban canopy layer (UCL) on urban boundary layer (UBL). A computer simulation was used to

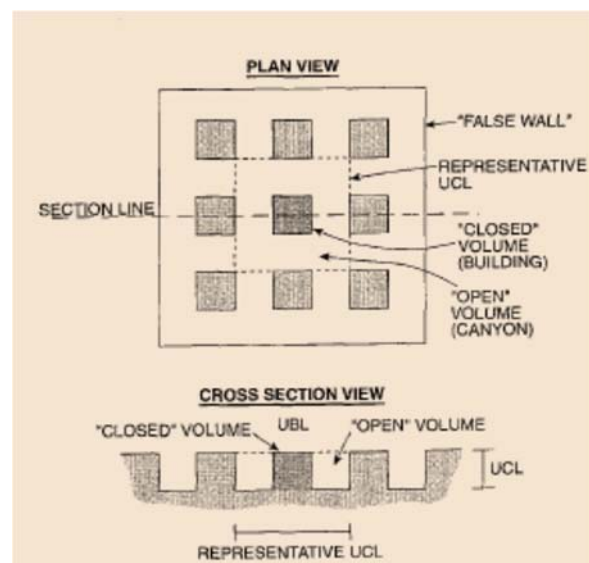


Figure 2.35: Model layout as viewed from above (plan view) and along a cross-section drawn through the UCL. Source: Mills (1997)

represent the thermal stresses of building configurations in different configuration structures. The natural heating of buildings was measured through daily sun exposure on structures. Sky view factor was used to assess cooling structures to compare different groups of building structures at various times of the year. The study concludes that the density of buildings has a significant impact on UCL/UBL interactions (Figure 2.35).

Charabi (2011) examined canopy-level UHIs in Muscat, Oman. The result of the study reveals that a UHI occurs during the night-time, especially in summer, 6 to 7 hours after the sun sets. This is because the local urban microclimate is distinguished by wind speed, high human activity, high density of buildings, and roads (Figure 2.34). The city is surrounded by mountains which cause the core of the city to be heated. The mountains isolate the cold breeze from the sea during the daytime and the warm air is trapped in the compact urban area of old Muscat.

2.12 Urban microclimate and urban geometry

Urban geometry is an important factor that affects the urban microclimate, particularly in cities with a hot dry climate. This topic and how it might modify the local urban microclimate has



Figure 2.36: Site maps of some study locations. Source: Shashua-Bar (2004)

been extensively studied. In general, an urban microclimate changes from different places in the same city because of various urban patterns (urban geometry) within the same environment. The local urban microclimate can be described as a specific environment that may change by

changing the urban geometry. Shashua-Bar and Hoffman (2000) examined the interrelationships between urban geometry and urban microclimate (Figure 2.36). The research represents urban geometry as the ratios (H/W), wooded area, and trees shading cover. Eleven different urban morphologies were studied using the analytical green CTTC7 model. The research compared urban site temperatures with metrological stations in open places. The study concluded that there was a 4K air temperature difference between wooded areas and open areas in hot, humid climatic regions. The cooling effect by surrounding sites with trees has become stronger in cities that have higher air temperatures. Certain researchers have explored the effect of urban form on microclimate by way of an analytical study of field measurements of different urban morphologies in the same city. Taleb (2012) measured the air temperature in two different urban geometries (traditional and grid-iron morphologies) in Dubai to represent the effect of different urban morphology form on altering the microclimate within the same city. The study determined that the wind speed in traditional morphology is lower than grid-iron, although air temperature records lower values. This is because the lower solar radiation in traditional morphology is a result of limited opening areas and the sky view factor.

The majority of researchers have proved that built form, vegetation, water body, and human activity change or influence urban microclimates, and, moreover, increase or decrease the air temperature in that urban microclimate. Bourbia (2010) examined different urban patterns which had different forms and levels of complexity and near water bodies. The aim of the research was to investigate the effect of different urban microclimate factors on the level of outdoor thermal comfort. This research found that people are more comfortable with increased evapotranspiration by trees than increased air flow (Bourbia & Boucheriba, 2010). However,

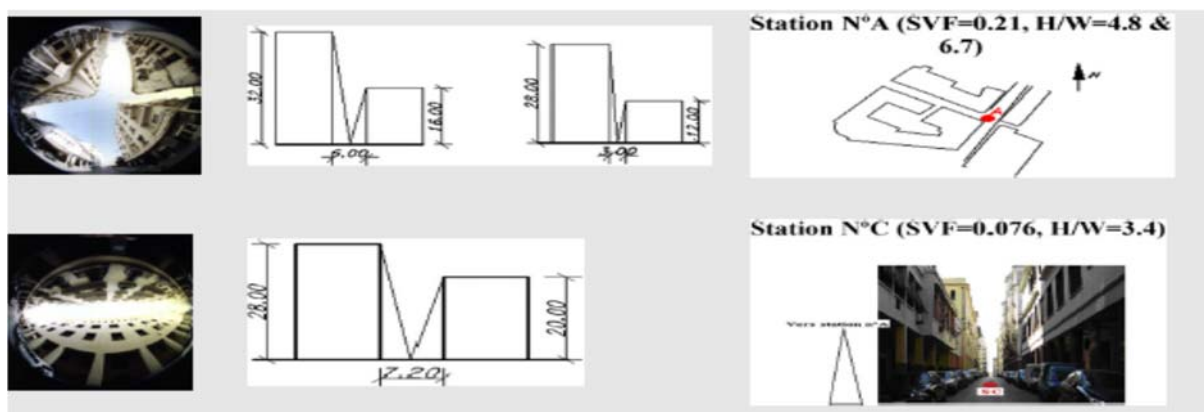


Figure 2.37: Site maps showing positions and canyons of the study. Source: Bourbia and Boucheriba (2010).

⁷ CTTC model: cluster thermal time constant.

people's acceptance of thermal comfort did not change with changes in airflow at high levels of air temperature. This means that the peak air temperature for summer days between 12:00 to 18:00 was not affected by changing wind speed. Ratti (2003) argued that the main variables of urban geometry that affect urban microclimate include: daylight accessibility to an urban canyon, surface to volume ratio, shadow area and sky view factor. The result of Ratti's research determined that thermal performance increased positively with surface volume ratio. Bourbia and Boucheriba (2010) discussed the urban geometry effect on solar incoming and long wave outgoing radiation. Solar radiation has a greater impact on streets and the surrounding environment in semi-arid climates. The study measured solar radiation (absorption and emission) through H/W aspects and sky view factor (SVF) with canyon orientation defined by its long axis (Figure 2.37). The research concluded that the difference in temperature of 3–6°C between urban areas and rural environment is a result of the solar radiation that enters the canyon.

Urban morphology has a significant impact on defining the differences in air temperature in an urban microclimate. This topic is extensively discussed in hot dry regions as the variation in air temperature between day and night is considerable. Solar radiation plays a crucial role in determining local microclimate in these urban areas. This variation depends on urban elements, such as urban surface materials, urban form, and urban greenery (Wong et al., 2011). Additional studies in relation to the impact of solar radiation on an urban microclimate have compared the traditional morphology (old city) with modern morphology (new development). These types of studies depend on the positive⁸ urban element of traditional urban morphology compared to modern morphology (Andreou, 2014; F. Bourbia & H. Awbi, 2004; Johansson, 2006; Morad & Ismail, 2017). Most of these studies ascertained that traditional morphology performs better thermally than modern morphology because of low solar radiation penetration into urban canyons. Mohammed (2015) found that the air temperature in shallow canyons (modern morphology) is warmer by 5–15% compared to narrow canyons (traditional morphology). Talep (2012) compared organic and structured urban morphology in the summertime in the UAE. The results indicated that organic morphology records lower air temperatures compared to the structured configurations. Traditional morphology is recommended not only because it performs better thermally, but it is a more sustainable configuration in terms of social and culture representation. Generally, it can be seen that

⁸ The positive urban elements include reducing solar penetration of urban areas by eliminating H/W ratios, using sustainable construction materials for building, and small façade windows and openings.

traditional urban morphologies perform better thermally, because traditional urban morphology is more sustainable than modern urban morphology, and the traditional form is designed to adapt to the local urban microclimate. Thermal comfort in traditional canyons is more acceptable than grid-iron (Johansson, 2012). Furthermore, the improved microclimate conditions in summertime will reduce energy demands in buildings.

2.13 Urban Heat Islands (UHI)⁹

Luke Howard initially described a UHI in 1818. It is one of the most important topics with respect to urban climate and considerable research has been completed on this subject (Erell et al., 2012). The topic of UHIs has been well studied and become the focus of architects, engineers, urban designers, and climatologists. This phenomenon is defined under certain weather conditions. UHIs involve significant differences in air temperature between a city and rural areas (Tim R. Oke, 1973). Literature on UHI mainly investigates the important factors relating to them. However, due to the complexity of UHI factors, it is challenging to control all the factors in one study. Thus, the most important factors that have been considered regarding each climate zone, for example the UHI factors for a hot, dry climate, are different to a UHI for hot and humid climates. Taled (2012) argued that urban configuration is one of the most important factors affecting air temperature variation, while Bokaie (2016) reported that vegetation and plantation is the most important factor of UHI. Generally, UHI can increase the temperature of a city by 2–5°C (T. R. Oke, 1987). A UHI causes differences in air temperature that reach 12°C in the evening time (EPA, 2009). Che-Ani (2009) and Taleb (2013) divided the factors affecting UHI into two categories:

1. Metrological factors, such as wind speed, orientation, relative humidity and cloud cover
2. Urban parameters, such as density, built-up area, sky view factor, building materials and urban structure.

Demand for cooling energy increases in summer with the peak temperature reaching 49°C in Erbil (Rasul et al., 2015). Higher air temperatures increase energy demands for cooling load. This demand can exceed grid capacity, resulting in local diesel powered generators being used which produce harmful emissions and increase ground level ozone (Okeil, 2010). Oke (1982) reported that an important factor affecting microclimate is sky view factor (SVF), which has a parallel relationship with heat loss, where narrow streets have lower heat loss.

⁹ later in the chapter a more detailed discussion of Urban Heat Islands will be given

Other factors affect microclimate wind flow between urban blocks. Wind flow is affected by the surface roughness of urban buildings and textures, and hence creates lower wind speeds in high density urban areas. In addition, vegetation is also another factor of microclimate due to the level of evaporation produced by plants. (Okie 2010) reviewed factors that affect the microclimate in an urban area (Table 2.8):

Table 2.8: Factors that affect an urban microclimate

Factors affecting urban microclimate			
1	Surfaces	Surface materials	Pavements, Asphalt, Dark Paints, Dark Plaster, Dark Cladding, Bricks and Concrete
2	Anthropogenic Heat	Industry	Plants and Electricity Power Stations
		Transportation	Cars and Public Transportation
		Building Temperature	The amount of energy absorbed or emitted by buildings into an urban environment
3	Vegetation	Evaporation	The amount of evapotranspiration which is produced by green area in urban morphology
4	Sky view factor	Width of street canyons	The amount of solar energy and solar radiation to urban facades
5	Lower urban wind speeds	Roughness of building aerodynamics	Density of buildings or urban blocks to overall site area

In contrast, hot, arid regions, urbanisation and man-made modifications, buildings, and green areas may cause Urban Cooling Islands (UCI) (Santamouris, 2014). This phenomenon can be seen in city centres compared with surrounding rural areas during the summertime (Rasul, Balzter et al., 2015). The researcher found that ‘built form, green areas and water bodies, all influence the urban microclimate and lower the air temperature’. Other researchers have established that wind speed is associated with a UHI (Unger, 2004). Morris and Simmond (2001) ascertained that UHI variation can be reduced by 0.14 °C if the wind speed is increased by 1m/s. Ratti (2003) studied the major variables of a UHI relating to urban microclimate which have a significant impact on urban air temperature, for instance SVF, surface to volume ratio, shadow densities, and day lighting. These factors have an impact on thermal comfort, urban air temperature and, finally, building energy consumption.

2.14 Types of Urban Heat Island UHI

UHIs can be observed and measured using two scales: firstly, by way of the temperature of the urban surfaces, in this case called surface heat islands, or by the atmosphere layer scale above the city, known as an atmospheric heat island. This classification is based on several categories, such as degree of homogeneity, urban intensity, temporal behaviour, and location of city (Gartland, 2008). The UHI is fundamentally generated as a result of the interaction between various physical processes. Both types of UHI have different properties and are not necessarily

generated at the same time or location (Oke, 1982). Chudnovsky (2004) argues that urban microclimate primarily depends on urban structure energy balance, which is dependent on urban layer properties. Thermal urban properties are determined by surface materials, sky view factor, and urban density. Both types of UHI are similar in terms of LST and how the air temperature changes between different layers of the atmosphere. A UHI causes a change in sensible heat and transfers the hot air from irradiated locations to shadow areas and lower air temperature zones by means of convection.

2.14.1 Urban Surface Heat Island (USHI)

This type of UHI forms when the urban surface temperature inside a city is higher than sub-urban and rural areas. This type of UHI commonly occurs when the urban areas are surrounded by moist soil and vegetated areas. Surface UHIs occur during the daytime rather than at night due to the solar radiation. However, the heat island phenomenon is opposite in hot and dry cities, where the urban areas are surrounded by desert or dry soil, and the urban surfaces temperature is lower than bare soil outside the city (Rasul et al., 2015). Weng (2004) described an urban surface heat island USHI as a variation in the air temperature of horizontal surfaces in urban areas, such as roofs, streets, pavements and green plot areas. From 1970, researchers have used remote sensing data, which can be represented as thermal satellite images or thermal infrared TIR. The satellites are used to obtain TIR data are TM/ETM+,¹⁰ MODIS,¹¹ TIRS¹² etc. These types of images are used to study and analyse the horizontal surfaces of any part of a city that appears in satellite images. The remote sensed satellite images are commonly used by researchers to study the microclimate of an urban area. Recent studies employed this technique because it has the ability to study a large area of a city. However, this technology has a few limitations associated with difficulties in measuring the amount of thermal energy that may be emitted by different urban surface materials. Table 2.9 shows the number of studies and different techniques using the satellite imaging process to predict and measure UHI.

Table 2.9 : Different factors and methods to measure USHI

Author	Technique used	Most effective factors	Climatic zone
(Tran et al., 2006)	Remote sensing	Land distribution and urbanisation	Tropical climate
(Weng, Lu, & Schubring,	Remote	Vegetation	Tropical climate

¹⁰ TM (Thematic Mapper) on board Landsat-5. ETM+ (Enhanced Thematic Mapper Plus) on board Landsat-7

¹¹ MODIS (Moderate Resolution Imaging Spectroradiometer) is an extensive program using sensors on two satellites that each provide complete daily coverage of the Earth.

¹² An airborne Daedalus scanner operated by NASA

2004)	sensing		
(Rasul et al., 2017)	Remote Sensing	Land use/land cover	Hot dry climate
(Rasul et al., 2016)	Remote Sensing	Vegetation and moisture	Hot dry climate
(Haashemi, Weng, Darvishi, & Alavipanah, 2016)	Remote Sensing	Land distribution and urbanisation	Semi-arid climate

The results from these studies identified that there are two types of Surface UHI: Hot Surface UHI and Cool Surface UHI. This primarily depends on climate zone and urbanisation. In hot and semi-arid climates during summer, the surface air temperature is lower than in rural areas, while in tropical climate zones, the urban area is hotter than in rural areas.

2.14.2 Atmospheric UHI

An atmospheric UHI can be defined as an increase in air temperature in urban areas more than rural areas surrounding a city. The general effect of this type of UHI appears after the sun sets directly, when the temperature reaches its maximum during the night. The heat mass exchange between the urban surface structures and the outdoor microclimate happens when air temperature in the surrounding buildings is lower than the external surfaces of urban structures. As a result of different variables in the urban structure in the same atmospheric environment, atmospheric UHI are divided as shown below.

a. Canopy Layer Heat Island (CLHI)

b. Boundary Layer Heat Island (BLHI)

2.14.3 Boundary Layer Heat Island (BLHI)

Oke (1976) found that the principal divide between both types of UHI is the difference in the main variables associated with the urban locations, geometry, intensity, orientation, physical and temporal characteristics of each urban area. Different techniques and instruments can be used to measure the impact of these types. Although UHIs are studied and observed primarily in the day time, this phenomenon can be observed at night, as well as in low latitude cities with a high level of heat flux produced as anthropogenic heat (Rasul et al., 2016).

BLHI can be defined as the layer of hot air that extends between a building's roof to a height of one km during the daytime. Moreover, this layer will shrink at night to 100m above the roofs. This air creates a dome of homogenous air that changes with changes in the air temperature of the canopy layer, which is directly located under this layer. Situ measurements

and special tools can be used to study this phenomenon, such as tethered balloons and aircraft (Timothy R Oke, 1976).

2.14.4 Canopy Layer Heat Island (CLHI)

CLHI refers to a scale layer between the ground surface levels to the average height of a building in an urban pattern. The air between buildings is affected by various factors including vegetation, surface materials, urban geometry and density, as well as human activities.

These different factors cause different canopy air heating, for instance a canyon with a prevailing wind direction typically cools more than a perpendicular canyon because the wind continuously releases the hot air (Balslev et al., 2015). This phenomenon can be measured through fixed or portable weather stations. The latter are fixed on a car and weather data can be collected regularly to investigate UHIs between city centres and rural areas (Brent C Hedquist & Anthony J Brazel, 2014). The majority of researchers have studied the urban microclimate, which is a combination of the effect of canopy and boundary heat islands (Ali-Toudert & Mayer, 2006; Andreou, 2013; Bakarman & Chang, 2015).

Bourbia and Awbi (2004) used field measurements with a shading simulation program (ShadowPack PC code v.2), as the methodology. The study analysed canyon geometry by measuring SVF and canyon aspect ratio H/W. They noticed that H/W aspect and canyon orientation had a greater effect on solar shading and the urban microclimate. The beneficial relationship between urban geometry and urban microclimate is helpful in generating urban design guidelines and eliminating energy consumption regarding housing projects. Table 2.10 summarises all of the additional papers that have been reviewed, creating a wide range of climates with a brief summary of their results. For hot dry climates the canyon geometry, solar access and shading were important climate factors and ENVI-met was widely used as a simulation tool.

Table 2.10 : Summary of additional papers reviewed creating a wide range of climates including a brief summary of their results

Author	Variables	Regions	Microclimate Factors	Methods	Results
(E. L. Krüger et al., 2011)	SVF, orientation and winds	Subtropical climate	Evaluate street geometry on ambient temperature	ENVI-Met, field measurement, comfort survey	Urban geometry has an impact on outdoor thermal comfort and air pollution
Moohammed Wasim Yahia & Erik Johansson, (2012)	Physiologically equivalent temperature (PET) outdoor standard effective temperature	Hot and dry climate	Old and new morphology effects on outdoor thermal comfort	Comprehensive micrometeorological measurements combined with questionnaires	Traditional morphology with deep canyons is more comfortable in summer than modern urban morphology, as a result of the lack of shade. Conversely, residential areas and parks in modern morphology are more comfortable in winter due to more solar access
Moohammed Wasim Yahia & Erik Johansson, (2010)	Street design as regards aspect ratio w/h -Orientation -Trees	Hot and dry climate	Detached or attached street canyons 1. Ground surface temperature 2. Thermal comfort	Software ENVI-met	Canyon aspect ratio H/W, orientation and vegetation has a great influence on thermal comfort in attached street canyon. Street with detached buildings; vegetation has a strong influence on surface temperature and weak interaction with orientation
Adeb Qaid & Dilshan R. Ossen (2014)	H/W ratio in a symmetrical street Different orientation Wind flow Solar radiation Building height	Hot humid climate	Examined symmetrical and low symmetrical street which offers conflict properties during the day and at night	Software ENVI-met	Changing street aspects W/H and street orientation act positively and negatively on urban microclimates. The aspect ratio of 0.8–2 reduces the morning microclimate and UHI, while an aspect ratio of 2–0.8 reduces air temperature by 4.7°C and surface temperature by 10 to 14°C
Naveed M, Robert D. Brown (2015)	1. Air temperature 2. Humidity 3. Solar radiation	Hot dry city	Air temperature and humidity in both spaces was similar	Simulate thermal sensation through the energy budget model COMFA	The research studied microclimate characteristics in two different outdoor spaces Shalimar Garden, and hard-surface courtyard houses. The study showed the same air temperature and air velocity in both places, but the solar radiation in the courtyard houses was much higher than in Shalimar Garden, which is considered the main factor of discomfort
(Andreou &	Air and surface	Tropical	Main microclimate	Analyse the effect of	The study compared two urban sites: traditional

Axarli, 2012)	temperature, air humidity and air velocity	climate	parameters that affect urban canyon are street geometry, street orientation and the effect of trees, horizontal surface albedo, wind speed and direction	parameters such as urban layout, street geometry and orientation on urban canyon microclimate using the Green Canyon tool	and contemporary. The study observed no significant difference in air temperature of street canyons with different orientations within each site, both in summer and winter. Street orientation does not affect air temperature
(Andreou, 2013)	Street geometry, orientation, wind speed, surface albedo and trees	Tropical climate	Thermal comfort analysis Physiologically equivalent temperature (PET) and Rayman v.1.2 tool. Experimental measurements	Different characteristics in terms of urban density, layout, and materials (street geometry)	Outdoor thermal comfort conditions in traditional environments with a compact layout are more favourable in the climatic zone examined, compared to conditions in typical contemporary settlements
Nastaran Shishegar (2013)	Street geometry (H/W ratio) and orientation on airflow and solar access in an urban canyon		Street design on the urban microclimate	Urban morphology and density, the properties of urban surfaces and vegetation cover	The study determined that street geometry H/W and orientation are the key factors to providing a pleasant microclimate at a pedestrian level in urban canyons
(van Esch et al., 2012)	1. Street width and orientation. 2. Building design parameters (roof shape and building envelop design on solar access	Temperate maritime	1. Design parameters (roof shape and building envelope design) on solar access to canopy. 2. Heat demand and solar heat gain is calculated with the aid of TRNSYS	Trigonometric equations (sun's position in sky and geometry of canyon	Solar access and passive solar heat on design parameters examined and analysed for individual houses to assess the relationship between indoor and outdoor thermal conditions
(Balslev et al., 2015)	Shade and wind velocity on thermal sensation, H/W ratio	Mediterranean climate	Psychological Equivalent Temperature PET	Shade or wind speed effect outdoor thermal sensation	This study established that streets that are orientated east-west experience double heat stress compared to north-south ones in summer. In winter, a higher H/W ratio can increase cold thermal sensation by 10°C PET on the EW and

					NS direction as a result of shading. Finally, the research found that solar radiation has more effect on thermal sonication than wind velocity in summer and winter. north-south orientated in Tel-Aviv provide a greater microclimate (Balslev et al., 2015)
(Brent C. Hedquist & Anthony J. Brazel, 2014)	Outdoor thermal comfort in a relationship with UHI	Hot and dry climate	Output data from ENVI-met model	Mean radiant temperature and predicted mean vote outcomes	This research studied 3 sites in Phoenix, Arizona and measured the data output from ENVI-met model. The results indicate in summer that UHI in a city centre is effective at night, and in the morning it is comfortable (cool island), whilst it is less comfortable from midday to evening time. In surrounding areas, the degree of comfort contrasts; discomfort during the daytime and comfortable at night. The surface heat can decrease dramatically by increasing tree, vegetation and structure shading and increasing outdoor thermal comfort. The conclusion of this study agreed with other studies regarding hot and arid cities
(Martinelli et al., 2015)	Daily shading pattern, SVF outdoor thermal comfort	Mediterranean climate	PET, RayMan model	PET values were significantly lower in shaded areas	The research concluded that minimum PET difference for the same locations was 2°C at 18:00, while the maximum difference was 7°C at 11:00
(Ali-Toudert & Mayer, 2006)	Height-to-width ratio Solar orientation	Hot and dry	Physiologically equivalent temperature (PET). The research attempted to design new canyons based on two factors: H/W ratio and solar radiation. Time and purpose of canyon usage also influence design choices	ENVI-met to study different h/w ratio to different solar orientation and numerical simulation	Study conducted in a hot dry climate. The study discussed urban canyons with different H/W (i.e. H/W=0.5, 1, 2 and 4) and various solar orientations (i.e. E-W, N-S, NE-SW and NW-SE) toward better thermal comfort at a street level using PET. The result of this study reveals that PET comfort level depends mainly on H/W aspects and canyon radiation. The study concluded that combining urban frequentation time usage and street usage can strongly mitigate heat stress

(W. Yang et al., 2013)	Sun sensation and solar radiation	Tropical climate	2036 effective questionnaire responses	Comparative analysis between outdoor and indoor thermal sensations	The study determined that the acceptable operative temperature range was 26.3–31.7 °C in outdoor urban spaces. Sun radiation and sun sensation is the most influential factor concerning human outdoor comfort. The study concluded that humans may expect higher temperatures in outdoor spaces compared with the same temperatures for indoor spaces
(Johansson, 2006))	Urban geometry compared shallow and deep street canyons	Hot and dry climates	Urban geometry on outdoor thermal comfort and its microclimate. Deep canyons cooler than shallow in summer	PET index	The result of this study shows a 6 to 10k difference between both canyons. The deep canyons have an acceptable level of comfort, while shallow canyons are extremely uncomfortable. In winter, solar access to shallow canyons produces more comfort. The study found that a compact urban design with deep canyons is preferable to shallow canyons. However, in winter, the canyon should be wider for solar access
(Lin et al., 2010)	SVF air temperature, relative humidity, wind speed and solar radiation	Hot and humid regions	12 field experiments to analyse outdoor thermal conditions and metrological data for a 10 year period	PET thermal index RayMan model	The result reveals that high SVF causes discomfort in summer and low SVF produces discomfort in winter. Moreover, the research concludes that shading an area with trees and buildings is important in hot summer. Outdoor space should avoid extensive shading in winter
(F. Bourbia & H. B. Awbi, 2004a) Part 1	Solar radiation, size and proportion of open spaces H/W on ground surface Orientations	Hot dry climate	The interrelation between canyon geometry and solar radiation	Size and proportion of open spaces has an enormous impact on solar access	The result of this study reveals that air temperature is different compared to surface temperature. Surface temperature principally depends on street geometry and sky view factor. There is a strong correlation between surface temperature with both street geometry and sky view factor in a hot dry climate

2.15 Microclimate in Erbil

Erbil has a hot and dry climate during the summer, when rural surfaces absorb heat more than in urban areas. The dry and large barren surface area which surrounds the city produces higher surface temperatures (Figure 2.38). Land surface temperatures are mitigated by increasing evaporation and shading effects on the land (House-Peters & Chang, 2011; Rasul et al., 2016; Weng et al., 2004), but this occurs in urban areas more than those surrounding the city. Rasul

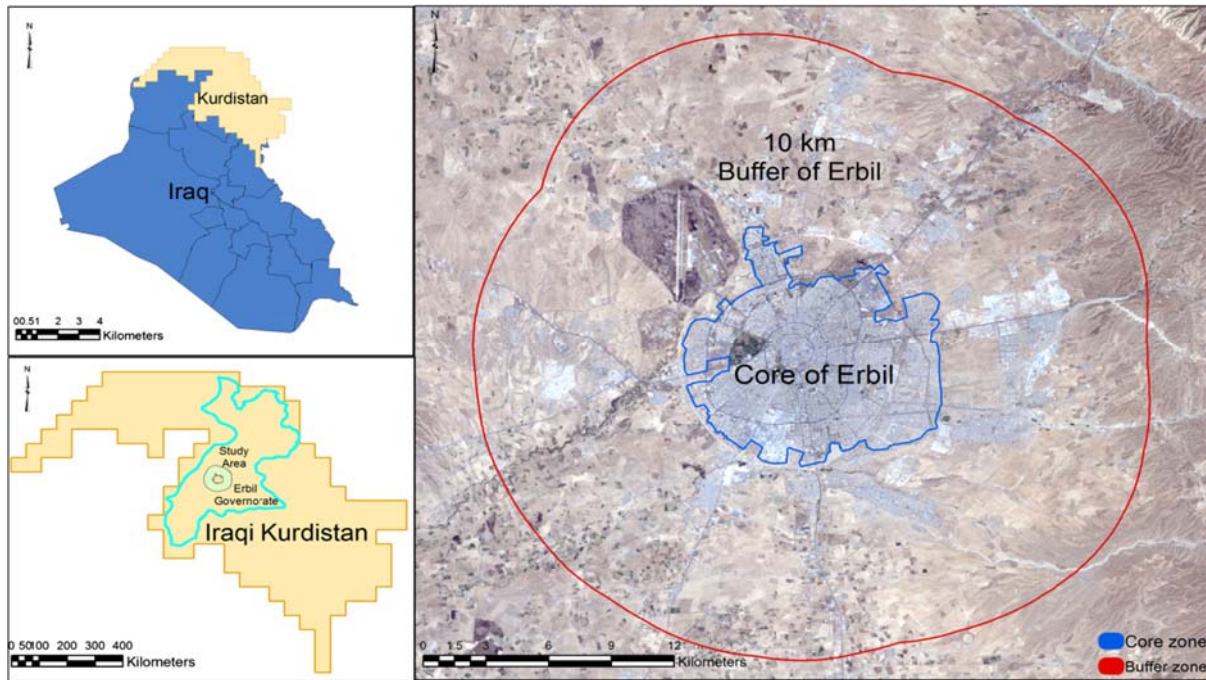


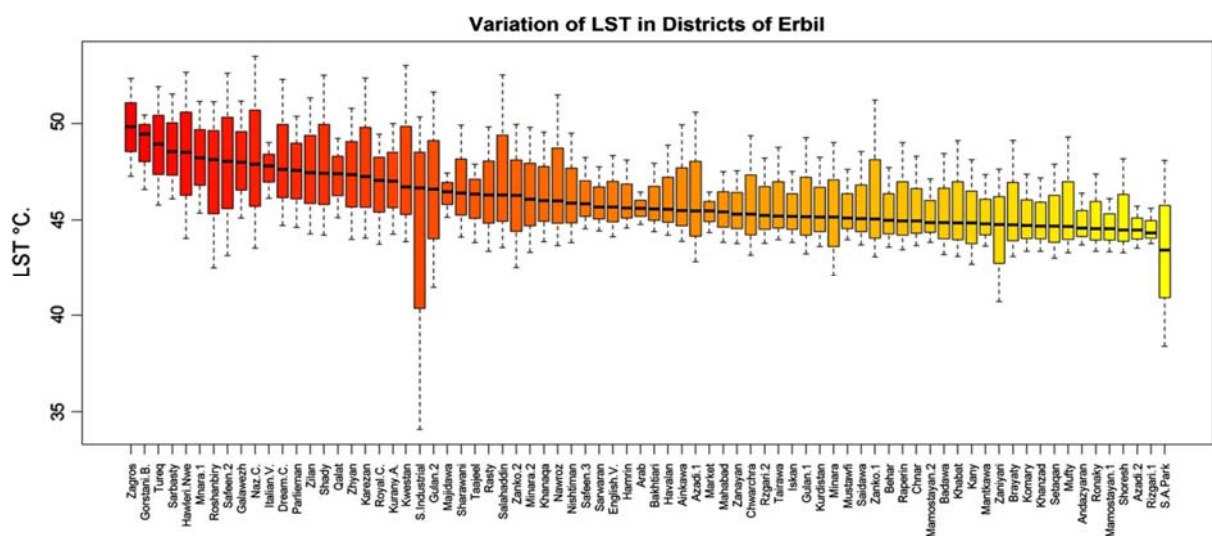
Figure 2.38: Map of Iraq, the Kurdistan Region and true colour Landsat of the study area.

(2015) examined the land surface temperature and surface urban cool island, and established that the land surface temperature is mainly affected by a high bareness index and green areas. Six satellite images were taken during the daytime to illustrate the surface urban cool island (SUCI) effect on Erbil. The thermal satellite images were used to identify land surface temperature (LST) and land use/cover (LULC), vegetation, green areas and water bodies. The study indicates that new developing open spaces and low density urban areas around the city are hotter than the city centre (Figure 2.38). The results reveal that during the daytime the residential urban areas recorded the lowest LST compared to rural areas (3.5 to 4.6 °C). Moreover, surface wetness (water bodies) is the main factor affecting urban cool islands and not vegetation cover (Rasul et al., 2015). The study also identified the maximum, mean, and minimum LST of Erbil, as shown in Table 2.11

Table 2.11: The max and min LST

Land surface temperature	City centre	Buffer zone 10 km surrounding city
Maximum °C	53.5	58.1
Mean °C	46.2	50.1
Minimum °C	34.1	37.6

The study similarly assessed LST and Surface Urban Heat Island Intensity (SUHII) by calculating zonal statistics, concluding that water bodies have lower LST (41.1 °C) compared to other hotter areas at the airport and on barren land (Table 2.12). In addition, the open green areas (trees and grass) recorded a medium LST higher than the water bodies and lower than the barren lands (Figure 2.39).

**Figure 2.39: Different air temperatures in all districts in Erbil. Source: Rasul, 2015****Table 2.12: Different high, low and mean LST for different zones in Erbil. Source: Rasul, 2015**

Zones	Highest surface temperature	Lowest LST	Mean LST
Lake 1 and Lake 2 (Figure 2.38)			40.22 °C ± 1.59 °C
Airport (outside the city)	53.11°C ± 2.6 °C		
Barren Lands	46.67°C ± 1.54°C		
North and South Industrial areas			48.1°C ± 2.46 °C 46.67 °C ± 1.54°C
Dense Trees		42.8 ± 1.91°C	
Grass		43.86 ± 2.46°C	

Table 2.13 shows the zonal LST analysis which indicates that its lowest value is in the old districts (high density), inside the 60m ring road, except for the city centre, Erbil citadel, with 47.4 ± 0.93 °C, as well as the modern part (low density) of the city, comprising Zagros in the north (49.83 ± 0.93 °C) and Sarbasty to the west of the city (48.54 ± 1.04 °C). The maximum LST was recorded at Zagros (49.83 ± 0.9 °C) and Turq (48.92 ± 1.16 °C), whereas the lowest

LST was recorded in Sami Abdulrahman Park (43.43 ± 2.06 °C), Rizgari 1 (44.32 ± 0.31 °C) and Azadi 2 (44.47 ± 0.44 °C). Finally, the mean LST was stable and close to the city's average temperature; Rasty (46.29 ± 1.31 °C) and Taajeel (46.34 ± 0.83 °C) (Table 2.13). (See Figure 2.40) for location of districts in Erbil).

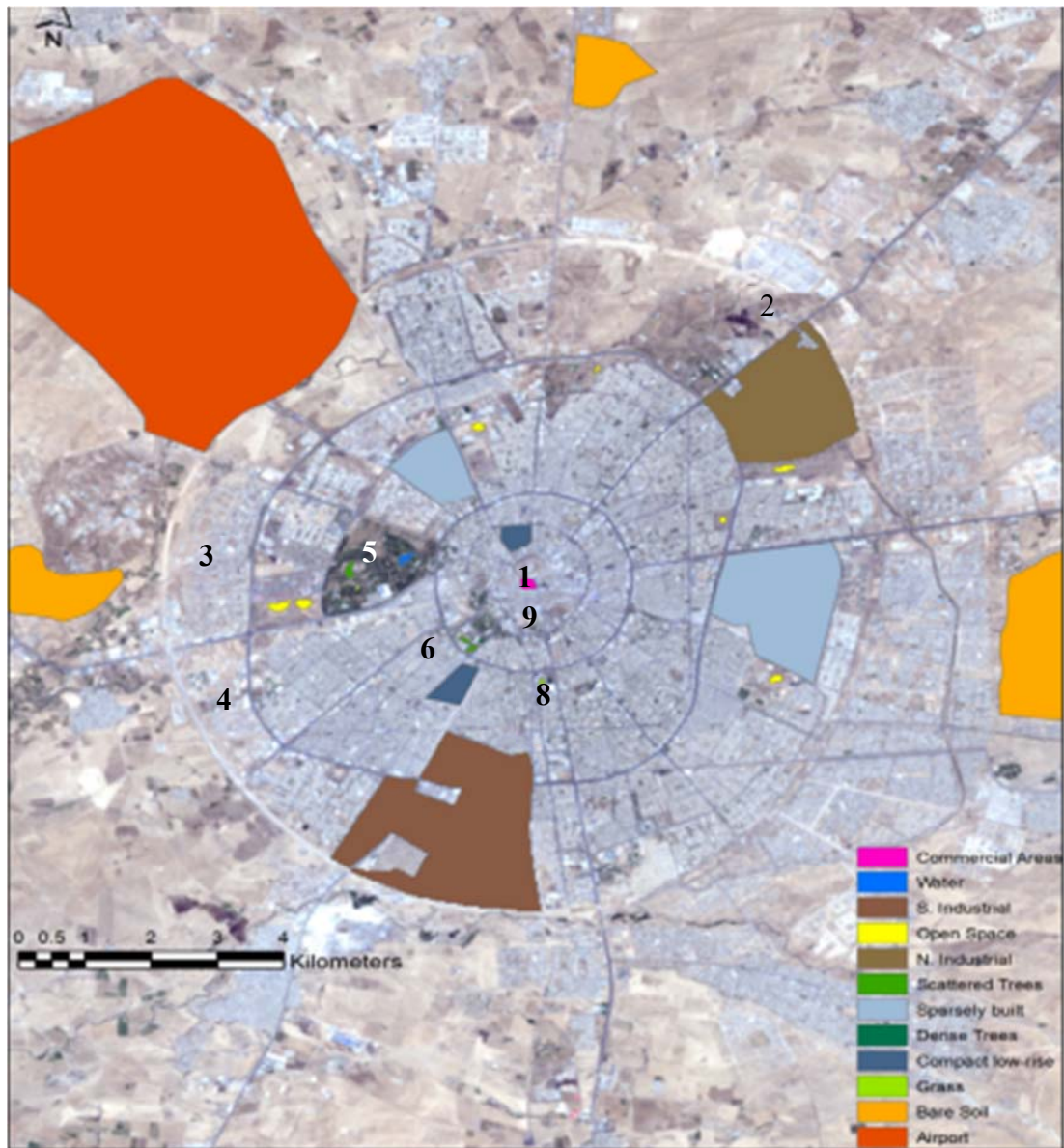
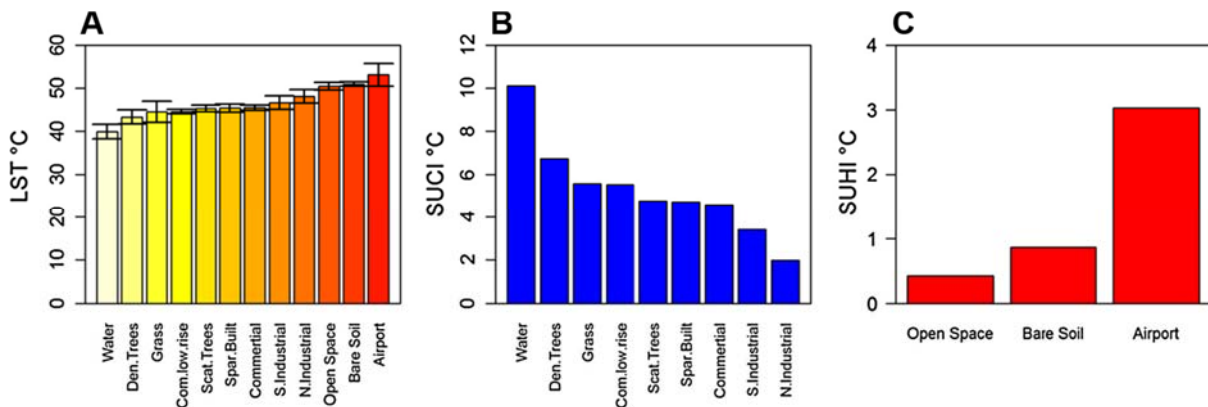


Figure 2.40: Samples of selected LULC with true colour Landsat OLI. Source: Rasul, 2015.

Table 2.13: Different LST in different districts in Erbil. Source: Rasul, 2015

Districts	Image reference	LST
Erbil Citadel	1	47.4 ± 0.93 °C
Zagroz	2	49.83 ± 0.93 °C
Sarbasty	3	48.54 ± 1.04 °C
Turq	4	48.92 ± 1.16 °C
Sami Abdulrahman Park	5	43.43 ± 2.06 °C
Rizgari 1	6	44.32 ± 0.31 °C
Azadi 2	7	44.47 ± 0.44 °C
Rasty	8	46.29 ± 1.31 °C
Taaheel	9	46.34 ± 0.83 °C

**Figure 2.41: Samples of selected LULC with true colour Landsat OLI. Source: Rasul, 2015**

The study indicates that in daytime in summer, especially in the morning, the average surface temperature in the city of built-up areas is lower compared to 10km outside the city boundary (Rasul et al., 2015). The Surface Cool Land Urban Island Intensity SCUII for the city centre ranges between 3.5–4.6°C. As a result of the findings and conclusion of this study (Rasul), the satellite thermal images identify that the LST in the city centre is lower than in rural areas (Figure 2.41), although the findings depend on the regional scale. Moreover, this study is essential to predict the general idea about the effect of build-up and urbanisation on Erbil's microclimate.

2.16 Urban microclimate modelling

The idea of using urban microclimate models to examine the correlation effects of urban design and urban microclimate in urban areas is relatively new. Historically, urban microclimate studies used in situ measurements, but recent developments in computer software can be used to assess and simulate urban microclimates. Urban microclimate modelling is important because it helps to reduce microclimate issues which affect not just thermal comfort but also human health and building energy consumption. To eliminate the impact of rapid urbanisation

and the UHI effect, most studies use urban microclimate modelling. These include urban factors, for instance vegetation, ground, and the surfaces of buildings, as well as microclimate parameters such as air temperature, relative humidity, wind flow, solar radiation and evaporation. Microclimate modelling allows the study of urban factors and urban microclimate parameters in one simulation package (Figure 2.42).

Additionally, the main advantage of modelling urban microclimates is that it allows different scenarios to be used and compared to the base case scenario (Blocken, 2015; Kanda, 2007). In addition, the model build-up is based on the information on specific points of the studied area (the site), while the simulation output provides information on any point in the computational domain (Blocken, 2014; Moonen, Defraeye, Dorer, Blocken, & Carmeliet, 2012; Rizwan et al., 2008).

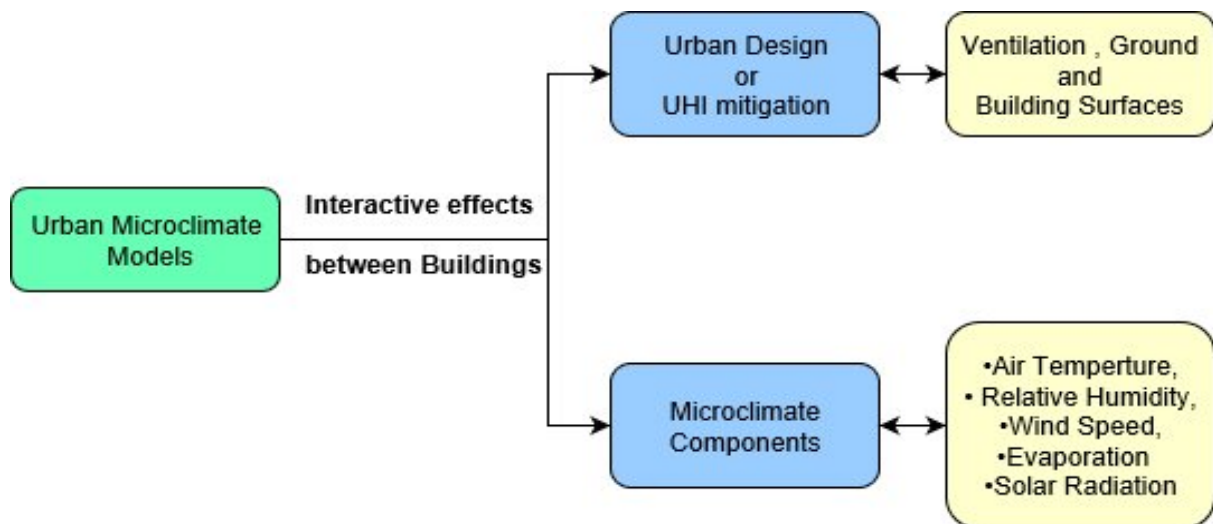


Figure 2.42: The urban microclimate model starting from UHI and measurements

G Mills 2009) divided the history of urban microclimate studies into six specific periods based on the urban microclimate research methodologies shown below:

1. First period, latter 1900s: This period gave descriptions of the urban effects on microclimate using conventional meteorological equipment such as (thermometers, hygrometers, etc).
2. Second period, latter 1960s: Urban microclimate was measured by means of process variables such as (heat exchange, turbulence and radiation). In addition, statistical methods were used to document results.
3. Third period, latter 1970s: For the first time, computer modelling techniques were used to predict urban microclimates. In addition, conventional (micro) meteorological was applied to model urban climates. Urban surfaces, scale, and urban effects were also defined.

4. Fourth period, latter 1980s: Urban microclimates were measured by the adoption of experimental approaches. Important urban forms were determined such as canyons instead of streets, and limited scale was used for models and direct measurements.
5. Fifth period, latter 1990s: The interaction between urban geometry and microclimate effect was studied using organised field projects.
6. Sixth period, latter 2000s: New realistic urban microclimate models were developed. Novel models and techniques were employed to study and analyse urban microclimate features.

In recent years, a wide range of models and simulations have been employed to study urban microclimate. Most important is the distinction between Computational Fluid Dynamics (CFD) and Energy Balance Models (EBM). Toparlar, Blocken, Maiheu, and Van Heijst (2017) demonstrated that CFD offers two advantages compared to EBM from the viewpoint of urban microclimates, as shown below:

1. CFD simulation coupling between wind speeds, air temperature and humidity.
2. CFD offers detailed analysis and representation of air flow comprising a smaller scale (building and human scale). However, CFD requires a high level of urban geometry representation, significant flow variables and powerful computing systems (Blocken, 2015; Moonen et al., 2012).

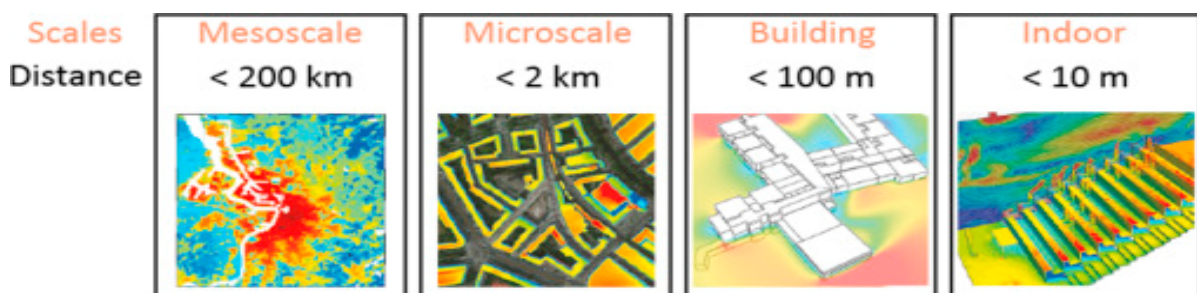


Figure 2.43: Horizontal dimension and representation of climate modelling scales

The scale is essential to determine the type of computational simulations, given that each model has limited boundary conditions. There are different scales in relation to studying urban microclimates ranging from mesoscale < 200 km to indoor scale < 10 metres (Figure 2.43).

The CFD modelling of urban microclimates can provide comprehensive information on air flow around buildings and other obstacles in that particular environment. the urban microclimate model using CFD parameters (i.e. air turbulence, energy balance) with thermodynamic processes evaluates the urban microclimate effect on ground level, walls, roofs and plants. In addition, CFD simulations are employed to study urban microclimates and can

be used to investigate wind flow around buildings, thermal and wind comfort at the pedestrian level, pollution and air quality, and rain and snow drifts, in addition to other topics.

Listed below are seven microclimate models that can be used for predicting urban microclimates.

Table 2.14: Microclimate methods ENVI-met simulation program as used by different researchers

Microclimate models				
No	Models	Developed by	Parameters measured	Results of significant studies
1	ENVI-met	Prof. M. Bruse Mainz University	Simulate surfaces of urban environments with resolution 0.5–10m and provide 250 grids. Based on fluid dynamic and thermodynamic laws. Using micro to local scale	Wong et al. (2011). Studied the impact of greenery using satellite images, field measurements and ENVI-met. The result of the study was the high impact of greenery on ambient temperatures. Fahmy (2009) investigated leaf area index (LAI) comparing two streets using ENVI-met to mitigate UHI. The result was a 0.1 to 0.3k reduction in both cases using ENVI-met. Thus, ENVI-met provides better evaluation than similar simulation programs
2	CTTC	M.E. Hofman	Predict urban temperatures through urban geometry	Shashua (2001) studied 11 sites and found a 0.5k difference when urban areas were with or without trees and increasing albedo from 0.5 to 0.7. The cooling increased by 4.5 K in streets and courtyards
3	PHOENICS CFD	CHAM company	Fluid flow, heat mass, chemical reaction, consumption engineering equipment	Dimondi and Nikolopoulou (2003) found that every 100m ² of vegetation reduces the temperature by 1 K
4	CitySim Pro	Kaemco 2016	Large scale building energy simulation tool which estimates energy fluxes at different scales. Simulates the energy flow of the building in an urban area. Effective radiation model. Can model the interaction between building environment variables, such as reflected radiation between buildings and surfaces, and complex mutual solar shading	(Walter & Kämpf, 2015). In this study, CitySim was used to calculate annual energy consumption and peak load for a building on the campus of the Swiss Federal Institute of Technology Lausanne (EPFL). (Coccolo, Mauree, Kämpf, & Scartezzini, 2016). The study aimed to build up a database platform for a sustainable city and human wellbeing. This study combined CityGML and Energy ADE to obtain integration of outdoor thermal comfort with a building energy simulation database.

5	Autodesk Thermal CFD	Autodesk 2016	Uses Finite Element Methods (FEM) and CFD to calculate urban environmental indices such as thermal comfort	(Naboni, Cocco, Meloni, & Scartezzini, 2018), compared four CFD simulations to estimate and calculate urban microclimate models in terms of computation time without compromising quality of output.
6	Grasshopper plug-ins Honeybee/Ladybug	Mostapha and Chris 2012	Grasshopper plug-ins are used for weather data, solar radiation, and other climatic analysis. It connects Grasshopper to energy simulation engines such as EnergyPlus and RADIANCE	(Calcerano & Martinelli, 2016). This study coupled genetic algorithms, parametric design and dynamic simulations to optimise the location of trees. The result showed that optimising tree location can reduce summer energy consumption by 11%. (Santos, Afshari, Norford, & Mao, 2018) This study used EnergyPlus and Rhino (Grasshopper, Honeybee and Ladybug plug-ins) to calculate the UHI in the UAE
7	OpenFOAM, Ansys Fluent and 'Saturne'	Developed for mechanical engineering applications	CFD programs that can be used for analysis of air flow in urban areas. These simulations depend on BSM such as CitySim, EnergyPlus and TRNSYS to simulate the boundary conditions of urban microclimate	(Y. Yang et al., 2019). Ansys Fluent was used in this study to demonstrate the UHI impact on air temperature. (Kubilay, Derome, & Carmeliet, 2018). In this study, OpenFOAM was employed to study the impact of rain on air flow in urban canyons. (Kadaverugu, Sharma, Matli, & Biniwale, 2019) used Code-Saturne to investigate the impact of urban landscape on air quality

There are a limited number of computer programs that can simultaneously model urban microclimate physical phenomena. Table 2.14 shows some of the CFD models that can simulate urban microclimates. These models are different in terms of resolution and physical and temporal bases. In addition, some models are complex and require a high level of computational skill to run (G. Mills, 1997). In contrast, some models are too simple in terms of microclimate outputs, such as CTTC (Liang, Meng, He, Ren, & Li, 2018). ENVI-met is the most appropriate software seen so far to model urban microclimates because it combines fluid and thermodynamic models to simulate solar radiation, exchange processes relating to heat and vapour, exchange at vegetation, bioclimatology and pollutant dispersion (Allegrini et al., 2015). Moreover, ENVI-met has a user-friendly interface and requires limited input data to generate detailed output data on urban microclimates. ENVI-met is one of the CFD and three-dimensional numerical models designed specifically to study and analyse the micro interaction

between urban design and microclimates. This model is considered one of the best models to calculate the fluid dynamics parameters of wind and turbulence in relation to thermodynamic processes which happen on the ground, walls, roofs or vegetation surfaces. The model's resolution is between 0.5–10 metres, which allows the model to simulate complex urban forms and various vegetation types. ENVI-met is a prognostic model based on thermodynamic and fluid dynamic laws (Ali-Toudert & Mayer, 2006; Erell et al., 2012). This enables the model to calculate the heat exchange process between wind flow and the surface air temperature; wind turbulence with vegetation parameters (Chen & Ng, 2012). The high capability of the program offers the simulation and prediction of the impact of urban geometry on modifying urban microclimates for specific urban areas within a daily cycle. This urban microclimate model is widely used to study urban microclimates in different climate zones and for calculating the interrelationship between urban design features and microclimate elements (Calcerano & Martinelli, 2016; Chow & Brazel, 2012; Huttner, Bruse, & Dostal, 2008; Lin et al., 2010).

In this section, we compare and evaluate 19 studies in different climate regions to select appropriate numerical software to model the urban microclimates in Erbil. In each study, we present microclimate factors, regional climate and application of numerical software. Studying their findings and microclimate factors reveals that ENVI-met is more appropriate in the simulation of urban microclimates. In the present study, ENVI-met is considered the most appropriate model to model and predict urban microclimate of Erbil.

2.17 Building Energy Modelling

Building energy consumption has generally increased significantly recently, and this has contributed to global warming and rising environmental pollution. Building Energy Modelling (BEM) is an important way to achieve and evaluate a building's energy saving from an early stage in the design process (Al-Homoud, 2001). In addition, it allows the designer to evaluate the impact of environmental factors on building performance, in order to offer optimised building design. Building energy models are used to measure a building's energy consumption or predict the total energy that will be used for cooling and heating systems. These models combine most of the factors that affect energy consumption, such as the building's location, geometry, construction materials, lighting and equipment, air conditioning systems, and daily operational patterns.

As well as measuring a building's energy efficiency via energy models, these programs are also useful for mitigating urban heat islands by evaluating the effect of urban heat island strategies, such as green roofs, tree shading, and ground cool paving around buildings. There are more than 400 computer applications to study the building energy performance (Maile, Fischer, & Bazjanac, 2007). According to (Dong, Lam, Huang, & Dobbs, 2007; Gao, Koch, & Wu, 2019), the main BEM tools can be classified into two groups, as below:

1. Calculation engines developed by the US Department of Energy (DOE), such as EnergyPlus, Autodesk Green Building Studio, Design Builder, and eQUEST
2. Calculation engines developed in-house using software such as Trace 700 and IES Virtual Environmental (IES-VE).

The capability of BEM mainly depends on the input data and simulation engine, which directly influence the model's output. Most of the research investigating BEM tools can be divided into three categories: 1. the capability of BES tools; 2. results reporting and validation (accuracy); and 3. user interface and limitations of BES (Crawley, Hand, Kummert, & Griffith, 2008; Gao et al., 2019; Maile, Fischer, Haymaker, & Bazjanac, 2010).

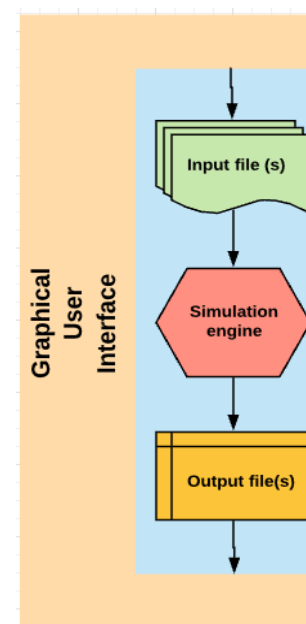


Figure 2.44: General structure of Building Energy Modelling tools

The general structure of BEM tools covers input and output data, and the simulation engine, as shown in Figure 2.44. The model's engine (e.g. IES-VE) employs input data to define the

simulation format and write output files, while the Graphical User Interface generates from the input, engine and output data a format file which illustrates the results graphically (Maile et al., 2007). Table 2.15 shows the input and output data ((Bahar, Pere, Landrieu, & Nicolle, 2013; Gao et al., 2019).

Table 2.15: The input and output data of Building Energy Modelling tools

Type	Input data	Output data
Building Energy Modelling tools	<ol style="list-style-type: none"> 1. Weather data, operating schedules, building geometry, internal loads, thermal zones, HVAC systems, components and simulation-specific parameters 2. Input data generated by BES tools (generated automatically without users' recreation) 	<ol style="list-style-type: none"> 1. Thermal performance assessment of building or spaces 2. Total or time-based building energy and utility costs 3. Lifecycle estimation of the energy costs for a specific building or any space inside it

Although BEM has been developed for decades and is widely applied in building design, construction, and operation, and for research purposes, it has limitations as described below:

1. The high cost of BEM simulation, due to the output data being labour and time intensive to produce;
2. Results only reliable under specific circumstances; output data not easily changed with changes to model settings;
3. The requirement that BEM needs an architectural and mechanical design (fundamental design) to start the simulation and generate the model;
4. “The issue of time-consumption of traditional BEM makes its results always lag in time behind the timing of design decision making” (Bazjanac, 2008);
5. The lack of consistency when preparing building geometry, which depends on the user's point of view instead of the original data resources;
6. The difficulty of preparing input data for simulation.

BEM has recently become an acceptable practical method for architectural design and building energy performance. On one hand, BEM tools have become a requirement for building design applications in order to determine cost and operation performance analysis. On the other hand, the achievement of accurate results with BEM simulation tools depends on input data, and the software program's capability, advantages, and drawbacks. For example, to gain accurate

results, significant time and expertise are needed to model the building's geometry, HVAC system, internal loads, and construction materials (Yezioro, Dong, & Leite, 2008).

(Mostafavi, Farzinmoghadam, & Hoque, 2015) state the different characteristics that should be taken into account when selecting a modelling tool from the available options, as below:

1. Usability model interface, which plays an essential role in good communication and information management between input and output data;
2. The model's capability to simulate the design framework, as integrated between detailed and complex building components with building geometry;
3. BEM interoperability and integration of the modelling procedure and building design process;
4. The user's requirements for the expected results (output data) in terms of details and format;
5. The level of output accuracy of the modelling procedure, by means of validation, as a main factor in selecting BSM for research or practice design purposes (Judkoff, Wortman, O'doherty, & Burch, 2008).

In addition to the above points, the accuracy of input data plays an important role in producing accurate output data. The input data are collected by the user (user responsibility), such as the building geometry, climatic data, and other missing data (dimension, and materiality). One important point that has to be raised here is that the weather data stored in the software's library should be efficient and strategic. This is because it employs historical weather data from the weather station nearest the building, and does not represent the exact urban microclimate around the building being simulated. To overcome this inaccuracy, detailed analysis of the urban microclimate around the simulated building is needed to generate new weather data that is more representative of the urban microclimate around the building. This assertion contradicts (Mostafavi et al., 2015), who report that "Although the microclimate around the building being analysed may not be reflected by the stored weather data files, unless an extreme microclimate exists, these data files are generally sufficient".

In the present study, a number of BEMs were analysed to evaluate their performance, the parameters measured, and their significant results. Table 2.16 shows common building energy models.

Table 2.16: Common microclimate methods used in research

Building Energy Models			
Models	Developed by	Parameters measured	Results of Significant Studies
DOE-2	US Department of Energy	Energy consumption	Akberi and Konopacki (2005) found that 75% of the energy that could be saved comes from cool roofs and tree shade
Energy Plus	US Department of Energy and the Lawrence Berkeley Laboratory	Thermal and visual comfort measured to nZEB target. Re-assessment of HVAC and lighting	(Ballarini, De Luca, Paragamyan, Pellegrino, & Corrado, 2019) found significant improvements in thermal performance, in terms of energy savings (- 37% of heating loads) and thermal comfort
TAS	US Department of Energy	Evaluating thermal analysis of buildings. Optimisation, energy and comfort performance	Yu and Wong (2007). The research showed that 10% of cooling loads can be saved when the building is surrounded by green areas such as park
HTB2	Cardiff University	Evaluating building energy, and energy demands for buildings in both design and occupancy period. Level of fabric, ventilation, solar gain, shading, occupancy, ground surfaces and outdoor environment	Li et al. (2007). Seasonal data were used to provide integration of the urban microclimate and building energy model
DIVA	US Department of Energy	Interaction between lighting and HVAC system to reduce energy consumption	(Alhagla, Mansour, & Elbassuoni, 2019) found a balance between natural lighting and solar heat reduced energy consumption
IES-VE	IES-VE company	Indoor: 1. Building energy calculation	(Skelhorn, Lindley, & Levermore, 2016) found that 2.7% of total cooling load can be reduced by adding four

		2. Human action on building energy consumption	trees to the north and four to the south side of a building; (Al Amoodi & Azar, 2018) found that the human actions can lead up to a $\pm 25\%$ variation in average energy consumption levels
		Outdoor: 1. SunCast to assess solar radiation 2. MicroFlo (CFD) to simulate wind speed and turbulence model	(Ghaffarianhoseini, Berardi, Ghaffarianhoseini, & Al-Obaidi, 2019). Investigate the thermal comfort. The study concluded that shading and ventilation strategies can achieve outdoor thermal comfort

The selection and suggestion of a BEM for simulation and analysis depends on certain variables, such as: the model's capability; how frequently the model will be used for simulation; user experience and profession (architect, engineer, developer etc.); the computer and system's ability (hardware to run the model); running time required by the model to provide accurate results; and other variables, such as the model's capability of connecting with other software e.g. 3D programs.

From Table 2 and the literature provided, the IES-VE was selected for the building scale simulation for this study, because it has advantages over the other simulation, given below:

1. A user-friendly interface, which is easy to learn for an architecture user; other models such as Energy Plus are more often used by engineers;
2. Virtually free for students and academic researchers. The software provides high quality data in terms of building materials and mechanical systems;
3. Large weather data files for various cities in the world;
4. Updated and modified weather data using special software developed by IES-VE;
5. Suitable for indoor and outdoor modelling as an effective research tool, for example using SunCast to determine the shading effect on the indoor environment (Skelhorn et al., 2016).

2.17.1 Integrated Environmental Solutions–Virtual Environment (IES-VE)

IES-VE is a computer fluid dynamic (CFD) model that is commonly used in BEM simulation. The model is well known as a significant practical information management tool. It is easy to learn, and the output data can be represented visually without enormous effort. This model can be used by architects because it also provides numerical data and schedules. As an information management tool, it gives an accurate simulation of the base case and responds well to other scenarios in a very short time, so that the quality of the simulation results can be examined quickly.

In addition, the model has a graphical interface and a large number of ready to use building materials that respond to user preferences, and it is easy to add new construction materials. The model engine can integrate various thermal information and performance in a short time, which gives the model the capability to be used as a research analysis tool in the early and post design stages (Attia, Beltrán, De Herde, & Hensen, 2009). Figure 2.46 shows the IES-VE engine and how the model integrates different sources of information to produce new information or output. The model can simulate solar radiation, airflow and climatic features, such as wind orientation and turbulence. In addition, it can be used to calculate energy costs and other

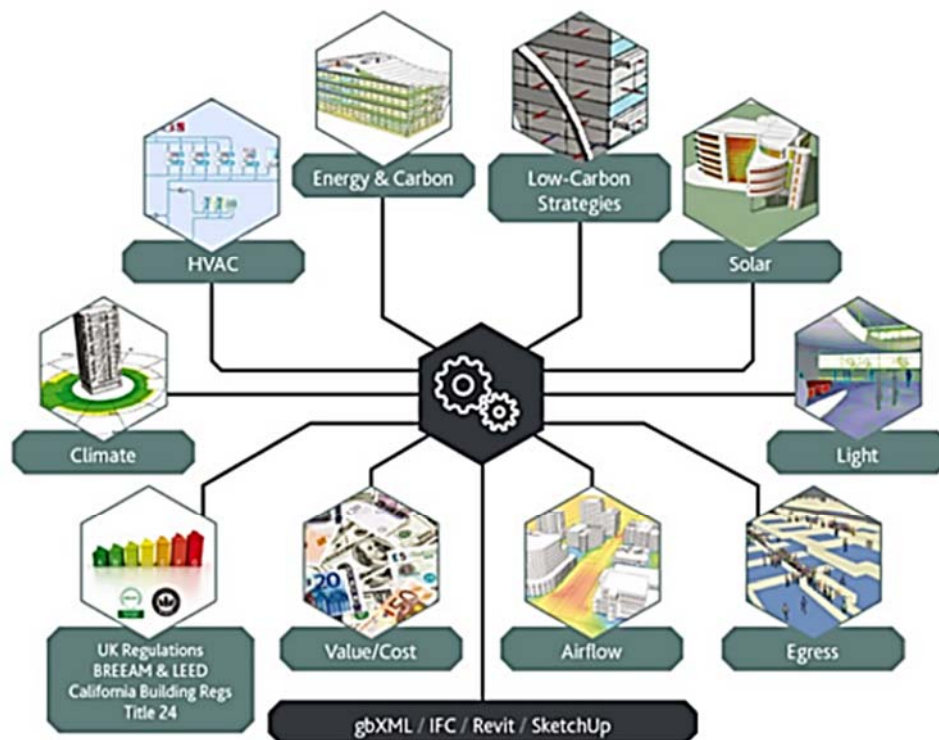


Figure 2.45: Integrated environmental solutions–virtual environment (IES–VE) engine

strategies, such as energy and low-carbon strategy, and provide report documents such as

BREEAM, and LEED. This research used HTB2 as a validation process through a direct comparison between IES-VE and HTB2 results.

2.18 Summary and conclusion of the literature review

This chapter presented an overview of the literature on Erbil's urban development and urban microclimate factors and modelling. The chapter was divided into four sections: Section 1 reviewed Erbil's climate; Section 2 is related to urban development in Erbil before 2003; Section 3 investigates urban microclimate modelling; and Section 4 discussed Building Energy Modelling (BEM).

The first section gave an overview of Erbil's climate and an analysis of urban microclimate factors: air temperature, wind speed for Kurdistan generally, and Erbil especially. In addition, satellite thermal imaging was critically reviewed to understand the urban characteristics (surface materiality and greenery) and Land Surface Temperature variation.

Based on previous literature, and analysing the local microclimate factors and thermal satellite images, the study concludes that Erbil experiences a Surface Urban Cool Island in summer time. This means that urbanised areas (high density) have lower LST compared to rural areas (low density) during daytime. In addition, urban LST variations may contribute to urbanisation and microclimate factors such as air temperature (T°), wind speed (WS), and solar radiation.

The second section covers the process of urban development of the city. This comprises the history of Erbil urban development, from a small castle to the third largest city in Iraq. This section reviews urban planning transformation from traditional to modern, and the master plans of the city from 1920 to 2006. Housing typology and associated problems are also briefly discussed. Before 1991, the urban development of the city was controlled by central government from Baghdad, and thus the urban development was designed without any consideration for the local identity of the Kurdish people. Moreover, urban development in Erbil experienced rapid expansion after 2003 as a result of geopolitics and socio-economic stability. The literature review concludes that the urban design process for housing projects in Erbil has not been studied well, and nor has how this process deals with the urban microclimate.

The third section reviews the local urban microclimate features and urban microclimate models. The urban microclimate in hot/dry climate cities is fundamentally different to other climate regions (tropical and humid). Moreover, solar radiation plays a crucial role in determining local microclimate in hot/dry urban areas. The literature shows that urban

microclimate can be modified by eliminating direct solar radiation (DSR), provide water bodies (fountains) and increase green areas. Urban and canyon geometry has been employed to eliminate DSR and reduce the sky view factor SVF. The narrow canyons (low SVF) and vegetation (evaporation) can reduce SVF and consequently air temperature, and improve thermal comfort for pedestrians during summer time.

In addition, urban microclimate modelling was also justified in this section. There are a limited number of computer programs that can simultaneously model urban microclimate, such as ENVI-met, CTTC, PHOENICS CFD, CitySim Pro, and Autodesk Thermal etc. Based on a critical evaluation of 19 studies undertaken in different climate regions, an appropriate numerical software was selected to model the urban microclimate in Erbil. In each study, microclimate factors, climate zone and the application of numerical software were present. This study concludes that ENVI-met is the appropriate research tool to model and predict the local urban microclimate of Erbil.

The fourth section discussed and evaluated Building Energy Modelling (BEM) types. BEM is a substantial technique to achieve and evaluate a building's energy saving from an early stage in the design process. The general structure of BEM tools covers input, output data, and the simulation engine. In this section, several BEMs were investigated (DOE-2, Energy Plus, TAS, DIVA, HTB2, IES-VE) to evaluate their performance, the parameters measured, and their significant results. The study concludes that IES-VE has advantages over the other BES because it has a user-friendly interface, is virtually free for students and academic researchers, provides its own weather data files, is capable of modifying weather data, and is appropriate for indoor and outdoor modelling as an effective research tool.

This chapter concludes that there is a lack of studies in regards to the how and why new residential developments in Erbil city impact on the urban microclimate. Further, how interventions into these residential developments influence the urban microclimate and how external shading will interact with both the urban microclimate and residential buildings. The main aim of this research is to investigate the impact of the urban form and shading on the urban microclimate and indoor dry bulb temperature.

Chapter 3 The Methodology

3.1 Introduction

The energy consumption in residential building is considered as a main sector of the final energy use in Erbil city (KRG 2012). This research is an open (inductive) study to clearly establish the link between the urban form and its microclimate and how interventions in the urban form can alter the microclimate. In turn the microclimate will impact on the internal building air temperature. Two parametric analyses will be undertaken, the first uses climate simulation software to model the urban microclimate and show how interventions alter this microclimate.

3.2 Over view of the research approach

The main methodology used was quantitative, comprising of two parametric studies one covering the modification of the microclimate and the second the modelling of a shaded dwelling

To understand the development of Erbil (Figure 3.1) a qualitative approach was used to inform the quantitative methods used. In addition, it helps to provide the study with additional information which could not be provide by the quantitative part of the study.

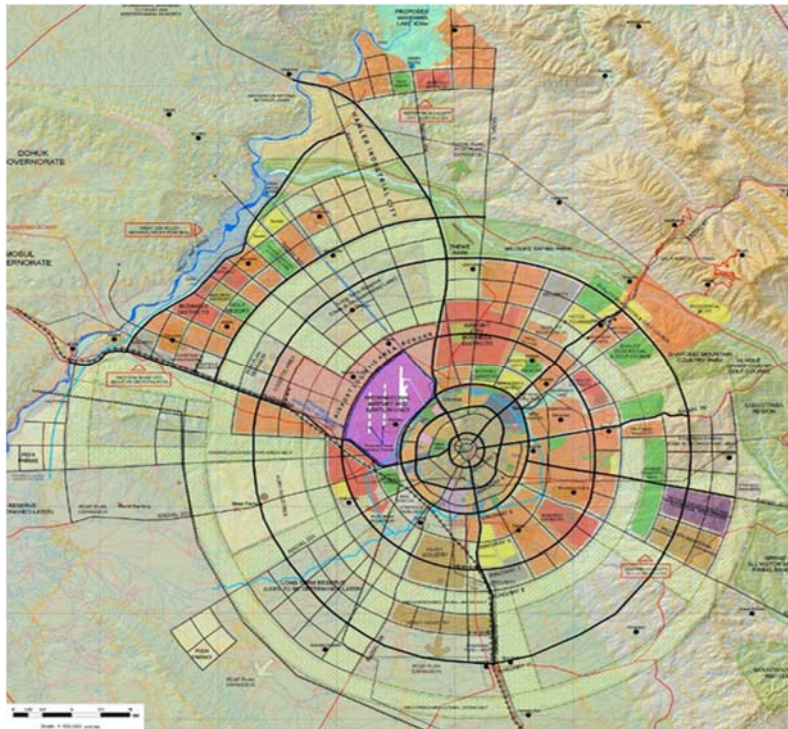


Figure 3.1: Erbil master plan, designed by Dar Al-Handasa

Based on the above, the study employed both methods (Qualitative and Quantitative) in order to respond to the objectives, as set out by this study in chapter 1. The qualitative research method was utilised to understand the pattern of urban development in Erbil via analysing government documents, maps, and images of Erbil. In addition, the qualitative research method was employed in collecting data about the urban housing design process in Erbil after 2003 by semi-structured interviews. Lastly, the quantitative method employed for the numerical modelling of local urban microclimate and individual building energy modelling. In the subsequent sections of this chapter the detailed description of each of the research methods

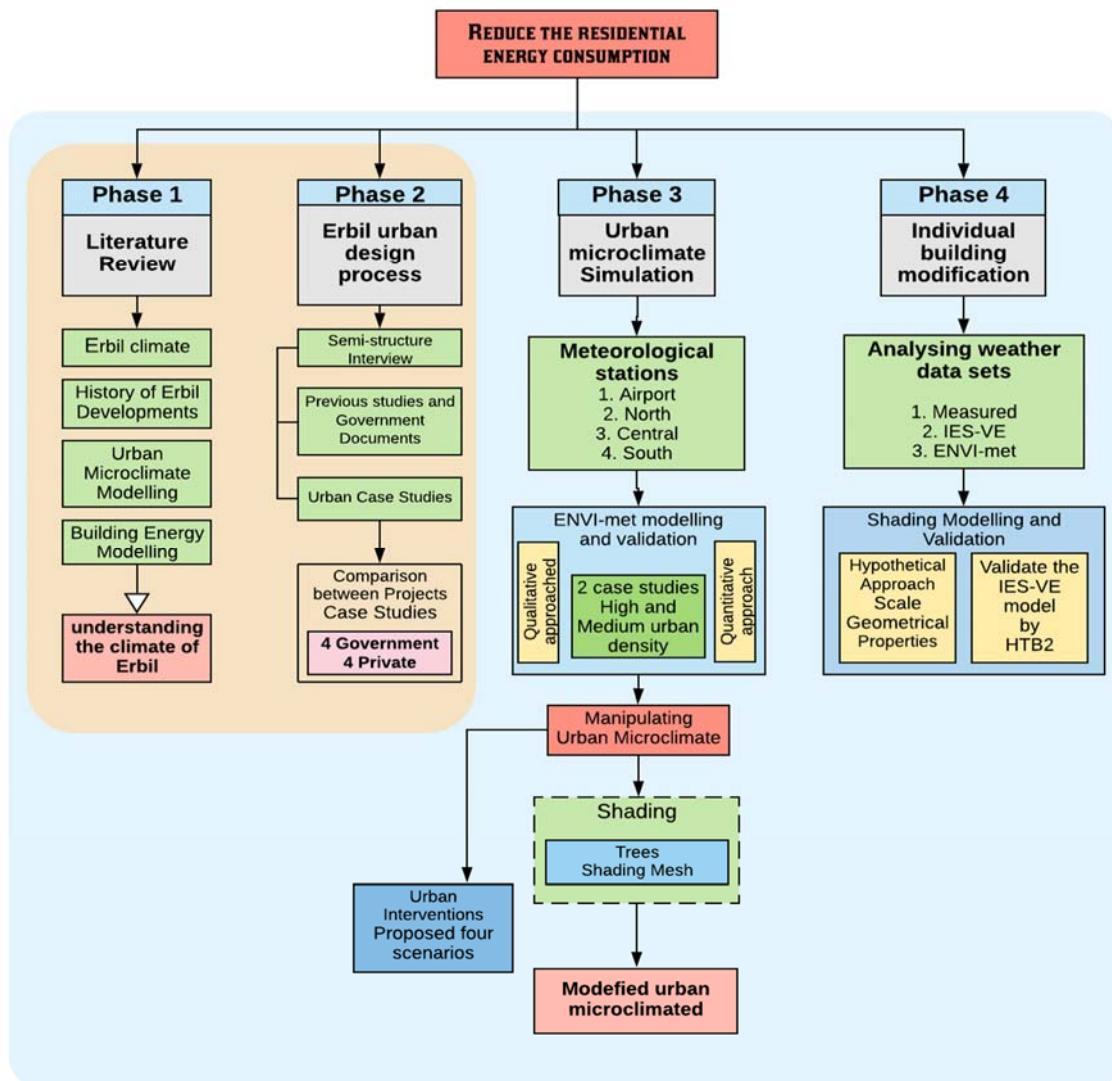


Figure 3.2: Thesis Structure – phases 1, 2, 3 and 4

employed for this study will be given. In view of the research method mentioned here, Figure 3.2 summaries how they are were utilised in this study.

3.3 The rational of using the methodology

The majority of this study depends on quantitative methods to achieve its aims. Two quantitative methods are used in this research: the first model's the residential urban microclimate and the second models individual buildings experiencing the microclimate. Qualitative methods were used as a secondary part of the study and were employed in responding to the aims, objectives and research questions arising in Chapter 1. The three qualitative research methods were used; semi-structured interviews, government documents (including maps and images), and housing development case studies.

The semi-structured interviews were used to investigate and understand the frame work of the process of urban design in Erbil city, for both Government and Private projects. This was done by collecting information during the interviews with urban planners and designers. The rational for the use of semi-structured interviews is based on the idea of collecting data about the topic from the main practitioners as there is very limited literature on this topic. Erbil urban housing design is a new topic, especially the Private Housing projects which only started after an Investment law was established 2006. In addition, the Government Projects were designed centrally from Baghdad before 1991 and after 2003 only local planners and designers could design the urban areas independently. These facts and lack of experience leads to limited studies and the lack of a clear frame work, for housing urban design in the city. The other reason for using semi structured interviews in this study was to provide information about Case Studies that were used in Chapter 4. This helps to understand the projects and explore the advantage and drawbacks of projects. The key benefit of this method is to obtain the data (the process of urban design) from the urban designers' point of view. This method is extensively described in section 3.4.

The Government documents (e.g. maps and images) were collected from government institutions. This method was used to provide additional data to understand the urban design process and to define the design frame work. In addition, the maps and documents were used to analyse the eight chosen case studies.

The case studies were used to demonstrate the level of environmental design used in the urban design. Four representative case studies were selected from the two urban design approaches.

3.4 Description of process used to collect and analyse data in respect of the qualitative research method utilised in this study.

The first part of the qualitative research method in this study reviewed literature in order to understand the history of urban development in Erbil. This included a review of the climate of Kurdistan in general and Erbil climate in specific. In addition, the review includes urban development and master plans of Erbil from 1920 to 2014. As well, the review covers the followings area listed below:

- Master plan of Erbil from Ministry of Municipality and Tourism.
- Buffer zone master plan from Ministry of Municipality and Tourism.
- GIS information (Erbil Expansion) from Erbil Governorate.

The second part of part qualitative method is concerned with the urban housing design process in Erbil after 2003 by semi-structure interviews and case studies. The process of the semi-structured interview is described below.

3.4.1 Samples

Semi-structured interviews were carried out with some government officials in 2017. The study includes 15 respondents in seven government institutes in Erbil. These respondents were chosen as they are responsible for urban and housing design projects. The institutes are Ministry of Municipalities and Tourism,

Local Municipality Department No 4, City Council, Erbil Governorate, Head of Municipalities, Department of Urban Planning and Investment Department, Figure 3.3. The 15 respondents are architects with their details provided in the Table 3.1.

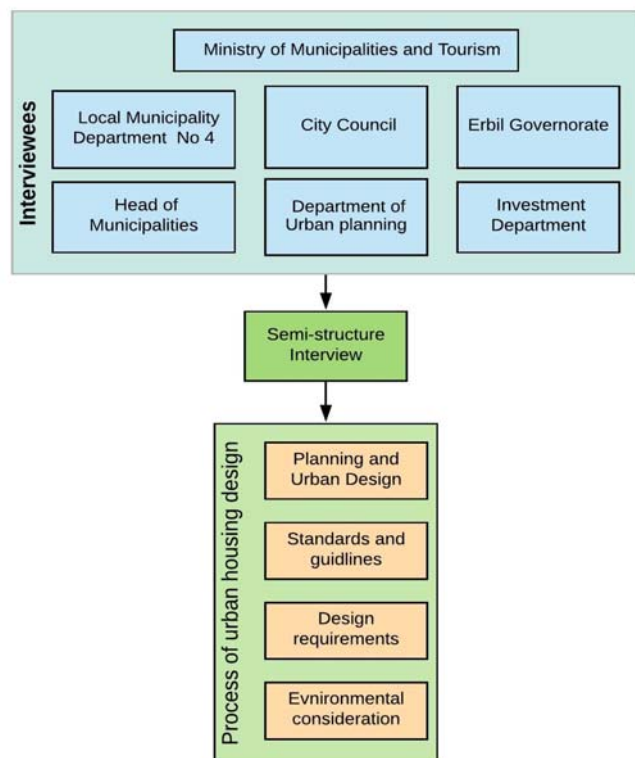


Figure 3.3: The interview structure

Table 0.1: Personnel interviewed, their positions and departments

NO	Names	Position	Place	Type of meeting
1	Architect	Head of Architecture office	Erbil Governorate	Semi-structure interview
2	Architect	Manager	Department of Urban planning of Erbil	General discussion
3	Architect	Head of Housing approval Department	Municipality Department Erbil No 4	Semi-Structure interview
4	Architect	Design Leader of planning office	Ministry of Municipalities and Tourism	Semi-Structure interview
5	Architecture	Manager of Buffer zone (Erbil)	General Director of planning and follow-up. Ministry of municipality and Tourism	General discussion about buffer zone.
6	Architecture	Manager of GIS centre (Erbil)	Erbil Governorate	Collecting maps and GIS information
7	Architect	Urban Services Designer	Place: Head of Municipalities of Erbil	Semi-Structure interview
8	Architect	Urban Services Designer	Place: Head of Municipalities of Erbil	Semi-Structure interview
9	Architect	Senior Architect at Approval department	Head of Municipalities of Erbil	Semi-Structure interview
10	Architect	Urban Designer	Head of Municipalities of Erbil	Semi-Structure interview
11	Architect	Architect in Investment of Kurdistan Department	Investment of Kurdistan Department	Semi-Structure interview
12	Architect	Head of Design Department	Head of Municipalities of Erbil	Semi-Structure interview
13	Architect	The Manager of Design Department	Head of Municipalities of Erbil	Semi-Structure interview
14	Senior Architect	The Manager of Design	Investment of Kurdistan Department	Semi-Structure interview
15	Senior Architect	Urban Designer	City council	Semi-Structure interview

3.4.2 The contents of semi-structured interview

The key questions in the semi-structured interview focused on four areas. These areas are; planning and urban design process, Urban design Standards and Guidelines of Erbil, Urban Design Requirements and Environmental consideration during design process in Erbil. See

Appendix A and B for more details of the key question used to carry out the semi-structured in the study.

3.4.3 Protocol of the semi-structured interview

The 15 respondents were interviewed after a preliminary meeting with each one of them prior to the beginning of the semi-structured interviews. At each interview, I meet them in their offices during work hours. The interviews varied in time duration between 1 hour to 3 hours. During each interview, I recorded the key responses of the interviewees with a pen and paper. The interview was done in Kurdish Sorani language. After each interview, I gave a vote of thanks. Because of the political situation in Kurdistan it was not possible to contact the respondents to confirm the contents of the interviews.

3.4.4 Analysis the data from the semi-structure interview.

The first steps utilised for analysing the data from the semi-structured interview was the translation of the key responses of the interviewees from Kurdish Sorani language to English language. The data concerning the responses of the interviewees was translated by paper and pen and stored on a computer before they were analysed. Afterwards, the data from the semi structured interviews were analysed based on content analysis with the results reported in chapter 4.

3.5 The urban Housing project case studies

In addition to the semi-structured interview described above, case studies of Government and Private housing projects in Erbil were carried out. A schematic of the methodology is given in Figure 3.3. Resent Urban Housing Design (UHD) were used as case studies to understand the application of the UHD process and analysis of planning style for new urban developments in the city after 2003. Moreover, they were used to show a overview on urban design practice in Erbil and how these projects reflect the local architecture features and environmental strategies. Both government and private housing projects were selected to balance the different planning and development processes. UHD projects are mainly designed by the government sector, which is represented by the Head of Municipalities designers and the Director General of Physical Planning of Erbil. For the private sector, projects are designed by architectural consultancies or by the developer's architect(s). Eight case studies were select for both types (i.e four for government and four for private), Figure 3.6. This was done by comparing eight case studies for both urban housing types Government and Private projects.

In each case study the basic information about the project were identified such as location, area, housing types, green area, building materials and others (See Chapter 4).

The criteria were used to select these projects, the first criterion was that they were representative of the development approach, and the second was that sufficient data could be collected to analyse them. The other criteria for selecting the case studies is provided in chapter 4 section 4.6, Figure 3.4 Shows the criteria that we used to select the projects.

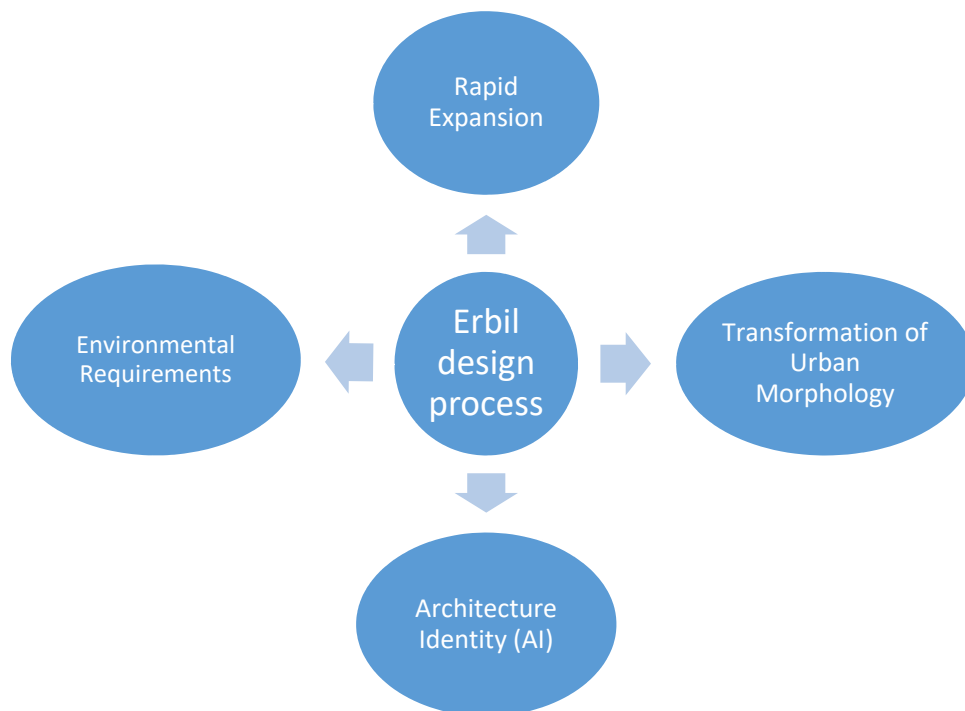


Figure 3.4: The relationship between the design process and associated problems

Furthermore, the housing projects were analysed by identifying their similarities and differences from urban planning process point of view following the criteria in chapter 4 section 4.9. The data used for the analysing the case studies obtained from the designer of project, Head of municipalities of Erbil and investment department of Erbil. The data is in the form of maps, drawings and images for both government and private housing projects.




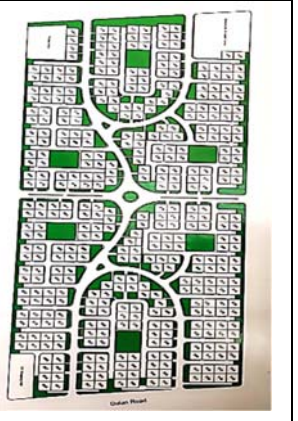




The Case Studies			
Government Projects		Private Projects	
			
Case study 1 Baxluw Manira	Case study 2 Grad Sor	Case study 5 Italian City 1	Case study 6 English Village
			
Case study 3 Gadjutiar	Case study 4 Rashkin	Case study 7 Italian City 2	Case study 8 Mass City

Figure 3.5: The Government and Private Case Studies.

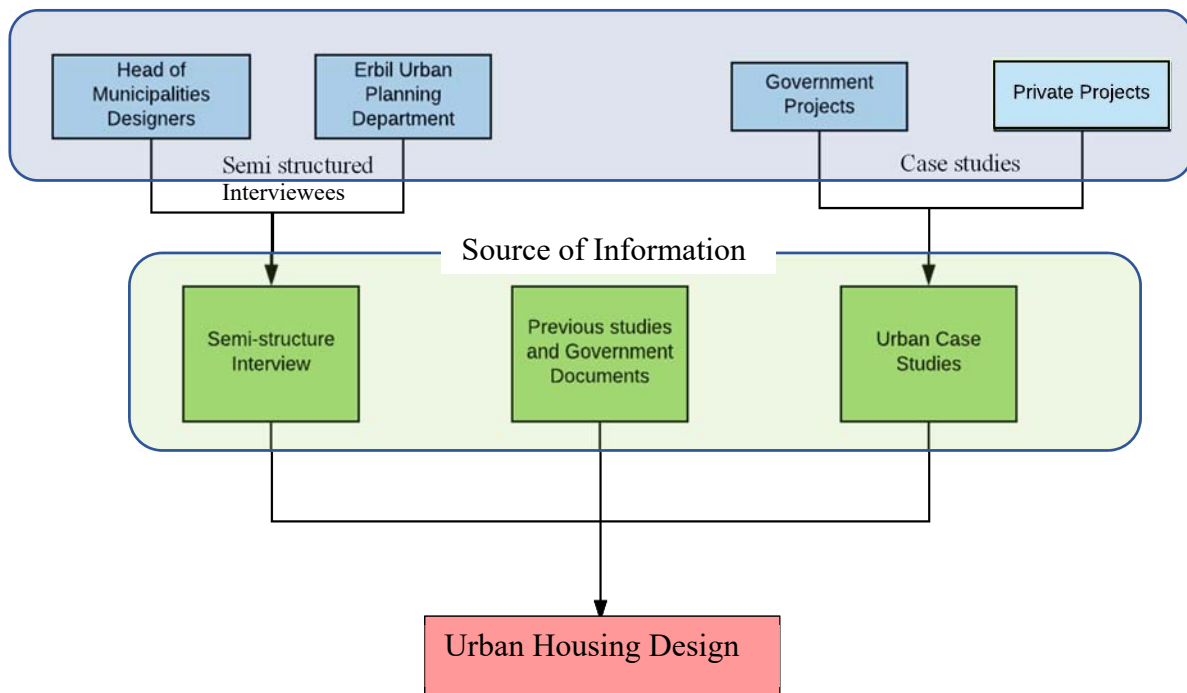


Figure 3.6: Erbil urban development methodology and the source of information

3.6 Climate Data for Erbil

The quantitative phases of the research, as depicted in Figure 3.2, starts with the weather observations in Erbil. The original methodology to be undertaken here was for there to be an extended site visit to Erbil during which *in situ* weather measurements were to be made, in both the organic urban morphology and the modern grid-iron morphology. However the geo-political situation in Kurdistan at the time, in particular the presence of ISIS some 50 km from Erbil, prevented extended visits. The University prevented both staff and students from travelling to Kurdistan. An alternative strategy was therefore devised, whereby existing weather stations were located and the data from these stations sourced.

3.6.1 Weather data stations in Erbil

Data from four weather stations in Erbil city were investigated: northern, airport, central, and southern weather data stations (Figure 3.7). The easiest weather station to obtain data from was the airport station situated to the north west of the city, which was available online; however, airport weather stations tend not to predict accurately the weather of their associated city. They are usually located way from urban conurbations in open

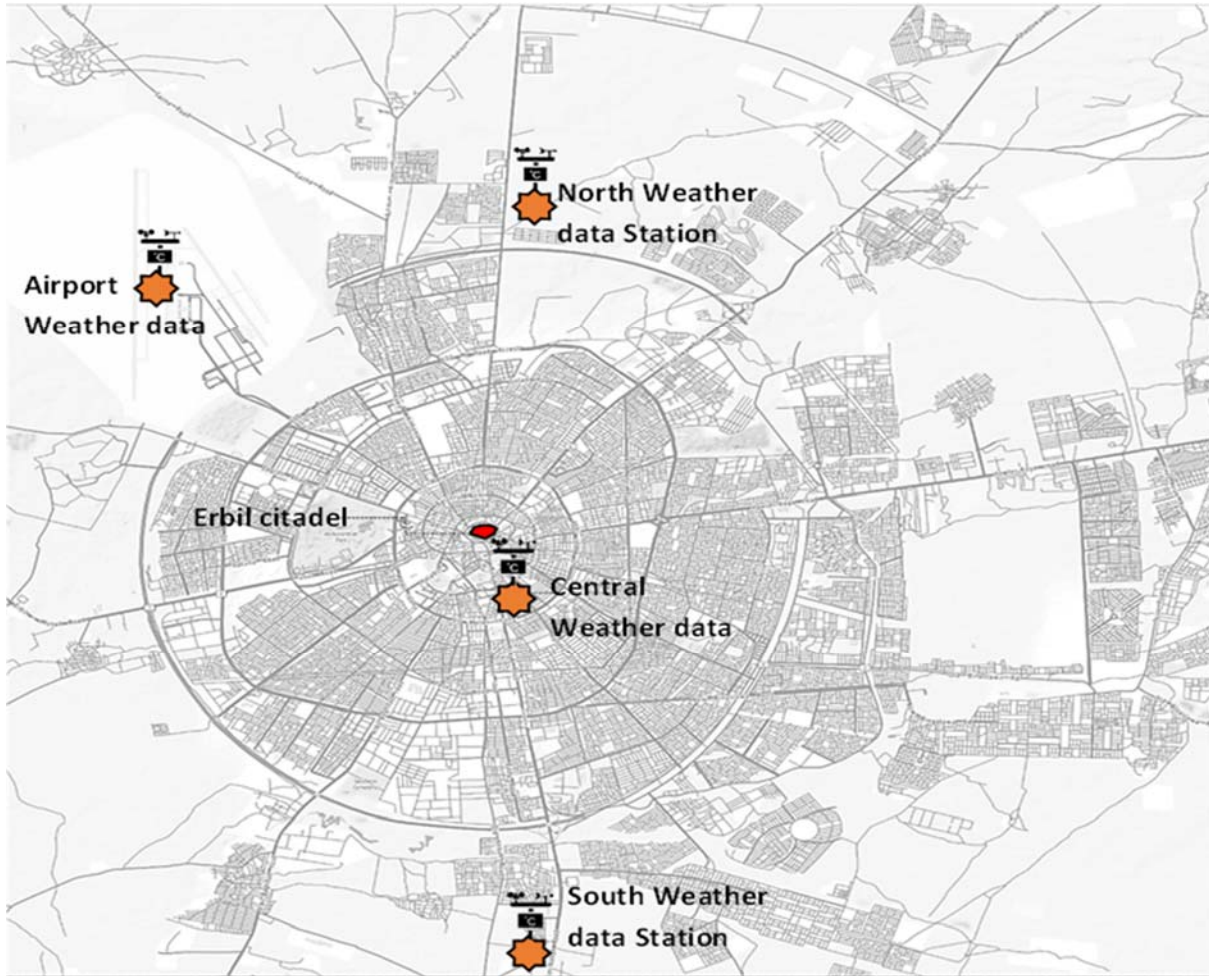


Figure 3.7: location of all weather stations; North, Central, Airport and South.

areas with large areas of unshaded concrete or asphalt, resulting in higher wind speed and lower air temperatures. This study required weather data from stations located in urban area within Erbil itself. Eventually, weather stations were located belonging to the Ministry of Agriculture, which collected data every 15 minutes. Data was obtained for three years 2014, 2015 and 2016. The four locations used in this study are: Aynkawa in the north, airport weather data in the north-west, Komary is 2km distant from the city centre, and Zhyan district in the south of the

city (Figure 3.7). The location of each source of weather data and other details are described as below:

3.6.2 Northern Weather Station

The Northern Weather Data station (NWD) is located in the northern part of Erbil (latitude 36.24 and longitude 43.99). The location has a low density urban area and is used for developing crops and agricultural purposes. The station is located in an open area and surrounded only on one side, with a few buildings, and the rest is agricultural fields. Originally, the station was isolated from Erbil, but as the city has expanded in the 21st century, the station is now on the edge of the city (Figure 3.7).

3.6.3 Airport Weather Station

The Airport Weather Data station (AWD) is located to the north-west of Erbil (latitude 36.22 and longitude 43.96). The location is within a low density urban area and the data is used for aviation purposes and metrological observation. The station is located inside the airport area, which is located outside the city (Figure 3.7). The urban density of the airport and the surrounding area is considered very low and does not represent the Erbil urban microclimate environment.

3.6.4 Central Weather Station

The Central Weather Data station (CWD) is located in the south-east part of Erbil near the city centre (Erbil citadel) (latitude 36.17 and longitude 44.01) (Figure 3.7). The location is within a high density urban area and the data are used for agricultural studies and research. The station is surrounded by traditional urban morphology to the north, a few open green areas to the east and west, and a high density residential urban area to the south and north-east. In general, the location of the station is the best case to represent the real urban microclimate of Erbil.

3.6.5 South weather data station

The Southern Weather Data station (SWD) is located in southern part of Erbil (latitude 36.11 and longitude 43.01). The location is considered a medium density urban area. As with the weather station located in the north of the city, this was once in a rural location but, as Figure 3.7 shows, the urban spread of Erbil has encroached on to its location. Further information concerning the weather data sets for Northern, Central and Southern weather stations is given in Appendix E.

3.7 The quality of the weather data

The weather data stations locations are surrounded by varying urban areas densities. Northern, Airport and Southern Stations are surrounded by very low or medium urban density compared to the Central Weather Station, which is located in high urban population area. The reliability of data can be seen through minor differences of data for all four stations, but the South Station data came with systematic error related to day-night timing and was corrected.

The Northern, Central and Southern Weather data stations were originally installed by a US company using modern sensors and data loggers. Temperature, wind speed, relative humidity, air pressure, rainfall, and specific humidity and soil temperature profile were measured. The measurement interval used was every 15 minutes between 2013–2016.

Table 3.2 shows a typical header from the weather data file, with the units used from measurement, air temperature is recorded in degrees centigrade along with the maximum and minimum temperatures, relative humidity is recorded as a percentage, air or barometric pressure is recorded in milli-bars, wind speed and gust speed is recorded in m/s and direction in degrees, solar radiation in kW/m² and total solar energy in MJ/m², soil temperature in degrees centigrade and finally rainfall in mm.

Table 0.2: The weather data header package

T O A5	C R 10 00	C R 1 0 0 0	28 89	CR 100 0.St d.06	CPU :ER RAS 002. CR1	81 49	MI N 15										
TI M ES T A M P	R E C O R D	I D	Pr og ra m	Batt _Vo lt_ Min	AirT C	Air TC _M ax	Air TC _M in	R H	B P _m ba r	WS _m s_ Av g	ws_ gus t_ Ma x	ws_ gust _T Mx	W in d Di r	Slr k W_ _A vg	Slr M J_ To t	Soil T10 _C_ Avg	Rai n_m m_ Tot
TS	R N			Volt s	Deg C	De g C	De g C	%	Mi lli ba rs	metres/sec ond			D eg re es	k W/ m²	M J/ m²	Deg C	mm
		S m p	S m p	Min	Smp	Ma x	Mi n	S m p	S M p	Av g	Ma x	TM x	S m p	Av g	To t	Avg	Tot

Figure 3.8 shows a plot of average air temperature taken for July 2015 for all four weather stations. The Northern, Central and Southern stations record roughly similar temperatures patterns throughout the month, but they do not correspond directly and this is a reflection of the different urban context of the weather stations. The fourth weather stations, the one located at the airport, shows a marked difference to those located in urban areas, and reflects the difficulty of using airport data to characterise urban microclimates.

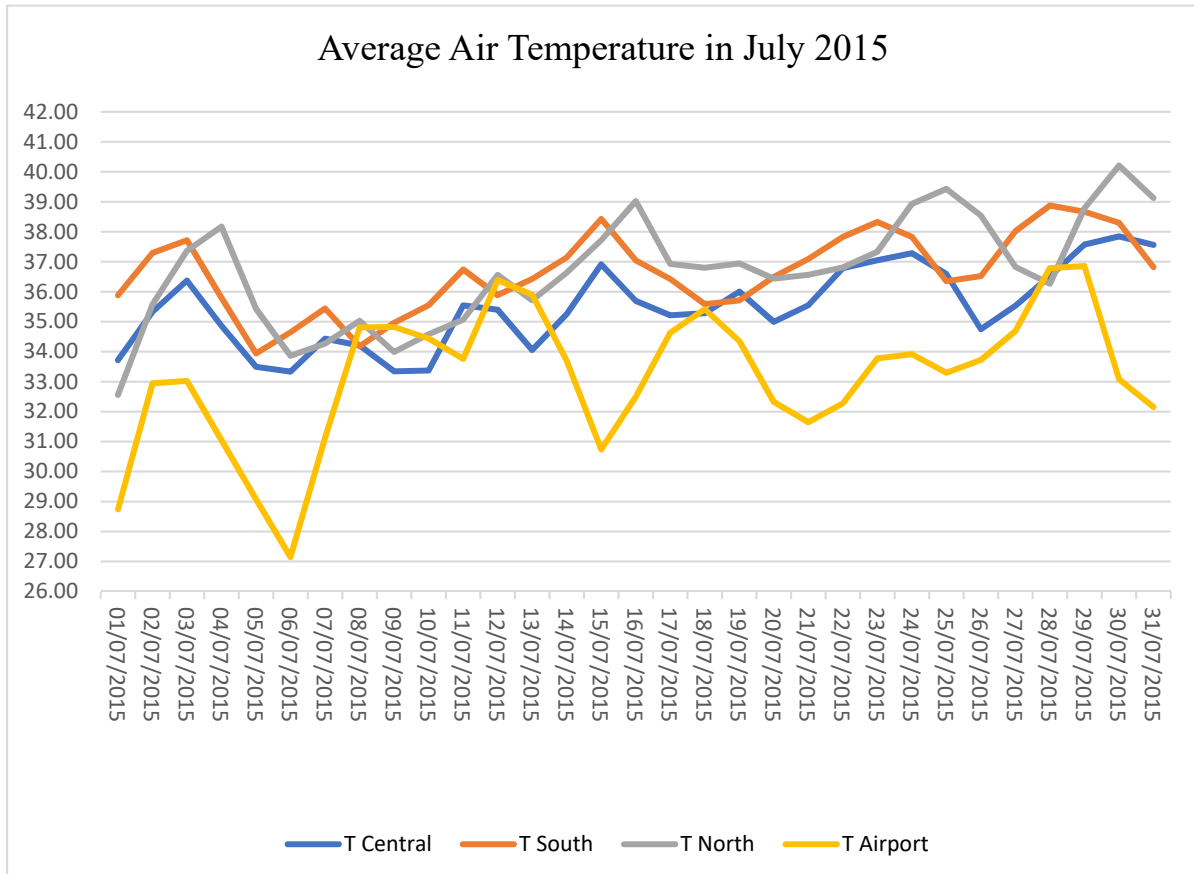


Figure 3.8: Average air temperature for Northern, Central, Airport and Southern stations

Figure 3.9 shows the average wind speed over the summer months of June, July and August 2015. The obvious observation here is the difference between the average wind speeds from the CWS with its high urban density, compared to those from the more open aspects of the other weather stations. This difference in wind speeds from urban to rural and semi developed areas is to be expected, as the surface roughness (referred to as the von Karman surface roughness in fluid flow) is much greater in urban than rural areas. This greater surface roughness acts as a drag on wind speeds relatively close to the surface. What is unexpected is the degree of reduction: conventional expectation would see wind speeds reduced by 20–30%. Here, the reduction is of the order of 80%. In descriptive terms, the wind speeds outside the

high density urban area would be termed, according to the Beaufort Scale, as a light breeze, whilst the description for the central urban area would be bordering on calm. This may explain the degree of reduction in wind speeds at the CWS; because the wind speeds are low outside the city centre, the friction offered by the city centre has a greater deceleration on wind speed than would be expected.

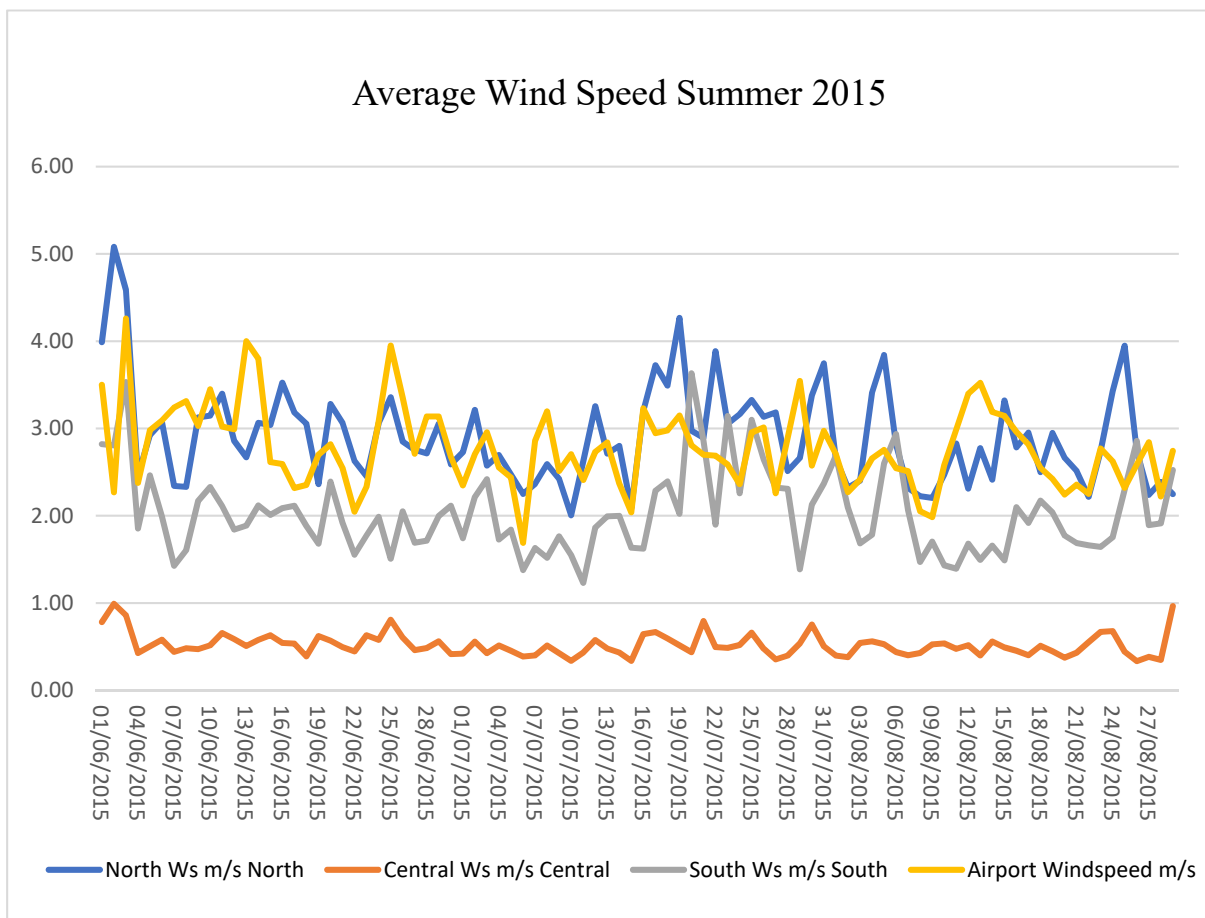


Figure 3.9: Average wind speed in June, July and August for Northern, Central and Southern stations

Further information concerning the measurement instruments and their accuracy used at the Northern, Central and Southern weather stations is given in Appendix D and F.

3.8 The quantitative method utilised in this study

The next stage of the quantitative phase is the modelling and validation of the urban microclimate.

ENVI-met simulation program is used to shape and define a microclimate model that matches real and local microclimates of Erbil city. To build a microclimate model which matches the reality of an urban environment is very difficult and complex process. ENVI-met programme is relatively modern and used by majority of researcher in this field. In addition, ENVI-met is not a well establish programme, but a research tool and the output data needs to be interpreted. ENVI-met is an analytic piece of software. Fundamentally, the model geometry incorporates air flow, heat (energy) balance and climate simulation with consideration of physical geography of location in order to predicate the urban climate. In this study two variables from the model simulation will be extracted, wind speed and air temperature and compared to the measured data from the weather stations located in Erbil. To compare the predicted with the observed (measured) values two methods will be used, Firstly by direct comparison between observed and modelled air temperatures in two urban areas of Erbil city, a qualified approach. Secondly, a quantified approach, based on systematic and unsystematic errors proposed by (Willmott 1982).

The study used an ENVI-met model to simulate microclimate model of modern urban area in a hot dry city. The simulation was difficult to control input data related to model simulation, such as relative humidity and soil moisture availability. The model was run for 96 hours to check the performance of software, the run takes 15 days to complete and the out-put was not accurate. This was caused by continuous heating energy input into the model, which caused the model to heat gradually day after day and there was no convergence. Hence the following issues were identified as problems during simulation:

1. Running time, to model 96 hours the model was need 15 days computer run time.
2. Input data, the model results is very sensitive to the input data.
3. The model heats up on a daily basis, with no convergence to a solution

As the programme is primarily a research tool it does require time to build up expertise in using the software. Many problems have been encountered and many false starts made. Help and advice has been sought from other users outside the UK and accessing user forum data base.

As previously mentioned two urban areas of Erbil were used to validate the climate model, the first area to be modelled was located around the central weather station and represents a high urban density of traditional

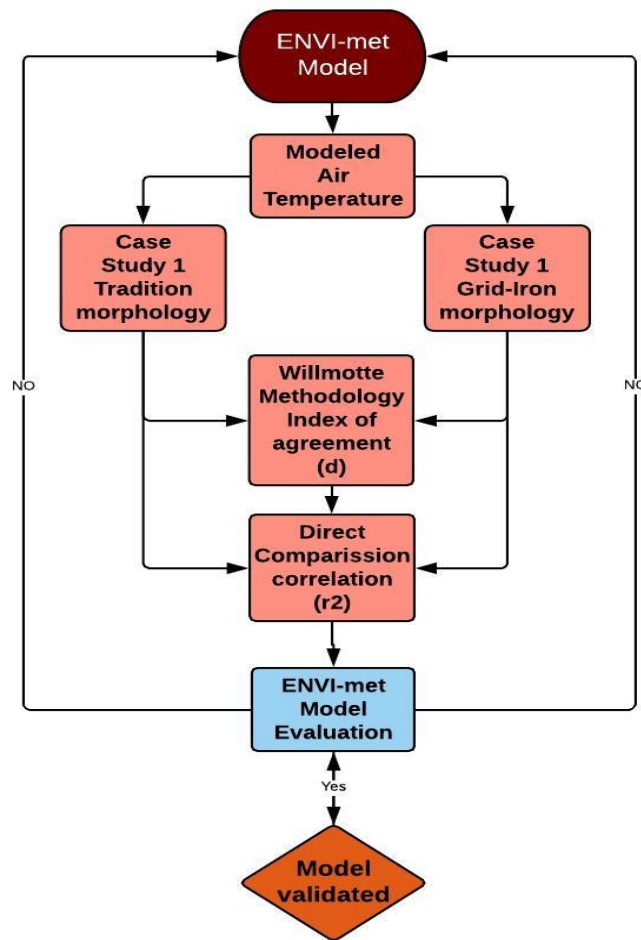


Figure 3.10: The schematic of the validation process.

organic form.

The second area was new proposed grid iron development close to the Southern weather station, Figure 3.7. Figure 3.11 show the organic and grid iron morphologies modelled, the image on the left is the urban development around the central weather station, while on the right is a proposed development adjacent to the Southern weather station.

The direct comparison correlation approach plot measured and predicted values and then calculates the correlation between the two sets of data. This comparison approach establishes a linear relationship between the measured and observed values. The closer the gradient of the regression line is to 1, the axis intercept is to zero and the regression coefficient approaches 1, the better the agreement. Of these three elements the regression coefficient provides the best indicator of agreement, whilst the others indicate systematic error.

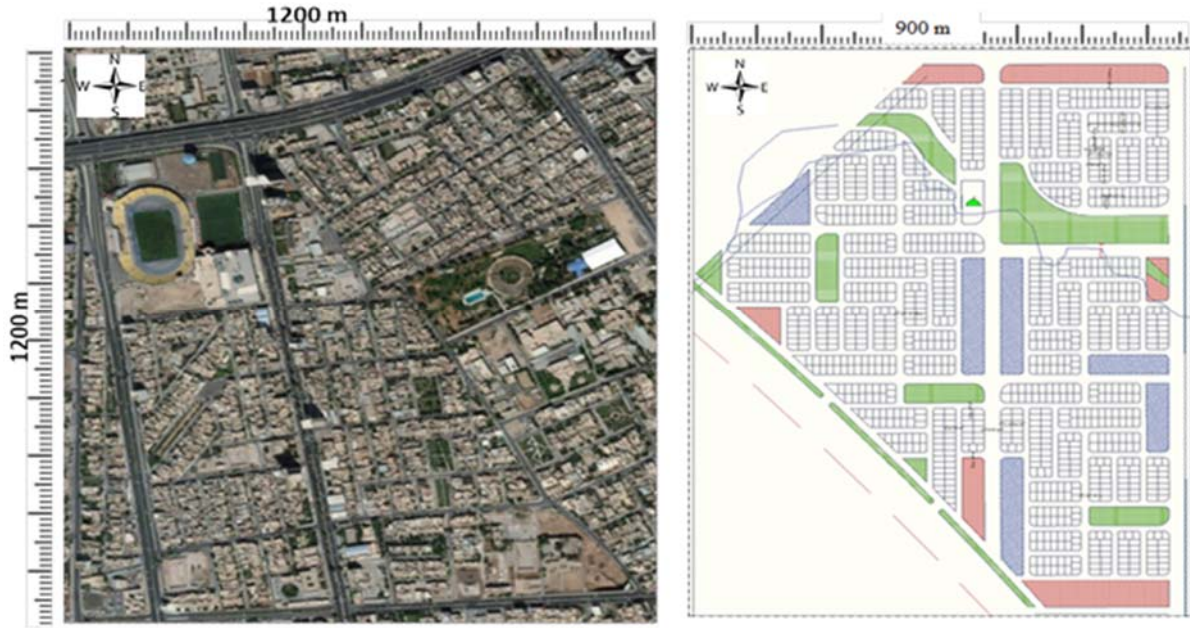


Figure 3.11: High and Medium urban density of Erbil were used to validate the climate model

The Willmott methodology defines the systematic and unsystematic errors between observed and predicted values and the index of agreement. Systematic errors can be thought of as a constant or proportional variant between observed and predicted, whilst the unsystematic errors may be considered as either unpredictable fluctuations in the measurements made by the instruments at the weather stations and/or inconsistencies' in the computer code or algorithms. The index of agreement was developed by Willmott to yield a standardised measure of the degree of error between observed and predicted values and varies between 0 and 1. A value approaching 1 indicates good agreement, whilst a value approaching 0 indicates no agreement. Figure 3.10 shows the schematic of the validation process.

Equation 1. MBE is Mean Bias Error, N is the number of cases, P is model predicated data, (O) observed data

$$\text{Mean Bias Error} = N^{-1} \sum_{i=1}^n (P_i - O_i)$$

The mean bias error is a measure of the overall systematic (bias) error.

Equation 2. Average "noise" or unbiased difference.

$$\text{Average "noise" or unbiased difference. } (sd^2) = (n - 1)^{-1} \sum_{i=1}^n (P_i - O_i - MBE)^2$$

Equation 3. Root Mean Square Error

$$\text{Root Mean Square Error} = N^{-1} \sum_{i=1}^n [(P_i - O_i)^2]^{0.5}$$

Root Mean Square Error is a measure of with the deviation from the true value.

Equation 4. Mean Absolute Error

$$\text{Mean Absolute Error} = N^{-1} \sum_{i=1}^n |P_i - O_i|$$

The mean absolute error measures how near a predication is to the measured value.

$$sd^2 \cong MSE - (P^- - O^-)^2$$

P^- and O^- the standard deviation of the predicated variable (S_p) and standard deviation of the observed variables (S_o), $P_i^- = a + bO_i$, where (a) and (b) intercept from slop of the latest – square regression.

Equation 5. Index of agreement'' between modelled and predicted data

$$\text{Index of Agreement } d = 1 - \left[\frac{\sum_{i=1}^n (p_i - o_i)^2}{\sum_{i=1}^n (|P_i| + |O_i|)^2} \right]$$

$$0 \leq d \leq 1$$

The index of agreement (d) is a standardised measure of the model prediction error, a value of ‘‘1’’ indicates a perfect agreement while a value of ‘‘0’’ would express no agreement.

To evaluate the accuracy of the ENVI-met model, a comparison made between its predication (modelled) and the measured weather data obtained from the local urban weather station (the observed value). The previously mentioned statistical parameters calculated according to Willmott (1982). The model ‘‘explain’’ the major traits of the measured weather data, but the Root Mean Square Error influenced by ‘‘Systematic’’ and ‘‘Unsystematic’’ errors and proportions of there that contribute to the Error.

A ‘‘good’’ model could be defined as one were the Systematic error approaches zero and the unsystematic error approaches the Root mean Square Error (Kong, Sun et al. 2016). Willmott proposed that the systematic error described by

$$\text{Mean Square Error systematic} = N^{-1} \sum_{i=1}^n (P^{\wedge} i - O_i)^2$$

And the Unsystematic Error by

$$\text{Mean Square Error unSystematic} = N^{-1} \sum_{i=1}^n (P_i - P^{\wedge} i)^2$$

By taking the Square root of both MSE_s and MSE_u these differences can be redacted to the units of temperature.

In parallel with the process of obtaining the weather data and the validation exercise, a study was undertaken to investigate how the ENVI-met models for a Traditional and Grid Iron urban morphologies perform. Both models used identical weather data so that any differences in prediction would be the result of morphologies. Figure 3.12 shows the organic morphology used on the left and an idealised grid iron morphology on the right.



Figure 3.12: Organic and grid iron morphologies

Once the validation exercises were completed and familiarity gained with using the ENVI-met software a series of climate mitigation strategies were employed on a proposed grid iron development. These strategies included rotation of the urban development in relationship to the prevailing wind direction, altering canyon geometries and increasing both the number and

size of urban open spaces. The overall aim of these mitigation strategies was to increase wind speed in the urban environment (increases natural ventilation) and reducing air temperature to aid thermal comfort and reduce cooling energy consumption.

In a hot dry climate, shade is an important consideration, so the next part of the methodology was to investigate how tree cover of open spaces impacts on the climate of these spaces. The provision of vegetation in ENVI-met is relatively straight forward, the program offers various options to model the tree canopy. However in a hot dry climate, the availability of water to irrigate a substantial tree canopy is a problem, to resolve this other methods of shading will be explored.

ENVI-met version 4.0 has a new modelling technique to simulate a building element. This includes elements which are not connected with a building form and are introduced as ‘single walls’. These single walls are building elements that not an integral part of a building, i.e. they are not part of the closed surface of the building. Single walls can best be described as elements that allow more accurately to recreate (simulate) building obstacles such as; small external walls, awnings or any structures that do not fill a whole grid cell.

The single walls have some physical properties as normal walls would have. For example, they

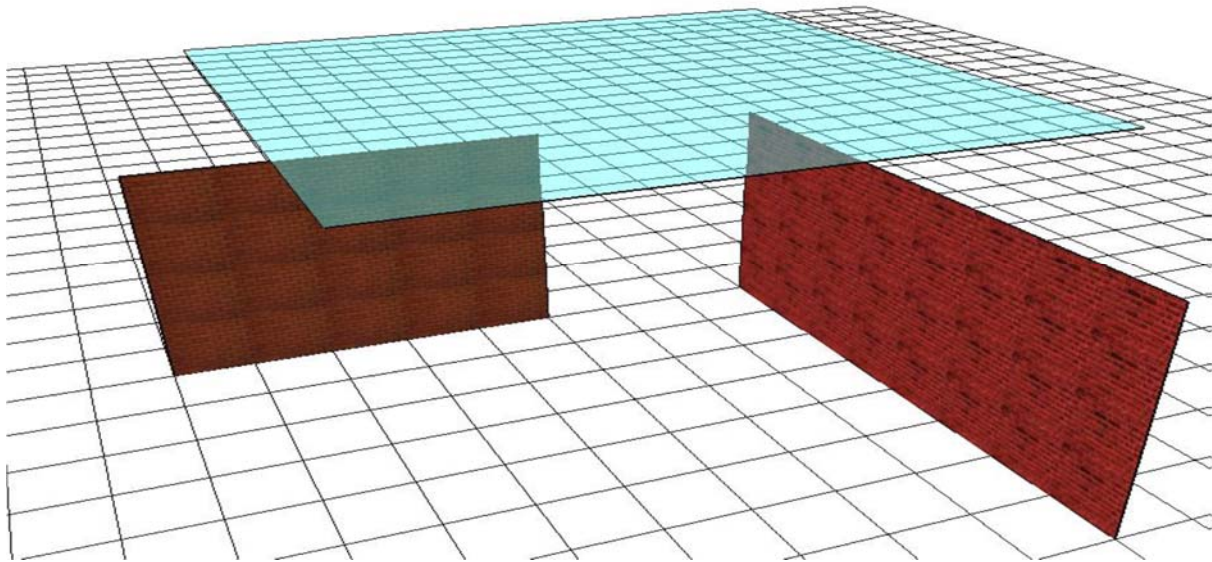


Figure 3.13: ENVI-met model showing single walls features.

are solid obstacle in terms of air flow but have no thermal properties. The main differences between the single walls and normal walls are; single walls can be horizontally modelled, with limited thickness, the very thin, not insulated, have low heat transfer coefficients and the air temperature is homogenously distribute across them.

In this study ENVI-met single walls have been used for modelling shading meshes. The difficulties with shading mesh modelling are that they have specific thermal properties which cannot be easily simulated. Shading meshes are extremely thin, less than one millimetre and horizontally laid out as shown in Figure 3.13. These single walls shading mesh have some corresponding physical properties which are highlighted below;

1. They allow radiation to be transmitted through the mesh.
2. They are thin with low thermal insulation (low heat transfer coefficient).
3. Not thermally integral with main model surfaces.

Shade mesh in this model interacts with solar longwave and shortwave radiation fluxes, reflections and re-radiates thermal energy during day and night time. In this study the shading mesh transmission is set to 50 % to allow natural lighting to enter open spaces during day time.

The next stage of the research, as shown in Figure 3.2, was to use a building simulation package to model an individual dwelling located in a modern grid iron urban plan. The simulation package chosen was IES-VE, it was selected as this package was well validated and support was available within the School. All building simulation programs need a weather data input file, three possible files were identified, the first option was a synthetic weather file generated by IES-VE. This file was compiled from several years of weather data to produce a 'representative year'. The second option was to generate a weather file using ENVI-met and the third option was to use one of the local weather stations to produce a suitable file. The three files were compared graphically and the obvious file to use was the third option, the local weather station data (See chapter 7 section 7.1 to 7.3).

The next step was to incorporate a horizontal shading mesh over a simple building, this required investigation of scale, shading coefficient and geometry (See chapter 7 section 7.4 to 7.7). This started by modelling the mesh relatively coarsely as a checker board, and gradually refining to smaller elements. The mesh was placed over a simple box, five sides of the box were heavily insulated to create an almost adiabatic boundary, with the top modelled as a typical flat roof of the region. The energy falling on the roof was measured together with computational time. This allowed an optimal solution to be obtained.

Once a successful method of incorporation a horizontal mesh into the model was achieved, a process by which validation of the approach was needed. Ideally the model should be validated against experimental measurements, but these experiments were beyond the scope and resources of this study. An alternative strategy was evolved were by a second building simulation program, HBT2, was used to simulate an identical simple building and by comparing the results a judgement can be made over the validity of the IES model (See chapter 7 section 7.7). This follows the well-established practice in Physics were two unrelated methods are used to measure a value of a parameter and if those two methods' agree, then there is an increased level of confidence that the value measured is correct. Figure 3.14 shows the schematic of this process.

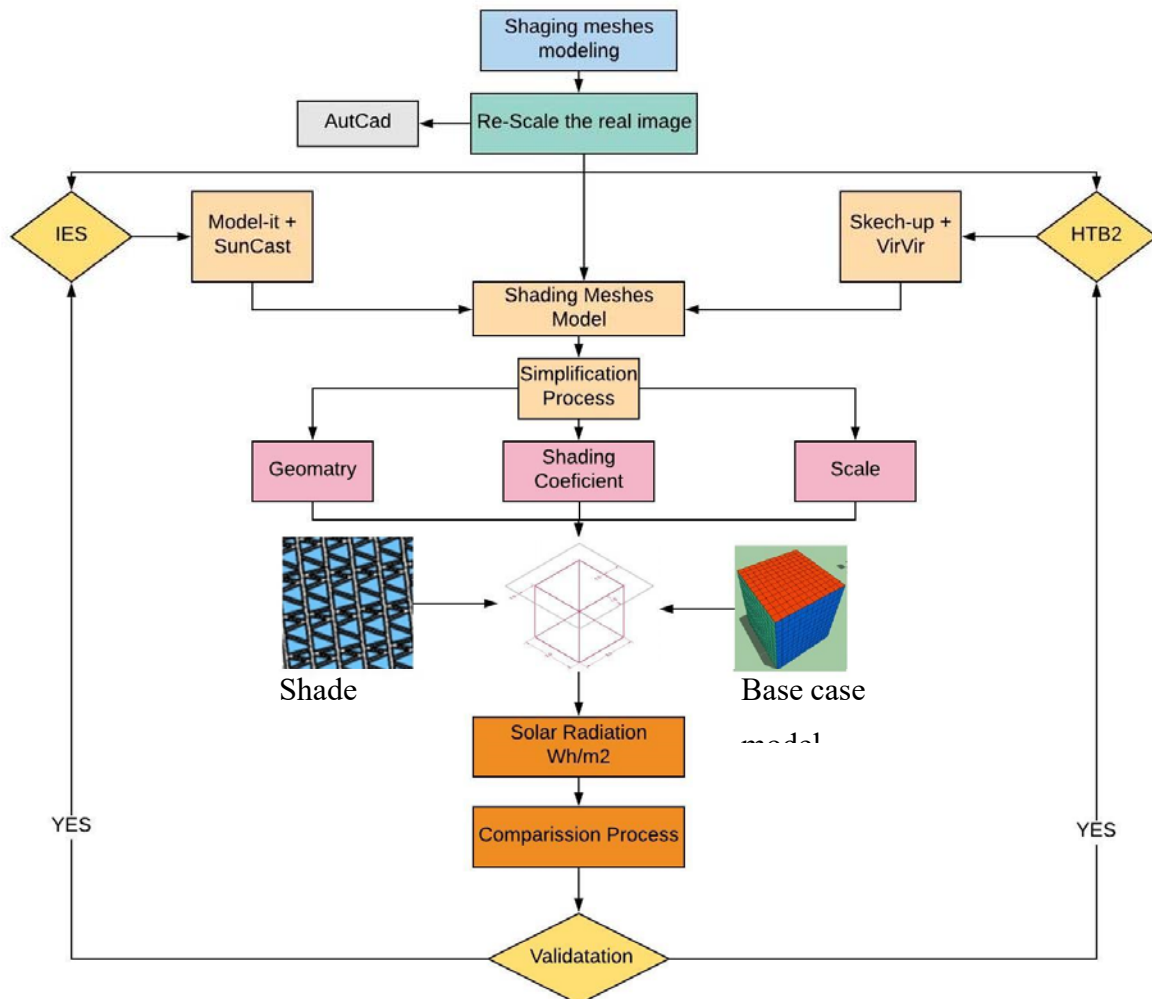


Figure 3.14: Schematic form the methodology of Shading Mesh Modelling process using both IES and HTB2 simulation model.

Having then established the validity of the modelling approach, the research could then proceed to model a prototype dwelling and explore the impact of shading has on this design. Building

simulation models often focus on just one building but in reality building are rarely isolated and interact with their neighbours'. Hence the modelling of this prototype dwelling in the context of an urban block in a grid iron formation will be explored (See chapter 7 section 7.8 to 7.11). This phase of the analysis will be concluded by a parametric study of the effects of exposing the prototype dwelling to different shading coefficients.

The final part of the research will explore a series of design strategies that would work with the shading mesh to reduce air temperature inside the proposed dwelling designs (Figure 3.15). These design strategies' centred on using night time ventilation to cool the interior of the prototype dwelling (See chapter 8).

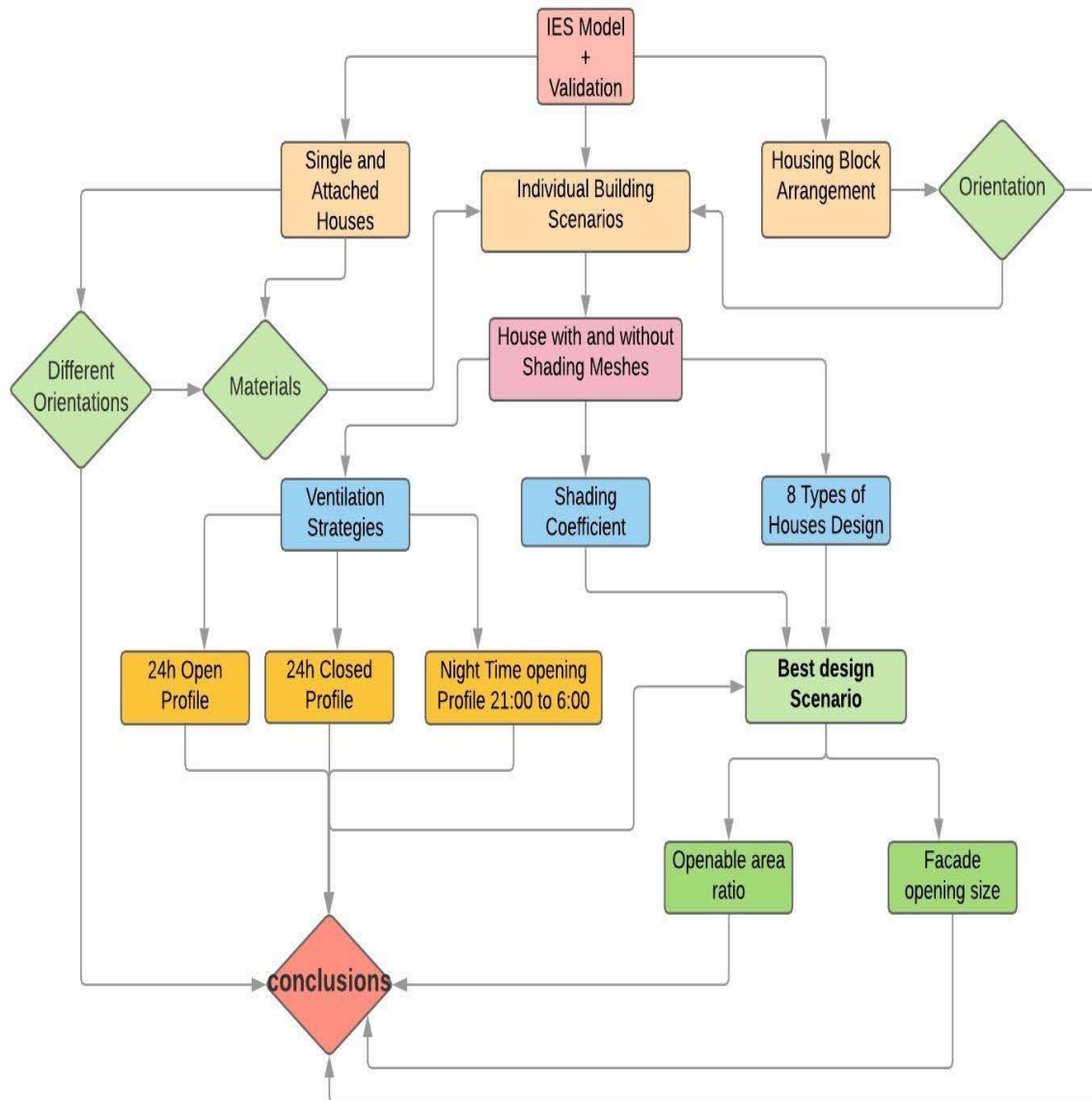


Figure 3.15: The process of prototype dwelling simulation structure using IES-VE model.

Chapter 4 Urban planning and regulations of Erbil city

4.1 Introduction

The emphasis of the chapter is the presentation of the case studies of Government and Private Projects this starts with the criteria for selecting the case studies. To balance the research four case studies were selected for the two development routes. For each case study, its location is declared, followed by the main features of the project and then a brief review of any environmental i.e. Microclimate considerations. For the Private projects additional comments were made about the appropriateness of the housing design for a hot dry climate. The chapter concludes by making a comparison between the Government and Private projects, and gives a direction for the subsequent chapters.

The purpose of Chapter 4 is to explain the context of the urban development of Erbil and how this influences the numerical modelling that will be detailed in later chapters. We begin with this quotation:

We have a book about the rules for investment in Kurdistan, but nobody refers to that. The works here is just temporal. For example, every manager has his own strategy to follow. In addition, every architect has his understanding of what the regulations are or how the act of investment should be followed. For that reason, to design any project we do not have any environmental standards or specific requirements, we are designing and we do not know what we are doing, it may work or may not be aligned with our environment (Senior Manager in KRG Investment Board, interviewed in 2017).

This quotation goes to the heart of the problem facing development in Erbil and the whole of Kurdistan, the lack of design guidance to produce a sustainable urban development in a hot dry climate.

This chapter uses three sources of information to identify the requirements of Urban Planning and Urban Development in Erbil after 1991. Semi-structured interviews with local government employees, government documentation (Appendix B), and Urban Housing Design (UHD) examples were used as research tools to draw the framework of the chapter.

Any urban design, new construction, or building renovation in the city requires formal documentation (Appendix C), which is used as an initial approval for starting the construction process (building approval). Head of Municipalities (HME) or Kurdistan Government documents (Formal documents) and maps are used to describe the formal building requirements used by the Investment Department and local municipalities for any construction and development projects.

Maps and other documents were used to collect information about the Master Plan history of the city and its urban expansion since 1991. UHD samples were used as case studies to understand the application of their process (Figure 3.6).

4.2 Erbil and Urban Design Process

A shortage of housing was the main problem for Iraqi cities from the 1980s until 2003. To combat this, in 2004 the Kurdistan government issued a five-year housing strategy to build 31,000 housing units, with 15,000 units in the city centre as multi-storey housing buildings. The first stage started with 1,000 housing units in Erbil, but only 400 units were completed due to the lack of infrastructure and construction materials. To overcome this issue, new legislation was enacted in 2006 to create two agencies for urban development. Together with these agencies, a new Master Plan of Erbil was issued up to 2030 for future development to follow (Figure 4.5). These new agencies for urban development, were Government or Private Company led, as certified in an in-depth interview with the Head of Design Department in Head of Municipalities of Erbil (AMM105-II). The Master Plan divides the lands around the city into three main zones: industrial, residential, and greenbelt. Any housing projects after 2006 must follow the Master Plan of the city, run by the Ministry of Municipality (Figure 4.2). Therefore, any developments regarding the housing sector must follow the Master Plan and will be designed either by the government or private sector (Figure 4.1 and Figure 4.5).

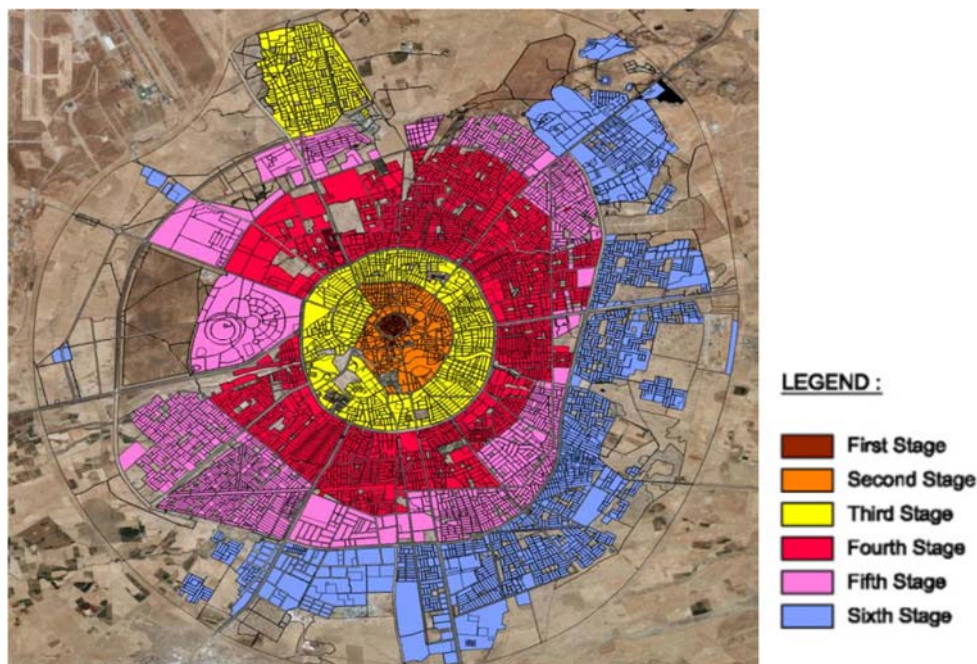


Figure 4.1: The stages of Erbil's development: HCECR, 2007

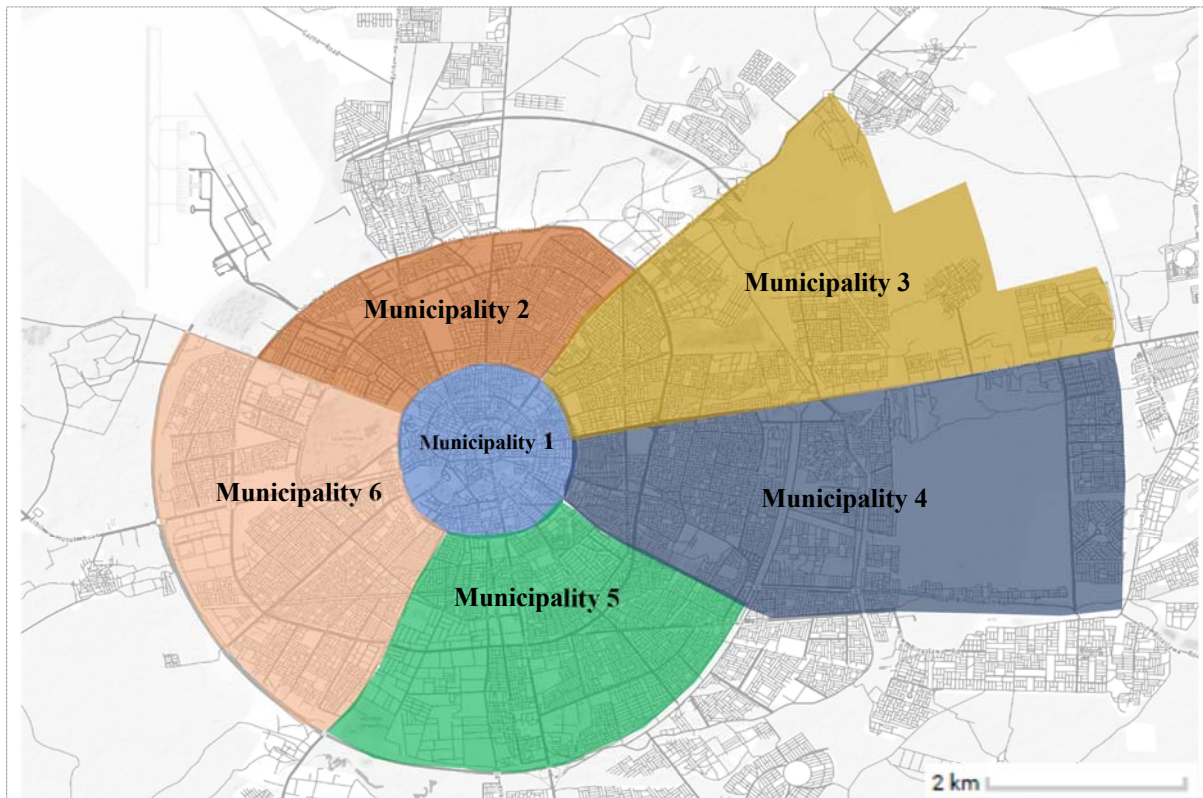


Figure 4.2: The six municipalities of Erbil: HCECR, 2007

(Reported from municipality interviews) To understand urban development in Erbil after 2003, the timeline of the urban design process will be explained in different steps for both the government



Figure 4.3. Informal housing, Badawa, Erbil

and private sector. There are similarities and differences between the urban design process for the

government and Private projects. There are four steps in the procedure for both types of projects; the fourth step is where they differ, as Figure 4.4 shows. The Government route is concerned with land ownership, design and infrastructure of the urban form, providing building plots for individuals to have designed and constructed housing. Whilst the private route follows the Government route but also designs and constructs the housing on the plots, a turnkey approach. The details of the common steps will be discussed in the next section.

4.2.1 Step one: Master Plan Approval

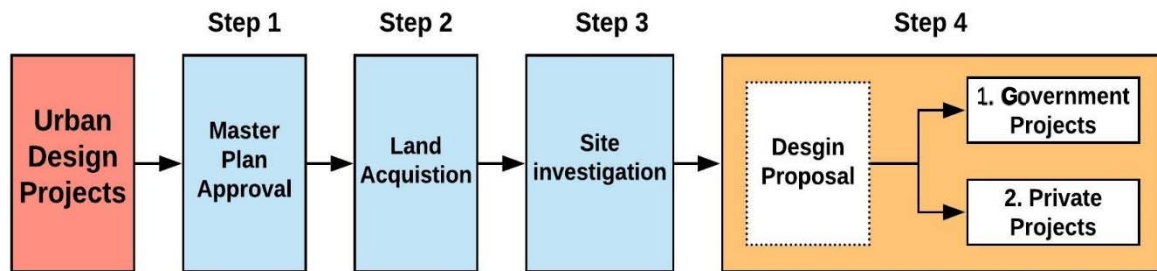


Figure 4.4: Similar Steps in Any Urban Design Housing Project Process in Erbil

The Master Plan department in the Ministry of Municipality of Erbil (MME) manages the master plan of the city (MOMT 2018), and any urban planning development projects within the city need approval from the Master Plan department (Figure 4.5). The department aligns proposed development projects with the master plan and land use policies: reported by a senior architect managing the approval department in the HME (AFM106-II). After approval, land acquisition is the second step in the urban design process.

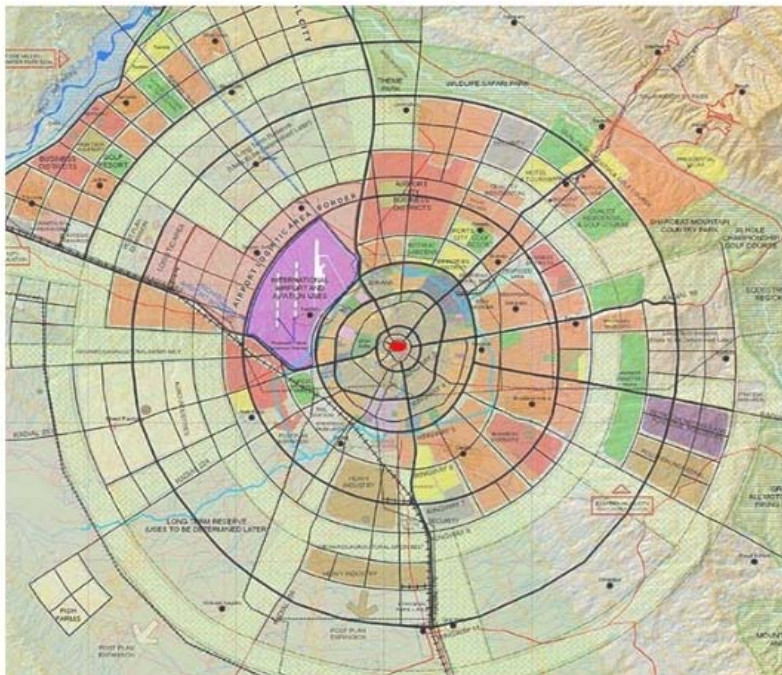


Figure 4.5: Erbil master plan until 2030

4.2.2 Step two: Land Acquisition

The acquisition of land for new developments which are located mainly outside urban areas of Erbil city starts with the Head of Municipalities (HME)¹ in the city. These lands are typically agricultural lands belonging to farmers and private owners. This was clarified after an interview with an architect at the design department at the head of the municipalities of Erbil:

Typically, the land belongs to private owners, and the HME changes the land ownership to the Government property by compensation the original (land) owner through the 15 % of the land area (in total). After the acquisition of the land by the government, the urban design process starts either by the government staff or private design companies. The proposal design will be reviewed later on by the Urban Planning Department before the final approval.

The process includes changing the ownership of the land to government ownership via compensation, which is usually in the range of 15% of the cost of the proposed land to be acquired for new developments.

4.2.3 Step Three: Site Investigation

The Head of Municipality of Erbil (HME) includes the departments of Urban Design, GIS, and Building Design. Typically, the HME sends an architecture and engineering team to survey the proposed site in collaboration with the GIS department. The physical dimensions and orientation for the proposed land will be investigated and then submitted to the Design Team to start the proposal for urban design. This investigation will refer to any existing building or any informal housing settlements (Figure 4.3). Primary site investigation helps designers to avoid clashes between the design proposal and the actual site (reported by an architect at the design department at the HME).

4.2.4 Step Four: Design Proposal

After the land ownership is changed to government property and the physical dimension has been investigated by the GIS department, the process of the urban housing design project starts with the government or private designers. The government designers are represented by

¹ Head of Municipalities: Is the main directorate and responsible of eight local municipalities of Erbil. Its include 20 departments such as planning and follow up, GIS, Law, Building licensing approval, Industrial, Traffics and roads, and other departments.

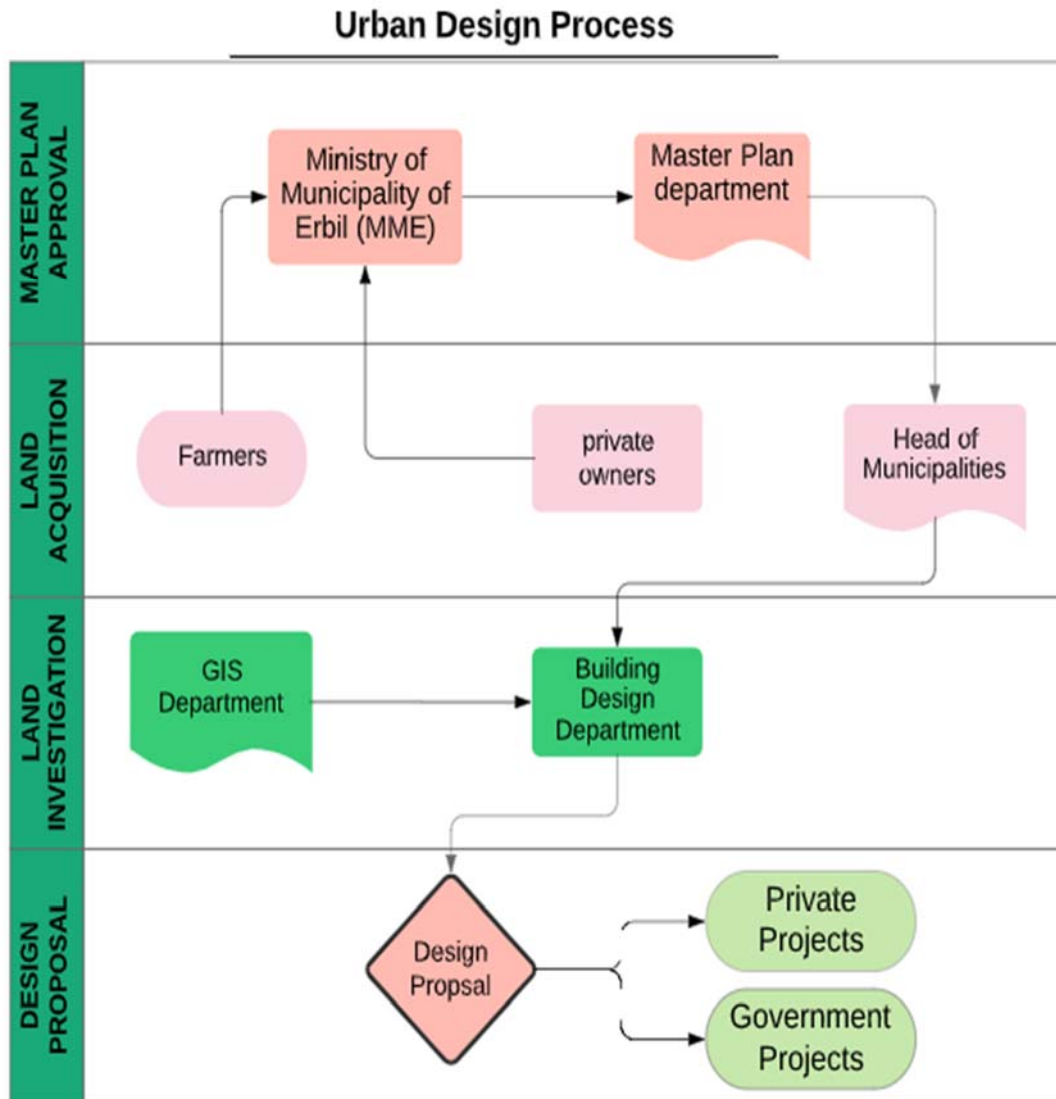


Figure 4.6: The process of urban design Government and Private projects

architects employed by the HME, and the private designers are represented either by architects from private construction companies or consultancies. Both sectors have a different approach to UDH projects. The design proposal mainly consists of a site plan of the housing project in which the lands for housing plots and services are identifiable. The Government and Private approaches are outlined in the following sections (Figure 4.6).

4.3 Government projects

In the majority of cases, the local government is responsible for providing housing units for communities; thus, the HME architects design housing projects to meet the housing needs of the new population. The UDH starts with a proposal for the site plan as discussed before. The government distributes housing plots among local citizens. Housing units are designed with the participation of the government and communities. The site plan is designed by HME

architects, while the housing units² are designed and constructed by either the plot owners or self-employed architects, Consultation companies are employed by the plot owners. Services and public spaces are designed by the Building Design Department (BDD) as a part of the HME (reported by an architect at the design department at the HME). The Urban Design Department uses the master plan to initiate new housing projects. A committee of designers is then activated to start the design proposal, including different government departments, as follows: Ministry of Municipality, Ministry of Planning, General Directorate of Urban Planning, and the City Council.



Figure 4.7: Government urban design projects

The site plan proposal design by HME and is sent to the General Directorate of Urban Planning to review all architectural and planning requirements before final approval (as certified in an in-depth interview with the Head of Design Department in HME). The first approval of the Urban Design Housing proposal is sent to the City Council³, and is made available for internal comment for 30 days to obtain feedback from the local community. After the legal time period, the project design is ready to implement (Figure 4.7).

Figure 4.8 shows the urban design stages from the proposal design stage to the land registration to the individual owners. The end point here is the provision of serviced plots and other community buildings, schools, hospitals etc. At no point in this urban design process is there and consideration of the impact of the design on the microclimate and no control on the environmental design of the houses to be constructed.

² Housing unit: The private residential construction needs advance approval from local municipality. The specific guideline for housing unit designed by HME and implement by local municipalities. This include information about building requirements (height of each floor, internal open spaces, and setbacks (Appendix C).

³ The City Council is made up of 17 members from various Kurdistan political parties, each serving a four-year term (Nagy 2006).

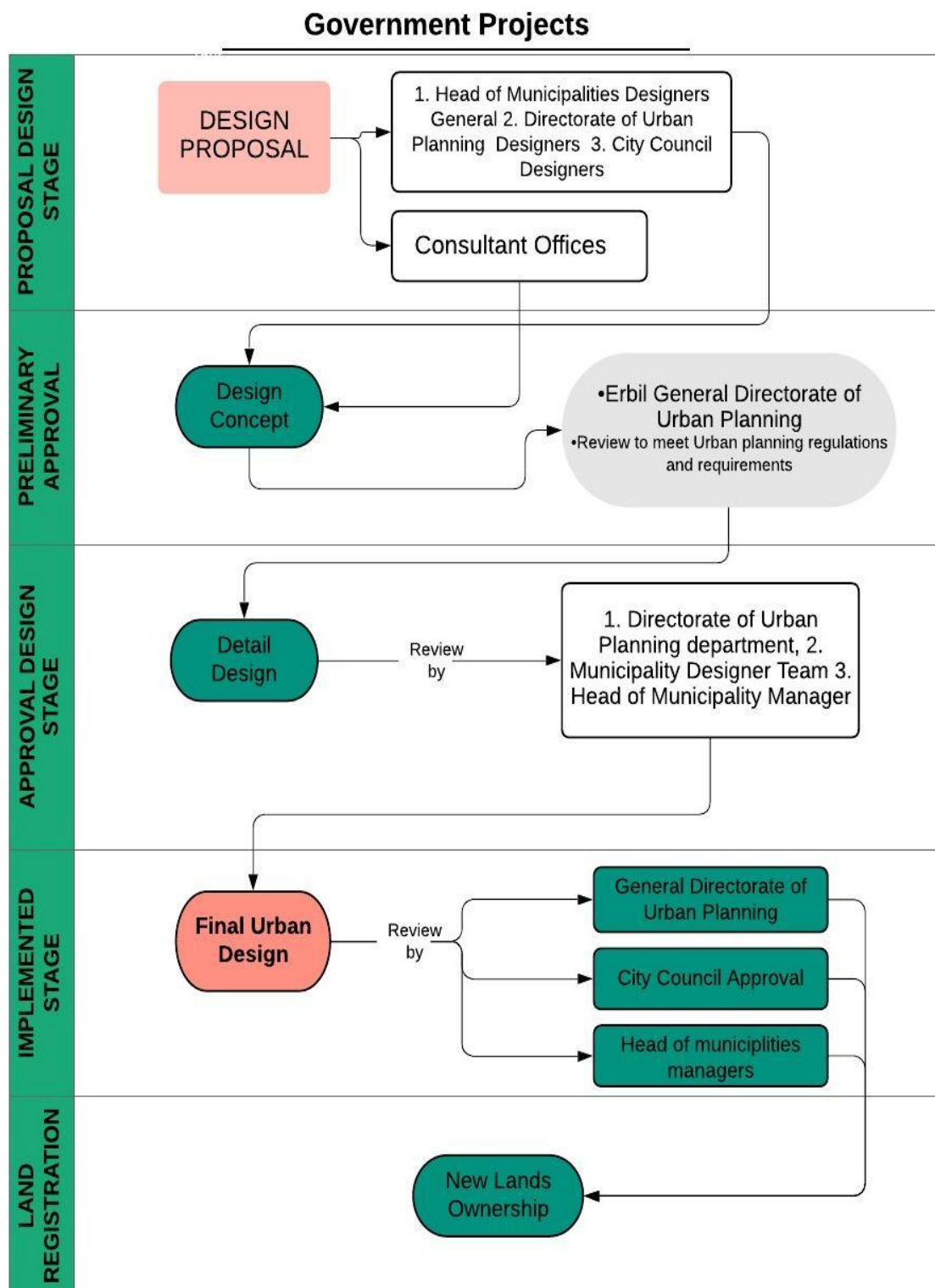


Figure 4.8: The process for government urban design projects

4.4 Private projects

Since 2006, the housing sector has been the most active investment sector and backbone of the Erbil economy. Housing projects are managed by the Kurdistan Investment Board (KIB) and implemented by local and international companies (Costantini 2013). In this section, we discuss the process of Private Urban Design Housing projects (PUDH) and the requirements associated with the housing project investment in Erbil. The process of PUDH projects is similar to government UDH projects in the earlier stages. However, the process of the former also contains the implementation stage. PUDH projects follow a different approach to government UDH projects after the initial stages. The main difference between government and private urban design housing projects is the construction stage, as government projects divide the land into housing plots and provide infrastructure for new housing blocks, while private housing projects focus on the design and construction of the housing units (Figure 4.9).

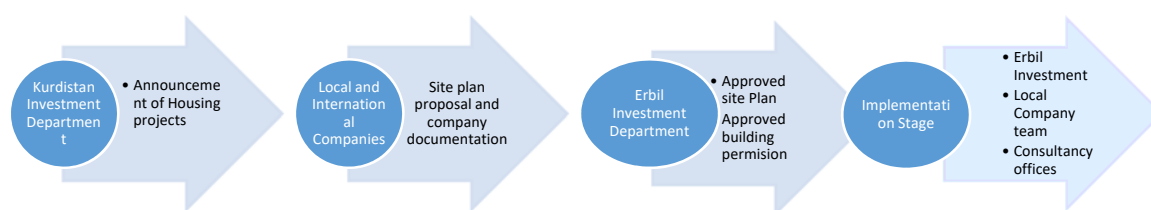


Figure 4.9: Process for private urban housing projects

The process of Private UDH starts by an announcement for the construction a housing projects from Kurdistan Investment Board up to new Master Plan of Erbil (Figure 4.10). International and local construction companies apply for the projects. Private UDH projects start from the design stage and continue until the project finishes. Most urban project investment is for housing projects, as there is a high demand for housing units. To understand the process of private UDH projects, this study reviewed government documents and used semi-structured interviews to shed light on the urban design process and its requirements in Erbil after 2003. The requirements for all Private UDH projects are similar, and follow the stages below:

- a. **Submission of the investment application.** In this stage, the formal documents are required for the investment company.
- b. **Eligibility Assessment:** The project's benefits to the public are assessed.
- c. **Land application and detailed planning:** At this stage, the investor company's documentation is assessed, such as previous work experience, financial resources, project plan and preliminary design proposal of the site plan.

- d. **Licencing Assessment:** After the acquisition of land and approval of the first proposal design, detailed designs are checked, such as the detailed site plan showing the design elements, land use and open spaces (green area) ratio, road networks, and detail design of housing types.
- e. **Construction:** This step uses the final design (design sets) approved by investment staff to construct the urban housing project. Three main bodies involved in this step are the investment department team, a local company, and an independent consultancy (activated in 2011), who review and report on the building process.
- f. **Operation:** This step considers the economic impact of the project and job creation.

The PUDH process starts with the proposed design of the investment company, who applies to the Investment Department to review all architectural and planning requirements before final approval. The process includes two stages of approval design. The first approval, is of the site plan during the Land application and detailed planning stage. The preliminary site plan is required to introduce the zoning and land use of the project. This site plan represents the concept of the project and introduction of the urban project, without details of the housing units or infrastructure and services.

The second stage of approval concerns the Licencing Assessment, which requires a detailed design of the site plan, the housing units, and all the services and infrastructure design for the proposed housing project. The detailed design includes detailed design sets for the architectural, construction, mechanical, and electrical designs of the project. Figure 4.11 shows both the urban design stages and the housing construction, from proposal design stage to individual registration of housing ownership. In contrast to the Government projects the private projects do include some elements of environmental design of the housing units but little consideration of the urban microclimate in the urban design.

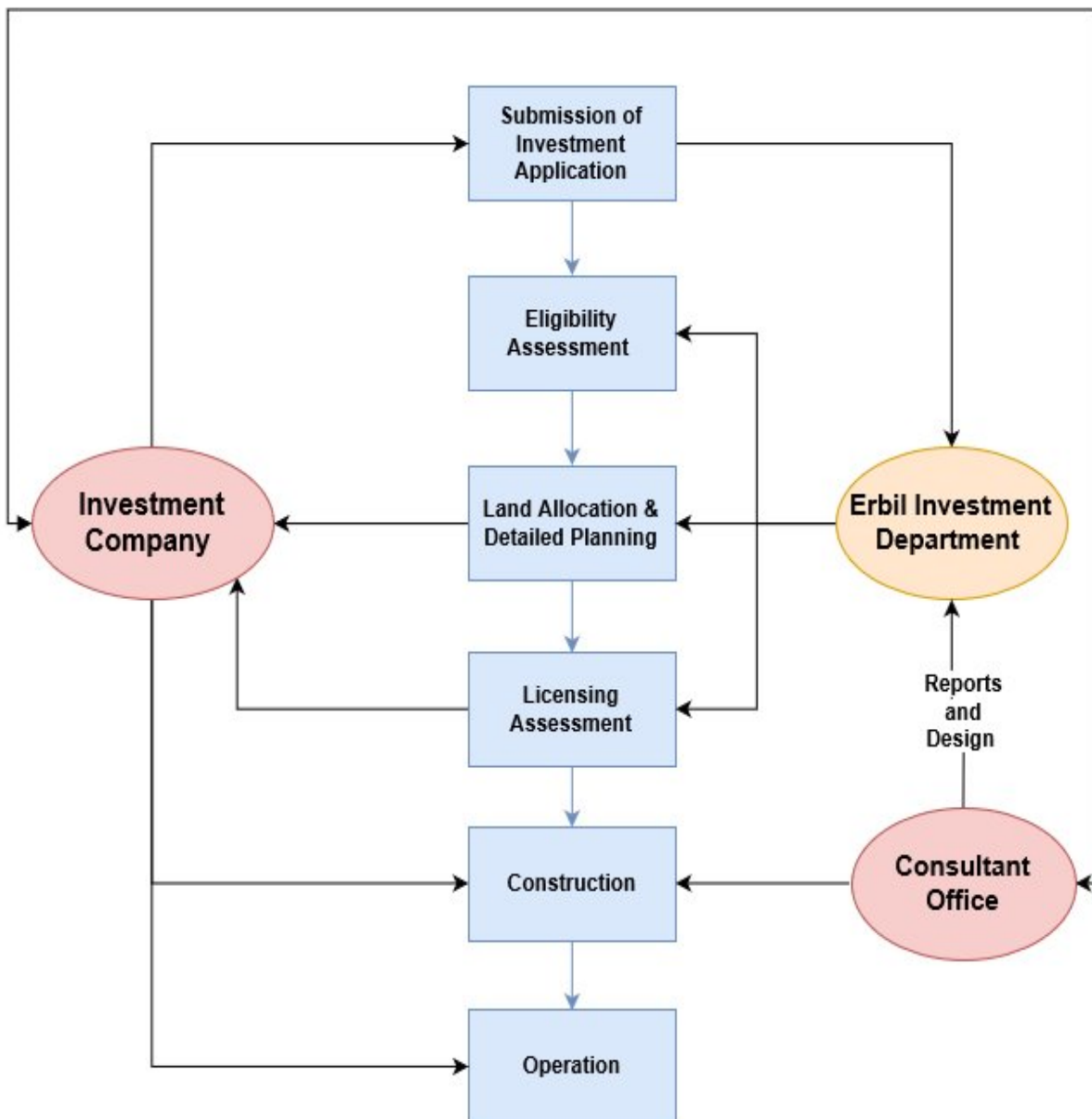


Figure 4.10: The investment licencing process

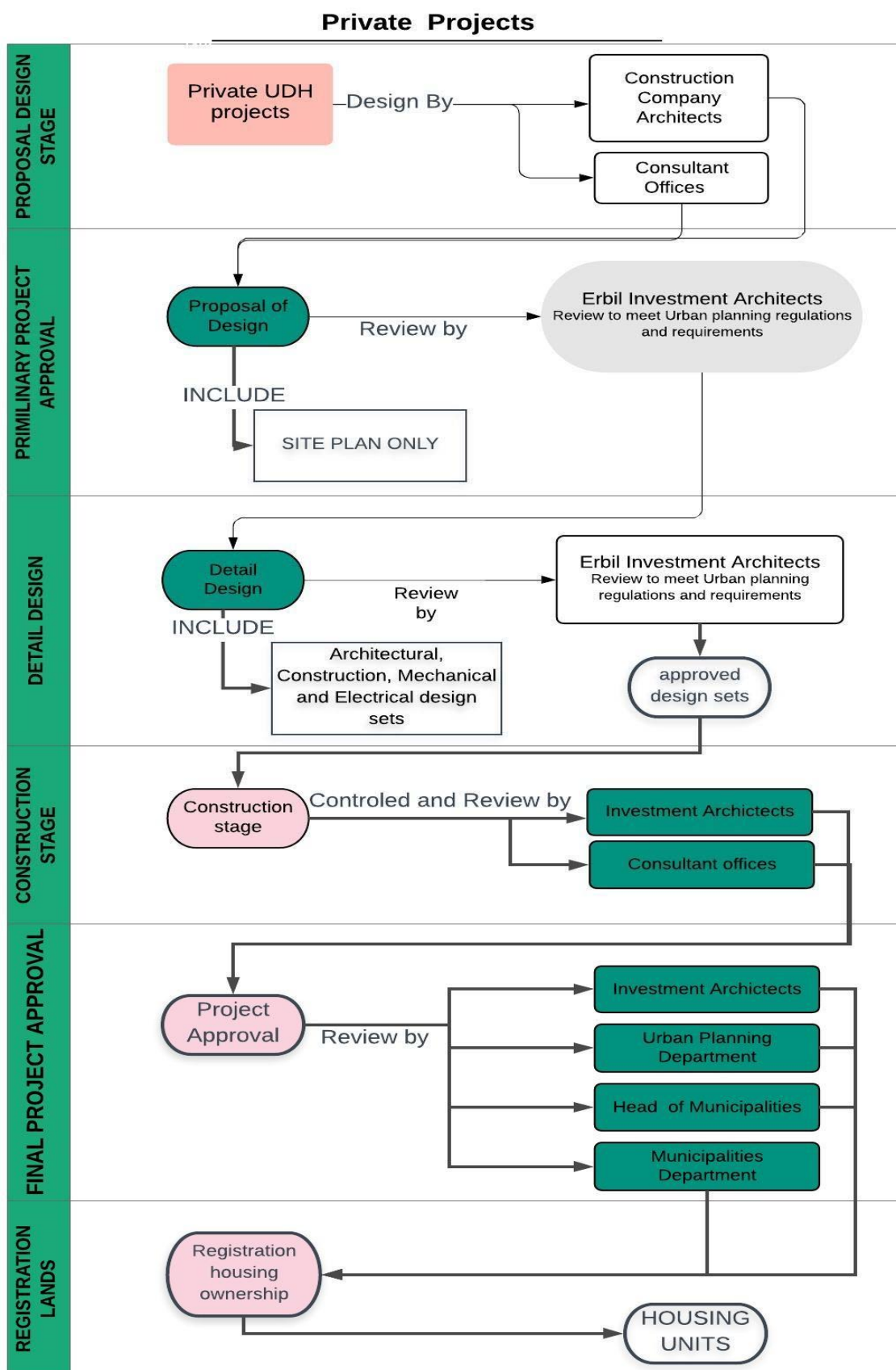


Figure 4.11: Private urban design projects

4.5 Case studies in Erbil Urban Areas

The case studies are focused on projects designed after 2003 by the government and private sector.

1. Government projects
2. Private projects.

4.5.1 Criteria for selecting the case study

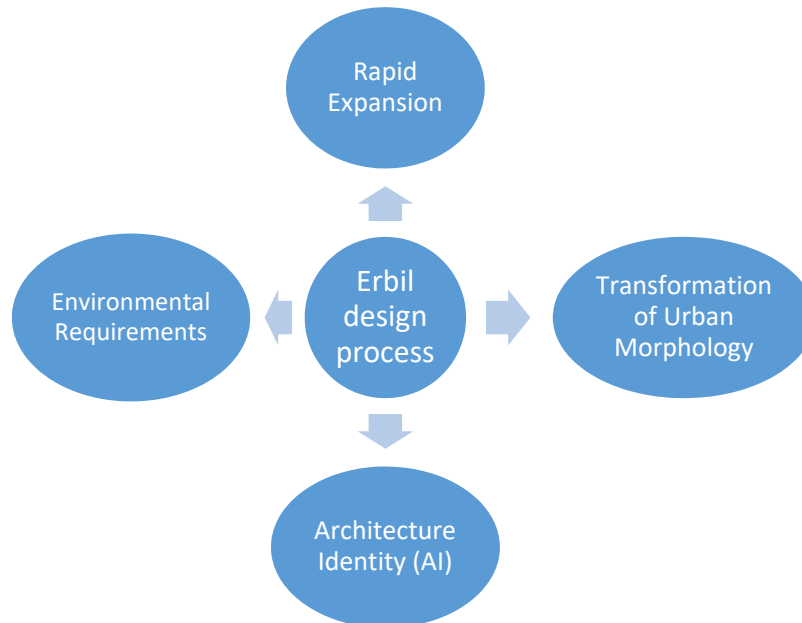


Figure 4.12: The relationship between the design process and associated problems

The criteria for selecting the case studies depended on four main issues mainly affecting the change in the city's urban physical environment: rapid expansion (RE) experienced in Erbil after 2003 in terms of the huge expansion of urban area; the transformation of the city's morphology (MF), environment requirements (ER); and architecture identity (AI) (Figure 4.12). Before 2003, the UDHPs in the city were mainly designed by government officers responsible for the process of urban design and distribution of plots. After 2006, it became possible for them to be designed by the government or investment companies. The high demand for housing, geopolitics, and socioeconomic factors helped the rapid expansion process in the city. Government projects were proposed as an attempt by the local government to respond to the high housing demands for new families, mainly represented by government employees. These projects focus on increasing plot numbers that can benefits more families, reported in an interview with a senior architect at the HME. The density and land use of the site plan is proposed by the design team in the Erbil Head of Municipalities and reviewed by the Department of Urban Planning and City Council before being distributed to the target people.

However, the private projects' design and construction process is done by investment companies to target new buyers. The site plan of private projects can be less dense in terms of housing plots. Either attached or detached, different sizes housing plots can be seen in private projects to attract families with different incomes.

Moreover, the main differences between these two types of project are that government projects provide plots and basic infrastructure, such as roads, water, and electricity, while investment projects can be described as a continuous process from the design stage to construction of housing units. This includes the design and construction processes.

The criteria for selecting case studies for both projects can be briefly described as:

1. **Rapid Expansion:** The new housing projects built after 2003 caused rapid expansion and changed the local urban microclimate of city. This expansion may be the main factor to highlight in the framework of this chapter, in terms of analysing some recent cases of UDH projects proposed by government and investment companies. Government-designed projects were proposed and implemented by the Ministry of the Municipality of Erbil, while the investment projects for housing designed and implemented by the private sector were through the Kurdistan Investment Board.
2. **Transformation Urban Morphology (TUM).** The city witnessed a transformation of urban form from traditional to grid-iron morphology. The citadel and surrounding urban areas (Arab and Bazaar) are a traditional urban form, while any development after 1920 is considered a grid-iron form. New developments follow X and Y axes without any consideration of the city's history.
3. **Environmental Requirements (ER):** Erbil is a hot dry climate and any urban development should adapt to the city's climate in both winter and summer. Thus, if the city is developed without consideration of the local urban environment, high energy consumption will be needed.

These case studies are used to analyse the new development in consideration of the environmental requirement and the level of adaptation to the local microclimate. The analysis is limited to the planning strategies and arrangement of the site plan.

4. **Architecture Identity (AI):** The local architecture identity of Erbil can be seen in the old city urban areas. The citadel and surrounding urban areas represent the Kurdish identity in terms of the architectural features on both the building and urban scales. The building plans, openings, locations, materials, and arrangements are similar and represent the long history

of the development process over hundreds of years. However, new developments lack the local architecture identity (Al-Shwani 2011), because they are mostly influenced by western architects and urban planners. New building plans, materials, and construction techniques have been used which have led to chaos and confusion in the architectural style (Ibrahim 2015).

Any case studies from the old traditional urban areas were not selected because they cannot be adapt to modern lifestyle and new ways of transportation in the city. Therefore, all case study samples are represented through those urban housing projects that may have caused the rapid expansion of the city and changed the local urban environment since 2003. Four samples were selected as case studies to represent government UDH projects designed by government employees, and four samples of private UDH projects were chosen to represent the private sector case studies designed and constructed by investment companies (Figure 4-13).

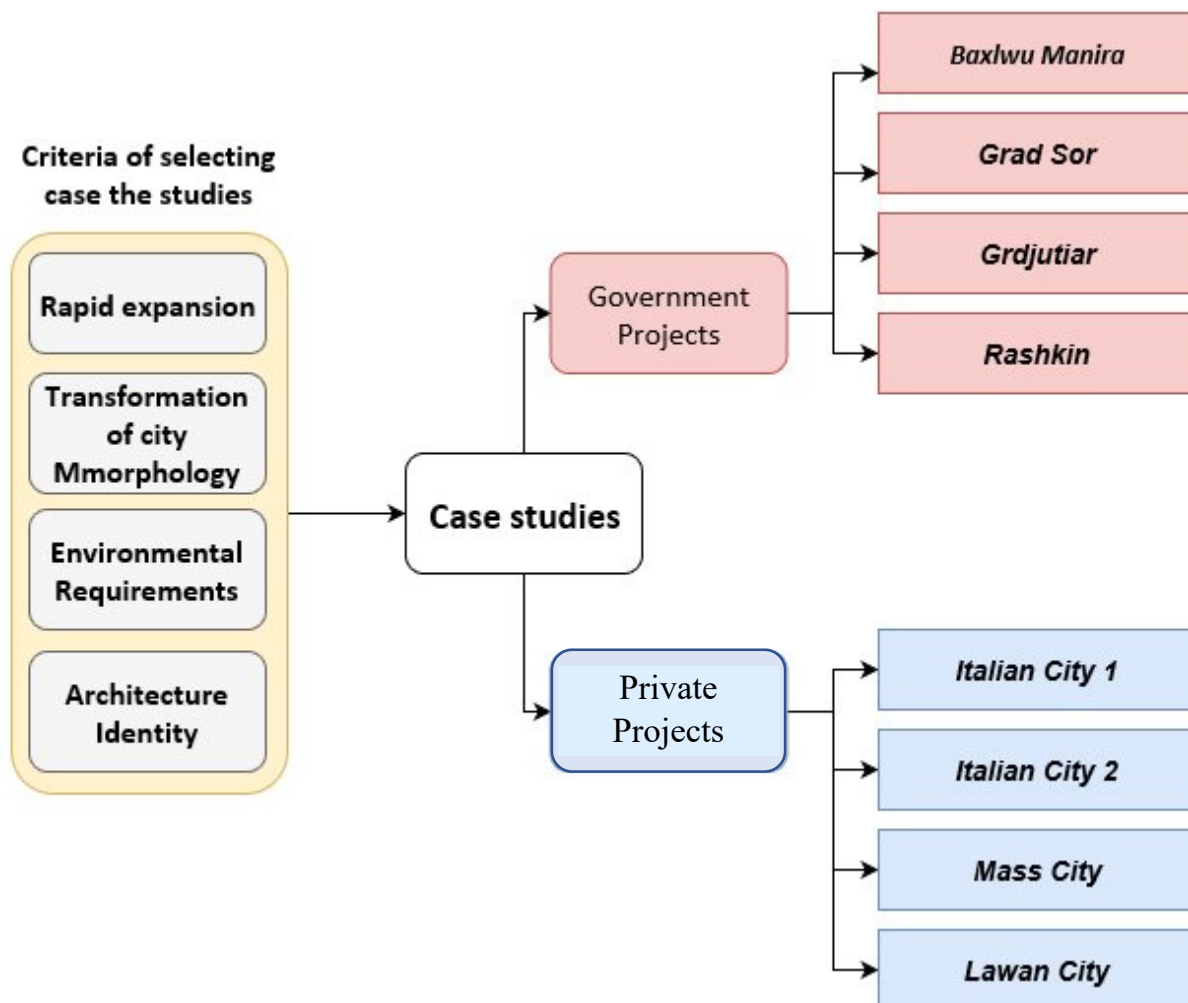


Figure 4.13: The criteria of selecting case studies and project samples for government and private projects

4.6 Government Project Case Studies

4.6.1 Baxlwu Manira

This project is located in the south west of Erbil and has an area of 34,604,600m² situated between two main ring roads at 100m and 120m⁴ (Figure 4-14). The main design concept of this project is opening spaces and green area, but high plot numbers have been used in the most recent projects in the city to cover the high demand for housing. The project covers a large area of open land which has been developed for the first time. A grid of road access connect the project with a main radial roads of Erbil and basic level of services provide to design to reduce the daily journey to city for basic needs of occupation. The project is mixed land use - between residential, commercial buildings⁵ and other services buildings.

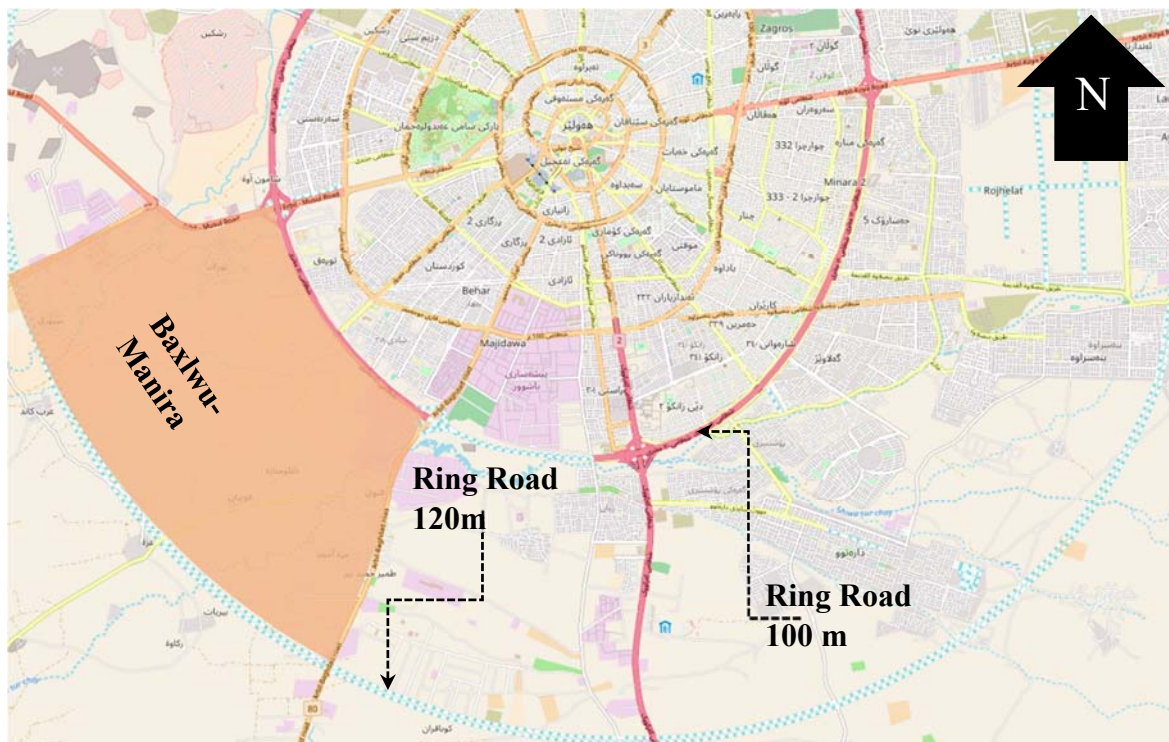


Figure 4.14: Baxlwu Manira project located in the south west of Erbil city

The services that project cover are commercial, health, religious, sports, educational, green area, and multi-story parking area. The site plan designed to cover the most essential services for occupancy in which they can adopt the project with its local services.

⁴ 100m and 120m: These are ring roads names which describe width in some case. The first ring road is 30m (30 m width) around the citadel, the second ring road 60m (60m width), the third ring road is 40m (40m width), the forth ring road is 100 m (100m width), and the fifth ring road is 120m (120m width).

⁵ commercial buildings: Retail

The main features of the project are:

- The site plan has mixed residential and commercial land use, as well as services.
- The commercial buildings are proposed to be 12 floors located in the centre of project, while the residential areas are on the boundary and of only two floors (Figure 4.15).
- The green area ratio is more than 30%, which is the minimum requirement of new urban developments in the city (Figure 4.15-C).
- The housing blocks have different orientations and every four blocks there is a central green area (Figure 4.15-A).
- Each block has two rows of housing and only one side faces the green area, while the back façade faces the opposite blocks. The green area is not equally distributed between the blocks (Figure 4.15-B).
- The green area is not distributed in a regular way and is designed to fill the shape (Figure 4.15-C).

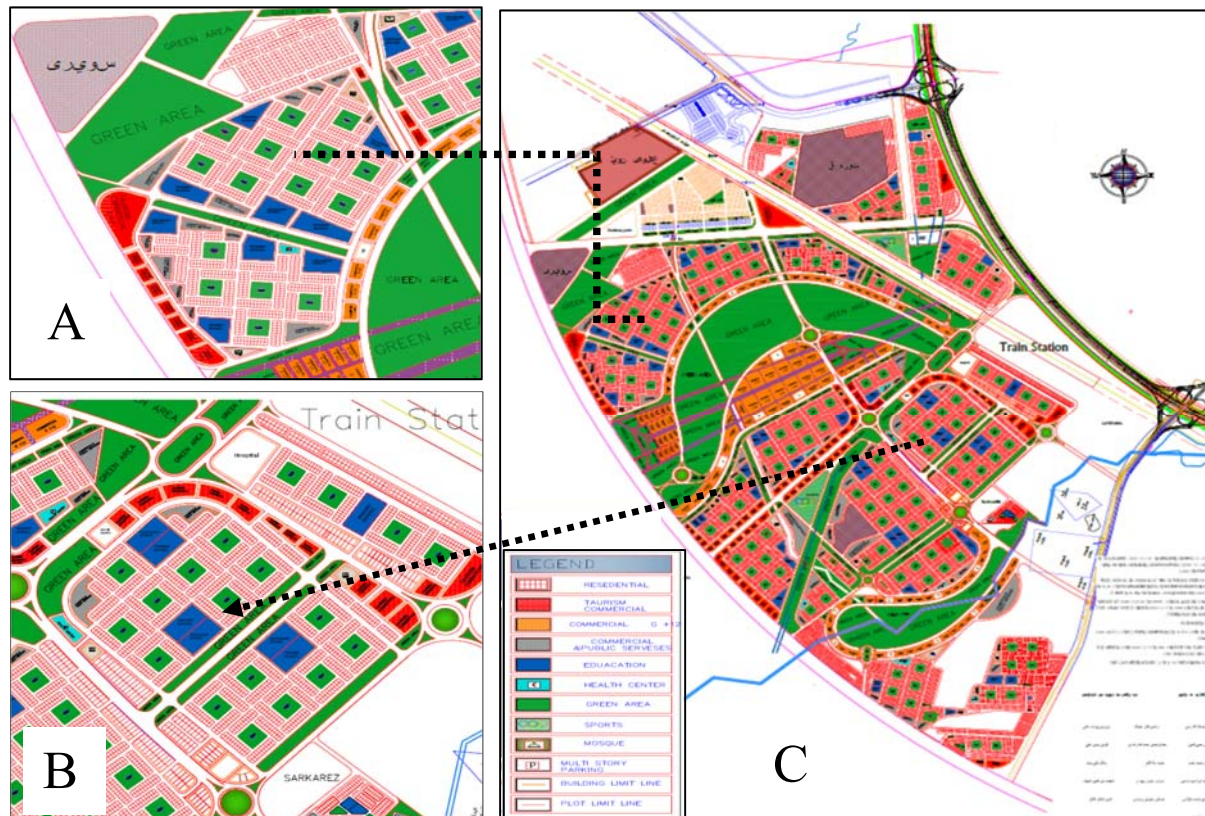


Figure 4.15: Baxluw Maira site plan – government-designed case study 1

4.6.1.1 Baxluw Manira Climatic conditions/observations

From Figures 4.15 and 4.16, the plans of the project, and the semi-structured interview with the designer, it was clear that the Baxluw Manira project was not designed to consider the local environmental features of Erbil. However, the project has more green areas than other housing projects in Erbil (both government and private). The project did not consider the housing

block's orientation towards the city's prevailing wind direction, and the blocks are designed to fill the spaces between the main roads (Figure 4.15). This type of project is designed to meet the increased housing demand and provided initial infrastructure (water and electricity). The designer attempted to increase the green areas and open spaces between the housing blocks and large parks in the middle of the project. The open green area can be used as an environmental strategy to manipulate the local urban microclimate (Tsoka, 2018), but this needs research and simulation of the proposal design before the construction stage. In so doing, well designed green areas can reduce the impact of the urban microclimate on the housing units.

4.6.2 Grad Sor

The area of this project is 12,598,973m². The architectural concept of the project is mixed between commercial⁶ and residential buildings, and the commercial blocks surround the housing blocks (see Figure 4.16-B). The commercial blocks are located on both



Figure 4.16: Grad Sor site plan – government design case study 2

⁶ Commercial: Retail and offices.

and vertical axes (main roads) of the site plan. Similarly, the housing blocks follow the two orientations vertical and horizontal axes and each group of blocks create a green core in the medial (Figure 4.16-A). The project includes other service areas for education, social needs, and other services.

The design has one shape of residential block (Figure 4.16-A), repeated in both directions with a similar shape and dimension. The commercial plots are different sizes positioned on the main roads and surrounded by green areas to reduce the mass ratio compared to the open spaces in the project.

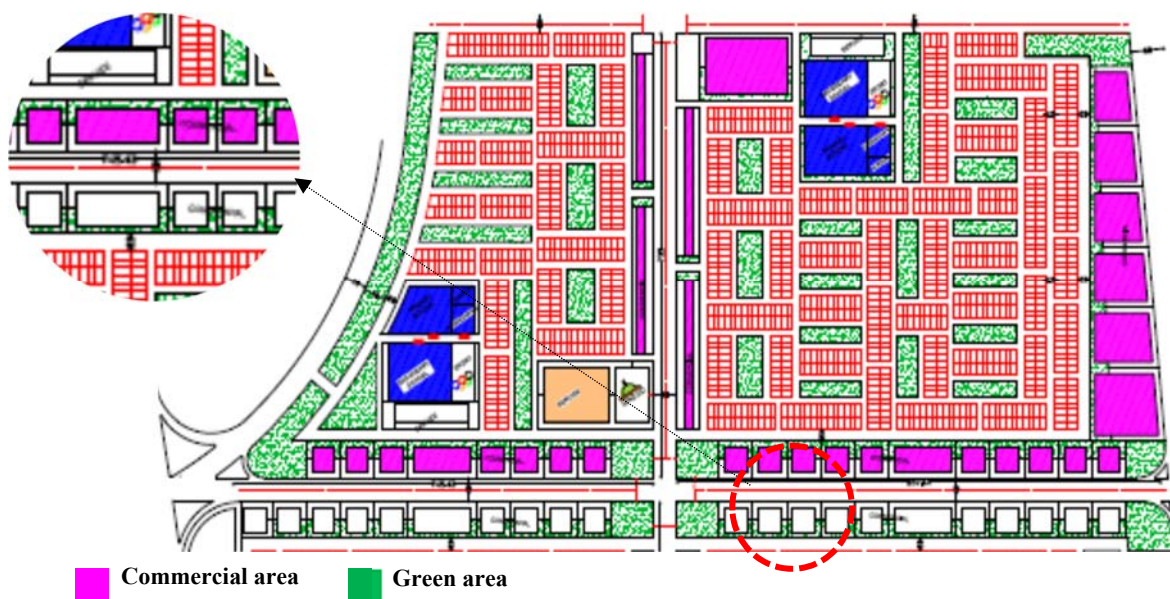


Figure 4.17: Part of Grad Sor site plan – commercial area surrounded by green areas

The main features of the project are:

- The site plan has mixed housing and commercial blocks, and open green areas (Figure 4.16-B).
- Each commercial building is surrounded by green area to increase green and open spaces (Figure 4.17) Each housing block unit faces an open green area, and the idea of designer was to increase green area and open spaces so that each housing unit would have plenty of green area equally.
- The site plan was designed without any consideration of environmental requirements, such as solar radiation and wind origin (as noted in an interview with the designer).
- The orientation of green spaces follows the housing block grids (X and Y axis).

- The orientation of both housing blocks and green areas follows the highway that surrounds the site (Figure 4.18-A).
- The natural element (the old river) of the site was taken as a design element to increase the open space (Figure 4.18-B).
- The streets are divided horizontally and vertically across the site plan of the project without any consideration of privilege wind direction and solar radiation (Figure 4.18).
- The residential block is only one standard shape that is repeated throughout the site plan, except for the location where natural elements appear, such as the river or borderline of the project land (Figure 4.18A and B).
- Each group of residential blocks has a similar services area that follows the same sequence of repetition as a standard block (Figure 4.18-B).
- The main road divides the project horizontally and vertically into two equal parts with a series of grid-iron roads parallel to the main roads that surround the site (Figure 4.18-A).

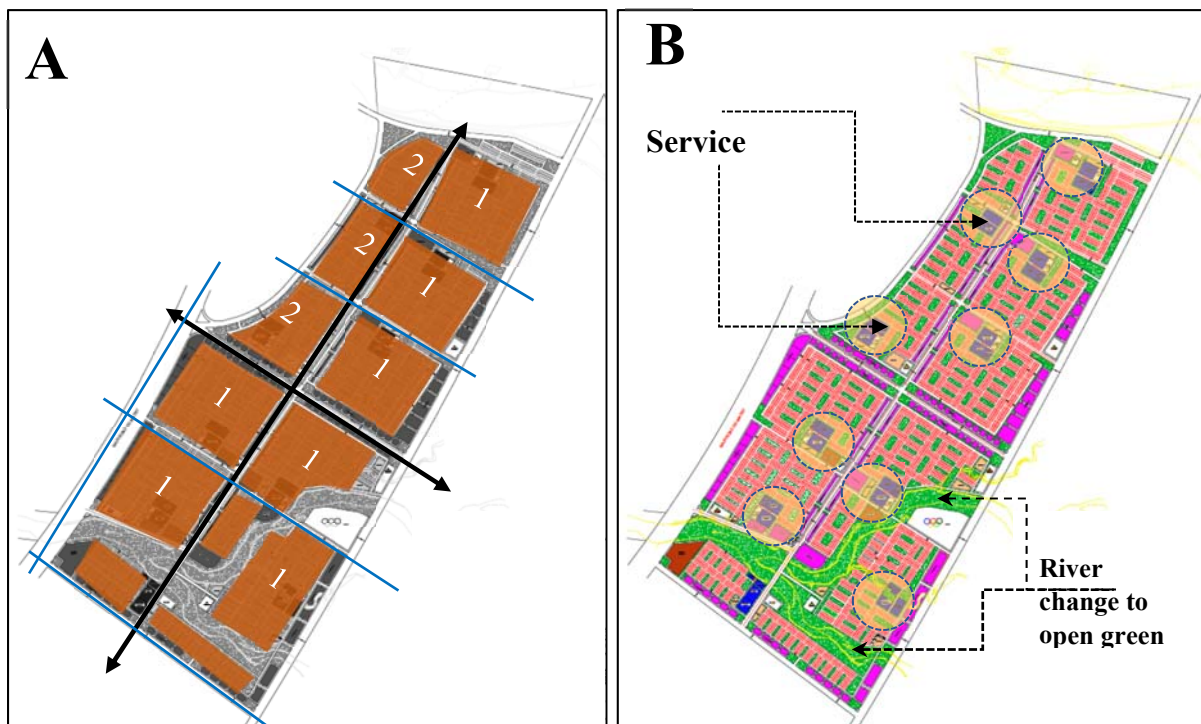


Figure 4.18: Grad Sor site plan – the residential block is one, repeated shape throughout the site

4.6.2.1 Grad Sor Climatic conditions/observations

Wind speed and block orientation may reduce the dry-bulb temperature (DT) of the outdoor urban areas if employed scientifically. Increased wind velocity between the canyons may work by convective heat removal. This helps to reduce DT and improve thermal comfort for outdoor urban areas (Lee, Mayer et al. 2019). In addition, the orientation of residential blocks may help to reduce both the amount of solar radiation falling on the canyon surfaces, and the energy

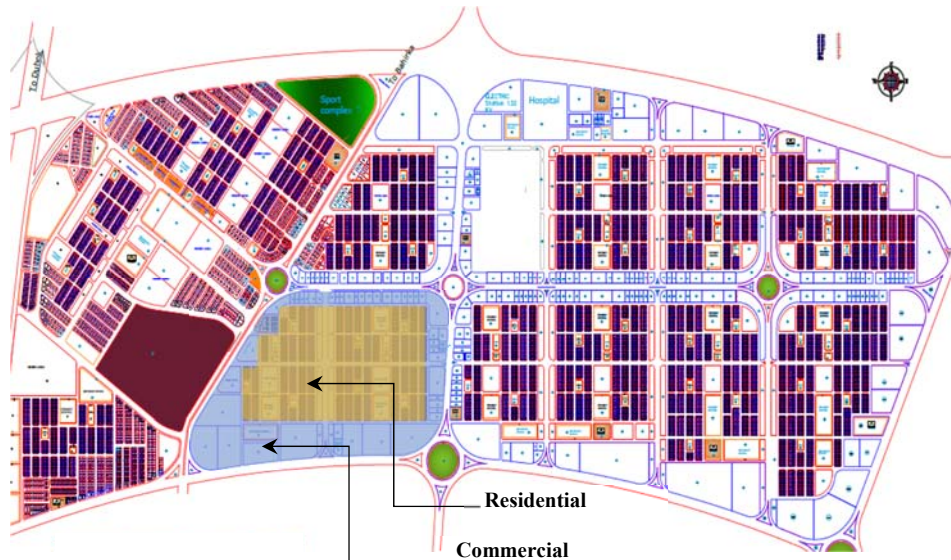


Figure 4.20: Gadjutiar site plan – government design case study 3, area 16,853,888 m²

In general, the housing blocks are surrounded by commercial blocks and other service buildings. Most residential blocks are oriented to east and west, and about 20% of the blocks are oriented toward 45° from the north (Figure 4.20).

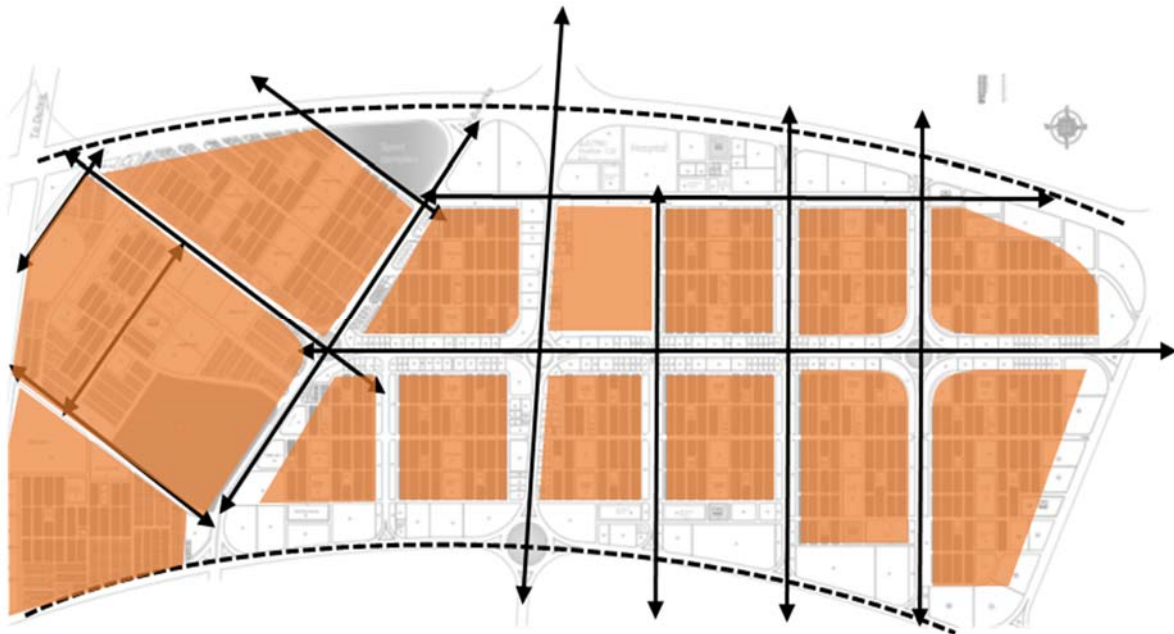


Figure 4.21: Gadjutiar site plan – the main axis of project

The main features of project are:

- The site plan mainly follows a grid-iron structure, with the streets directed to the north and south or east and west (Figure 4.21).

- The green areas have a similar direction as the residential blocks and are not equally separated between the blocks (Figure 4.20).
- The commercial plots are located on the main roads at 20 to 50m widths, while the residential canyon is just 10 and 12m (Figure 4.20).



Figure 4.22: Gadjutiar site plan – the old main roads crossing the project

- The services and public buildings are located on the main roads and the residential blocks are located in the centre of the residential blocks (Figure 4.20).
- The residential blocks are represented by one shape of block, which is repeated throughout the site (Figure 4.23).
- The residential housing blocks include three types of plot (250, 350, 450, 500, 600 and 850 and 1000 m²). The plots of 250, 450, 500, and 600 m² are located toward east-west, while the other plots are rotated 45° from the north. The commercial and services plots are of different shapes and areas (Figure 4.25).
- The vertical axis divides the project area to two parts and around 30% is rotated 45 from the north axis. This was planned to adapt to the two old roads (Bairka) which connect Erbil to the Bairka district and then Erbil to Mosul and Duhok province (Figure 4.22).



Figure 4.23: Gadjutiar site plan – the main direction of residential blocks (East-West) in the project



Figure 4.24: Gadjutiar site plan – the old main roads crossing the project

- The site plan has high density residential areas with limited green, open spaces. The commercial blocks and public services ratio is greater than residential areas (Figure 4.24).
- The canyons between residential blocks are 12m width, while the main roads range from 15 to 50m width (Figure 4.24).



Figure 4.25: Gadjutiar site plan – the site plan land use

4.7.3.1 Gadjutiar Climatic conditions/observations

From Figures 4.21–4.25, the plans of the project, and the semi-structured interview, the Gadjutiar project was not designed to consider local environmental features. The urban planners and designers used Iraqi urban planning standards and some international styles of urban planning to produce this product.

Therefore, the site plan is divided horizontally and vertically without any consideration for the local identity of the city or any other factors, such as the topography of the land. The old roads and boundary lines of the project are reflected in the site plan division. This can be clearly seen in the network of roads in the southern part of the project (Figure 4.21).

The ratio of open, green areas is limited and not separated equally between the residential urban areas. The horizontal and vertical axes of the blocks help to act as a channel to increase wind speed in parallel canyons, which may reduce the air temperature during summer time. In addition, the south façade gains less radiation. In spite of well-known simple features of environmental principles for urban design and urban planning, this project did not consider sun radiation and other environmental principles. The orientation of the majority of the residential blocks does not face south, which is the best façade direction (Figure 4.25).

The best direction for the residential blocks is the direction which is not parallel to the city's prevailing wind, but 255° from the north. This helps to remove the heat mass from the canyon during summer time, especially at night time. The prevailing wind direction of Kurdistan is move from the west, south-west to north (Husami 2007). Thus, the site plan is in the best position regarding wind direction, because the prevailing wind will distribute equally between the horizontal and vertical blocks. The best equal distribution of wind in both directions in the vertical and horizontal canyons will have a limited impact on the local microclimate, because wind speed in the urban area in Erbil is very low, estimated at between 0.55–1.0 m/s. The site plan for the project was not designed to cope with the environmental features of a hot dry climate city such as Erbil; instead, it was designed to meet the high shortage of housing units and high demand for housing and commercial plots in the city.

The site plan for the project was not designed to cope with the environmental features of a hot dry climate city such as Erbil; instead, it was designed to meet the high shortage of housing units and high demand for housing and commercial plots in the city.

4.6.4 Rashkin

This project is located in the north-west of Erbil in an area of 486,050 m². The plot is located between two ring roads at 60 and 100m and lies around 4km to the north-west of Erbil citadel (Figure 4.26). In this case study, the designer was provided with limited information about the plot from the master plan department, as shown in Figure 4.26. The plot was proposed as a complex of luxury hotels, but this type of project is in high demand because tourism in the city attracts many tourists from the middle and south of Iraq. The plot is located in between two high ways which are easy to access from the rest of the city and which are also close to the city airport from the north side of the plot (Figure 4.26).

In addition, green area was proposed to surround the plot from the outside of the ring road 100m, as shown in Figure 4.26. The green area was proposed to increase outdoor air quality, because of sound pollution from the airport sound and air pollution from the main road (Figure 4.41).

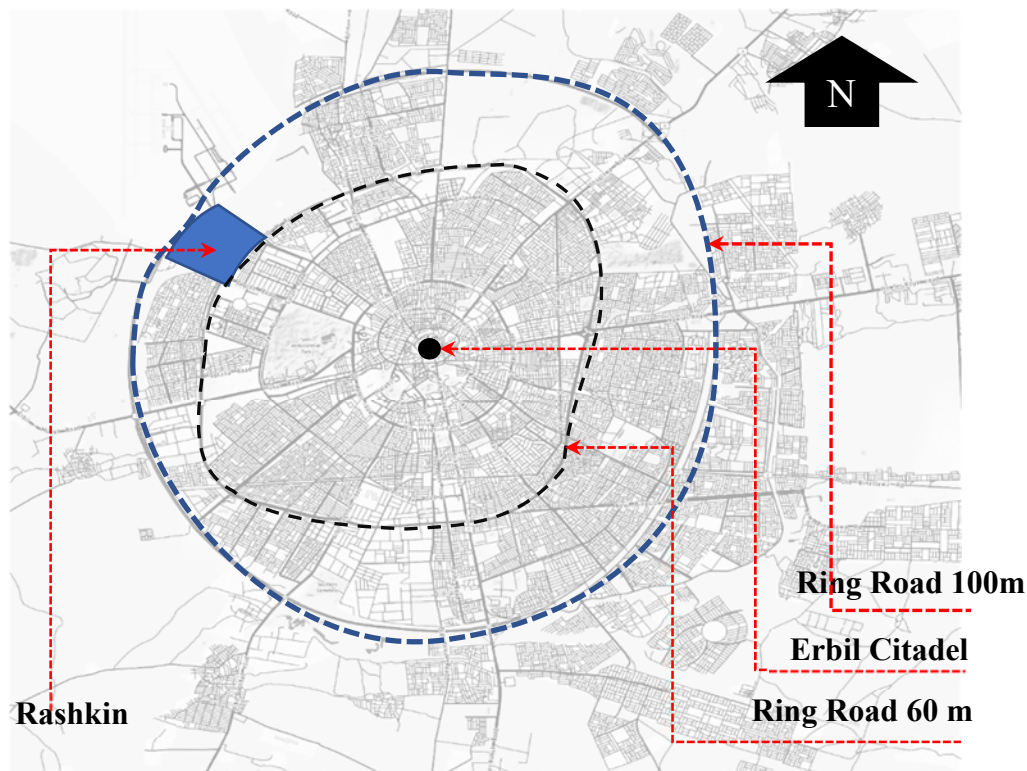


Figure 4.26: Rashkin site plan – the location of project in the city site plan

Erbil government is in charge of the urban design process of the land and it then distributes the land to investors to build hotels and other services. The land use of the plot is a complex of hotel buildings up to the master plan of the city. The design team in the Head of Municipalities of Erbil was chosen to design this plot. After urban planning by the design team, the small plots receive investment from local and international investment companies.



Figure 4.27: Rashkin site plan – the location of the project and City Airport

The first proposal for the plot design was influenced by the surrounding green belt (Figure 4.28-A). The plot is divided by 50% open green space and 50% building blocks, which include: 11 hotel buildings plots, service buildings plots, and a petrol station. The decision makers did not accept the first proposal design because of the high demand for plots and the expensive price of commercial plots in the city.

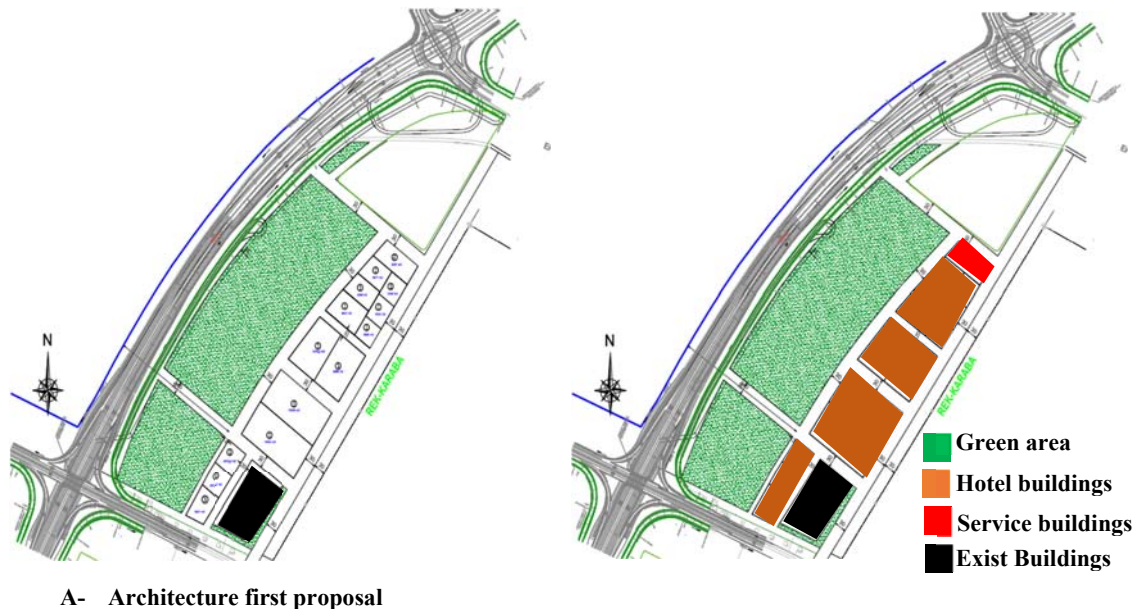


Figure 4.28: Rashkin site plan- Government design case study-4.

The first proposal was not accepted by the Head of Municipalities of Erbil. Therefore, the designer redesigned the second proposal with more plots and reduced the green areas in

response to the high demand for commercial plots around the city (Figure 4.29-B). Green belt was reduced in this location to increase plot numbers.

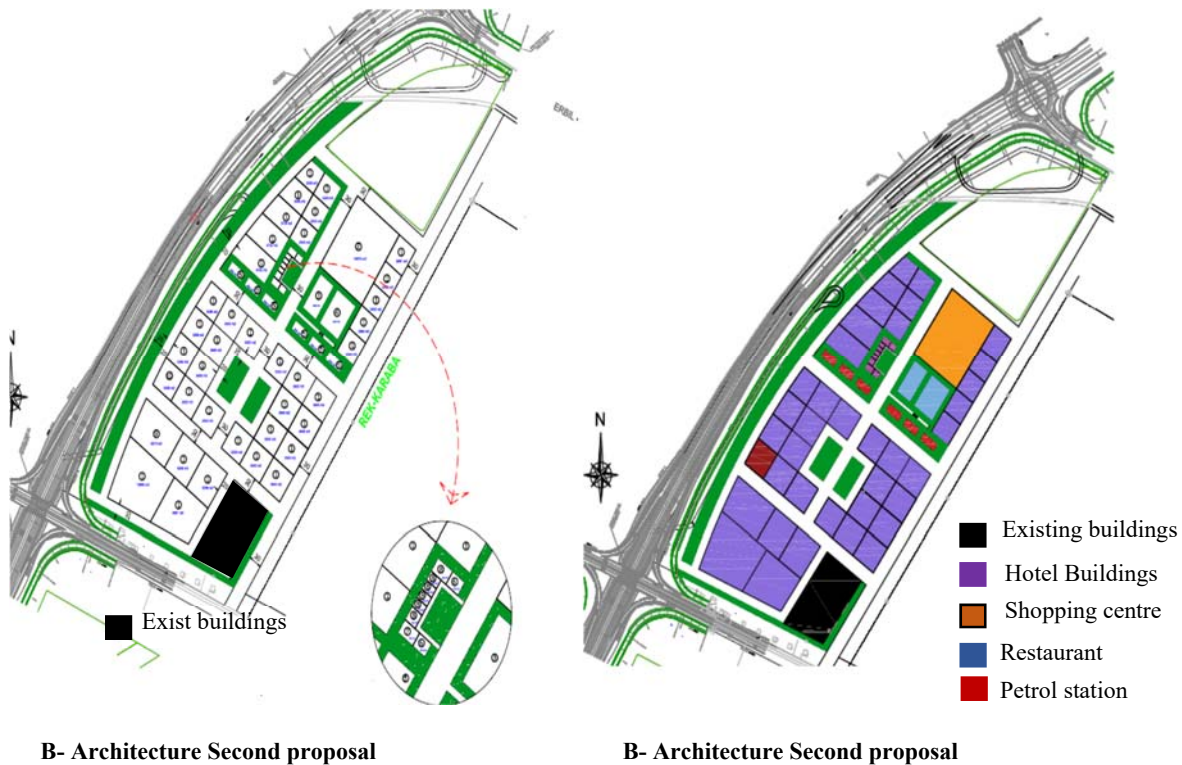


Figure 4.29: Rashkin site plan – government designed case study 4

The main features of the project are:

- The site plan is mixed commercial and investment projects (hotels and offices), as well as services (Figure 4.29).
- The commercial buildings were proposed to be 12 floors located in the centre of project, while hotel building plots were located on the boundary of the project.
- The green areas ratio was more than 50% in the first proposal design, and around 20% in the second, even though the minimum requirement for new urban developments is 30%.
- The blocks have a different orientation and most blocks have a central green area (Figure 4.29-B).

4.6.4.1 Rashkin Climatic conditions/observations

From Figures 4.27–4.29, the design options, and the semi-structured interview with the designer, the project was not designed to consider environmental features. The influence of western architecture is clear from the grid-iron street pattern. The blocks are divided up by the surrounding main roads in the first design option, while the second option is a more detailed design with a mix of green areas and building blocks to reduce building density and increase

green, open spaces. However, the first option was designed with more green area and open spaces, but the second mixed buildings and green, open spaces. This mixture may have a sensible effect on solar radiation during summer time by providing evaporative water and reduce air temperature. Wind speed and block orientation were not taken into account in the design process, even though they may have a minimum impact on DT because of the wind velocity, which is 0.55 to 0.6m/s. Nevertheless, this kind of proposal needs a simulation before final approval to address the environmental impact of the design on the local environment of the city.

4.7 Private Project Case Studies

Private projects represent more than 50% of modern developments in Erbil. Most of the projects were built by local and international companies as investment projects in Erbil after 2003. In this chapter, some projects are presented and compared with government housing projects to determine the similarities and differences of urban design criteria in these projects, and investigate the urban planning design elements and issues for private housing projects.

4.7.1 Italian City 1

This project is located in the west of the city and has an area of 386,400 m² (Figure 4.30). Italian City 1's position is 3km west of the citadel. It is considered one of the most famous

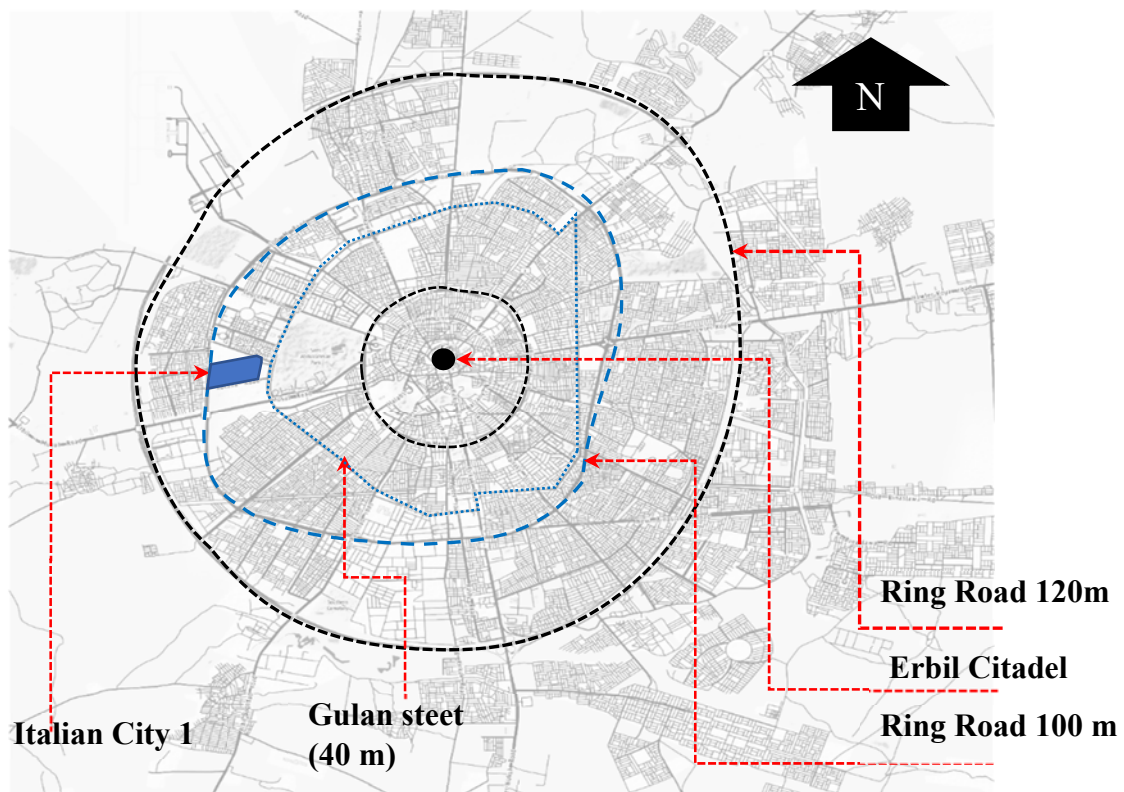


Figure 4.30: Italian City 1 – the location of the project in the city site plan

private housing projects that was designed and built through investment by private company for first time in Erbil (Figure 4.30). The Italian City was designed and constructed by a local company called *Hemn Group Companies* in 2008 (Figure 4.31). The city consists of attached and detached housing types, services, and facilities, as below:



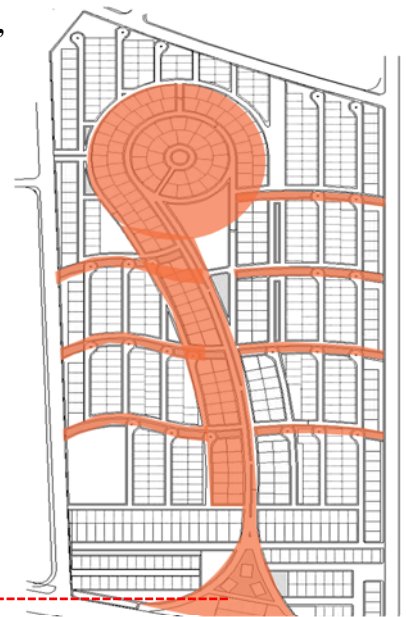
Figure 4.31: Italian City 1 site plan – local and international investment project 1

1. Housing types – Four types can be seen in this project, labelled A, B, C, and D (Figure 4.35). Where possible two images are shown, the designers' intent and its actual construction. The designers' tend to decorate their images with greenery (Figure 4.33).



Erbil Citadel site plan – the road network looks like a tree with a single main entrance for safety and security reasons.

Italian City 1 – Site plan, semi-organic shape site plan with single main entrance



Single main entrance

Figure 4.32: Italian City 1 – architectural concept, and the similarity between both site plans

2. Facilities and services, such as schools, supermarkets, public parks, and administration and office buildings, showing a high level of infrastructure compared to other local and government housing projects.
3. The site plan design represents a modern style which appeared after 2003 in the city. Most of the housing projects are grid-iron shape and contain just two axes, X and Y. This project was an attempt to design in different way to government projects, as the rigid grid-iron form was loosened and the housing style was intended to appeal to residents from overseas. The percentage of open space and green area ratio is limited compared to the buildings area. The minimum green area should not be less than 30% of total site area, so each house has its own garden and the large green area outside the houses used a road shoulder (Figure 4.33)



Figure 4.33: Italian City I – houses have their own gardens, and the large green area



Figure 4.34: Italian City 1 four types of individual houses A, B, C and D

The architecture and urban planning design concept developed from a tree shape that started with the main entrance axis and separated into side branches, right and left. The main axis divided the grid of houses into two and separated the residential and public zones into the shape of a tree. The idea of a tree shape has an historical architectural background in Erbil's citadel,

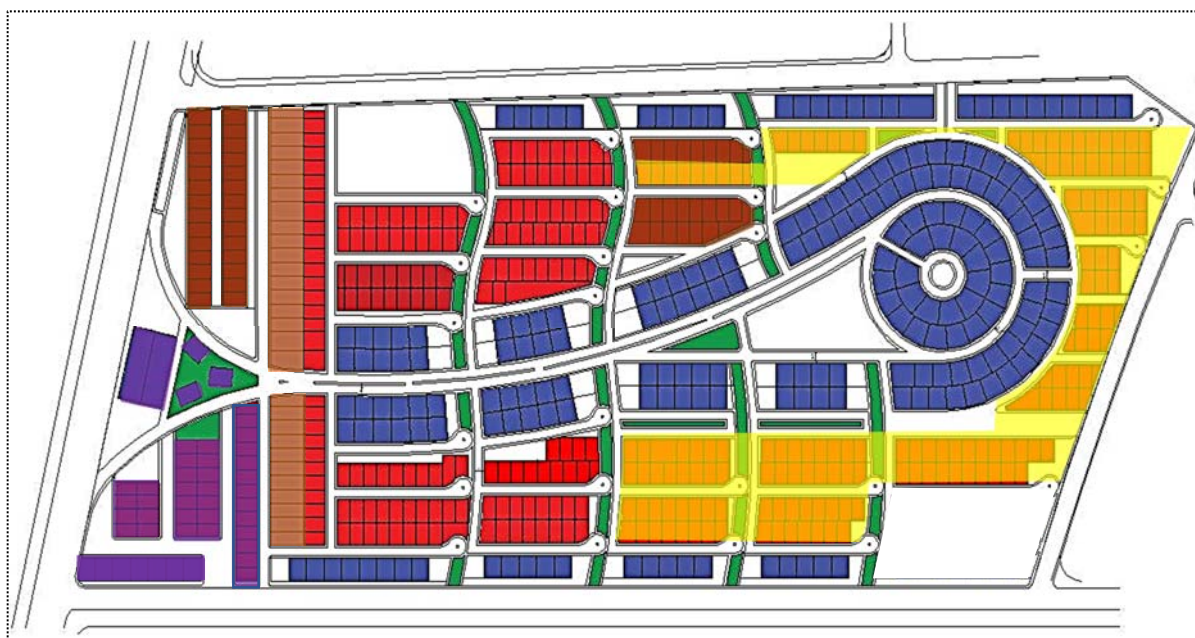


Figure 4.35. Italian City 1: types of individual housing units A, B, and C and D

Housing Plots	Number of houses	Area of Plots	Housing Type	Colour
Private Villas	35	Not regular	Detached	Purple
House type A	263	320 m ²	Semi-detached	Blue
House Type B	155	250 m ²	Attached	Red
House Type C	39	140 m ²	Semi-detached	Orange
House Type D	194	200 m ²	Semi-detached	Yellow

in the main entrance of the city and upregulated network of narrow allies that lead to closed branches (Figure 4.32). The Italian City 1 project reflects the idea of a tree and branches to connect housing units and separate them with a core area, which includes service buildings and offices. The design attempts to break down modern grid-iron morphology through the main axes and curved branches on both sides of the project.

There are 659 housing units classified up to the plot area, and finishing material quality. The total area of the project is 386,400 m², which represents a housing area of 183,671.65 m², public green area of 17,740 m², roads and pavements of 147,070.35 m², and a services area of 15,809 m². Other building areas such as administration offices, motels, restaurants, and commercial areas represent 25,466 m².

The project was designed in cooperation with the Hemn group and Italian companies. The housing units are designed to reflect western houses (Italian houses). The building materials and construction used Italian technics of construction (Parow 2017). Isolation building materials and precast hollow core concrete slabs were used for the ceilings (Figure 4.36).



Figure 4.36: Italian City 1: ceiling materials (precast concrete)

The main features of the project are:

- The site plan contains five types of housing unit and different average sizes of plot area.
- Each housing block building is surrounded by green area to increase green and open spaces (Figure 4.35).
- Most housing block units face each other and there is a high density of buildings; the idea of the designer was to increase green area through linear curved shapes of green areas placed vertically between horizontal housing blocks.
- The site plan was designed without consideration of the local environment, such as solar radiation and wind originations, but the housing units were designed to resist summer heat and winter cold through high quality building materials (Parow 2017).

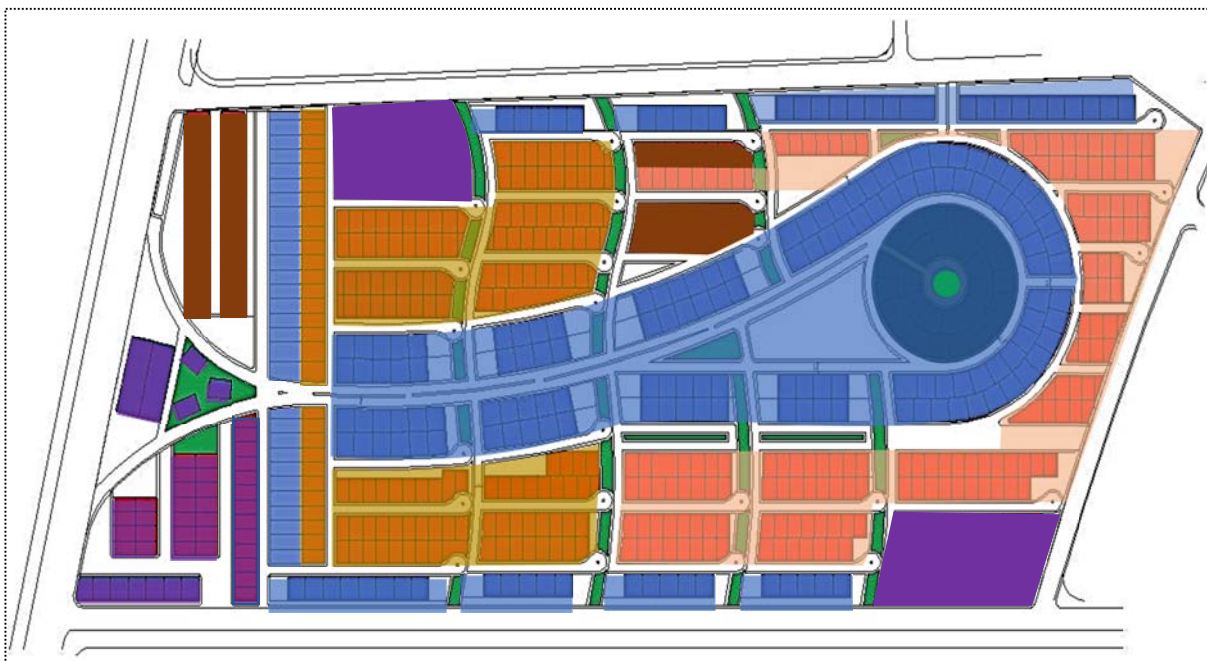


Figure 4.37: Italian City 1: zonal types of individual housing units A, B, C and D

- The walls and ceilings are constructed with high insulation material for heat and sound. The exterior walls are covered with 500mm thick expanded polystyrene (EPS) (Parow 2017).
- The orientation of the housing blocks and green areas does not follow the (X and Y axes) and boundary line roads like other housing projects (Figure 4.37).
- The residential block is not just one standard shape repeated throughout the site plan, but instead works as a system of road networks using cul-de-sacs to control traffic. The project may have considered certain environmental factors in terms of the housing units using insulation materials, but the project did not use urban planning environmental strategies.

4.7.1.1 Italy city 1 Climatic conditions/observations

From Figures 4.32–4.37, the design site plan, images, and the semi-structured interview with the project manager of the construction company (Hemn Group), it is clear that the project was designed to consider some environmental features. The construction materials and building procedure used Italian techniques of construction. This includes insulating building materials and precast hollow core concrete slabs being used for the ceilings (1st and 2nd floors), while the third floor (truss ceiling) was added to reflect western architecture features (Figure 4.34). This can reduce direct solar radiation to the second floor ceiling and reduce thermal mass.

The influence of western architecture is clear from the housing unit's design (truss ceiling), while the grid-iron and street pattern is an attempt to design differently to most government projects, as the rigid grid-iron form was loosened. The site design attempts to break down the modern style of grid-iron morphology through the main axes and curved branches on both sides of the project. The open, green spaces are limited, but have been well designed and maintained until now (Figure 4.33). Each housing unit has its own garden, which can help to reduce the direct solar gain falling on surfaces and increase outdoor thermal comfort. Neither wind or air temperature effects were considered during the design of the project, even though insulating materials are used. This type of project needs an environmental simulation modelling process before implementation the project to minimise heat gain during day time and maximise heat loss at night time.

4.7.2 English Village

The project is located in the west of the city and has an area of 278,014 m². The English Village's position is 3.2 km west of the citadel (Figure 4.38), and it is another well-known private housing project designed and built by private companies. It was built at a time when the housing project was one of the earlier projects in the city (Figure 4.39). Designed and

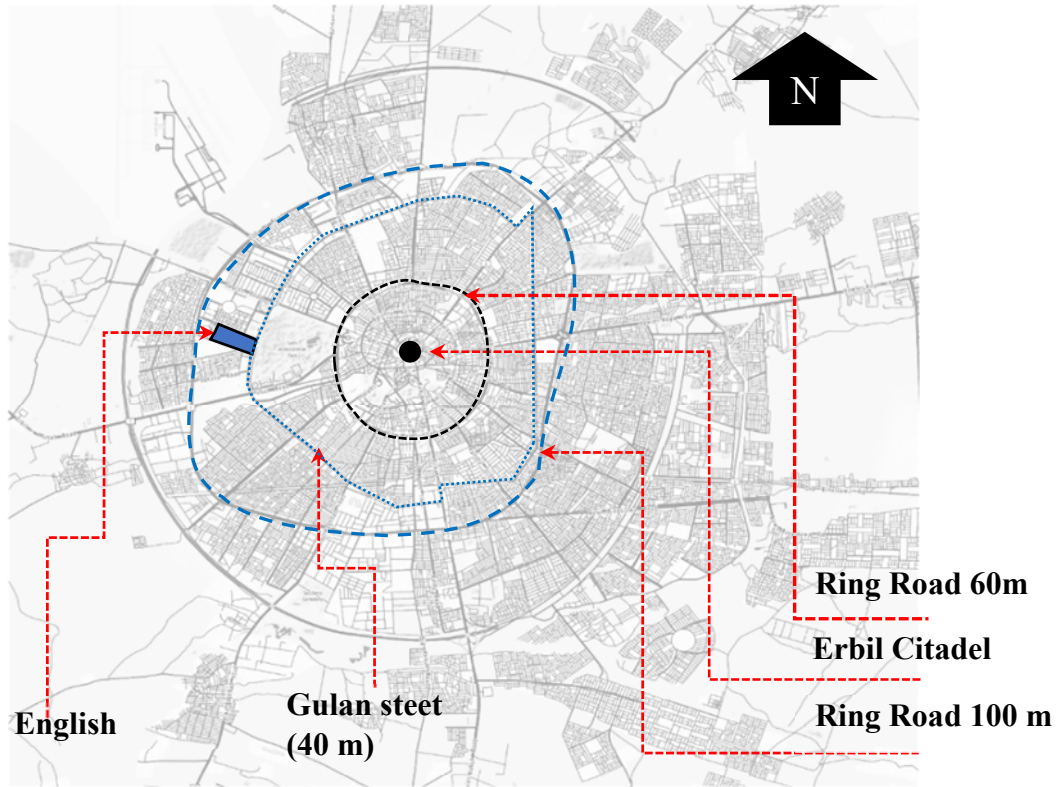


Figure 4.38: English Village – the location of the project in the city site plan

constructed by a local company called *Hawler* and British property development company J.M. Jones and Sons in 2006, the city consists of 420 identical detached villas with services and facilities. The green area represents around 30% of the total project area.



Figure 4.39: English Village site plan – local and international investment project 2

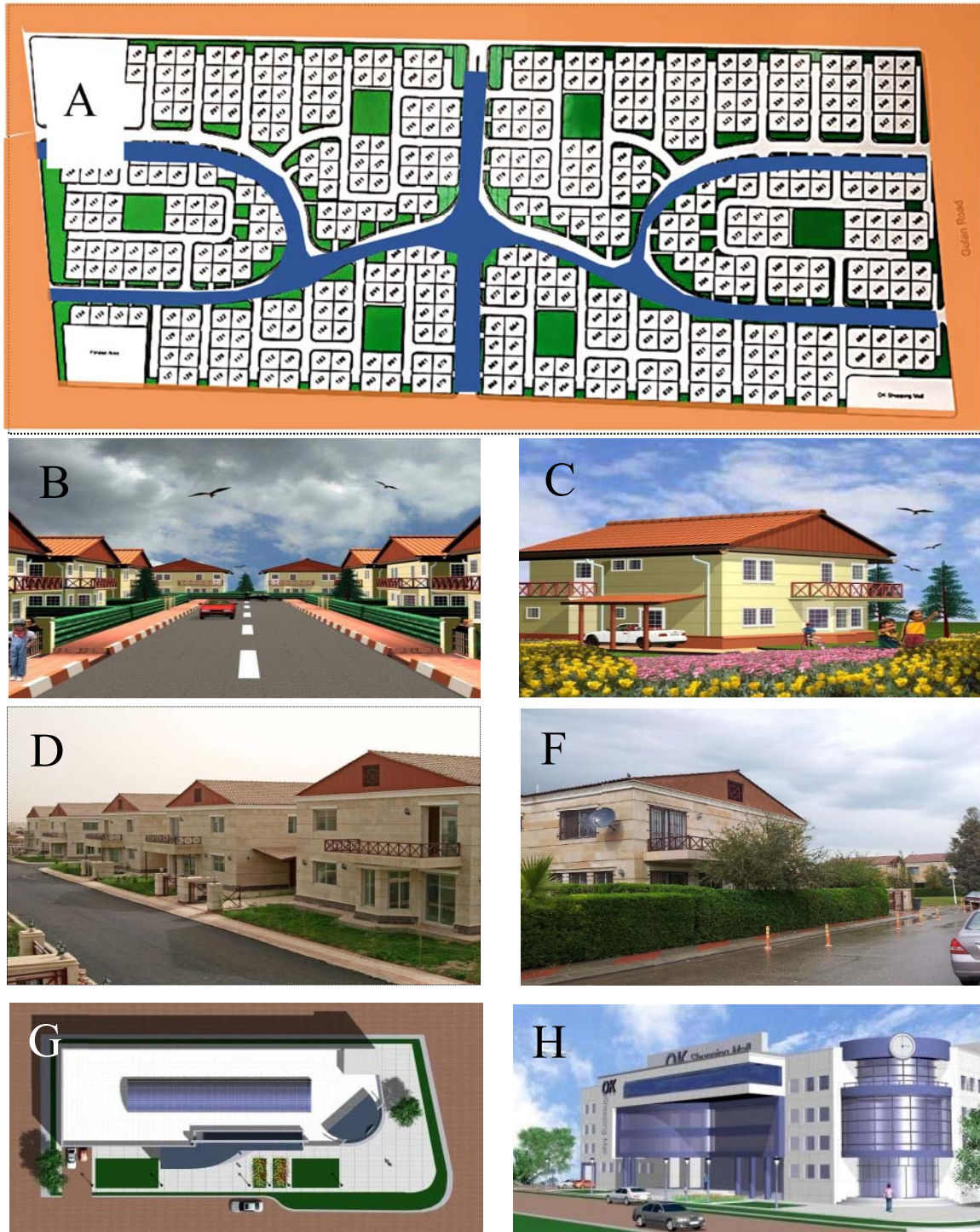


Figure 4.40: (A) The site plan of English Village and one type of individual villa (B, C, D and F) showing there is no fence between the villas. (G, and H) the supermarket at the project site

The site plan design represents an English design style influenced by a design company based in the UK (J.M. Jones and Sons). Most of the housing projects in Erbil are grid-iron style with just two axes, X and Y. This project attempted to reflect the English lifestyle and design using a disrupted street grid, which would help to attract investors and families to buy these villas. The style of the houses and road network is different from other housing project patterns and the local patterns of the old city in the city centre (the citadel). The planning style is western,

which separates equal open green areas between housing blocks. The road networks do not rigidly follow X and Y grids, as the government designed projects do. The percentage of open spaces and the green area ratio are acceptable compared to the buildings area ratio. The minimum green area should not be less than 30% for residential projects, and this project has an open green ratio represent of around 30% of the total project area (Figure 4.39).

The architecture and urban planning design concept was developed from constructing a secure residential environment, starting with the main entrance axis and separating into right and left side branches. The main axes divided the block of houses into two equal parts with similar housing units and blocks. The English Village housing project reflects the idea of the western style in terms of housing blocks, open spaces, road networks, and building design and architecture style. The houses are separated from the street via a soft fence (greenery), and this is unique among the other housing projects in Erbil (Figure 4.39).

The main features of project are:

- The site plan contains only one type of housing unit and only one plot size, unlike other projects, which have at least two plot sizes.
- Each housing unit (villa) is surrounded by a green area to increase green and open spaces.
- Most housing villas face each other, depending on the road network, and the idea of the designer was to increase the green area by connecting housing units and roads via green areas (greenery fence) (Figure 4.40).
- Although the site plan was designed without consideration of the local environment, such as solar radiation and wind originations, the villas were designed to resist local environment through high quality building materials.
- The orientation of the housing blocks and green areas does not follow the X and Y axes and boundary line roads, like other housing projects (Figure 4.39).
- The residential blocks are not one standard shape repeated throughout the site plan, but it works as a system that has one, two, four, six, eight, and ten villa plots (Figure 4.41).
- The project considered the environmental factors in terms of the housing units by using high quality materials, and also used some urban planning strategies such as open space and green areas.

4.7.2.1 English village Climatic conditions/observations

This project reflect the western style in term of urban planning and housing unit (Figure 4.40). This happen because two main reason; firstly to attract investors and high class families to buy these villas, and secondly it's designed by J.M. Jones and Sons design company based in the UK. The project mainly constructed with high quality materials and using a disrupted street grid instated of grid-iron morphology. The housing unit surrounded by green area and used truss ceiling. The project mainly not designed based on local environmental consideration, but it has high percentage of green area compare to government projects. This type of projects needs environmental urban consideration and calculating total energy demands for each housing unit. This help to employ the local environmental strategies during construction and after construction process.

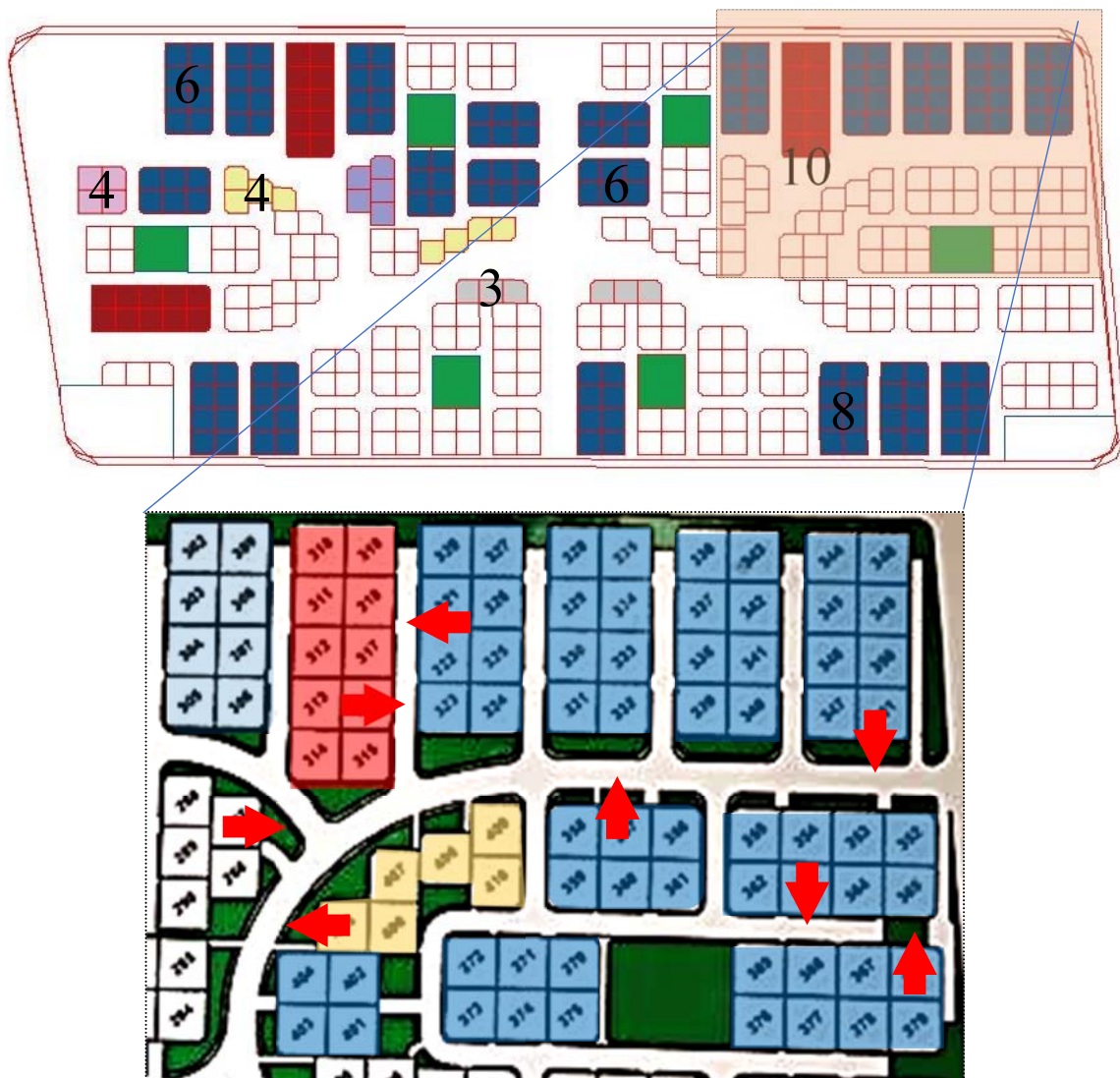


Figure 4.41: English Village housing unit type

4.7.3 Italian City 2

This project is located in the north east of the city and has an area of 750,000 m² (Figure 4.42). Italian City 2's position is 6.53 km west of the citadel. As in Italian City 1, this project is a well-known private housing project designed and built with the investment of a private local company (Figure 4.42). The Italian City-2 designed and constructed by local company, *Hemn Group Companies*. The company invested in two housing projects, Italian Cities 1 and 2, the project consists of 1,561 housing units on the 120 ring road, which is a newly built ring road. The housing units have plot sizes of 200 m², 240 m², and 320 m².

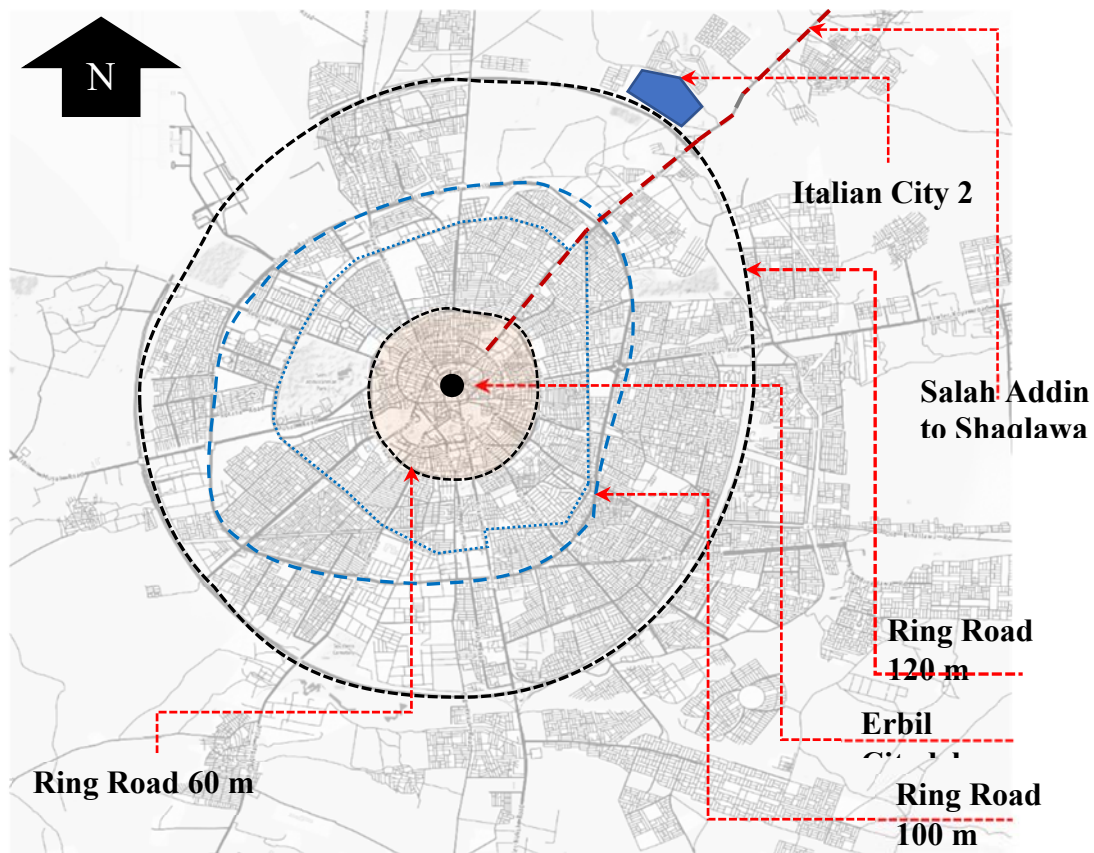


Figure 4.42: Italian City 2 – the location of the project in the city site plan

The project started in 2012 and was finished in 2015. Moreover, the project location distinguishes itself compared to other residential projects, as it is directly positioned on the 120m ring road. This position provides easy access to any location in the city and a direct connection to the city centre via the 120 ring road and Shaqlawa Road from the north of the city (Figure 4.43).



Figure 4.43: Italian City 2 site plan – local and international investment project 2

The project is surrounded by four roads and green belt from the main entrance side (Figure 4.44). In contrast with Italian City 1, the site plan of this project divides the housing blocks into vertical and horizontal objects (Figure 4.44). Most type A houses have 320 m² or more and are located at the beginning of blocks, as the variable area of plots is caused by irregular shapes, while house types B and C are located in the middle of the project. Type A houses are located on the wider 15m street, and types B and C are on narrow 12m streets (Figure 4.44). The project has a high density building ratio (650,000 m²) and a low density of green and open spaces (100,000 m²).

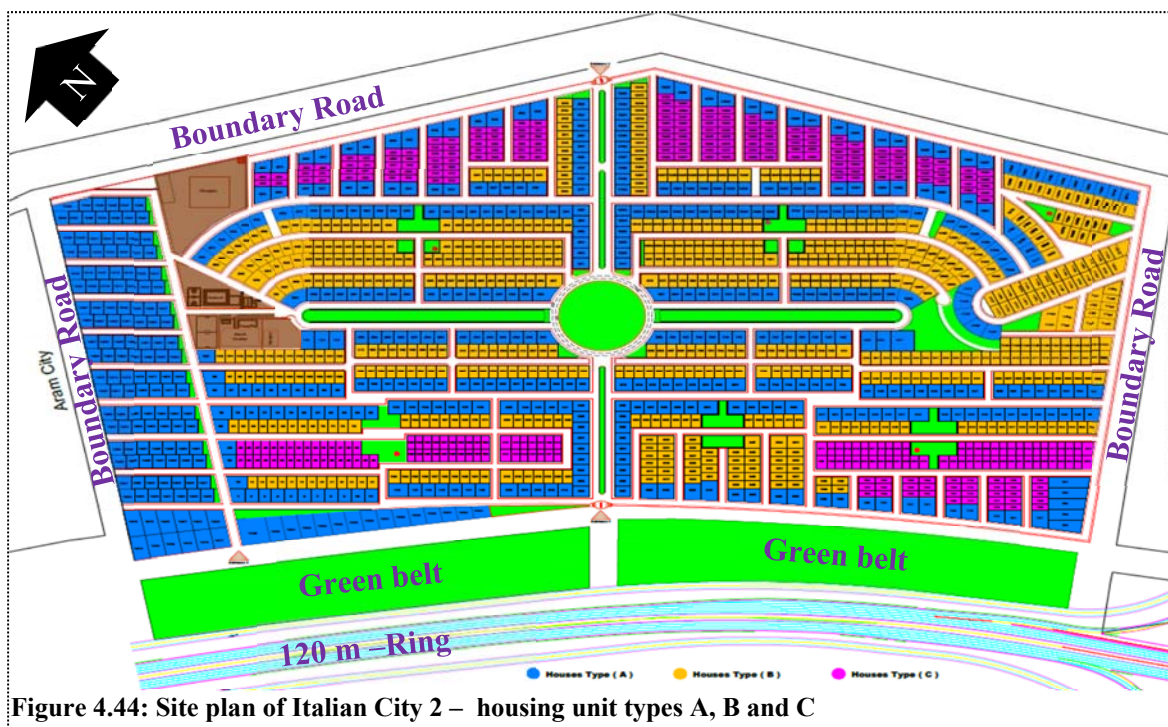


Figure 4.44: Site plan of Italian City 2 – housing unit types A, B and C

The city consists of attached and detached housing types, and services and facilities, as below:

Housing Plots	Number of Houses	Area of Plots	Housing Type	Colour
House Type A	569	320 m ²	Detached housing	Blue
House Type B	657	240 m ²	Attached housing	Yellow
House Type C	323	200 m ²	Attached housing	Purple
Green Area		+/- 100,000 m ²		Green
Services		21,022 m ²		Red



Figure 4.45: House types A, B, and C, Italian City 2

The main features of the project are:

- The site plan contains three types of housing units and different average plot areas (Figure 4.46).
- Some housing blocks are surrounded by green areas to increase green and open spaces (Figure 4.44).
- Most housing blocks face each other, resulting in a high density of buildings (Figure 4.46). The designer's idea was to provide green areas adjacent to the ring road at the entrance to the project (Figure 4.45).
- The site plan was designed without consideration of the local environment, such as solar radiation and wind originations. The design blocks rotate in different directions horizontally and vertically.
- The design of the project was made with due consideration of the topography of the site, i.e. (the site plan respected the difference in the topographical levels of the land) (Figure 4.46).

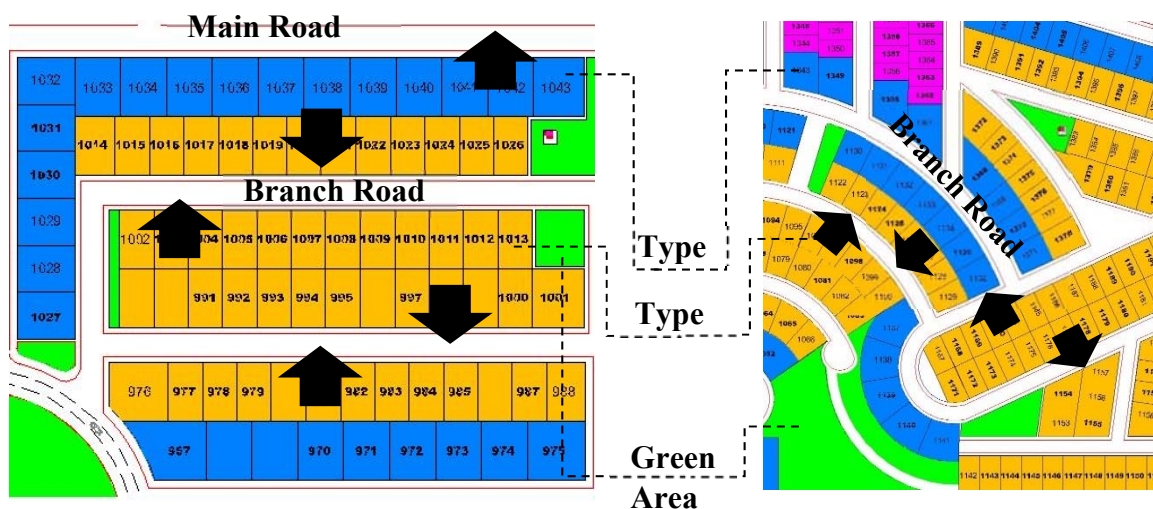


Figure 4.46: House types A, B, and C, Italian City 2 – blocks built facing each other

- The walls and ceilings are constructed with high insulation material to minimise heat and sound penetration. The exterior walls are covered with 50mm thick expanded polystyrene (EPS).
- The orientation of the housing blocks and the green areas follows the X and Y axes and boundary lines of roads, as in other housing projects (Figure 4.44).
- The streets divide the site plan into housing plots and a network of roads without any consideration of the prevailing wind direction or solar radiation. The site plan is designed as physical objects rather than environmental features (Figure 4.43).



Figure 4.47: Italian City 2 – recycled water used for irrigation



Figure 4.48: Italian City 2 – the consideration of the site's topography

- The residential block is not only one standard shape repeated throughout the site plan, but works as a system of network roads horizontally and vertically, with only one cul-de-sac (Figure 4.46).



Figure 4.49: Italian City 2 – Power station and water treatment plant on the project

- The project considered the environmental features in terms of housing units (building scale) by using insulation materials. In addition, the project used urban planning scale environmental strategies, such as for water treatment (Figure 4.49), and the electrical power plant. The waste water is divided into two types, heavy and light waste water; the light waste water from domestic usage is recycled to irrigate the green areas, of around 100,000 m² (Figure 4.47).
- The project design has attempted to adapt to the local urban environment in terms of the geographical topography of the site, the reduction of heat gains and losses (insulation materials), and by the provision of a local power station and water treatment plant (Figure 4.48).

4.7.3.1 Italy city 2 Climatic conditions/observations

From the design site plan, images, and semi-structured interview with the project manager of the construction company Hemn Group (Parow 2017), it is clear that this project considered environmental features in terms of housing units (building scale) and urban environmental strategies. This includes high insulation material to minimise heat and sound penetration⁷, water treatment, the local electrical power plant, and recycling waste water for irrigation (Figure 4.49). The project is considered one of the best in Erbil in terms of environmental features, but these environmental features are individual attempts and not based on specific research or a standard for Erbil or the region.

These types of projects need more environmental strategies, such as microclimate adaptation to housing block orientation. Microclimate simulation for an urban housing project before the construction stage is important to reduce the energy demand for each housing unit and project as well.

⁷ Hemn Group has a factory to produce the ready-to-use polystyrene building materials (EPS panels). This building material can be used for walls, roofs and partitions. The factory uses Italian systems and machinery which meet European standards. EPS panels is easy to install for construction, economic, high thermal energy saving, and sound insulator. (www.hemngroup.com)

4.7.4 Mass City

The project is located in the north east of the city and has an area of 1,054,720 m². Mass city is 8 km north east of the citadel (Figure 4.50). Like Italian City 1 and Italian City 2, this project is a well-known private housing project designed and built using private investment (Figure 4.50), and is a joint venture between local and international companies, the Trillium Group and Mass Group (Abu Hamad 2014). As a Trillium Group project, Mass City has 5,000 residential housing units in the north east of the city on the main road from Salah Addin to Shaqlawa. The project contains 11 house prototypes divided into five zones. The first zone is 400 villas started

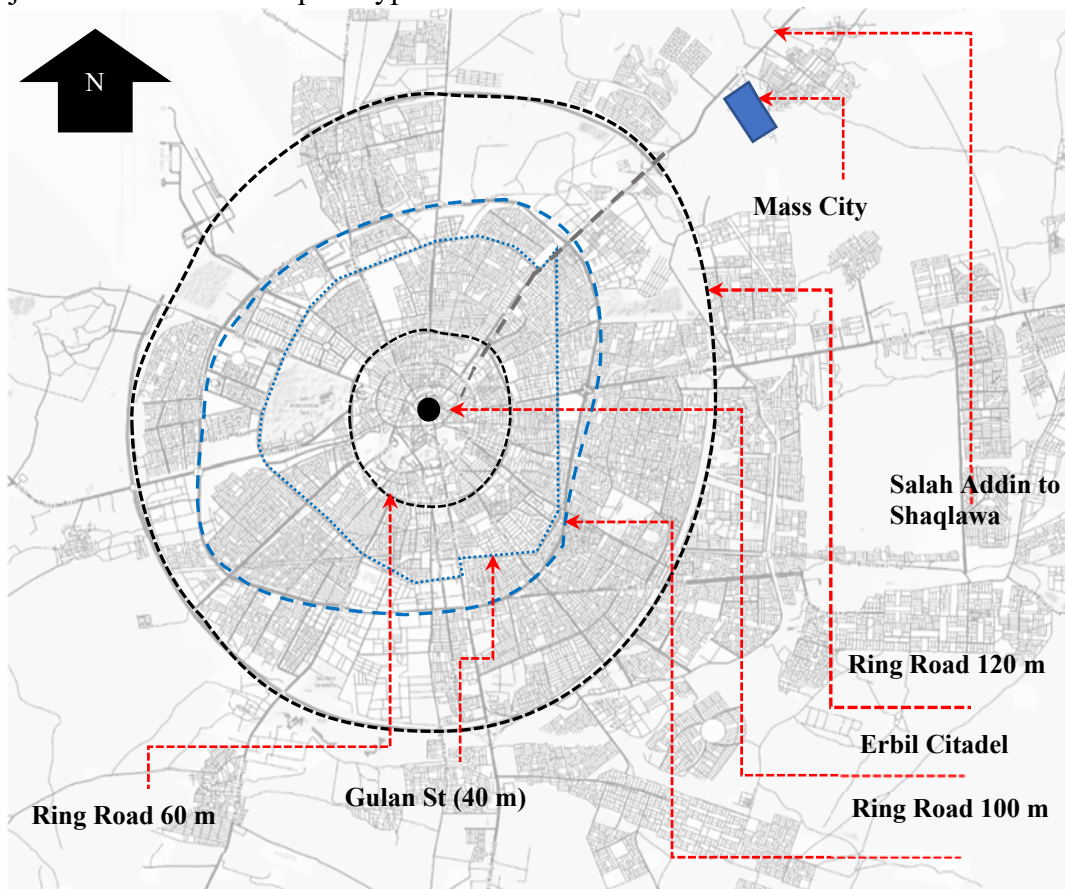


Figure 4.50: Mass City – the location of project in the city site plan and citadel

in 2013, and which were supposed to be finished in 2017 on a budget of \$1 billion. The project's concept maintains the local architecture of the city through using similar architectural features in its housing facades. In addition, the project used high quality materials and provided infrastructure services to the site (Figure 4.51).

4.7.4.1 Project Concept

The project is surrounded by green areas from all directions, which help to reduce sand storms during the dry season. The design utilises the natural land topography to site the housing blocks, green areas and open spaces, and this correct land management means the blocks are integrated

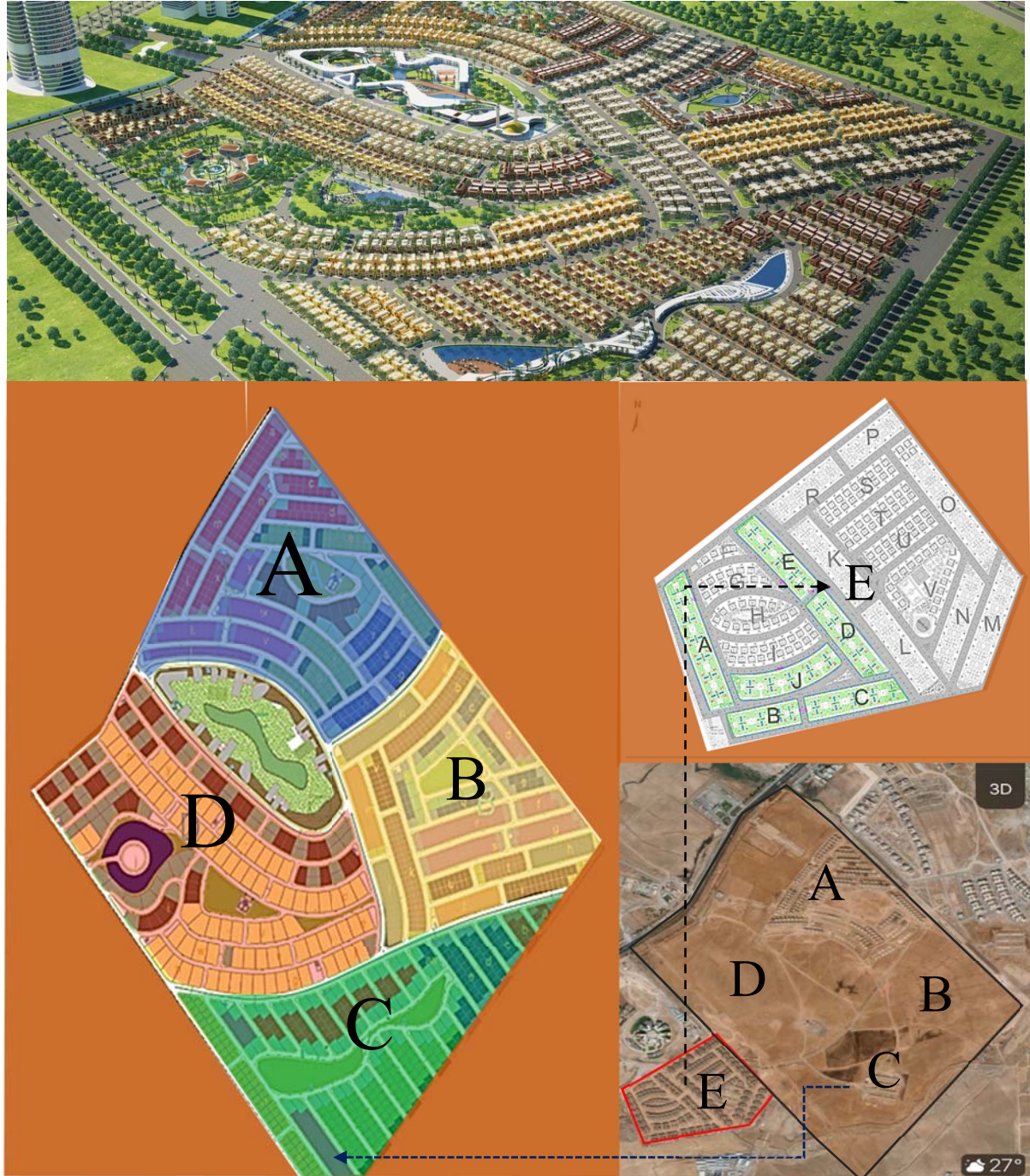


Figure 4.51: Mass City – local and international investment project 3

with other facilities in the project, such as green areas and public services (Abu Hamad 2014). The modern and western architectural style can be seen to a limited extent, as the housing block arrangements and wide roads contrast with the historic and local architecture of Erbil (Figure

4.51). However, individual housing units are a mixture of modern and traditional styles (Figure 4.52). The building materials and construction process used a modern method, but the local identity can be seen in the building façades. The designer borrowed architecture elements from houses in Erbil citadel and re-used them in housing façades (Figure 4.52).



Figure 4.52: Mass City – prototype housing units

There are 16 housing prototypes depending on plot areas of 240m², 320m², 600m² and 1000m², rather than the quality of the construction (Mass city 2019). Similar construction materials and techniques were used for all villa types, and these are targeted at medium and luxury home buyers. The villas are semi-detached and detached with building areas of 240–700m². The project includes other non-residential developments such as cafes and restaurants, a hospital, shopping malls, a school, and two towers with 30 floors. The design and construction process of this project was different from other projects in Erbil, as shown below:

1. Site adaptation

The project started with a site survey and geotechnical services to consider the natural and environmental elements of the site. The project is outside Erbil towards the north east of the city and the site is distinguished by hills and valleys, which were not flattened or filled in during the design process; these natural features were integrated in the design without any effect on the occupants' safety and privacy.

2. Construction Materials

High quality materials were used to construct the housing units, such as external insulation cavity brick walls and an insulated roofing system to reduce heat transfer in the hot summer. This helps to reduce heat gain during summer and heat loss in winter.

3. Concept of the Design

Local architecture details were employed through the repetition of the traditional façade elements borrowed from Erbil citadel houses (Figure 4.52).

4. Infrastructure

The project provided a high level of infrastructure for all housing units. These services include road networks, water supply, a reservoir and pump station, a sewage network, a water treatment plant, waste management, a storm management system, electrical works, firefighting, an IT network, and a security, safety and control system.

The main features of the project are:

- The site plan contains four types of plot and 16 prototype housing units (Figure 4.52).
- The housing blocks are surrounded by open green area to increase green and open spaces (Figure 4.51).
- Most housing block units face each other and there is a low density of building (Figure 4.52). The idea of the designer was to increase the green areas and open spaces (Figure 4.52).
- The site plan was designed without consideration of the local environment, such as solar radiation and wind origination. The design blocks are rotated in different directions and axes depending on the natural features of the site.

- The design of the project was made with due consideration of the topography of the site, i.e. the site plan respected the differences in the topographical levels of the land (Figure 4.52).
- The walls and ceilings are constructed with high insulation material for heat and sound protection. The exterior walls are 240mm masonry brick covered with 50mm thick EPS.
- The orientation of housing blocks and green areas does not follow the X and Y axes and boundary line roads as in other housing projects (Figure 4.52), but does follow the natural features of the site.
- The residential blocks are not just one standard shape repeated throughout the site plan, but work as a system of network roads following the natural features of the site.
- The project considered the environmental features in terms of housing units at the building scale by using insulating materials. In addition, the project used urban planning scale environmental strategies, such as water treatment and an external electrical power plant of 2500 kw.
- The project attempted to adapt to the local urban environment in terms of the geographical topography of site, reduction of heat gain and loss of housing insulation materials, open green areas, blue areas (fountains), and high quality infrastructure services.

4.7.4.2 Mass city Climatic conditions/observations

From the design site plan, images, and semi-structured interview, the project considered the environmental features for both urban and housing unit scale. This includes adaptation of the site plan to the natural topography of the land, and high quality infrastructure (road network, recycling wastewater, and waste management) (Abu Hamad 2014). In addition, the housing unit reflects Erbil's traditional housing features in terms of façade only, while building materials are modern (reinforced concrete) (Figure 4.52). In term of adaptation with local environment, the project consider one of the best project in Erbil city compare to government and other private projects. In addition, the project employed many environmental strategies during design and implantation process, but these strategies are not depend on specific research or design expertise (Microclimate wind and air temperature). These type of project needs intensive research and simulation on both scales (Urban and Building) to estimate the total energy consumption and how environmental strategies can reduce the cooling energy during the summer and heating energy during winter.

4.8 Comparison between Government and Private Projects

This section compares private and government projects in Erbil. These two types of housing projects are similar in some ways, but have major differences. Mainly, the government projects are concerned with the division land and provision of initial infrastructure (roads, water, and electricity). The housing units (plots) were designed by the occupant (self-design and built) or self-employed architects, which results in an urban fabric of different styles of housing units in terms of shape, size, design elements, and finishing materials. These types of project cannot be controlled by the government and the plot owner has as a high degree of flexibility of design preferences (plans and façades), social and psychological preferences, economic preferences, building techniques and materiality (Omer, 2018), and construction time limit. Most of these government projects for housing units have local authority approval (i.e. a building licence), which is assessed by the local municipality based on the building requirements (see Appendix C). The government's building licence is a requirement based on basic urban planning guidance, such as setbacks, open space sizes, and the height of housing units, without any consideration of the architecture details relating to the building environment or local architecture identity (design elements).



Figure 4.53: Government housing project in Erbil city, different housing design, height and building materials

Therefore, government project housing units are different in terms of design, architecture elements, and façades, and can be described as raw housing without a specific identity or unity of appearance (Figure 4.53). On the other hand, the private housing projects can be described as a more systematic process of design and construction (See section 4.8). The housing units in private projects are designed and constructed by consultant offices or private architecture companies, and this resulted in a unified style of housing unit in terms of design (plans and façade) and construction materials. Private housing projects are controlled by three working bodies; the Investment Department, Consultant Office, and the investor company, all of which help to unify the housing project in terms of the design approach, building technique, and construction time. Private housing projects have a different approach to designing housing units as described in the previous sections, and all housing project designs must be approved before any construction process starts (KRG Investment Board, 2017). Although the process of approval of private projects does not include the building environment and local architecture identity elements during the process of the design, project approval, or project construction, the housing units are more unified than the government projects regarding the design, façades, building materials, and infrastructure (Figure 4.54).



Figure 4.54: Private housing project in Erbil, with similar housing design, height, and building materials

Table 4.1 contrasts the similarities and differences of private and government housing projects designed after 2003 in Erbil.

Table 4.1: Government and private projects in Erbil

Criteria	Government Projects	Private Projects
Process of Design	<ul style="list-style-type: none"> • Covers site plan design stage • Distributing lands and plots and main services (zoning design) • Design by mostly government staff 	<ul style="list-style-type: none"> • Covers both the site plan design and detail design for construction stage • Distribution of lands and detail design for all buildings and integrated infrastructure • Design by private construction company or consultant office
Implementation	<ul style="list-style-type: none"> • Does not include construction stage (not systematic process) • No maintenance plan for the future 	<ul style="list-style-type: none"> • Includes the construction stage (systematic process of design, construction, and operation) • Maintenance plan for the future
Design Elements	<ul style="list-style-type: none"> • The housing units are different in the design and construction materials used 	<ul style="list-style-type: none"> • The housing units are united in the design and construction materials used
Project Time Limit	<ul style="list-style-type: none"> • There is no time limit for finishing the project. Each housing unit starts and finishes independently 	<ul style="list-style-type: none"> • The time limit for finishing the project is considered and controlled by the Investment Department
Urban Design Elements	<ul style="list-style-type: none"> • Highly influenced by modern and western planning (grid-iron morphology) 	Highly influenced by modern and western planning (Italian City 1, and 2), and there are attempts to have the design fit into the local identity (Mass City)
Open Space to Buildings Ratio	<ul style="list-style-type: none"> • Housing units' green areas not controlled by government and designers (no guidance) 	<ul style="list-style-type: none"> • Controlled by the Investment Department and designers (open spaces and green areas \geq 30%)
Individual Housing Design Elements	<ul style="list-style-type: none"> • Not controlled by local authorities and municipalities (various plans and facades) 	<ul style="list-style-type: none"> • Controlled by the Investment Department and has similar plans and facades.
Construction Materials	<ul style="list-style-type: none"> • Not controlled by government and local authorities 	<ul style="list-style-type: none"> • Controlled by the Investment Department

	<ul style="list-style-type: none"> • Various types of materials have been used depending on economic, social and psychological preferences (no guidance) 	<ul style="list-style-type: none"> • Specific type of building materials used or may vary depending on housing type in the project (no guidance)
Infrastructure	<ul style="list-style-type: none"> • Basic infrastructure • No basic infrastructure used in some government projects 	<ul style="list-style-type: none"> • Integrated infrastructure is required by the Investment department before the construction process • Water treatment plants and power stations can be seen in some private projects (Italian City 2)

Table 4.1 above shows that both private and government projects have similarities and differences in the design and construction process. The main differences between both types of project are that government projects focus on the division of housing plots (the zoning plan) and may provide the initial infrastructure (water and electricity), but the private projects are concerned with the systematic design and construction process of the housing units and providing an acceptable level of infrastructure compared to the government projects (water treatment plants and power stations). However, both types of projects used grid-iron morphology and a western approach in the design of the site plan. The main similarity for both government and private projects is the lack of or limit to the environmental approach or local microclimate consideration during the design and construction process at both urban and building scales. Missing government regulations and guidance on housing projects for both government and private projects led to a lack of control over the buildings, urban environment, and application of environmental strategies.

4.9 Conclusion

This chapter describes and analyses the housing projects built in Erbil after 2003. Three types of resources were used: semi-structured interviews, government documents, and case studies. Two types of housing projects were used as case studies, government and private, to show the similarities and differences between housing projects in terms of the application of the process of design and construction.

These projects demonstrated some similar steps in terms of the urban design process, such as land acquisition and the master plan approval stage, although they have different approaches in the urban design and approval process. For instance, the private projects included a construction step while the government Projects focused only on the design of the site plan and distribution of the housing plots.

Housing project designs in Erbil have mainly been influenced by western urban design approaches (grid-iron) without any consideration of the local architectural identity. The alignment of grid-iron morphology has been driven by geometry rather than local urban microclimate needs.

This chapter has shown that consideration of the microclimate was not employed during both the urban design and housing construction process. Although the private projects attempted to employ local architectural elements in Mass City, used environmental elements such as water treatment plants and power stations in Italian City 2, and used insulation building materials in Italian Cities 1 and 2, these attempts were individual efforts without government guidance or practical research to address the building environment problems during the design and construction process of housing projects.

As Erbil has experienced rapid urban expansion, the absence of government environmental regulations and guidance has led to the urban fabric being exposed to the harsh climate, especially during the summer months. Therefore, in the next chapter of this study, the research simulates and predicts climatic variables in the modern grid-iron housing block pattern to address the local microclimate issues of the urban design in the city. An ENVI-met simulation is used to identify the wind speed, orientation, and air temperature between the buildings.

Chapter 5 Urban Microclimate Validation

5.1 Introduction

Erbil witnessed rapid expansion after 2003 as a result of socio-economic and geo-political factors. The urban area in the city developed by way of government and private housing projects. However, the developments were designed and constructed without consideration for the local urban microclimate or local design features that were used in the historical architecture of the city. The aim of this chapter is to investigate the urban microclimate of modern urban morphology and strategies to reduce the impact of outdoor urban microclimate on open spaces which surround buildings. The first section of this chapter determines and Analyses four weather data stations. These weather data stations are located in various urban density areas: low, medium, high and rural areas. Air temperature, Wind speed and Relative humidity were compared and analysed. These data were used as input data to simulate the local urban microclimate of the city using ENVI-met. The second section validates the ENVI-met model. This study chose two case studies in high and medium density urban areas for the validation process. The validation process in this study used two methods; specifically, a direct comparison between measured and modelled air temperature, and Willmott's methodology (Index of agreement). The third section pertains to the microclimate modelling of traditional and modern morphologies. Air temperature and wind speed were compared as a result of the simulations. Subsequently, wind speeds for a modern urban area using three scenarios of wind direction 180°, 225° and 270° from the North were modelled. This simulation aims to understand the wind behaviour in open spaces and urban canyons.

5.2 Weather data stations in Erbil city.

Data from four weather stations in Erbil were investigated, specifically the north, airport, central and south weather data stations (Figure 5.1). These weather stations are located in different densities of urban development, representing lightly developed, minimal development, heavy development and medium development, respectively. The weather data stations belong to the Ministry of Agriculture, which collects data every 15 minutes, except for the airport weather data which is obtained from an online source. The accuracy of the weather data and its location is important to evaluating the local microclimates using ENVI-met. Therefore, this research compares four sources of data to simulate the base case scenario. The location of each weather data source and other details are shown in chapter 3 section 3.6.



Figure 5.1: Four Weather Data Station locations in Erbil City

5.2.1 North weather data station

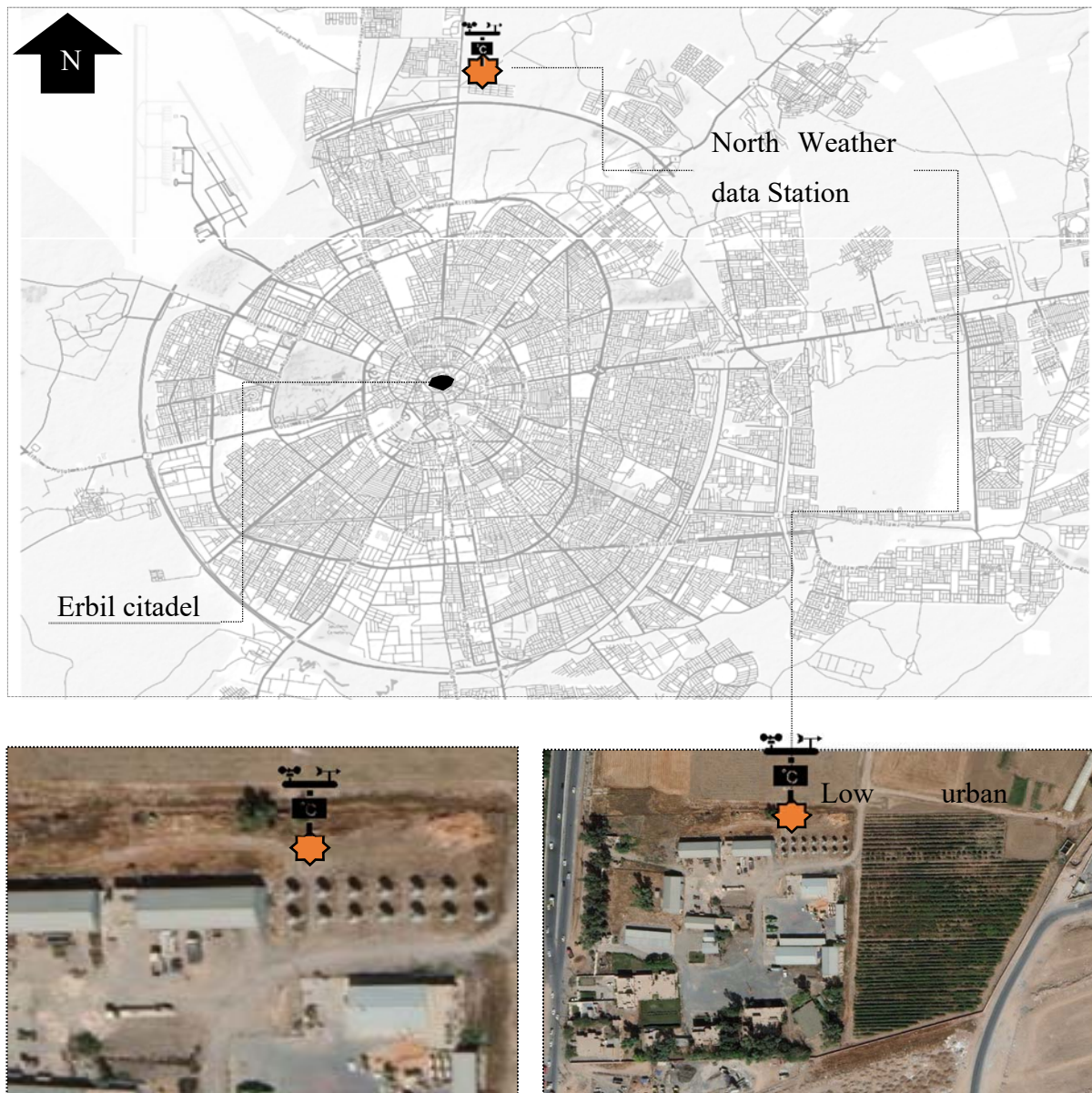


Figure 5.2: North Weather Data Station in Erbil City

The north weather data (NWD) is located in a low density urban area used for crops and agricultural purposes. The station is located in an open area surrounded by a few buildings and agricultural fields (Figure 5.2).

5.2.2 Airport Weather Data Station

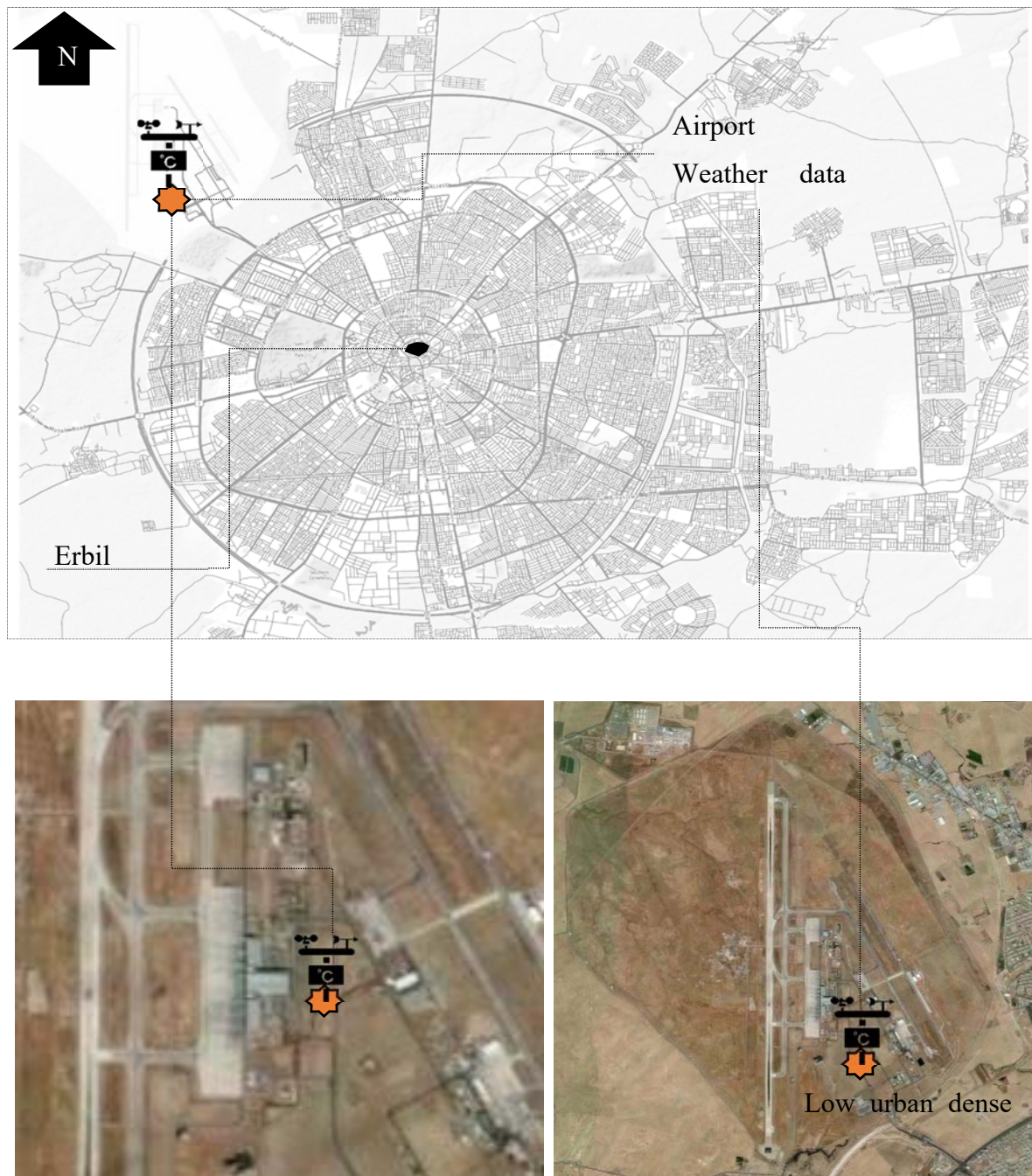


Figure 5.3: Airport Weather Data Station in Erbil City

The station is located inside the airport area, on the edge of the city (Figure 5.3). The urban density at the airport and surrounding area is considered low. Therefore, the station is important for air navigation, but does not represent Erbil's urban microclimate environment.

5.2.3 Central weather data station

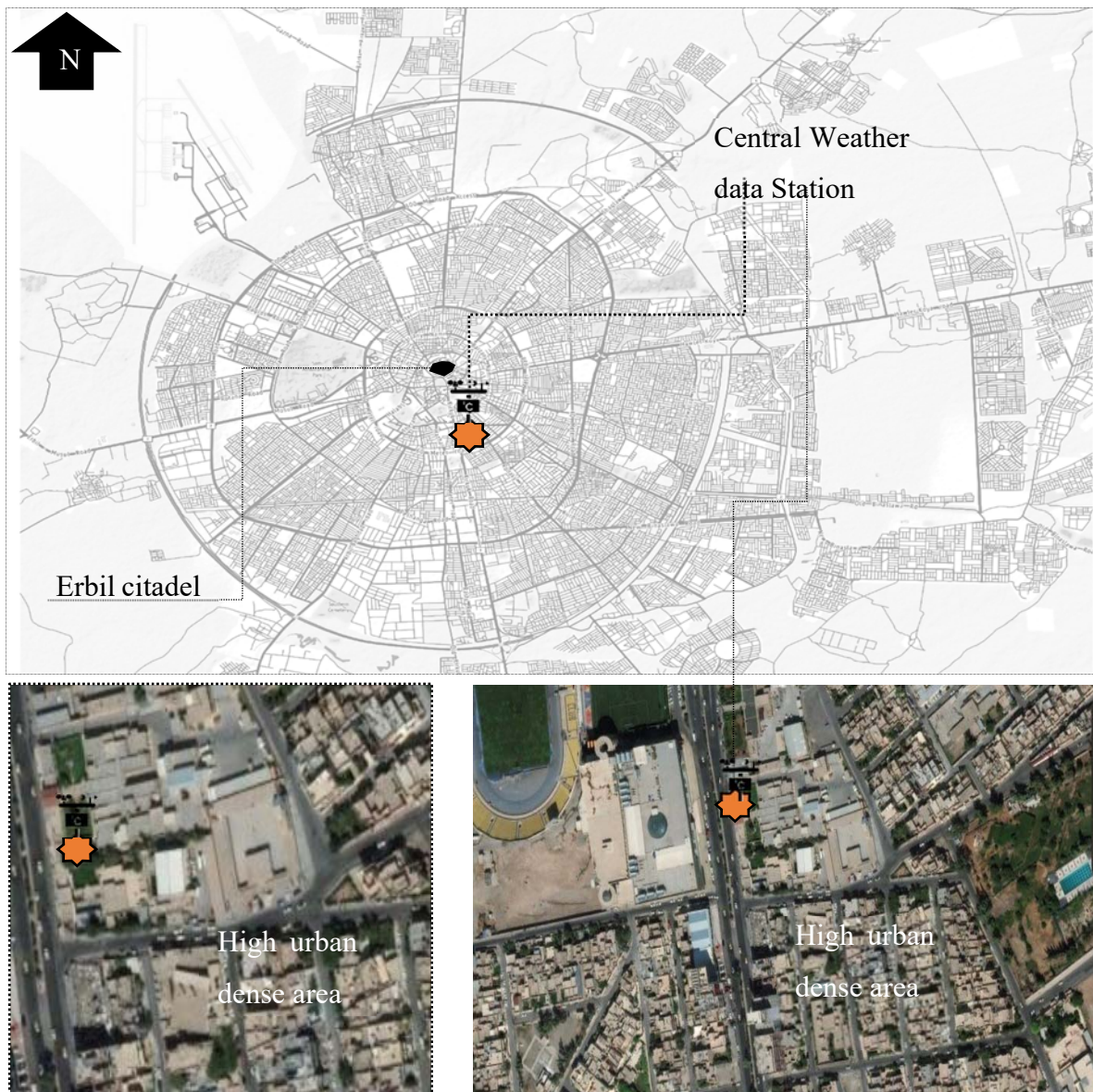


Figure 5.4: Central Weather Data Station in Erbil City

This station is situated within a high density urban area. The data are used for agricultural studies and other research (Figure 5.4). CWD is located in a well-established urban area near the city centre, surrounded by traditional urban morphology in the north, a few open green areas in the east and west, and high density residential urban areas in the south and north-east. In general, the location of the station represents the real urban microclimate of Erbil (Figure 5.3).

5.2.4 South Weather Data Station

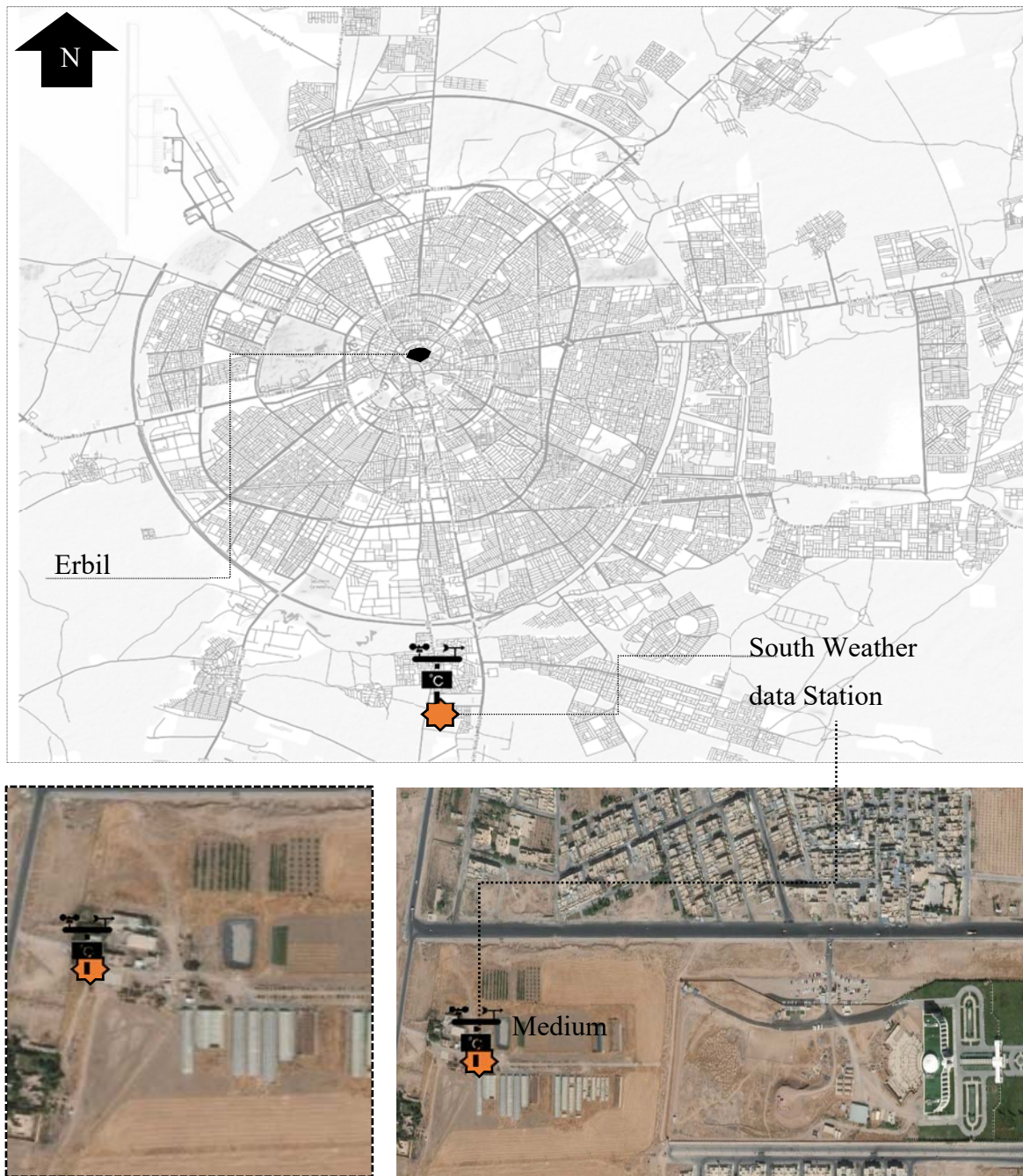


Figure 5.5: South Weather Data Station in Erbil City

The location is considered a medium density urban area and the data are used to serve agricultural crops in the south of the city (Figure 5.5).

5.2.5 The quality of data and locality in urban context of Erbil

The reliability of data can be seen through minor differences pertaining to data in all four stations. However, the south station data came with systematic errors related to day-night timing, and hence were corrected¹. The three weather data stations (south, central and north) were originally installed by a company from the US using modern sensors and data loggers. No information is available about sensors or the company that installed the airport weather station. Air temperature, wind speed, relative humidity, air pressure, rainfall, specific humidity, and soil temperature were measured. The measurement interval used was every 15 minutes for the hot summer months of June and July for the four years between 2013–2016 (Table 5-1). June and July is peak summertime, when the air temperature reaches 44 °C.

¹ The correction needed was to adjust to data collection time such that the maximum day time temperature occurred at the same time as the Northern and Central weather stations.

Table 5-1: shows the weather data package.

TOA5	CR1000	CR1000	2889	CR1000. Std.06	CPU:ERRA S002.CR1	8149	MIN_15										
TIMES TAMP	REC ORD	ID	Prog ram	Batt_Volt_Min	AirTC	AirTC_Max	AirTC_Min	RH	BP_mbar	WS_m/s_Avg	ws_gust_Max	ws_gust_TMx	WindDir	SlrkW_Avg	SlrMJ_Tot	SoilT10_C_Avg	Rain_mm_Tot
TS	RN			Volts	Deg C	Deg C	Deg C	%	Millibars	meters/second			Degrees	kW/m	MJ/m	Deg C	mm
		Smp	Smp	Min	Smp	Max	Min	Smp	Smp	Avg	Max	TMx	Smp	Avg	Tot	Avg	Tot

The symbols for weather data package explained in detail in appendix J. These data are used as input data for ENVI-met program to propose new design scenarios that may modify both air temperature and wind speed in urban areas of a city with a hot/dry climate. For this reason, this section will interpret three climate elements in Erbil and compare all four stations. Regarding the four weather stations, three weather measurements will be presented.

1. Air temperature
2. Relative humidity
3. Wind speed.

5.3 Microclimate Measurement:

In this section, daily average air temperature (Ta), relative humidity (RH), and wind speed (WS) are presented for the summer of 2015. In addition, summaries of monthly Ta, RH and WS were compared for all stations. This section analyses weather data to understand and choose appropriate input data to represent the local urban microclimate of the city.

5.3.1 Air Temperature

These data was obtained from measurement points (Figure 5.1.). (Figure 5.2 to Figure 5.3), in four different urban densities (very low, medium and high) in Erbil (Figure 5.5). The data reveal that there are differences in average air temperature between the northern, central and southern weather stations compared to the airport weather station (Figure 5.6), which is positioned in a very low density urban area. These differences in Ta between locations could be because the urban density varies between locations, and the central weather station is surrounded by a high density urban area in contrast to the north and south weather stations.

The maximum daily Ta was 40.21 °C at the weather station in the north, while the minimum Ta was 27.15 °C for the airport weather station (Figure 5.6).

The data from the airport weather station were in poor agreement with other stations and recorded a lower average Ta for the month of July. This could have occurred because the other three weather stations have similar sensors for collecting data or the local microclimate of the airport weather station includes a very low urban area compared to the other three stations (high, medium and low). The airport weather data represents the microclimate of Erbil Airport only and might require correction factors when used as input data to represent the local urban microclimate (Bourikas, James et al. 2016). From this viewpoint, average hourly, daily and monthly data for all weather stations data were analysed.

In terms of the impact of Built-up Area (BUA) on urban microclimate within different urban densities, hourly air temperatures (Tah) were analysed (Figure 5.6). The data in Figure 5.6 show average Tah for all four weather stations from 00:00 to 23:00. The airport and northern weather stations have similar day profiles, reflecting low urban developments, while the southern and central weather stations have similar day profiles reflecting higher urban developments.

The maximum air temperature was 45.88 °C at 16:00 at the northern weather station, while the minimum air temperature recorded was 22.7 °C at the northern weather station; the central and south weather stations had similar values for air temperature (Figure 5.6). Many studies have been completed on the effect of Urban Heat Islands and how urban areas are hotter than rural areas. The airport weather station recorded almost similar patterns to other stations during daytime, while during the night it recorded lower Ta (Figure 5.6). This may possibly be related to urban density and the effect of the heat mass of the buildings, as a similar pattern was also displayed for the northern weather station, reflecting the low urban densities at this location.

Table 5-2: Maximum and minimum air temperatures in July 2015 for the four stations

	North	Central	South	Airport
Max- Tah	45.88 °C	44.32 °C	43.88 °C	49.5°C
Min- Tah	22.7 °C	29.13 °C	27.98 °C	17.2°C
ΔTah	23.18	15.19	15.9	32.3

The maximum hourly air temperature difference (ΔT_{ah}) was 32.3 °C, recorded at the airport weather station with very low urban density. This difference represents how the radiation energy from the sun increases the air temperature in urban areas during daytime compared to

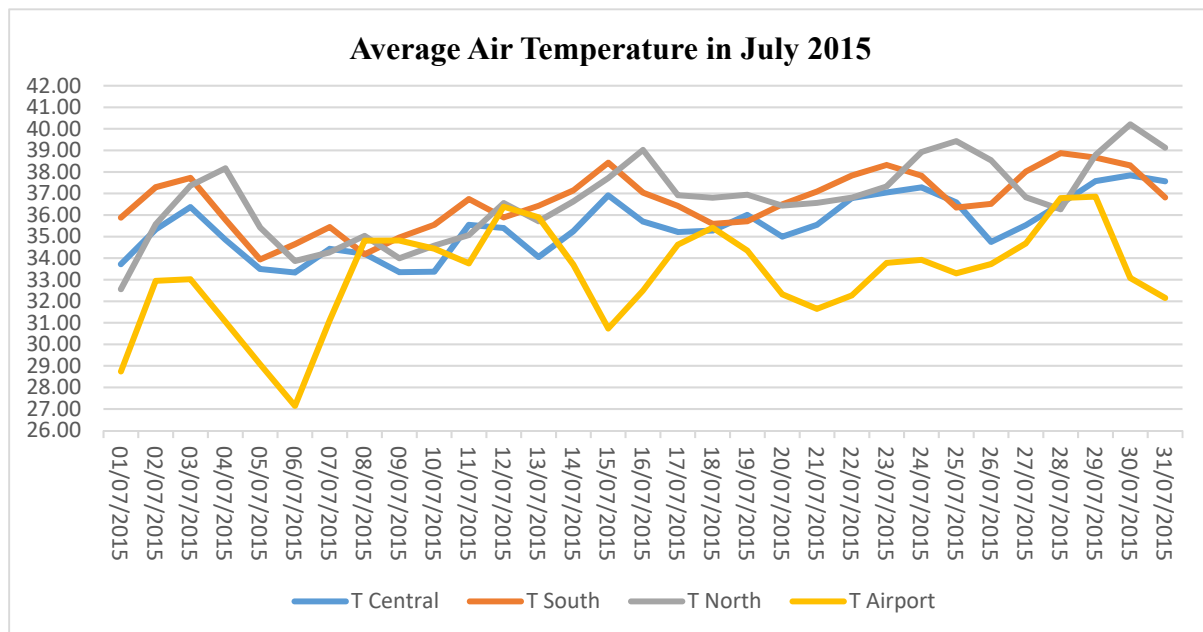


Figure 5.6: Average air temperature for Northern, Central, Airport and Southern stations

night time (Table 5-2). This variation in air temperature was observed to be less at the central and southern weather stations for 24 hours (Figure 5.5), because an urban area microclimate is slightly cooler during daytime owing to shaded areas from urban elements and higher relative humidity. This result corresponds with Denise (2015), who assessed the micro scale cooling effect of vegetation in urban environments (Duarte, Shinzato

et al. 2015) and (Chatzidimitriou and Yannas 2015). As would be expected, different temperatures were recorded by all four weather stations. To explore these differences further, the measurement error needs to be declared. As the error in measurement of the northern, central and southern weather stations is known, comment can be made on the significances of the differences between individual measurements from these stations

Table 5-3: Hourly average, maximum and minimum air temperatures for four weather stations 1 July 2015

Time	Ta °C North Station	Ta °C Central Station	Ta °C South Station	Ta °C airport Station
00:00	27.5	34.47	34.92	24.4
01:00	28.27	33.44	32.35	28
02:00	26.39	31.48	32.31	27
03:00	23.98	30.66	30.92	26
04:00	22.81	30.19	29.6	25.1
05:00	22.7	29.13	27.98	24.8
06:00	23.51	30.22	28.18	24.3
07:00	30.62	31.89	28.58	26
08:00	33.35	34.22	28.49	29.4
09:00	37.23	34.88	32.53	33.1
10:00	39.86	38.56	34.75	38.6
11:00	41.53	39.81	38.58	42.5
12:00	43.22	41.86	40.11	41.5
13:00	44.4	42.98	41.46	41.8
14:00	45.11	43.89	42.45	42.2
15:00	45.55	44.29	42.78	42.8
16:00	45.88	44.32	43.11	42.3
17:00	44.81	43.43	43.6	41.8
18:00	43.46	42.63	43.88	41.1
19:00	41.14	41.07	43.83	39.7
20:00	38.71	39.18	43.18	32.8
21:00	34.24	38.4	41.13	27
22:00	32.93	36.8	38.24	25.6
23:00	30.53	36.02	35.66	24.8
Average	35.32	37.24	36.61	33.03
Mix	45.88	44.32	43.88	42.8
Min	22.7	29.13	27.98	24.3
ΔT_{ah}	23.18	15.19	15.9	18.5

At peak air temperatures, the sensors error is $\pm 0.65\text{k}$ (for 45°C). When comparing two sensors with an error associated with the measurements, a root mean square approach is used (Pentz 1988). When comparing these temperatures, the comparative error will be $\sqrt{2} \times 0.65 = 0.92\text{k}$. In other words, if the temperature difference is equal to or less than the error differences, we can confirm that both sensors are recording the same temperature.

The maximum hourly average air temperatures (Table 5-3), for the northern, central and southern weather stations were 45.88°C , 44.32°C and 43.83°C , respectively. Statistically, the central and southern weather stations recorded the same temperatures. However, the northern station is recording statistically higher temperatures than the central and southern stations. The difference in temperature is 1.56 and 2.05K. When examining the minimum temperatures, wider variations in temperature are observed. However, the error of the individual sensors is temperature dependent and a different comparative error needs to be calculated.

The minimum temperatures for the northern, airport, central and southern weather stations are 22.7°C , 24.3°C , 29.13°C and 27.98°C , respectively (Table 5-3). The differences in minimum air temperature exceed the 0.7 K (the error at 27°C) value so there is confidence that the weather stations are recording different minimum air temperatures.

The denser urban areas have higher temperatures than the less dense urban areas, with the central weather station recording the highest minimum temperature, reflecting its surrounding urban densities. This demonstrates the Urban Heat Island (UHI) effect, where the more developed locations, central and southern, do not cool to the same extent as the rural northern

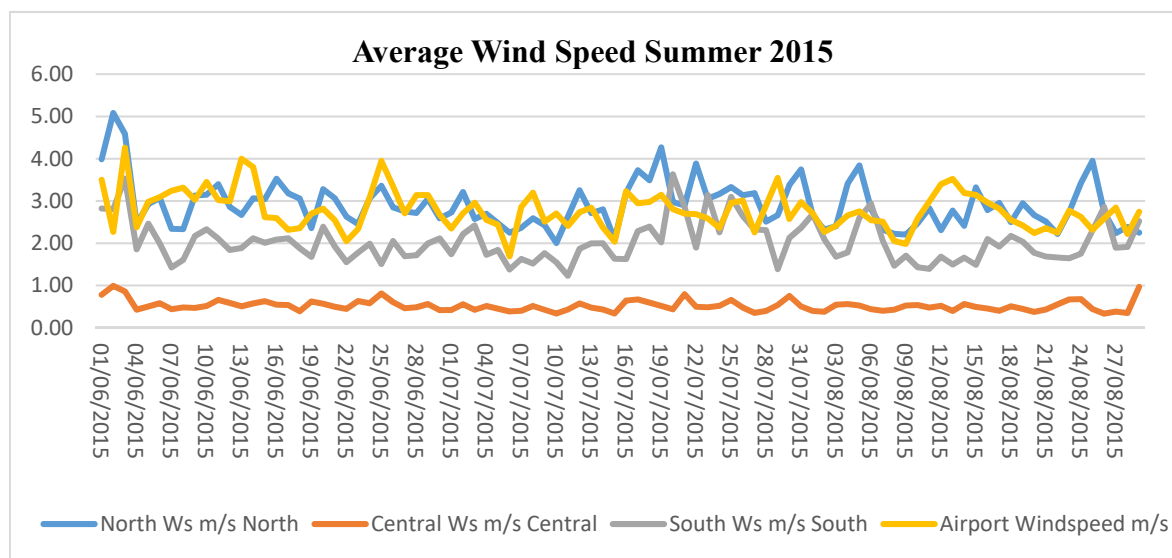


Figure 5.7: Average wind speed in June, July and August for Northern, Central and Southern

and airport stations (Figure 5.6). It can also be observed that, in the early morning, the southern weather station indicates a significantly lower temperature than the central station (Table 5-3).

From the point of view of microclimate, the average air temperature between 12:00 and 18:00 is less affected by urban density (Table 5-3). Figure 5.6 shows that differences in ΔT_{ah} generally decrease during the daytime and increase during the night. The maximum ΔT_{ah} between the northern and central stations was 9.02 K at 06:00 before sunrise, while the minimum was 1.36 K at 12:00 when the angle of the sun becomes more vertical.

5.3.2 Wind Speed

Local urban microclimates are influenced by alterations in wind patterns, wind direction and speed. High density urban morphology reduces wind speed and increases air temperature around buildings due to the heating energy trapped between the urban areas. Measurements of wind speed at all stations in Erbil are shown in Figure 5.7. The central weather station with high density urban areas recorded wind speeds of less than 1m/s, while the southern weather station displayed the next lowest, with medium density urban areas compared with the northern and airport weather stations. Wind speed is higher in rural areas or suburban areas – 3 to 4 m/s compared to 0.2 to 0.8 m/s in the city centre. Figure 5.7 shows average wind speed from June to August for Erbil. Wind speed affects T_a significantly, and this phenomenon can be seen more during the night compared to daytime. Air temperatures at the northern and airport

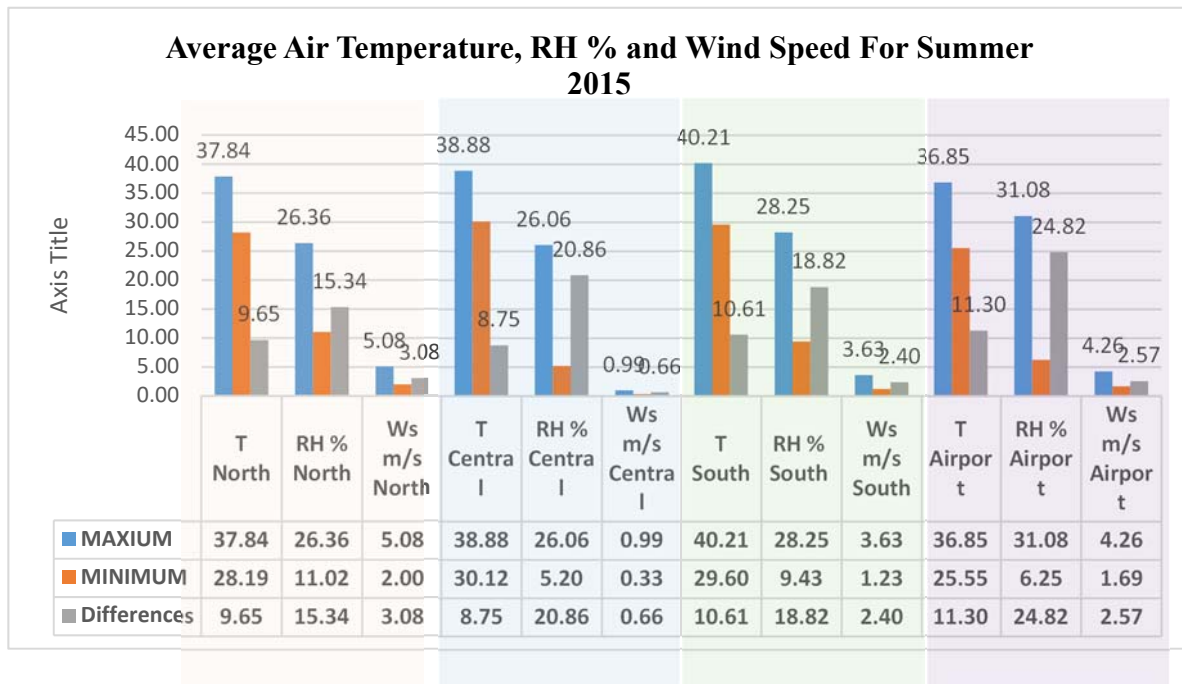


Figure 5.8: Average Air temperature, Relative Humidity and Wind speed in June, July and August 2015 for Northern, Central and Southern stations

stations are lower than the central and southern stations, with the wind speeds noticeably higher at the northern and airport stations (Figure 5.8).

Figure 5.8 shows the average monthly maximum, minimum and difference in air temperature, relative humidity and wind speed for all locations during June, July and August for Erbil. The average wind speed at the northern weather station recorded the highest level with 5.08 m/s, whereas the lowest level was 0.33 m/s documented at the central weather station. The average wind speeds recorded at the southern and airport weather stations were 3.63 and 4.26 m/s, respectfully. The average maximum air temperature at the southern and central weather stations recorded 40.21 and 38.88 °C compared to the northern and airport weather stations, which recorded 37.84 and 36.85 °C.

Regarding the three urban weather stations, the general pattern is for the wind speed to increase during daylight hours and decrease after sunset (Figure 5.8). The airport wind speed suddenly drops at 09:00 and then rapidly increases and exhibits the same phenomenon at 21:00. This change at 09:00 and 21:00 may have been caused by external not weather-related interactions. These results indicate that urban microclimate and air temperature depend on wind speed, corresponding with Morris and Simmonds' study on UHI. This found that an increase in wind speed of 1 m/s reduced the UHI variation by 0.14 °C (Morris, Simmonds et al. 2001).

Wind speed reduces the air temperature in the morning and night time, but this reduction was not considerable from 12:00 to 18:00 for all locations. Wind speed at the airport weather station does not follow a similar pattern to other weather stations. During daytime and night time Figure 5.8, shows the wind speeds for all four weather stations. The basic pattern is low wind speed during the night, which increases during the day. However, the high urban density surrounding the central weather station significantly reduces the daytime increase.

5.3.3 Relative Humidity

Concerning average relative humidity, the weather stations recorded different figures, with a maximum of 31.08% and 28.25%, respectively, for the airport and southern stations. The northern and central weather stations have a similar average in relation to RH with 26.36 and 26.08%, respectively, as the temperature falls Relative humidity reduces during daytime with increasing air temperature and increases during the night. The relative humidity values do not vary much from station to station as shown in figure 5.9.

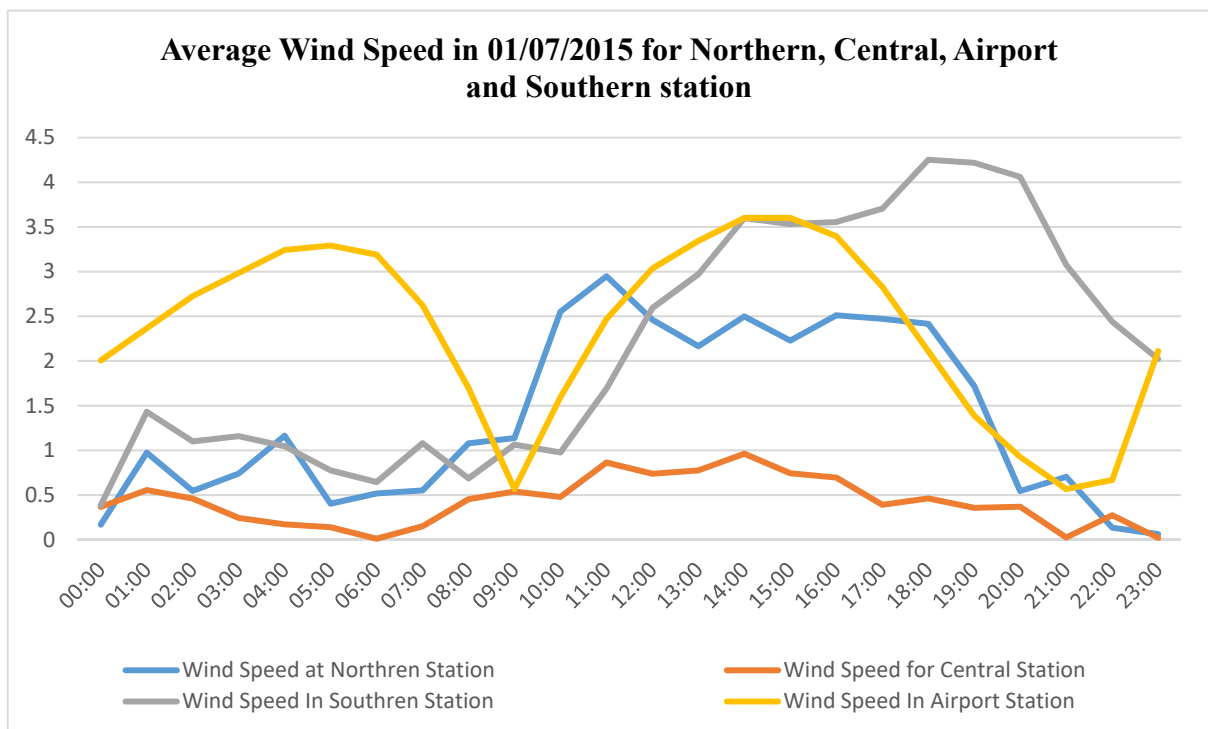


Figure 5.9 Hourly average wind speed in 1st of July 2015 for Northern, Central and Southern stations.

5.4 Summary of weather data for June, July and August 2015

5.4.1 Air temperature

Central and southern weather stations are comparable in terms of air temperature, while there is a significant difference between these weather stations and the weather station located to the north of Erbil (Figure 5.10).

During the hottest part of the day, the two weather stations (southern and central) recorded

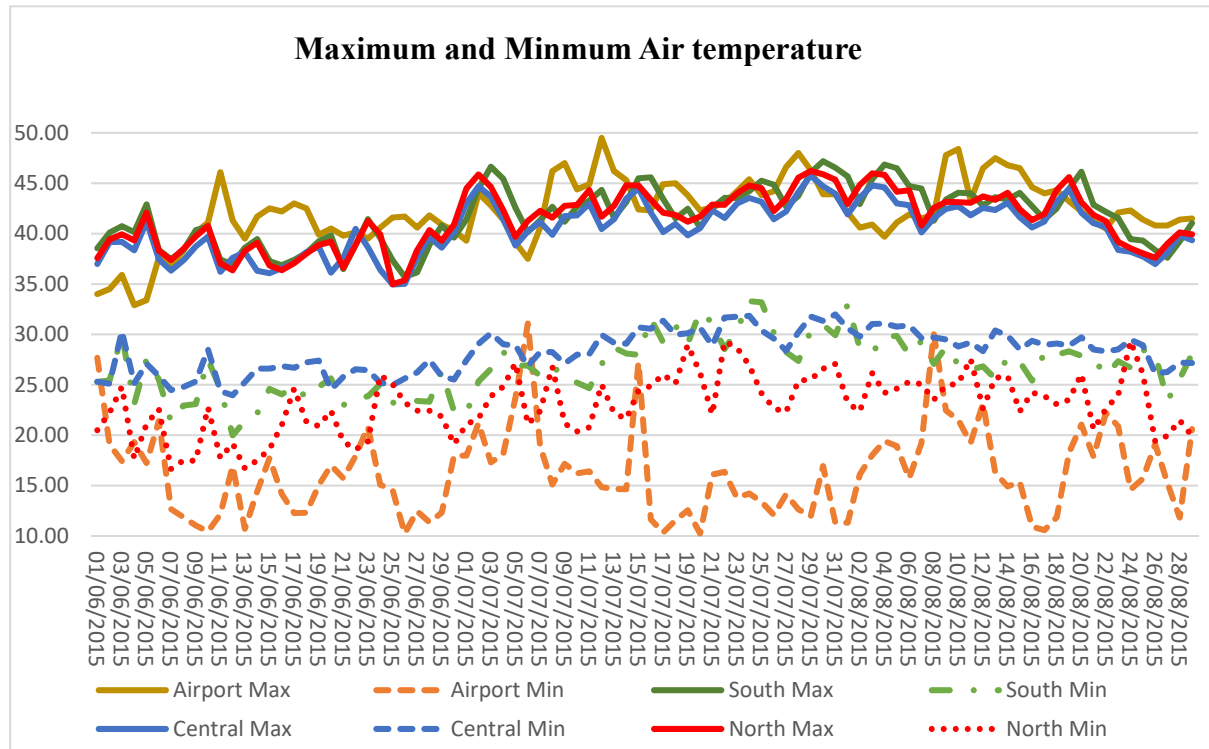


Figure 5.10 The maximum and minimum air temperatures for North, Central and South weather stations in June, July and August 2015.

similar air temperatures, while the northern and airport stations differed. In the early mornings and evenings, there was a significant difference in air temperature between all four weather stations (Figure 5.10).

In relation to the central weather station, located within a high density urban configuration, the solar energy is stored in the urban fabric and this moderates the air temperature, especially during the evening and earlier morning (Table 5-3). The northern weather station is located within a low density urban area (Figure 5.10), and may be considered a rural area. Here, the air temperature falls to below 30°C at night and increases to 45°C at peak daytime (Figure 5.10). This phenomenon is typical for desert climate rural areas. The air temperature at the southern weather station, whose urban density lies between the central and northern weather stations, closely follows the central weather station.

In terms of the urban locations and the relationship between the data for all sites, the weather stations recorded different values. For simulation reasons, the central and Southern weather stations were chosen to compare and evaluate results from the ENVI-met predictions because of two factors. Firstly, the central station with high urban density and southern station located in medium urban areas which moderates urban air temperature especially during night-time. Secondly, the validation case studies located within the high and medium density urban areas.

5.4.2 Relative Humidity

The maximum relative humidity (RH) at the central and southern weather stations recorded similar values; they have high and medium urban densities. The northern weather station recorded higher RH during all the summer months (Figure 5.11). The maximum RH between all locations was 68.8%, 48.42%, 46.24% and 45.67% for airport, northern, central and southern locations, respectively (Table 5-4). On 22nd August 2015, the airport weather station recorded a maximum RH of 68.8%, with an average of 34.37%. This is similar to the northern station. This high level of RH may be related to rain falling on that specific day, because on the days before, and on, August 22nd, 63.0% was recorded (Figure 5.11). The northern weather station is located close to green areas with trees (Figure 5.1), which help to increase the RH and decrease air temperature by evapotranspiration during the daytime. These green areas work as an urban park and produce shaded places during daytime. In addition, green areas help to change the balance of urban surface energy by absorbing latent energy and reducing soil heat storage (Takebayashi and Moriyama 2009, Hsieh, Jan et al. 2016).

Table 5-4: Average, maximum and minimum relative humidity for four weather stations (Summer 2015)

Average	Airport RH %		South RH %		Central RH %		North RH %	
	Max	Min	Max	Min	Max	Min	Max	Min
	34.37	6.98	26.58	9.37	26.27	8.88	34.49	8.14
Max during all summertime	68.8	12.6	45.67	17.63	46.24	14.75	48.42	13.98
Min during all summertime	10.7	3.2	13.26	3.437	14.32	3.856	20.1	3.357
Differences all summertime	58.1	9.4	32.41	14.193	31.92	10.894	28.32	10.623

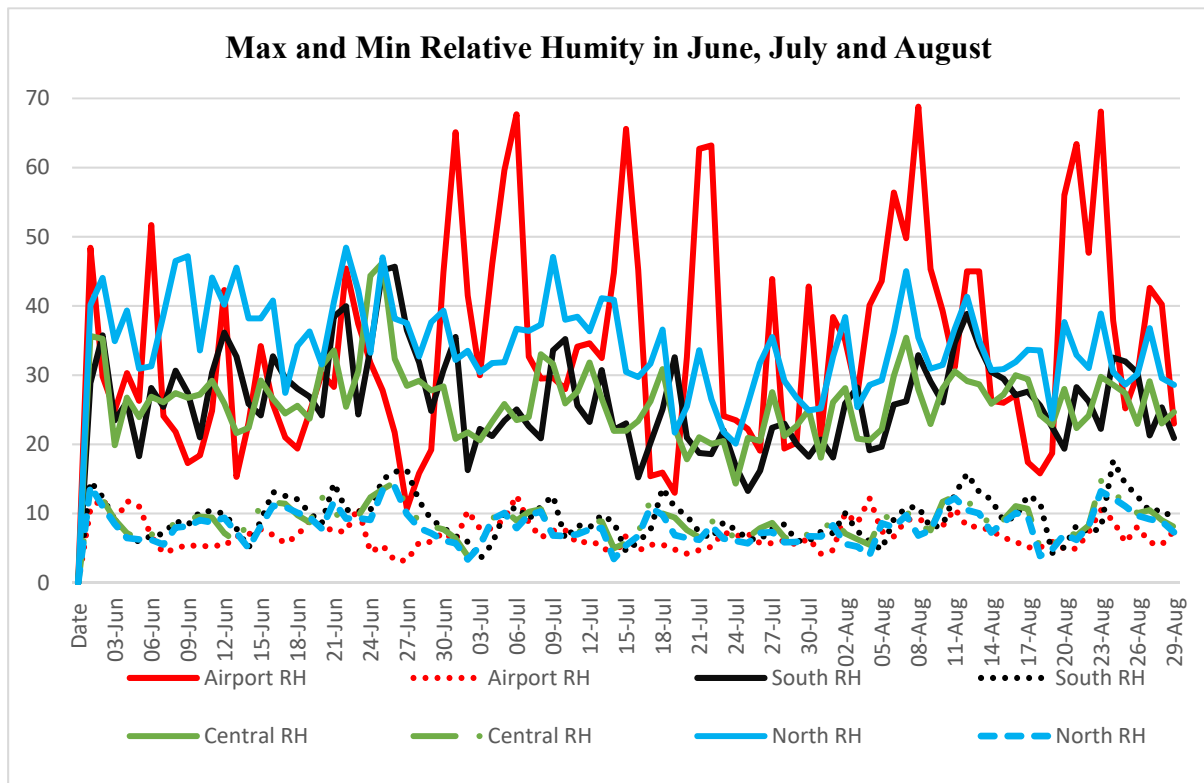


Figure 5.11: The maximum and minimum Relative humidity for North, Central and South station in June, July and August 2015.

Southern and central weather stations recorded relatively lower RH (17.63% and 14.75%), because of large masses of concrete in these urban areas (high and medium urban density). Short wave radiation direct from the sun increases urban surface temperatures and generates a reduction in RH. The maximum RH was recorded at the airport station, whereas the minimum RH were 3.2%, 3.35%, 3.41% and 3.85% for the airport, north, south and central weather stations. There is little variation in the minimum RH values (Table 5-4).

Similar to air temperature, the airport and northern weather stations recorded averages in RH almost similar at 34.37% and 34.49%, while the southern and central stations documented 26.58% and 26.27%, respectively. This confirms how urban microclimate variables change for different locations within a similar city and how the density of the urban areas affects the average RH in a city with a hot/dry climate.

5.4.3 Wind Speed

Wind speed and direction were measured at all three locations continuously using Campbell sensor 5106, at a height of 2metres. Figure 5.12 shows daily maximum and minimum wind speeds at the Northern, Central and Southern weathers stations. The maximum wind speed recorded was 11.6 m/s at the Northern weather station, while the minimum wind speed was

between 0.00 to 0.33 m/s at Central weather station. Commonly, wind speed in Centre of Erbil city are very low compare to Airport, Northern and Southern parts of the city reflecting the density of central urban area (Table 5-5).

Table 5-5: Average, maximum and minimum wind speed for four weather stations (Summer 2015)

	Airport	Central	North	South
Max	7.46	3.51	11.60	6.58
Min	0.10	0.00	0.00	0.00
Average	3.78	0.55	5.8	2.83

In general, regarding summer 2015, the average maximum wind speed ranged between 1.27 to 11.60 m/s for the northern weather station, medium wind speed range for the southern weather station 1.7 to 10.01 m/s and for the central weather station, lowest wind speed ranged between

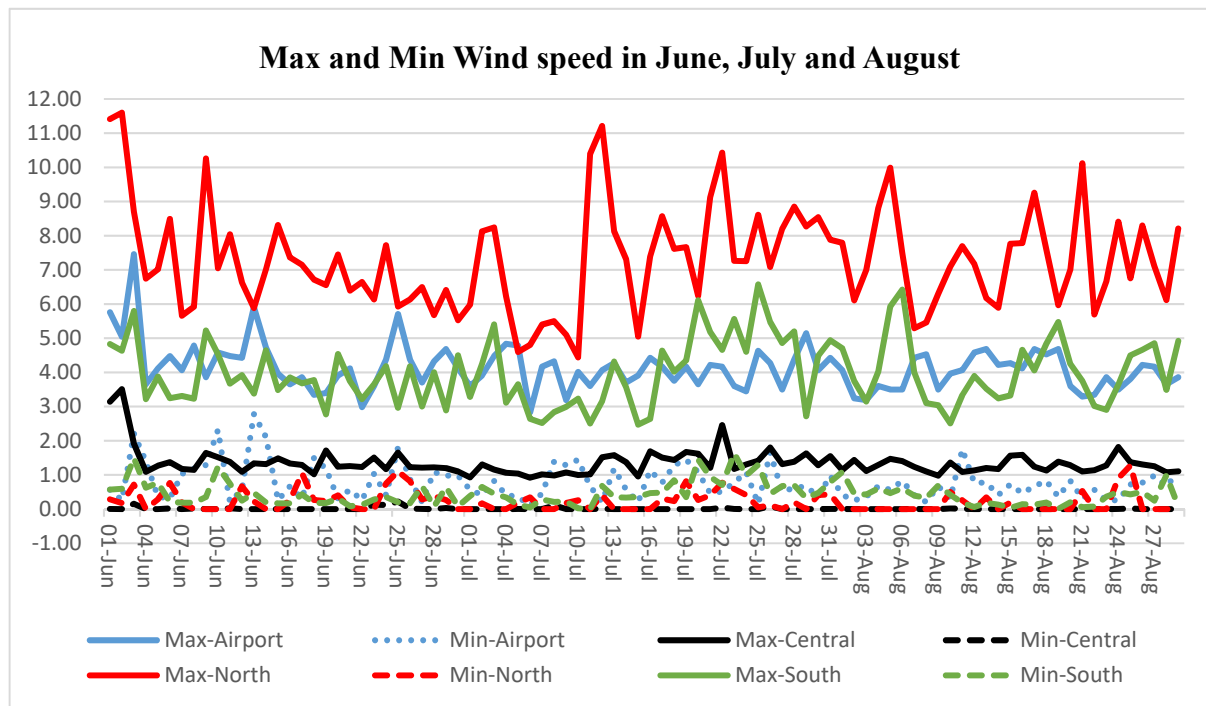


Figure 5.12: The maximum and minimum Wind Speed for North, Central and South station in June, July and August 2015

1.53 to 3.05 m/s for all three summer months (Figure 5.12).

The prevailing wind direction for Erbil is from the south-west primarily and west partially. Regarding the northern weather station, located in a low density urban area, wind speeds will be at maximum value during all the summer months. The southern weather station, in the south-west of the city in a medium density urban area, recorded an average 2.83 m/s. The central weather station had the lowest wind speeds with an average 0.55 m/s during summer as regards the high urban density (Table 5-5).

From analysing the four weather stations in different locations of the city (northern, airport, central and southern) and presenting the data hourly, daily and monthly for three microclimate variables (wind speed, air temperature and relative humidity), the urban microclimate is moderated by urban density in different ways. For example, wind speeds in rural and suburban areas recorded higher levels compared to the city centre with high urban density during day and night times.

The results reveal that each specific location has its own urban microclimate. The airport and northern weather stations are almost the same (low urban density), while the southern and central weather stations (high and medium urban density) recorded similar variables when compared. As previously mentioned in Section 5.4.1, for simulation reasons and the use of ENVI-met, the central and southern weather stations were chosen as the initial input data and to evaluate the modelled variable prediction. The central and southern weather stations represents an urban microclimate for high and medium urban morphologies in Erbil because of two factors. The central weather station is located in a high density urban area, and the Southern weather station is located in a medium to low urban density. The area around the central weather station is a mature site and unlikely to see further development, whilst area around the southern weather station is being developed.

5.5 Climate Simulation

The methodology of the thesis mainly contains four phases: collection and analysis of local urban weather data, local urban microclimate modification, individual building modification. In this phase of the study, the ENVI-met numerical simulation program was used to shape and define a microclimate model that matches the real microclimate of Erbil by means of validation; however, building such a microclimate model is very difficult and complex. The ENVI-met programme is relatively modern and used by the majority of researchers in this field. In addition, ENVI-met is not a well-established programme, but a research tool that requires interpretation of the output data. ENVI-met is analytical software. Fundamentally, the model geometry incorporates air flow, heat balance and climate simulation with consideration of the physical geography of a location in order to predict urban climates. This study will simulate wind speed and air temperature in an urban morphology and validate this against data observed in an urban area of Erbil (using central and southern weather data). To validate air temperature, the research proposed by Willmott (1982) based on systematic and unsystematic errors will be used.

The study used an ENVI-met model to simulate the microclimate model of a modern urban area in a hot/dry city. It was difficult to control input data related to the model simulation, such as relative humidity and soil moisture availability. The model was run for 96 hours to check the performance of the software; it took 15 days to run and the output was imprecise. This is because of the continuing input of heating energy into the model, which caused the model to gradually heat up. The microclimate model (ENVI-met) experienced various problems during the simulation such as:

1. Running time: to model 96 hours, the model needed 15 days
2. Input data: the model result changes enormously with small changes of input data
3. The model heats up gradually. For these reasons, the model must be validated with observed data from an urban area (central weather data).

As the program is primarily a research tool, it does require time to build expertise in using the software. Numerous problems were encountered and many false starts made, and so help and advice was sought from other users outside the UK, and by accessing a user forum database.

5.6 ENVI-met

ENVI-met is a three dimensional program that simulates and analyses urban microclimate environments. The typical resolution of the ENVI-met microclimate model is 0.5 metres to 10 metres (Huttner, Bruse et al. 2008). It uses fluid dynamic fundamental laws to calculate the dynamic of the microclimate of urban areas during day and night (Huttner 2012). This study selected ENVI-met 4.1.0 to simulate the urban microclimate model, developed by Bruse in 2010. ENVI-met simulates soil, surfaces and vegetation within an urban scale canopy layer (Chow and Brazel 2012), and can accurately simulate the physics of atmospheric boundary layers of any urban area around the world (Bruse 2004). Simulation is normally between 24–48h, with ten seconds as the maximum time step. The model can also present the energy balance for all types of urban surfaces, for example buildings and plants. ENVI-met can simulate the interactions between urban elements such as weather, soil, plant and buildings on an urban scale (Bruse 2004). Every single structure or building, vegetation, and soil layers can be simulated. These properties enable ENVI-met to be the ‘perfect tool’ for researchers and designers for both planning and urban design processes. ENVI-met contains the following sub-models (Huttner 2012):

1. 1 D boundary model represents the boundary conditions between 0 to high 2500m
2. 3 D atmospheric model signifies building structures and plants

3. 3D/1D soil model represents soil temperature and moisture content in different layers.

The program calculates interaction between urban elements (weather data, soil, vegetation and building materials) on a microscale level, and has been well studied and validated by different researchers around the world. ENVI-met is good as a research tool to predict local urban microclimates and simulate future mitigations during the design process.

It must be emphasised that ENVI-met is a research tool that is under development and is updated regularly, and has some limitations which inhibit the accuracy of the prediction process. The major limitations of the program are shown in the list below:

1. Turbulence

ENVI-met has a tendency to overestimate the turbulent production of the flow around buildings. The local exchange coefficient (k) and the diffusion coefficients (ϵ) used by ENVI-met can be responsible for high acceleration or deceleration of the wind flow. There is some research on mitigation of k - ϵ , but these modifications need reprogramming in ENVI-met, which is not applicable or causes lower k near the stagnation points. In addition, Hong Jin (2017) observed that if the initial wind speed (input data of wind speed) is lower than 2m/s, the program perfectly matches the measured wind, while if the initial wind speed is higher than 2m/s, the modelled wind speed is slightly higher than the measured wind speed.

2. Radiation

The ENVI-met program is the only program that simulates all three radiation elements together (*analysis tools to calculate distribution of short-wave direct, diffuse and reflected solar radiation*), although this calculation does not perfectly simulate radiation fluxes. Firstly, the program considers both upward and *downward diffuse radiation* as similar. Secondly, plants appear not to be influenced by Short Wave Diffuse Radiation (SWDR) in terms of absorption and creation. Thirdly, Short Wave Radiation generated via the ground and plants is not considered. Finally, average instead of individual surface temperature is used to estimate objects (surfaces and plants). This leads to an overestimation of colder surfaces and underestimation of warmer surfaces.

3. Soil model

The programme cannot simulate the irrigation process relating to soil and plants.

4. Fair Weather Model

The program cannot simulate environment below freezing point or conditions where precipitation exists. Many studies have validated the ENVI-met outputs. For example, Samaali et al. (2007) simulated a radiative model using ENVI-met. In addition, using the ENVI-met program requires the user to have some background knowledge concerning the program's limitations and atmospheric physics to be able to assess the quality of results and run the model efficiently.

The unique abilities of the program have encouraged a large number of researchers to assess and validate results to produce new hypothetical scenarios for urban designs and the future development of cities. So far, ENVI-met is one of the only free available programmes that can numerically simulate the urban microclimate with this range of accuracy.

5.7 Erbil City Climate Simulation

According to the literature review, microclimate researchers have made use of two approaches to study the UHI effect:

- a. The first approach is termed 'observational approaches'. These types of studies use data from *in situ* measurements, remote sensing, and wind-tunnels to measure outdoor microclimates
- b. The second approach is known as the 'Simulation approach' and employs *Computational Fluid Dynamics* (CFD).

This study used the second approach to simulate an urban microclimate and compared the modelled data with observed data by means of validation. In addition, this approach can compare any relevant or irrelevant variables to produce new scenarios. However, the main disadvantage in relation to simulation is the application of several simplifications to model a complex urban microclimate dependent on fluid dynamic calculations. Therefore, an understanding of building physics and 'careful validation' is essential. Building a microclimate model that matches the real environment is very complex. Fundamentally, the geometry of the model incorporates air flow, heat balance and climate simulation in consideration of the physical geography of a location in order to predict urban climates.

This study simulates and validates air temperature in two urban morphologies² (high and medium density). The study validates the model in two ways: through direct comparison between observed and modelled air temperatures in two urban areas of Erbil (central and

² Urban morphologies: Housing urban area well discussed in chapter 4.

southern weather data stations); and, analyses based on systematic and unsystematic errors between observed and predicted air temperatures as proposed by Willmott (1982). The model was run for 96 hours (4 days), and the simulation took 15 days to run. The first 24 hours is discounted as this allows the initial conditions to be worked through. The second 24 hour period was used for analysis. Running the program saw a gradual heating up of the microclimate, so after 48 hours the results were erroneous and not used. The ENVI-met input data should be well studied and analysed prior to use, because the programme is designed to simulate local urban microclimate using initial input data (a specific area in the city). During this research time, we found that using airport data (airport weather stations) does not represent all of the city's urban microclimate or a specific case study area. For this reason, the input data should be taken from inside the study area and not weather stations outside the city.

5.8 Validation the Microclimate model

To create a digital model representation of Erbil's microclimate, the ENVI-met simulation program was used. Moreover, two case studies were used to validate this model. Most studies

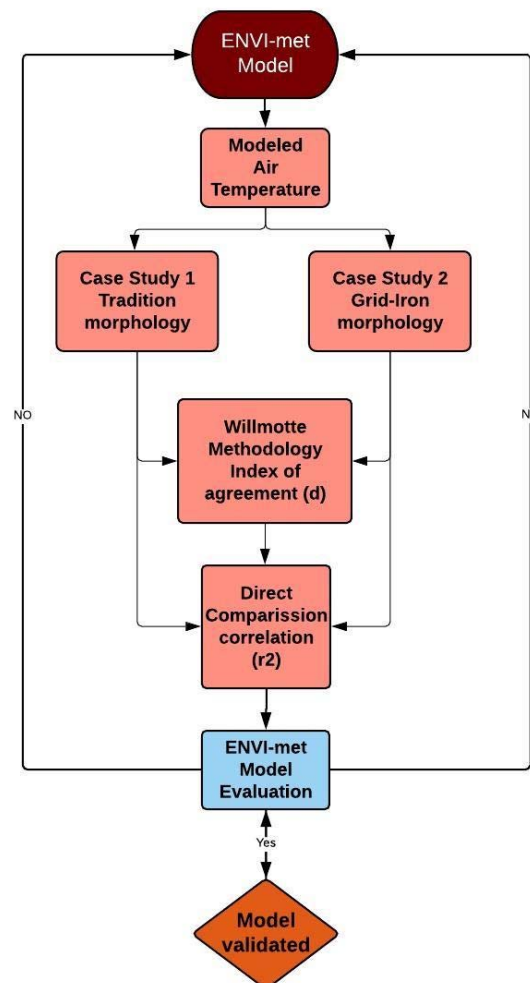


Figure 5.13: ENVI-met model validation

have validated the ENVI-met model through direct comparison between modelled and measured air temperature, while other studies employed root mean square error (RMSE) and index of agreement (d). In this study, the validation process of the environmental model used both methods to carefully validate the simulations. Figure 5.13 shows the process of validation for both case studies, and the comparison approach plots measured, predicted and then calculated the correlation between the two sets of data.

The Willmott methodology defines the systematic and unsystematic errors and index of agreement. Systematic errors can be thought of as a constant or proportioned variant between observed and predicted, whilst the unsystematic errors may be considered as unpredictable fluctuations in measurement by the instruments used at the weather stations and inconsistencies in computer code or algorithms. The index of agreement developed by Willmott (1981) is a standardised measure of the degree of error between the predicted and observed values and varies between 0 and 1. A value approaching 1 indicates good agreement, whilst a value approaching 0 indicates no agreement.



Figure 5.14: Position of the case studies in Erbil

Air temperature was modelled in two different locations as shown in Figure 5.14. The first located is in a high density urban development near the city centre, while the second located is in the south of city is a medium density urban development (Figure 5.14).

For any ENVI-met model, the user needs the initial input data to create a configuration file and (initial metrological conditions). To precisely model the local urban area, this study used two different sets of initial data taken from south and central weather stations (Figure 5.14).

5.8.1 Case Study1- Tradition Urban Morphology (High density)

This case study is located in the central part of Erbil (36.17° N, 44.01° E). The area of study is 1200m x 1200m, which is a mixed urban area with open green areas. The location has high density traditional urban form and modern developments, such as the stadium in the north-west. The streets between residential blocks are 10 to 12 metres wide, with widths of 15 metres for the main streets and 30 to 40 metres for the ring roads. The blocks are directed toward the centre of the city (citadel) (Figure 5.15).

The central weather station is located in the northern part of the simulated area, as shown in Figure 5.15. The site is located between two ring roads of 60 metres and 40 metres. The residential blocks are divided horizontally and vertically or rotated 45° from the north. Open green areas can be seen in various sizes and shapes between housing blocks (Figure 5.15). The two main open green spaces are the stadium, which is north of the weather station, and the park, which is east of it (Figure 5.15).

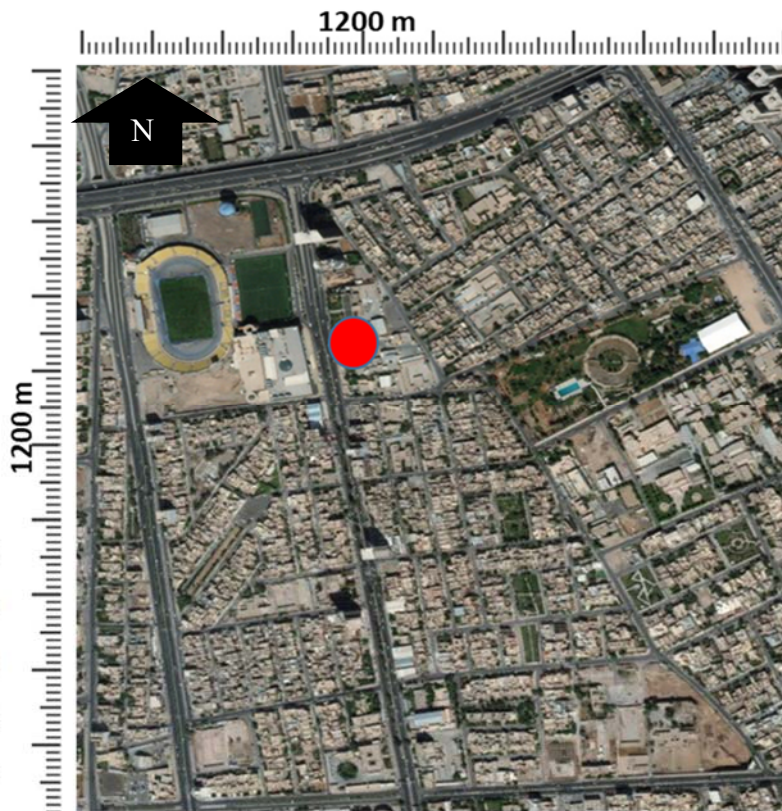


Figure 5.15: Case Study 1 urban configuration. Red circle represent Central Weather Station

By simulating this site, we can predict the local urban environment for areas around the city centre with high density urban development and use high quality measured data collected from inside the simulated urban area as initial data (input data) (

Table 5-6). Figure 5.16 has the ENVI-met physical model on the left with an aerial view of the area to the right.

Table 5-6: ENVI-met input data for case study 1.

Parameter	Units	Values	
Initial air temperature	C°	33.62	
Wind speed	m/s	0.55	
Wind direction	0 from the north and 180 from the south	225°	
Relative humidity at a 2m height	%	15.4	
Specific humidity at top of model	2000m g/kg	4	
Maximum air temperature at 15:00	C°	40.15	
Minimum air temperature at 05:00	C°	26.27	
Soil temperature at a depth of	(K)		
1. 00 to 5 cm		311.23	
2. 20 to 50 cm		306.07	
3. 50 to 200 cm		300.77	
4. Below 200 cm		298.81	
Building fabric used in ENVI-me model			
Urban blocks			
Materials	Reflectivity	Emissivity	Height
Walls layers (From inside to outside)			
1. Gypsum (2 cm)			6.40 m
2. Hollow concrete blocks (20 cm)	0.73	0.9	
3. Cement rendering (2 cm)	0.35	0.9	
Roofs layers (from top to bottom)			
1. Concrete tiles (10 cm)	0.5	0.9	
2. Fine soil (10 to 15 cm)	0.53	0.89	+ 6.40 m
3. Reinforcement concrete (20 cm)	0.8	0.91	
Pavements types			
1. Road Asphalt	0.19	0.9	
2. Concentrate pavement	0.29	0.9	+ 0.2 m
3. Green areas (grass)	0.26	0.9	
Shading mesh			
Shade mesh	0.4	0.07	+ 7.0 m
Building Properties			
Parameter	Units	Values	
Inside Temperature	K	297	
Heat Transmission Walls	W/m²K	0.74	
Heat Transmission Roofs	W/m²K	0.67	
Albedo Walls		0.3	
Albedo Roofs		0.15	



Figure 5.16: Case Study 1 Illustrates the ENVI-met physical model on the left with an aerial view of the area to the right

5.8.2 Microclimate model evaluation of Case Study 1

This section evaluates air temperature prediction accuracy by comparing data from the central station (measured data) with the ENVI-met results (modelled data) for 01/07/2015 (Figure 5.17). The maximum air temperature at the central station was 40.12°C recorded at 16:00 over an 18 hour observation period, while the maximum air temperature for the ENVI-met model temperature was 39.54°C (Figure 5.17) recorded at 15:00 for the observation period.

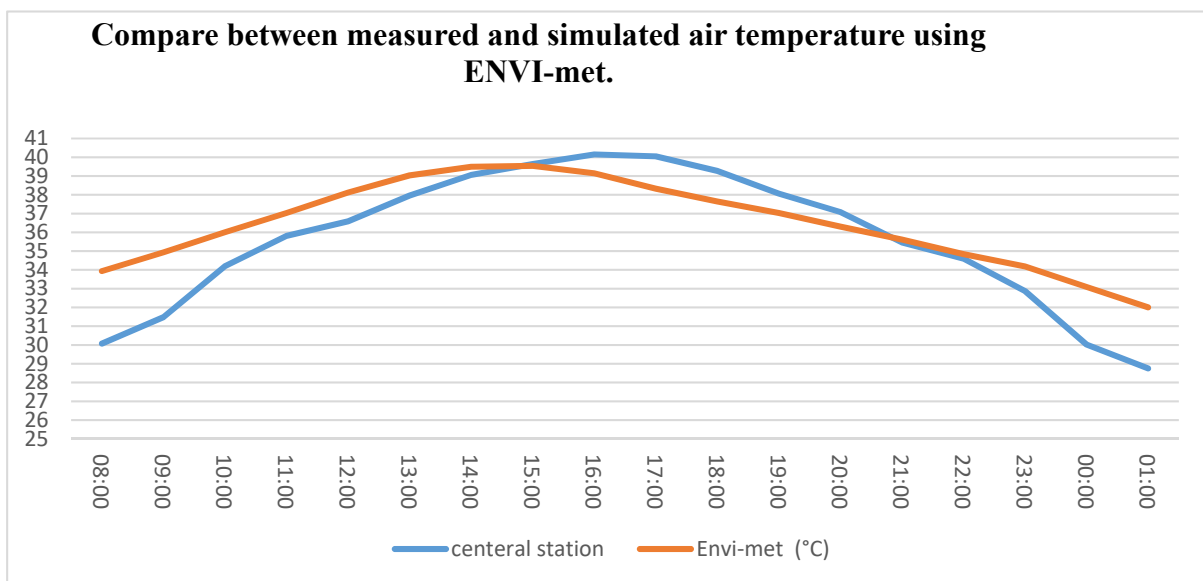


Figure 5.17: Modelled and measured air temperature for Case Study 1

In general, other researchers have established that the ENVI-met model underestimates the minimum and maximum air temperatures (Chow, 2012). To evaluate the accuracy of the modelled air temperature, we used Willmott's (1982) methodology, as discussed previously (see the Methodology chapter).

Figure 5.18 plots the measured against the predicted air temperature. The correlation is 0.8735, which indicates strong agreement between measured and predicted air temperature. The value of Mean Bias Error (MBE),³ Mean Average Error (MAE)⁴ and RMSE⁵ were acceptable with low magnitudes (0.79, 1.45, and 2.58), respectively. The RMSE Root mean square error Systematic (RMSEs)⁶ and Unsystematic (RMSEu) is given with a lower magnitude for the latter (Figure 5.18).

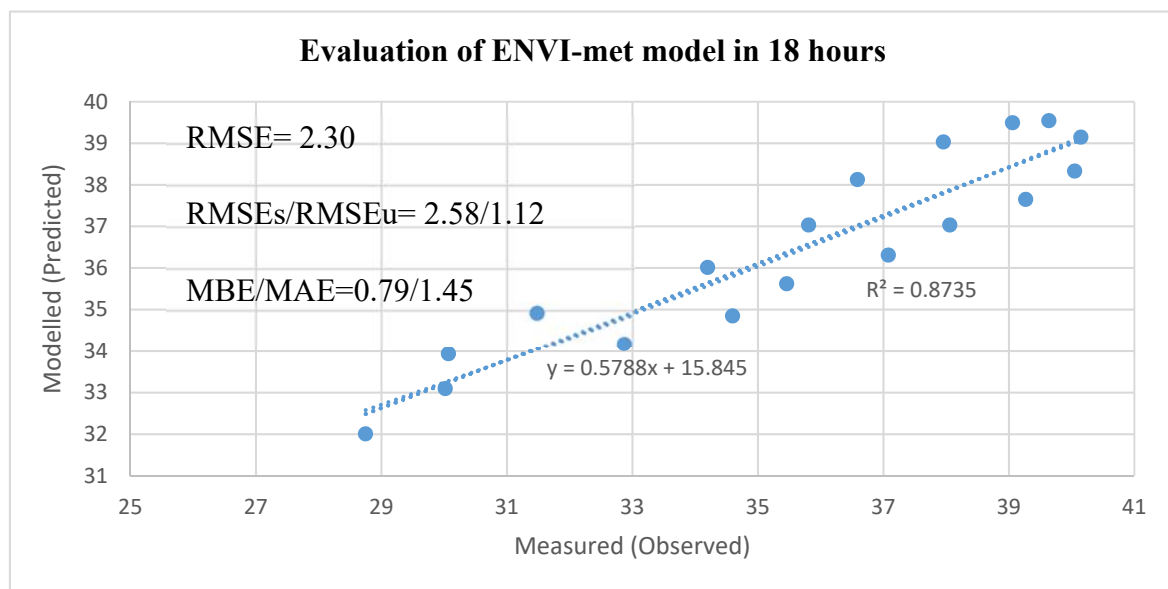


Figure 5.18: Correlation and index of agreement for modelled and measured air temperature in 18 hours

³1. If the absolute value is not taken (the signs of the errors are not removed), the average error becomes the mean Base Error (MBE) and is usually intended to measure the average model bias, as positive and negative values can cancel each other, resulting in a lower prediction of error.

⁴ The Mean Absolute Magnitude Error (MAE) measures the average magnitude of its error in a set of predictions without considering their Root Mean Square Error.

⁵ The RMSE is a quadratic scoring rule that also measures its average magnitude of the error.

⁶ The Root Mean Square Error has two components: specifically a systematic element, which is consistent with deviation between predicted and observed,. The second element of the RMSE is unsystematic errors, produced by the predictive process and measurement of the observation. A low RMSEu value is desirable.

For more specific results regarding the validation process, this study evaluates daytime (08:00 to 17:00) at the specific station (Figure 5.19). Previous studies have indicated that ENVI-met overestimates and underestimates microclimate data. For this study, daytime modelled data is the core of this study, and therefore daytime air temperature was evaluated for both case studies.

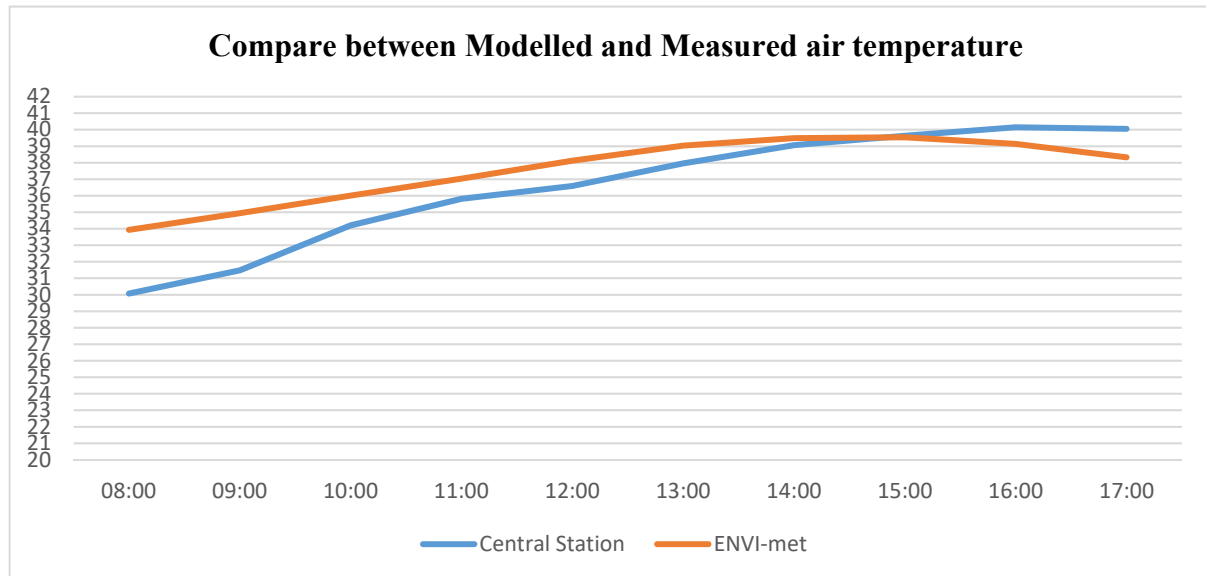


Figure 5.19: Modelled and measured air temperature for Case Study 1 during daytime hours
The correlation for the daytime prediction yielded a much closer relationship between measured and predicted. For daytime simulation, the values of Mean Bias Error (MBE), Mean Average Error (MAE) and (RMSE) were more acceptable and with lower magnitudes than the 18h simulation. MBA, MAE and RMSE were 1.05, 1.62, and 1.98, respectively. The Root

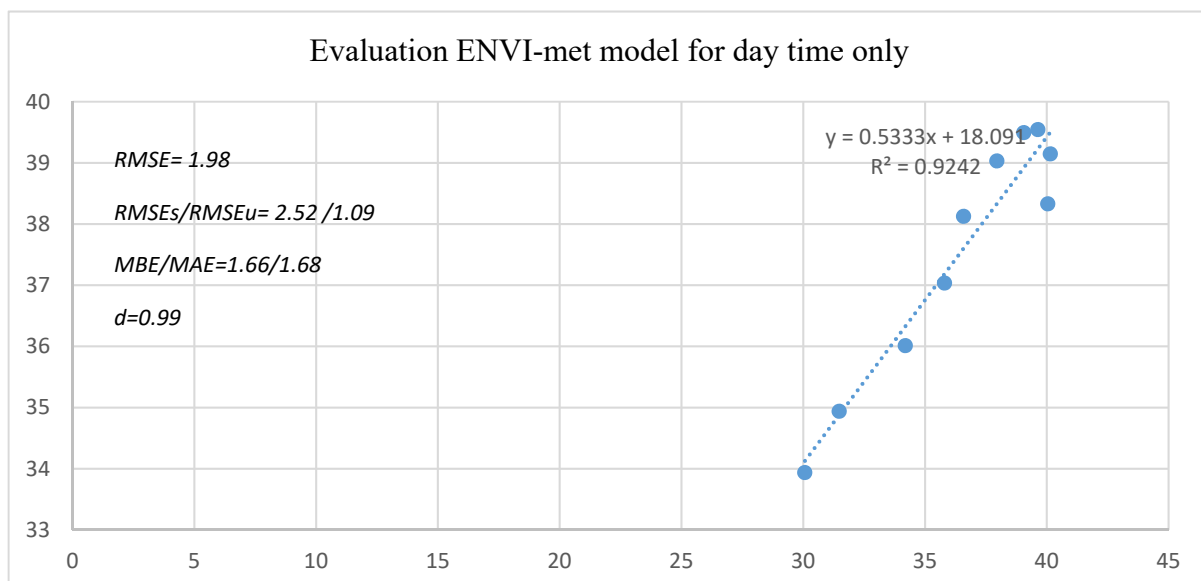


Figure 5.20: Shows the correlation and index of agreement for modelled and measured air temperatures during daytime hours only

mean square error Systematic RMSEs was 2.52 and Unsystematic (RMSEu 1.09, with a lower magnitude for the former than the prediction of 18 hours (Figure 5.20).

Table 5-7: ENVI-met validation for case study 1 using ENVI-met program (day time and 24 houses)

For both the 18 hour simulation and day-time (08:00 to 17:00) simulation, the ENVI-met (P) modelled data exhibited generally ‘good agreement’ in contrast to observed data for the central station (O), both correlations ($r^2=0.87$) for 18 hours and ($r^2= 0.92$) for daytime (08:00 to 17:00). In addition, the index of agreement ($d= 0.89$) and ($d= 0.99$) for both 18 hours and the daytime period is good (

Table 5-7). The index of agreement (d) is 0.89 and 0.99 indicates that the ENVI-met model captured measured data well (air temperature) during the 18 hour period and very well during the daytime (08:00–17:00). The 18 hour simulation comprises a large Systematic Root Mean Square Error (RMSEs) at 2.58 compared to daytime of 2.52.

For the 18 hour case simulation, modelled air temperature at a height of 2m underestimated afternoon (15:00 to 21:00) and overestimated night-time and early morning. The model showed better agreement during daytime simulation with limited over and underestimation. Day time (08:00 to 17:00) simulation has limited overestimation and this becomes less as the model continues to run into the afternoon, until the model equals simulated air temperature at 15:00.

Validation Air temperature results (ENVI-met) compare to Central station				
		variables	18 hours	Day time (08:00 to 17:00)
1	Average ENVI-met predication	P	36.46	37.56
2	Average Observed (measured) data	O	35.62	36.50
3	Correlation	r^2	0.87	0.92
4	Mean bias error	MBE	0.79	1.66
5	Mean average error	MAE	1.45	1.66
6	systematic Root mean square error	RMSEs	2.58	2.52
7	Unsystematic Root mean square error	RMSEu	1.12	1.09
8	Index of agreement ⁷	d	0.89	0.99

In the late afternoon, the model starts to underestimate the observed air temperature (Figure 5.19). The model showed underestimation during daily peak temperature and overestimation at night-time, because it (ENVI-met) cannot predict the thermal mass phenomenon at night and during the early morning. These results correspond with a study completed in Phoenix,

⁷ Index of agreement proposed by Willmott measures the overall accuracy of the prediction process and ranges between 0 and 1, with 0 being poor predictions and 1 excellent predictions.

Arizona, which found an overestimation of results after midnight and early morning. Furthermore, regarding underestimation, the results obtained in Phoenix are partially in agreement with the result of this study, which found that ENVI-met underestimated afternoon to midnight (Chow, 2012).

Chow (2012) modelled two urban areas of Phoenix, Arizona. One of these areas bordered a large recreational park. The park influenced the weather station but was outside the modelled area and had no influence on the prediction. The other modelled area had no external influences and achieved satisfactory agreements. The results generally overestimated the night and underestimated daytime air temperature modelled using ENVI-met.

ENVI-met overestimation of air temperature during night-time and early morning might be because of the limited ability of ENVI-met to model the heat storage of individual buildings. Moreover, indoor air temperature is equal to all the buildings in the ENVI-met model and this temperature is constant throughout the simulation period. In addition, the one dimension soil model used by the ENVI-met model cannot cope with *horizontal heat transfer* within the ground because that underestimation might have occurred during late afternoon (Figure 5.19).

5.8.3 Case Study 2: Modern Urban Morphology (medium urban density)

This case study is located in the southern part of Erbil (36.2063° N, 44.0089° E). The area of study is 1200m x 900m which contains three types of buildings: commercial, residential and public services (Figure 5.21 - A). The study uses a residential area as the main target. As showed in the most case studies in chapter 4 and for this case study, the local streets have 12 metre widths between residential blocks and 15 metre widths for the main streets (Figure 5.21 - B).

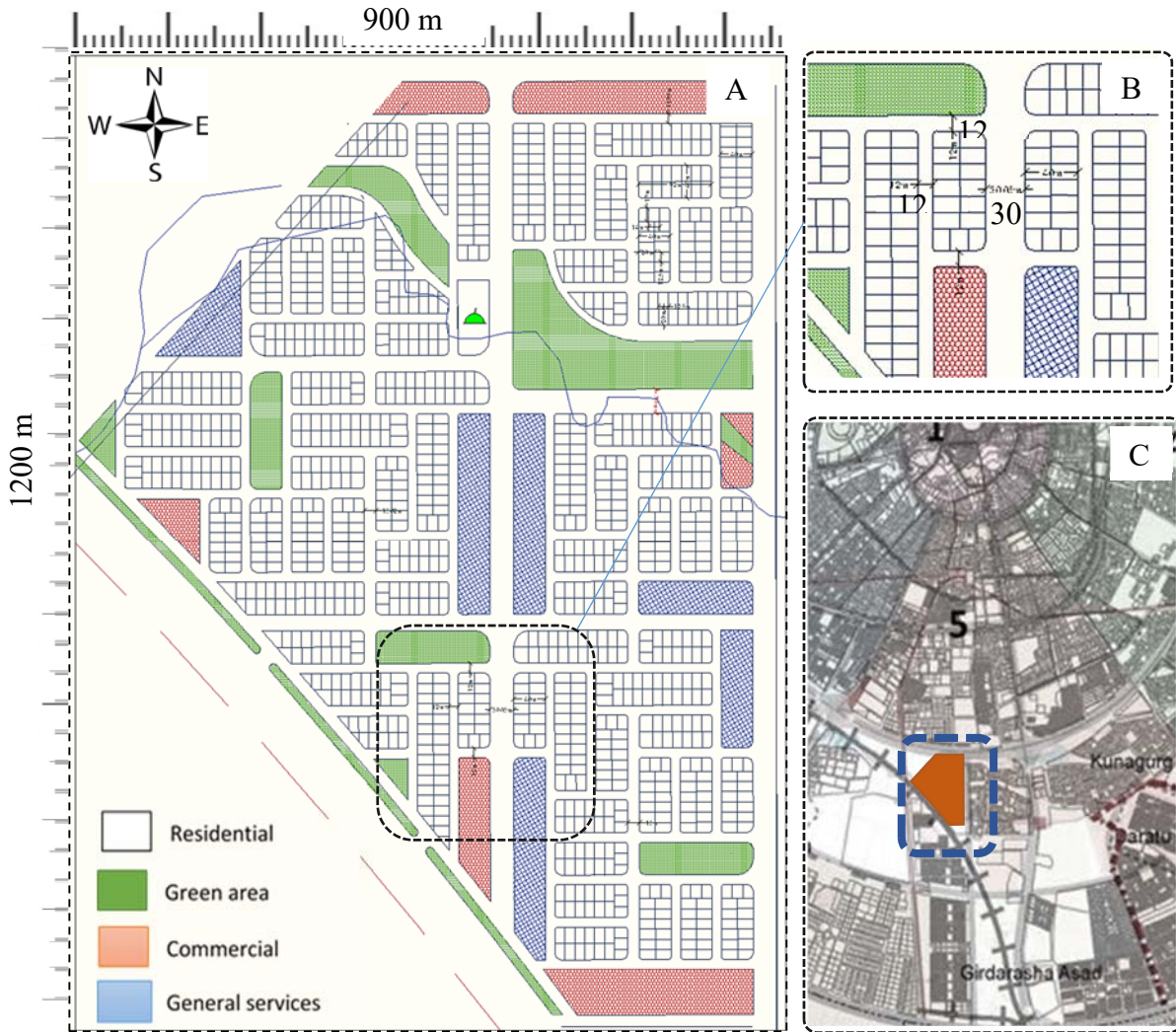


Figure 5.21: Case study area to the south of the city centre

The case study area is considered a modern urban development. The urban area was designed by local architects and planners employed by Erbil's Governor (government projects⁸). The design is based on poor urban planning guidelines issued in Baghdad in 1967 (see Chapter 4), which divided the area into a grid of individual blocks and each block into a variety of 200m² plot arrangements (Figure 5.21-A). Street alignment is north-south, east-west without any concern for climatic and environmental approaches (Figure 5.21-B).

The southern weather station is located to the south of the simulated area, as shown in (Figure 5.22). The site is located on ring road 100m. It consists of open green areas of various sizes randomly distributed between housing blocks. The main open spaces are situated in the northern part and other green areas distributed across the location (Figure 5.21-A). By simulating this site, we can predict local urban environments for modern urban areas far away

⁸ Government projects: This type of housing projects well described in chapter 4.

from the city centre. The site has medium urban density development and measured data from the southern weather station located near the simulated urban area will be used (Figure 5.22).



Figure 5.22: Southern Weather Data Station locations in Erbil City

This case study will be used to address the model the urban microclimate of this part of the city and analyse it .

Table 5-8: ENVI-met input data for Case Study 2

Parameter	Units	Values
Initial air temperature	C°	36.33
Wind speed	m/s	3.00
Wind direction	0 from the north and 180 from the south	225°
Relative humidity at a 2m height	%	14.5
Specific humidity at top of the model	2000m g/kg	5
Maximum air temperature at 15:00	C°	41.41
Minimum air temperature at 05:00	C°	22.18
Soil temperature to a depth of	(K)	
9. 00 to 5 cm		311.23
10. 20 to 50 cm		306.07
11. 50 to 200 cm		300.77
12. Below 200 cm		298.81

**Figure 5.23: Real urban plan and configuration model using ENVI-met (left), Zhyan district area on the right**

5.8.4 Microclimate model evaluation for Case Study 2

This section evaluates the accuracy of air temperature prediction for Case Study 2 with medium dense urban development by comparing data from the southern weather station (measured data) with ENVI-met results (modelled data) for 1 July 2015 (Figure 5.24). The maximum air temperature at the southern station was 41.41°C recorded at 17:00 during a 24 hours observation period, while the maximum air temperature for ENVI-met modelled air temperature was 39.13°C at 15:00 (Figure 5.24).

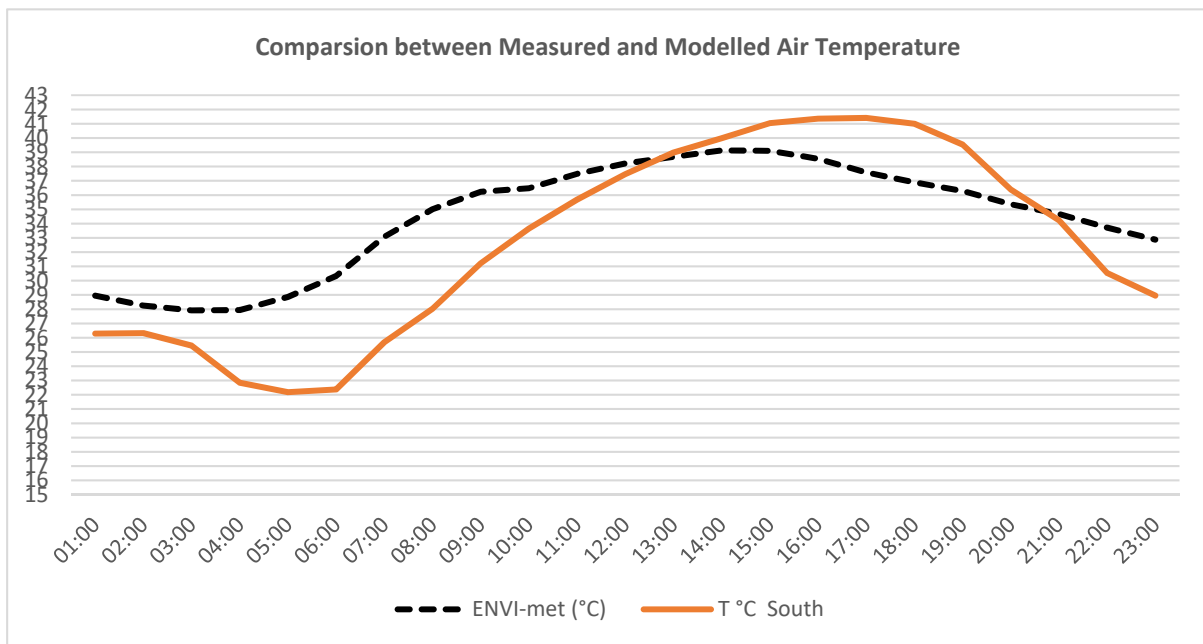


Figure 5.24: Case Study 2. Modelled and measured air temperatures for Case Study 2

In general, Chow (2012) and other researchers have established that the ENVI-met air temperature model underestimates or overestimates the minimum and maximum temperatures depending on time of day. To evaluate the accuracy of modelled air temperature we used Willmott's (1982) methodology, which uses systematic and unsystematic root mean square ($RMSEu/RMSEu$). ENVI-met 4 was used to model medium urban density (Case Study 2), as shown in Figure 5.23 with input data taken from the southern weather station, as indicated in Table 5-8.

Figure 5.25 plots the measured air temperature against predicted for the 24 hours period and yields a correlation coefficient of 0.7901. The values of Mean Bias Error (MBE), Mean Average Error (MAE) and RMSE were acceptable and had low magnitudes (2.94, 4.34, and 5.29), respectively. The Root Mean Square Error Systematic (RMSEs) was 5.05 and $RMSEu$ 1.72, giving a lower magnitude for the former, as desired (Figure 5.25).

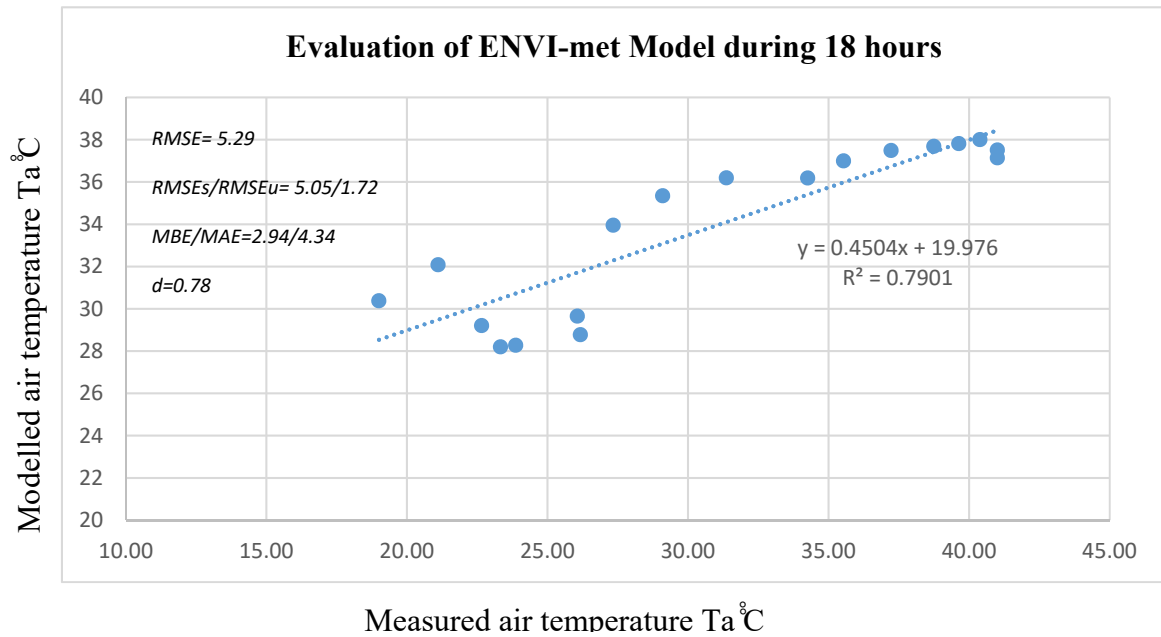


Figure 5.25: Correlation and index of agreement for modelled and measured air temperature for 18 hours

This study also evaluated the daytime (08:00 to 17:00) validation for Case Study 2 using the southern weather station.

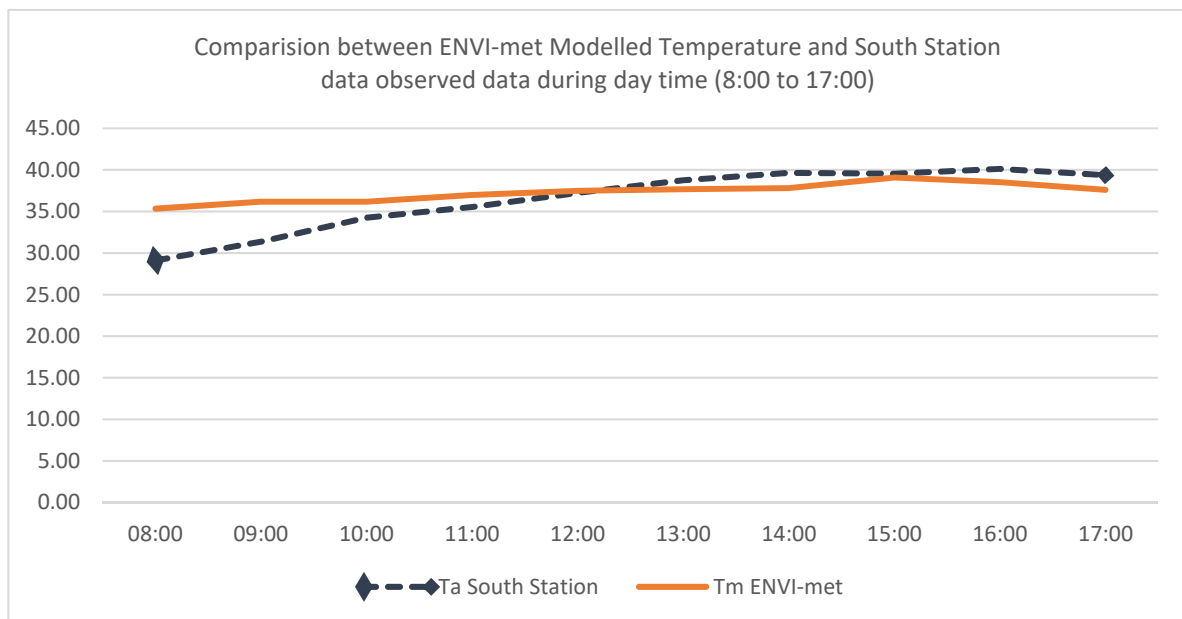


Figure 5.26: Case Study 2. Shows the Modelled and Measured air temperature during daytime (7:00 to 18:00)

For daytime air temperature (08:00 to 17:00), the maximum air temperature at the southern station was 41.36°C recorded at 15:00 for the daytime hours observation period, while the maximum air temperature for the ENVI-met modelled air temperature was 39.13°C (Figure 5.26) at the same time. Figure 5.27 shows the relationship between measured and modelled for

the daytime period and is similar to the first case study, where the correlation coefficient increased to 0.8523.

For daytime simulation (ENVI-met), the values of Mean Bias Error (MBE), Mean Average Error (MAE) and RMSE were more acceptable with lower magnitudes than the 24 h simulation (southern Case Study 2). MBE, MAE and RMSE were 2.14, 0.79 and 2.80, respectively. The Root Mean Square Error Systematic (RMSEs) was 2.68 and Unsystematic (RMSEu) 0.45. A lower magnitude for the former is desired and shows an improvement on the day time prediction (Figure 5.27).

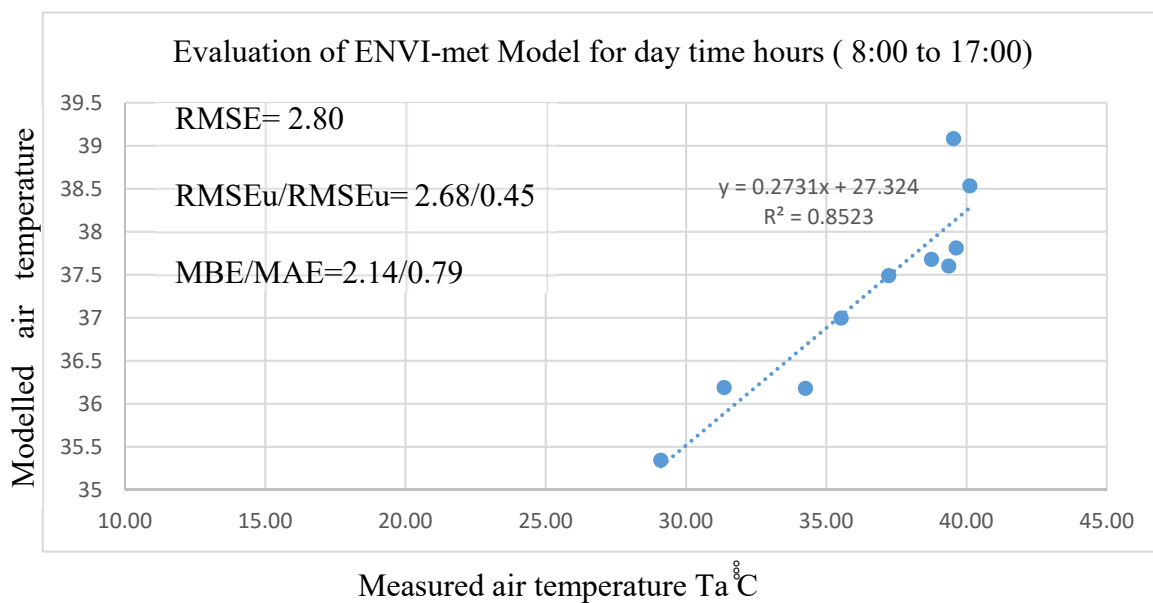


Figure 5.27: correlation and index of agreement for modelled and measured air temperature during daytime (07:00 to 18:00) – Case Study 2

In relation to Case Study Two, both the 24 hours simulation and daytime simulation (08:00 to 17:00) and the ENVI-met (*P*) modelled data showed generally ‘acceptable agreement’ compare to observed data in southern station (*O*), both correlation ($r^2 = 0.79$) for 24 hours and ($r^2 = 0.85$) for daytime (08:00 to 17:00). In addition, the index of agreement is ($d = 0.78$) and ($d = 0.99$) for both the 18 and daytime period, respectively (Table 5-9).

The index of agreement (d) is 0.79 and 0.99 indicates that the ENVI-met model is capturing measured data (air temperature) during the daytime better than the 24hours simulation. In both cases, (d) is considered to be well representative of the case studies. The 24 hours simulation had a higher Systematic Root Mean Square Error 5.05 compared to day time of 2.68.

Table 5-9: ENVI-met validation for Case Study 2 using the ENVI-met program (daytime and 24 hours)

Validation of air temperature results (ENVI-met) compared to the south weather station				
		Variables	18 hours	Day time (08:00 to 17:00)
1	Average ENVI-met predication	<i>P</i>	33.81	37.28
2	Average Observed (measured) data	<i>O</i>	30.99	36.28
3	Correlation	<i>r</i>²	0.79	0.85
4	Mean bias error	MBE	2.94	0.79
5	Mean average error	MAE	4.34	2.14
6	Systematic Root Mean Square Error	RMSEs	5.05	2.68
7	Unsystematic Root Mean Square Error	RMSEu	1.72	0.45
8	Index of agreement	<i>d</i>	0.78	0.99

Simulation Case Study 2 with medium urban development for 24 hours, using ENVI-met to model air temperature at a height of 2m, reveals that modelled air temperature was underestimated during the afternoon from (15:00 to 21:00) and overestimated at night and from early morning to afternoon (Figure 5.24). This result corresponds with the study undertaken in Phoenix, which found overestimated results after midnight and early morning. The model showed underestimation during daily peak temperature which starts at 13:00 and reached a peak at 17:00, the hottest time during the 24 hours period. This underestimation decreases with sunset. After sunset the overestimation starts at night and increases gradually to reach its peak in the early morning (06:00) and converges to disappear at noon (Figure 5.24). This overestimation of the air temperature occurs because the ENVI-met model cannot predict the thermal mass phenomenon at the night-time and early morning. In real environments, urban elements absorb heat energy during the daytime and release this heat after sunset until a balance is reached. Moreover, air temperature drops from midnight to sunrise (in summertime). ENVI-met cannot correctly model this phenomenon. Additionally, regarding underestimation, the Phoenix results are partially in agreement with the results of this study, as they found that the ENVI-met model results underestimated the period from afternoon to midnight. The limitation of this study is daytime during summer months only.

The ENVI-met air temperature model confirmed a better agreement during daytime simulation (08:00 to 17:00) with limited over and underestimation compared to the 24 hours simulation.

In addition, Middel (2013) explained that the ENVI-met overestimation during night-time and early morning regarding air temperature might be because of the incapability of ENVI-met to

incorporate veering winds (wind speed and wind direction). Even though the ENVI-met configuration file takes into account wind speed and direction, this remain stable during the simulation process. The warm or cool atmosphere caused by thermal wind systems is not considered by the ENVI-met model. Thus, the thermal wind phenomenon that warms or cools the local environment is not considered by ENVI-met.

5.9 Summary of the validation process

In this study, two cases were evaluated and validated: the central and southern case studies. The main differences are local microclimate and urban development densities. Central Case Study 1 (traditional) investigates the microclimate of a high urban density area close to Erbil citadel, while the southern Case Study 2 (modern) represents existing and future medium urban development of the city between the ring roads⁹ (150m and 200m) (Figure 5.14). The simulation employed ENVI-met and was run for 96h. However, only the second 24h were used due to software limitations in the first 24h of the simulation. The results show that the central Case Study 1 has a better index of agreement than the southern Case Study 2. In addition, both case studies represent a ‘good agreement’ between modelled and measured (observed) air temperature using a direct comparison with microclimate data from the weather stations, using Willmott’s methodology (Willmott 1982). The validation process for the microclimate simulation involved overestimation and underestimation of modelled data compared to observed data from site. This discrepancy might be a systematic or unsystematic error. Moreover, ENVI-met can cause other discrepancies as a result of the limitation of the program to model all microclimate elements. Thermal mass, heat storage, soil and air temperature, wind veer and thermal wind system etc. are not thoroughly simulated by ENVI-met and are beyond the capability of the program. The results of the validation are compared with the observed temperatures and other studies which used a similar approach within similar urban microclimate regions, such as the study conducted in Phoenix, Arizona, which has a microclimate that is similar (hot/dry).

In conclusion, the validation of this study concerning different urban developments in Erbil was considered adequate. In general, microclimate elements, such as the air temperatures of both case studies, were well captured in the simulation and showed a high index of agreement (*d*). The results of the validation show good agreement during daytime rather than the 18h/24h simulation. Starting with the validated model, this research employed southern Case Study 2

⁹ Ring roads 100m and 150m: These roads are disrobed in chapter 4 and we showed how these roads have an impact of current development of Erbil.

as a base case to produce other design scenarios, with the aim of enhancing the local urban microclimate around residential buildings in Erbil.

Chapter 6 Urban Microclimate Modelling

6.1 Introduction

In Chapter 5 the modelling of the urban micro climate using ENVI-met was investigated and validation undertaken. In this chapter, ENVI-met will be used to investigate the impact of different urban morphologies on the urban climate. Four studies will be performed.

The first study will compare a modern grid-iron to a traditional urban morphology. For the grid-iron morphology, the more road structure would allow greater air movement but provide less shade. Whilst the traditional morphology will restrict air movement but will have better utilisation of shade.

The second study will investigate the effect of prevailing wind direction has on a wind speeds within a grid-iron morphology. Here a proposed development, (Section 5.8.3), was selected, this development was scheduled to be constructed in the Southern part of Ebril, close to the Southern weather station) (Figure 6.13). The grid-iron morphology is aligned with the rad pattern, North- South and East-West. Three wind directions were chosen, winds from the South, South-West and the West. These directions can be mirrored or translated to represent wind directions from all the cardinal points.

The third study takes the grid-iron urban morphology studied in the previous section and investigates a series of design interventions that could be made in the urban grid. The urban grid was divided into three zones, but only one zone was subjected to these interventions. This allowed the study of the impact of an intervention on the adjacent zones to be made. Three interventions were undertaken, the first increased the number of open spaces, the second increased the East-West canyon widths and the third intervention, placed green areas around the housing blocks. The aim of these interventions was to minimise air temperature around buildings and maximise wind speeds within the urban grid. By reducing the air temperature around buildings, the heat gain would be reduced, thus reducing the amount of additional cooling required. Maximising wind speeds helps to promote ventilation and this again will reduce the additional cooling load that maybe required.

In the final study, the impact of shading will be investigated. In a hot, dry climate, shade either by vegetation or man-made devices is a well-established principle to reduce direct.

6.2 Compare between Grid-iron and Tradition urban Morphology.

Note: At the time of undertaking this part of the study in 2016, the original intention was to travel to Erbil to measure climate data. Due to security reasons, this plan was not executed. The sourcing of climate data used in the previous researches was problematic and time consuming. To gain experience in using ENVI-met, the airport climate data were used, and these included higher wind speed compared to the more urban-based weather stations described previously.

This section of study was not repeated after validation, because it take long time to re-simulate. This part of study was undertaken to gain experience with the model, and the higher wind speed were used because it was the only climate data available at that time.

This part of study is not in chronological order with previous part of study. The findings of this section are qualitatively correct, but quantitatively is slightly different. It is used to get familiar with the urban microclimate and using the model process. This scenarios was not repeated after validation, because it is a comparison study and the magnitude of wind speed can be changed, but the relationship between the morphologies (Grid-iron and Tradition) are valid.

This section compares two scenarios from urban areas in Erbil using ENVI-met. The simulation is concerned with residential block areas in two different urban morphologies (traditional and grid-iron). The proposed grid-iron morphology comprises plot areas of 200m² and 10m canyon widths (Figure 6.1). The site contains residential blocks and attached houses. Each block has 26 housing units, comprising two floor buildings with 6 metre high units. The houses are open at the front only, while the other three directions are attached to other units. The construction materials for building consist of hollow concrete blocks (40cm x 20cm x 20cm) for walls and reinforced concrete slabs for ceilings. The street is covered by a layer of asphalt. The air temperature was measured for both scenarios at six positions (east-west and north-south) at a height of 1.8 metres Figure 6.4.

“The water and vegetation factors are eliminated by excluding them from the simulation models. This is to ensure that factor of urban configuration is strictly the influencing factor of urban microclimate temperature variation”(Taleb and Abu-Hijleh 2013).

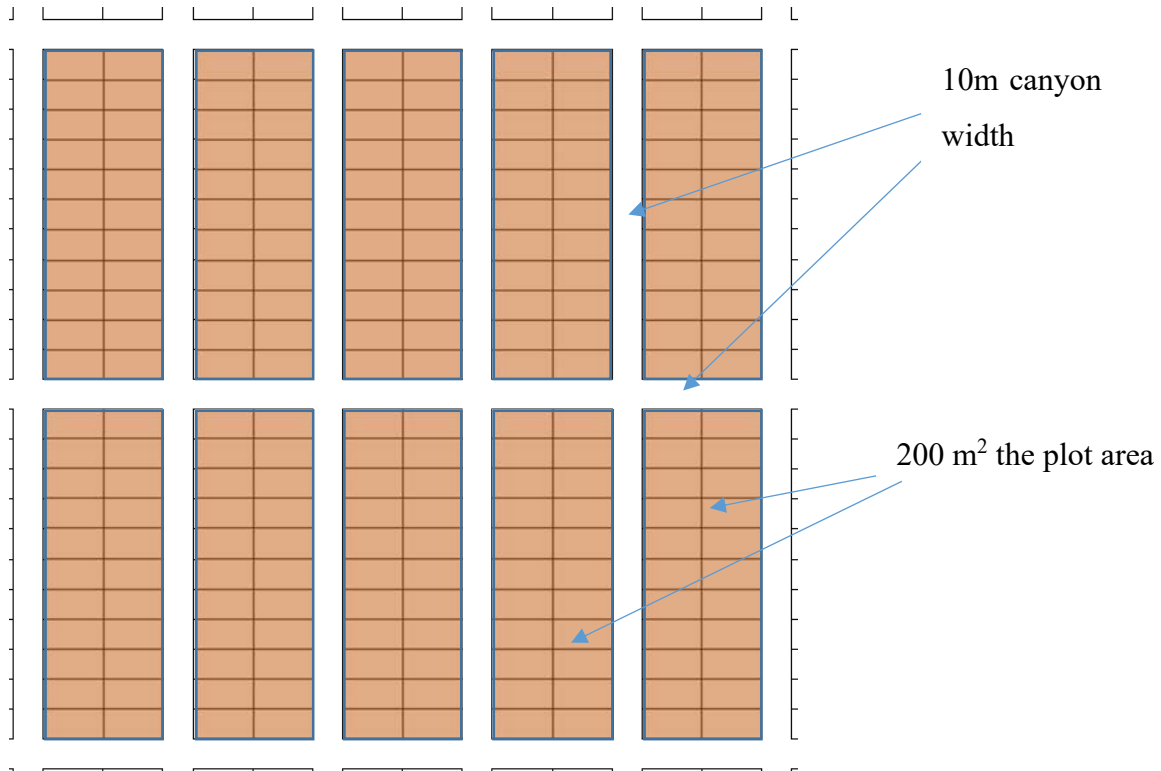


Figure 6.1: The residential blocks, 200 m² plot area and 10m canyon widths

The traditional morphology has different plot areas that are more or less than 200m² and different canyon widths, typically less than 5m. The investigated site is a high density residential block with attached houses (Figure 6.2). Most of the houses have one floor in general, 4 metres high, whilst the housing units' have courtyards surrounded by rooms. The houses are open to the central courtyard connected by an entrance only. The construction materials are bricks for load bearing walls (24cm x 12cm x 8cm) and wood or steel (I Section), with bricks for the ceiling. The streets are covered with concrete or bricks.



Figure 6.2: The residential blocks of traditional urban morphology, with different plot areas and canyon widths

ENVI-met was used to simulate both case studies with input data shown in Table 6-1.

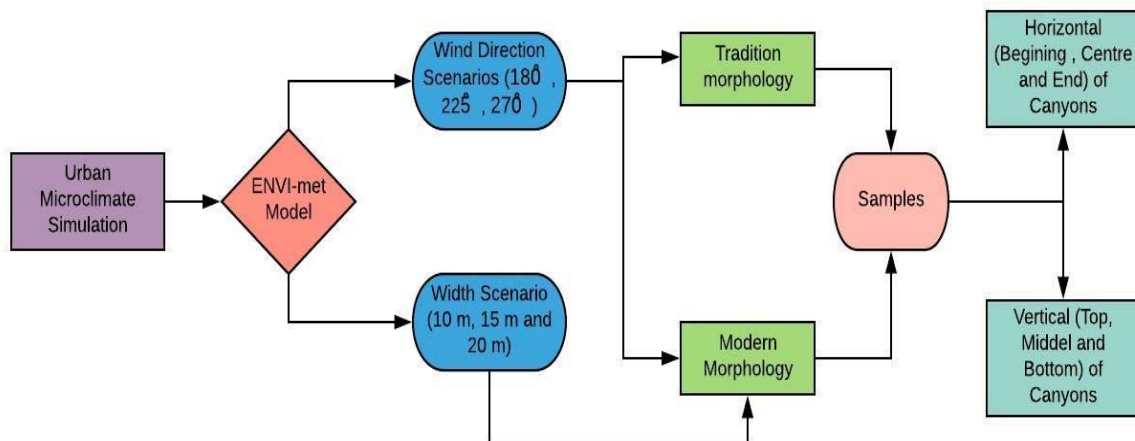


Figure 6.3: The ENVI-met model and samples for all scenarios for both traditional and Modern urban morphologies

Table 6-1 : ENVI-met input data for both modern and traditional urban morphology cases

Parameter	Units	Values	
Initial air temperature	C°	33.62	
Wind speed	m/s	0.55	
Wind direction	0 from the north and 180 from the south	225°	
Relative humidity at a 2m height	%	15.4	
Specific humidity at top of model	2000m g/kg	4	
Maximum air temperature at 15:00	C°	40.15	
Minimum air temperature at 05:00	C°	26.27	
Soil temperature at a depth of	(K)		
1. 00 to 5 cm		311.23	
2. 20 to 50 cm		306.07	
3. 50 to 200 cm		300.77	
4. Below 200 cm		298.81	
Building fabric used in ENVI-me model			
Urban blocks			
Materials	Reflectivity	Emissivity	Height
Walls layers (From inside to outside)			
1. Gypsum (2 cm)			
2. Hollow concrete blocks (20 cm)	0.73	0.9	6.40 m
3. Cement rendering (2 cm)	0.35	0.9	
Roofs layers (from top to bottom)			
1. Concrete tiles (10 cm)	0.5	0.9	
2. Fine soil (10 to 15 cm)	0.53	0.89	+ 6.40 m
3. Reinforcement concrete (20 cm)	0.8	0.91	
Pavements types			
1. Road Asphalt	0.19	0.9	
2. Concentrate pavement	0.29	0.9	+ 0.2 m
3. Green areas (grass)	0.26	0.9	
Shading mesh			
Shade mesh	0.4	0.07	+ 7.0 m
Building Properties			
Parameter	Units	Values	
Inside Temperature	K	297	
Heat Transmission Walls	W/m²K	0.74	
Heat Transmission Roofs	W/m²K	0.67	
Albedo Walls		0.3	
Albedo Roofs		0.15	

This section of the study compares the two urban morphologies (Figure 6.3). For research purposes and further investigation on local urban microclimate, two variables were analysed: air temperature (C°) and wind speed (WS m/s).

The proposed scenarios were divided into two sections to test the two variables:

1. Wind direction: Three wind directions (180°, 270° and 225°). This scenario is applied to both traditional and modern morphologies (Figure 6.3).
2. Canyons widths: Three different widths (10 m, 15 m and 20 m) were applied to the modern morphology only (Figure 6.3).

Note: Only one scenario¹ will be presented in this chapter. The rest of the data can be seen in the Appendix I. Both studies will be presented as shown in Table 6-2. The simulation period is 24 hours for 1st July, 2015. Wind direction applied is 225° from the north.

¹ This scenario comprises 225° wind direction and 10 m canyon widths for the modern morphology. The other scenarios can be seen in the Appendix I.

Three cases of wind direction applied over a residential block for both traditional and modern morphology. The modern morphology case also investigated three canyon widths 10m, 15m and 20m. The different wind directions are 180°, 270° and 225° from the north.

Table 6-2: ENVI-met outputs with data from two case studies traditional and grid-iron 1

ENVI-met Model	Properties of Morphology
Grid-iron canyons	10m canyon width & 200m ² plot area
traditional canyons	Different width and different plot areas

In this section, two variables for the ENVI-met outputs for grid-iron and traditional morphologies were investigated (air temperature and wind speed). The study was based on one wind direction (225° from the north) and two environmental factors, specifically air temperature TC° and wind speed WS (m/s). The section ends with a direct comparison between traditional and grid-iron urban morphologies.

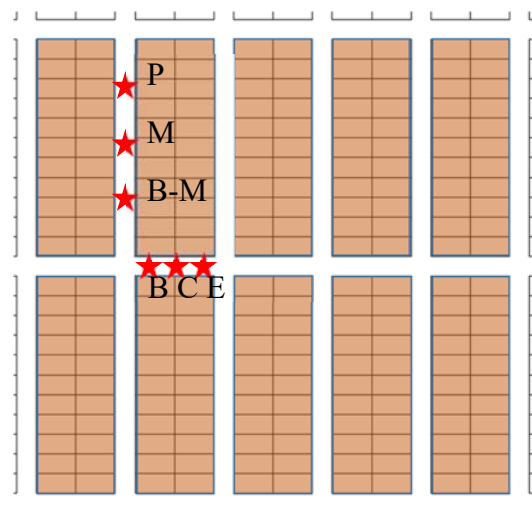
6.2.1 Grid-iron morphology

ENVI-met was employed to simulate the grid-iron (modern) morphology using the input data presented in Table 6-3. The results include air temperature and wind speed measurements for the grid-iron morphology at different times of the day, as shown in Table 12. The simulation was run for 24 hours on 1st July, 2015. However, only four times during that 24 hours period are presented.

Table 6-3: ENVI-met outputs data for Grid-Iron 1.

ENVI-met outputs	Wind Direction	Time of measurement				Urban morphology
		9:00	12:00	15:00	18:00	
T °C	225°	●	●	●	●	●
WS m/s	225°	●	●	●	●	●

The sample is located in the east-west and north-south canyons (see Figure 6.4). The east-west samples were taken at three positions in the canyon: Beginning (B), Centre (C) and at the End (E) of the canyon. The north-south samples were taken at the Top (P), Middle (M) and Bottom (BM) of the canyon (Figure 6.4).

**Figure 6.4: Shows the position of Horizontal and Vertical sample positions**

6.2.1.1 Air temperature and wind speed for grid-iron morphology

Air temperature was simulated and obtained using ENVI-met as shown in Figure 6.5. The results show air temperature for both the east-west and north-south canyon samples are similar during the night, while the results are slightly different during the daytime. The maximum air temperature is 41.40 °C at 13:00 for the BM sample in the north-south canyons, while the minimum air temperature is 33.3 °C at 04:00 for the BM sample. There are slight differences in air temperature for the east-west and north-south canyons during the daytime for both samples, as a result of different sun radiation falling onto the canyons.

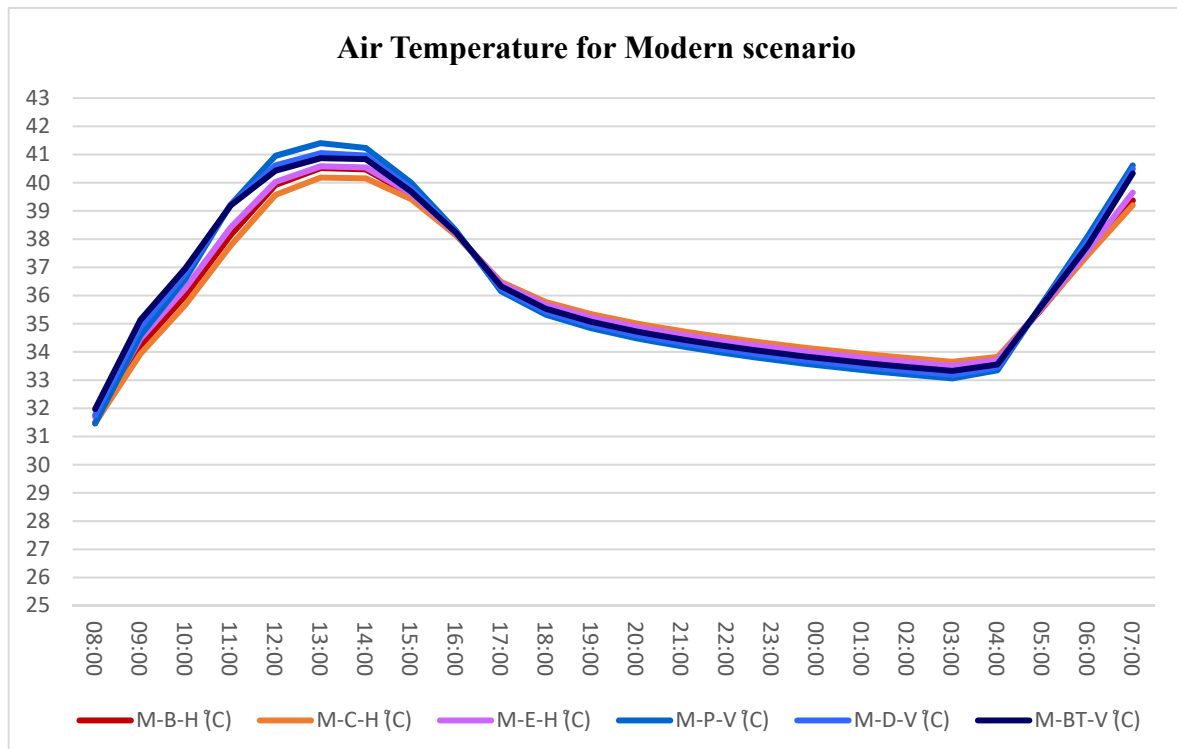


Figure 6.5: Air temperature for the east-west and north-south samples

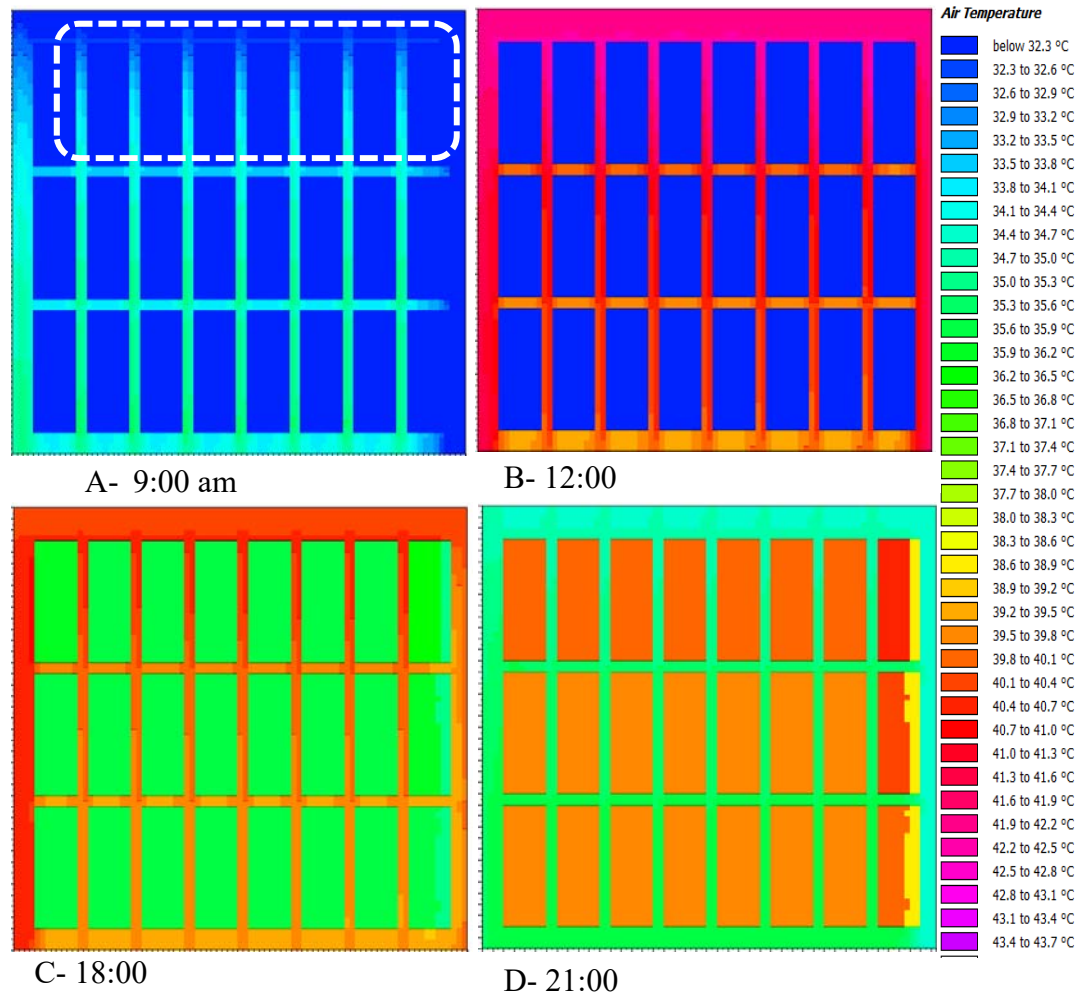


Figure 6.6: Air temperature using the ENVI-met simulation for the modern morphology at 09:00,

Figure 6.6 shows the air temperature for modern morphology with 10 metre canyon widths. The results indicate that air temperature varies between day and night-time (Figure 6.6). The air temperature between the east-west and north-south canyons has a similar colour distribution at the four times, as shown in Figure 6.6. The air temperature of canyons does not alter between the east-west and north-south canyons except for the 09:00 sample, where the top canyons (north-south) recorded lower temperatures compared to the middle and lower canyons. However, the other canyon samples are similar in air temperature during the day and night. This may be related to the boundary condition of model.

The wind speed for the first case scenario² shows that the horizontal canyons recorded lower wind speeds in contrast to the vertical canyons (Figure 6.7). Wind speeds for day and night-time are similar, as shown in Figure 6.7. The vertical canyon samples are divided into three

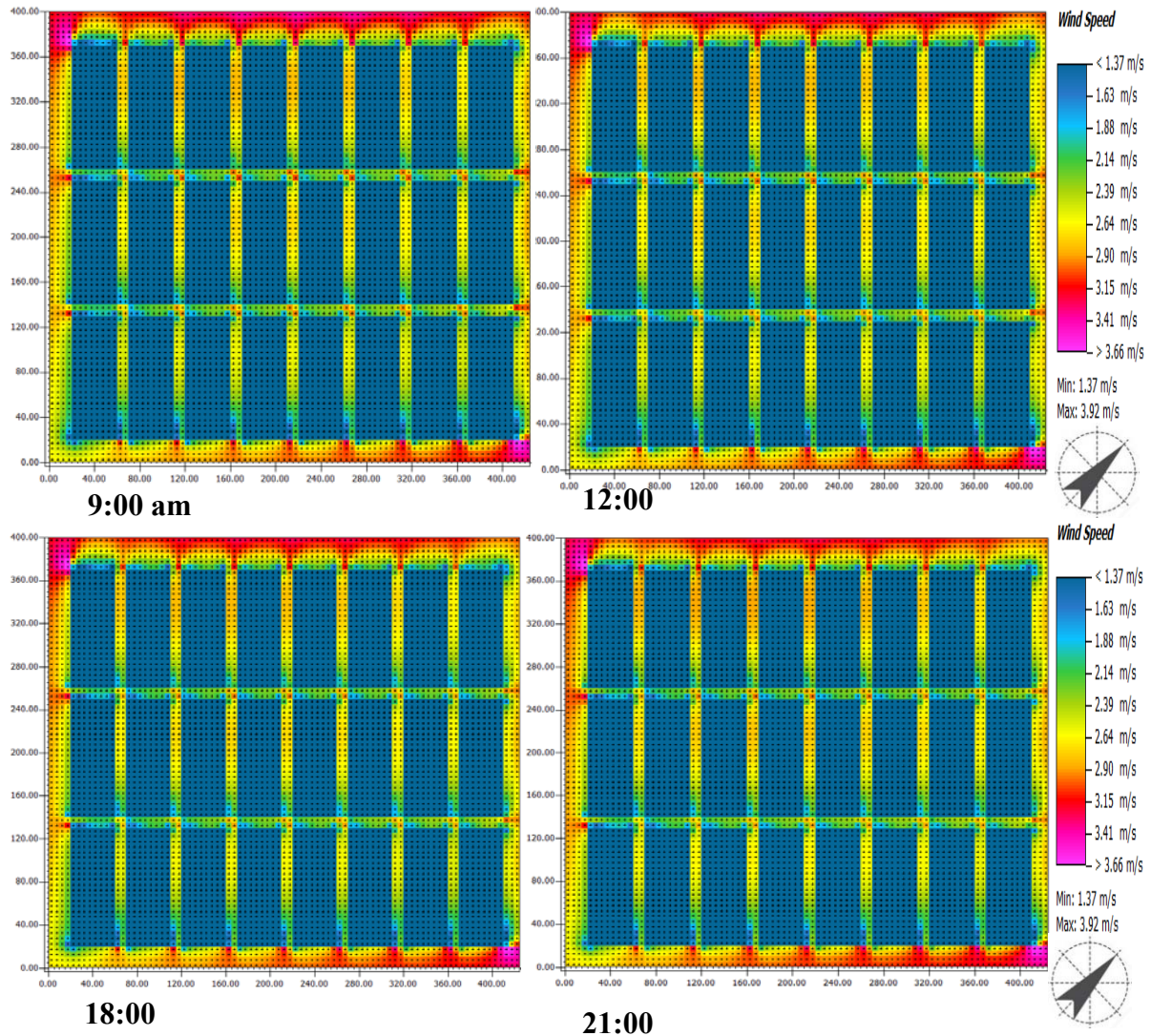


Figure 6.7: Wind speed using ENVI-met for modern morphology at 09:00, 12:00, 15:00 and 21:00

parts (Top, Middle and Bottom) of the canyons. Wind speeds for the Top and Middle locations were 2.64 m/s, while the Bottom canyon was relatively lower at a wind speed of 2.14 m/s, whilst the boundary condition of the site recorded higher wind speeds of 3.66 m/s (Figure 6.7).

² Modern morphology with 10m canyon width.

6.2.2 Traditional morphology

ENVI-met was used to simulate the traditional morphology with the input data shown in Table 6-4. The results include air temperature and wind speed measurements for traditional morphology at different times of the day, as shown in Table 6-4. The simulation was run for 24 hours on 1 July 2015, though they are presented only four times during that 24 hours period.

Table 6-4: ENVI-met outputs for Tradition morphology

ENVI-met outputs	Wind Direction	Time of measurement				Urban morphology
		9:00	12:00	15:00	18:00	Tradition
T °C	225°	●	●	●	●	●
WS m/s	225°	●	●	●	●	●

The samples for the traditional scenario were taken from east-west and north-south (see Figure 6.8). The east-west samples were taken in three places in the canyon, specifically Beginning (B), Centre (C) and at the End (E) of canyon. The north-south samples were taken at the Top (P), Middle (M) and Bottom (BM) of the canyon (Figure 6.8).

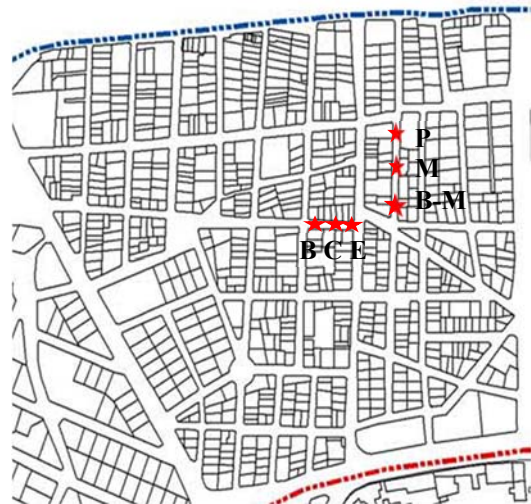
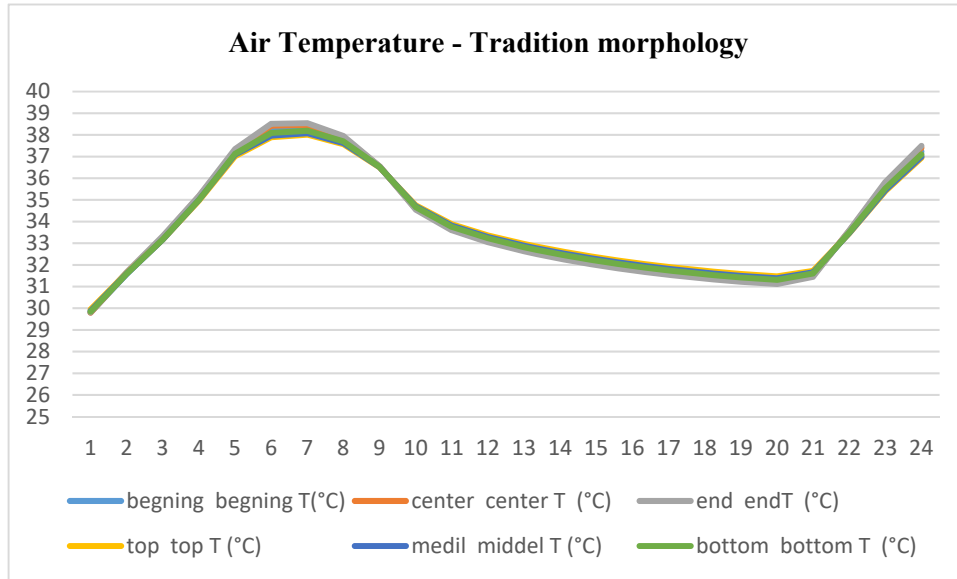


Figure 6.8: Illustrates the sample positions of the horizontal and vertical samples for the traditional scenarios

6.2.2.1 Air temperature and wind speed for Tradition morphology.

Air temperature simulated and obtained using ENVI-met is shown in Figure 6.9. The results reveals that the air temperature for both (east-west and north-south) samples recorded similar results (Figure 6.8). The maximum air temperature is 38.54 °C at 14:00 for the E sample in the east-west canyons, whereas the minimum air temperature is 29.79 °C at 8:00 am in the C sample. There are slight differences in air temperature for east-west and north-south canyon samples during daytime, less than 1 °C (Figure 6.9).



6.9: Air temperature for east-west and north-south samples

Figure 6.10 shows the air temperature for the traditional morphology with different canyon widths (less than 5 metres). The results explain that the air temperature varies between day and night-time (Figure 6.9). The air temperature between the east-west and north-south canyons

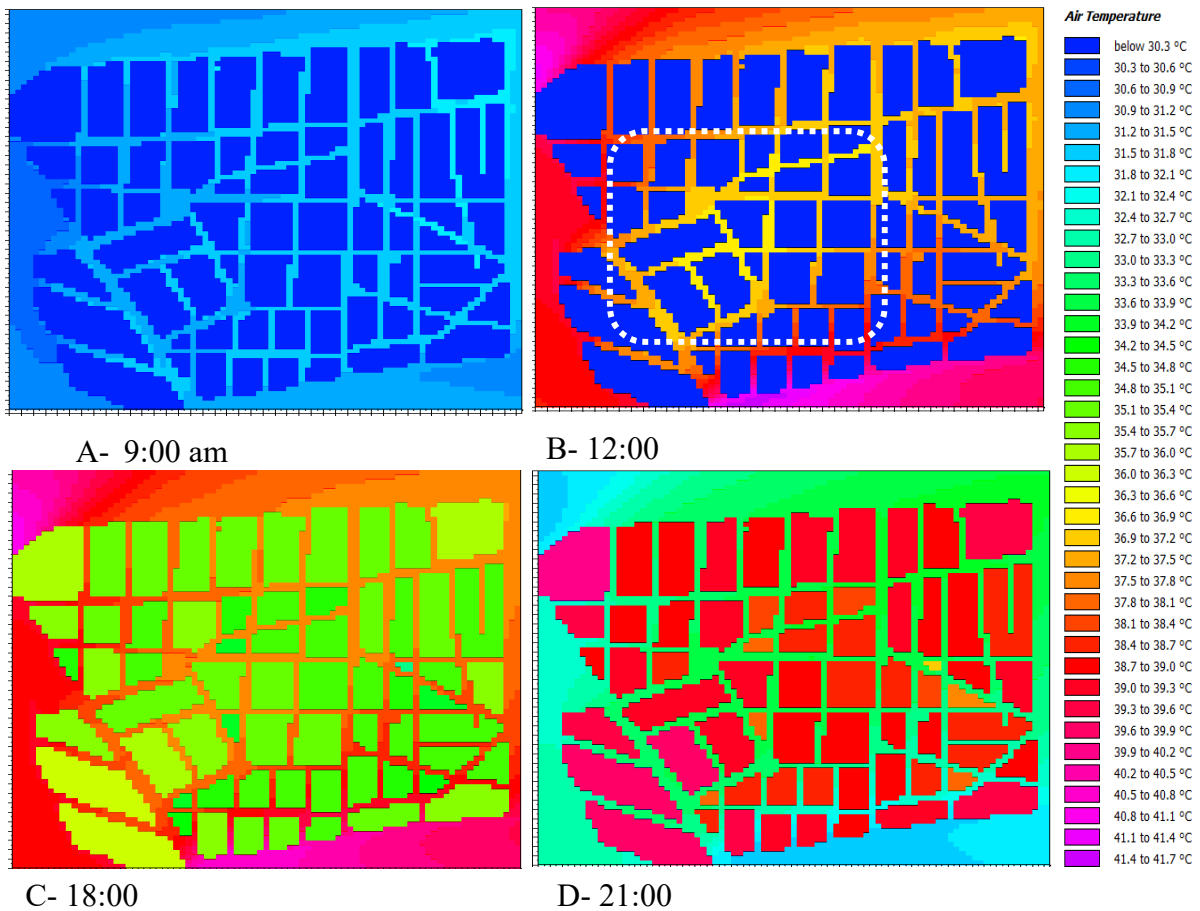


Figure 6.10: Air temperatures for the traditional morphology using the ENVI-met morphology at 09:00, 12:00, 15:00 and 21:00

recorded a similar range of temperatures (colour) at the four times, as shown in Figure 6.10. Moreover, the air temperature of the canyons does not change with canyon direction (vertical and horizontal) except for the 12:00 sample, where the middle canyons recorded higher air temperatures compared to the canyons above and below the highlighted white box (Figure 6.11-B) the highlighted white box. However, the other canyon samples (09:00, 18:00 and 21:00) have similar air temperatures.

The wind speeds for the second case scenario³ indicate that the horizontal canyons recorded similar wind speeds in contrast to the vertical canyons (Figure 6.11). Wind speeds for day and night samples were similar except in the middle of the canyons (Figure 6.11-B). The middle canyons recorded 2.29 m/s (red colour) compared to other canyons 1.63 m/s (yellow colour). In addition, three north-south canyons also recorded higher wind speed in comparison to the east-west canyons (Figure 6.11 -C-18:00).

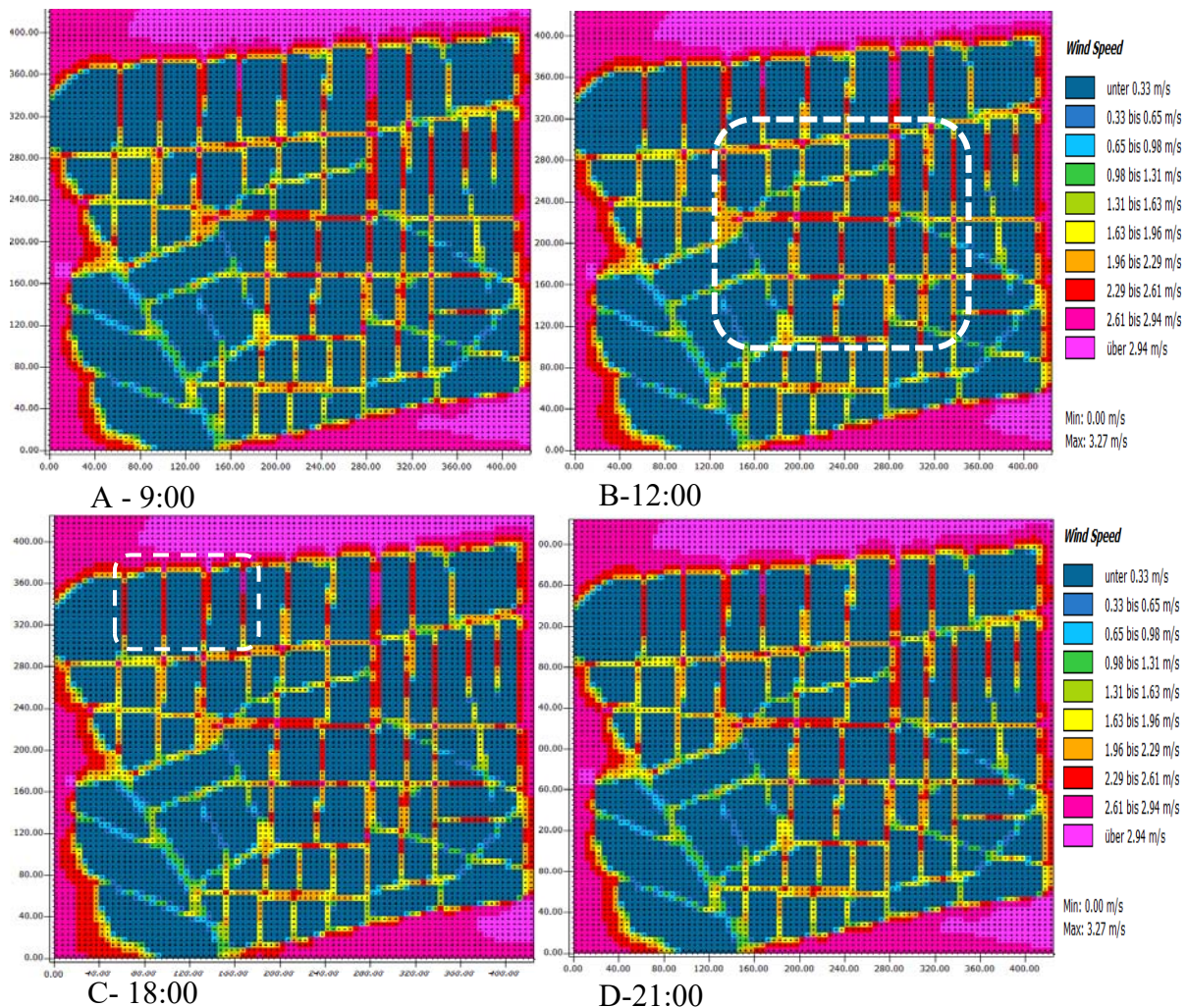


Figure 6.11: Shows wind speed for tradition morphology at 9:00, 12:00, 18:00 and 21:00.

³ Traditional urban morphology with narrow width canyons (less than 5 metres).

6.3 Comparisons traditional and modern morphologies

The ENVI-met model for both traditional and modern urban morphologies was simulated with a similar configuration file (Table 6-1). The air temperature was measured for both scenarios

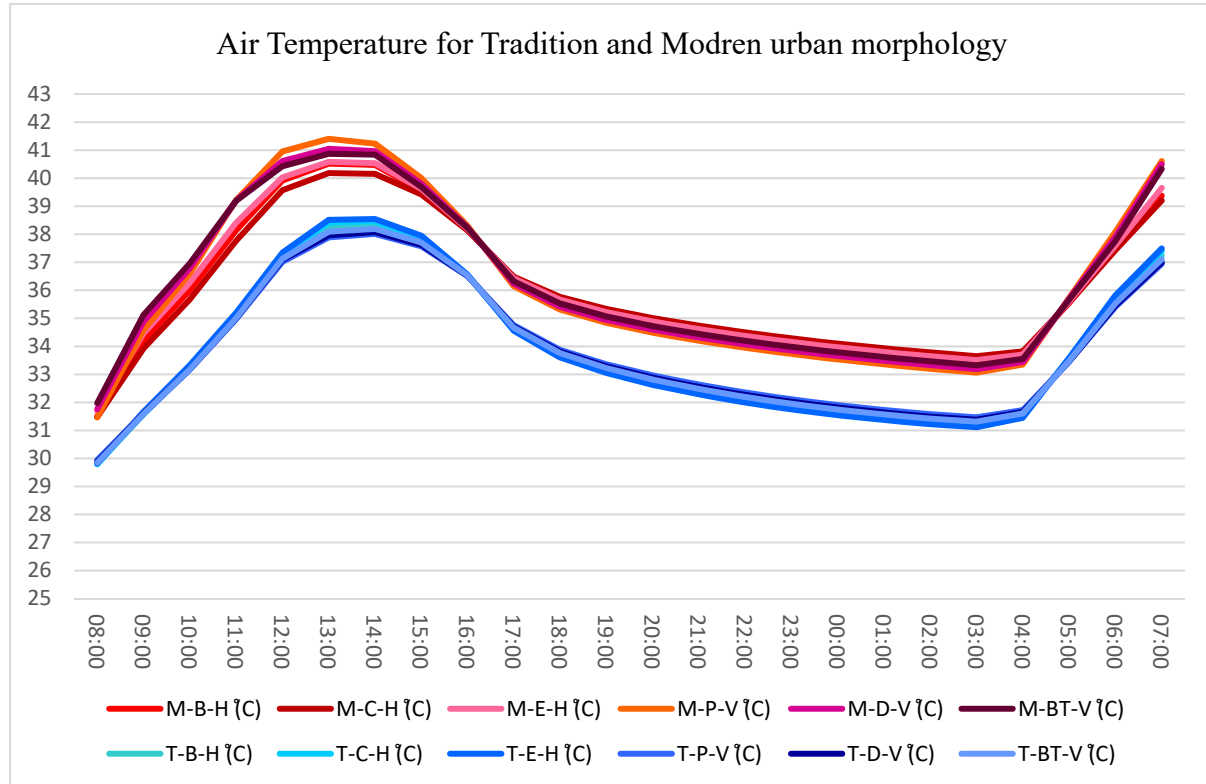


Figure 6.12: Shows air temperature for both tradition and modern morphology for horizontal and vertical samples.

in six positions (east-west and north-south) at a height of 1.8 metres. The results demonstrate that the air temperature for the modern morphology is higher than the traditional morphology in both the east-west and north-south samples during the day and night. The maximum air temperature is 41.40 °C at 13:00 for the top position (north-south canyons), while the minimum temperature for a similar scenario is 33.18 °C for the middle position (north-south samples). The maximum air temperature for the traditional morphology is 38.54 °C at 14:00 at the end of the east-west canyons, while the minimum temperature is 31.31 °C for a similar scenario.

Figure 6.12 shows that there is a difference of almost 2 °C in each position between the traditional and modern urban morphologies. The difference in air temperature ($\Delta \bar{T}_C$) for the modern east-west and north-south samples is more than the differences in air temperature ($\Delta \bar{T}_C$) for the traditional morphology. The different morphologies have little effect on wind speed, although they do have an effect on air temperature.

6.4 Wind direction simulation

In this section of the study, wind speed and its direction were simulated by means of the CFD program embedded within ENVI-met, using input data from a weather station located in the northern part of Erbil⁴. The aim of this set of simulations is to understand wind speed properties surrounding buildings and open-green spaces for the modern⁵ morphology in Erbil. To achieve this aim, three wind direction scenarios were proposed and analysed as below:

- A. First scenario with 180° wind direction from the north
- B. Second scenario with 225° wind direction from the north
- C. Third scenario with 270° wind direction from the north

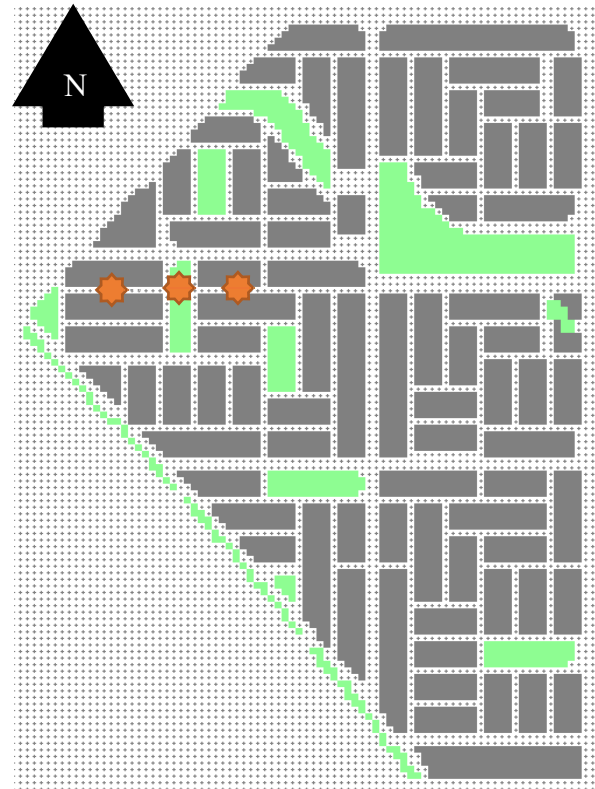


Figure 6.13: Case study Scenario modelled using ENVI-met.

In this simulation, wind direction was only changed to investigate wind speeds using ENVI-met. In addition to wind speed, air temperatures were measured for the canyons before the centre and after the open spaces (Figure 6.13).

⁴ The north weather data station is located in a rural area. Wind speed is higher than the city centre weather station. For this set of simulations, we used a wind speed 4 m/s from the north weather station.

⁵ Modern morphology refers to any development of Erbil which does not follow organic morphology. For the case study, this research used the proposed design and ran all simulation scenarios.

6.4.1 First scenario with 180° wind direction from the North.

6.4.1.1 Air Temperature for First Scenario.

Air temperatures were taken from the three points as shown in Figure 6.14. The samples were taken at a height of 1.8 metres, for three positions (before, centre and after) in the open green space.

The results revealed that the maximum air temperature is 42.68°C and the minimum air temperature 28.97°C. Both maximum and minimum air temperatures are for the centre of the open space. This means after the open space is either hotter or cooler than the canyons, depending on the time of day (Figure 6.15).

The air temperature in the centre of the open space appears to be dependent either on the SVF, gaining solar energy during the daytime and losing energy to the night sky during the evening. The canyons either side of the open space are less influenced by solar gain and night-time losses or the temperature in the centre of open space depends on orientating the open spaces, as the open space aligns with the wind direction (Figure 6.14). The canyons either side are sheltered from the prevailing wind and respond less to the diurnal variation of the air temperature.

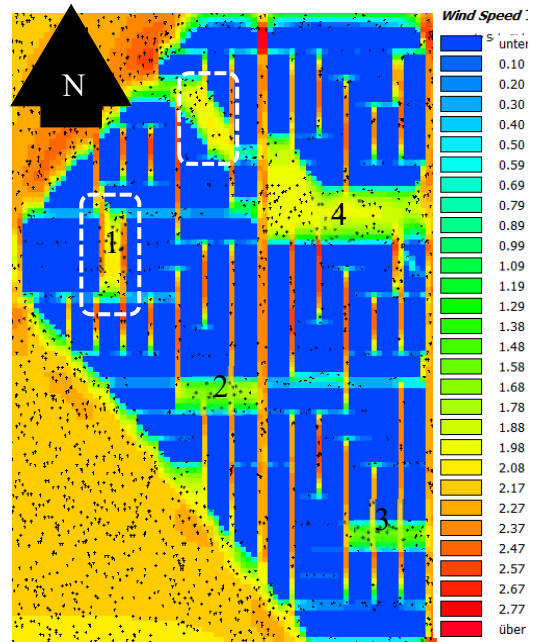


Figure 6.14: ENVI-met output showing wind speed for the first scenario, wind direction 180° from the north

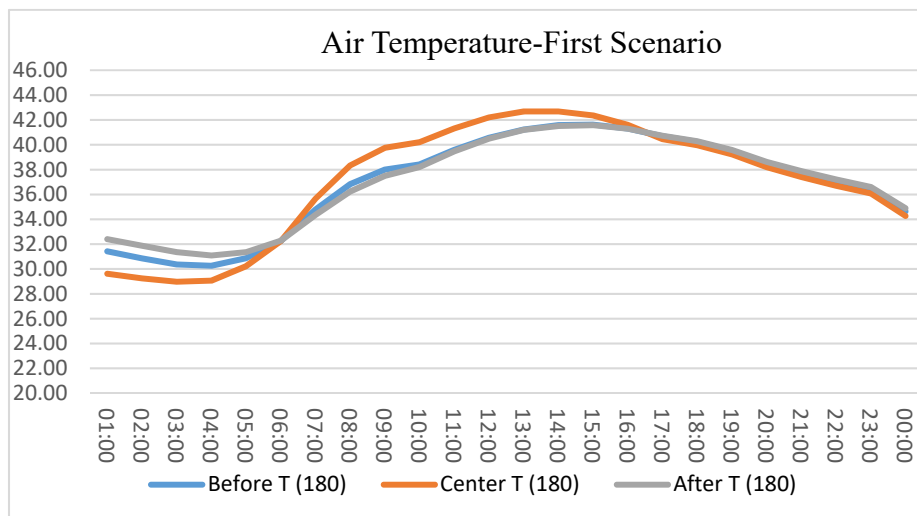


Figure 6.15: Air Temperatures for the first scenario when wind direction is 180° from the North

6.4.1.2 Wind Speed for the first scenario

Wind speed measured for three points Before, Centre and After the open space (Figure 6.16). The results show that the north-south canyons work as a channel for the wind, with wind speeds higher than other urban areas (Figure 6.16). The north-south canyons were predominately (red colour) more than 2.57 m/s compared to the east-west canyons less than 0.3 m/s (blue and grey colour) (Figure 6.14). The wind speed in this scenario can be explained further by means of the points below:

1. The north-south canyon is parallel to the wind direction and works as a channel for the wind, with wind speeds higher than other urban areas (Figure 6.14).
2. Canyons with 15 metre (main roads) widths have higher wind speeds than those with widths that are 10 metres wide (branch roads), specifically canyons which are perpendicular to the wind direction (Figure 6.14).
3. Green and open spaces have higher wind speeds compared with the east-west canyons and are lower than the north-south canyons.
4. The two open spaces on the eastern part of the model have the largest values for wind speed, as their direction corresponds with the wind direction 180° from the north (Figure 6.14).
5. East-west canyons recorded the lowest wind speed as they are perpendicular to the wind direction (Figure 6.14).
6. Wind speeds around the buildings in urban canyons vary depending on canyon directions and the width of the canyon. North-south canyons generally recorded higher wind speeds than the open spaces, while the wind speeds in open spaces were higher than the east-west canyons.
7. Wind speeds depend primarily on the urban environment and canyon characteristics. The branch roads running in an east-west direction (shorter), generally start with higher wind speeds, are lower in the middle, and become higher again when connecting with the north-south canyons (Figure 6.14).

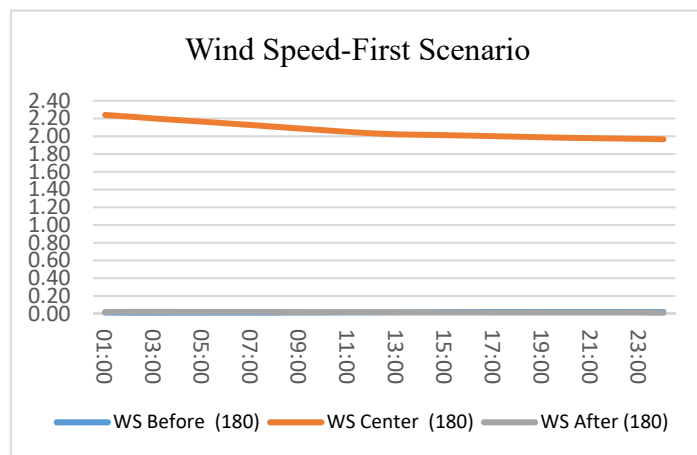


Figure 6.16: Wind Speed for first scenario when wind direction is 180° from the North

8. Road junctions regularly record higher wind speeds and created a tunnel effect where dense built-up areas remain in the wind's shadow. The last canyon on the top north east part of the model shows the lowest wind speed, where the flow chooses the shortest path to escape.
9. Wind shadow can be seen clearly on the edge of the model in all directions except north-south. This occurs because the wind that comes from boundary conditions at high speed is reduced by built-up urban features (Figure 6.16).

6.4.2 Second scenario with 225° wind direction from the north

6.4.2.1 Air temperatures for the second scenario

Air temperatures were taken from three points as shown in Figure 6.13. The samples were taken at a height of 1.8 metres for three positions (Before, Centre and After) the open green space. The maximum air temperature is 42.47°C and the minimum 29.35°C. The maximum air temperature is for canyons before the open space, while the minimum air temperature is recorded for the centre of the open space (Figure 6.18). Overall, the air temperatures for the open space and canyons before and after the open space are similar. Moreover, the air temperature is not showing any difference during daytime and night-time for all points (similar range) (Figure 6.18).

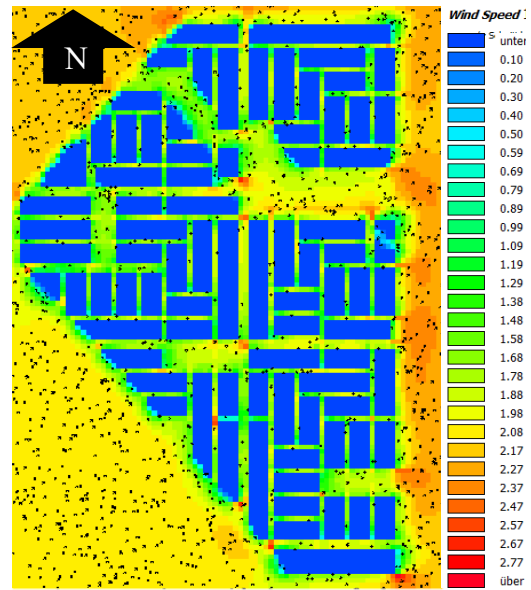


Figure 6.17: ENVI-met output for Wind speed for the second scenario when wind direction is 225° from the North

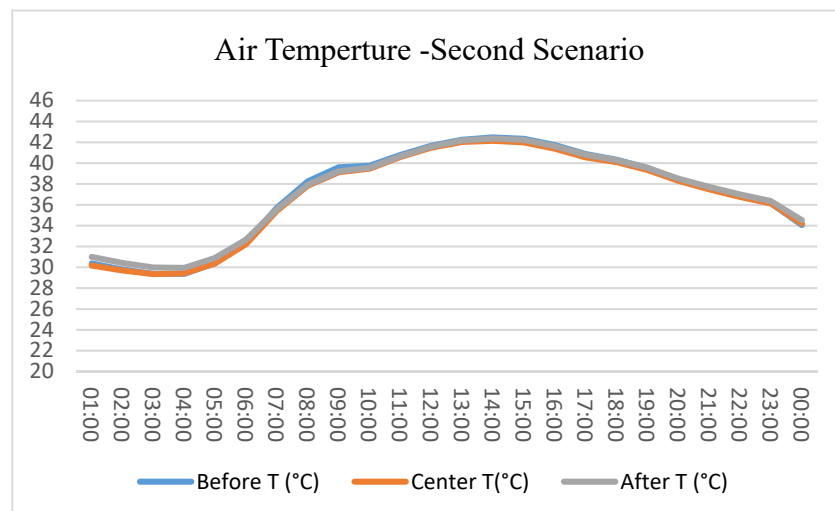


Figure 6.18: Air Temperature for the second scenario when wind speed is 225° from the north

6.4.3 Wind speed for the second scenario

Wind speed was measured for the three points Before, Centre and After the open space (Figure 6.13). The results show that the north-south and east-west canyons work as a channel for the wind (Figure 6.17). The north-south and east-west canyons coloured yellow and light green (1.78 to 2.08 m/s) are similar to the open spaces (1.78 to 2.08 m/s). The wind speed in this scenario is explained through the points below:

1. Wind speeds are generally distributed between urban areas better than the previous scenario (wind directions 180°) from the north, for both canyons and open spaces.
2. Open spaces and canyons after the open space have slightly higher wind speeds compared with the canyons before the open space (Figure 6.19).

3. Wind speeds recorded higher values for the canyon with a 20m width and are lower for canyons with a width of 10m, except for the canyons with a 20m width on the southern part of the model (Figure 6.20). This occurs because of the wind shadow of higher buildings located in the wind flow direction.

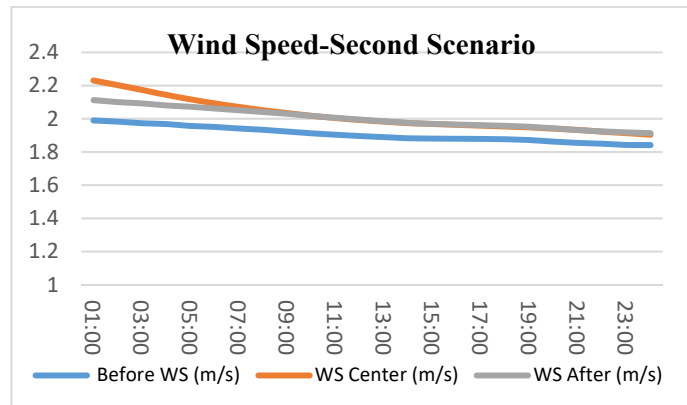


Figure 6.19: Wind Speed for second scenario when wind direction is 225° from the North.

4. Wind speeds in this scenario are higher in the longer canyons. This means that the wind speed in any canyon depends on the features of the canyon and not just the wind direction.

5. Wind speed is slightly lower on road intersections owing to the wind direction and as the canyon orientation is not parallel to the wind flow (225°), whereas in the middle of the canyon the wind flows directionally along it (Figure 6.20).

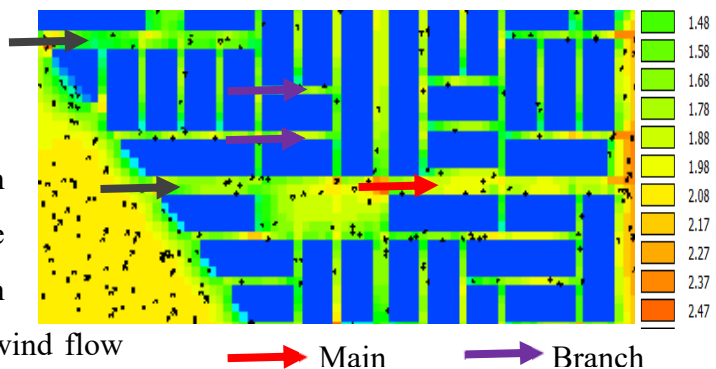


Figure 6.20: ENVI-met image shows wind speed for main roads and branch roads

6. In general, this scenario indicates that the north-south canyon records similar wind speeds with east-west canyons and open space (Figure 6.19).
7. Wind speed in all urban areas (canyons and open spaces) is distributed equally.

6.4.4 Third scenario with 270° wind

6.4.4.1 Air Temperature for third scenario (270° from the north).

Air temperatures were taken for the three points, as shown in Figure 6.13. The samples were taken at a height of 1.8 metres for three positions (Before, Centre and After) the open green space.

The results indicate that the maximum air temperature is 43.66 °C and the minimum air temperature is 29.06 °C. Both maximum and minimum air temperatures are for the canyon before the open space (Figure 6.22). Figure 6.22 shows the air temperatures at the three measurement locations. The wind direction is now parallel with the canyons, whilst the temperature profiles are similar.

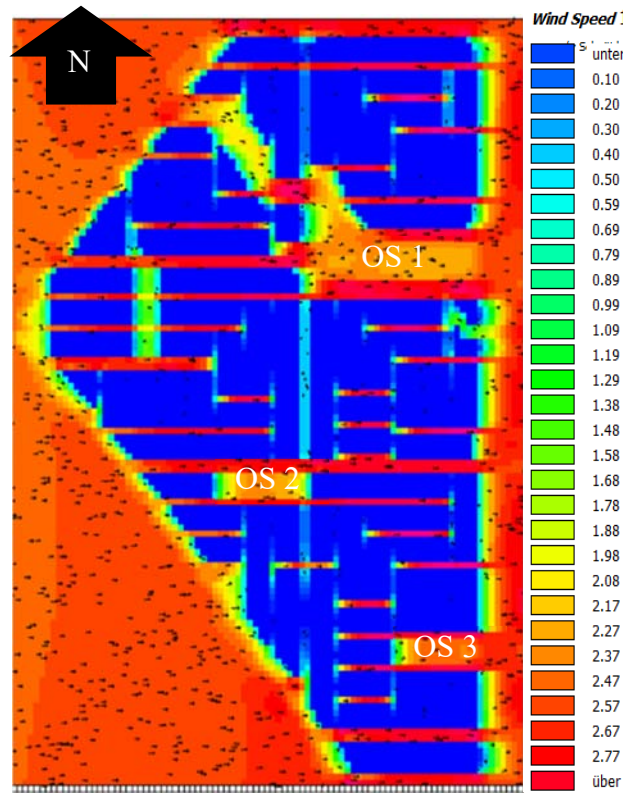


Figure 6.21: ENVI-met output for the third scenario when wind direction is 270° from the north

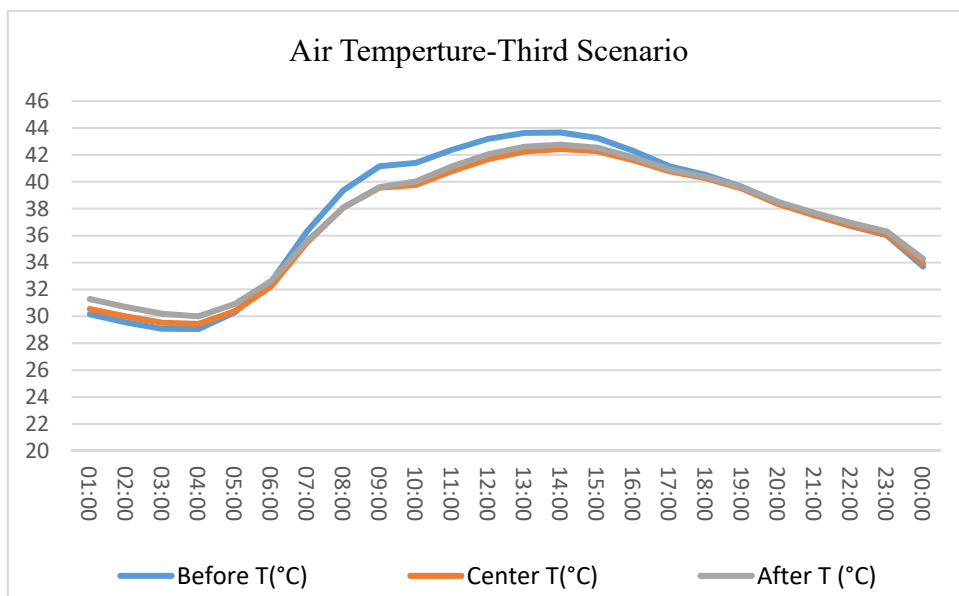


Figure 6.22: Air temperature for the third scenario when wind direction is 270° from the north

6.4.4.2 Wind speed for third scenario (270° from the north).

Wind speed was measured for the three points Before, Centre and After the open space (Figure 6.13).

The results show that the east-west canyon works as a channel for the wind Figure 6.24, because they are parallel to the wind direction. The east-west canyons are red colour (2.57 m/s and above) compared to the open spaces, coloured light green-yellow (lower than 1.9 m/s) (Figure 6.23). The wind speed in this scenario can be explained by means of the points below:

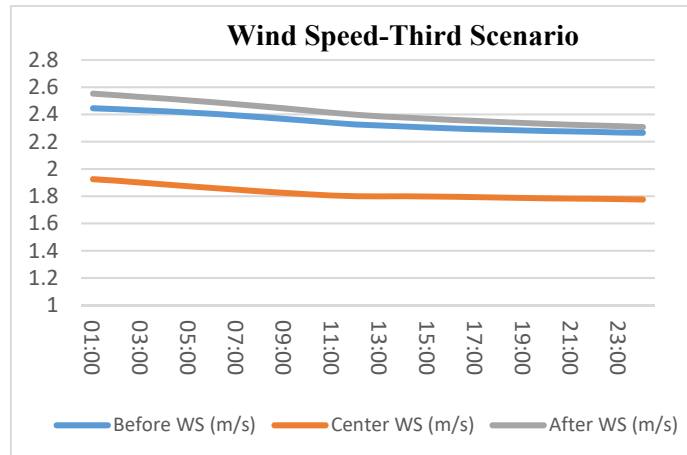


Figure 6.23: Wind Speed for third scenario when wind direction is 270° from the North.

1. The east-west canyons work as channels for the wind, with the wind speeds higher than other urban areas (open spaces and north-south canyons) (Figure 6.21).
2. Canyons with 20m width (main roads) have very similar wind speeds as the 10m and 15m wide canyons depending on wind direction (Figure 6.24).
3. Green and open spaces have higher wind speeds compared to north-south canyons and lower than the east-west canyons (Figure 6.24).
4. The three open spaces on the eastern part of the model have the largest values for wind speed as their direction corresponds with the wind direction (Figure 6.21).
5. The open spaces (OS) are rectangular shapes located parallel to the wind, and this direction recorded higher values in contrast to the other OS perpendicular to wind direction in this scenario.
6. The three OS in the eastern part of the model (1, 2 and 3) have higher wind speed values as their direction corresponds with the wind direction (Figure 6.24).

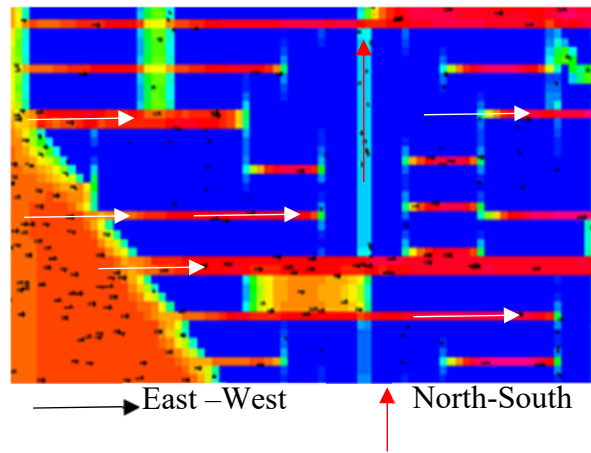


Figure 6.24: Showing the differences between East-West and North-South canyons.

7. Wind speeds around the buildings in the urban canyons vary, depending on canyon directions. north-south canyons record the lowest wind speed as they are perpendicular to the wind direction.
8. Wind speeds depend primarily on urban microclimate and canyon characteristics, and the branch roads in east-west directions that are generally shorter start with higher wind speeds compared to longer canyon (north-south) directions. Canyons perpendicular to the wind direction have lower speeds in the middle and increase when connected with the east-west canyons.
9. Road junctions regularly recorded higher wind speeds and created tunnel effects, whereas high density built-up areas remained in wind shadows (Figure 6.24).
10. Wind shadow effects can be seen clearly on the edge of the model in all directions except east-west. This occurs because the wind speeds that come from boundary conditions are high and are reduced by built-up urban areas (Figure 6.21).

6.4.5 Comparisons between all scenarios for wind directions (180°, 225° and 270°) from the north.

6.4.5.1 Air Temperature for all scenarios

Air temperatures for the nine samples are compared in Figure 6.25. The samples represent the three wind direction scenarios (180°, 225° and 270°). The results confirm that the maximum air temperature is 43.66°C and the minimum 28.97°C (Figure 6.26).

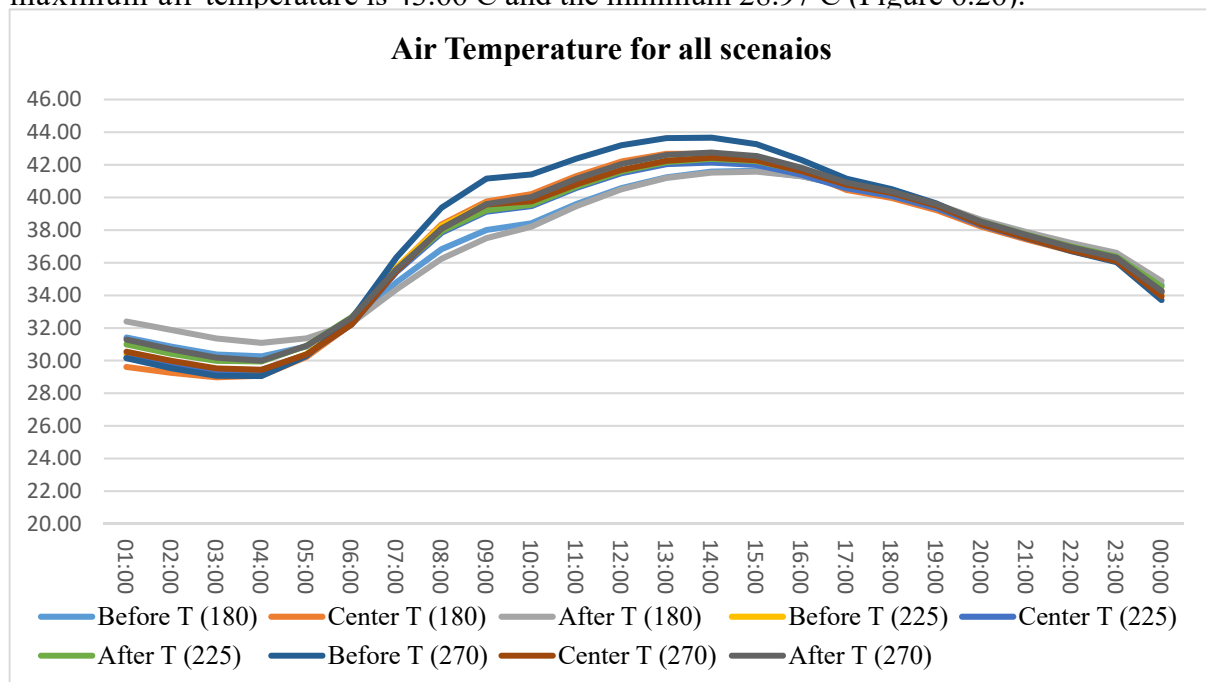


Figure 6.25: Air temperature for all wind direction scenarios (180°, 225° and 270°) from the north

The maximum air temperature recorded within the canyon is located before open spaces for the 270° wind direction scenario, while the minimum air temperature was recorded for the canyon that is located after the open space for the scenario with the 180° wind direction from the north. The maximum (ΔT) between daytime and night-time was 14.61°C and the minimum was 10.49°C Table 6-5.

Table 6-5: Compare between all seniors (180°, 225°, and 270°)

	Scenario 1: 180°			Scenario 2: 225°			Scenario 3: 270°		
	Before	Centre	After	Before	Centre	After	Before	Centre	After
Max (°C)	41.63	42.68	41.58	42.477	42.14	42.36	43.66	42.43	42.76
Min (°C)	30.26	28.97	31.09	29.37	29.35	29.95	29.06	29.44	30.00
ΔT	11.37	13.71	10.49	13.11	12.80	12.41	14.61	13.00	12.76

The maximum difference in air temperature between scenarios was at 09:00 for the sample located before open spaces for the 270° scenario and the canyon that is located after the open spaces for the 180° scenario. In general, canyons and open spaces for all three scenarios recorded different values depending on the location and characteristics of the canyon. Overall, the air temperature in the second scenario (225°) recorded more stable patterns in terms of maximum and minimum air temperature compared to the other two scenarios (180° and 270°) (Table 6-5).

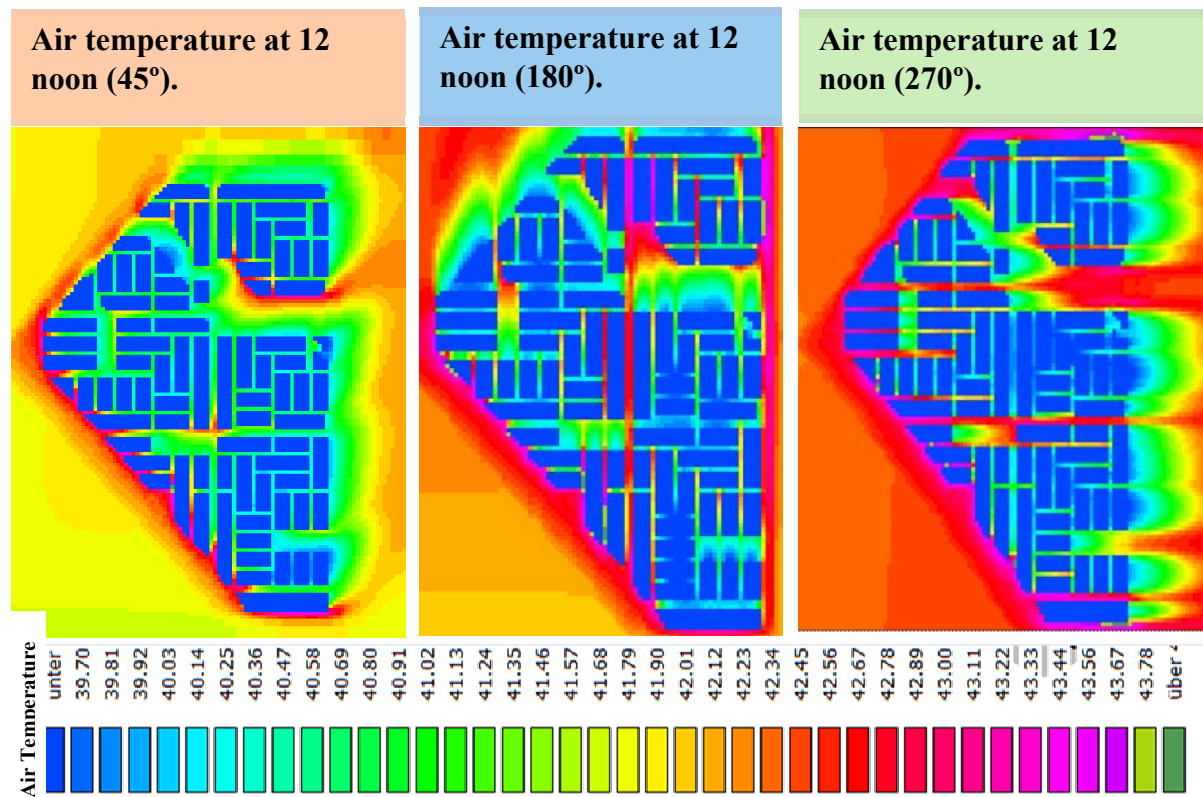


Figure 6.26: Air temperature for all three scenarios (45°, 180°, and 270°).

6.4.6 Wind speed for all scenarios

Wind speed (WS) for the nine samples is compared in Figure 6.27. The samples represent three wind direction scenarios (180°, 225° and 270°). The results reveal that the maximum wind speed is 2.55 m/s and the minimum wind speed is 0.01 m/s. The maximum wind speed was recorded for the canyon located after the open space for the 270° wind direction scenario, while the minimum wind speed was recorded for any canyons perpendicular to the wind direction for both scenarios, 180° and 270°, respectively. Generally, open spaces recorded average wind speed values for all scenarios. WS for the first and third scenarios (180° and 270°) recorded high WS for canyons parallel to the wind direction and low WS values for canyons perpendicular to the direction of the wind (Figure 6.27). The simulation result for all scenarios shows that the 225° wind direction is more stable for both north-south and east-west canyons. In addition, the open spaces recorded an average level of wind speed for similar scenarios. WS for the 225° scenario is distributed better for all urban areas compared to other scenarios. From the simulation results, WS and air temperature are more stable for urban areas (canyons and open spaces) when wind direction is 225° from the north.

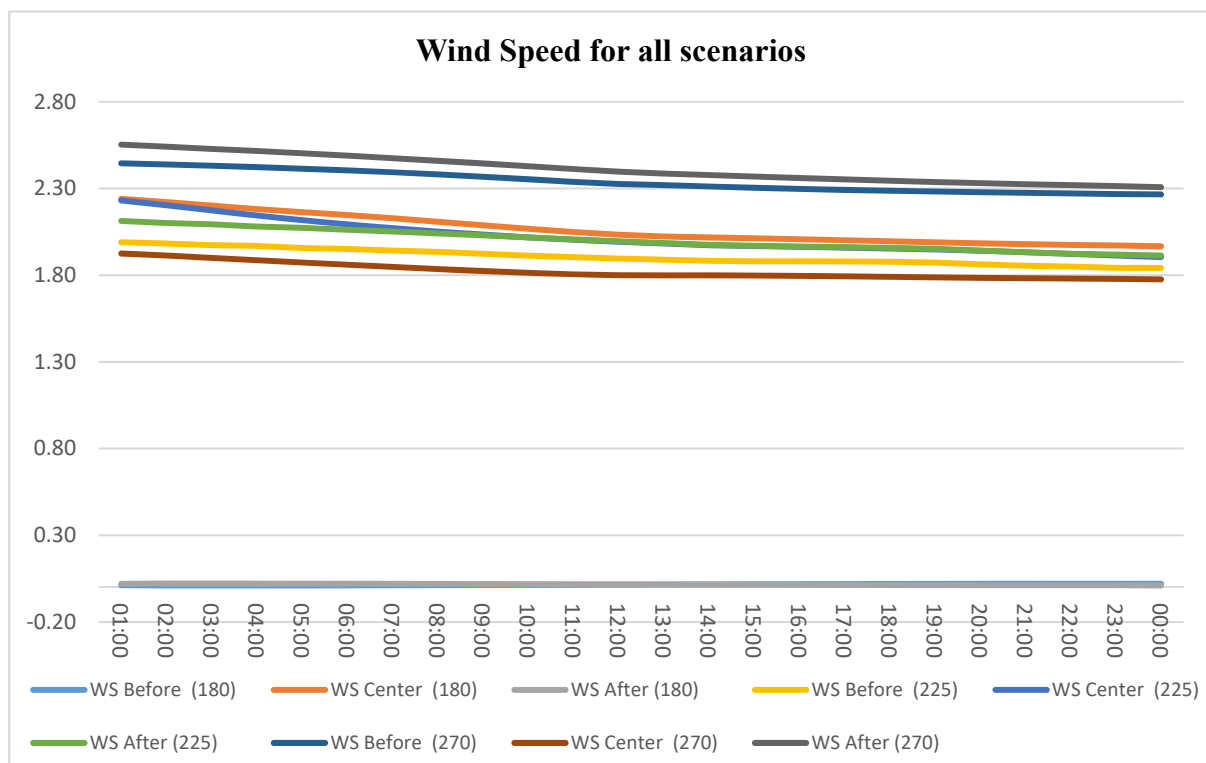


Figure 6.27: Compare Wind Speed (WS) for all scenarios (180°, 225° and 270°) from the North.

6.5 Proposed Design Interventions (Erbil Case Study)

The purpose of the urban design interventions in this study aims to decrease the air temperature and increase the wind speeds in urban areas. Three different design scenarios were proposed aiming to minimise air temperature and maximise wind speed in urban areas.

Air temperature and wind speed for each simulation were calculated for 1st July 2017. The three design scenarios are described below:

1. Adding central open-green areas (Figure 6.29 - A).
2. Increase width of east-west canyons from 12 to 20m (Figure 6.29 - B).
3. Adding individual open-green areas between housing units (Figure 6.29 - C).

In this section, the proposed design scenarios are simulated and analysed using the ENVI-met program with wind direction 225° from the North. The Designed scenario was discussed in Section 5.5. This case study was selected because:

1. It is the proposed design and can be edited to enhance an urban microclimate using simulation (Figure 6.28).
2. The case study location is in the southern part of Erbil with medium dense urban development. The location is on the border line of new and existing developments which may help to predict the future development of the urban microclimate outside Erbil's existing urban area.
3. Typical urban morphology (grid-iron) (Figure 6.28). Most of the new developments in the city will use a similar approach. This issue is explained in detail in Chapter 4.

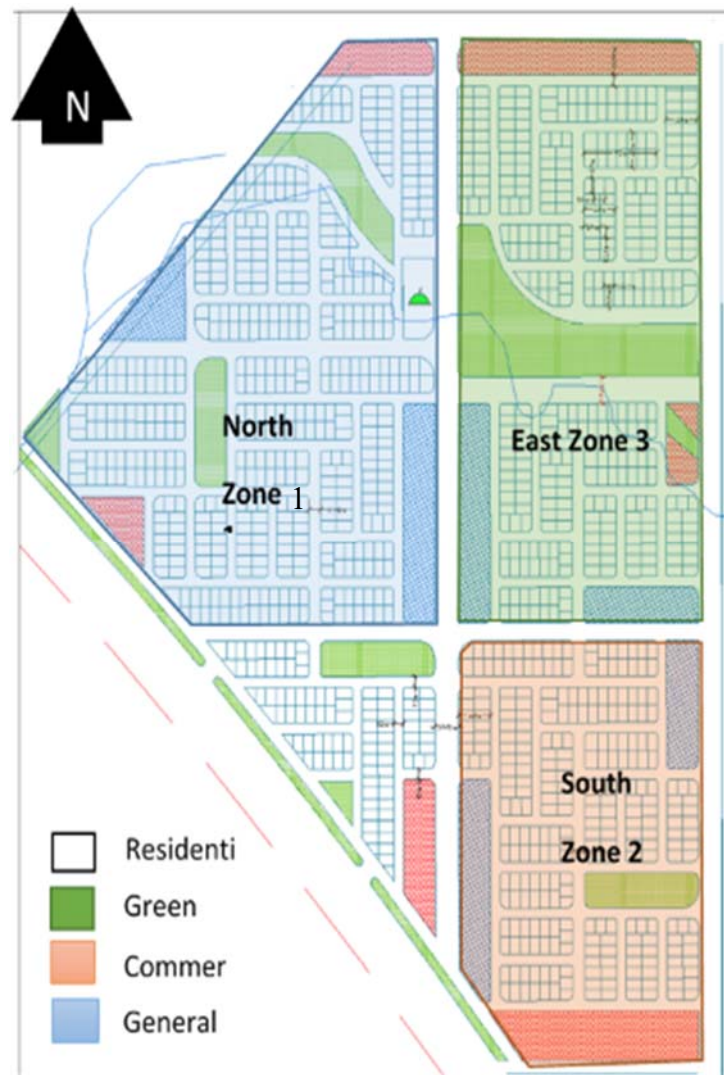


Figure 6.28: Designed scenario, typical grid-iron urban morphology for low rise residential buildings in Erbil

Three scenarios are compared with a Designed case study. The comparison will compare three zones⁶ in each scenario (Figure 6.29).



Figure 6.29: Designed case scenario and three proposed design interventions using ENVI-met

⁶ The site plan was divided into three zones: 1, 2 and 3. Each zone was measured under similar environmental conditions. However, the design intervention only took place in Zone 1. Figure.56.

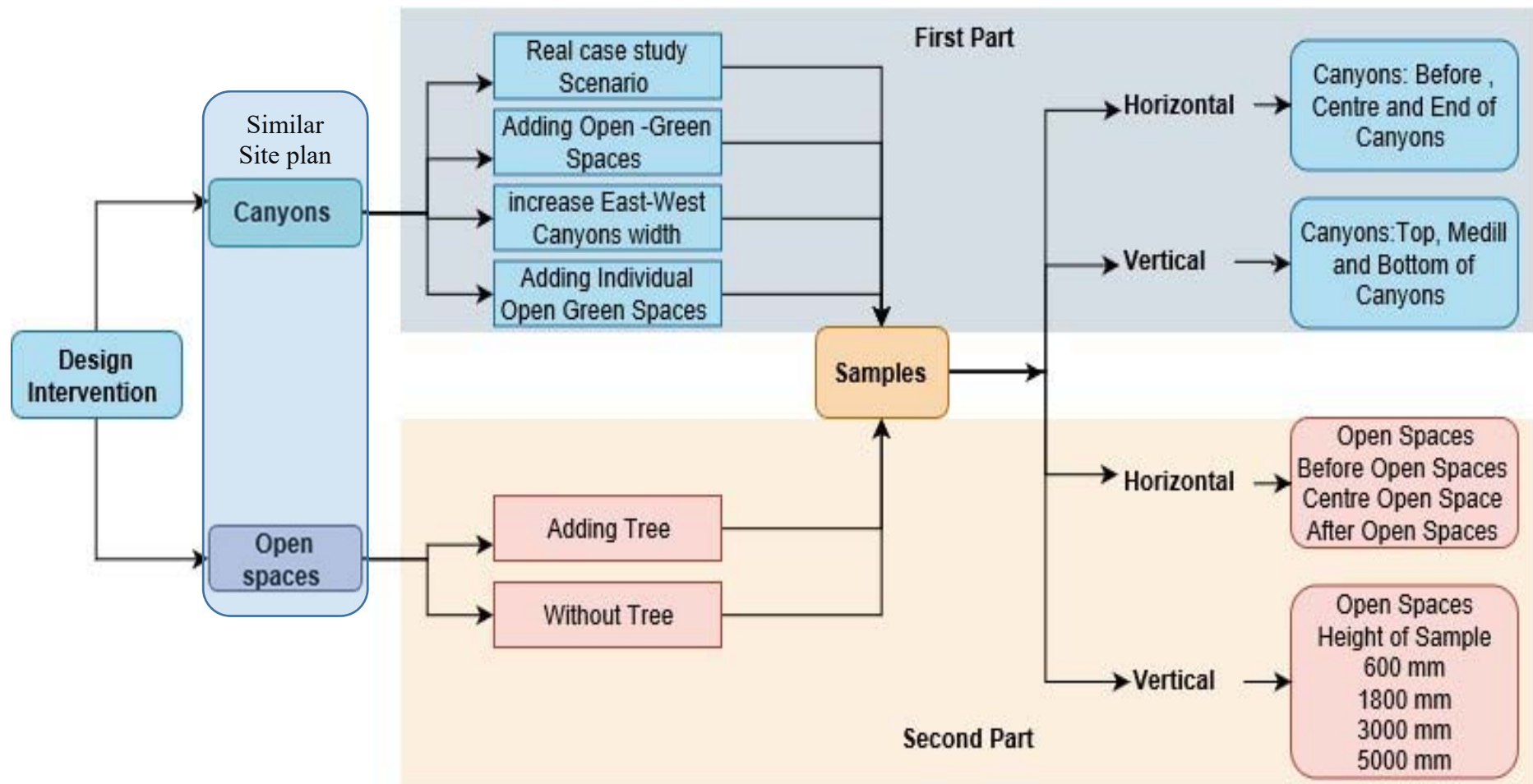


Figure 6.30: Shows the plan of work undertaken to investigate the impact of interventions

The site plan in each scenario will be divided into three zones, numbered 1, Zone 2 and Zone 3 (Figure 6.31). In each zone, six samples will be selected to measure air temperature (T) and wind speed (WS). Both north-south and east-west canyons will be considered. The Beginning, Centre and End of each canyon will be measured.

Figure 6.30 illustrates the full investigation plan, which is divided into two parts. The first part covers the aforementioned scenarios, detailed in blue in Figure 6.30. The second part to be introduced in Section 5.17 investigates the use of trees as shading devices in the open spaces, detailed in pink (Figure 6.30).

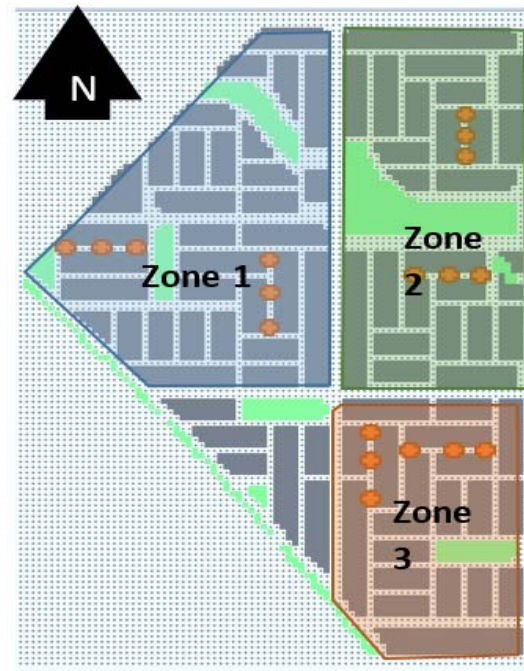


Figure 6.31: Designed Scenario, showing the location of the samples within the zones

6.5.1 Designed case study scenario

The case study is located in the southern part of Erbil. Air temperature samples were taken from three points NS and EW in three positions, the Beginning, Centre and End of canyons. ENVI-met was used to simulate all zones, as shown in Figure 6.31. All samples points were taken at a height of 1.8 metres at the Beginning, Centre and End of canyons for the east-south canyons and Top, Middle and Bottom for north-south canyons (Figure 6.31).

a. Air temperature and WS for east-west canyons (Designed case study).

Table 6-6: Air temperature and WS in the Designed Case Scenario for a horizontal canyon⁷ – Zones 1, 2 and 3

Designed case scenario ⁸ – east-west samples																		
Zone 1							Zone 2						Zone 3					
Time	T (°C)			WS (m/s)			T (°C)			WS (m/s)			T (°C)			WS (m/s)		
	B	C	E	B	C	E	B	C	E	B	C	E	B	C	E	B	C	E
09:00	40.7	39.6	40.2	1.6	1.9	1.9	38.6	38.7	38.7	1.4	2.0	1.8	38.1	38.2	38.3	1.5	2.1	2.0
12:00	42.5	41.7	41.3	1.6	1.9	1.9	41.1	41.2	41.2	1.4	1.9	1.8	40.9	41.1	41.2	1.5	2.1	2.0
15:00	42.8	42.3	42.1	1.5	1.9	1.9	41.8	41.9	41.9	1.4	1.9	1.8	41.7	41.8	42.0	1.4	2.0	2.0
18:00	40.3	40.3	40.3	1.5	1.9	1.9	40.3	40.3	40.3	1.3	1.9	1.8	40.3	40.3	40.3	1.4	2.0	2.0
21:00	37.5	37.6	37.7	1.5	1.9	1.9	37.8	37.8	37.9	1.3	1.9	1.7	37.8	37.8	37.9	1.4	2.0	2.0
00:00	33.8	34.1	34.3	1.5	1.8	1.8	34.8	34.9	34.9	1.3	1.9	1.7	34.6	34.6	34.8	1.4	2.0	2.0

⁷ Horizontal and Vertical canyons mean East – west and North – South canyons respectively.

⁸ T °C: Air Temperature, WS (m/s) Wind Speed, B: Beginning of canyons, C: Centre of Canyons and E: End of canyons

Table 6-6 shows air temperature ($T^{\circ}\text{C}$) and wind speed (WS) for east-west canyons in Zones 1, 2 and 3 and is graphically displayed in Figure 6.32 - Figure 6.34. The site plan is divided into three zones to address the relationship between zones and how changes in Zone 1 may have an impact on Zones 2 and 3. The samples demonstrated Air Temperature (T) and Wind

Speed (WS) for the Designed case scenario with slight differences for all zones. The research was simulated for 24 hours for the Designed case study scenario, though only six sample times were analysed (09:00, 12:00, 15:00, 16:00, 21:00 and midnight). The maximum air temperature was recorded at 15:00 (41.7°C – 42.8°C), while the minimum air temperature was recorded at midnight for all zones (33.8°C – 34.9°C). Overall, there is a difference in air temperature between the zones during daytime, and this difference decreased during night-time (Figure 6.33).

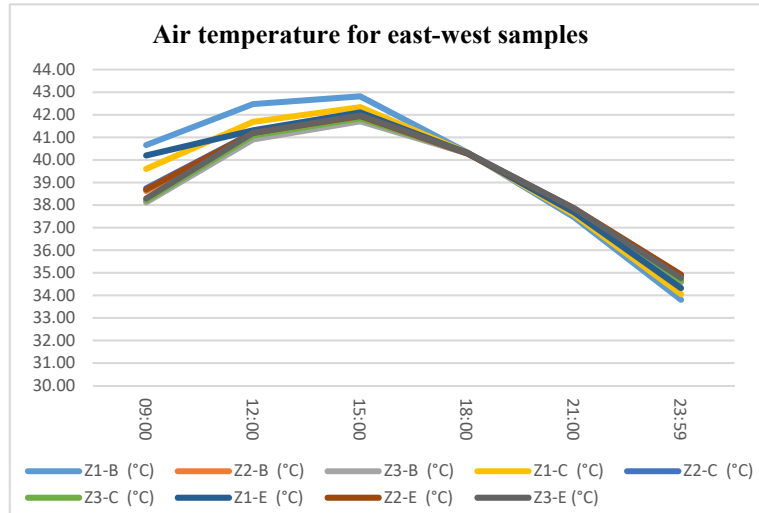


Figure 6.32: Air Temperature for the Horizontal samples for all zones

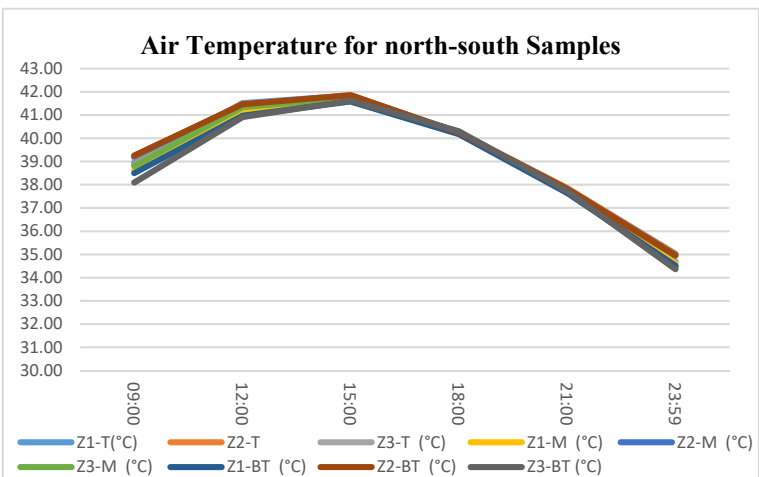


Figure 6.33: Air temperature for the Designed Case Scenario for Vertical canyon –Zone 1, Zone 2 and Zone 3

b. T and WS for north-south canyons (Designed case study).

Table 6-7: Air temperature and WS in the Designed Case Scenario for north-south canyon – Zones 1, 2 and 3

Designed case scenario ⁹ – north-south samples																		
Zone 1							Zone 2						Zone 3					
Time	T (°C)			WS (m/s)			T (°C)			WS (m/s)			T (°C)			WS (m/s)		
	T	M	BT	T	M	BT	T	M	BT	T	M	BT	T	M	BT	T	M	BT
09:00	39.0	38.6	38.5	1.8	2.0	1.5	39.2	39.2	39.3	1.4	1.9	1.4	38.9	38.8	38.1	1.8	1.9	1.5
12:00	41.5	41.2	41.0	1.8	2.0	1.5	41.5	41.5	41.5	1.4	1.9	1.4	41.4	41.3	40.9	1.8	1.9	1.4
15:00	41.8	41.6	41.6	1.7	2.0	1.5	41.8	41.7	41.9	1.4	1.9	1.4	41.7	41.7	41.6	1.7	1.9	1.4
18:00	40.3	40.2	40.2	1.7	2.0	1.5	40.3	40.2	40.2	1.4	1.9	1.3	40.3	40.3	40.3	1.8	1.8	1.4
21:00	37.8	37.7	37.6	1.7	2.0	1.4	37.9	37.8	37.8	1.4	1.9	1.3	37.7	37.7	37.7	1.7	1.8	1.4
00:00	34.7	34.6	34.5	1.7	2.0	1.4	35.0	35.0	34.9	1.4	1.9	1.3	34.5	34.4	34.4	1.7	1.8	1.4

Table 6-7 exhibits the air temperature (T°C) and WS for the north-south canyons for zones 1, 2 and 3 and is graphically displayed in Figure 6.34. The samples reveal Air Temperature (T°C) and WS for the Designed case scenario with a low difference for all zones (Figure 6.33 and Figure 6.34). The research simulates 24 hours for the Designed case study scenario, although only six sample times were analysed (09:00, 12:00, 15:00, 16:00, 21:00 and midnight) (Figure 6.33). The maximum air temperature was recorded at 15:00 ranging between (41.6°C–41.9°C), while the minimum air temperature was recorded at midnight for all zones ranging between (34.4°C–35°C). Zone 1 is a large built up area compared with Zones 2 and 3. Moreover, air temperature (T°C) and WS displayed a similar range for all zones. The comparison between both east-west and north-south for all three zones for the Designed case scenario exhibited slight differences for T (°C) and WS (m/s) for the east-west samples during daytime and almost similar air temperatures for the north-south samples. The subsequent set of simulations investigates new design interventions to judge how these may affect air temperature and wind speed.

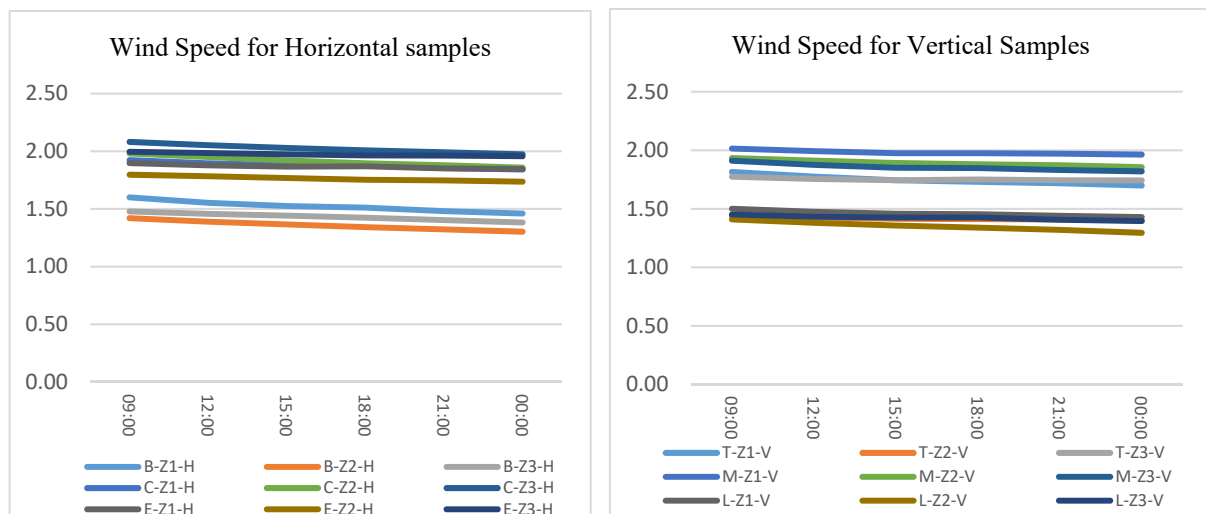


Figure 6.34 Wind speed for vertical and horizontal canyons (all zones).

⁹T (°C): Air Temperature, WS(m/s) Wind Speed, B: Beginning of canyons, C: Centre of Canyons and E: End of canyons

6.5.2 Adding central open-green areas (first scenario)

The first design intervention increased the number of central open-green spaces in the Designed site plan (Figure 6.35). Two open-green spaces were added aiming to enhance the urban microclimate of the city. In this scenario, urban density is reduced by adding central open-green areas. The aim of this simulation is to investigate the effect of open-green areas on the surrounding canyons and the effect of adding open-green areas in other zones, as shown in Figure 6.35. In this study, central open-green areas were added aiming to reduce air temperature and increase wind speed.

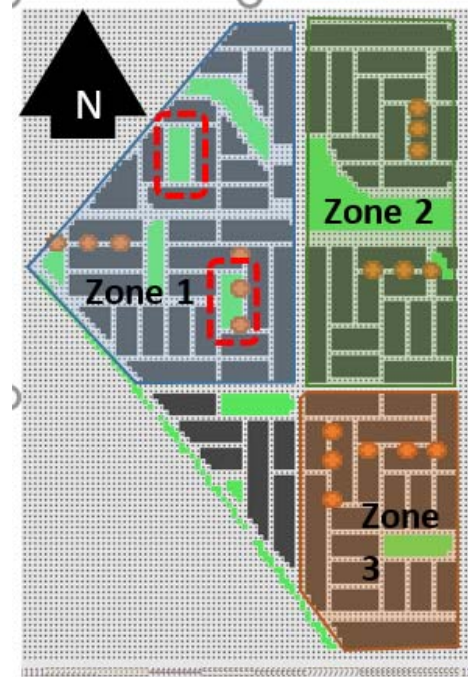


Figure 6.35: Scenario 1: adding open green spaces to the Designed case study

a. Air Temperature and Wind Speed for east-west canyons (First scenario)

Table 6-8 presents air temperature and wind speeds for all three zones for the first scenario. The maximum air temperature is 43.00 °C, whilst the minimum air temperature is 33.7 °C.

Table 6-8: Air temperature and WS for the first scenario (adding central open green areas) for east-west canyon samples

Adding central open green areas ¹⁰ –east-west samples																		
Time	Zone 1						Zone 2						Zone 3					
	T (°C)			WS (m/s)			T (°C)			WS (m/s)			T (°C)			WS (m/s)		
	B	C	E	B	C	E	B	C	E	B	C	E	B	C	E	B	C	E
09:00	41.0	39.6	38.9	1.5	1.9	1.9	38.6	38.7	38.7	1.4	2.0	1.8	38.7	38.4	38.3	2.1	2.1	2.0
12:00	42.9	41.7	41.3	1.4	1.9	1.9	41.1	41.2	41.2	1.4	1.9	1.8	41.3	41.2	41.2	2.0	2.1	2.0
15:00	43.0	42.3	42.1	1.4	1.9	1.9	41.8	41.9	42.0	1.4	1.9	1.8	42.0	41.9	42.0	2.0	2.1	2.0
18:00	40.3	40.3	40.3	1.4	1.9	1.9	40.3	40.3	40.3	1.3	1.9	1.8	40.3	40.3	40.3	2.0	2.1	2.0
21:00	37.4	37.6	37.7	1.3	1.9	1.9	37.8	37.8	37.9	1.3	1.9	1.7	37.8	37.8	37.9	2.0	2.1	2.0
00:00	33.7	34.1	34.3	1.3	1.8	1.8	34.8	34.9	34.9	1.3	1.9	1.7	34.6	34.7	34.8	1.9	2.1	2.0

Table 6-8 shows air temperature (T °C) and WS for east-west canyons in Zones 1, 2 and 3. The samples showed that the Air Temperature (T) and WS for the first scenario (adding open-green areas) with only small differences for all zones. The research simulated 24 hours for this scenario, although only six samples times were analysed (09:00, 12:00, 15:00, 16:00, 21:00 and midnight) (Figure 6.36). The maximum air temperature was recorded at 15:00 and ranged

¹⁰ T (°C): Air Temperature, WS(m/s) Wind Speed, B: Beginning of canyons, C: Centre of canyons and E: End of canyons.

between (43.0°C to 41.9°C), while the minimum air temperature recorded at midnight for all zones ranged between (33.7°C to 34.9°C). Zone 1 has a large built up area compared with Zones 2 and 3 so open-green areas were added. The air temperature (T°C) for all zones showed a similar temperature range with the exception of the Beginning sample for Zone 1. This may be due to its proximity to the boundary condition of the model.

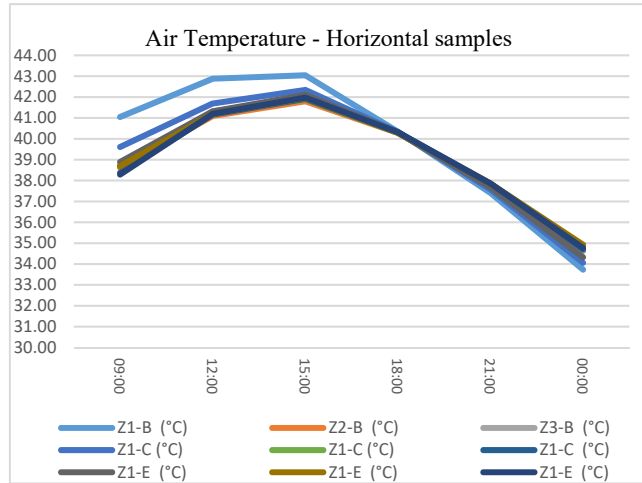


Figure 6.36: Air temperature for second scenario (adding open-green areas) – horizontal samples

The air temperature for this zone starts at 41.0°C compared to Zones 2 and 3 between (38.6°C and 38.7°C), respectively. The sample at the Beginning of the east-west canyons exhibited higher temperatures compared to other samples (Figure 6.36). The differences in air temperature for this sample are greater during the daytime than at night.

Wind speed recorded a similar range for all zones between (1.3 m/s to 2.10 m/s). In general, Zone 3 recorded higher wind speeds compared to Zones 1 and 2 for all three sample positions. The difference is insignificant and does not influence air temperature, as shown in Table 6-8.

b. Air temperature and wind speed for north-south canyons (first scenario)

Table 6-9 compares air temperature and wind speed for the north-south canyons sample in the three zones for the first scenario. The results show that the maximum air temperature is 42.5°C, while the minimum air temperature is 34.30°C.

Table 6-9: Air temperature and WS for the first scenario (adding central open-green areas) for vertical canyon samples

Adding central open green areas –north-south samples																		
Time	Zone 1						Zone 2						Zone 3					
	T (°C)			WS (m/s)			T (°C)			WS (m/s)			T (°C)			WS (m/s)		
	T	M	BT	T	M	BT	T	M	BT	T	M	BT	T	M	BT	T	M	BT
09:00	40.0	39.8	38.8	1.6	1.8	1.4	39.2	39.2	39.3	1.4	1.9	2.0	38.9	38.8	38.5	1.8	1.9	1.9
12:00	42.4	42.2	41.3	1.5	1.8	1.4	41.5	41.5	41.5	1.4	1.9	2.0	41.4	41.3	41.2	1.8	1.9	1.9
15:00	42.3	42.5	42.0	1.5	1.7	1.4	41.8	41.7	41.9	1.4	1.9	2.0	41.7	41.8	41.8	1.7	1.8	1.8
18:00	40.2	40.1	40.1	1.4	1.7	1.3	40.2	40.2	40.2	1.4	1.9	2.0	40.3	40.3	40.3	1.7	1.8	1.9
21:00	37.7	37.5	37.6	1.4	1.7	1.3	37.8	37.8	37.8	1.4	1.9	2.0	37.7	37.7	37.7	1.7	1.8	1.9
00:00	34.6	34.4	34.4	1.4	1.7	1.3	35.0	35.0	34.9	1.4	1.9	2.0	34.5	34.5	34.3	1.7	1.8	1.9

The north-south samples revealed T and WS for the first scenario with only small differences for all zones (Table 6-9). The research simulated 24 hours for the first scenario, although only six samples times are presented (09:00, 12:00, 15:00, 16:00, 21:00 and midnight) (Figure 6.37). The maximum T°C was recorded at 15:00 and ranged between

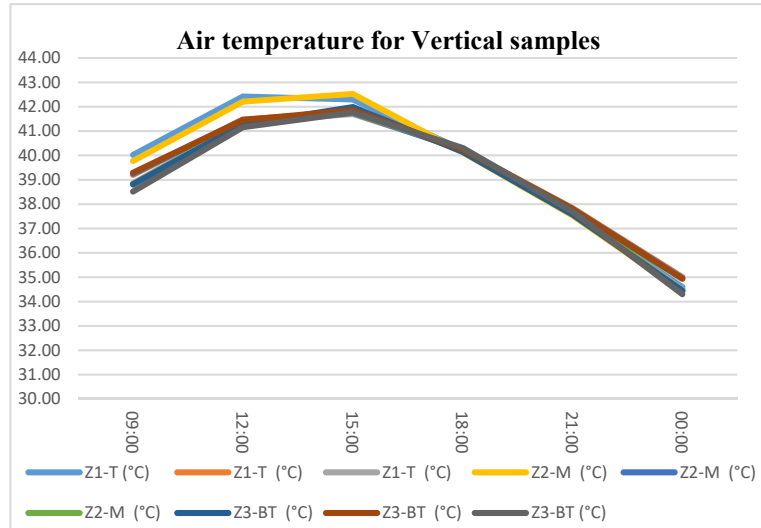


Figure 6.37: Air temperature for the second scenario (adding open-green spaces) – Vertical samples

(42.5°C to 41.7°C), while the minimum T°C was recorded at midnight for all zones, ranging from 34.30°C to 34.97°C. Zone 1 has a large built up area compared to Zones 2 and 3. Nevertheless, the T°C and WS recorded an almost similar range for all zones. WS for all zones in these scenarios ranged between 1.43 m/s to 2.00 m/s (Table 6-9).

The sample at the Middle of the vertical canyons shows a higher temperature in Zone 1 in contrast to other samples (Figure 6.37, yellow line). The difference in air temperature for both samples is more during daytime than at night-time. This increase in air temperature of these sample points may be related to the new open spaces added as a design intervention. Moreover, the amount of solar radiation that enters these spaces is more than other zones.

The comparison between both the east-west and the north-south canyon samples for all three zones in the first scenario (adding open-green spaces) shows a slight difference T (°C) and WS (m/s) for the east-west samples during daytime and an almost similar air temperature for the north-south samples (Figure 6.37).

6.5.3 Increasing east-west canyons widths (second scenario)

The second design intervention increased the east-west canyons from 10–20 metres, (Figure 6.38). All the main east-west canyon (Zone 1) widths were increased to enhance the urban microclimate. In this scenario, urban microclimate was measured via T°C and WS. The aim of this simulation is to investigate the effect of canyon width on the canyon's microclimate and surrounding canyons and, moreover, to investigate the effect of changing canyon widths on other zones, as shown in Figure 6.38. In this study, increasing the widths of east-west canyons aims to reduce the air temperature and increase the WS.

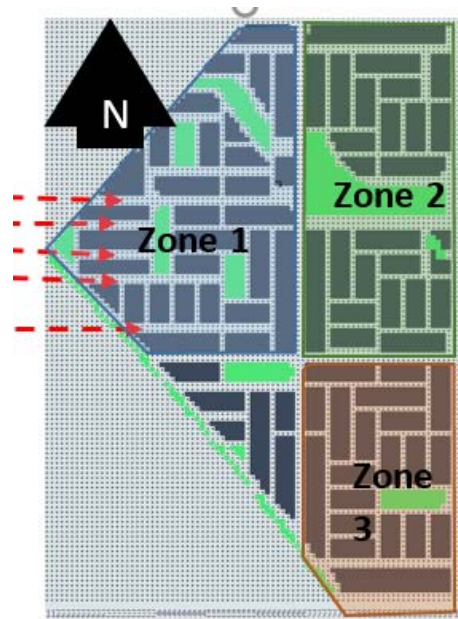


Figure 6.38: Shows Scenario 3, increasing East-West canyons

a. Air Temperature and Wind Speed for Horizontal¹¹ canyons (Second scenario)

Table 6-10 shows air temperature and wind speed for all three zones for the second scenario. The maximum air temperature is 43 °C and the minimum air temperature is 33.5 °C. Table 19 shows the air temperatures (T °C) and wind speed (WS) for horizontal canyons (east-west) in all zones (Figure 6.38). In general, the samples indicated that the T and WS for the second scenario (increasing east-west canyon width) with only small differences for all zones. The research simulated 24 hours for this scenario, though only six samples times are shown (09:00, 12:00, 15:00, 16:00, 21:00 and midnight) (Figure 6.39). The maximum air temperature was recorded at 15:00 with (43.0 °C to 41.9 °C), while the minimum air temperature was recorded at midnight for all zones with (33.5 °C to 34.9 °C).

Table 6-10: Shows Air Temperature and WS for the second scenario (increasing east-west canyons) for horizontal canyon samples

Increasing east-west canyons ¹² – horizontal sample																		
Zone 1							Zone 2						Zone 3					
Time	T (°C)			WS (m/s)			T (°C)			WS (m/s)			T (°C)			WS (m/s)		
	B	C	E	B	C	E	B	C	E	B	C	E	B	C	E	B	C	E
09:00	41.2	40.1	39.5	1.6	1.8	1.9	38.7	38.8	38.7	1.4	1.9	1.8	38.8	38.4	38.3	2.1	2.2	2.0
12:00	43.0	42.0	41.7	1.6	1.8	1.9	41.1	41.2	41.2	1.4	1.9	1.8	41.4	41.2	41.2	2.0	2.2	2.0
15:00	43.0	42.3	42.2	1.6	1.8	1.9	41.8	41.9	41.9	1.4	1.9	1.8	41.9	41.9	42.0	2.0	2.1	2.0
18:00	40.2	40.1	40.1	1.6	1.8	1.9	40.3	40.3	40.3	1.3	1.8	1.8	40.3	40.3	40.3	2.0	2.1	2.0
21:00	37.2	37.3	37.4	1.5	1.8	1.8	37.8	37.8	37.8	1.3	1.8	1.8	37.8	37.8	37.9	2.0	2.1	2.0
00:00	33.5	33.7	34.0	1.5	1.8	1.8	34.8	34.9	34.9	1.3	1.8	1.7	34.6	34.7	34.8	1.9	2.1	2.0

¹¹ Horizontal and Vertical canyons mean East – west and North – South canyons respectively.

¹²(°C): Air Temperature, WS(m/s) Wind Speed, B: Beginning of canyons, C: Centre of canyons and E: End of canyons.

The air temperature ($T^{\circ}\text{C}$) for all zones recorded a similar range except Zone 1, which is located at the Beginning of the canyons before the open space (Figure 6.39).

The air temperature for Zone 1 starts at 41.24°C compared to Zones 2 and 3, between (38.67°C and 38.78°C), respectively. The beginning of the east-west canyons shows higher temperatures compared to other samples (Figure 6.39). The

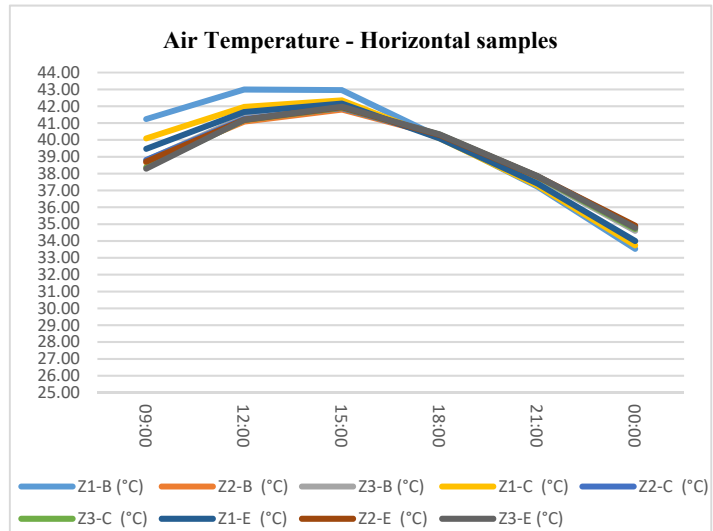


Figure 6.39: Air temperature for the second scenario – horizontal samples

differences in air temperature for this sample are greater during the daytime than at night. This abnormality as regards the air temperature of this sample point (Zone 1– Beginning east-west canyon sample) may be related to the boundary condition of the model that may influence this point, seeing as it is very close to the boundary condition. WS recorded a similar range for all zones and ranged between 1.3 m/s to 2.2 m/s. In general, Zone 3 recorded higher wind speeds compared to Zones 1 and 2 for all three sample positions. The difference is an insignificant amount and does not influence air temperature, as shown in Table 6-10.

b. Air Temperature and Wind Speed for the north-south canyons (second scenario)

Table 6-11 compares air temperatures and wind speeds for all three zones for the second scenario (increasing east-west canyons). The maximum air temperature range is 42.6°C and the minimum air temperature is 34.3°C .

Table 6-11: Shows T and WS for the second scenario for vertical canyon samples

Increasing east-west canyons –the north-south ¹³ sample																		
Zone 1							Zone 2						Zone 3					
Time	T ($^{\circ}\text{C}$)			WS (m/s)			T ($^{\circ}\text{C}$)			WS (m/s)			T ($^{\circ}\text{C}$)			WS (m/s)		
	T	M	BT	T	M	BT	T	M	BT	T	M	BT	T	M	BT	T	M	BT
09:00	40.0	39.9	38.9	1.6	1.8	1.3	39.2	39.2	39.3	1.4	1.9	1.4	38.9	38.8	38.5	1.8	1.9	1.9
12:00	42.4	42.3	41.3	1.5	1.7	1.3	41.5	41.4	41.4	1.4	1.9	1.4	41.4	41.3	41.2	1.8	1.9	1.8
15:00	42.3	42.6	42.0	1.5	1.7	1.3	41.8	41.7	41.9	1.4	1.9	1.4	41.7	41.8	41.8	1.8	1.9	1.8
18:00	40.2	40.1	40.1	1.4	1.7	1.3	40.2	40.2	40.2	1.4	1.8	1.3	40.3	40.3	40.3	1.8	1.8	1.9
21:00	37.7	37.5	37.6	1.4	1.7	1.2	37.8	37.8	37.8	1.4	1.8	1.3	37.7	37.7	37.7	1.7	1.8	1.8
00:00	3.6	34.4	34.4	1.4	1.6	1.2	35.0	35.0	34.9	1.4	1.8	1.3	34.5	34.5	34.3	1.7	1.8	1.9

¹³ T ($^{\circ}\text{C}$): Air Temperature, WS(m/s) Wind Speed, B: Beginning of canyons, C: Centre of canyons and E: End of canyons. T= Top of the canyons, M= Middle of the canyons, BT= Bottom of the canyons.

Table 6-11 illustrates the air temperatures ($T^{\circ}\text{C}$) and wind speeds (WS) for the north-south canyons in all zones (second scenario). The samples revealed that $T^{\circ}\text{C}$ and WS for the second scenario have only small differences for all zones. The research was simulated for 24 hours for the second scenario, but only six sample times are shown (9:00, 12:00, 15:00, 16:00, 21:00 and midnight) (Figure 6.40).

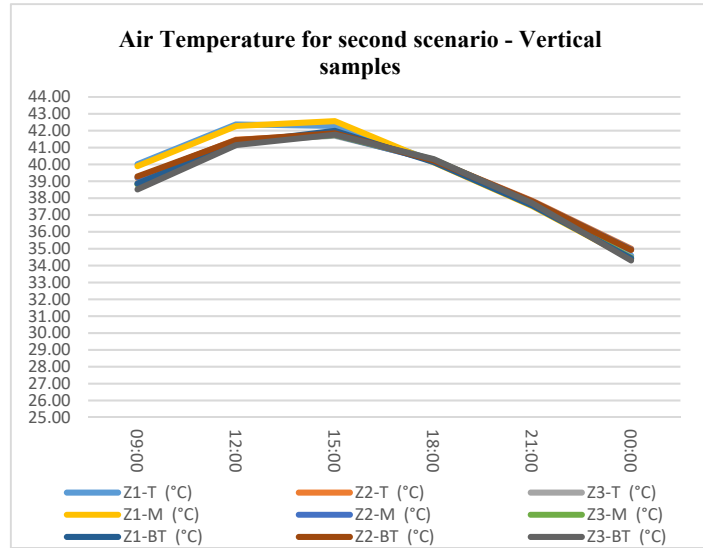


Figure 6.40: Air temperature for the second scenario – vertical samples

Zone 1 recorded the highest air temperature at 15:00 and lowest air temperature at 00:00 compared to Zones 2 and 3, with a maximum air temperature difference of less than 2.0°C .

The sample at the Beginning and Middle of the north-south canyons shows slightly higher temperatures in Zone 1 compared to the other samples (Figure 6.40). The differences in air temperature for both samples is greater during the daytime than at night. This higher air temperature for these sample points may be related to the canyons (increasing east-west canyons) that were added as a design intervention. Moreover, the amount of solar radiation that enters into these canyons will be more than other zones as a result of increasing the width of the canyons from 10–20 metres. This will allow solar radiation to enter the canyon during daytime more than other zones.

The comparison between both east-west and north-south samples for all three zones in the second scenario (increasing east-west canyons) shows slight differences in the $T^{\circ}\text{C}$ and WS (m/s) for the east-west samples during daytime and similar air temperatures for the north-south samples.

5.8.4 Adding Individual Open-Green areas (Third Scenario)

The third design intervention is adding individual open-green space between residential blocks (Figure 6.41). The east-west canyons divided by adding individual open-green spaces and canyons are shortened by half their original length, aiming to enhance the urban microclimate. In this scenario, the urban microclimate was investigated by measuring the T^{°C} and WS. The aim of this simulation is to investigate the effect of individual open-green areas on the canyon's microclimate and surrounding canyons, in addition to the effect of this on other zones, as shown in Figure 6.41. In this study, the increase in open-green areas may reduce the air temperature and increase the WS.

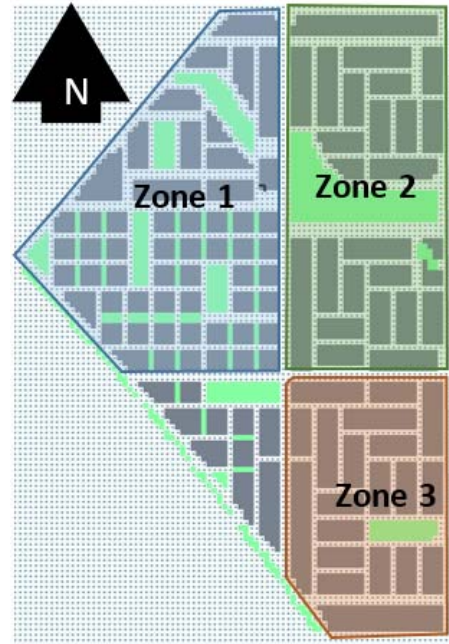


Figure 6.41: Shows Scenario 3, Adding Individual Open-Green Areas

a. Air Temperature and Wind Speed for east-west canyons (third scenario)

Table 6-12 compares air temperature and wind speed for all three zones for the third scenario (adding individual open-green areas). The maximum air temperature is 43.0^{°C} and the minimum air temperature is 33.7^{°C}. Table 6-12 shows T^{°C} and WS for horizontal canyons (east-west) in all three zones (Figure 6.41).

Table 6-12: Air temperature and WS for the third scenario (adding individual open-green areas) for horizontal canyon samples

Adding Individual Open ¹⁴ – Green areas – Horizontal Samples																		
Zone 1							Zone 2						Zone 3					
Time	T (°C)			WS (m/s)			T (°C)			WS (m/s)			T (°C)			WS (m/s)		
	B	C	E	B	C	E	B	C	E	B	C	E	B	C	E	B	C	E
09:00	41.1	39.3	38.5	1.4	1.6	1.7	38.7	38.8	38.7	1.4	1.9	1.8	38.7	38.4	38.3	2.1	2.1	2.0
12:00	42.9	41.5	41.1	1.4	1.6	1.7	41.2	41.3	41.2	1.4	1.9	1.8	41.3	41.2	41.2	2.0	2.1	2.0
15:00	43.0	42.1	41.9	1.3	1.6	1.7	41.8	41.9	41.9	1.4	1.9	1.8	41.9	41.9	42.0	2.0	2.1	2.0
18:00	40.3	40.3	40.2	1.3	1.6	1.7	40.3	40.3	40.3	1.3	1.8	1.8	40.3	40.3	40.3	2.0	2.1	2.0
21:00	37.4	37.5	37.6	1.3	1.5	1.7	37.8	37.8	37.8	1.3	1.8	1.7	37.8	37.8	37.9	2.0	2.1	2.0
00:00	33.7	34.0	34.3	1.3	1.5	1.7	34.8	34.9	34.9	1.3	1.8	1.7	34.6	34.7	34.8	1.9	2.1	2.0

¹⁴ T (°C): Air Temperature, WS(m/s) Wind Speed, B: Beginning of canyons, C: Centre of Canyons and E: End of canyons

In general, the samples confirm that T °C and WS for the third scenario have the least possible differences between all zones. The research simulated 24 hours for this scenario, but only six samples times were shown (09:00, 12:00, 15:00, 16:00, 21:00 and midnight) (Figure 6.42). The maximum air temperature was recorded at 15:00 with (43.0 °C to 41.8 °C), while the minimum air temperature was recorded at midnight for all zones between (33.7 °C to 34.9 °C) (Figure 6.42). The beginning of Zone 1 recorded higher temperatures than the other samples. Once again, its location near the boundary may account for this.

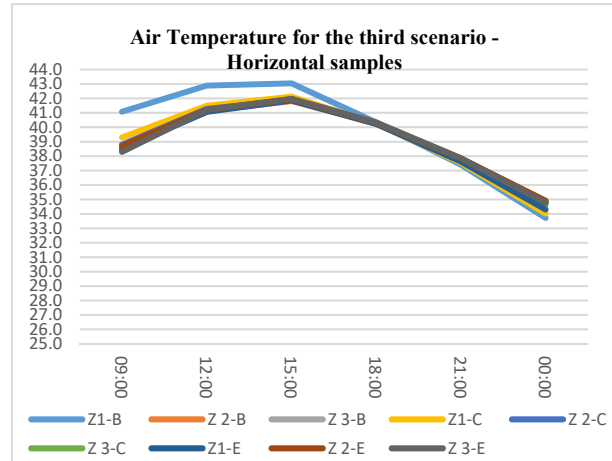


Figure 6.42: Air Temperature for the third scenario- Horizontal samples

WS recorded a similar range for all zones between 1.3 m/s to 2.2 m/s. Similar to the second scenario, Zone 3 recorded higher wind speeds in contrast to Zones 1 and 2. The difference is slight and does not influence air temperature, as shown in Table 6-12.

b. Air Temperature and Wind Speed for the north-south canyons (third scenario)

Table 6-13 compares air temperatures and wind speeds for all vertical canyons in three zones for the third scenario. The maximum air temperature is 42.4 °C and the minimum air temperature is 34.3 °C.

Table 6-13: Air temperature and wind speed for the third scenario (adding individual open-green areas) for the north-south canyon samples

Adding Individual Open – Green Areas – north-south samples																		
Time	Zone 1						Zone 2						Zone 3					
	T (°C)			WS (m/s)			T (°C)			WS (m/s)			T (°C)			WS (m/s)		
	T	M	BT	T	M	BT	T	M	BT	T	M	BT	T	M	BT	T	M	BT
09:00	39.6	39.8	39.2	1.5	2.2	1.3	39.2	39.3	39.4	1.4	1.9	1.0	38.5	38.8	38.5	1.9	1.9	1.9
12:00	42.0	42.1	41.6	1.4	2.1	1.3	41.5	41.5	41.6	1.4	1.9	1.0	41.2	41.3	41.2	1.8	1.9	1.9
15:00	42.0	42.4	42.1	1.4	2.1	1.3	41.8	41.7	42.0	1.4	1.9	0.9	41.6	41.7	41.8	1.8	1.9	1.8
18:00	40.2	40.1	40.1	1.4	2.1	1.2	40.2	40.2	40.2	1.4	1.9	0.9	40.3	40.3	40.3	1.8	1.9	1.9
21:00	37.6	37.5	37.5	1.3	2.0	1.2	37.8	37.8	37.8	1.4	1.9	0.9	37.8	37.7	37.7	1.8	1.9	1.9
00:00	34.6	34.3	34.4	1.3	2.0	1.2	35.0	34.9	34.9	1.4	1.9	0.9	34.6	34.5	34.3	1.8	1.9	1.9

Table 6-13 shows the T^{°C} and WS for the north-south canyons in three zones. The results clarify that the T^{°C} and WS for the third scenario have only a slight difference for all zones. The research simulated 24 hours for this scenario, though only six samples times were presented (09:00, 12:00, 15:00, 16:00, 21:00 and midnight) (Figure 6.43).

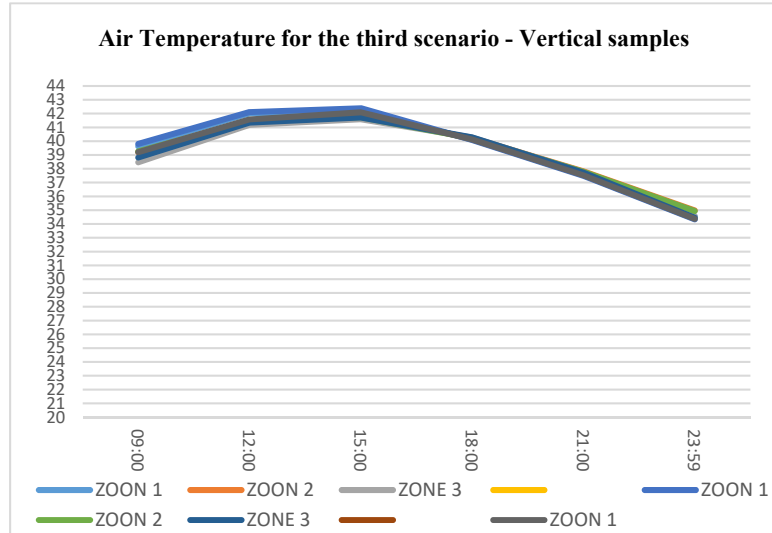


Figure 6.43: Air temperature for the third scenario – vertical samples

The maximum air temperature was recorded at 15:00 with a range of 42.4°C to 41.6°C, while the minimum air temperature was recorded at midnight for all zones with a range of 34.30°C to 35.0°C. Zone 1 recorded the highest air temperature and lowest air temperature in contrast to zones 2 and 3 with a maximum air temperature difference of 1.6°C. The Beginning and Middle samples in Zone 1 of the north-south canyons show a slightly higher air temperature compared to the other samples (Figure 6.43). The differences in air temperature for both samples is greater during the daytime than at night. This may be related to the design interventions which increase the amount of solar radiation that enters into this canyon more than those in other zones. Increasing the width of the east-west canyons from 10–20 metres allows more solar radiation to enter the canyon during the daytime than in other zones.

The comparison between both canyon types in the third scenario shows slight differences in the T (°C) and WS (m/s) for the east-west samples during daytime only compared to night-time and similar air temperatures for the north-south samples.

6.6 Comparison of Designed case study and all design intervention scenarios

Air temperatures were measured and analysed for the Designed case study and all design scenarios using ENVI-met (Figure 6.29). The site plan was divided into three zones to compare the interventions on the canyon design impact on a similar zone and other zones within the site (Figure 6.28). The results from the last section indicated that air temperature and wind speed

record almost similar values for all three zones in each scenario. This means the design interventions did not have a significant impact on other zones within the same site.

In this section, only results for Zone 1 for all scenarios are compared. The aim of this section is to investigate the impact of design scenarios on the canyon and open spaces microclimate for a similar zone. Air temperature and wind speed are compared for zones only for each scenario. Air temperature and wind speeds were measured at a height of 1.8 metres.

1. Air Temperature¹⁵ for east-west and north-south canyons in Zone 1

Table 5-23 and Table 5-24 shows air temperatures in Zone 1 at East-West and North-South canyons for all intervention scenarios. For the East – West canyons both temporal and special influences can be detected. Dealing with the temporal influences first: here the differences between day and night are clear, once the sun has set, after 18:00, the difference in temperature between the Designed case and all others is small, at all canyon positions. The day time temperatures do indicate more significant changes. Starting with the beginning of the canyon first, none of the interventions yield lower air temperatures than the Designed scenario, however the differences are small. The worst performing intervention is the increasing of the East – West canyon widths' the temperature increase being greater during the morning than the afternoon. The temperature at the beginning of the canyon is strongly influenced by the adjacent boundary condition, so may not reflect the impact of the intervention greatly. Looking at the Centre and End of the canyon, a more consistent picture emerges; adding an open space has no impact on air temperature, increasing the East – West canyons increases the air temperature during the morning, though in the afternoon has no effect. Adding additional open green spaces does lower the air temperature at both Centre and End locations with the maximum difference in the morning and decreasing during the day. However the maximum difference is only 0.4 K, and when the air temperature itself is around 40 °C, a 1% change, and has little impact.

For the North – South canyons, the temporal differences is again evident, after 18:00 there is little impact from interventions. During the daytime none of the interventions lower the canyon

¹⁵ R = Designed case scenario, O = Adding Open Spaces, I = Increase East –West canyons, V = Adding Individual Open Green Spaces

Z1 = Zone one, P = Sample position at the Top of the Canyons, M = Sample position in the Middle of the Canyons, BT = Sample position at the Bottom of the Canyons

air temperature at the three positioned sampled. There is no clear picture from the data as to whether any intervention has the least bad performance.

Table 6-14: Air temperature for Zone 1 for the Designed case study and design intervention scenarios in east-west canyons

East-West Canyon Samples													
Time	Zone One – Four Scenarios T(°C)				Zone One – Four Scenarios T(°C)				Zone One – Four Scenarios T(°C)				T(°C)
	Beginning of the canyon samples				Centre of the canyon samples				End of the canyon samples				Δ°C
	R	O	I	V	R	O	I	V	R	O	I	V	
09:00	40.7	41.0	41.2	41.1	39.6	39.6	40.1	39.3	38.9	38.9	39.5	38.5	2.7
12:00	42.5	42.9	43.0	42.9	41.7	41.7	42.0	41.5	41.3	41.3	41.7	41.1	1.8
15:00	42.8	43.0	43.0	43.0	42.3	42.3	42.3	42.1	42.1	42.1	42.2	41.9	1.1
18:00	40.3	40.3	40.2	40.3	40.3	40.3	40.1	40.3	40.3	40.3	40.1	40.2	0.2
21:00	37.5	37.4	37.2	37.4	37.6	37.6	37.3	37.5	37.7	37.7	37.4	37.6	0.3
00:00	33.8	33.7	33.5	33.7	34.1	34.1	33.7	34.0	34.3	34.3	34.0	34.3	0.6

Table 6-15: Air Temperature for case study and design intervention scenarios for the north-south canyons

North-South Canyon Samples													
Time	Zone One – Four Scenarios				Zone One – Four Scenarios				Zone One – Four Scenarios				T(°C)
	Top samples				Middle Samples				Bottom Samples				Δ°C
	¹⁶ R	O	I	V	R	O	I	V	R	O	I	V	
09:00	39.0	40.0	40.0	39.6	38.6	39.8	39.9	39.8	38.5	38.8	38.9	39.2	1.4
12:00	41.5	42.4	42.4	42.0	41.2	42.2	42.3	42.1	41.0	41.3	41.3	41.6	0.6
15:00	41.8	42.3	42.3	42.0	41.6	42.5	42.6	42.4	41.6	42.0	42.0	42.1	0.9
18:00	40.3	40.2	40.2	40.2	40.2	40.1	40.1	40.1	40.2	40.1	40.1	40.1	0.2
21:00	37.8	37.7	37.7	37.6	37.7	37.5	37.5	37.5	37.6	37.6	37.6	37.5	0.3
00:00	34.7	34.6	34.6	34.6	34.6	34.4	34.4	34.3	34.5	34.4	34.4	34.4	0.4

¹⁶ R = Designed case scenario, O = Adding Open Spaces, I = Increase East –West canyons, V = Adding Individual Open Green Spaces.

Z1 = Zone one, P = Sample position at the Top of the Canyons, M = Sample position in the Middle of the Canyons, BT = Sample position at the Bottom of the Canyons.

2. Open Spaces Air Temperature for all Scenarios¹⁷

Open spaces in Zone 1 were investigated to understand the impact of canyon design intervention on open spaces. Air temperature was measured in open spaces (Zone 1) for all scenarios at a height of 1.8 metres using the ENVI-met simulation program (Figure 6.44).

The results show that air temperature for the open spaces are almost similar for all scenarios (Figure 6.44).

The difference in air temperature for the open spaces is greater during the daytime than at night, which is similar to the performance of the canyons.

The maximum difference ($\Delta^{\circ}\text{C}$) is 0.8°C at 9:00 for the Designed case study and adding individual open green spaces (Figure 6.44). The design interventions on the canyons for all scenarios had a limited impact on open space air temperatures, as shown in Figure 6.44.

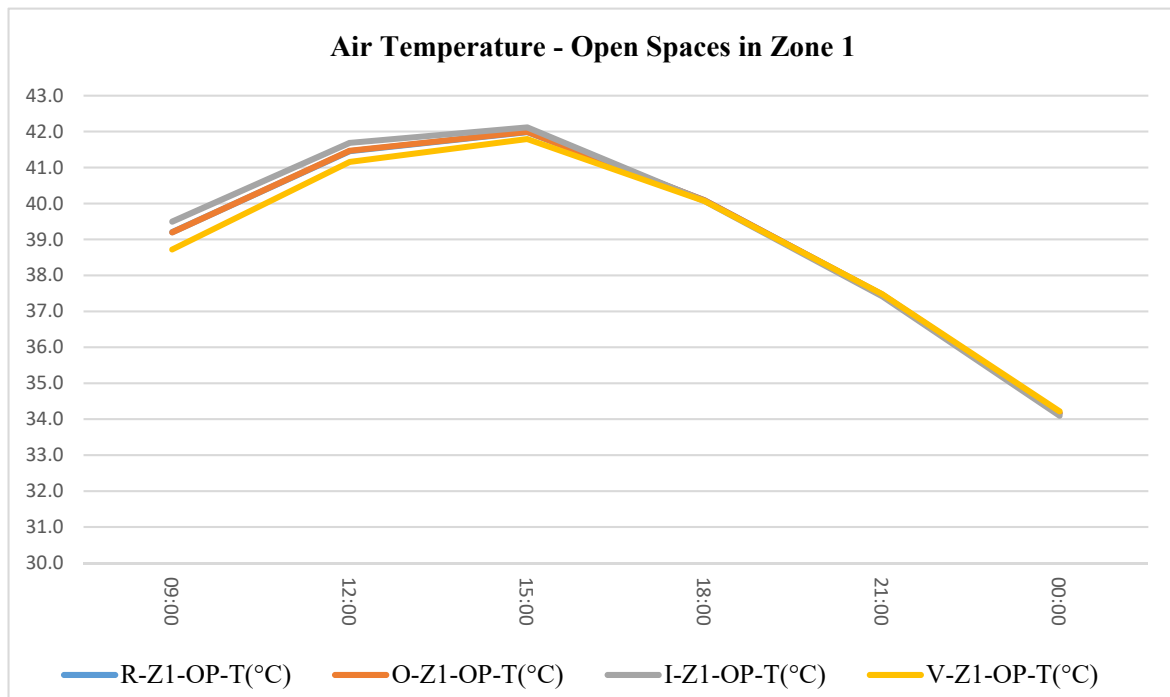


Figure 6.44: Air Temperature for open space in Zone 1 in the Designed case study and all design scenarios

¹⁷ **Z1** = Zone one, **OP** = Sample Position in the centre of the **Open Spaces**.

R = Designed case scenario, **O** = Adding Open Spaces, **I** = Increase East –West canyons, **V** = Adding Individual Open Green Spaces.

3. Wind Speed¹⁸

Wind speed measured for both east-west and north-south canyons at the sample positions illustrated in Figure 6.45.

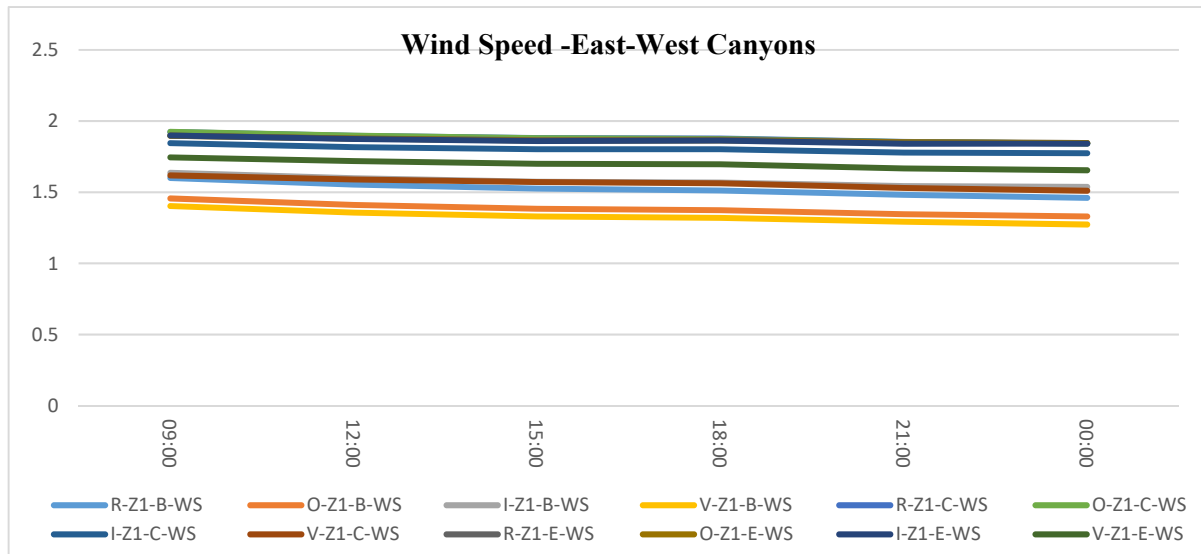


Figure 6.45: Wind Speed in Zone 1 for open space in the Designed case and all design scenarios (East-West canyons)

Figure 6.45 shows the wind speeds for east-west canyons and Figure 6.47 explains wind speeds for north-south canyons. The results show that wind speed ranged between 1.3 m/s to 2.13 m/s for all scenarios. The maximum wind speed recorded for north-south canyons was 2.13 m/s at 9:00 am for the position of the middle canyon sample compared to 1.89 m/s for the maximum wind speed for east-west canyons.

¹⁸ **Z1** = Zone one, **R** = Designed case scenario, **O** = Adding Open Spaces, **I** = Increase East –West canyons, **V** = Adding Individual Open Green Spaces. **WS** = Wind Speed (m/s).

B = Sample position Beginning of the Canyons, **C** = Sample position in the Centre of the Canyons, **E** = Sample position at the End of the Canyons.

P = Sample position in the Top of the Canyons, **M** = Sample position in the Middle of the Canyons, **BT** = Sample position at the Bottom of the Canyons.

Wind speed in the open spaces¹⁹ was also measured to investigate canyons design intervention impact on open spaces wind speeds.

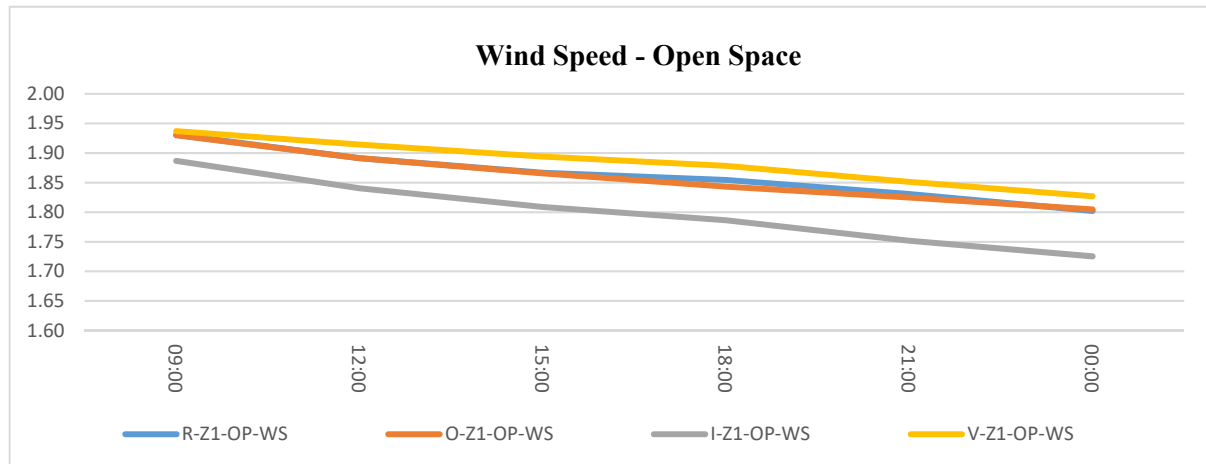


Figure 6.46: Wind Speed for the Designed case study and all design scenarios in zone one (open space)

Figure 6.46 illustrates wind speeds for the same open space for all scenarios. The results show that there is a limited difference in wind speed for all scenarios with a maximum wind speed of 1.94 m/s and minimum of 1.73 m/s.

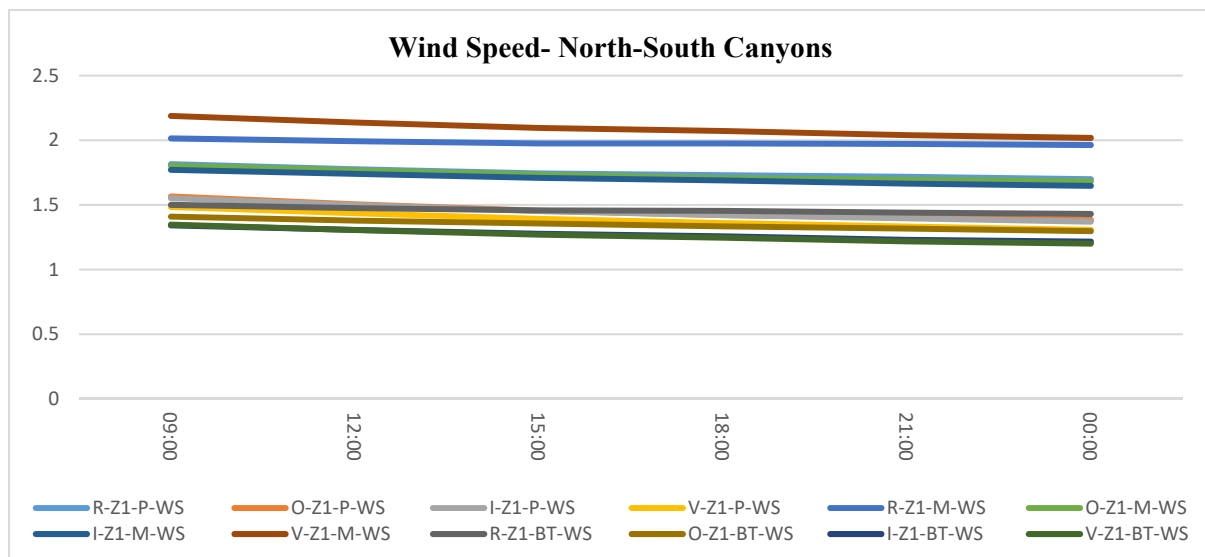


Figure 6.47: Wind speed in Zone 1 for the Designed case and design scenarios (north-south canyons)

The results show that wind speed recorded higher values in canyons in contrast to open spaces (Figure 42, Figure 43 and Figure 6.44). Additionally, canyon design intervention has a limited effect on open spaces wind speeds.

¹⁹ **Z1** = Zone one, **OP** = Sample Position in the centre of the **Open Spaces**.

R = Designed case scenario, **O** = Adding Open Spaces, **I** = Increase East –West canyons, **V** = Adding Individual Open Green Spaces. **WS** = Wind Speed (m/s).

Air temperatures and wind speeds for east-west and north-south canyons were measured in the same locations for all scenarios. The results confirmed that there is a slight difference in air temperature ($\Delta^{\circ}\text{C}$) between east-west and north-south canyons at the Beginning of the samples. These differences may be related to the boundary condition of the model, with this sample being located near a boundary condition compared to other sample locations.

Wind speed for measured canyons and open spaces recorded similar values. This suggests that the canyon design intervention did not have a significant impact on the urban microclimate for canyons and open spaces. This section concludes that the design interventions did not have a significant impact on air temperatures and wind speeds, as shown in the results for all scenarios.

The design interventions (all scenarios) did not have a significant impact on air temperature and wind speed within the modified zone or on other zones within the site. The difference in air temperature for all measured samples is limited. This leads the research to investigate more effective strategies to reduce the effect of daytime solar radiation.

In the following section, the research explores more investigations on the impact of solar radiation on the open spaces and how a reduction in solar radiation impacts on the urban microclimate of urban areas.

6.7 Adding trees for green spaces

In the last section, the study showed that design interventions on canyons have a limited impact on the Air Temperature (T) and Wind Speed (WS) for Zone 1 and other adjacent zones. In this section, the study simulated only Zone 1 using ENVI-met (Figure 6.48). The simulation explores new strategies to enhance the local urban microclimate of open space in the urban areas.

In a hot, dry climate, shade either by vegetation or a manmade device is an obvious choice.

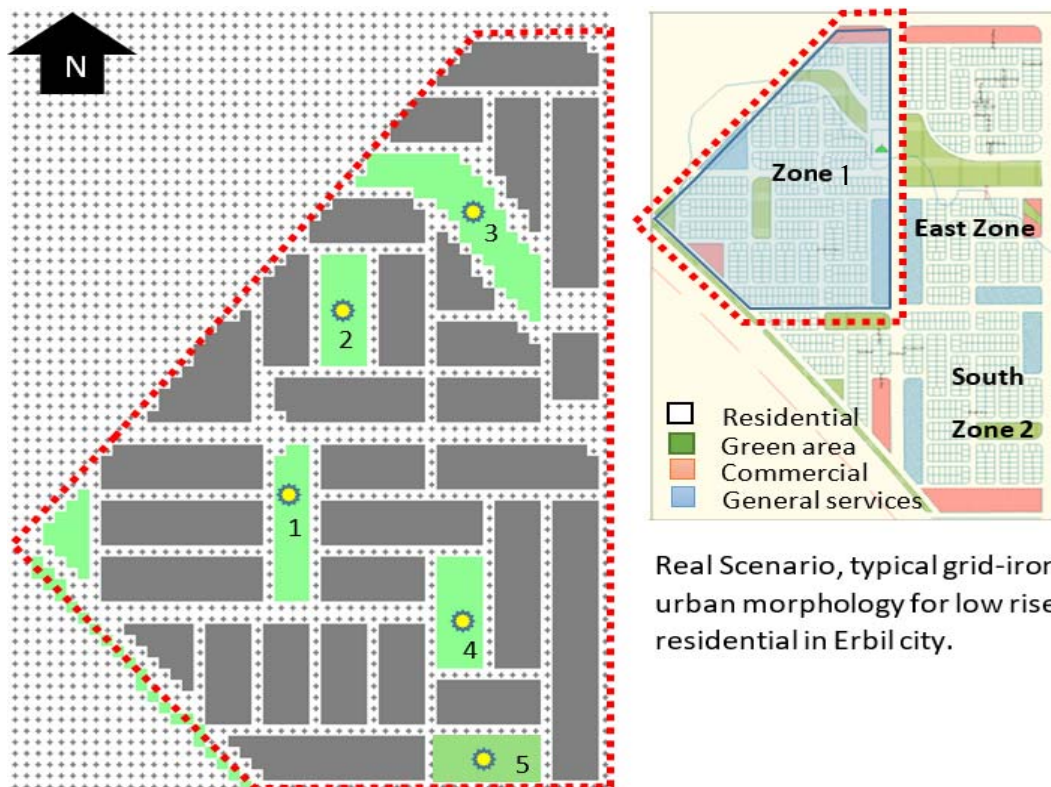


Figure 6.48: ENVI-met Zone 1 model. Three points in east-west canyon samples represented by red stars

Whilst the lack of precipitation in Erbil does limit tree growth, it is a strategy worth exploring. The aim of the simulations is to investigate the impact of adding trees into the open spaces. The simulations include different scenarios as below:

1. Open spaces without trees
2. Open space with trees.

Method of analysis: in this simulation samples are taken in two different directions for each scenario as below:

- a. **Horizontally**, Air temperature, Mean Radiant Temperature and Wind Speed are taken in the centre of open spaces (Figure 6.49).
- b. **Vertically**, Air Temperature, Mean Radiant Temperature (MRT) and Wind Speed are taken at four heights for Open Space 1 at **600mm, 1800 mm, 3000 mm and 5000 mm** (Figure 6.49).

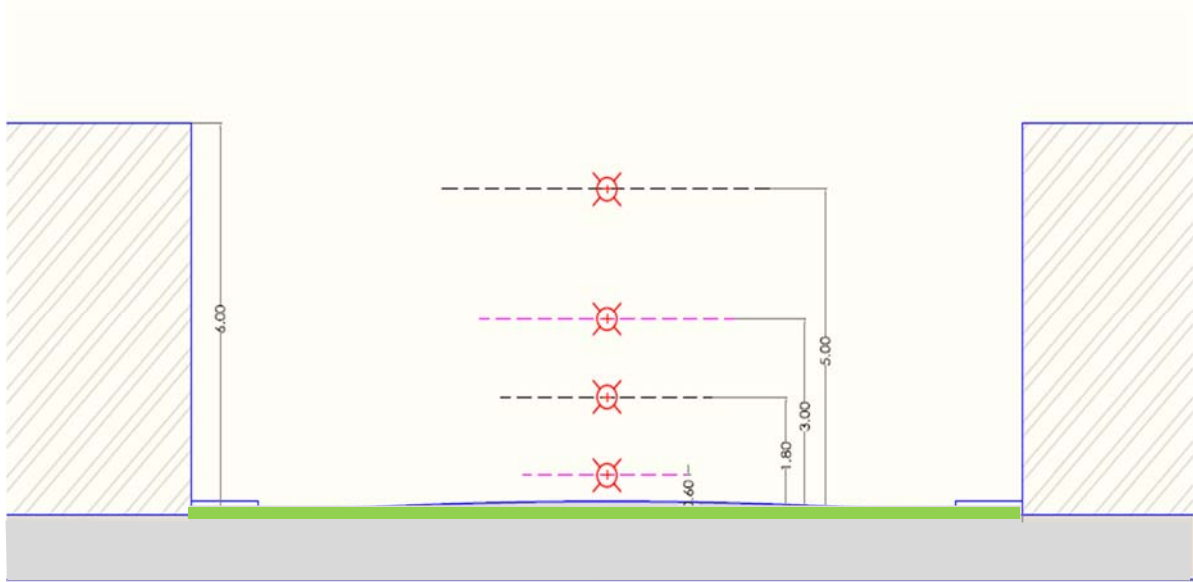
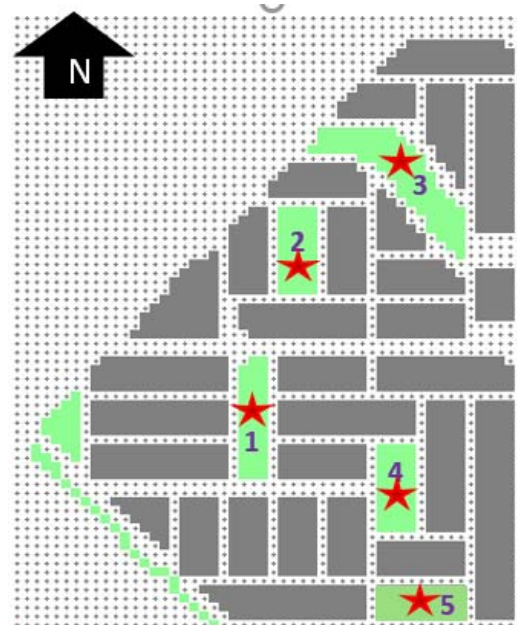


Figure 6.49: Measurement point in the centre of canyon with different heights

6.7.1 First scenario, Open spaces Without Trees

The open spaces in this scenario are without trees (Figure 6.50). This simulation was run for 24 hours for modern morphology in Erbil to simulate the Air Temperature, Wind Speed and Mean Radiant Temperature in open spaces only. The weather data was taken from a local weather station (central station) with a low wind speed of 0.5 m/s and 225° wind direction. The position of samples is shown in Figure 6.50.



★ Samples Position in the Open Spaces

Figure 6.50: The horizontal sample position for both types of canyon and

6.7.1.1 Air Temperature – First Scenario

1. Horizontal Samples²⁰

In this scenario, Air temperature, Wind Speed and Mean Radiant Temperature were measured in the five open spaces, as shown in Figure 6.50. The results are compared for 23 hours for the 1st July 2017.

Figure 6.51 Shows the air temperature for all five open spaces. The samples are taken at a height of 1.8 metres for the five different open spaces (Figure 6.49). The maximum air temperature was 39.02 °C and the minimum air temperature was 31.54 °C recorded for open space 1. The results explain that the air temperature for all five samples record similar values (Figure 6.51).

2. Vertical Samples (Zone one – 600mm, 1800mm, 3000mm and 5000mm

²⁰ These samples refer to the position of samples and the samples taken in the middle of the open spaces.
WOT = First Scenario Open Spaces without Trees.

In this simulation, the air temperature was taken in the centre of Open Space 1 (Figure 6.51). The samples were taken and measured at four heights: 600 mm, 1800 mm, 3000 mm and 5000 mm (Figure 6.49). This simulation compared air temperature for four samples in the centre of Open Space 1. Figure 6.52 depicts the air temperature for the vertical samples in Open Space 1. The results show that the air temperature for all four samples recorded similar values at different heights (600 to 5000 mm) (Figure 6.52). The results exhibit similar values for all samples during night-time and daytime, with a maximum air temperature of 38.65 °C and minimum air temperature of 31.75 for the Open Space 1 sample at 600 mm and Open Space 1 sample at 5000 mm, respectively (Figure 6.52).

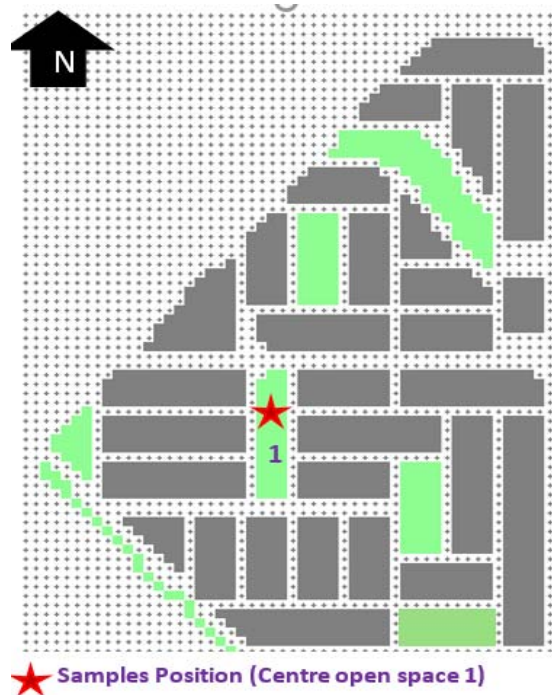


Figure 6.51: Vertical sample positions for Open Space 1

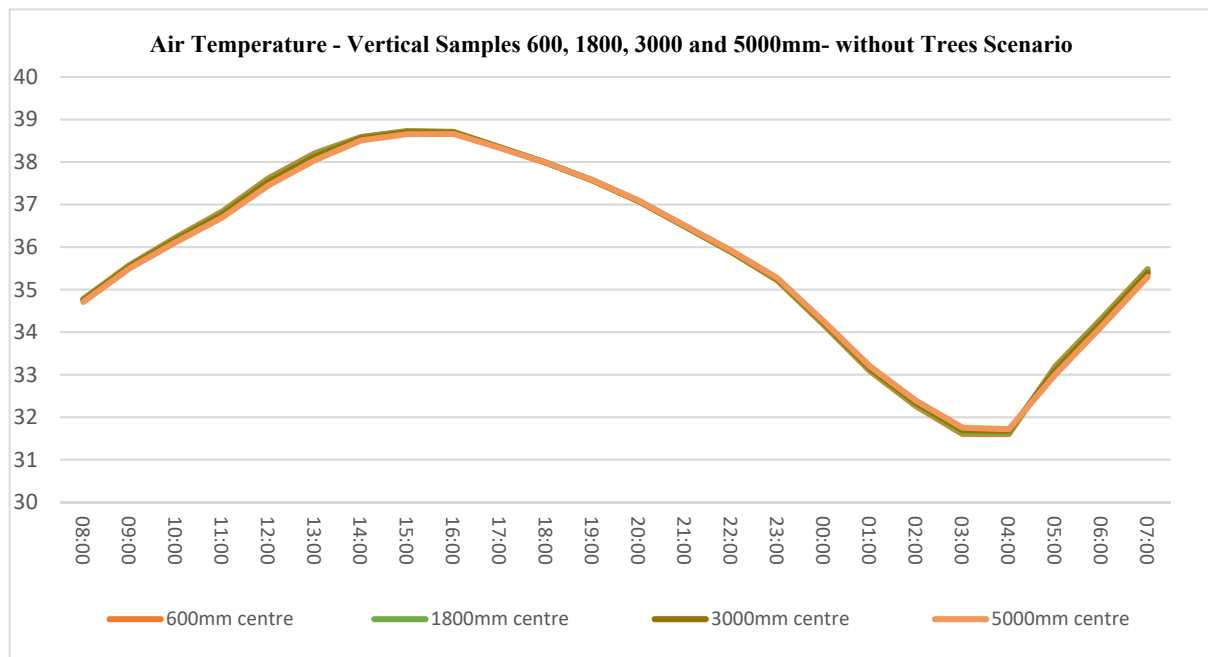


Figure 6.52: Air Temperature for vertical samples (600mm, 1800 mm, 3000 mm and 6000 mm).

6.7.1.2 Wind speed – First Scenario (Open Spaces without Trees)

6.7.1.3 Horizontal samples (First Scenario)

Wind speed was simulated in five open spaces without trees, as shown in Figure 6.53. The maximum wind speed was recorded in Zone 5 (0.36 m/s) in contrast to minimum wind speed in Zone 1 (0.21 m/s) (Figure 6.53). The position of Zone 5 is near the boundary condition from the south. This may be related to higher wind speed values compared

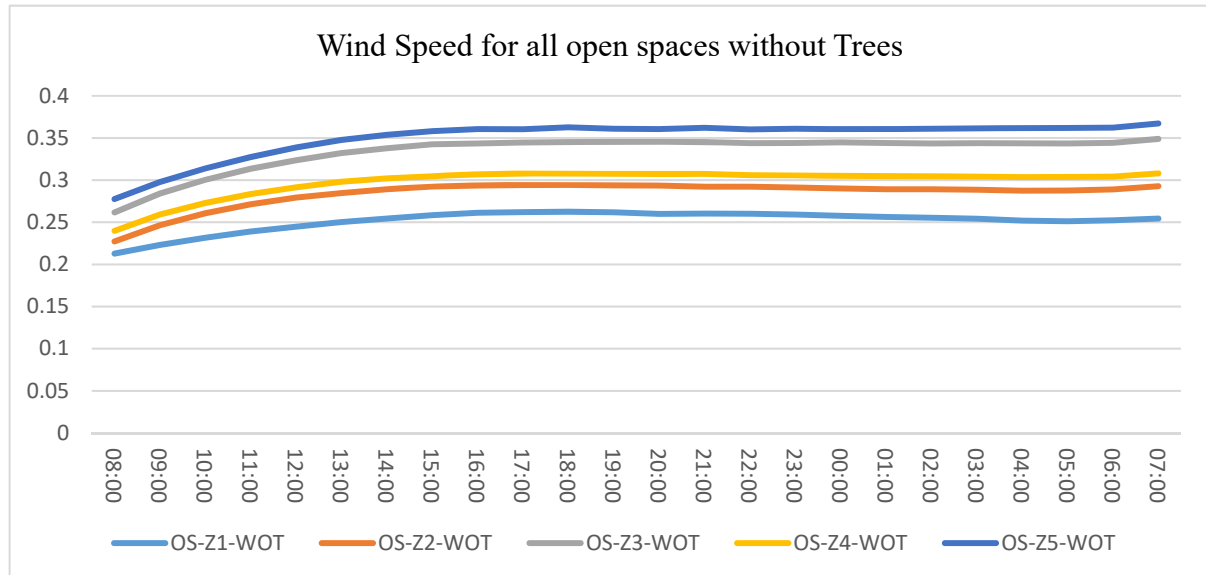


Figure 6.53: Wind speed for horizontal samples (east-west) and (north-south) canyons

to other zones, where housing surrounded the open spaces from all directions. Zone 3 recorded higher wind speeds than Zones 1, 2 and 4. This may occur because of the position and area of open space 3 compared to Zones 1, 2 and 4. It is located in a position where the eastern direction opens directly onto the boundary condition similar to Zone 5 (Figure 6.53). Overall, the wind speed is similar for all open spaces.

6.7.1.4 Vertical samples (First Scenario)

The second group of wind speeds were measured for the vertical samples in Open Space 1 at different heights, as shown in Figure 6.49. The samples were taken at 600 mm, 1800 mm, 3000 mm and 5000 mm. The results show that wind speed for vertical samples are between 0.33 m/s to 0.21 m/s for all four samples (Figure 6.54). The wind speed increases with height. The maximum wind speed was recorded at 5000 mm, while the minimum wind speed was recorded at a height of 600 mm.

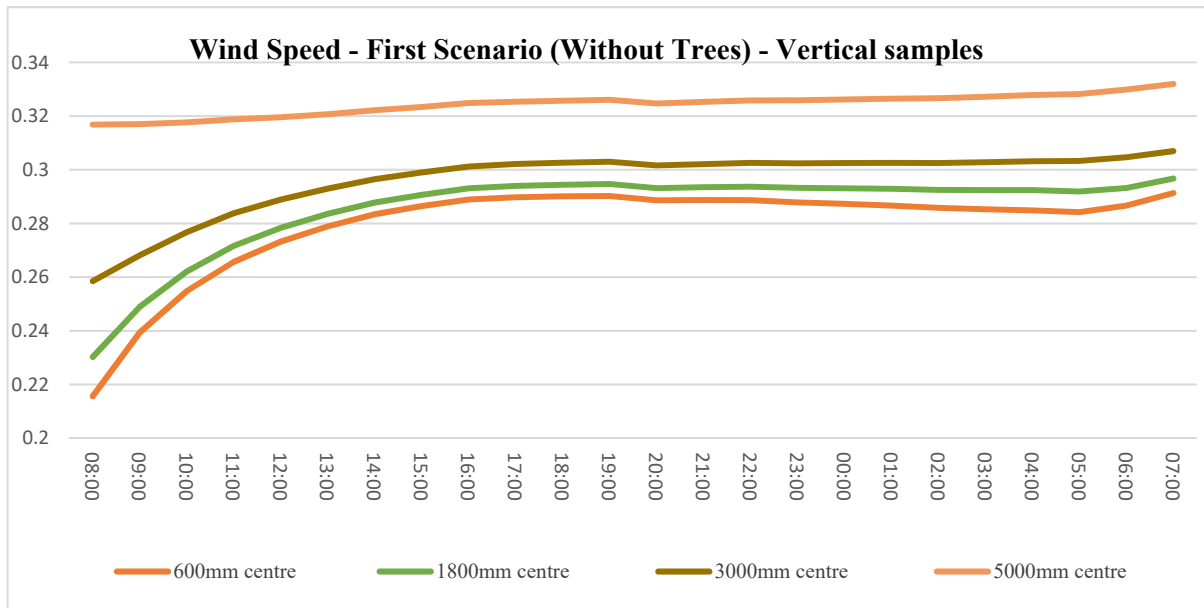


Figure 6.54: Wind speed for vertical samples in similar positions in the centre of Open Space 1

6.7.1.3 Mean Radiant temperature²¹ – First Scenario

The introduction of shade into any environment will have little or no effect on air temperature but will impact on wind speed and radiant energy exchange. One measure of this exchange is the Mean Radiant Temperature, this is a measure of the average temperatures of the surfaces that surround a point and if the point is located outside, this will include solar radiation. External shading will therefore reduce both the radiant energy emitted by the building surfaces and direct solar gain.

²¹ Mean Radiant temperature is defined as the “uniform temperature of an imaginary enclosure in which the radiant heat transfer from the human body equals the radiant heat transfer in the actual non-uniform enclosure” (ASHRAE, 2001)

6.7.1.5 Horizontal Samples

Mean Radiant Temperature (MRT) was measured in five open space positions at 1800 mm height, as shown in Figure 6.4. The results illustrate that the MRT during the daytime is higher than at night. The maximum MRT is 82.40 °C at 14:00, while the minimum MRT is 20.60 °C at 03:00 (Figure 6.55). The MRT for all samples recorded similar values during the daytime and night-time.

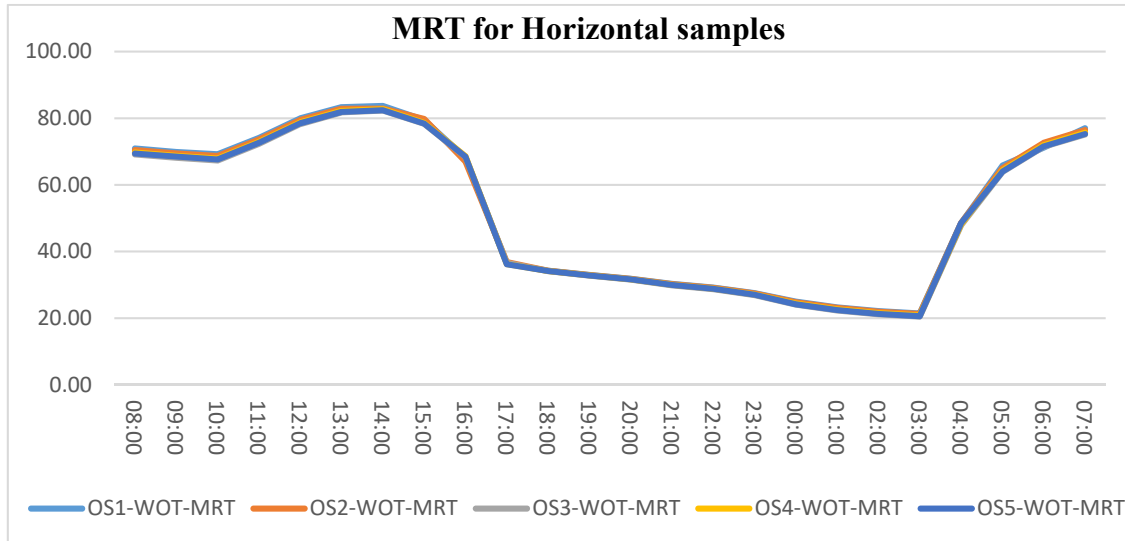


Figure 6.55: Mean Radiant Temperature for Horizontal samples from Open Spaces 1, 2, 3, 4 and 5

6.7.1.6 Vertical Samples

Mean Radiant Temperature (MRT) was measured in Open Space 1 only at four heights, as shown in Figure 6.49. The result shows that the MRT during the daytime is higher than the night-time. The maximum MRT is 84.23 °C at 14:00, while the minimum MRT is 20.60 °C at 3:00 (Figure 6.56). The MRT for all samples recorded similar values during the daytime and night-time (Figure 6.56).

For both horizontal and vertical samples the MRT show similar profiles: during the day time the MRT is strongly influences by solar gain, both direct and radiation from adjacent buildings. After sun set the direct component disappears and the open spaces see the night sky resulting in a slow reduction of the MRT until early morning.

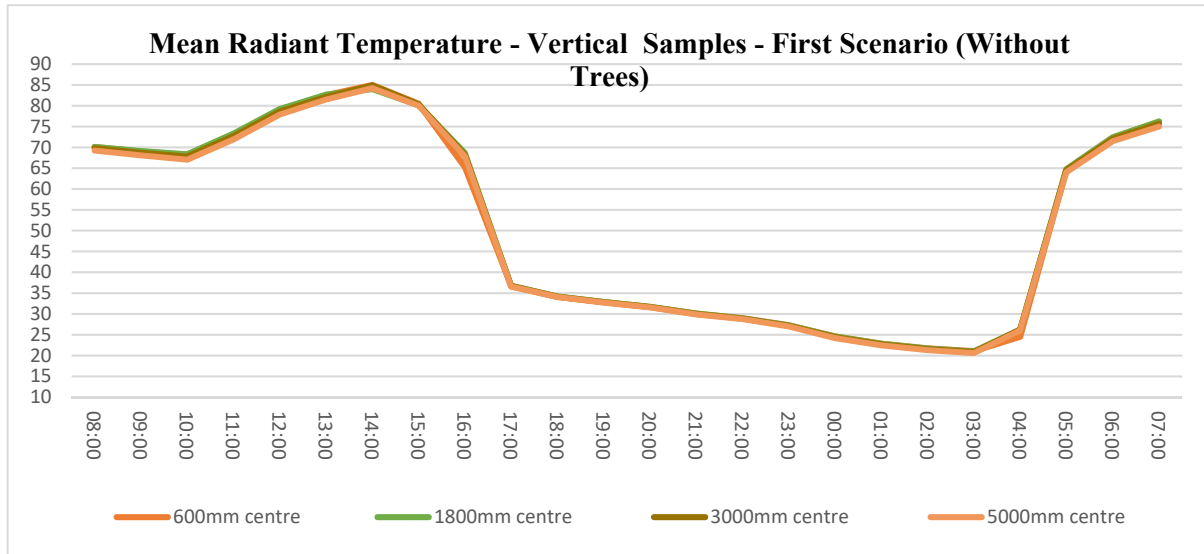


Figure 6.56: Mean Radiant Temperature for vertical samples

6.7.2 Second Scenario (Open Space with trees)

The open spaces in this scenario are fully covered with trees (Figure 6.51). The simulation was run to measure the Air Temperature (T), Wind Speed (WS) and Mean Radiant Temperature (MRT) in all five open spaces (Figure 6.56). The weather data were taken from the local weather station with a low wind speed of 0.5 m/s and 225° wind direction. The aim of this simulation was to evaluate the impact of trees (shading) on the urban microclimate of open spaces.

6.7.2.1 Air Temperature – Second Scenario

1. Horizontal Samples

Air temperature simulated for the five open spaces were taken at a height of 1.8 metres, as shown in Figure 6.57. The results show that the air temperature for all five samples had small differences (Figure 6.57). During the day-time (06:00 to 17:00) the air temperature for Open Space 5 was higher than Open Space 1, while during night-time the differences in air temperature increased and Open Space 5 recorded the lower value (Figure 6.58).

The maximum air temperature is between 41.15°C and 39.19°C and the minimum air temperatures are 31.11°C to 28.82°C.

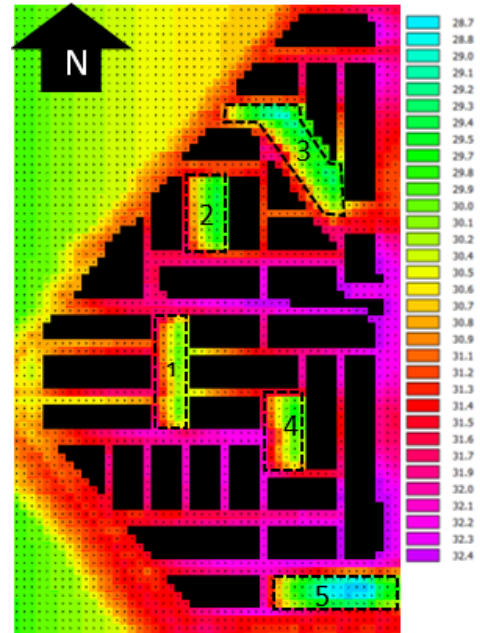


Figure 6.57: Air Temperature for second scenario showing the open spaces air temperature differences at 4:00 am

Open Space 5 is located close to the boundary of the simulation, Figure 6.58 and will be directly influenced by the boundary conditions. Hence, it will be hotter during the daytime and cooler at night compared to the other open spaces.

Open Space 1 recorded the minimum air temperature during daytime with maximum air temperature during the night-time.

Overall, air temperatures for open space samples increase or decrease because of wind speed and thermal mass. However, the difference in air temperature by adding trees into open spaces does not have a significant impact on air temperature.

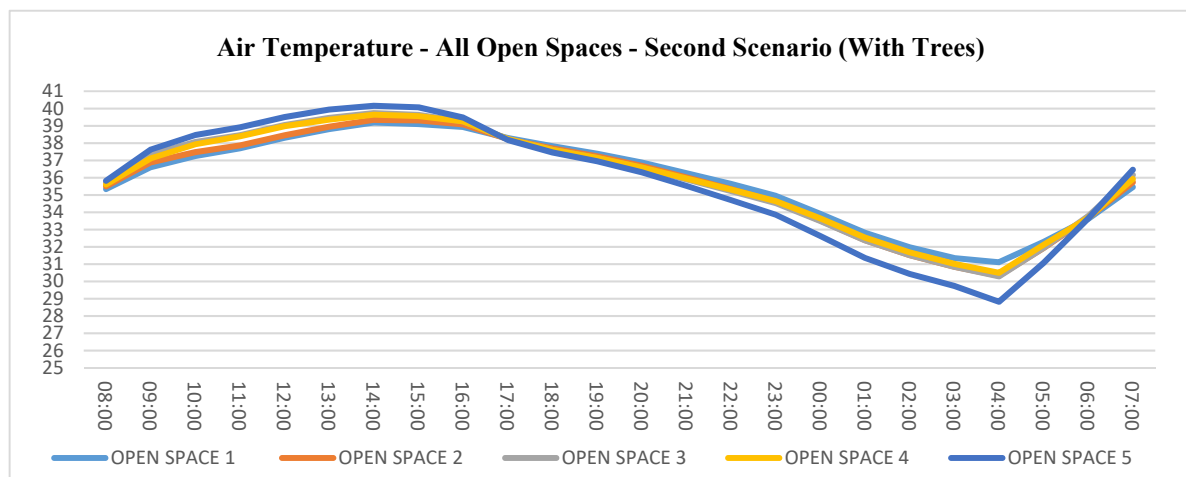


Figure 6.58: Air temperature for the second scenario (open spaces)

2. Vertical Samples (Zone One) – 600mm, 1800mm, 3000mm and 5000mm

In this simulation, air temperatures were compared for four samples located in the centre of Open Space 1 (Figure 6.49). The samples were measured at four heights: 600 mm, 1800 mm, 3000 mm and 5000 mm.

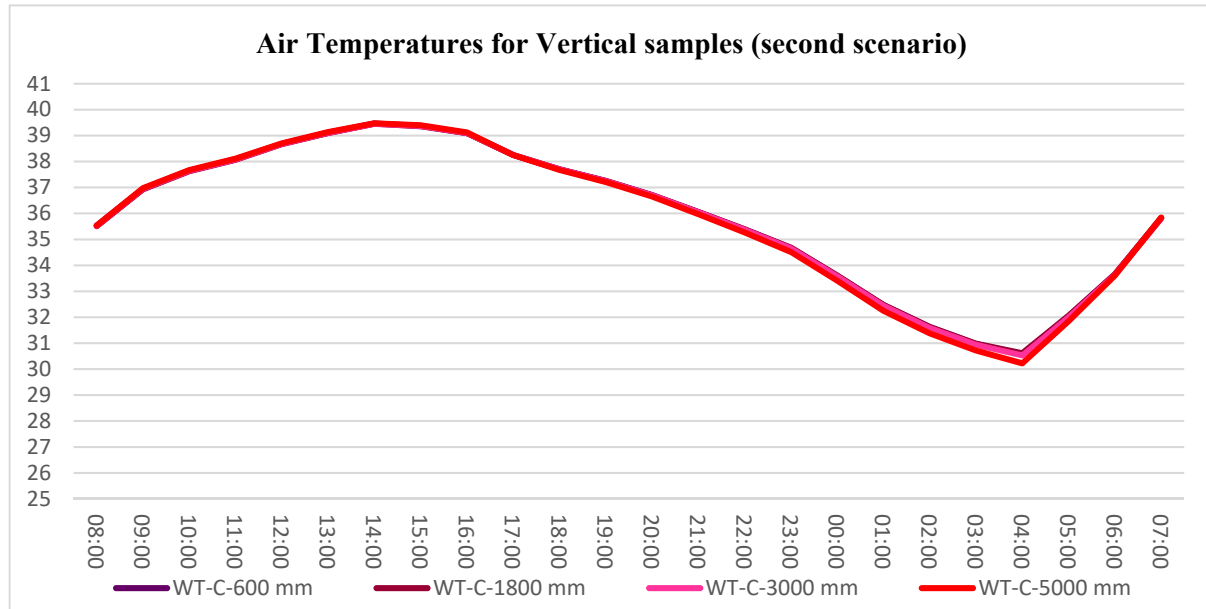


Figure 6.59: Air temperature for vertical samples in three sample positions with four sample heights (Second scenario)

There is a small difference between the daytime and night-time temperature with maximum air temperature of 39.48°C, and minimum air temperature of 30.22°C. The maximum air temperature and maximum ($\Delta^\circ\text{C}$) were recorded for open spaces samples (Figure 6.60). The trees do not allow the wind to flush out the air temperature (heat energy will be trapped) inside the open spaces, while in the canyons the wind flushes out the heat energy from the canyon (Figure 6.60).

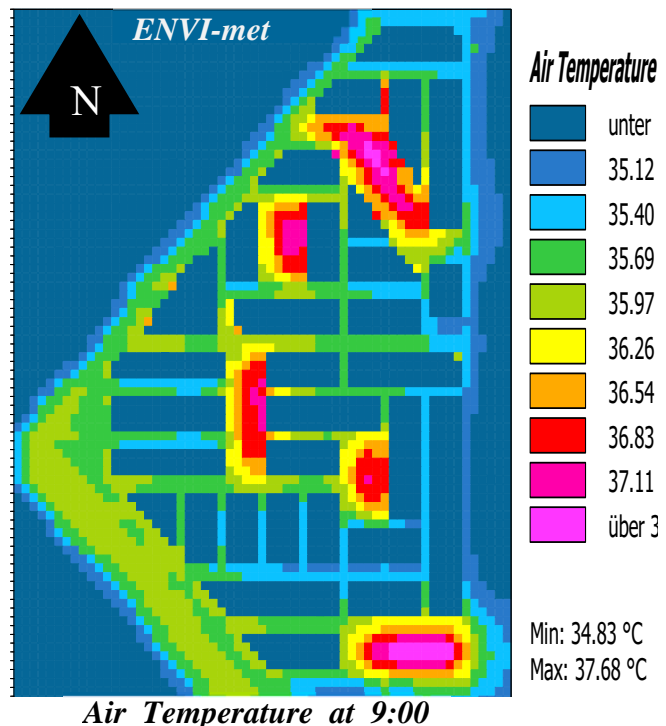


Figure 6.60: Air temperature for the second scenario (with trees)

6.7.2.2 Wind Speed – Second Scenario

In this scenario (with trees), wind speeds were measured horizontally and vertically for open spaces (Figure 6.48 and Figure 6.49). The maximum wind speed is 0.25 m/s for Open Space 3 compared to 0.17 for Open Space 5 (Figure 6.61).

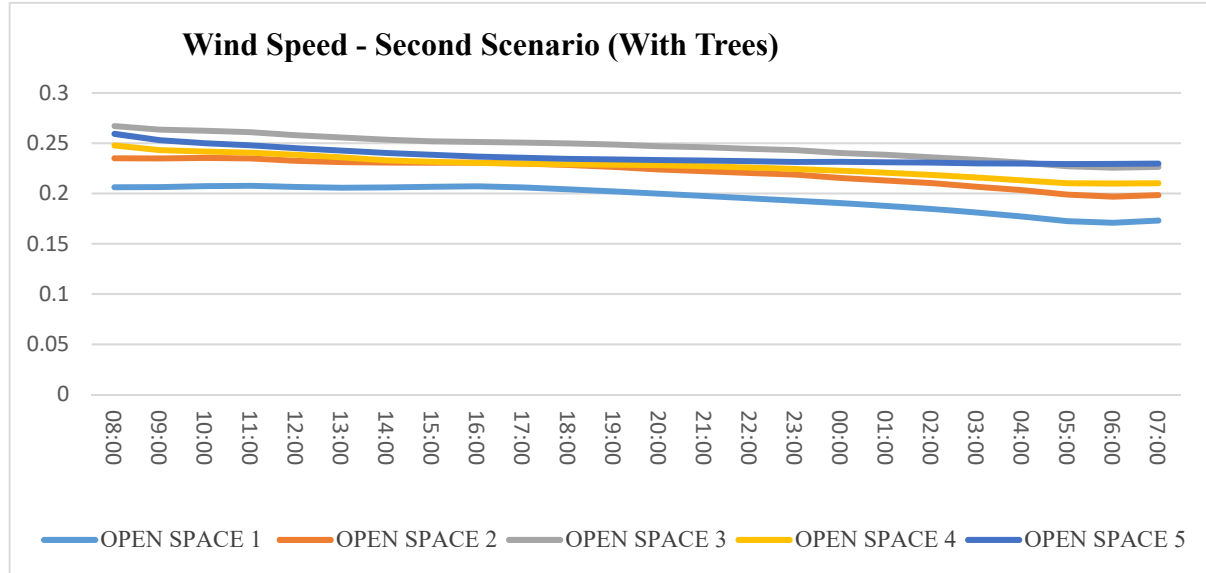


Figure 6.61: Wind speed for horizontal samples in the centre of all open spaces; second scenario open spaces with trees.

Figure 6.49 shows the position of the vertical samples of wind speed in Open Space 1. The samples indicate that Open Space 1 at a height of 5000 mm recorded the lowest wind speed compared to samples taken at heights of 600 mm, 1800 mm and 3000 mm (Figure 6.62).

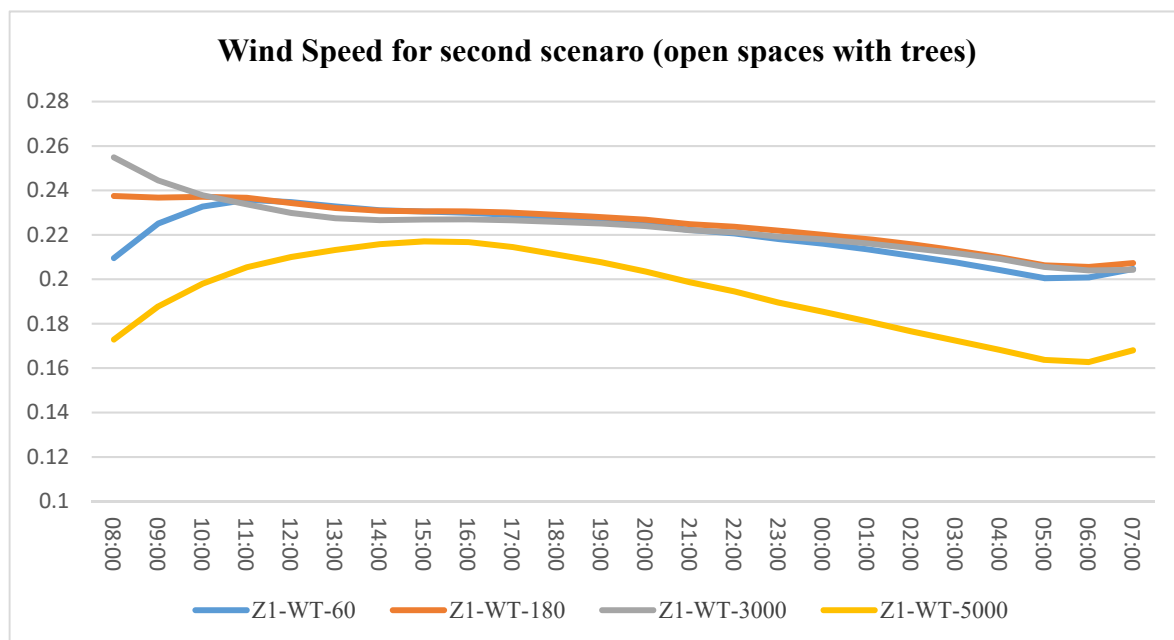


Figure 6.62: Wind Speed for the second scenario (with trees), Vertical samples for Open Space 1

The results indicate that wind speeds for the vertical samples are between 0.24 m/s to 0.18 m/s for all four samples (Figure 6.62). Wind speed for samples from Open Space 1 at heights of 600 mm, 1800 mm and 3000 mm recorded higher values compared to the 5000mm sample point (Figure 6.62). Open Space 1 is full of trees below 300m only isolated tree trunks are present providing little wind resistance, but at 5000mm the tree canopy is fully developed, Figure 6.63, and does significantly reduce the wind speed at this height points.

Wind speed for samples from Open Space 1 at heights of 600 mm, 1800mm and 3000mm record higher values compared to the 5000mm sample point, Figure 5.94. Open Space 1 is full of trees, below 300m only isolated tree trunks are present providing little wind resistance, but

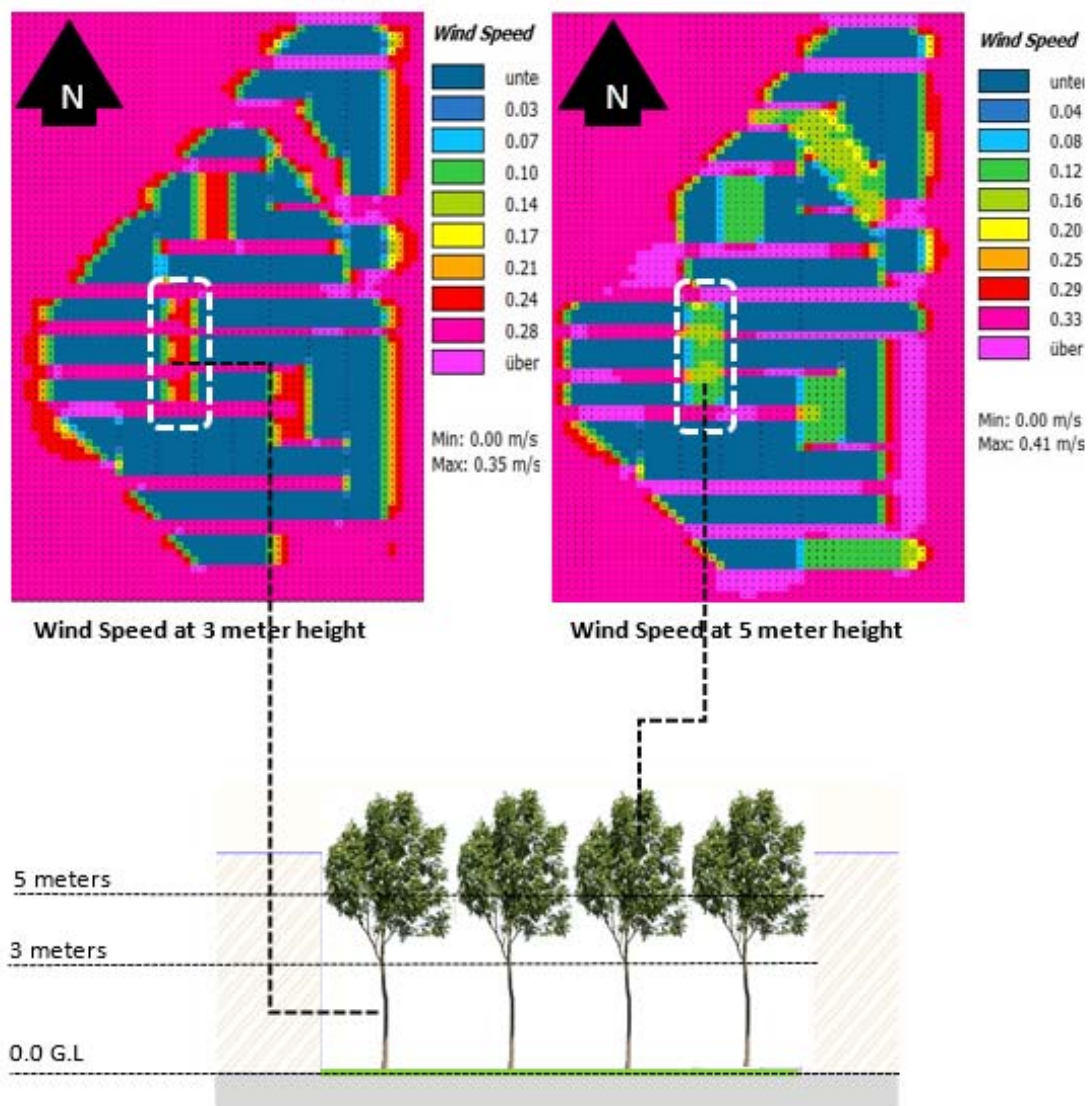


Figure 6.63: ENVI-met images showing wind speed at different heights for the second scenario (open spaces with trees).

at 5000mm the tree canopy is fully developed, Figure 5.95, and does significantly reduce the wind speed at this height

6.7.2.3 Mean Radiant Temperature – Second Scenario

6.7.2.3.1 Horizontal samples

Figure 6.64 displays the Mean Radiant Temperature (MRT) for horizontal samples (5 samples) at a height of 1.8 metres for all five open spaces. The results signify that the MRT for all samples in the open spaces is similar during daytime and night-time.

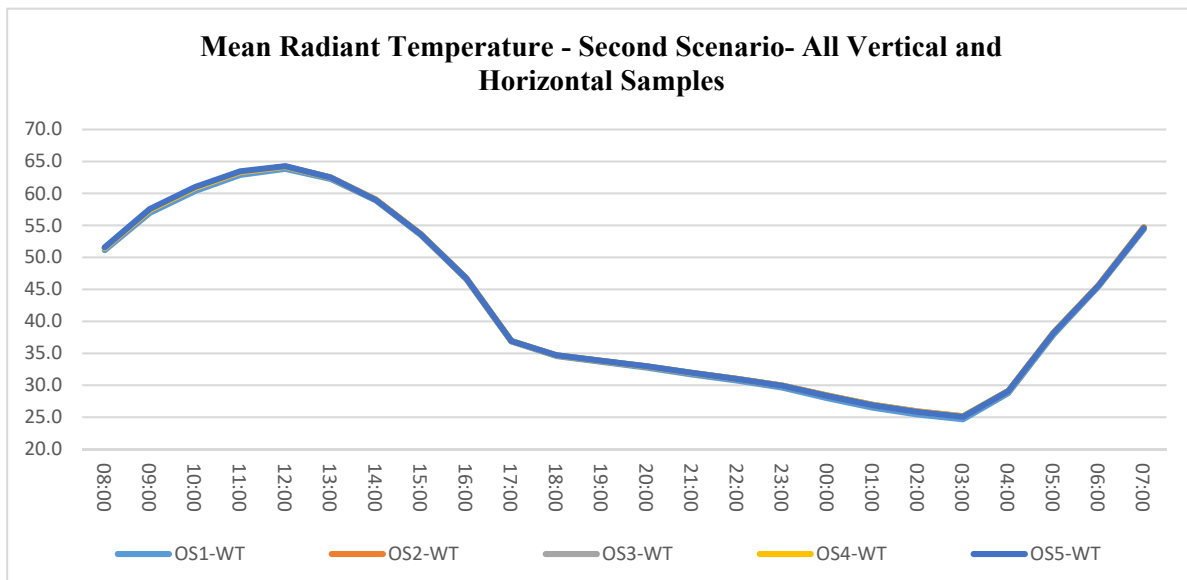


Figure 6.64: Mean Radiant Temperature for horizontal samples for the second scenario (open spaces with trees)

The samples show similar MRT during the night-time, but there are slight differences in MRT during the daytime (Figure 6.64).

Mean Radiant Temperature for open spaces with trees recorded lower values in contrast to open spaces without trees. This occurs as a result of shading by trees which cover all the open spaces. Shading by trees has a significant impact on MRT reduction for the open spaces (Figure 6.65).



Figure 6.65: ENVI-met image showing Mean Radiant Temperature for canyons and open spaces (second scenario) at 12:00 noon

6.7.3.4 Vertical samples

Mean Radiant Temperature (MRT) was measured in the second scenario (open spaces with trees) for vertical samples at Open Space 1 (Figure 6.66). The results show that MRT during the daytime is higher than at night.

The maximum MRT is 66.05 °C at 14:00, while the minimum MRT is 25.47 °C at 03:00 (Figure 6.66). The differences in MRT increase during daytime between samples, while the values for all samples consist of a noticeable smaller difference during night-time.

Generally, the MRT temperature for open spaces for the second scenario (open spaces with trees) is different during day-time and with a slight difference during night-time when compared to the first scenario (open spaces without trees).

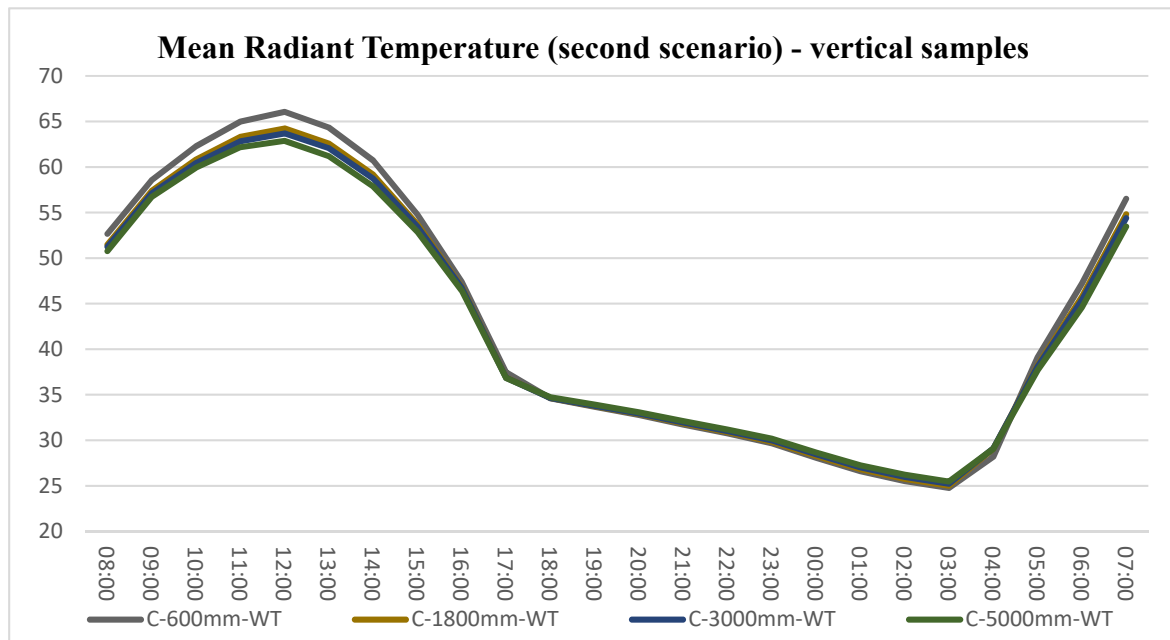


Figure 6.66: Mean Radiant Temperature for vertical samples (second scenario)

Figure 6.67 illustrates how the height of the buildings impacts on shading and MRT in relation to the canyons. Canyon samples at a height of 5,000 mm is not shaded by building blocks, while canyon samples at a height of 3 metres are partially shaded.

Tree heights and two buildings (circled with hidden lines) in the north-east and south-west (Figure 6.67) are higher than 6 metres, so the shading area for these cases is more than the other residential blocks (Figure 6.67).

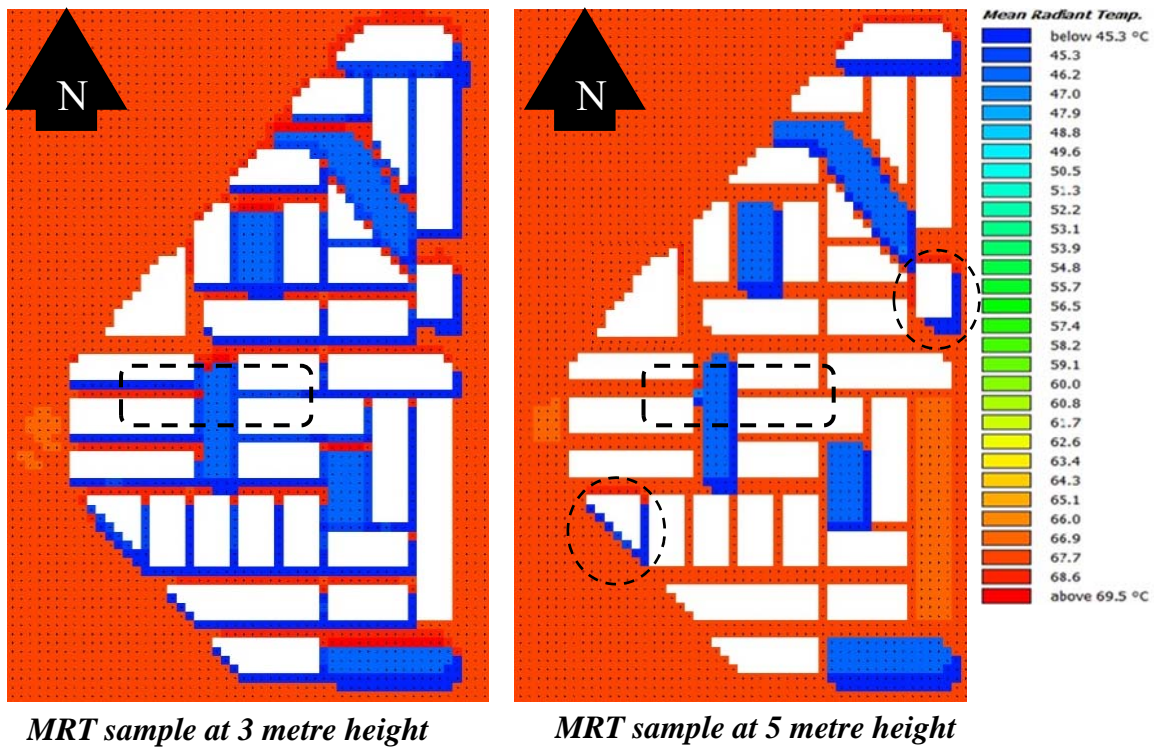


Figure 6.67: Mean Radiant Temperature for second scenario (open space with trees) at 16:00 showing the shading effect at different heights

6.8 Compare two scenarios

In this section, the air temperature (T), wind speed (WS) and mean radiant temperature (MRT) for all five open spaces for both scenarios (open spaces with and without trees) are compared.

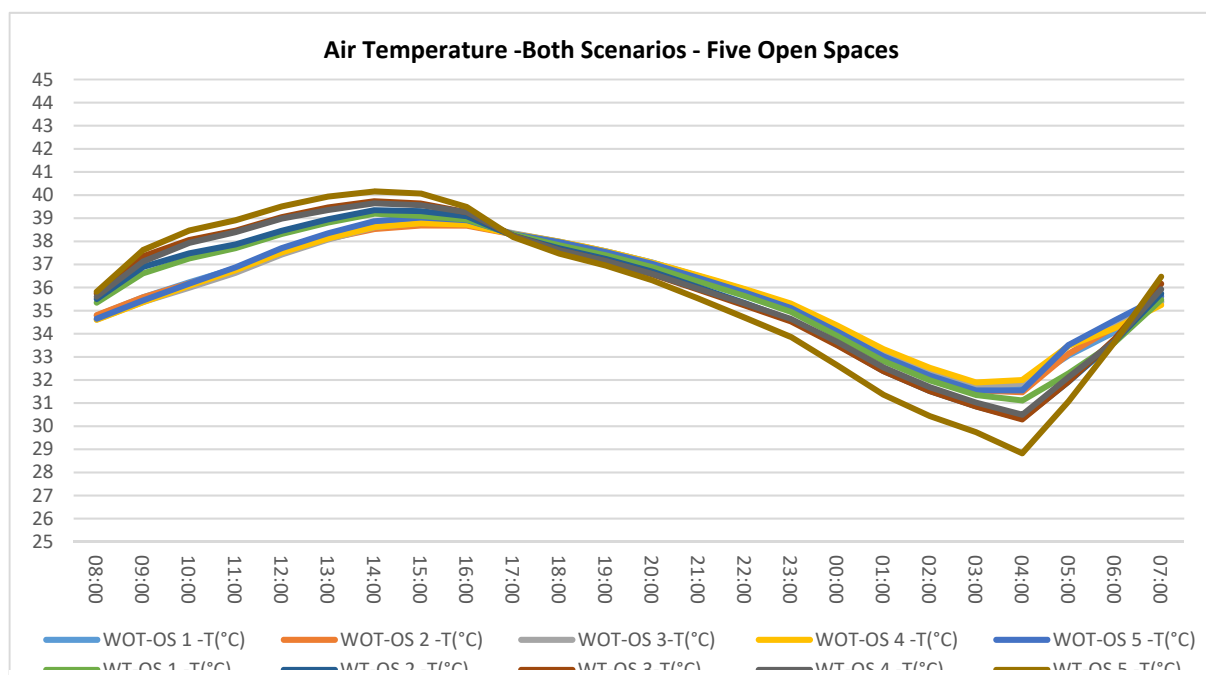


Figure 6.68: Compare all five open spaces, air temperatures for both scenarios (open spaces with and without trees)

6.8.1 Air Temperature (Open Spaces with Tree and Without Trees)

Air temperatures in Figure 6.68 compare both scenarios for all five open spaces. The results show that adding trees into the open spaces had no significant impact on air temperature. The air temperature is approximately the same for both scenarios, with only slightly differences. Air temperature for open spaces without trees recorded lower values compared to open spaces with trees, for the reason that the trees impact on wind speed, resulting in higher air temperatures (Figure 6.69).

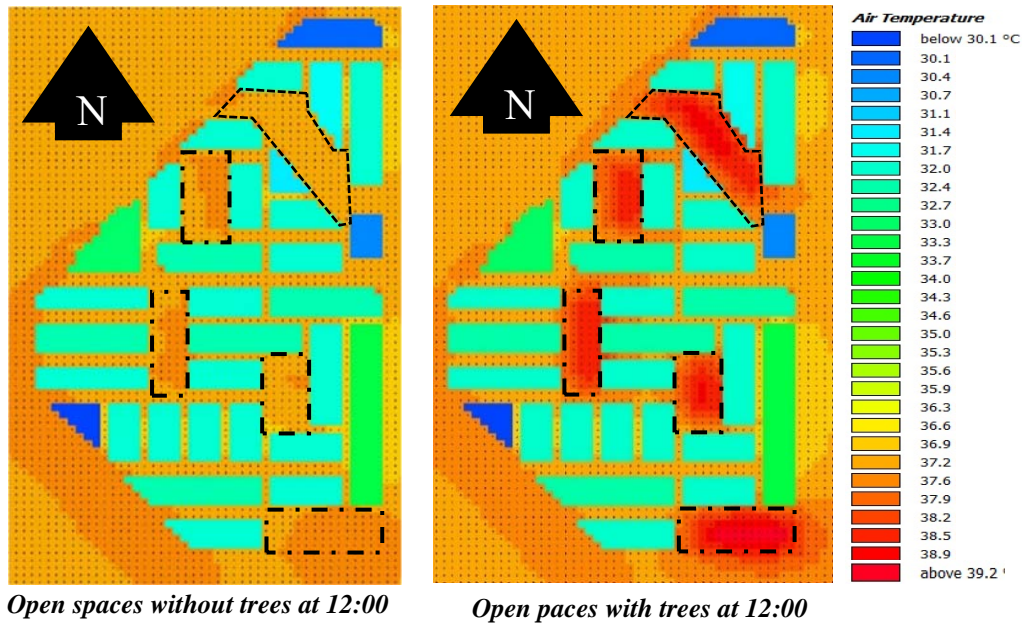


Figure 6.69: Air Temperature for all open spaces for both scenarios at 12:00

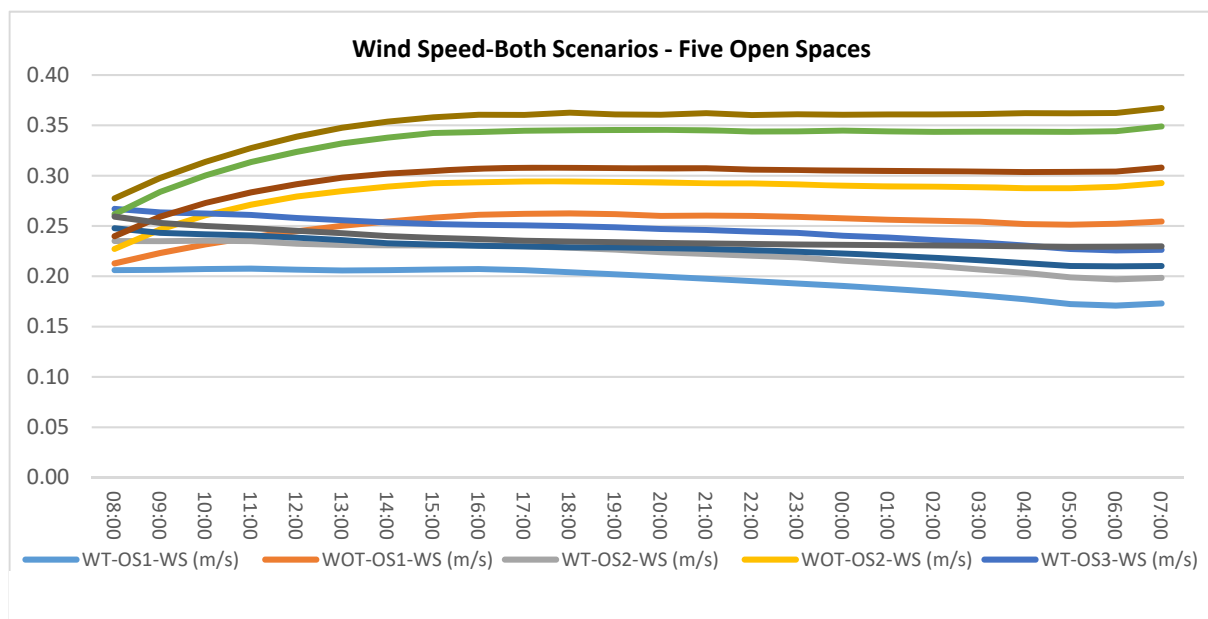


Figure 6.70: Compare all five open spaces wind speed for both scenarios (open spaces with and without trees)

6.8.2 Wind Speed (Open Spaces with Tree and Without Trees)

Wind speed in this section is compared for all five open spaces in both scenarios (open spaces with and without trees). The results show that there is an impact on wind speed by adding trees into the open spaces. Wind speed for open spaces without trees is higher than open spaces with trees (Figure 6.70 and Figure 6.71).

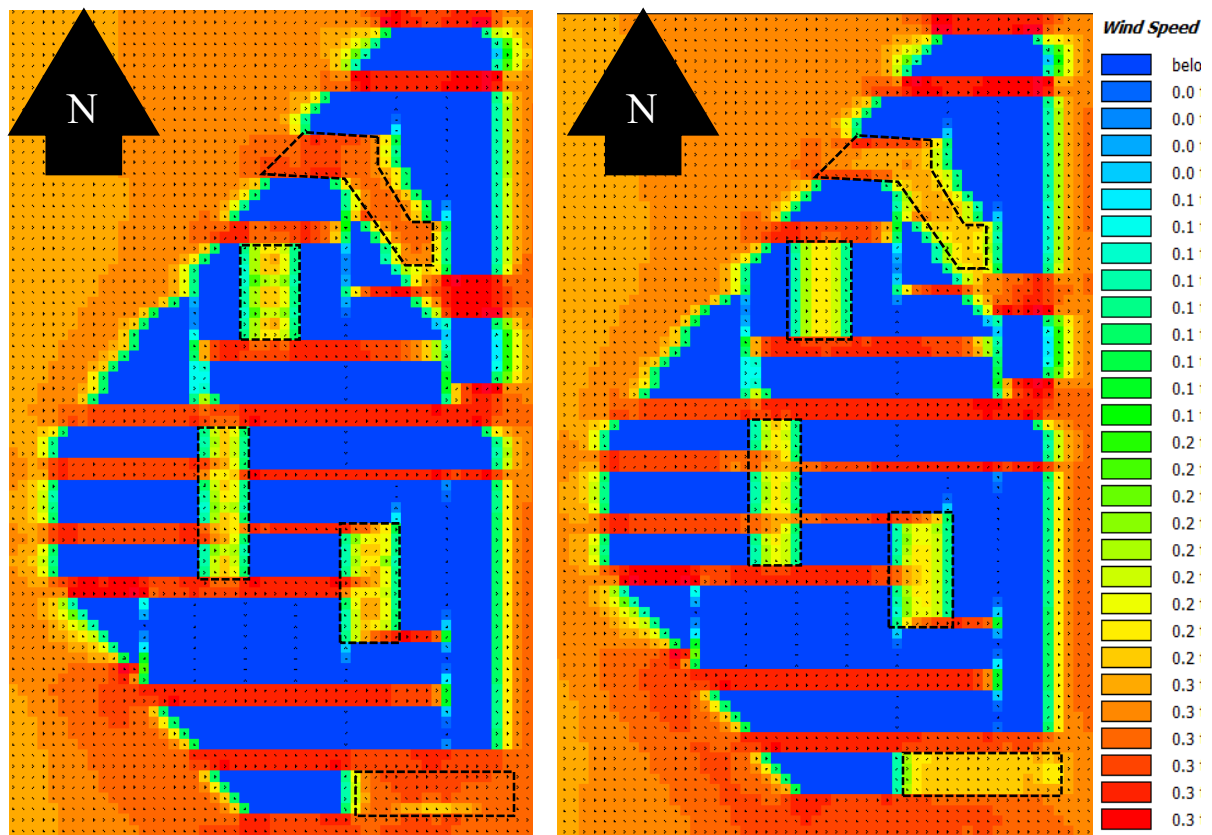


Figure 6.71: Wind Speed for all scenarios (open spaces with and without trees)

6.8.3 Mean Radiant Temperature (Open Spaces with and Without Trees)

Mean Radiant Temperature (MRT) was measured at a height of 1.8 metres in the centre of all five open spaces in both scenarios (open spaces with and without trees).

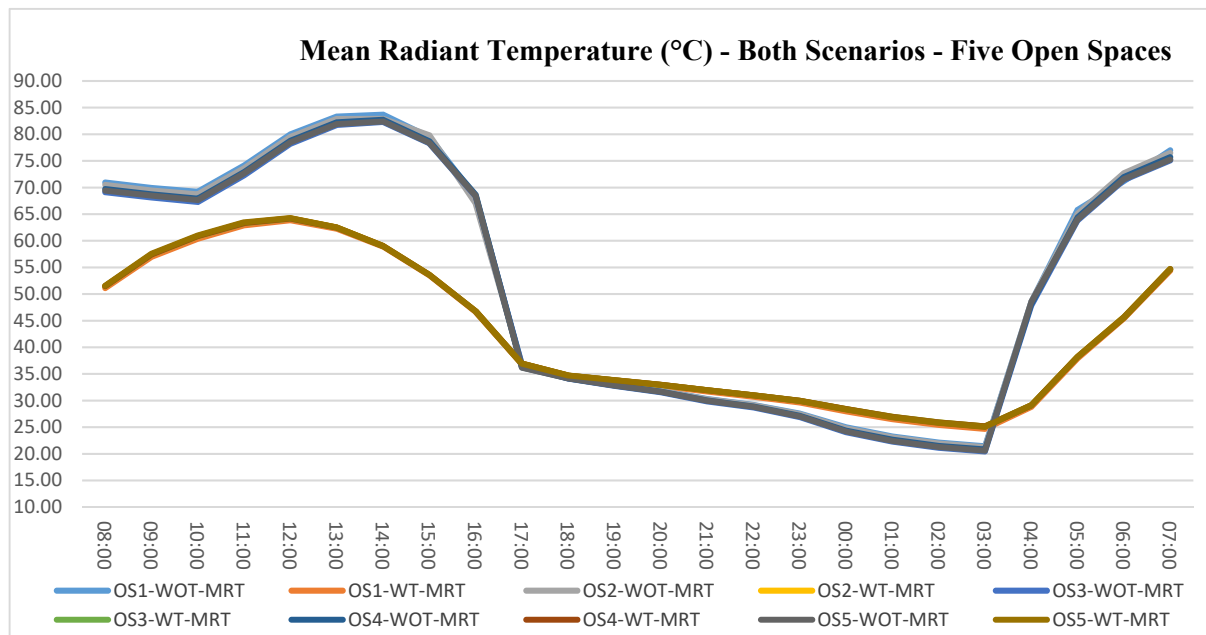


Figure 6.72: Compare all five open spaces Mean Radiant Temperature for both scenarios (open spaces with and without trees)

The results suggest that open spaces for the first scenario (open spaces without trees) recorded higher MRT during daytime in contrast to the second scenario (open spaces without trees).



Figure 6.73: Mean Radiant Temperature for both scenarios at 12:00 showing the impact of tree shading on MRT on open spaces

There is a significant difference in MRT between both scenarios during daytime from sunrise to sunset (Figure 6.72). Trees provide shade for the open spaces in the second scenario, which prevents the solar radiation reaching the open spaces. This leads to reduced MRT in open spaces beneath the trees. The maximum MRT recorded at 14:00 for open spaces without trees was 83.69 °C, while maximum MRT for the second scenario (open spaces with trees) at 12:00 was 64.26 °C.

The results suggest that adding trees into the open spaces has a limited impact on MRT during night-time. Open spaces without trees recorded lower MRT during night-time. This difference increased gradually from zero at 17:00 to a maximum at 03:00 (Figure 6.72). During the night-time, the trees limit radiation loss to the night sky, and hence there is an increasing difference after sunset.

Shading strategies can be used in urban areas (open spaces) as an effective strategy to reduce solar radiation during the daytime, which reduces thermal energy present in outdoor open spaces (Figure 6.73). The results of this section confirmed that adding trees to the open spaces has a limited impact on air temperature and wind speed for canyons and open spaces, while adding trees (shading) to open spaces has a significant impact on MRT during daytime and limited impact during night-time.

6.9 Conclusion

In this chapter, both traditional and modern urban morphologies were simulated. The results signify that air temperature is lower for the traditional urban area compared to the modern urban morphology, with a maximum air temperature of 38.54 °C and 41.40 °C, respectively (See section 6.11 and 6.12).

One of the important findings in this chapter is having the wind direction parallel to North-South or East – West canyons increase the wind speed in those canyons but decrease the wind speed in the perpendicular canyons. Moreover, having the wind direction in 225° from the North will distribute equally between both North-South (Vertical) and East – West (Horizontal) canyons (See section 6.13). The impact of having this orientation provides higher wind speeds in both canyon directions and that in turn will increase building ventilation rates in both canyon directions.

The design scenarios showed that there is a limited impact related to the design interventions on air temperature ($T^{\circ}\text{C}$) and a noticeable impact on wind speed (WS m/s) by way of modifying canyon directions according to wind direction. The high density urban areas in Erbil have a low wind speed 0.5 m/s , so any design scenario to increase the wind speed may not have a significant impact on the urban microclimate (because the wind speed is originally low). These differences are not enough to have an impact on the design of new urban planning projects (See section 6.14).

For this reason, new design scenarios were employed (adding trees into the open spaces), whilst ENVI-met was used to simulate Air Temperature ($T^{\circ}\text{C}$), Wind Speed ($\text{WS}^{\circ}\text{C}$) and Mean Radiant Temperature ($\text{MRT}^{\circ}\text{C}$) for the Horizontal and Vertical samples. The results exhibited that adding trees into the open spaces does not have a significant impact on the $T^{\circ}\text{C}$ and WS m/s for both canyons and open spaces (See section 6.16).

MRT can be reduced by adding trees into the open spaces. The maximum MRT for Open Space1 (without trees) was 83.69°C compared to Open Space 1 (with trees) 63.85°C . The significant impact of adding trees to MRT caused by shading from trees, reduces the solar radiation entering into open spaces. The shading strategy can be used as an effective design feature to reduce thermal energy during summertime in cities in hot/dry climates.

Chapter 7: The Impact of Shading Mesh

7.1 Introduction

This chapter discusses the application of shading strategy to control solar access and wind speed in urban areas (open spaces and canyons). The amount of solar exposure from solar radiation is one of the main factors to control urban microclimate conditions.

In the first section of this chapter, the history of shading in the traditional urban morphology of Erbil was explained. The second section illustrates the modern use of shading in recent projects. The third section explains the simulation procedure for shading mesh using ENVI-met. The final section explains the impact of using shading mesh as an effective strategy to reduce solar radiation in hot, dry climate urban areas.

Shading has been used for a long time in hot, dry climates to help people cope with hot summers. This can be seen in the narrow canyons in the traditional morphology of most Middle-East cities (urban scale). In addition, a shading device called a *shanshol* or *shanashil* (building scale) is used in house windows.

The narrow and vertical canyons are decorated with *shanashil* which eliminate direct solar radiation from entering house spaces directly located in the canyon. The *shanshol* consists of a grid of small halls used as a mechanism to reduce direct solar radiation and provide a level of privacy for houses. The traditional way to reduce direct solar radiation was by means of reducing canyon width (reduced sky view factor), although this strategy is not applicable for modern urban housing projects. This is due to modern transportation (cars) and placing infrastructure under the streets. This study investigates the impact of urban shading strategy by covering canyons and open spaces with shading mesh. In order to simulate this, ENVI-met is used to model shading mesh over the urban areas.

7.2 History of shading

Radiation is an important factor; it is extremely variable and a dominant component of the thermal energy balance of outdoor urban microclimate. Inside buildings, the air temperature is described by simple temperature without regard to radiant field surroundings, because the room temperature is influenced by the internal surface temperature of a room already shielded from intense solar radiation.

The design of outdoor spaces is fundamentally responsible for the urban microclimate and differs from the microclimates in indoor spaces, and pedestrians experience a wide range of thermal sensations through radiation. There are two forms of radiation that affect an outdoor urban environment, namely, short wave and long wave radiation. In hot, dry climate regions, radiation was an important subject in relation to creating urban microclimates (Johansson 2006). These urban design strategies to reduce radiation can be seen in both buildings and urban scale (Figure 7.1). For example, housing units in Erbil were built to adapt to the hot environment by eliminating direct contact between outdoor and indoor environments (Abdulkareem 2012, Amin and Al-Din 2019). In this section, the historical strategies of Erbil's microclimate are explained. The environment building element can be divided into two main categories for both buildings and urban scale:

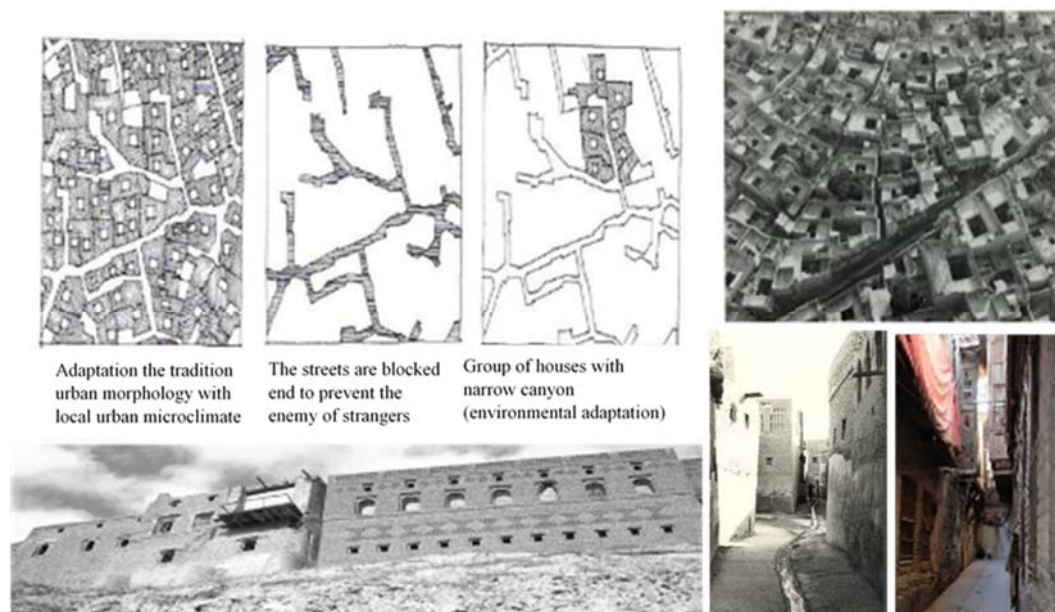


Figure 7.1: Traditional urban planning showing the horizontal design elements of an old city in a region with a hot-dry climates. Sources <https://thetravelingi.com/2017/10/20/iraq-dining-in-erbil-kurdistan/>, (Khaled 1993), SadikG/123RF.com

1. Horizontal urban design elements: this strategy aims to reduce the sky view factor of canyons by reducing their width of canyons and open spaces, to reduce the penetration of direct solar radiation (short wave radiation) and increase shaded areas (Figure 7.1).
2. Vertical design elements: this strategy employed vertical architecture features to generate a unique design element which adapts to the local urban environment and reduces the penetration of direct solar radiation into the indoor environment (Figure 7.2). This type of design element is divided into two main categories:

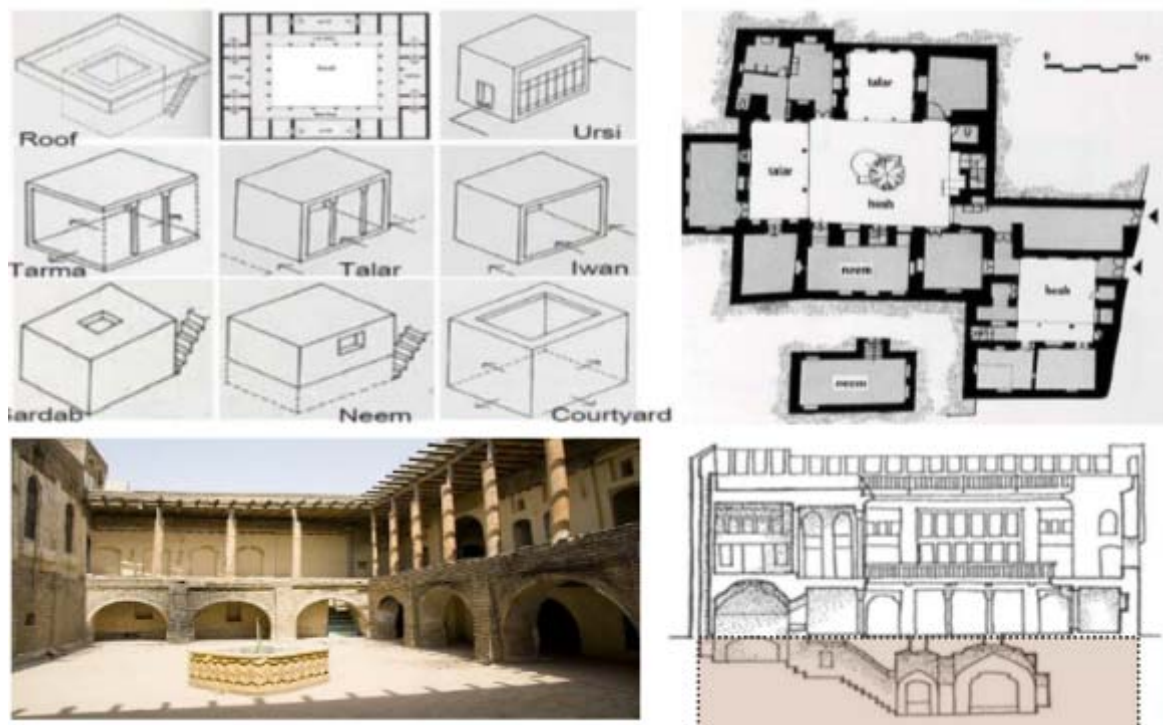


Figure 7.2: Housing unit shows the environmental elements of historical housing in Erbil. Sources (Al Jaff, Al Shabander et al. 2017) (Morad and Ismail 2017)

a. Arrangement plan for house units

The main architecture building elements in traditional housing in Iraq are the courtyard (core of the house), Ursi, a closed room with three walls, a shaded corridor (*Tarma*), as well as the Talar, Neem and Sardab (basement) (Ayyash 2015). The idea of these architectural zones is to provide essential shade using 3D geometry (length, width and height) (Al-Azzawi 1996). Additionally, to prevent occupants from thermal energy balance basements or half basements (Neem) are used during daytime in hot summers and as a convenient storeroom in winter (Figure 7.3).

b. Architectural treatment of openings and façade details



Figure 7.3: Shanasheel in traditional neighbourhoods in Iraqi cities. Source of image <https://thereaderwiki.com/en/Mashrabiya>, <https://www.alamy.com/stock-photo/old-basra.html>

The opening in traditional houses in a hot, dry climate region is relatively small to restrict the amount of daylight to penetrate and eliminate direct solar radiation from entering. In housing units, the shading element is employed vertically on the first floor to provide shading and privacy for the bedroom (Baiz and Fathulla 2016). This shading device, called a '*al shanasheel*' is located at the opening and made from wood. It contains small holes approximately 50 mm square all over the opening and the individual unit is attached to the external wall service (Figure 7.3). The *shanasheel* is an important element in traditional architecture not only in Iraq but throughout the Middle East. It has an environmental function both inside and outside the traditional housing unit (Akram, Ismail et al. 2015). It provides privacy and eliminates solar radiation indoors and provides shade for the narrow canyons by casting a shadow on canyon walls and floors. The narrow alleys in traditional urban areas are wider on the first three metres above the ground and become narrower as the shading devices overhang the external walls of the first floor. The buildings are attached together along the alleys and the overhanging shading level (fairly wide), whilst at the same time direct sunlight is eliminated by reducing the SVF (Figure 7.4). Shading devices continue to be used in traditional areas of Erbil even now. The city centre (Erbil citadel) is surrounded by traditional urban morphology, primarily traditional markets (Bazar) (Al-Hashimi and Bandyopadhyay 2015).

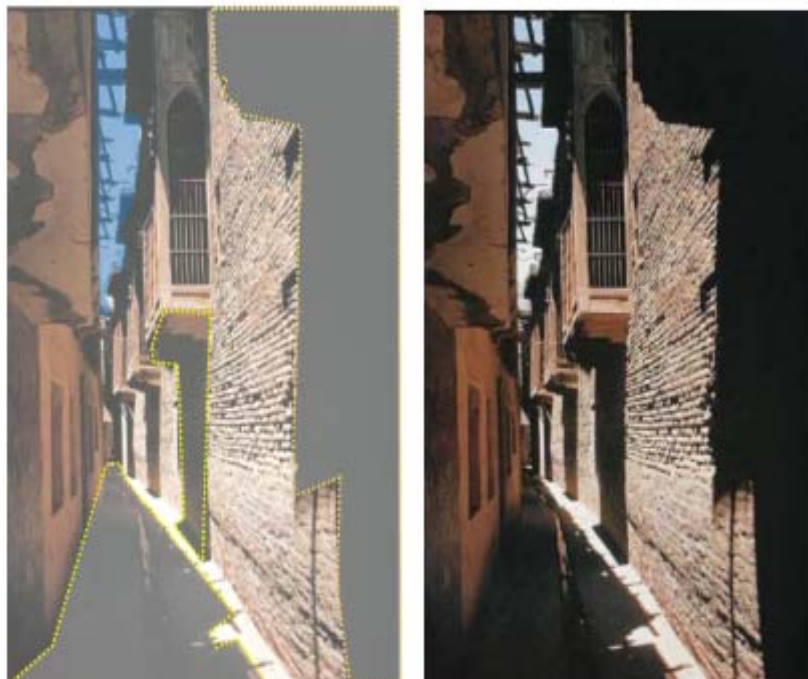


Figure 7.4: Traditional ally showing the shaded area and SVF through employing the *shanasheel*

Most traditional markets (Qaisaria¹) are fully covered by arches and domes to maximise the shading and protect indoor environments from outdoor and solar radiation (Figure 7.5). Several of the modern markets in Erbil also avoid direct solar radiation by using shading textiles or plastic corrugated sheet).

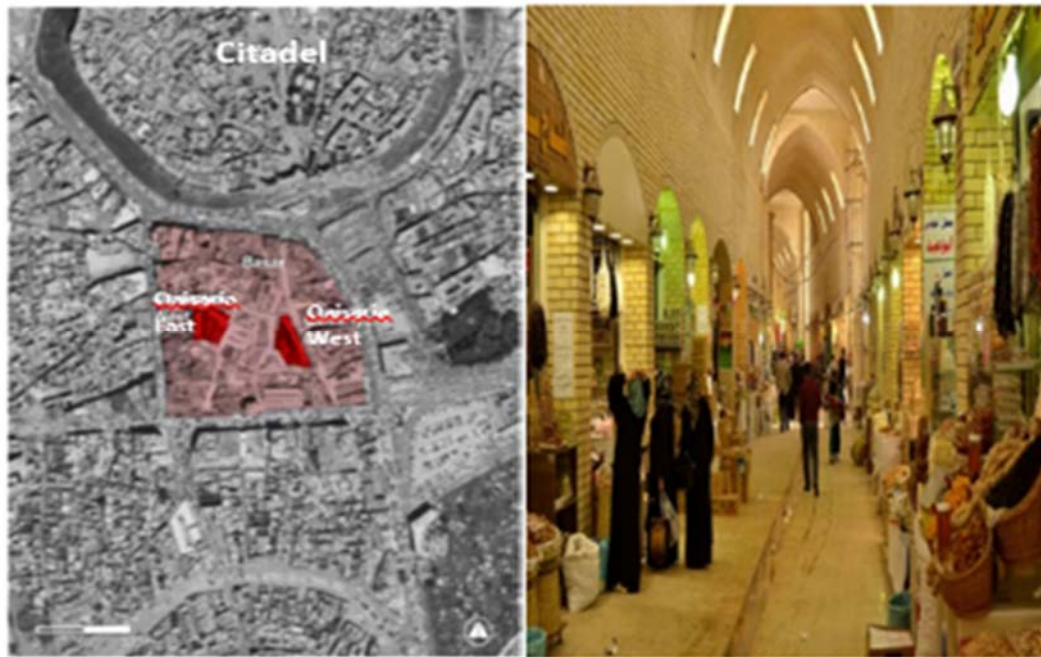


Figure 7.5: Location of a traditional bazar in Erbil and the inside Qaisaria

The casual shade can be movable or fixed and corrugated plastic sheets installed with steel frames are used during summer and winter (Figure 7.5). Textile shading devices are movable and used only in summertime to devices reduce the SVF of the canyons (Mortada 2003). Pedestrians can move easily at ground protect shoppers (Customers) from direct sun radiation.

¹ The Qaisaria (east and west) is a traditional market constructed using traditional masonry and domes that can be seen in some cities in Kurdistan. The construction has two stories (ground and basement) with controlled gates which close at night. The lower floor contains small linear shops that open inwards, while ground shops open outwards. This arrangement plan provides a comfortable environment for lower storeys.

7.3 Modern shading devices

Solar radiation exposure and the degree of that exposure is the main factor for controlling urban microclimate conditions in hot, dry climate regions. Exposure to solar radiation varies from streets to semi-closed and open spaces. Modern shading devices are used to prevent outdoor open spaces from the intensity of solar radiation and provide thermal comfort for pedestrians. In mid-latitude regions, more than any other regions, the occupants of open spaces are suffering from thermal stress because of overheating during summer time (Erell, Pearlmutter et al. 2012). During daytime hours between (10:00 to 17:00), especially, solar radiation (short wave) is

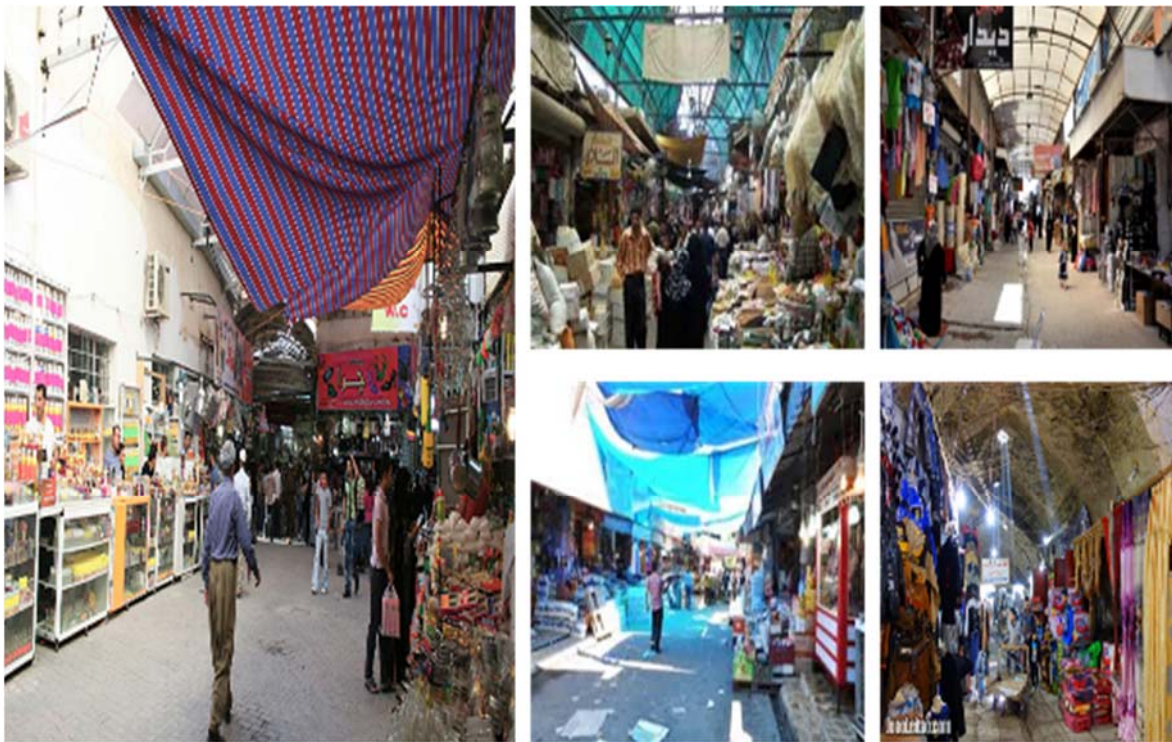


Figure 7.6: Using Shading devices in modern Erbil city markets

severe in city spaces and creates an uncomfortable environment for pedestrians exposed to the sun, and the over-heating of urban surfaces. The body absorbs heat from direct solar radiation or diffuse radiation (reflected radiation) from urban surfaces and buildings (Pearlmutter, Bitan et al. 1999, Mohajerani, Bakaric et al. 2017). The solar radiation which people absorb varies depending on the location of sun in the sky, the geometry of the body and the physical characteristics of surfaces (Oke 2002, Yang and Li 2015).

To eliminate direct solar radiation, shading devices can be employed more than trees to provide shade in hot, dry climates, for the reasons outlined below:

1. There are low water resources in hot climate cities in summertime for irrigation, as there is no rain in summer
2. The shading from trees does not provide sufficient shade for locations in urban areas (Zhao, Sailor et al. 2018)
3. The trees cannot be modified to provide shade or removed in response to weather conditions, for example in wintertime
4. Trees reduce wind speed near buildings (Kang, Kim et al. 2017, Chew and Norford 2019).

Shading devices (shading mesh) have fixed physical properties, such as shading coefficient, shading area geometry, and position. Furthermore, trees can change their shape and opacity over the course of their lifetimes, while shading devices have a fixed shading geometry and



Figure 7.7: Horizontal shading device across the canyon's width providing shade to pedestrians

position over the life of the building. The shading device reduces energy consumption by reducing radiant load on buildings enclosed in hot climates by shading building surfaces (Mirraimi, Mohamed et al. 2016). Additionally, shading devices reduce solar gain and heat flux during day time (Li, Qu et al. 2016). Therefore, less energy is required due to reduced heat gain and the operation of air-conditioning systems can be reduced. The shading devices in urban areas can be divided into two main types upon their installation direction.

a. Horizontal shading devices

Shading devices can be used on residential and commercial buildings for both canyons and open spaces in individual houses (Figure 7.1 and Figure 7.8). Human thermal comfort and radiation absorbed by the body in the centre of a canyon depends on specific factors: the height of point (pedestrian H_b), shading coefficient (SC_{sv}), height (H) and width (W) of street, canyon orientation and solar angles (Erell, Pearlmutter et al. 2012). The shading coefficient (SC_{sv}) is defined as:

Equation 7-1 Shading coefficient in the regular symmetric street canyon

$$SC_{sv} = \frac{[H - \frac{W}{2}(\tan ALT_{bp})]}{H_b}$$

Where $\tan ALT_{bp} = \tan ALT / \cos (AZ - AZ_w)$.

The solar altitude angle is $\partial LT = (90 - \theta_z)$, ∂Z is the solar azimuth angle, and AZ_w the azimuth angle. The measured angle is between the normal line of casting shadow and the north wall. This angle can change 180° over 24 hours.



Figure 7.8: Shading devices for open spaces in individual housing

The second type of horizontal shading device can be seen in open spaces in individual housing units (Kirimtat, Koyunbaba et al. 2016). It covers a limited area outside the house that cannot be shaded by walls or adjacent buildings (Figure 7.8).

b. Vertical shading devices

An atmosphere sustainable sunscreen is an important design feature, used for new and existing buildings (Figure 7.9), as it reduces the impact of solar radiation entering into the building by up to three quarters. Therefore, the energy consumption for cooling will be reduced by reducing the working hours of air conditioning units to achieve comfort levels. The main function of

vertical shading devices is to reduce the direct solar radiation being transmitted through the external openings and windows. It is used primarily outside buildings to limit the entry of solar



Figure 7.9: A systematic facade element which provides the occupants with maximum daylight and minimum solar radiation

radiation in hot summers (Kim, Lim et al. 2012, Gupta and Tiwari 2016).

Additionally, such a sunscreen can be used to articulate the building envelope or cover part of the building using different materials. The negative impact of façade elements is the reduction in daylight, which means that the occupants of a dwelling may not have sufficient lighting. To control the lighting impact of these elements, a series of perforated elements have a textural feature to allow daylight beyond the external envelope of the building (Figure 7.9).

Architects use these shading devices to improve buildings with sustainable features that reduce energy consumption (Cimmino, Miranda et al. 2017). The shading devices can be modified by changing their profile, colour, and the covering part of the façade (Figure 7.10). A number of studies have been carried out in a hot, dry climate to improve daylight and reduce the impact of solar radiation by analysing the porosity of an element's 'perforations'. The researchers found that south facing façades should be treated differently to achieve positive results (saving energy consumption). Sherif (2012) established that adding screens to south and west facing façades in a desert climate can reduce energy consumption by 30%. Omidfar (2015) assessed

the performance of complex geometry solar screens to optimise indoor daylight and energy consumption. The results exhibited an annual reduction in the energy consumption of 30% and 40% for both south and west façades.

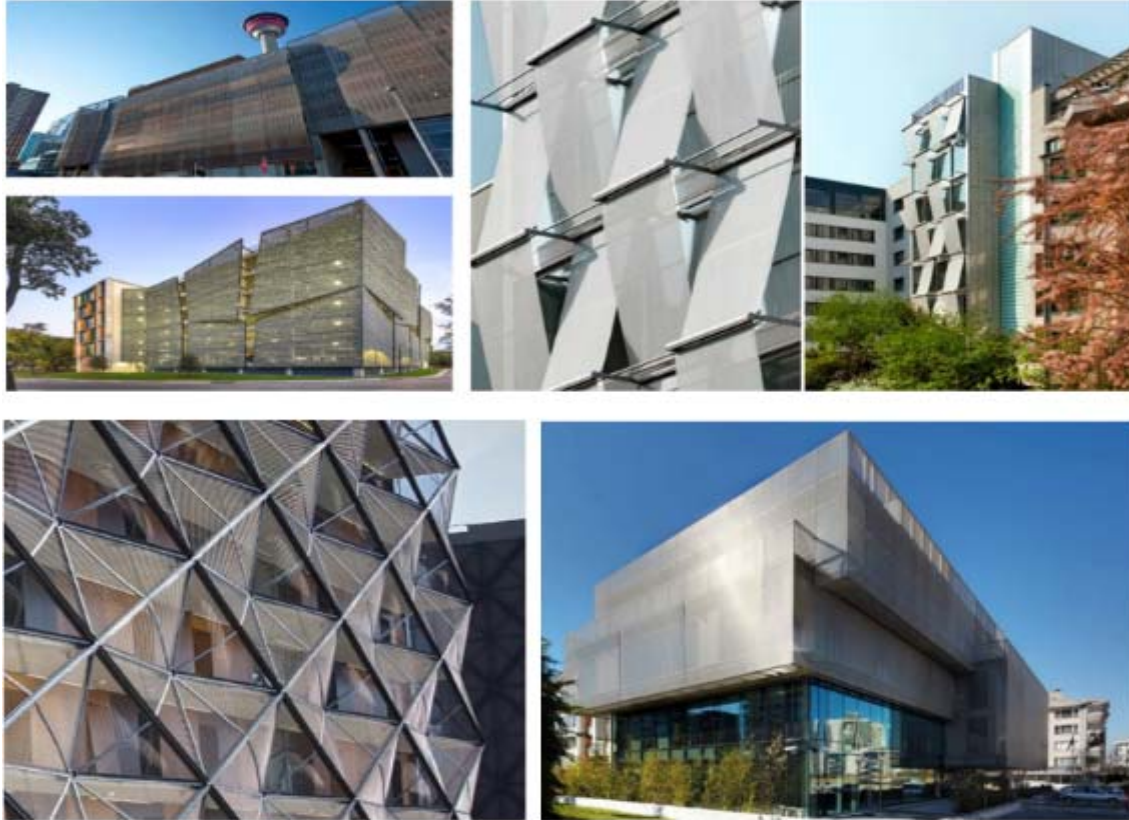


Figure 7.10: Vertical shading devices.

Researchers used Genetic Algorithms² (GA) to simulate solar screen and assess the performance of daylight and energy consumption (Omidfar, Torghabehi et al. 2014). Positive results were obtained from the study undertaken by Calsas (2002), which employed GA to optimise the size and placement of external window to measure daylight and thermal energy.

² 'Genetic Algorithms (GA) are a powerful method in the process of finding optimised solutions for a large number of problems, and have been widely studied in the field of the built environment. They mimic the process of natural selection, where the most powerful individuals are expected to prevail in a highly competitive environment, and a fitness value is utilised in order to assess how good these individuals are.'

This method can also provide a preferred solution for designers to select. González and Fiorito (2015) discovered that energy consumption and daylight can be improved by enhancing shading devices for northern façades by utilising GA to minimise direct solar radiation without affecting natural light levels. Moreover, Karamata and Andersen (2014) developed a vertical shading device based on the Mashrabiya design to adapt to hot, dry climates. The aim of the study was to develop a new system which can eliminate or block direct solar gain and transform it into diffuse light. They used GA as the method to optimise solar radiation and daylight through different shading devices. Positive results were obtained.

The main feature of organic urban morphology in a hot, dry climate region regarding modern shading devices is to employ a shading strategy to minimise direct solar radiation and improve natural lighting (daylight). Therefore, this study takes the benefits from both sides concerning historical and modern shading concepts and applies it to the modern urban areas to generate a new concept for shading a strategy that might be adapted for existing and new housing developments in Erbil.

The aim of the current chapter is to model a horizontal shading mesh using ENVI-met and apply it over open spaces and canyons to manipulate the urban microclimate, but still allow enough daylight to pass through (sufficient allowance of daylight). This will reduce direct solar radiation in order to reduce MRT, and thus improve the thermal comfort of occupants by reducing PET³, which leads to reduced energy consumption by buildings. Air temperature, wind speed and Mean Radiant Temperature will be simulated for both shaded and unshaded open spaces.

In the literature, there are limited studies which quantitatively measure the impact of shading mesh (Shashua-Bar, Pearlmutter et al. 2009). These studies used genuine shading mesh to measure the physical properties of mesh such as transparency, absorption and reflection. In the last decade, shading mesh has been used primarily for agricultural crops and to cover greenhouses (Castellano, SCARASCIA et al. 2008). In addition, this type of shading is limited

³ Physiological Equivalent Temperature

for use in urban areas and open space in cities in a hot, dry climate, although its impact on urban microclimates has not been widely studied with relation to other building environmental strategies. There are a few studies which have investigated the impact of shading mesh on ambient air temperature and surface temperature (Pearlmutter and Rosenfeld 2008, Shashua-Bar, Pearlmutter et al. 2009).

In addition, shading mesh is useful to adopt and apply for shading in cities in a hot, dry climate because it allows sufficient daylight to pass through during the daytime and allows wind to easily penetrate, which is important for night ventilation and removing urban pollution. Based on the extensive studies and literature pertaining to hot, dry climates, it was seen that a reduction in SVF is the one of the most effective ways to improve an urban microclimate. This can be undertaken by way of increasing building heights or narrowing canyons (Bakarman and Chang 2015). These studies found that low SVF in typical urban settings increases comfortable conditions for occupants through sufficient protection from direct solar radiation (Ali-Toudert and Mayer 2007). In this study, a horizontal shading mesh will be used to reduce the SVF by covering the open spaces and protect urban areas from direct solar.

As shown in Chapters 2 and 5, ENVI-met is an effective research tool in relation to studying urban microclimates, and therefore this study used ENVI-met to model shading mesh and measure its impact on an urban microclimate.

7.4 Model of shading mesh

ENVI-met version 4.0 consists of a new modelling technique to simulate building features. This includes design features which are not connected with the main building form, introduced as a ‘single wall feature’.

These single walls are building elements that are not an integral part of a building, i.e. they are not part of the closed surface of the building. Single walls can be described as features that recreate (simulate) building obstacles, such as small external walls, awnings or any structures that do not fill a whole grid cell more accurately (Figure 7.11).

Single walls have various physical properties like normal walls. For example, they are solid obstacles for wind speed and turbulence.

Conversely, these walls are not used for thermal calculations as normal enclosure walls are. The main differences between the single walls and normal walls are that single walls can be horizontally modelled with limited thickness (thin) and are poorly insulated, they have a low heat transfer coefficient, and the air temperature homogenously distributes through them. The thermal balance equation for single walls is calculated as follows:

$$Q_{sw,net}^{abs} + Q_{lw,net}^{abs} \sigma T_{4w}^* + (4 + 4v_1)(T_{air,1} - T_w^*) + (4 + 4v_2)(T_{air,2} - T_w^*) \\ = \frac{c_{wall} \rho_w \Delta x}{\Delta t} (T_w^* - T_w).$$

T_w^* is the temperature of the single wall at the next time step, v_1 , v_2 , $T_{air,1}$ and $T_{air,2}$ the wind speed and air temperature at the grid cells separated by the single wall. This equation can be converted to:

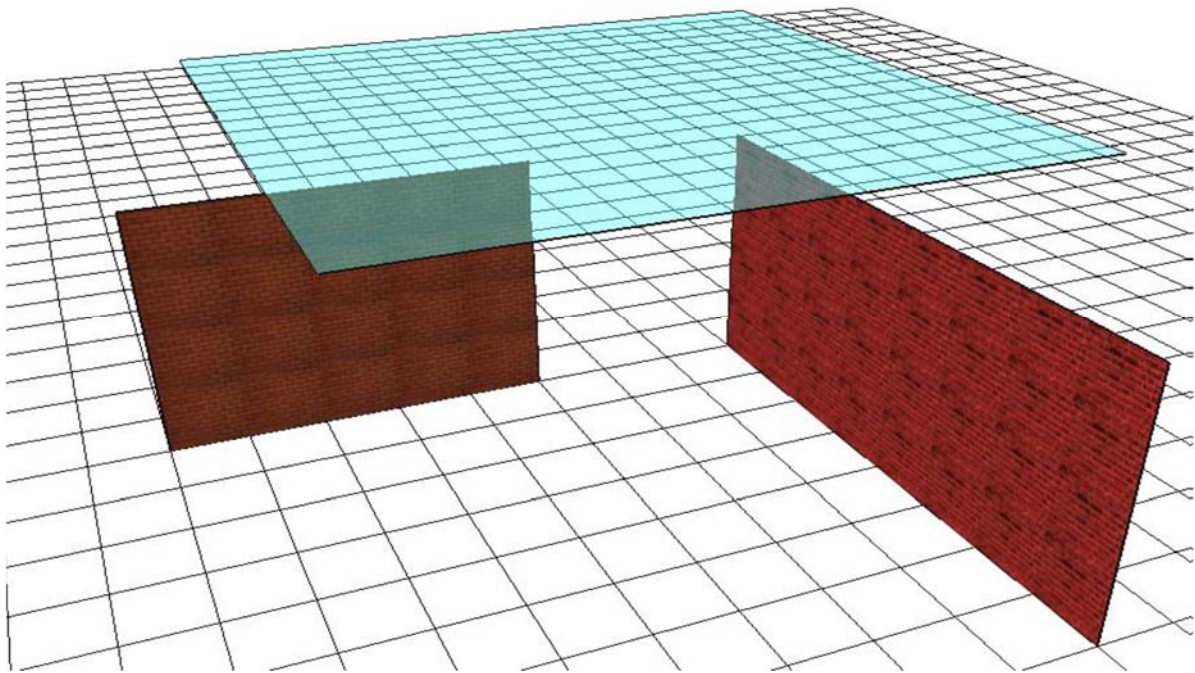


Figure 7.11. ENVI-met model showing single walls features

$$2\epsilon\sigma T_w^* + T_w^*((4 + 4v_1) + (4 + 4v_2) + \frac{c_{wall} \rho_w \Delta x}{\Delta t} T_w - (Q_{sw,net}^{abs} + Q_{lw,net}^{abs} + \frac{c_{wall} \rho_w \Delta x}{\Delta t} T_w + (4 + 4v_1) T_{air1} + (4 + 4v_2) T_{air2})) = 0$$

The convective heat transfer coefficient (W/m²K) for either side of the single wall/roof is calculated according to the German Din 6946 (DIN 2008) = 4+4v, where v is the wind speed in m/s adjacent to the surfaces of the single wall/roof.

In this study, ENVI-met single wall features have been used for modelling shading mesh. The difficulty with shading mesh modelling is that it has specific thermal properties that cannot be easily simulated. Shading mesh is thin, less than one millimetre, and horizontally laid out, as shown in Figure 7.11. Single walls and shading mesh have some corresponding physical properties, highlighted below;

1. Radiation can pass through
2. They are thin with low thermal mass (low heat transfer coefficient).
3. They are not thermally integrated with the main model surfaces.

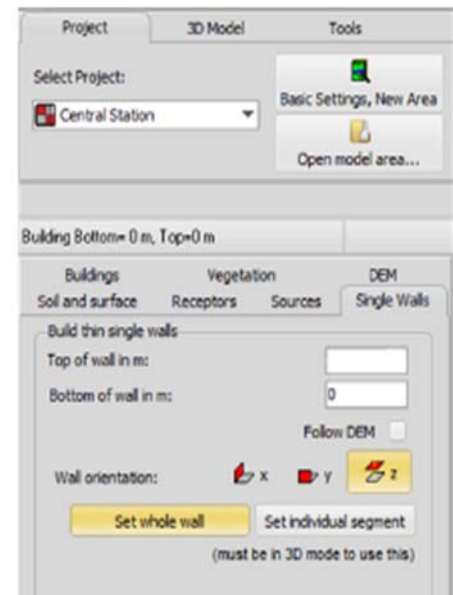


Figure 7.12. View of ENVI-met interface showing single walls variables

The shading mesh can be simulated using the ENVI-met model by way of the steps presented below:

1. Using single walls to form the shading mesh.

The model starts by activating 3D tools in the ENVI-met interface view and selecting 'set whole wall'. The single wall is applied on the Z axis with adjustable heights (Figure 7.12). The option of using the Z axis to create single walls is an appropriate way to achieve similar physical properties to shading mesh.

2. Creating materials which have similar physical properties to shading mesh.

ENVI-met.4 has the capability to change building materials to user preferences. New material properties have been added to the ENVI-met database to simulate shading mesh with specific thermal properties. These include: absorption, transmission, reflection, density, and thickness of materials (Figure 7.13).

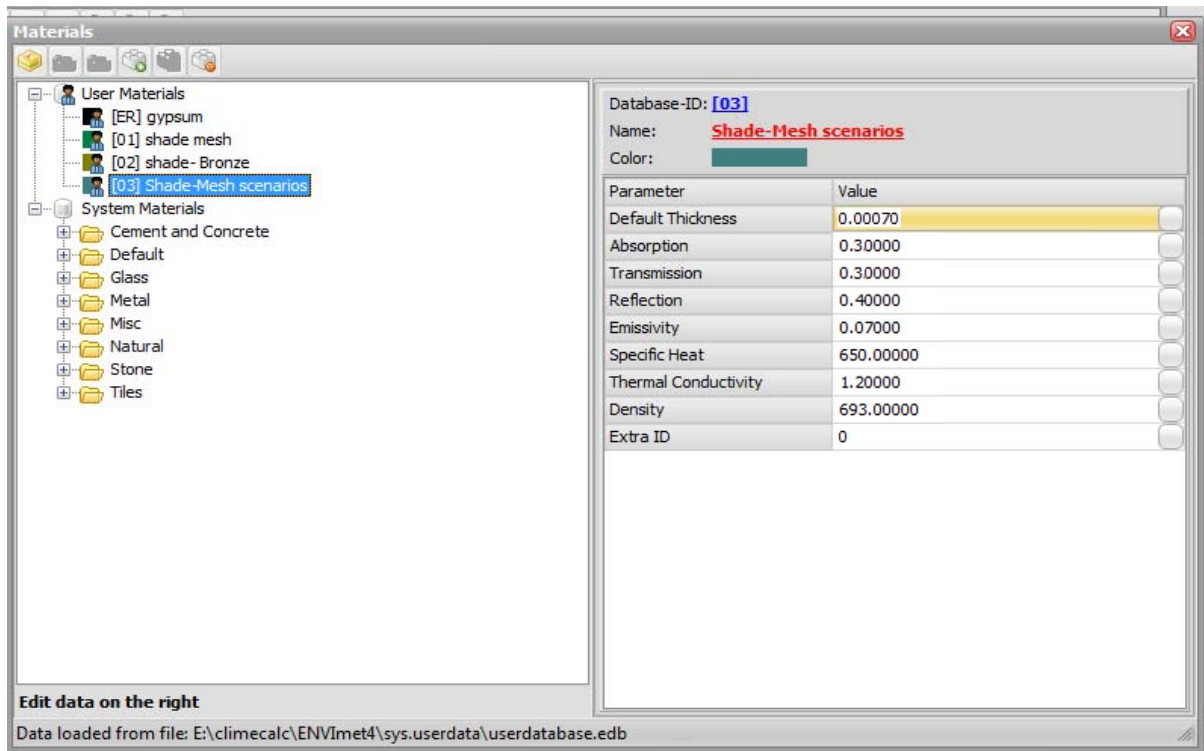


Figure 7.13 Adding new materials to the ENVI-met model database

For the first set of modelled shading meshes, the study used values as physical properties. These are shown below:

- a) Absorption 30%
- b) Transmission 30%
- c) Reflectance 40%
- d) Emissivity 0.07 W/m²
- e) Density 963 kg/ m³
- f) Thickness 0.7 mm

3. Apply new materials to these horizontal single walls.

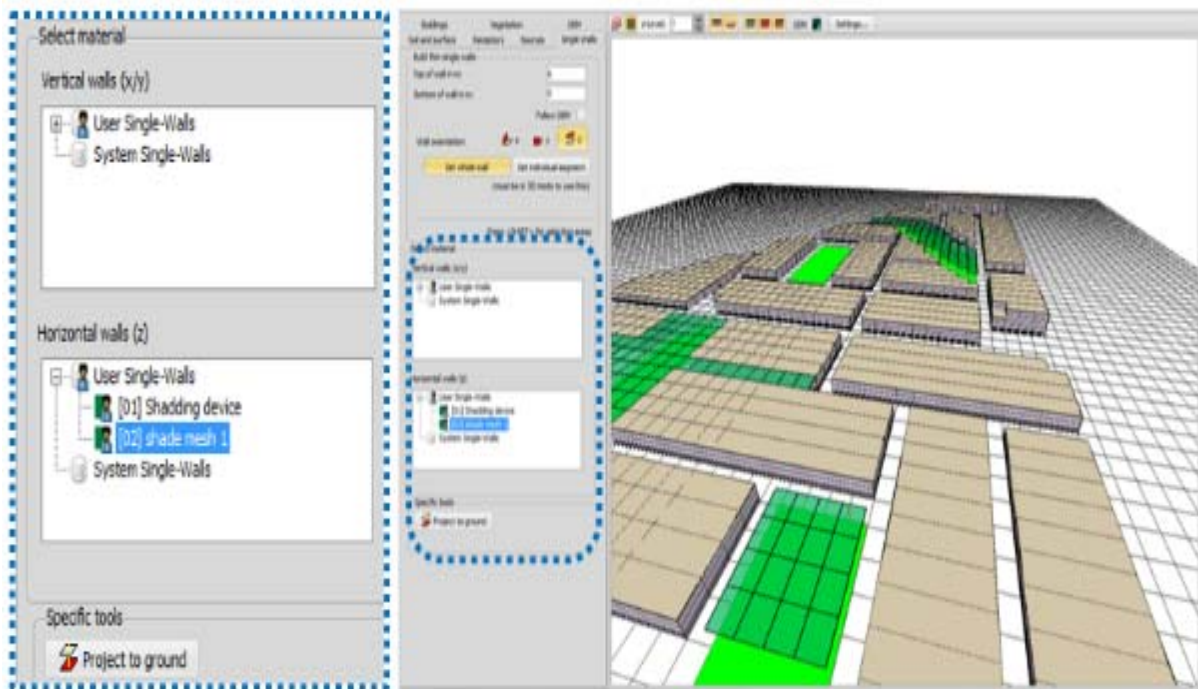


Figure 7.15 Horizontal single walls model and selected materials

The new materials must be saved in the ENVI-met database prior to being assigned as a material. They will have physical properties corresponding to the real shading mesh (Figure 7.13). Figure 7.15 illustrates horizontal single walls over open spaces and over a canyon in Zone⁴ 2, which can transmit radiation and light. The shading mesh in this model will interact with solar longwave and shortwave, radiation fluxes, reflection, and re-radiation of thermal energy during day and night-time. In this study, the shading mesh transmission is set to 50% to allow natural lighting to enter open spaces during daytime.



Figure 7.14: Shows shading mesh over certain parts of the site plan and sample position of the three zones: Zone 1, Zone 2 and Zone 3.

⁴ In chapter 5, Zone 1 is modelled. Split into 3 new zones, now labelled Zone 1, 2 and 3.

7.5 Adding Shading Mesh

In this section of the study, the ENVI-met simulation is used to represent the shade mesh which will be presented. The site plan is divided into three zones, numbered 1, 2 and 3. Zone 1 represents an open green space with a larger area, surrounded by residential blocks compared to other open spaces. Zone 2 includes sample points for both canyons and open green areas, while Zone 3 is half shaded by the shading mesh and half unshaded, is open (Figure 7.14). In the last chapter, it was concluded that adding trees has a significant impact on Mean Radiant Temperature (MRT). In this chapter, shading mesh is employed as an alternative to trees, to cover both open green spaces and canyons. Shading mesh is considered economic as well as easy to construct and maintain. In addition, trees cannot easily be used as a long-term strategy in cities in a hot, dry climate due to the limited water resources. The purpose of this simulation is to investigate the impact of shading mesh on an urban microclimate of canyons and open green spaces. Six sample positions are taken for each scenario, at a height of 1.8 metres. The locations of the samples are shown in Figure 7.14. The simulations proposed three different scenarios, as highlighted below:

1. Modify (Optimise) the height of the shading
2. The impact of shading and no shading on canyons and open spaces, with reference to MRT and PET.

The simulations used input data to create the configuration file used during the running of the program (Table 7-2). The weather data are taken from an urban area with relatively low wind speed 0.55 m/s and hourly air temperature and relative humidity, as presented in Table 7-1.

Table 7-1: Air temperature and relative humidity used for simulation input data

Time	00:00	01:00	02:00	03:00	04:00	05:00	06:00	07:00	08:00	09:00	10:00	11:00	12:00	13:00	14:00	15:00	16:00	17:00	18:00	19:00	20:00	21:00	22:00	23:00
RH %	17.05	30.02	21.32	23.21	25.67	27.03	26.56	22.76	24.66	20.56	16.05	13.15	12.26	11.1	9.22	8.60	7.95	9.76	8.50	8.54	8.78	10.56	11.70	13.26
T (C)	30.02	28.75	27.96	27.63	26.99	26.30	28.76	29.07	31.20	34.20	34.20	35.81	36.59	37.96	39.06	39.64	40.15	40.05	39.27	38.06	37.08	35.60	34.60	32.87

For each scenario wind speed, air temperature and Mean Radiant Temperature were measured at a height of 1.8 metres for 24 hours.

Table 7-2: Shows ENVI-met input data to generate the simulation configuration file

Parameter	Units	Values
Initial air temperature	C°	33.62
Wind speed	m/s	0.55
Wind direction	0 from the north and 180 from the south	225°
Relative humidity at a 2m height	%	15.4
Specific humidity at top of model	2000m g/kg	4
Maximum air temperature at 15:00	C°	40.15
Minimum air temperature at 05:00	C°	26.27
Soil temperature at a depth of	(K)	
1. 00 to 5 cm		311.23
2. 20 to 50 cm		306.07
3. 50 to 200 cm		300.77
4. Below 200 cm		298.81
Building fabric used in ENVI-met model		
Urban blocks		
Materials	Reflectivity	Emissivity
Walls layers (From inside to outside)		
1. Gypsum (2 cm)		
2. Hollow concrete blocks (20 cm)	0.73	0.9
3. Cement rendering (2 cm)	0.35	0.9
Roofs layers (from top to bottom)		
1. Concrete tiles (10 cm)	0.5	0.9
2. Fine soil (10 to 15 cm)	0.53	0.89
3. Reinforcement concrete (20 cm)	0.8	0.91
Pavements types		
1. Road Asphalt	0.19	0.9
2. Concentrate pavement	0.29	0.9
3. Green areas (grass)	0.26	0.9
Shading mesh		
Shade mesh	0.4	0.07
Building Properties		
Parameter	Units	Values
Inside Temperature	K	297
Heat Transmission Walls	W/m²K	0.74
Heat Transmission Roofs	W/m²K	0.67
Albedo Walls		0.3
Albedo Roofs		0.15

7.5.1 Modify (Optimise) the height of the shading mesh from 6, 7, 8, 9, 10, 11 and 12m

In this scenario, six different heights for the shading mesh were simulated to investigate the thermal impact of shading mesh (Figure 7.16) and its height on the local urban microclimate beneath it (Figure 7.17).



Figure 7.16 Sample position of the first simulation set

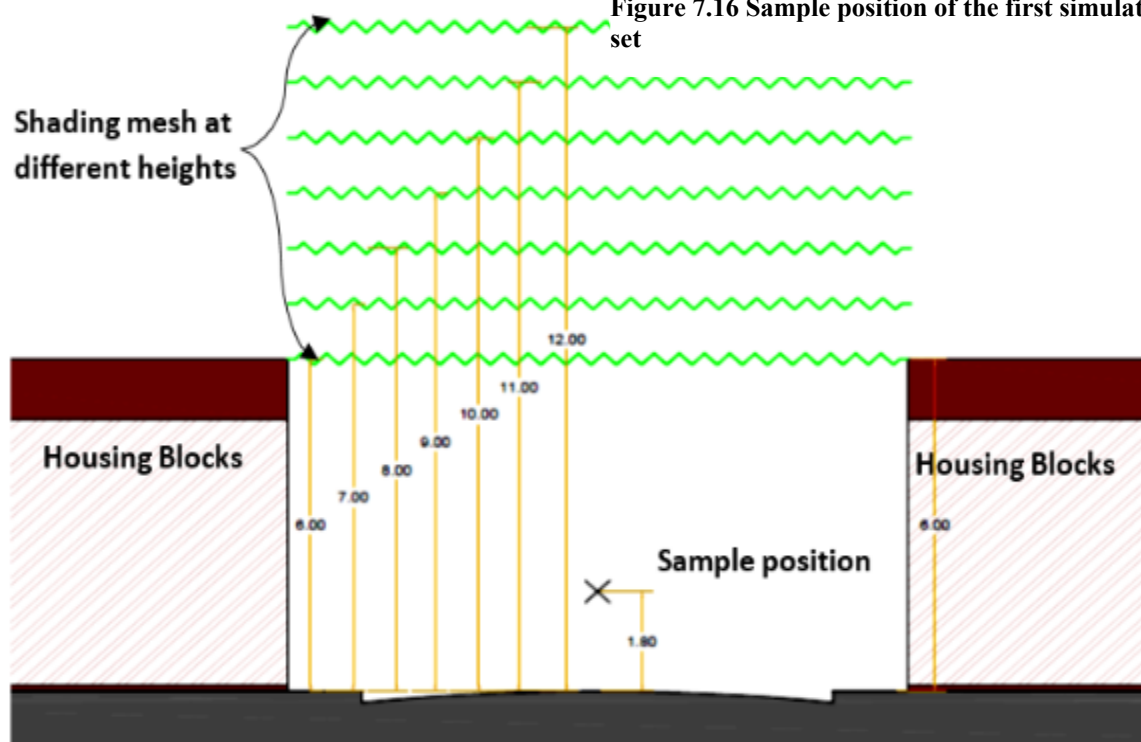


Figure 7.17: Shading mesh at different heights 6-12 metres from ground level

Figure 7.18 shows the air temperature for the six sample positions at six different heights starting from 6–12 m. The air temperature is measured in the centre of two canyons and four open spaces, as shown in Figure 7.16. This simulation aimed to investigate the impact of shading mesh height on air temperature for both canyons and open spaces. The maximum air temperature was 39.12 °C and the minimum was 29.49 °C (Figure 7.18). The results show that air temperature record higher values in canyons during daytime and lower values during night-time compared to open spaces. At 15:00, the sample position before the open space in Zone 2 recorded the maximum air temperature and at 03:00 the same position recorded the minimum air temperature (29.5 °C). In contrast, air temperature in open spaces covered by shading mesh in Zone 3 recorded the lowest air temperature during night-time (29.49 °C) and a relatively high temperature during the daytime (38.63 °C), compared to the canyon sample. Overall, changing the height of the shading mesh had limited impact on canyon and opens spaces air temperature. The air temperature recorded lower values during night-time.

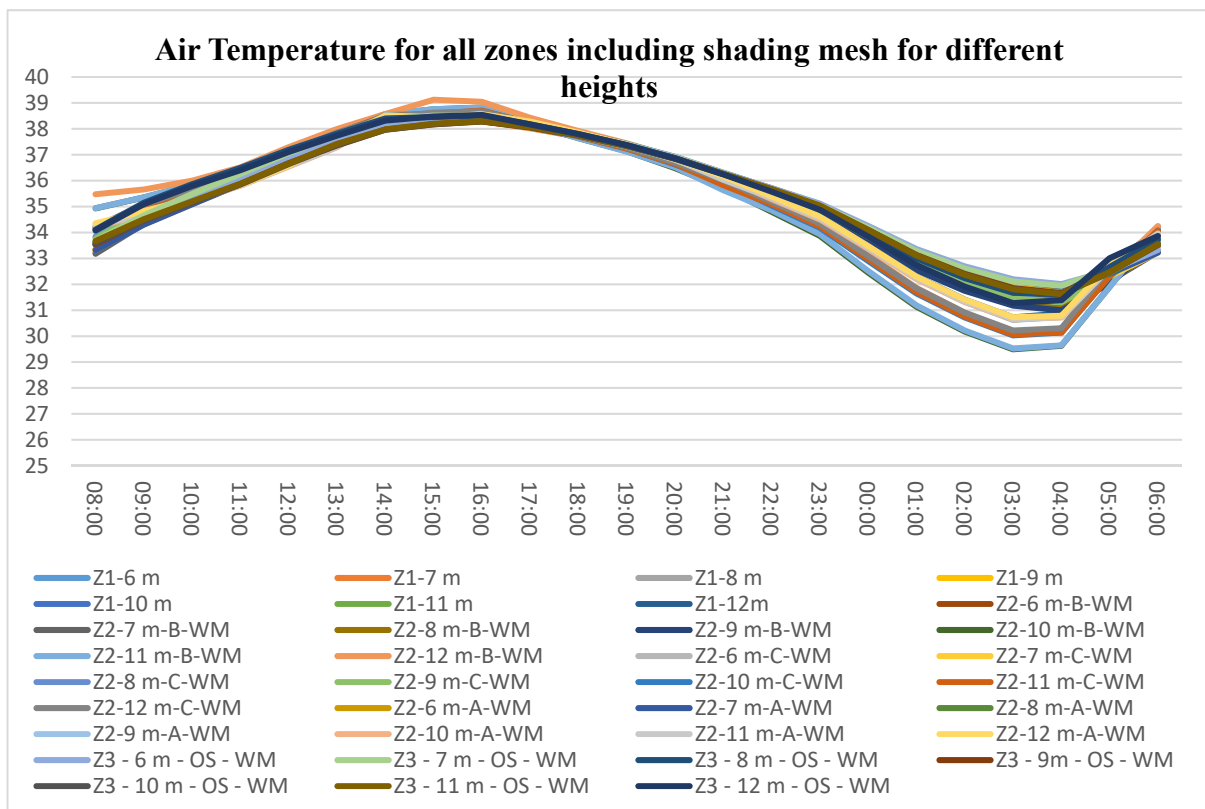


Figure 7.18: Air Temperature for all zones at different heights (6–12 m)

These differences in air temperature may be related to differences in wind speed in different spaces more than the impact of the shading mesh. Wind speed was measured at a height of 1.8 metres for seven scenarios with different shading mesh heights. The results showed that the wind speed in canyons recorded higher values in contrast to open spaces. Zone 2 – 12m maximum wind speed recorded was 0.48 m/s and minimum wind speed was 0.28 m/s for the central open space in Zone 2 – 6m.

The wind speed is significantly influenced by changing shading mesh heights (Figure 7.20) The maximum wind speed was with the shading mesh at a height of 11–12 metres compared to minimum values with shading mesh at heights of 6 and 7 metres.

The wind speed can be categorised by the heights of the shading mesh, when the shading mesh is at 6 and 7 metres, the wind speed is similar – 8 and 9 metres are higher than the first group and lower than heights of 10 and 11 metres. Therefore, shading mesh at a height of 12 metres records the maximum values (Figure 7.20)

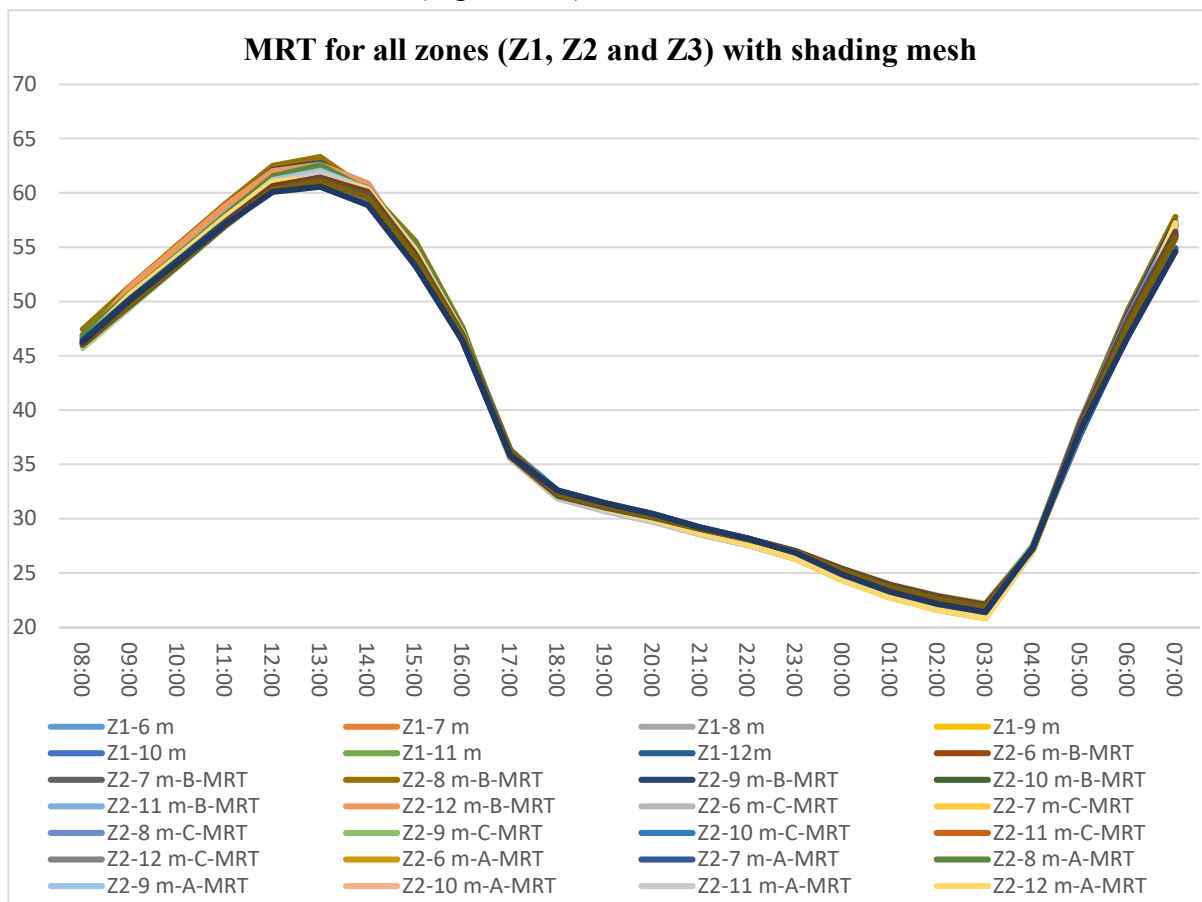


Figure 7.19: Mean Radiant Temperature for all zones at different heights 6–12 metres

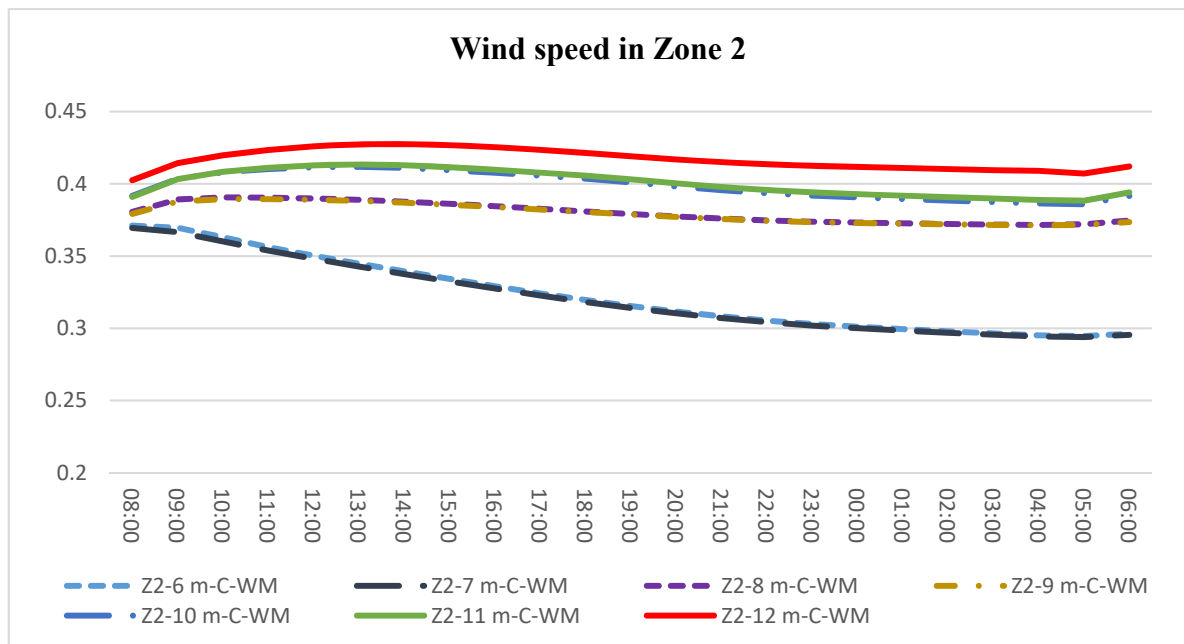


Figure 7.20 Wind speed for all zones at different heights 6–12 metres

MRT values when covered by shading mesh at different heights. These simulation sets show that changing the shading mesh height (6–12 metres) has a limited impact on air temperature and MRT, while wind speed is significantly influenced by increasing the shading mesh height (Figure 7.20). Even though the shading mesh reduced wind speed, this reduction is considered to have a limited influence on the overall urban microclimate of open areas because the maximum wind speed was 0.55 m/s, and any change of wind speed cannot individually have an impact on urban microclimate. This means that the shading mesh can be installed at any height between 6–12 m without having a significant impact on air temperature (T°) and Mean Radiant Temperature (MRT). However, other factors should be taken into consideration, such as the porosity of the shading mesh to allow dust and natural lighting (sufficient daylight) to pass through the shading mesh which covers any spaces beneath.

7.5.2 Shading mesh transparency at 30% and 50%, with shading mesh at two heights (6 and 8 m)

This section investigates the impact of increasing the transparency of shading mesh on air temperature (T), wind speed (WS) and Mean Radiant Temperature (MRT). Two different shading mesh transparencies were selected: 30% and 50% (Figure 7.22). T, WS and MRT were measured for only one position (A) in Zone 1, with two different shading mesh heights (6 and 8 metres) (Figure 7.21).

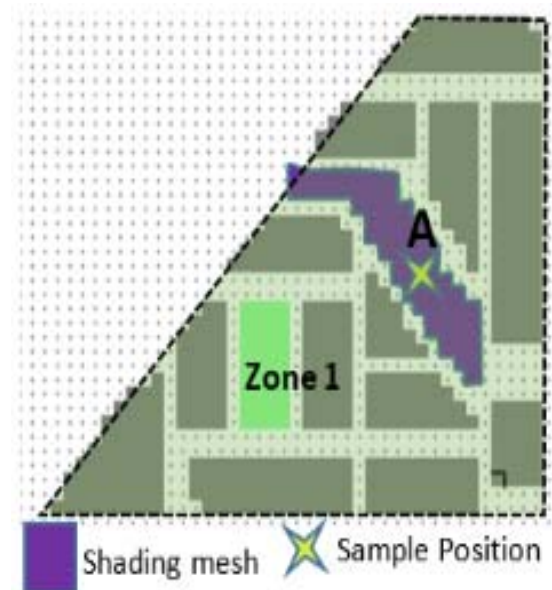


Figure 7.21: Sample position in Zone 1

Figure 7.24 shows the air temperature for both shading mesh scenarios (30% and 50%). The simulation results show that air temperature is similar for both scenarios at different heights during daytime and air temperature records lower values for the sample with 30% transparency at a height of 8 metres (Figure 7.24). The maximum T is almost similar for all samples at 15:00 and 16:00, while the difference in air temperature (ΔT °C) is 0.93 °C, less than 1 °C.

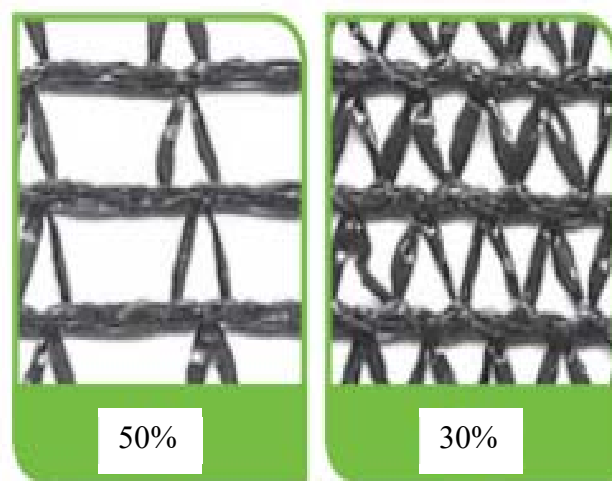


Figure 7.22: Shading mesh transparencies of 30% and 50%

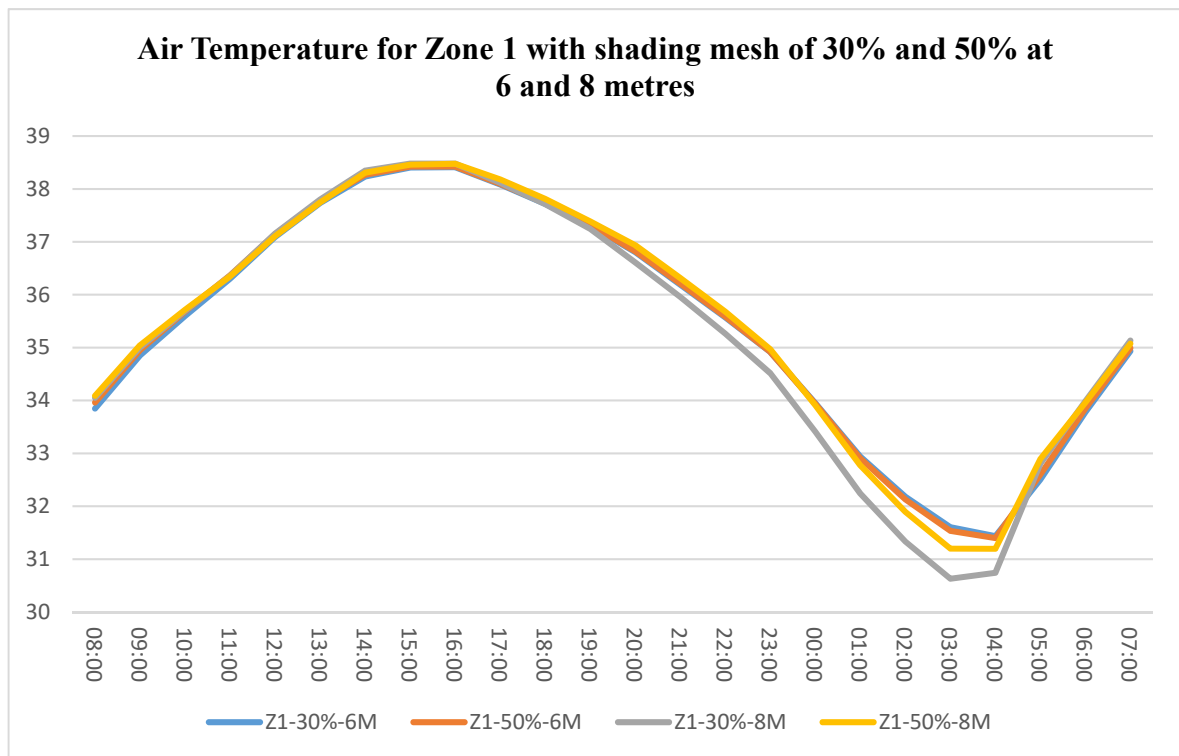


Figure 7.23 Air temperature for Zone 1 with different shading mesh transparencies (30% and 50%) at heights of 6 and 8 metres

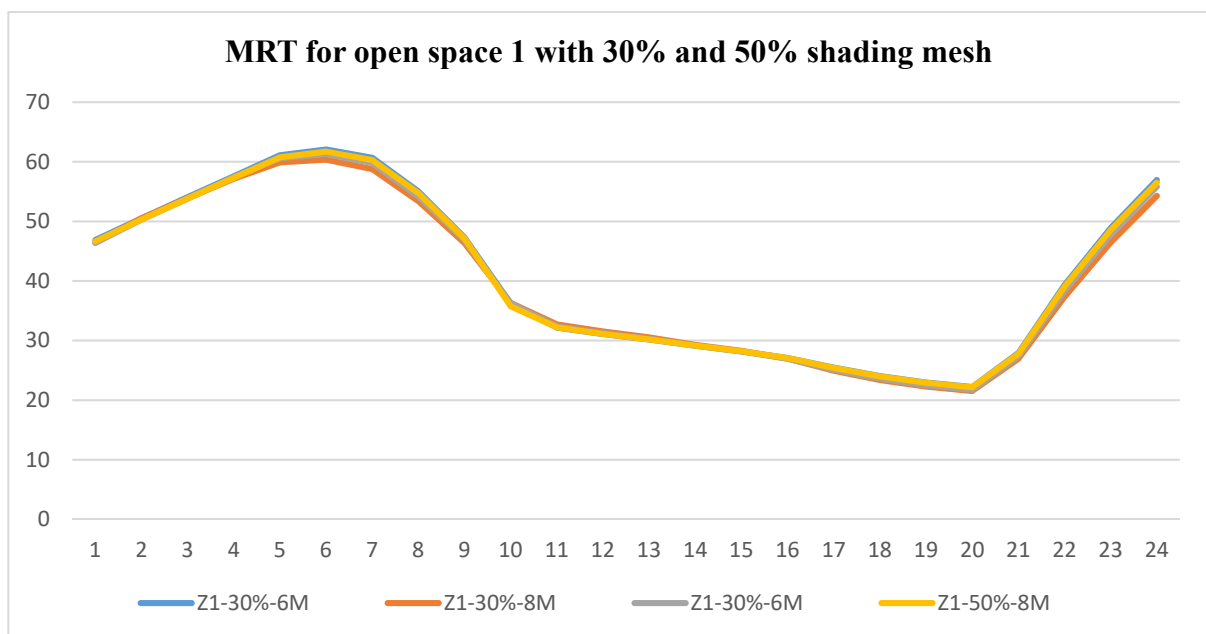


Figure 7.24: Mean Radiant Temperature for Zone 1 with different shading mesh transparencies (30% and 50%) at heights of 6 and 8 metres

Figure 7.26 shows the WS at Zone 1 for both shading mesh 30% and 50% transparency at heights of 6 and 8 metres. The results show that increasing the shading transparency increases the wind speed for Zone 1. The maximum WS was 0.5 m/s recorded for the sample with 50% shading mesh transparency at a height of 8 metres, whereas the minimum WS was 0.44 m/s for the sample with 30% shading

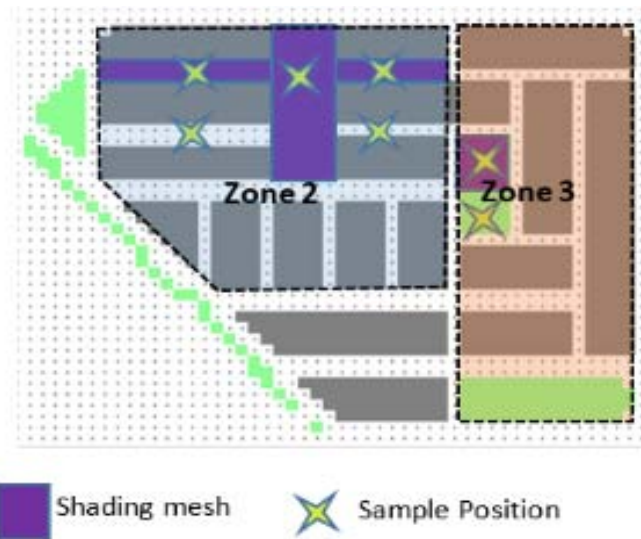


Figure 7.25: Sample positions for canyons and open spaces with and without shading mesh in two zones, Zones 2 and 3

transparency at a height of 6 metres (Figure 7.26). The results confirm that the performance of the shading mesh with 50% transparency is better with 30% transparency over open spaces.

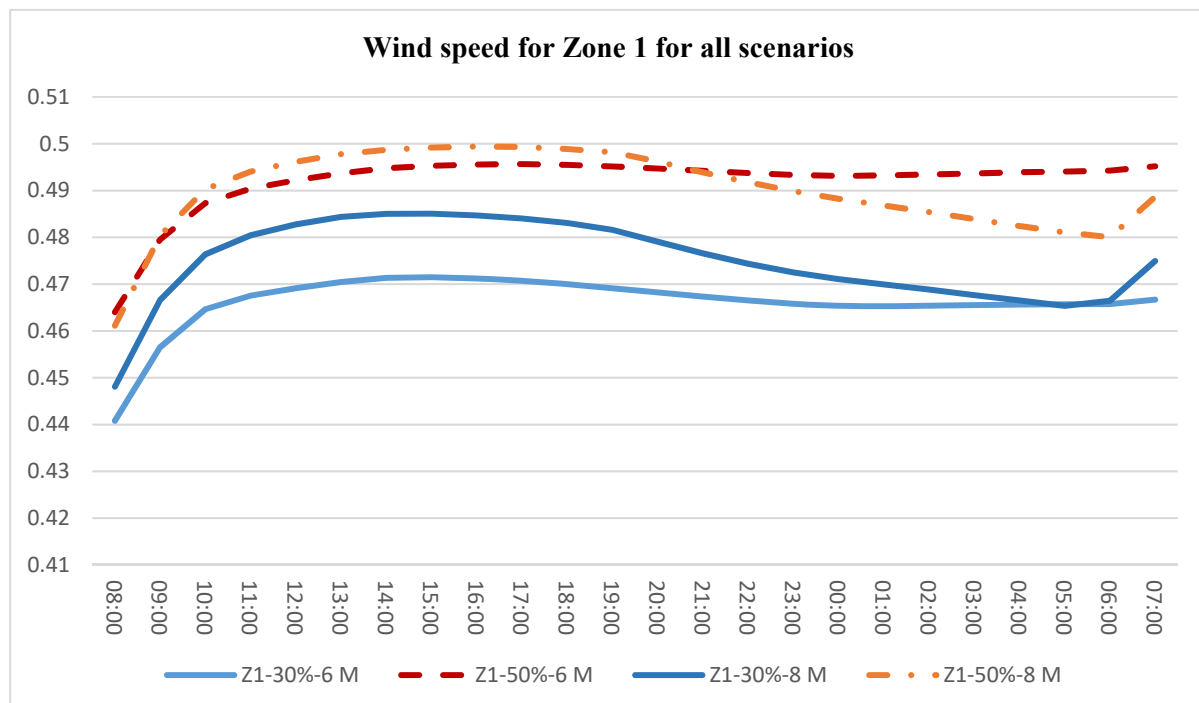


Figure 7.26 Wind speed for Zone 1 with different shading mesh transparencies (30% and 50%) at heights of 6 and 8 metres

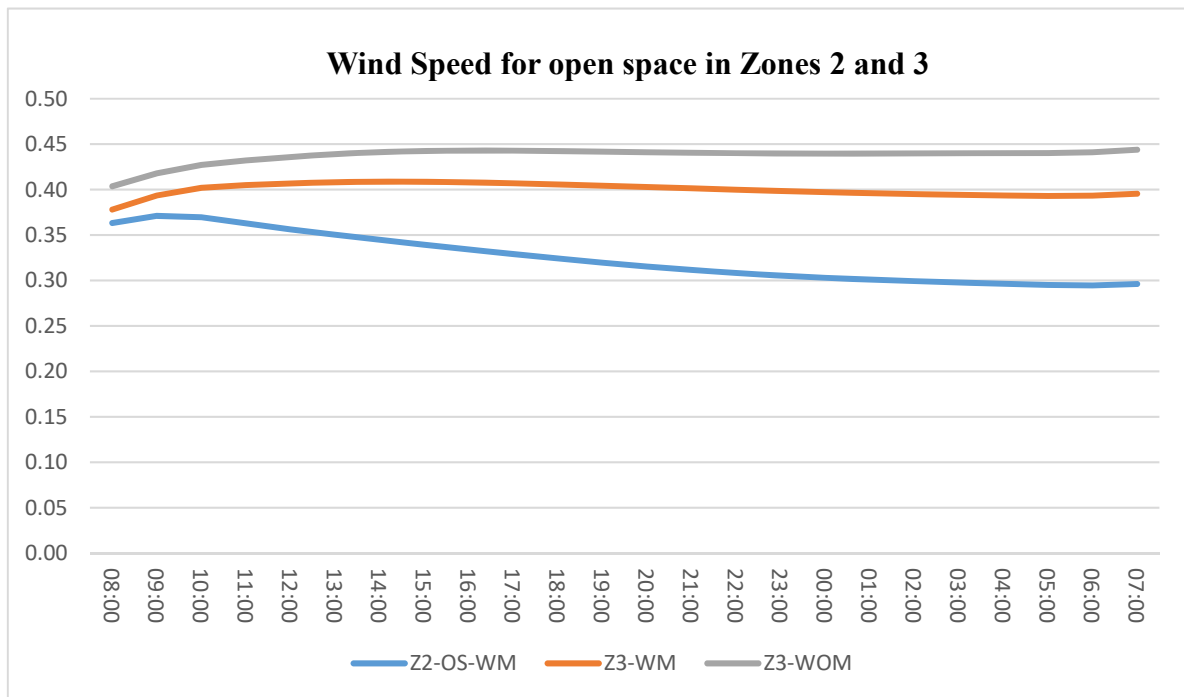


Figure 7.27: Wind speed for open space in Zones 2 and 3 with and without shading mesh

Figure 7.23 shows that changing the shading transparency of both heights had no impact on MRT for both scenarios. The overall simulation results demonstrate that shading mesh

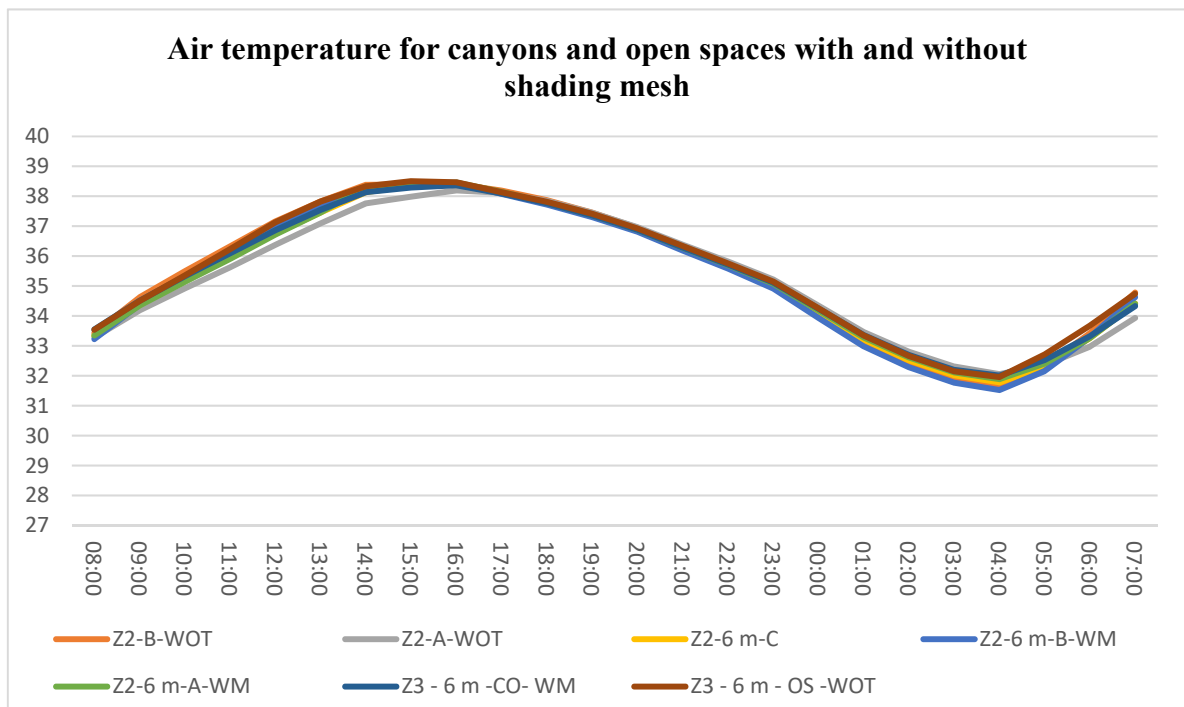


Figure 7.28: Air temperature for canyon and open spaces in Zones 2 and 3 with and without shading mesh

transparency (30% and 50%) has a limited impact on T, WS and MRT. However, the WS reveals differences between the values for different scenarios, although this is because of the height of the mesh and not the transparency (Figure 7.26).

7.5.3 Mean Radian Temperature (MRT) and Physiological Equivalent Temperature (PET)

7.5.2.1 Shading mesh impact on urban spaces

In this set of simulations, the MRT is measured in both canyons and open spaces (Figure 7.25). To reduce solar gain, shading mesh was explored to reduce the Mean Radiant Temperature. MRT is measured in seven sample positions for urban areas in Zones 2 and 3 (Figure 7.25). The shading mesh in this section covered open spaces and east-west canyons. The aim of the simulation is to investigate the impact of shading mesh on MRT in canyons and open spaces. Similar to previous simulation sets, Air temperature (T), Wind Speed (WS) and Mean Radiant Temperature were measured (MRT). There are slight changes in T for the canyon after the open space in Zone 2, but this is less than 1 °C (Figure 7.27). The results show that the air temperature is not significantly impacted by adding shading mesh for both canyons and open spaces with and without shading mesh.

Figure 7.28 illustrates wind speed for open spaces in Zones 1 and 2 with and without shading mesh. The results show that adding shading mesh on the top of open spaces reduces wind speed. The maximum WS was recorded for open spaces without shading mesh in Zone 3, while minimum WS was recorded for open spaces with shading mesh at Zone 2 (Figure 7.28). Figure 7.29 shows that MRT can be reduced by adding shading mesh to any canyons and open spaces. The maximum MRT was recorded for samples without shading mesh, while the minimum MRT was recorded for samples with shading mesh for both canyons and open spaces. The maximum and minimum MRT was 82.11 °C and 20.1 °C recorded for open spaces without shading mesh during day and night-time.

The results⁵ show that during daytime the shading mesh has a significant impact on MRT reduction (Figure 7.29). MRT for open space and canyons at 14:00 recorded the maximum impact compared to open spaces and canyons which were not covered by shading mesh. The sample position in the canyon before the open space in Zone 2 was recorded at 84.62 °C at 14:00 in contrast to 60.25 °C when covered by shading mesh. A few canyon samples without shading mesh recorded values similar to canyons with shading mesh between 14:00 and 15:00. This occurs because the angle of sun is reduced and canyon shading covers the sample position, which means lower MRT were recorded, even in the canyon not covered by shading mesh (Figure 7.29). During night-time, both canyons and open spaces with and without shading mesh recorded almost similar values (Figure 7.29).

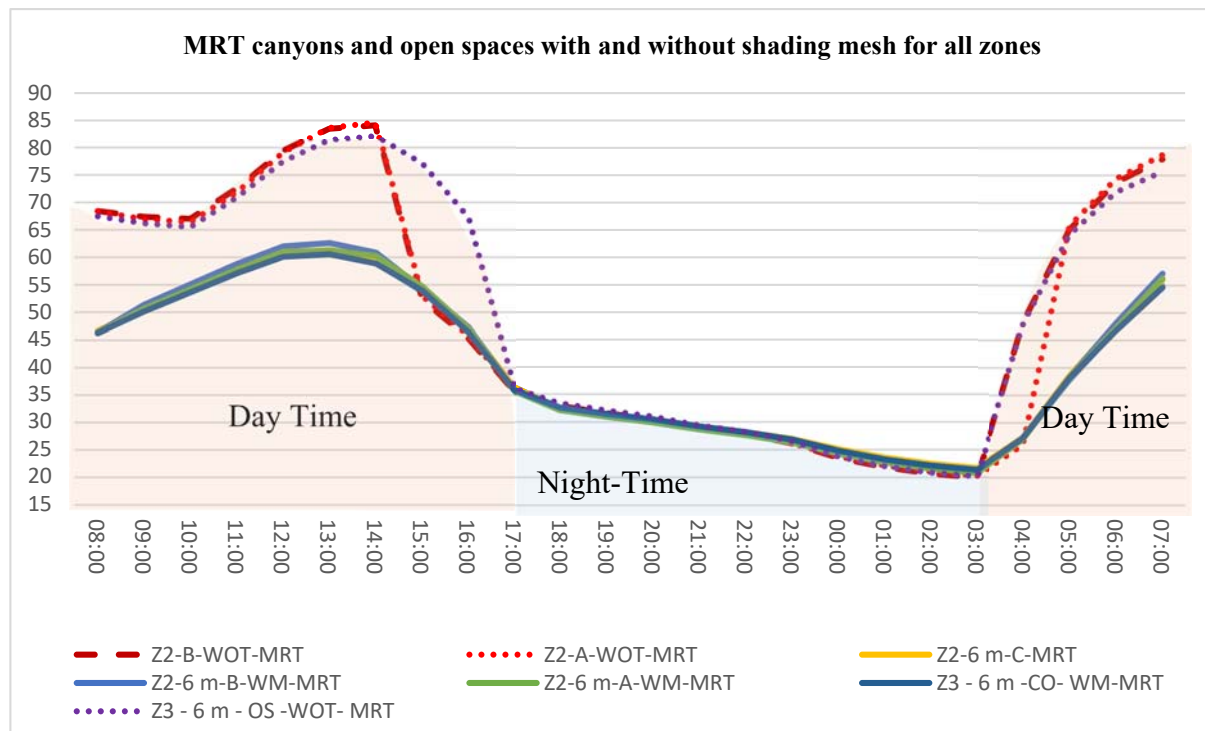


Figure 7.29 Mean Radiant Temperature for canyons and open spaces in Zones 2 and 3 with and without shading mesh

⁵ The symbols in the figure 6.29 are Z2: Zone 2, B: Before the open spaces, WOT: Without shading mesh, 6 m: the sample taken at height of 6 meters, C: centre of canyon, WM: with shading mesh, A: After of open spaces, OS: open spaces.CO: covered open space with shading mesh

Figure 7.29 shows MRT at 12:00 noon and wind speed distribution in all areas which were simulated. The results indicate that MRT at daytime can be reduced by adding shading mesh. In addition, Zone 3 the open areas not covered by shading mesh recorded lower values compared to canyons. The open spaces in Zones 1 and 2 recorded maximum MRT 64.63 °C, while the maximum MRT of the canyons was 68.31 °C (Figure 7.29). This is because the open spaces are covered with grass, while the canyons are covered with asphalt. Additionally, the wind speed recorded maximum values in canyons not covered with shading mesh (Figure 7.30). The open spaces not covered with shading mesh recorded lower wind speeds than canyons and higher wind speeds than shaded open spaces. The shading mesh thus works as an obstacle for

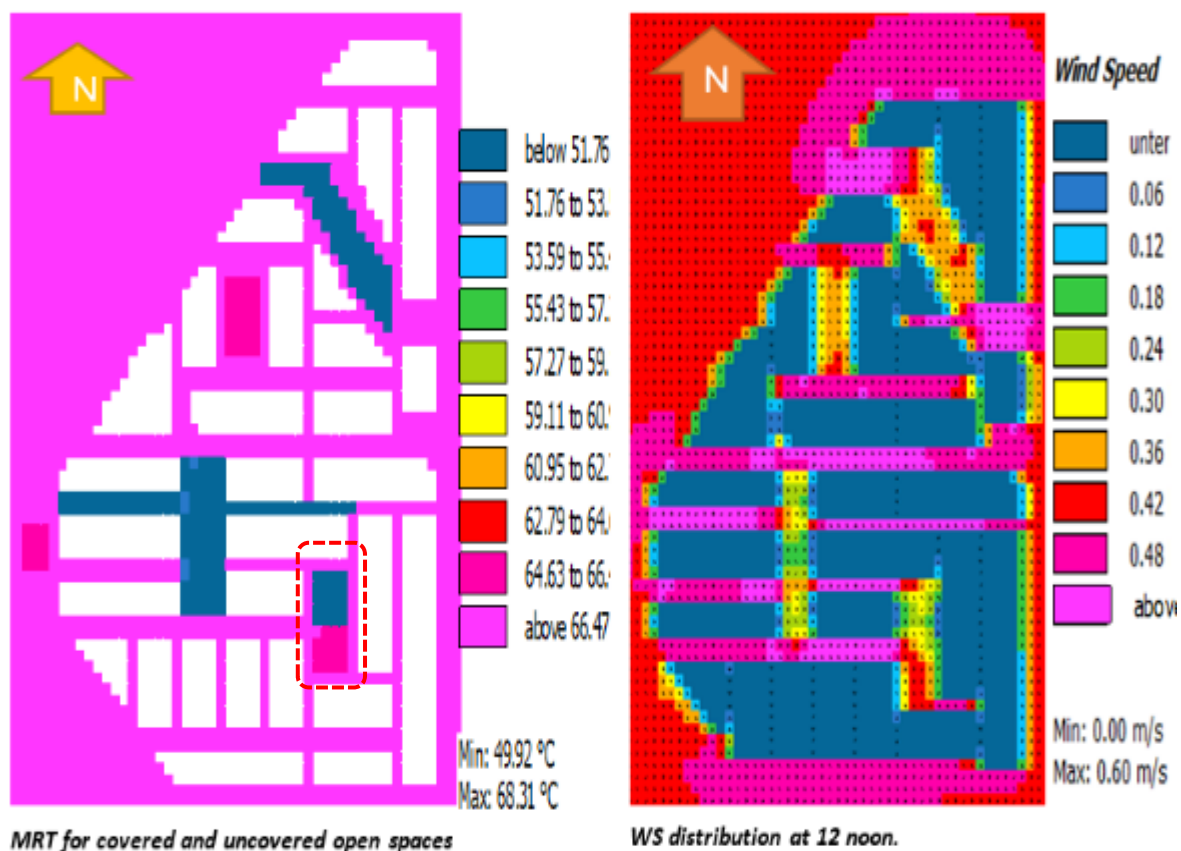


Figure 7.30: Mean Radiant Temperature and WS for open spaces and canyons with and without shading mesh

wind speed, as shown in Section 7.5.2.

As mentioned before the maximum value of MRT is recorded for open spaces that received direct sun light, while open spaces that have shading recorded lower values in general. The minimum values of MRT recorded in night or after sun set until sun rise. The results shows

that open spaces with shading mesh can significantly reduce the MRT during day time without reducing wind speed. This results correspond with other studies in hot dry climate cities, for instance Al Hafith (2018) measured the MRT in courtyard houses at summer time. He found that maximum MRT is reduces by 20 °C in shaded courtyards compare to unshaded once.

This study shows the importance of applying the shading mesh as a sustainable strategy to modify the urban microclimate in canyons and open spaces. In addition, it can be used as design guidance for architects and urban planners during the design or renovation existing urban areas. The other benefit of apply shading mesh is, it can be easily removed in winter time to maximise the direct sun light and increase the occupant thermal comfort. While other research depend on vertical walls and orientation of building blocks to provide shading area for internal spaces such as courtyards. These vertical walls reduce the wind speed and this can lead to entrapment heat energy in those semi-closed urban areas. While shading mesh allow the wind penetrate though and flush out the heat energy and increase night time ventilation.

7.5.4 Physiological Equivalent Temperature (PET)

PET is defined as the air temperature at which, in a typical indoor setting (without wind and solar radiation), the heat budget of the human body is balanced with the same core and skin temperature as under the complex outdoor conditions to be assessed, Hoppe P 1999. Matzarakis (1999) produced the following categories' of thermal perception and PET Table 7.3. The physiological equivalent temperature – a universal index for the biometeorological assessment of the thermal environment (Matzarakis, Mayer et al. 1999).

Table 7.3 Ranges of the physiological equivalent temperature

Thermal Perception	PET
Very Cold	
	4
Cold	
	8
Cool	
	13
Slightly Cool	
	18
Comfortable	
	23
Slightly warm	
	29
Warm	
	35
Hot	
	41
Very Hot	

The physiological equivalent temperature (PET) is used to assess the 'thermal component of microclimate'. This simulation is used to calculate the PET using data from ENVI-met and to assess the impact of shading on outdoor PET.

PET was measured using RayMan software. This method is widely used in the literature (Cheung and Jim 2018, Sharmin, Steemers et al. 2019). Linear correlation was used to assess the results and compare PET and MRT (Figure 7.31). Mean Radiant temperature was measured by ENVI-met for Zone 3 for open space with and without shading mesh, as shown in Figure 7.32. The data from ENVI-met was reused as input data for RayMan software to calculate PET.

results verify that using shading mesh not only reduces the MRT, but significantly reduces PET. The urban microclimate can thus be improved in terms of the thermal sensation for pedestrians. Figure 7.33 shows that PET for the open space with shading is significantly lower than the open space without shading mesh. The maximum PET for the uncovered open space was 63.4°C compared to 50.6°C for the open space covered with shading mesh (Figure 7.33).

Urban microclimate improvement can have an important impact on pedestrian thermal sensation (Sharmin, Steemers et al. 2019). Therefore, the importance of shading mesh as a strategy is to improve the local urban microclimate and the thermal comfort of outdoor urban areas.

7.6 Discussion and Conclusion

This chapter briefly reviewed historical and modern shading to understand the impact of shade on an urban microclimate. Shading mesh is not easy to model on an urban scale,

and therefore ENVI-met was utilised to model and analyse the data. Shading mesh properties were used to generate new materials and applied to cover urban open spaces and canyons in order to compare shading and no shading open spaces.

Radiation exchange is the one of the principle factors that influence urban microclimate for hot dry climate city (Zhao, Sailor et al. 2018). In residential neighbourhood the most significant factor that manipulates occupancy thermal comfort is Mean radiant Temperature (MRT) (Shashua-Bar, Pearlmutter et al. 2011).

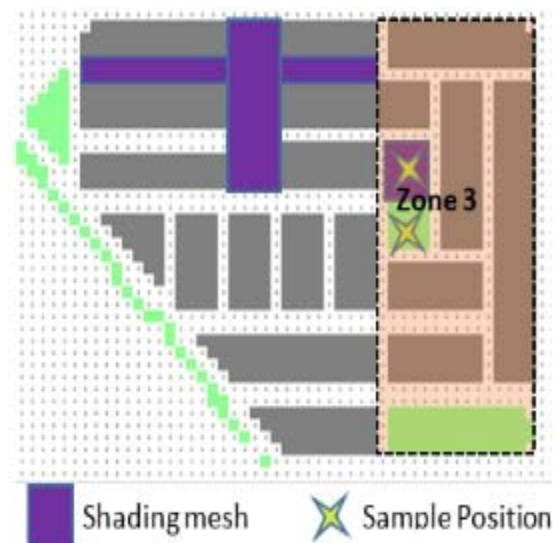


Figure 7.31: Sample position in Zone 3 with and without shading mesh

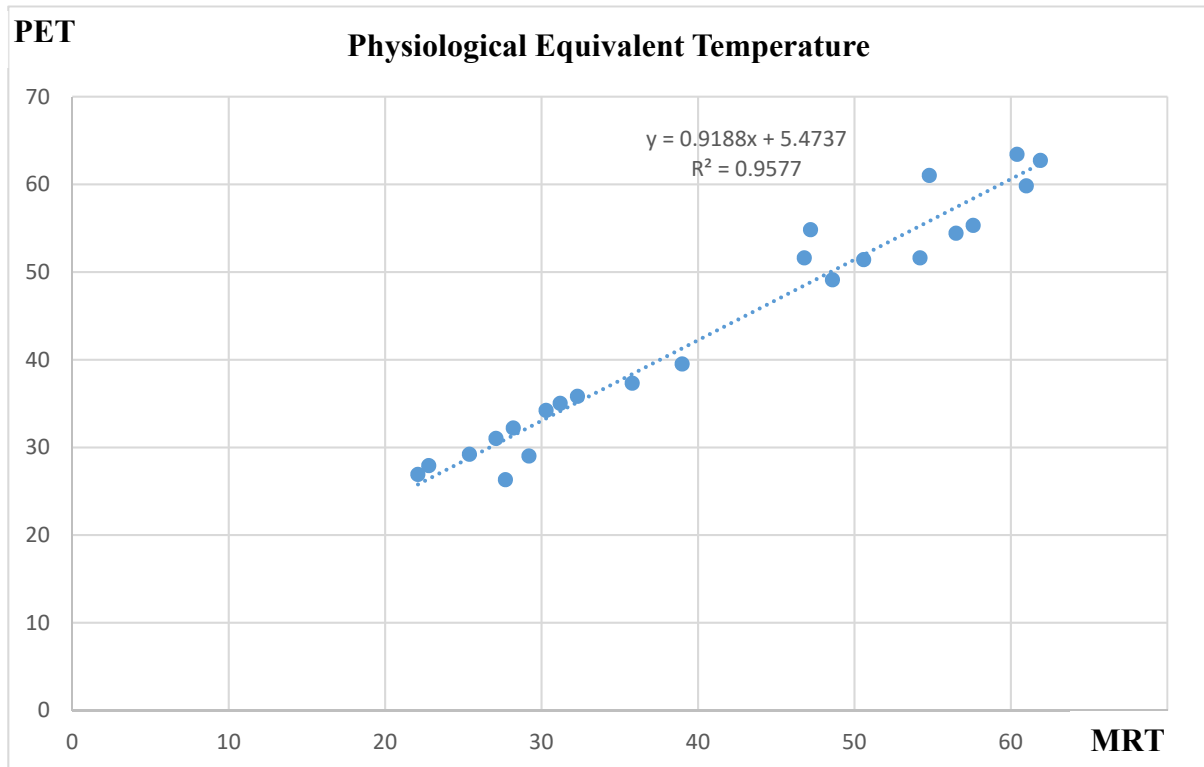


Figure 7.32: Correlation between PET and MRT

Shading mesh is used mainly to cover greenhouses and agricultural crops (Castellano, Mugnozza et al. 2008). Shading mesh has limited used for shading purposes in the modern urban areas and its impact on the local urban microclimate has not been widely studied. There are a limited studies that investigate the impact of shading mesh on air temperature and surface temperature such as (Pearlmutter and Rosenfeld 2008, Shashua-Bar, Pearlmutter et al. 2009), but these studies and their finding differ with present study because of the following points; firstly, the studies based on practical tests and limited scale of measurement. Secondly, different climatic profiles with the present study, these studies were in Israel and the present study in Kurdistan-Iraq.

Shading mesh can applied to provide shading in hot dry climate cities, because during day time it allows sufficient daylight to pass through, and allows air movement which is important for ventilation and removing urban pollution. Based on literature, the researchers found that reduction in sky view factor (SVF) is one of the most effective ways to improve urban microclimate. This can be done through increase building heights or narrowing canyons

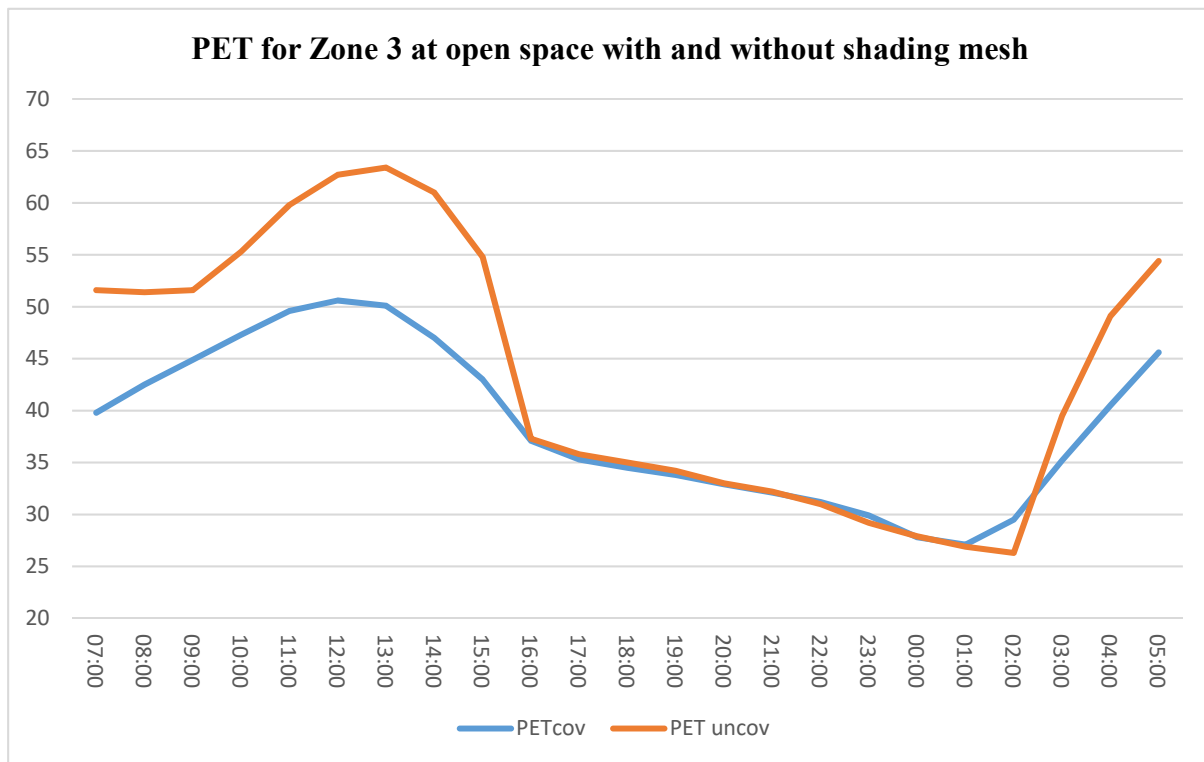


Figure 7.33: PET for open space at Zone 3 with and without shading mesh

(Bakarman, Chang. 2015). These studies found that low SVF in typical urban settings improve thermal comfort for occupants by sufficient protection from direct solar radiation (Toudert, Mayer. 2007). In this study horizontal shading mesh is used for similar principle, which is reduces the SVF by covering the open spaces by shading mesh to protect these urban areas from direct solar radiation and allow sufficient day light and air to pass through it.

The strategy of shading urban open spaces can be used in new and exist housing projects. Thus, this kind of strategy can be employed at any time or in any part of the city; Traditional and modern morphologies. Through simulating shading mesh within an urban microclimate, this study found that MRT for open spaces can be reduced significantly, while limited reduction on air temperature and wind speed. Reduction of MRT using shading strategy agrees with other research such as (Shashua-Bar, Pearlmutter et al. 2011, Zhao, Sailor et al. 2018).

The current study found that local urban microclimate for modern grid-iron morphology mainly depend on solar radiation and secondary on wind speed in hot dry climate, especially at summer time. To control and improve local urban microclimate, it is important to propose a new design product that meets comfortable needs. Shading in urban areas helps to improve urban local

the impact of shading mesh on urban microclimates and how urban microclimates can be modified. The next chapter will explain the impact of shading on individual building units and explain how the modified urban microclimate (ENVI-met) weather data file can be used.

Chapter 8 Modelling the shade mesh

8.1 Introduction

The previous chapter on urban scale climate analysis was explained and conducted. This chapter uses the local microclimate information from the previous chapters to test the climate effects on the building scale. This chapter explains the building scale simulation using IES software. The chapter is divided into three main sections.

The first section is on IES modelling input and output. Similar to other Building Energy Simulation software, IES uses a weather data file as the main input data to provide thermal analysis of a building. Three types of weather data will be explained and compared to determine the representative set of data.

The second section is on shading meshes and validating the model. The shading mesh model is not easy to model using BEM because of the size of mesh. IES is used to model the shading mesh through a series of simplifications of the shading mesh regarding size and shape. The modelling approach is validated using a second BEM software package called HTB2, developed by Cardiff University, UK.

The third section is on models the prototype housing units and analyses their thermal performance using IES. The prototypes are simulated with and without a shading mesh to determine its impact on indoor dry bulb air temperature.

The fourth section is about housing block arrangements and their orientations on indoor dry bulb temperature (DT). The modelling process include 12 housing block arrangements were compared with similar climatic boundary and building materials. In addition, North-South and East-West blocks façade were modelled with IES-VE.

8.2 Numerical modelling and validation (building scale) using IES

The energy consumption in a residential building is a main sector in the final energy use in Erbil. The Iraqi Ministry of Electricity announced that 45% of the demand for energy is from residential buildings. In Iraq and the Kurdistan region, there is a shortage of electricity, especially during summer months, as the government can only produce 45% of the total energy demand. The remaining demand is generated by the private sector or imported from neighbouring countries (Iran and Turkey). Kurdistan aims to reduce energy demand in order to respond to growing urban developments by reducing the energy consumption in new and existing buildings. Calculating energy consumption using Building Energy Simulation (BES) models is a modern way to reliably estimate the energy demands for any type of building. This study uses the IES building simulation program to estimate the indoor air temperature of prototype housing in Erbil. The previous chapter used a shading mesh as an effective strategy to reduce the Mean Radiant Temperature of outdoor microclimate urban areas, while in this chapter IES is employed as a research tool to model the shading mesh and estimate house performance with and without a shading mesh.

8.2.1 IES model input and outputs

IES is an energy system model which uses a mathematical model to describe the behaviour of buildings. This BEM has three main pillars: input variables, model structure, and output variables (Figure 8.1). The output variables of IES BEM can be determined when information about the first two pillars is available (Input and Model structure). The input variables (forcing variables) can be divided into two types, controllable and uncontrollable. Controllable variables include the engineering system of the buildings (e.g. thermostat settings and building materials, etc.), while uncontrollable variables are outdoor variables that directly affect the energy modelling, such as solar radiation, air temperature, and wind speed. The uncontrollable input data can be forecasted or modified through systematic techniques.

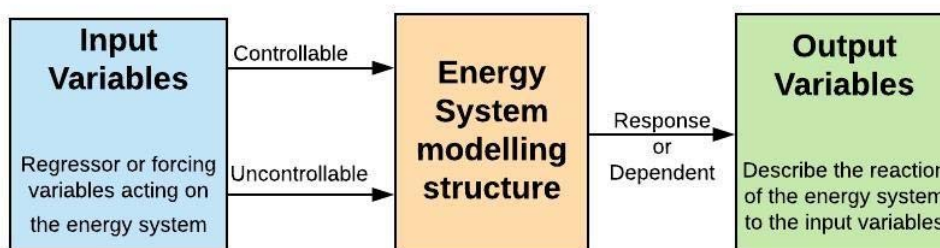


Figure 8.1: Building Energy Modelling structure. From Hao Gao (2019)

The model structure is the hydrothermal discretion of building energy simulation. This part provides all the mathematical equations that BES needs for energy transfer during the simulation process.

The output data in this case are represented by indoor air temperature, air velocity, and relative humidity for the measured space and building energy consumption. These variables are a result of the reaction between input data and the model structure (building modelling system). IES models use a large database of files to provide information for the weather data file for different locations around the world. These weather data files can be uploaded as input data by the user without knowing what the original file includes. These weather data files come as a specific extension file to be used as input data, but they have a significant impact on simulation outputs. The structure of the BES model mainly depends on the weather data file to produce the output data, which is important to the end user. Thus, great attention should be taken to understand the weather data file ingredients before any BES calculations. This study compares three different sources of weather data to justify the appropriate set of data (Figure 8.2).

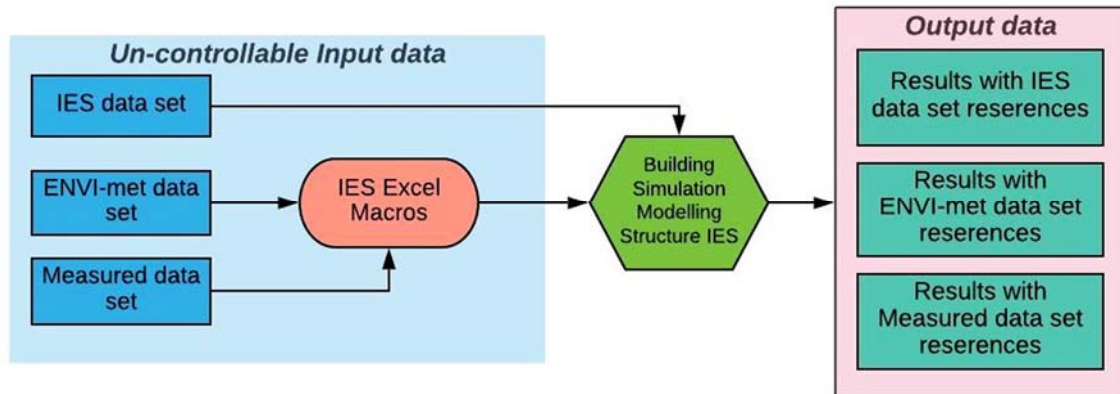


Figure 8.2: The process of simulating three difference sources of weather data

8.2.2 IES and weather data file

Most Building Energy Simulation (BES) software uses a typical weather data file taken from the original company which generated the software. The typical weather data are normally generated through a statistical process of multiyear observation of weather data measured by weather stations outside the urban area in peripheral zones.

The weather data file is influenced by microclimate variables and urban densities. The typical weather data used by IES includes climatic variables such as solar radiation and wind speed, but not urban density. In Chapter Five, the study showed how air temperature and wind speed

differs between urban areas. Previous studies have shown that urban areas have higher air temperatures and lower wind speed compared to areas outside the city centre (low and medium urban density). These differences in air temperature are caused by Urban Heat Islands (UHI). However, in Erbil this phenomenon is different with regard to air temperature, as the air temperature in urban areas during daytime is lower than in open areas outside the city as a result of intensive solar radiation in open spaces and shading in urban areas. This phenomenon is called an Urban Cool Island (UCI). During the night time, air temperature is higher than outside the city.

As a result of different climatic variables for different urban areas, the energy performance of any building inside a specific urban area will differ. Therefore, a calculation which uses typical weather data for different urban areas, for example airport (low density) and city centre (high density), can lead to inaccurate estimation of energy consumption. IES weather data files, as with any other BES model, depend on climate variables such as dry bulb and dew point temperature, wind speed, and solar radiation. Any differences in these variables strongly influences the heating and cooling calculation loads. In this study, different weather files were generated and compared to reduce this discrepancy and increase the accuracy of the building simulation model. The aim of this section is to determine the most accurate source of climatic variables to generate a typical weather data file that can be used for IES simulation.

The new weather data file includes all local variables ignored by a typical weather data file, such as solar radiation, wind speed, building materials, and vegetation etc. Three sources for climatic variables were used to generate a specific IES weather dataset, as below:

1. IES weather dataset with IES references (IES dataset)
2. IES weather dataset with ENVI-met references (ENVI-met dataset)
3. IES weather dataset with local site measured references (Measured dataset).

For two datasets (ENVI-met and measured) similar computational process was used to generate the weather IES datasets, while the original IES weather data file was generated by the IES company.

8.2.3 IES weather dataset with IES references (IES dataset)

IES weather data utilise site information which contains values for latitude, longitude and height above sea level, and a range of sites published by CIBSE and ASHRAE Standards (Figure 8.3).

The database for the IES simulation program allows the user to design the weather data file for cooling and heating loads through the individual entries called **Design Weather Data Source and Statistics**. These data include monthly minimum and maximum dry bulb temperature, dry bulb time lag, and daily wet bulb temperature at maximum dry bulb temperature, as shown in Figure 8.4-A. These monthly weather data can be used to estimate the heating and cooling loads, but for accurate heating and cooling loads, hourly datasets are needed. To produce long term datasets, the research used monthly datasets generated hourly

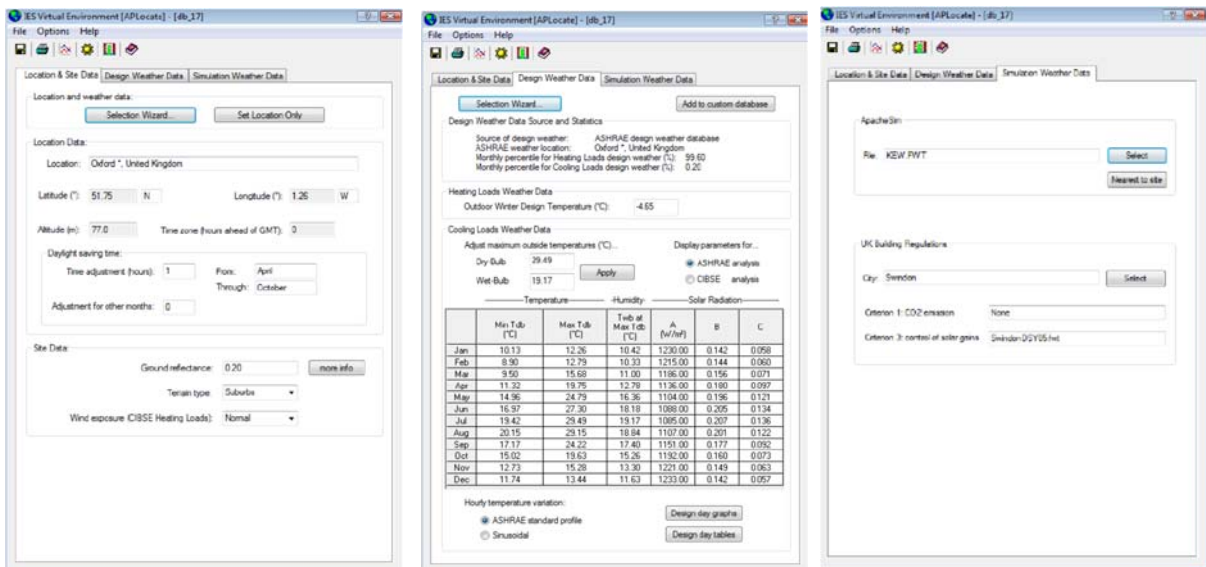


Figure 8.3: IES weather data information published by CIBASE and ASHRAE

data through Meteonorm¹ software (Radhi 2009) (26²). The other source of weather data for Erbil is not published in CIBSE and ASHRAE Standards. The IES can also simulate those regions that are not published in the standards through a specific option shown in Figure 8.4-B, which allows the uploading of a customised weather data file for climate configuration during heating and cooling calculations. The customised IES weather dataset is weather data for 12 months generated by the IES Company, composed of taking typical months from 15 years of observed weather data. These data represent a Typical Metrological Year (TMY) for

¹ Meteonorm software is a special program used to generate hourly weather data sets from monthly average weather data sets.

² Meteotest, Meteonorm, Global Meteorological Database, Version 7.1, Handbook Part I (2015).

a specific location such as Erbil, and can be used for BES of typical rather than extreme weather conditions.

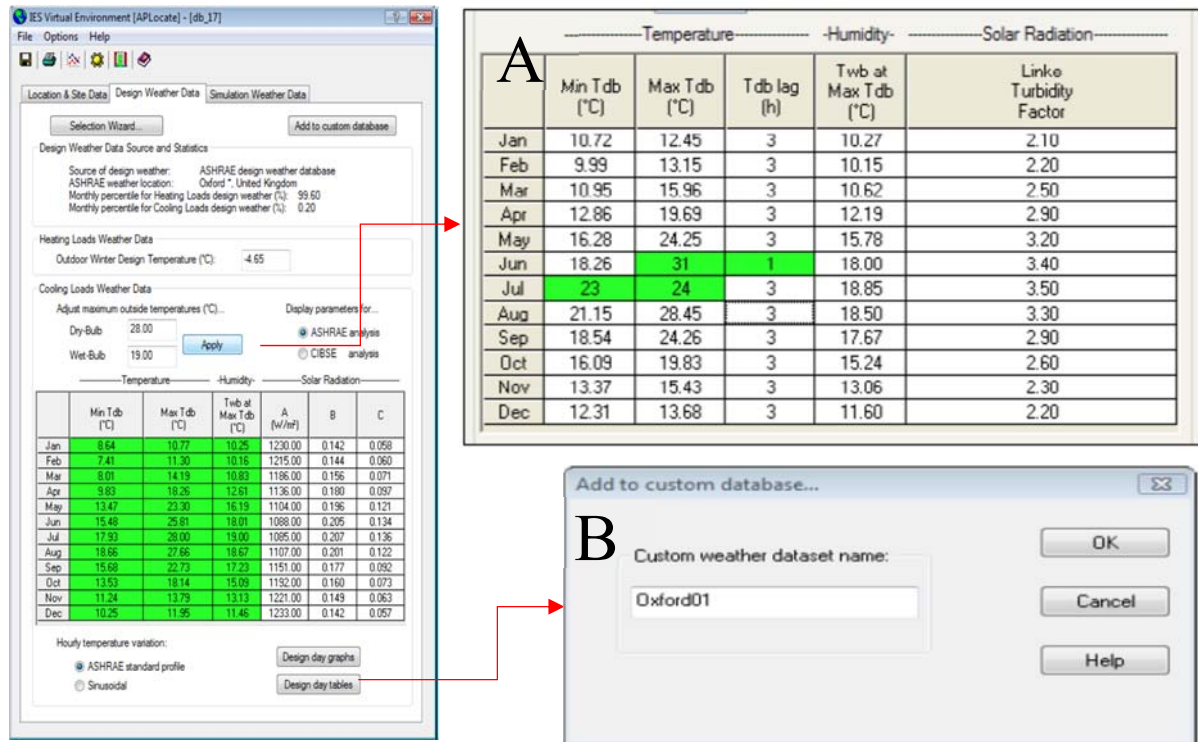


Figure 8.4: IES Design Weather Data Source and Statistics. A: Design of monthly weather data. B: Add unpublished weather data file for locations not included in the IES program database.

As mentioned in Section 7.2, this type of weather dataset is inaccurate for urban BES. In the literature, we found that there is a lack of studies which raise this issue. One recent study published in 2018 by Tsoska found that simulating a building inside a specific urban microclimate with Typical Metrological Year (TMY) is not considered an accurate simulation. The results of the study showed that the urban microclimate for a specific area had a higher dry bulb temperature and lower wind speeds compared to a TMY at the reference location. In addition, they found that climatic factors (air temperature and wind speed) strongly affect the output of energy simulations, and this influences the heating and cooling loads of buildings within a specific urban context. In this study, IES Excel Macros were used to generate weather data files suitable for IES software. These weather data files were modified to represent the local urban microclimate context of Erbil in such a way that urban microclimate elements participate in the thermal energy simulation.

8.2.4 IES weather dataset with ENVI-met references (ENVI-met dataset)

ENVI-met is one of the best fluid dynamic simulation software programs for evaluating local microclimate conditions. The program can simulate the micro scale for 24–72 hours, but after this the model will become too hot and the output is considered incorrect. This limitation of the program makes the provision of a years' worth of data different. Hence, the evaluation of Erbil's microclimate conditions was set for 24 hours, or one diurnal cycle. Therefore, a specific day³ was selected for each month for simulation by ENVI-met.

The configuration file of the model includes data that represent the urban surface, vegetation, and meteorological variables. In addition, the programme can use a set of data (air temperature and relative humidity) from the nearest meteorological station and force the program to use only that data as its configuration file, to generate more accurate and realistic data for an urban area. ENVI-met can produce a dataset which includes air temperature, wind speed, and mean radiant temperature. Modelling the urban microclimate of a typical residential area of Erbil and validating it using two methods helped to generate a weather dataset for a specific urban area in Erbil (Section 5.5). The model used hourly air temperature, wind speed, and relative humidity from the central station. The model and wind direction for the boundary condition correspond to real site parameters. The urban residential blocks are made of hollow concrete blocks and the roofs from reinforcement concrete, to represent actual local building materials. Figure 8.5 shows the ENVI-met model simulated with the local urban microclimate. The results of the ENVI-met model were collected for the sample position at 2 m between the east-west canyons using LEONARDO software, which allows the simulation results to be displayed in plan and elevation. Table 1 shows some of the parameters for the urban microclimate of in the ENVI-met model which can be used to produce a weather data file for the IES model.

³ Three type of studies have been used in ENVI-met, as below:

1. ENVI-met without any description of the reasons for using specific days, or a random selection
2. ENVI-met with extreme days in summer (hotter days)
3. Use of a typical characterised day of the year.

Table 8.1: Urban microclimate parameters from the ENVI-met model

Time	Wind Speed (m/s)	Air Temperature (°C)	Mean Radiant Temp. (°C)
08:00	0.58	33.3	47.3
09:00	0.59	34.3	50.9
10:00	0.59	35.1	54.5
11:00	0.60	35.8	58.1
12:00	0.60	36.7	62.0
13:00	0.60	37.4	63.3
14:00	0.60	38.3	62.0
15:00	0.60	38.4	56.0
16:00	0.60	38.4	47.8
17:00	0.60	38.2	35.6
18:00	0.60	37.8	31.7
19:00	0.60	37.4	30.6
20:00	0.60	36.9	29.6
21:00	0.60	36.3	28.6
22:00	0.60	35.7	27.6
23:00	0.60	35.1	26.5
00:00	0.60	34.2	24.9
01:00	0.60	33.3	23.5
02:00	0.61	32.7	22.4
03:00	0.61	32.2	21.6
04:00	0.61	32.0	27.9
05:00	0.61	32.4	68.6
06:00	0.61	33.2	49.8
07:00	0.61	34.3	58.3



Figure 8.5: ENVI-met model and sample position

Air temperature recorded a maximum value at 15:00 and minimum value at 04:00 of 38.4°C and 32.0°C, respectfully (Figure 8.6).

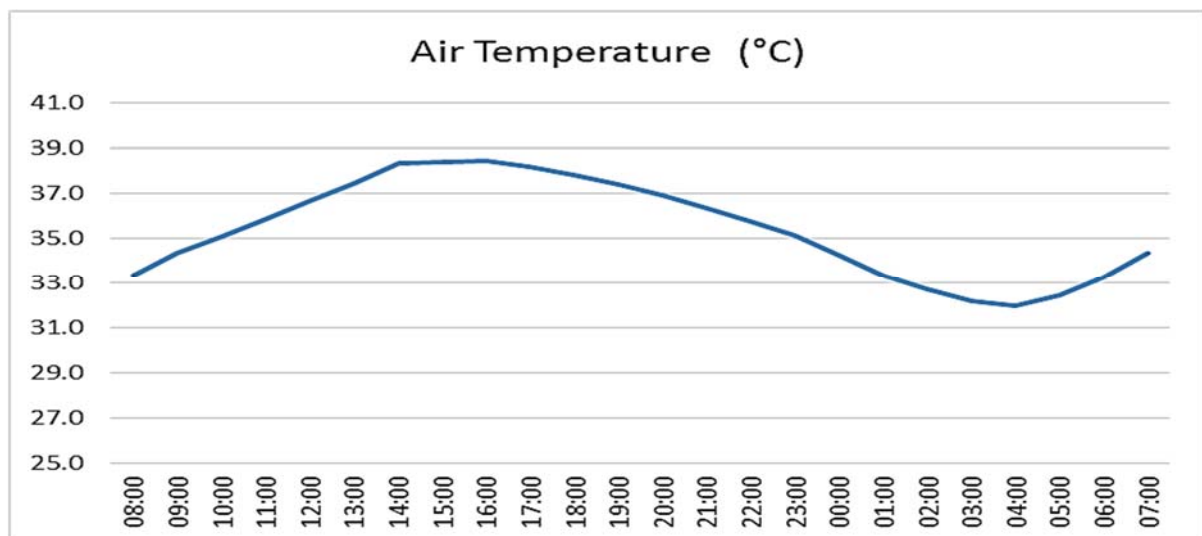


Figure 8.6: Sample of air temperature for sample position in ENVI-met

8.2.5 IES weather dataset with local site measured references (Measured dataset)

Four weather stations in Erbil were used and analysed for 2014, 2015, and 2016 (Figure 8.7). Air temperature, wind speed and relative humidity were compared to understand the urban microclimate of the city (Section 5.2).

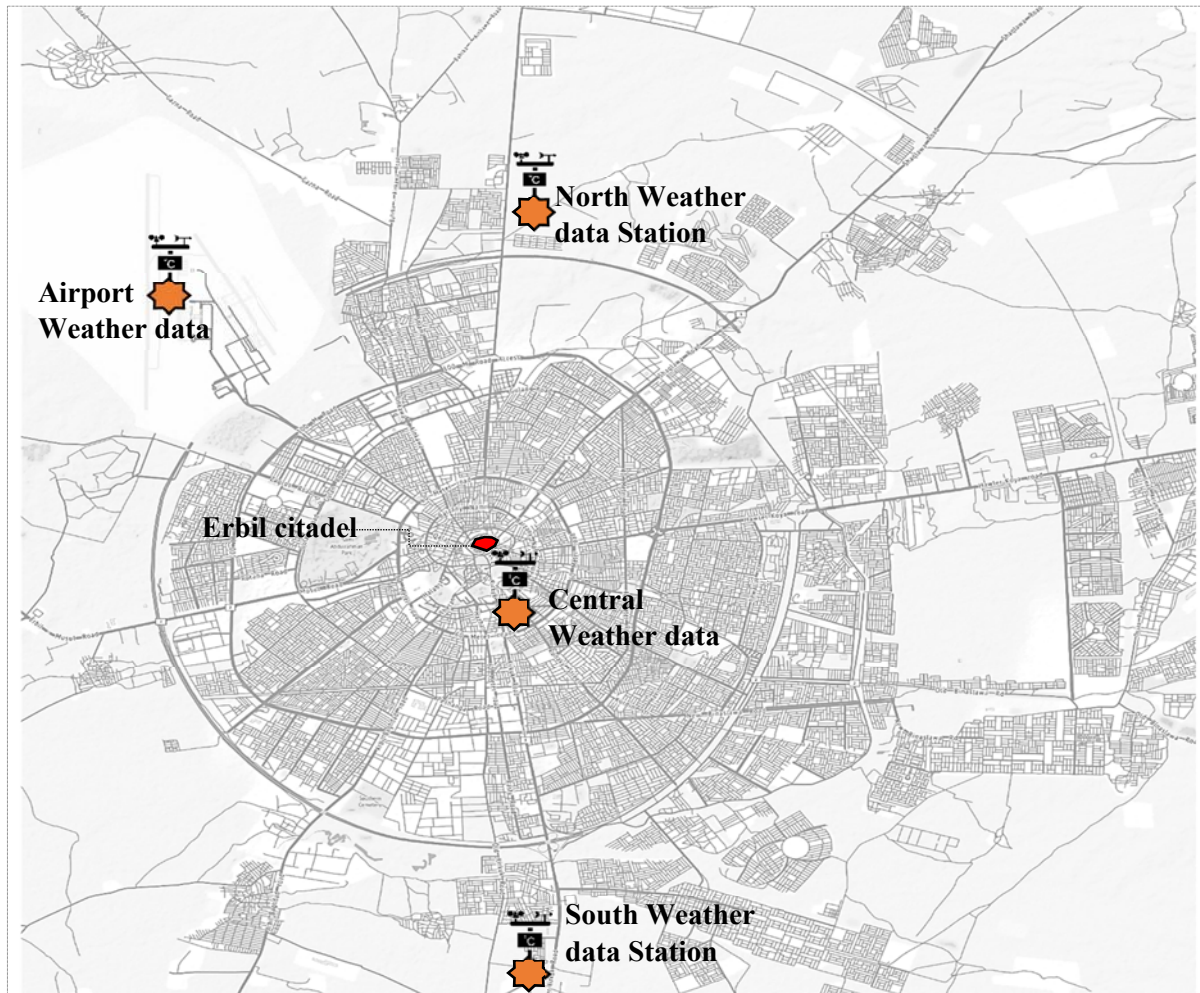


Figure 8.7: Four weather data station locations in Erbil

The results show that the Central Weather Station (CWS) is more representative of the urban microclimate of Erbil because it is located in high density urban area, while the airport, and north and south weather stations are located in the rural area outside the city, with a lower urban density than the predominately urban areas. Air temperature, relative humidity, and wind speed were manipulated to re-generate the weather data file used as the input data for the simulation process using IES.

8.3 Generation of the weather data file for IES

BES has been used as a research tool by architects, engineers, and designers to estimate building energy calculations. These energy models use a weather data file as input data to build a configuration model. The desired configuration model for energy simulations should be based on accurate weather data file. This strongly influences annual energy consumption, air conditioning system size, and the annual cost of energy.

This study employed three sources of data (IES, ENVI-met, and measured data) to produce weather data files which were used as an input data for the process of simulation. These three weather data files were used as a research tool to justify the most appropriate weather dataset to use (Figure 8.8).

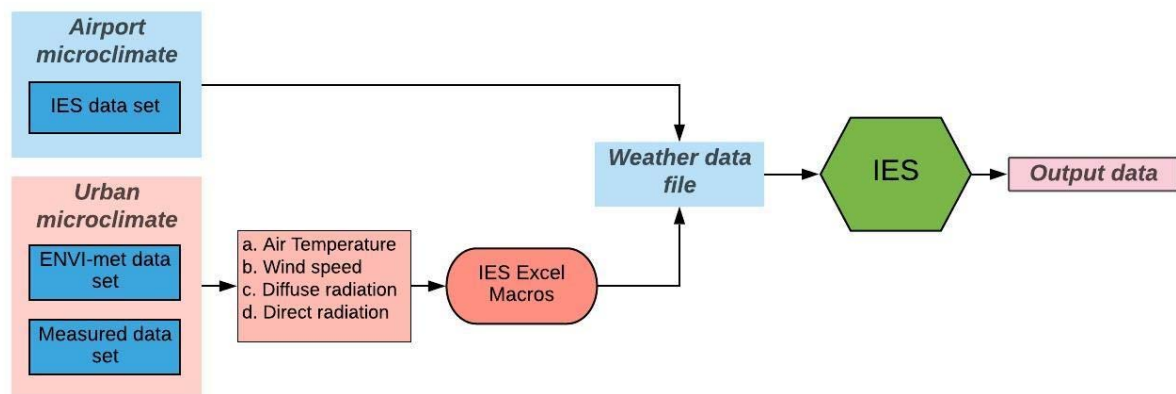


Figure 8.8: The process of producing a new weather data file

As mentioned in the previous section, using an IES weather data⁴ file does not correctly represent the urban microclimate of the Erbil urban area. Thus, this study used IES Excel Macros to facilitate the manipulation of weather data, and using Measured data⁵ and ENVI-met⁶ outputs to generate IES weather data (Figure 8.8).

In addition, two methods were used to justify the most representative urban microclimate weather data file, as below:

1. Direct comparison of air temperature for the three sources of data for 1st July 2015 (Figure 8.10).
2. The IES model⁷ for dry bulb temperature of three different weather data files (Figure 8.9).

⁴ The IES weather data file is a weather data set produced by the IES Company through the selection of long term typical data over 15 years.

⁵ Measured data taken from the central station.

⁶ Simulation urban residential case study outputs.

⁷ In this test, IES was run three times with three weather data files (Measured, IES, and ENVI-met).

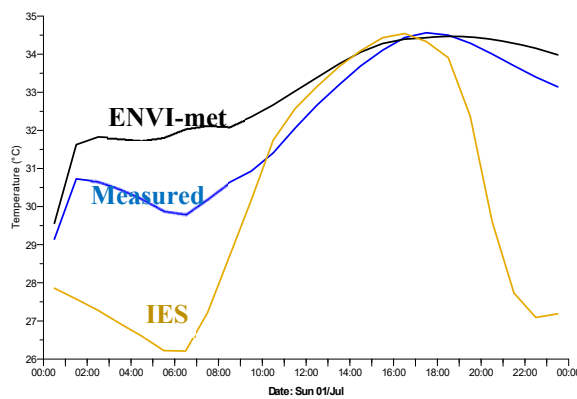


Figure 8.9: IES simulation output using three sources of information

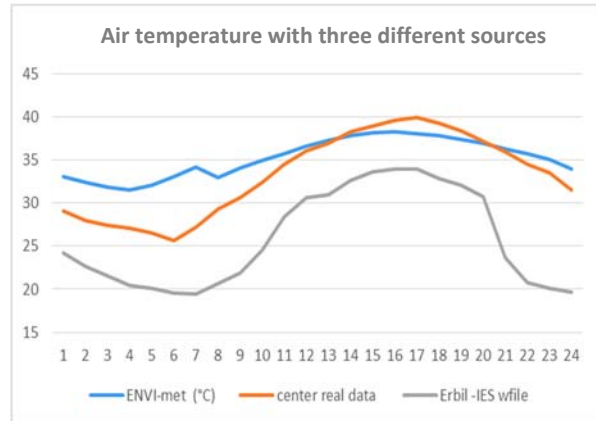


Figure 8.10: Sample of air temperature using three sources of data: ENVI-met, IES weather file and Measurement data

Figure 8.10 shows that for air temperature in the three sources of data, IES records lower values compared to ENVI-met and Measured air temperature. Measured and ENVI-met models recorded nearly similar values during the daytime, but Measured data recorded lower values than ENVI-met during the night (Figure 8.9).

The IES model was run three times, and the weather data files were changed for each simulation. The dry bulb air temperature was modelled and compared for 24 hours for 1st July 2015. The results show that the IES model is significantly impacted by changing weather data files (Figure 8.9). ENVI-met recorded higher dry-bulb temperatures for the day and night compared to the IES and Measured data models. During the day between (10:00–18:00) the three models recorded almost similar values, while during the night these values changed significantly. The dry bulb temperature did not decrease during the night as the IES weather data did, and this result is due to the UHI effect, which is ignored by the IES file. ENVI-met is therefore more desirable for simulation than IES during daytime but performs poorly once the sun has set, the measured data file replicates both daytime and night time well and is superior to the other two.

The performance of the IES model for any building in a specific urban microclimate depends mainly on weather datasets (uncontrollable variables). The synthetic weather data file produced by the IES Company assumed the climate conditions at the airport. These data represent a rural area with a low density urban microclimate, and not a high urban density area (city urban microclimate). The solar radiation effects for a high density urban area are altered by the complex urban geometry and building materials. This complex urban

environment influences air temperature, wind speed, and solar radiation, leading to new building microclimates in the cities called UHI or UCI.

To start the simulation of a building in a specific urban area using the IES model, three weather datasets were used. The IES weather data file produced an erroneous result and the ENVI-met data were also not perfect, but more accurate than IES. Therefore, Measured data for the site is the most accurate (Figure 8.9), and for this reason it will be acceptable to use measurement data rather than ENVI-met and IES weather data.

8.4 Modelling Shade Mesh using IES

In hot and sunny regions, low-cost high density polyethylene (HDPE) nets are widely used for shading purposes in agriculture. Shading mesh can also be used for external and internal shading to reduce the intensity of solar radiation. The mesh works as a radiation barrier, by reflecting and absorbing direct solar radiation. The mesh then re-radiates the energy but at a much lower temperature, and hence the environment beneath the mesh is much cooler than the environment above. Some of the absorbed solar energy of the mesh is lost via convection either back into the environment or below the mesh. In order to reduce the effect of solar radiation heat loads in hot climates, shading mesh is used in residential and industrial buildings and areas, such as car parks, playgrounds, and swimming pools (Abdel-Ghany and Al-Helal 2011).

8.4.1 Plastic shade mesh types

Plastic shading meshes are classified by their properties, such as material, type and dimension of thread, mesh size, texture, colour, density, and porosity/solidity. It also has radiometric properties, for example transmissivity, reflectance, and absorption, as well as mechanical

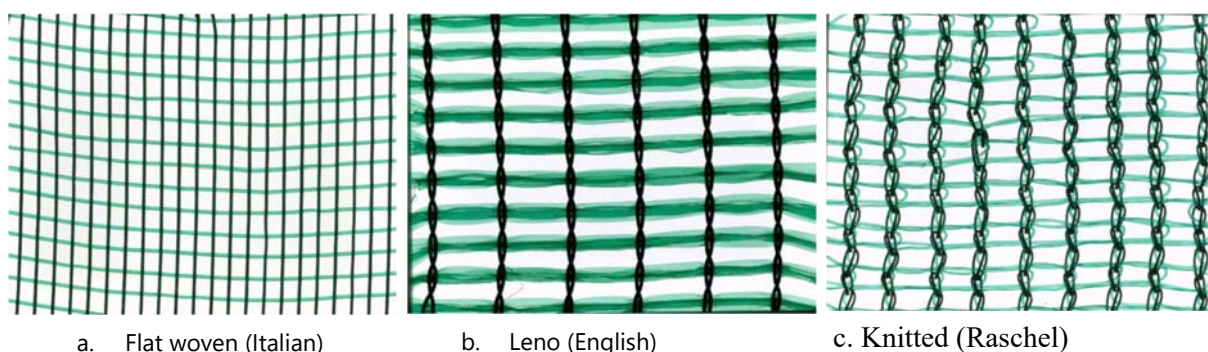


Figure 8.11: Types of plastic shade mesh

properties like strength, tensile stress, elongation at break, and durability. Plastic shading mesh differs in both length and width, depending on factory and customer preferences, from

1–6m, 12–20m and 20–300m. High density polyethylene is mainly used for the production of plastic shading mesh, as it is non-toxic. There are two main types of thread for plastic shading meshes: round monofilaments, and flat tapes (Hemming, Swinkels et al. 2008). Figure 8.11 shows three types of plastic shade mesh categorised by their texture: flat woven (Italian), Leno (English), and Knitted (Raschel). Shade mesh size, porosity, and density depend on net texture, and the connection between single threads that generate a regular porous geometric structure. Mesh size is the distance between two threads in the same single weft direction. The mesh size is normally given in mm, and for shading purposes the shade meshes are between 2.5–4 mm, while the thickness of the shading mesh is measured by the thickness of single threads (mm). Porosity is normally represented by the percentage of open area of shade mesh divided by total area of shade mesh. Cohen and Fuchs (1999) showed that porosity can be measured by three methods: radiation balance, interception and solar radiation, and analysis of images of the materials. Moreover, the density of the shading mesh depends on the texture, size, and thickness of the mesh. This study compares different shading mesh porosities (shading coefficient) and shade mesh size (Scale) and shape (Geometry), to test the mesh's ability to reduce direct sun radiation over the roofs of buildings.

8.4.2 The shading mesh model

Shading mesh thermal energy analysis requires essential knowledge of solar and thermal radiation exchanges between the shading mesh and surfaces they cover. Several studies have examined the solar radiative properties and behaviour of shading mesh using different methods. Most studies have examined the physical properties of plastic meshes (net porosity, colour, and shading density) as the main subjects of their studies. Here, we focus on both shade mesh arrangements and solar radiation on the surfaces underneath (roof surfaces). Different methods have been used to measure the solar properties of plastic meshes. A light model was used by Hemming (2008) to analyse the radiometric performance of structures covered by mesh (Hemming, Swinkels et al. 2008). However, Ahmed (2014) argued that 'It is impossible to directly measure the thermal radiative properties of shading nets because of the net's surfaces' (Ahmed, Ibrahim et al. 2014). The researcher tested the shade mesh thermal properties under natural conditions using horizontal black substrate covered by shading mesh fixed by a wooden frame. Thermal radiation flux and temperature were measured above and below the shading mesh (Ahmed, Ibrahim et al. 2014). In addition, Ahmad (2014) found that the solar radiation absorbed by the net (Shading mesh) did not equal the emitted radiation. Castellano, Russo et al. (2006) measured ultraviolet, visible, and

infrared spectrum wave energy to examine the construction parameters (porosity, colour, and shading factors) of plastic shading mesh. In other studies, solar radiative properties under natural conditions were measured (Abdel-Ghany and Al-Helal 2011), and a few laboratory studies have compared the thermal radiative properties of both plastic mesh and metallic shade screens (Andersson 2010, Abdel-Ghany and Al-Helal 2012). Mainly, these studies are limited to the thermal radiation exchanges with plastic shade mesh (solar radiation, thermal radiation, and convective heat). In general these studies are associated with agricultural research on how solar radiation performs in greenhouses. In addition, plastic mesh has been used to examine the effect of solar radiation on the physical properties of the plastic mesh itself. There have been many studies on the solar thermal and radiative effects on vertical building elements, such as double skin façades (DSF), but few studies have measured solar radiation behind the shading mesh. However, these studies measured these effects under real conditions. Understanding this impact is important for this study, and so in this section the aim is to model and validate the shading mesh used to modify microclimate direct solar radiation on both the urban and single building scales. Shading mesh thermal analysis is not well understood and there are no specific international standards to test the various types of plastic mesh on the market. Although Italy and France has standards to test, there are as yet no European standards to test agriculture nets (Díaz-Pérez 2013). In general, plastic shading mesh has been studied by agricultural researchers to develop and enhance plant production or protect crops from frost or sun spots (Hemming, Swinkels et al. 2008).

The bulk of the literature on horizontal Shading has been taken. From agricultural sources, there is little to no literature a horizontal shading of buildings (Pearlmutter and Rosenfeld 2008, Shashua-Bar, Pearlmutter et al. 2009). Shade mesh is can be used in architecture horizontally (shading mesh) and is widely used vertically (shading screens). Recently, the façade of some buildings has included metal mesh grids as a second skin above the building envelope. These secondary skins are used as a design element, to reduce daylight, solar radiation, and solar gain. Geometry, texture, and other physical properties such as porosity, transparency, colour, and thickness have a huge impact on shading device performance. Another important factor that affects solar gain through shading screens (shading devices) is the angle of solar radiation on the shade mesh/screen.

8.4.3 Modelling shade meshes

In hot dry climate regions, solar radiation is one of the most important factors affecting the internal environment of a building. To minimise this effect, the solar shade created by shading meshes can improve building performance by reducing the direct solar load. Solar shading may affect dwelling energy consumption through lighting, cooling, and heating energy. Solar radiation in hot dry climates increases the heat gain of the buildings during summer months. In hot dry regions shading devices are widely employed in windows and courtyards, and on narrow roads (canopies) to reduce direct solar radiation load. However, these strategies have been ignored in modern building construction methods using artificial cooling systems to achieve thermal comfort, such as an air conditioning system. Traditional and modern architecture can use shading devices to control daylight and thermal energy by modifying direct solar radiation and thermal exchanges through the building envelope.

Most studies that have examined external perforated solar screens (PSS) have measured solar radiation through vertical surfaces, in order to reduce energy consumption and achieve thermal comfort, where reducing solar gain through the fenestration is important. However, studies to quantify the amount of solar radiation on the horizontal surfaces are rare. On these horizontal surfaces, a combination of insulation and reflective surfaces has been used, but in hot dry climates, insulating the roof will reduce energy flow to the top of the building in winter, leading to overheating, and dust will absorb the reflective surfaces. Modelling shading meshes with a ‘real scale’⁸ is difficult in terms of CFD models, as most CFD programs use thermodynamic calculations to generate output data for close 3D spaces (length, width, and height). The simulation of solar radiation through extremely fine meshes such as shade mesh is not an easy task for these programs. In this field, two kinds of research have studied shade analysis:

1. Agriculture studies – this kind of research used natural conditions to test and explore the effect of plastic shade mesh on plants.
2. Architecture and building physics studies – this group of researchers used CFD simulation programs to simulate Perforated Solar Facades (PSF) mainly on vertical building elements, such as a double skin façade (DSF).

In both groups of studies, the simulation of plastic shade mesh and façade elements is problematic because of the element scale. The simulation time for building environmental

⁸ The shading mesh has very tiny holes (2mm x 2mm) with a thinness of less than 1mm, so the CFD program cannot easily model very tiny shapes laid out on a large area.

performance simulation tools to obtain accurate results needs ‘considerable time and iterations’ (Chi, Moreno et al. 2017). In addition, CFD simulation programs and energy performance tools cannot easily model complex geometry such as perforated solar screens and plastic shading meshes. The process of designing the model and simulating these kinds of complex geometrical patterns is sophisticated and needs high performance computers. For these reasons, a hypothetical test room with simplified geometrical objects was used to represent the complex geometries of a perforated solar screen. Chi et al. (2017) used simple objects such as circles, hexagons, rectangles and triangles in a matrix to model complex geometries to calculate the energy consumption and daylighting of the perforated solar screen. Using the EnergyPlus simulation program, one of the commonly used programs to simulate and model energy consumption in buildings, Kim (2011) reassessed the energy performance of buildings to test the accuracy of the energy transformation that accrues in complex geometries, using a DSF as a case study. The Energyplus program is very efficient for both daylighting and thermal energy transmission compared to on site measurements (Kim and Park 2011).

In addition, some authors have developed simulation methods and integrated different simulation packages to simulate both daylighting and energy consumption. Both horizontal and vertical building geometries at the fine and micro scale, such as in shading mesh and perforated solar screens, require a new way to be represented in CFD models. New studies have linked Grasshopper⁹/Rhino¹⁰ to Radiance/Daysim¹¹ to assess the design parameters, such as window opening size and materiality (González and Fiorito 2015). Moreover, to calculate solar radiation based on a climatic-based matrix, DIVA¹² was used to calculate daylight (Board 2011, González and Fiorito 2015). The studies that used Grasshopper as a simulation tool manipulated the hourly shading coefficient of a hypothetical screen. Then, yearly lighting energy consumption was generated and loaded into the Design Builder¹³ program for thermal simulation.

In order to model the micro scale geometry of shading mesh threads using the IES simulation program, we proposed a hypothetical method of simplifying the shade mesh was employed

⁹ Grasshopper is a graphical algorithm editor which integrated with Rhino's 3-D modelling program.

¹⁰ Rhinoceros is 3D computer – aided design (CAD) software use for drawing curves and freeform surfaces.

¹¹ Radiance/Daysim is analysis software which model the annual amount of daylight inside and outside of buildings (<https://daysim.ning.com/>).

¹² DIVA Daylighting Simulations with Radiance using Matrix-based Methods.

¹³ Design Builder is an ‘Energy-Plus based software tool used for energy, carbon, lighting and comfort measurement and control’ (<https://www.altensis.com/en/services/designbuilder-software/>).

(Figure 8.12). In this test various factors were tested; shading coefficient (porosities), geometry, and the scale of the shading mesh. Moreover, the shading coefficient range on direct solar radiation was compared in the simulation. The method quantified different shading coefficients to test the effect of solar radiation load on roof surfaces. In addition, a 50% shading coefficient was selected as the main case, which provides sufficient daylight under the shade mesh. Different scale mesh threads and geometry were compared to examine the effect of mesh scale on model accuracy outputs. These proposed scenarios were limited to examining the scale of threads, and the geometry of the shade mesh. The latter has a minor effect on thermal analysis and the amount of solar radiation that falls on the roofs compared to the shading coefficient. The simulation also compared the inputs of the shading coefficient, scale, and geometry of mesh with solar radiation on the horizontal surfaces and the dry bulb temperature of the test room.

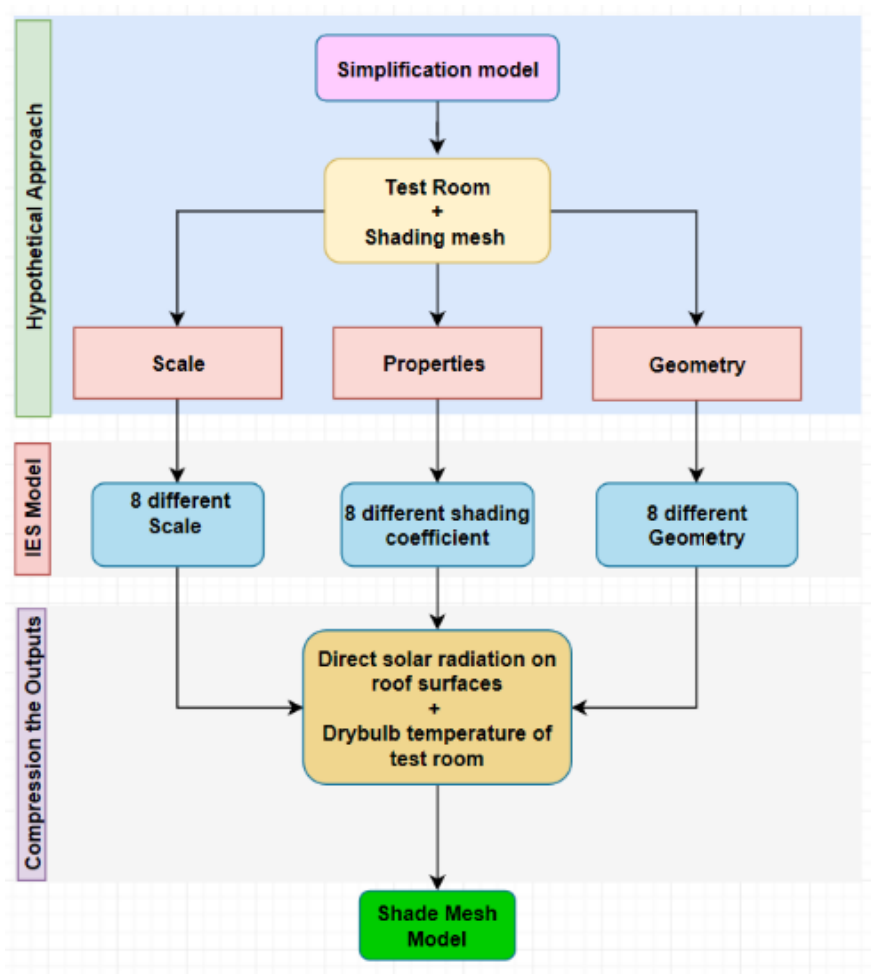


Figure 8.12: Model the shading mesh using IES-VE

8.5 Shading mesh model and validation

In order to simulate the shading mesh and validate the accuracy of the model, two simulation programs were used: IES and HTB2. The model and validation process for both programs used similar boundary conditions to examine the hypothetical test room.

The model and validation in this research was divided into two parts as below:

1. First part using IES model only, to simulate the test room and shading mesh (simplification model)
2. Second part using IES and HTB2, to model and validate the shading mesh.

8.5.1 IES shading mesh model

IES was used to simulate four basic points:

1. Quantify Roof Solar Radiation (RSR) on roof building surfaces with and without shading mesh
2. Simulate the shading coefficient
3. Compare different shading mesh geometry (SMG) types with a similar shading coefficient of 50%, to provide an acceptable level of daylight under the shading mesh
4. Model surface solar radiation and dry bulb temperature for the hypothetical test room.

A hypothetical residential test room was used to examine the performance of the shading mesh. The shading mesh was re-scaled and modelled using Auto Cad software, as shown in Figure 8.13. To test the model's accuracy, different scenarios of shading model were performed and a similar weather data file for a hot dry climate region was used, as discussed in Section 7.4. The simulation was for peak summer time on 1st July, 2017. The maximum and minimum daily air temperature in July is 40 °C and 27 °C, respectively, as shown in Figure 8.14.

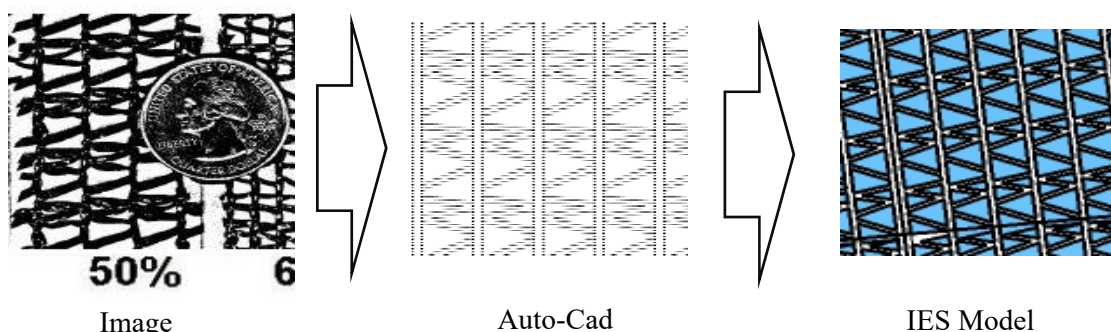


Figure 8.13: Process of rescaling the shading mesh from a real image to the IES model

The shading mesh threads are measured in millimetres and so are extremely small compared to the scale of the hypothetical test room (Figure 8.15). Moreover, the simplification model (Figure 8.12) was used to examine the capability of the IES program to simulate shading mesh as a design approach for the reduction of heat gain and energy consumption in a hot dry climate.

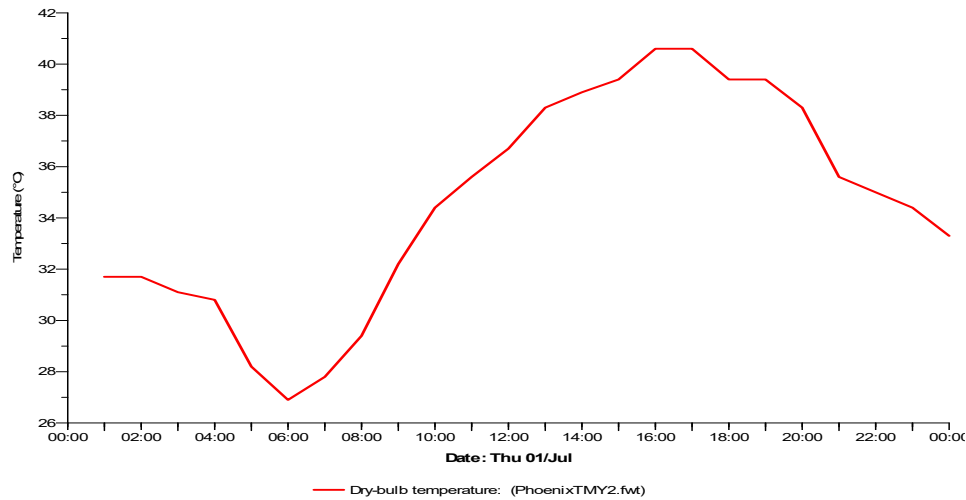


Figure 8.14: Dry bulb temperature of weather data file

The IES simulation was used to test the performance of the shade mesh model in two ways, to compare simulation running times (SRT), and compare output data (solar radiation and the dry bulb temperature of the test room).

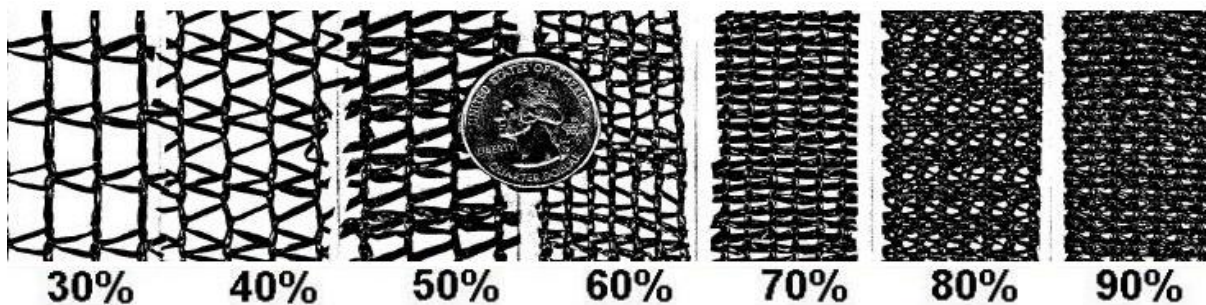
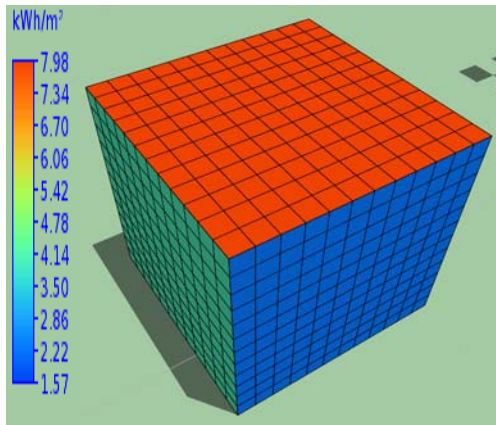


Figure 8.15: The scale of the shading mesh with different shading coefficient compared to a 5 pence coin

In order to simulate the shade mesh used by IES, the mesh segments were re-drawn and rescaled by Auto Cad using a real image, shown in Figure 8.13. Specific building input parameters were applied to the test room, as below:

1. Employ a hypothetical test room with 3m cube, without any openings (Figure 8.16)
2. Control heat gain through the roof only, using insulation materials with a thickness of 600mm applied to the ground floor and exterior walls.



The roof is the part of the building most affected by direct solar radiation compared to the exterior walls and ground floor

Figure 8.16: The surfaces most affected by direct solar radiation in buildings

The roof structure is comprised of concrete slab with roof tiles, and the U values of the envelopes that make up the test room are shown in Table 8.2. The heat flux through the walls and floor is thus minimised.

Table 8.2: Building materials for the hypothetical test room

Test Room	Material	U value W/m ² K	Surface Area (m ²)	Thickness (mm)	Density Kg/m ³	Cooling/ ventilation mechanism
Roof	Concrete Tile	4.3807	9	100	2100	Natural Ventilation
External Walls	Cellular polyisocyanurate	0.0381	36	600	32	
Ground floor	Cellular polyisocyanurate	0.0381	9	600	32	

3. Proposed scenarios are characterised below:

- a. First type, to test the Simulation Running Time (SRT)
- b. Second type, to test the shading coefficient (porosity) ranges starting with 40% to 100%
- c. Third type, to test shading mesh geometry. In this simulation, mesh segments are changed to test the efficiency of the model

4. Quantify the hypothetical test room's dry bulb temperature with and without shade mesh for all proposed scenarios.

8.6 IES shading mesh simplification model (scale, shading coefficient and geometry)

This section of the study presents the process of simulating the hypothetical test room with different shading mesh scales, shading coefficients, and geometry. The output of these simulations (generated scenarios) is compared with the unshaded cube. The next section explains in detail the shading mesh simplification model.

8.6.1 IES shading mesh model with 8 Scale

The first set of modelling presents the process of the model hypothetical test room and compares it with the base case model (Figure 8.17). This section concerns changing the size of the mesh scale. The shading mesh size and shape will affect the direct solar radiation that falls onto the horizontal and vertical surfaces of buildings. The porosity of the shading mesh was maintained constant at 50%, and the shading mesh extended over the test room as shown in Figure 8.17.

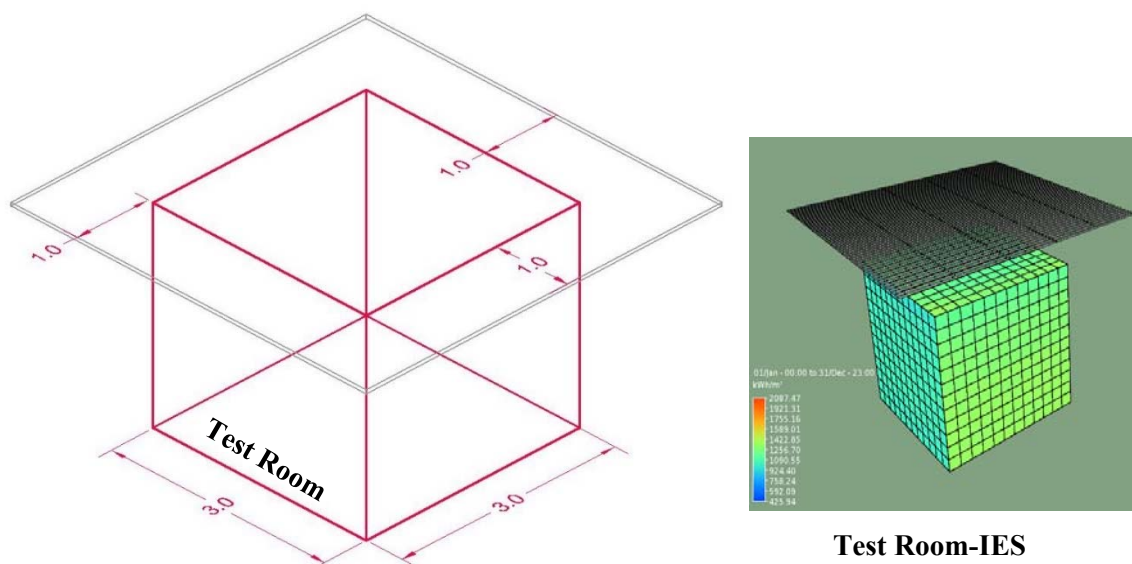


Figure 8.17: The test room with shade mesh

Eight different mesh thread sizes were modelled (Figure 8.18), starting with a crude checker board style mesh in which the thread width was 500 mm (shape 1, Figure 8.18). The final mesh thread size was 1.6 mm and produced an almost solid looking shade over the test room (shape 8, Figure 8.18).

As the thread size gradually reduced, the simulation time increased due to the number of surfaces being modelled. Table 8.3 shows this progression, with shape 1 having a simulation run time of three minutes, while shape 8 had a simulation run time approaching 24 hours.

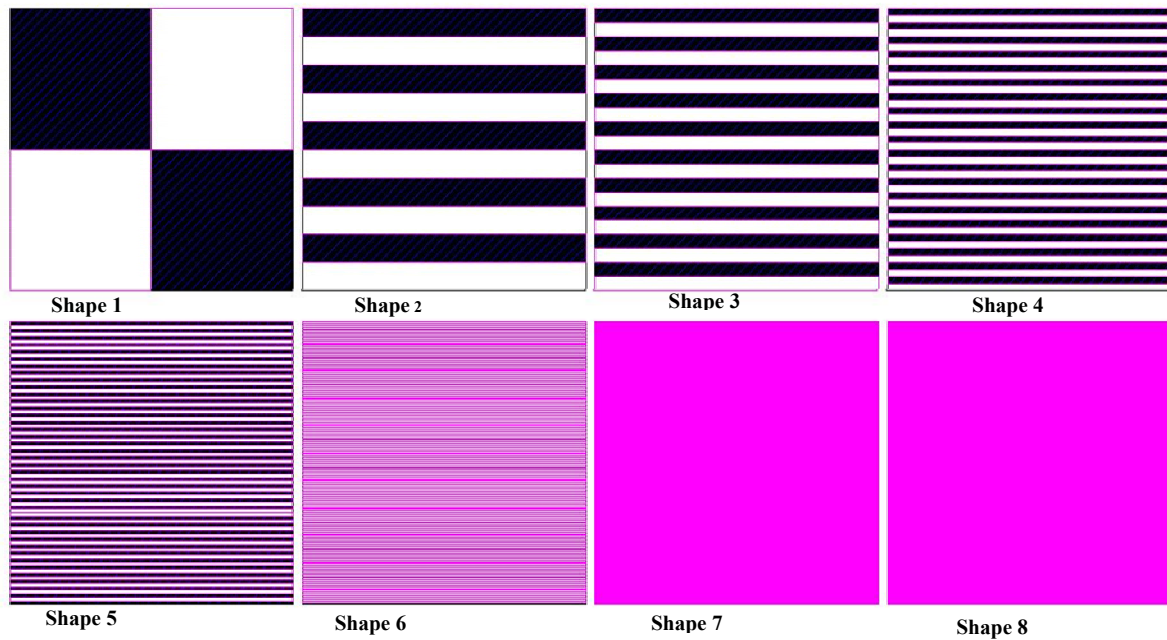


Figure 8.18: The shade mesh scale in 8 different scenarios. The scale of mesh segments reduced gradually from 500 mm to 1.6 mm

8.6.2 IES shading model with 8 shading coefficient.

8.6.3 IES shading model with 8 shading geometry.

Table 8.3: Shape patterns of shade mesh, showing the number of mesh segments in each scenario

Porous shape	Thread size (width of threads)	Simulation run time (Min)		Model surfaces (shade mesh surfaces)
		SunCast ¹⁴ simulation	Apache ¹⁵ simulation	
Shape 1	500 mm	2	1	50
Shape 2	100 mm	5	2	125
Shape 3	50 mm	24	5	250
Shape 4	25 mm	30	6	500
Shape 5	12.5 mm	50	8	1000
Shape 6	6.25 mm	80	10	2000
Shape 7	3.1 mm	3h	20	4000
Shape 8	1.6 mm	23:12	25	8000

8.6.4 Solar Shading Analysis

¹⁴ SunCast one of IES-VE parts which used for design process to model shading and solar insolation studies by generating images from 3D models.

¹⁵ Apache simulation is dynamic thermal simulation model which based on mathematical model of heat transfer process inside and around buildings (www.iesve.com).

The IES simulation program uses SunCast for solar insolation studies and shading analysis. It can be used to perform shading at any stage of the design process by generating images and modelling the solar effect on the surfaces using IES Model Builder. In addition, SunCast can be used to investigate the effect on energy demand of outdoor obstruction, self-shading of buildings, solar mapping, and building orientation. Sun position in this program is defined by date, time, orientation, latitude, and longitude of site. Moreover, it is able to produce shadows and internal solar insolation for any building or object defined by its position. SunCast can be used for passive solar design studies and is essential in the planning stage to identify the effect of sun shadow on the surrounding environment. More importantly, solar surface shading and insolation statistics can be modelled through this application. Table 8.3 shows that increasing the mesh density has an impact on simulation time. Figure 8.19–21 show the effect these different mesh sizes had on the radiation energy distribution on the roof of the hypothetical test room. For each mesh shape shown in Figure 8.19–21, showing two images, the upper image represents the shading mesh with the test room beneath. The lower image shows the solar radiation distribution over the roof surface (IES output). This is best understood by looking at shape 1, where the crude checker board pattern of the shading mesh is

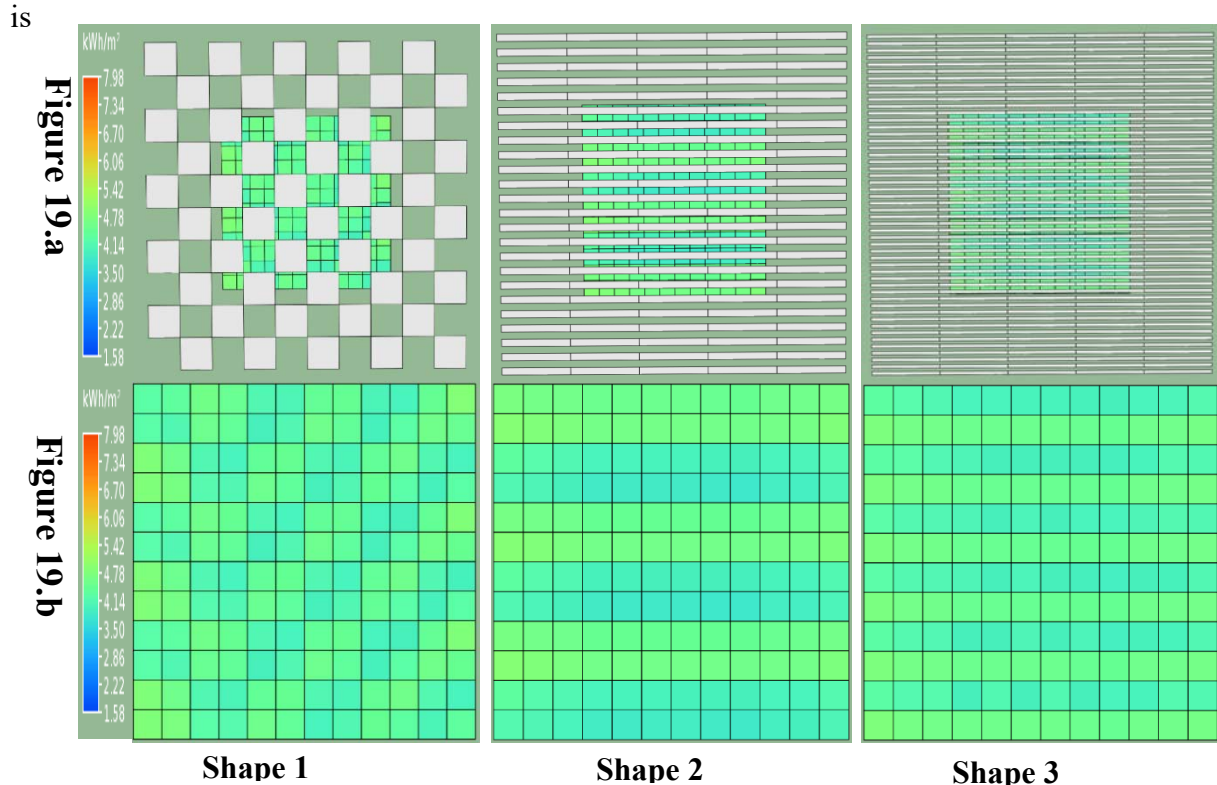


Figure 8.19: The top perspective view Showing the shade mesh mode for three scenarios, with solar radiation configuration image that fallen on the roof surfaces. Shape 4, 5 and 6 with similar 50% shading coefficient

replicated by the checker board pattern of the solar radiation distribution. Moving to shape 8, the checker board pattern disappears and an even solar radiation distribution is shown (Figure 8.19 - Figure 8.21).

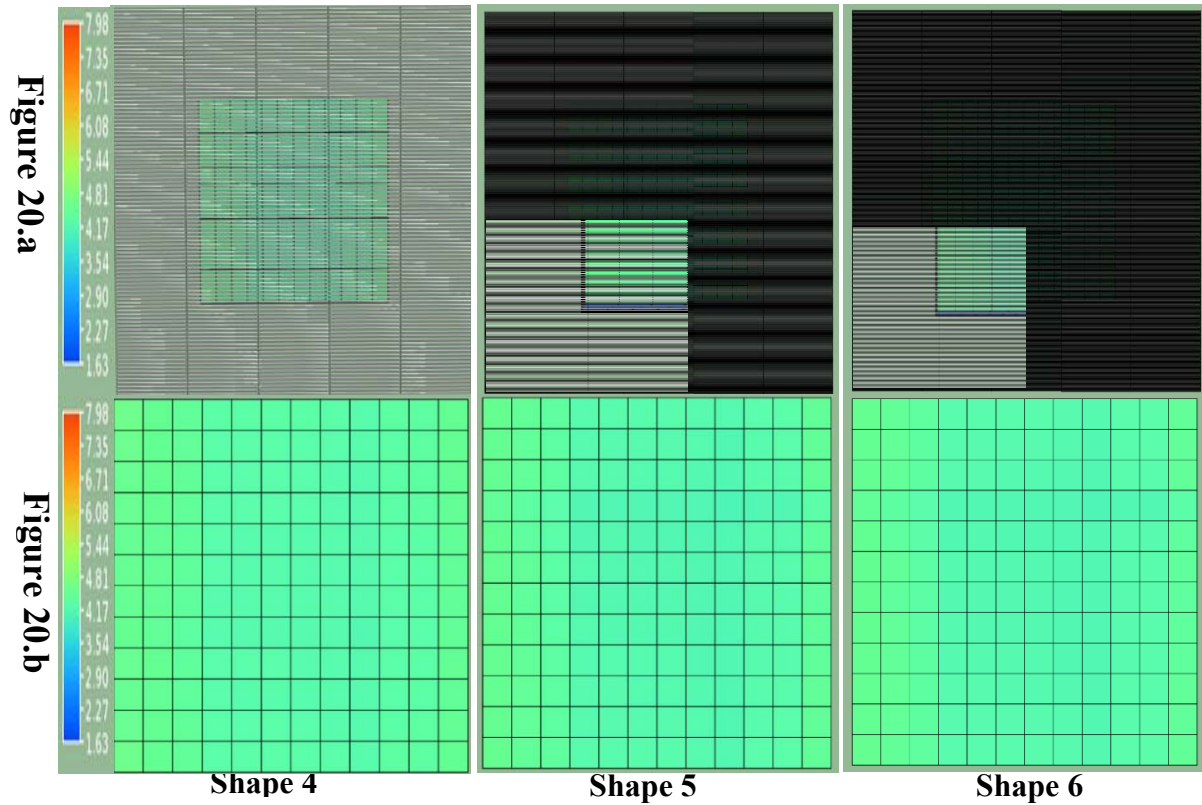


Figure 8.20: The shade mesh mode for three scenarios, with the solar radiation configuration image falling on the roof surfaces. Shapes 4–6 have a similar 50% shading coefficient

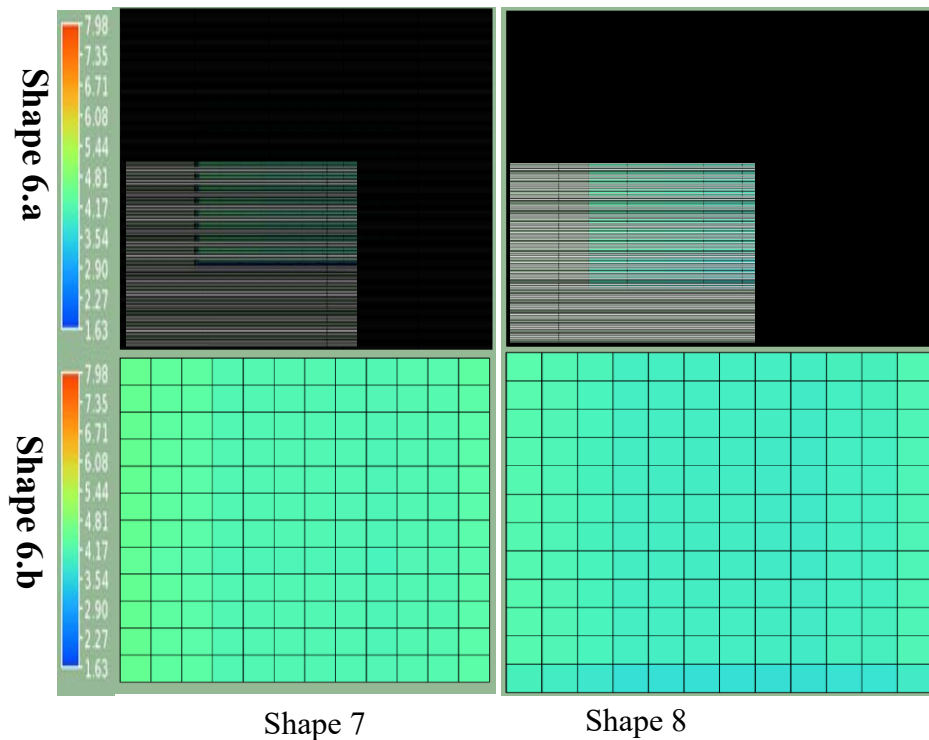


Figure 8.21: The shade mesh mode for two scenarios, with the solar radiation configuration image falling on the roof surface. Shapes 7 and 8 have a similar 50% shading coefficient

8.6.5 Thermal analysis simulation

Table 8.4: Dry resultant temperature and roof solar radiation for the base case and 8 scenarios. The IES model was used to generate (T) 4 times a day

Scenario and shape number	Roof solar radiation on roofs (kWh/m ² day)	Dry bulb temperature (T) of test room °C			
		6:00	12:00	18:00	24:00
Shape 1	4.38	30.31	38.13	44.38	33.11
Shape 2	4.30	30.31	38.13	44.37	33.1
Shape 3	4.33	30.31	38.13	44.38	33.11
Shape 4	4.33	30.31	38.13	44.37	33.11
Shape 5	4.32	30.31	38.14	44.38	33.11
Shape 6	4.32	30.31	38.12	44.33	33.1
Shape 7	4.23	30.3	38.09	44.27	33.08
Shape 8	4.28	30.27	37.96	43.9	32.96

Thermal analysis or Apache¹⁶ in the IES program use thermal input data, such as building location, weather data, and properties of building fabric to generate the thermal model. The hypothetical test room was designed to test the thermal analysis (3x3m, and 3m high), without any opening to control thermal analysis (Figure 8.17). The hot dry climate location and weather file were used, and the building properties are as shown in Table 2. In this simulation, the shade mesh effect on roof surfaces and room internal temperature were predicted. The hypothetical test room was used as the base case and modelled without

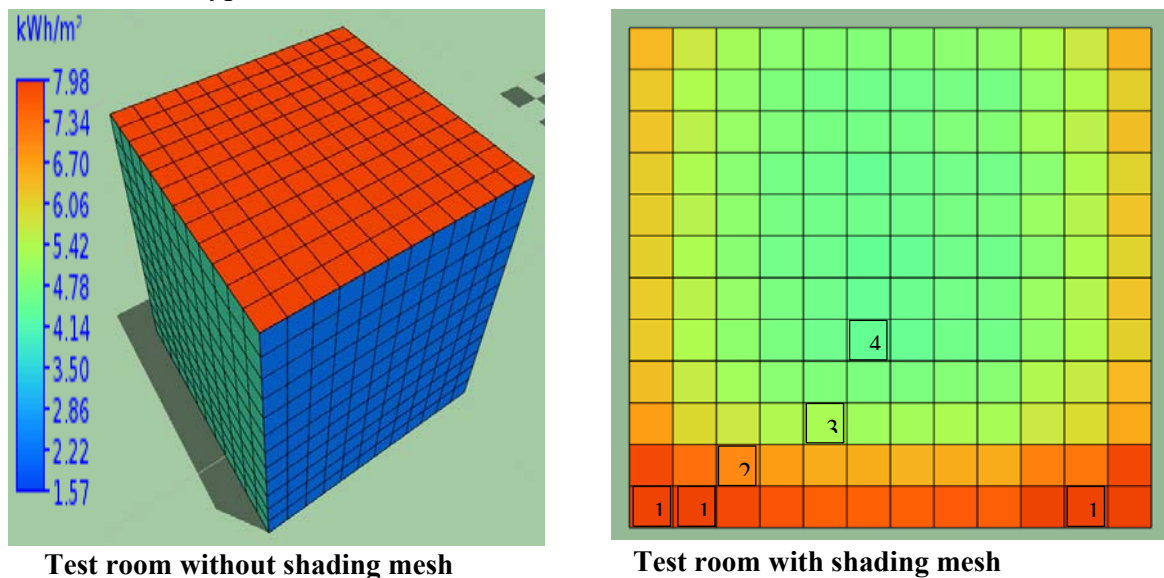


Figure 8.22: Roof solar radiation for the base case on the left hand side. A high resolution grid was applied on surfaces to accurately match the grid colour and colour chart

¹⁶ Apache simulation is dynamic thermal simulation model which based on mathematical model of heat transfer process inside and around buildings (www.iesve.com).

shading mesh, while the other eight scenarios were covered by shading mesh (Figure 8.19–21). A high resolution of 0.25 m² grid were applied to calculate direct solar radiation on the roof surface (Figure 8.22). The roof area of 9 m² was divided into 144 segments that received various levels of solar radiation when the shading mesh's pattern was altered in each scenario. To calculate solar radiation upon a specific surface, the grid was used to categorize the exact amount of solar radiation falling on a specific area measured in kWh/m². In Figure 8.22, each grid was measured and the colour chart on the left hand side represents the solar radiation value on the surface, according to the legend colour, and divided by the total number of grids.

Equation 1 calculates the solar radiation on the floor of the test room

$$\text{Solar radiation of any surface} = \frac{n1+n2+n3+n4...}{\text{all grid number}}$$

Where n is the surface grid with a specific colour. Each colour represents a radiation heat flux. The process enabled the total radiation on the roof surface to be estimated.

Dry resultant temperature was predicated for all eight scenarios with the shading mesh four times a day, and for the base case. The aim of this calculation is to represent the effect of the shade mesh on the room temperature (Table 8.4 and Table 8.5). In Table 4, for roof shape 1, the total radiation heat flux was 4.38 kWh/m² day, while the more intensive model, shape 8, had a total radiate heat flux of 4.28.

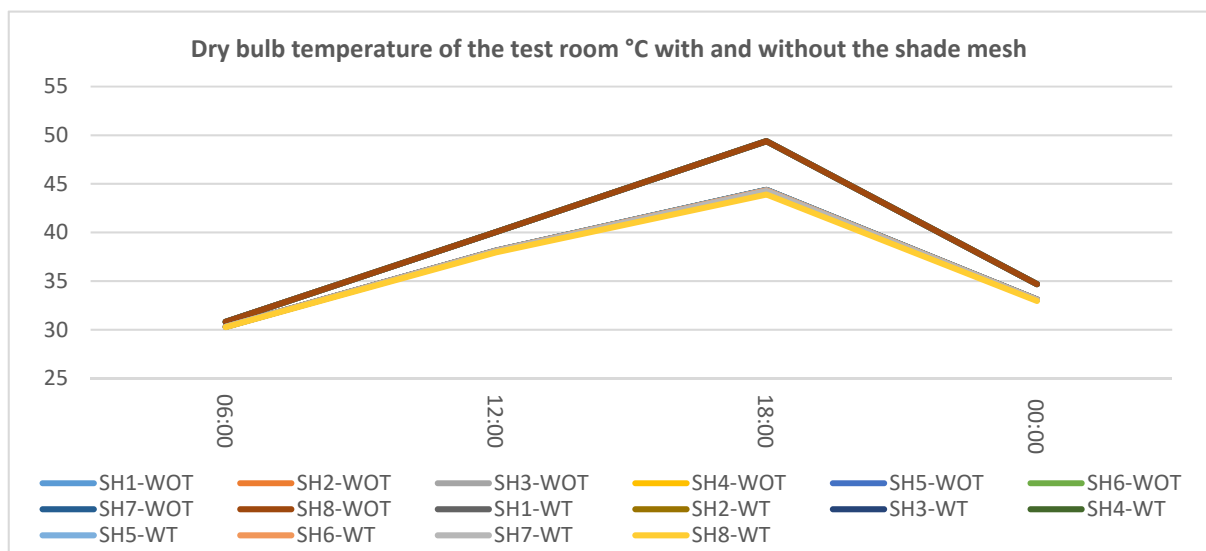
For dry bulb temperature predicted in the room, the variation from shape 1 to shape 8 was small. At 6:00 in the morning, the difference was 30.1°C–30.27°C, and the 0.04 K is negligible. At 12:00 midday, the difference was 38.13°C–37.96°C, 0.17 K, at 18:00 the difference was 0.48 K, and at 24:00 midnight the difference was 0.15 K (Table 8.4).

To Table 8.5 shows the impact of shading mesh modelling scale on the indoor dry bulb air temperature, the change of scale has only a small impact on the predicted values. However, the shading mesh is effecting the test rooms Dry Bulb temperature when the simulation results compare between hypostatical test room with and without shading mesh. No impact is seen at 6:00 and 24:00 but at 12:00 and 18:00 the impact is marked, at 18:00 the differences is greater than 5K. Figure 8.23 shows the test room dry bulb temperature with and without shading mesh. The maximum air temperature was recorded at 18:00 for the test room without the shading mesh

Table 8.5: Comparison of dry resultant temperature for the base case and 8 scenarios. The IES model was used to generate (T) 4 times a day

Scenario and shape number	Dry bulb temperature of test room °C without shade mesh				Dry bulb temperature of test room °C- with shade mesh			
	6:00	12:00	18:00	24:00	6:00	12:00	18:00	24:00
Shape 1	30.82	40.05	49.39	34.7	30.31	38.13	44.38	33.11
Shape 2	30.82	40.05	49.39	34.7	30.31	38.13	44.37	33.1
Shape 3	30.82	40.05	49.39	34.7	30.31	38.13	44.38	33.11
Shape 4	30.82	40.05	49.39	34.7	30.31	38.13	44.37	33.11
Shape 5	30.82	40.05	49.39	34.7	30.31	38.14	44.38	33.11
Shape 6	30.82	40.05	49.39	34.7	30.31	38.12	44.33	33.1
Shape 7	30.82	40.05	49.39	34.7	30.30	38.09	44.27	33.08
Shape 8	30.82	40.05	49.39	34.7	30.27	37.96	43.9	32.96

The graph shows a gradual increase in temperature difference between the shaded and unshaded areas during the day time, reaching a peak time at 18:00. The effect of the shading mesh on dry bulb air temperature started to reduce after 18:00 when the sun sets (Figure 8.23).

**Figure 8.23: Dry bulb temperature for hypothetical test room with and without shading mesh**

In this set shading coefficient is fixed. The results show that the shading Mesh Segments Scale (MSS) has a minor effect on model performance (Table 8.5), but a significant effect on Simulation Run Time (SRT) (Table 8.3). The shading mesh can be modelled with a large MSS without affecting the solar radiation on the roof and the inside dry bulb temperature.

8.6.6 IES shading mesh model with 8 shading coefficient

Shading mesh coefficient can be defined as the distance between any two threads (mesh segments) in the similar weft direction. The porosity of shade mesh can be defined as the percentage of open area in the mesh body divided by the total area of the shade mesh. The porosity of shading mesh may be affected by the direct solar radiation (DSR) that falls onto

the horizontal and vertical surfaces of buildings. DSR passes through the porous mesh and falls on the roof surfaces, while closed areas of the mesh body (shade mesh segments) reflect and absorb the rest of the DSR, and then re-radiates or convects, conducts or stores the

surplus energies. The mesh size is normally given by mm, and for shading purposes the shade meshes are between 2.5 to 4 mm, while the thickness of the shading mesh is measured by the thickness of single threads (mm). In this simulation, both the size and thickness were fixed, because there is a minor effect of the mesh segments scale (MSS) on model performance and results, as shown in the previous section (shading mesh scale simulation). The aim of this simulation is to determine the effect of the shading mesh coefficient on roof solar radiation (RSR) that falls onto the roof surfaces, with and without shading mesh. The simulation process starts with a comparison of shading meshes, from 40% to 100% (Figure 8.24 and 28).

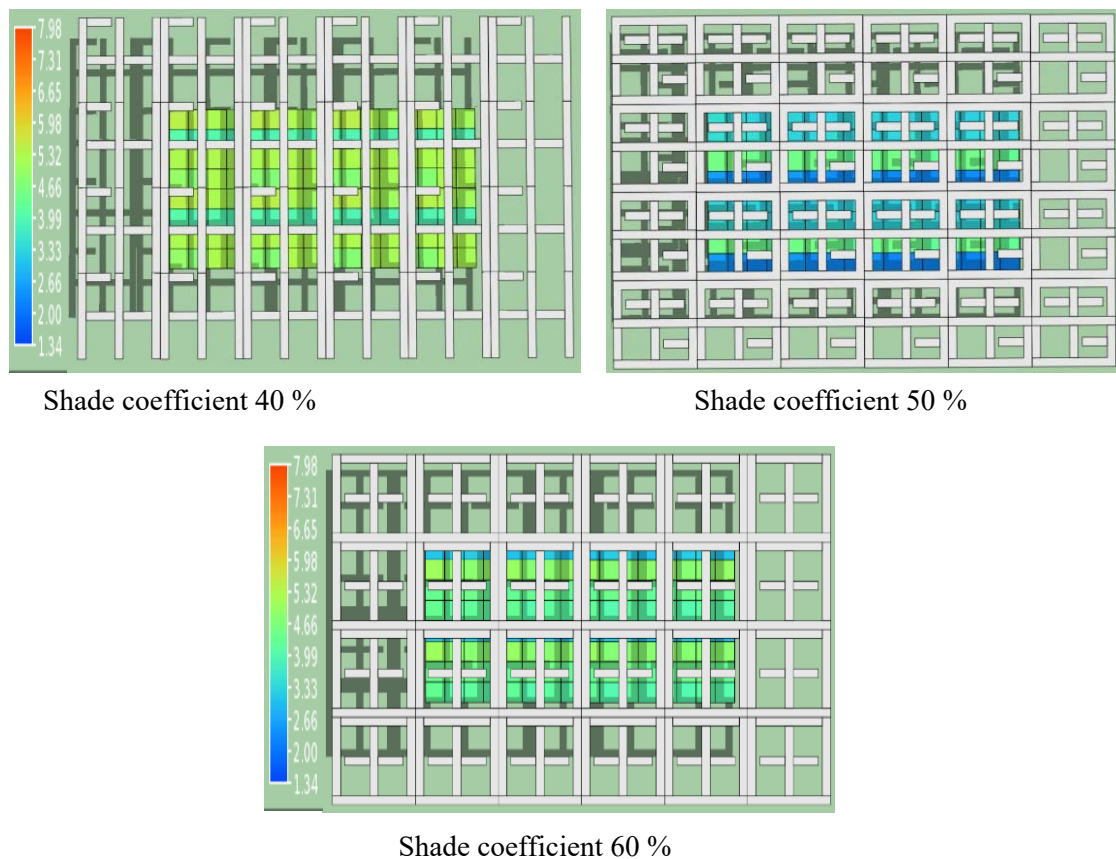


Figure 8.24: Test Room with 40%, 50% and 60% shading coefficient

8.6.7 Shading mesh coefficient types

The process of simulation for different shading coefficients is divided into two parts. The first part compares three different shading coefficients of 40%, 50% and 60%, while the second part of the simulation compares five types of shading coefficients at 50%, 60%, 70%, 80%, 90% and 100%. In the first part of the simulation, three different shading coefficients were simulated with similar mesh texture (see Figure 8.24). The results compared both thermal analysis and solar radiation over the roof. Dry bulb temperature for both the weather data file and test room with shading mesh were first compared to show the efficiency of the IES model. Figure 8.25 displays the external dry bulb temperature and the internal predicated dry bulb temperature for the unshaded room, for the first two days of July. The black solid line in Figure 8.25 indicates the internal unshaded dry bulb temperature, which will be used to compare the effectiveness of different shading mesh coefficients. The results show that the base case test room record higher dry bulb temperatures and a small shift time (Figure 8.25). All three diffident shading meshes with 40%, 50%, and 60% coefficients were compared with the base case test room (without shading mesh) (Figure 8.26). The results show that as the coefficient increases, the maximum dry bulb temperature decreases and there is a displaced time shift. The minimum dry bulb temperature shows only a small change and time shift.

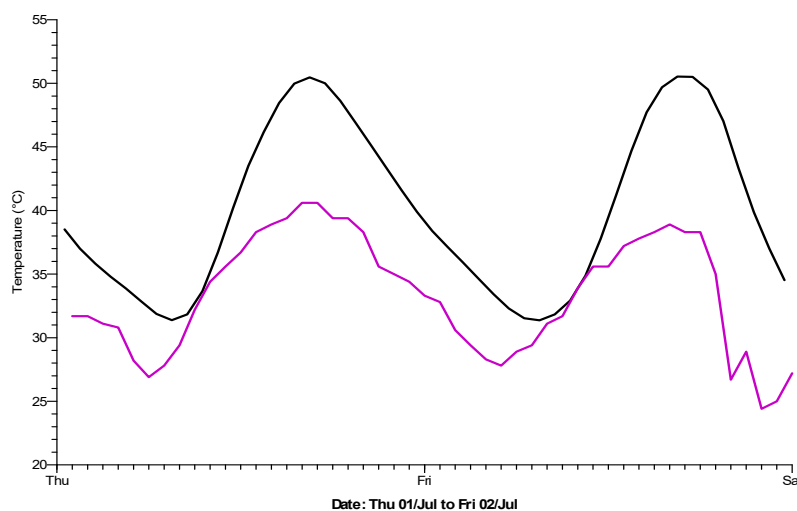
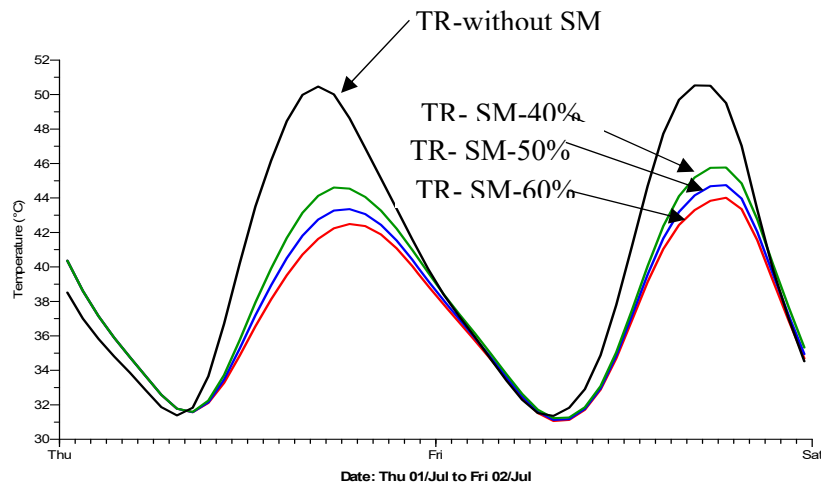


Figure 8.25: Comparison of dry bulb temperature for the test room and weather data file

The second part of this scenario determined how increasing shading coefficient reduces both the Roof Solar Radiation (RSR) and the dry bulb air temperature of the test room through a reduction in direct solar load falling on the roof.



1. Dry bulb temperature for test room without shade mesh
2. Dry bulb temperature for test room with shade mesh and 40% shading coefficient
3. Dry bulb temperature for test room with shade mesh and 50% shading coefficient
4. Dry bulb temperature for test room with shade mesh and 60% shading coefficient

Figure 8.26: Dry bulb temperature for the test room with and without shading mesh for 1st and 2nd of July 2017

The second part of the simulation tested six shading coefficient types –50%, 60%, 70%, 80%, 90% and 100% (see Figure 8.27). The shading coefficient ratio in this simulation is the

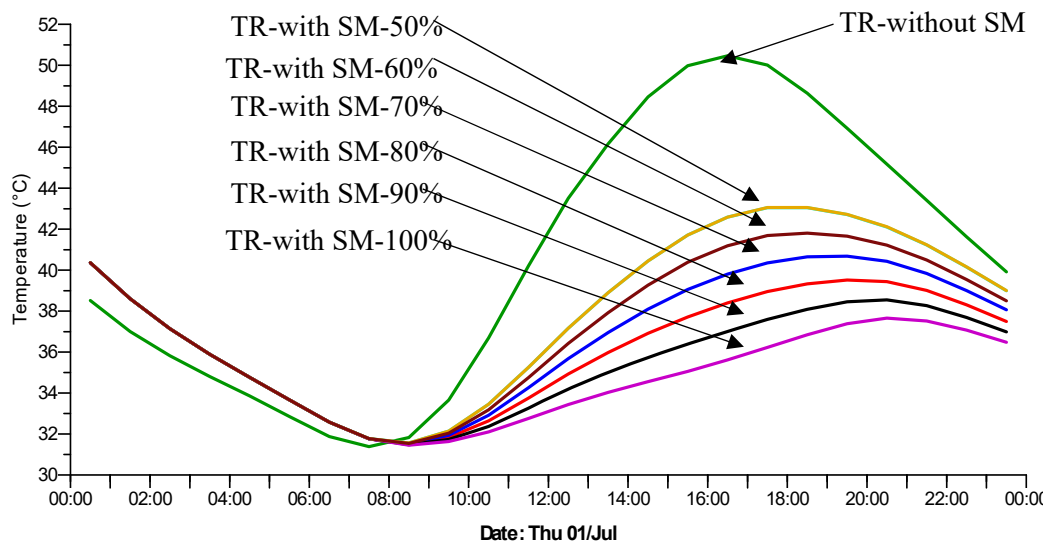


Figure 8.27: Dry bulb temperature for the test room with and without shading mesh, 1st July 2017

amount of space between shading segments. For example, with the 50% shading coefficient, 50% of the DSR passes through the shading mesh and 50% is reflected and absorbed by the shading mesh body.

Figure 8.28 shows the shading configuration used to achieve these coefficients. Figure 8.27 shows the results for 1st July 2017 only. As would be expected, increasing the shading coefficient decreased the peak dry bulb temperature, with no effect on the minimum dry bulb temperature. A less obvious aspect of the increased shading coefficient is the time delay of the peak dry bulb temperature. In Figure 8.27, the unshaded part has a peak dry bulb temperature at 16:00, while the lower peak for the 100% shading coefficient occurs after 20:00. This reflects the thermal mass of the test room heating up more slowly due to reduced solar gain. The simulation set shows that increasing the shading mesh coefficient reduced the DSR on the roof and decreased the dry bulb air temperature of test room.

8.6.8 IES shading mesh model with 8 Geometry

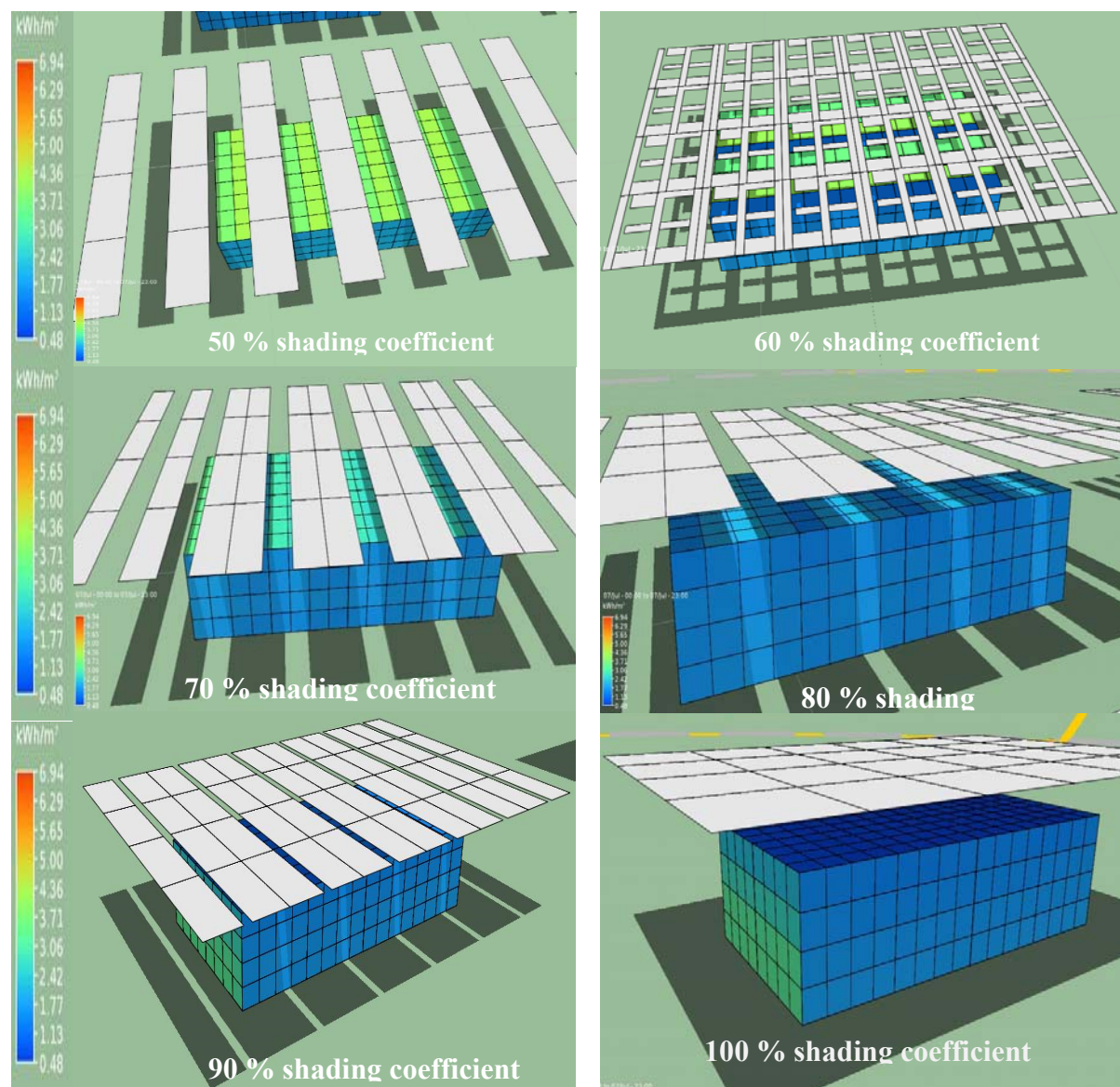


Figure 8.28: Test Room with 50, 60, 70, 80, 90 and 100 % shading coefficient

Shade mesh geometry or mesh segment shape may have an effect on the thermal analysis and solar radiation of any surface under the shade mesh. The aim of this simulation is to determine the effect of shade mesh geometry on the thermal properties of the test room. The simulation started by comparing eight different geometries of shade mesh with the same shading coefficient of 50%, as shown in Figure 8.29. The DSR spots can be altered by changing the row and column of mesh segments. Day lighting is also taken into account through the process of designing the shade mesh, and a shading coefficient of 50% will allow enough day light to enter the space. This test used eight types of mesh geometry to determine the effect of mesh-geometry on the solar radiation and dry bulb temperature of the test room. The test room's building fabric properties are shown in Table 8.2. In addition, similar environmental conditions and climate location were applied for all scenarios.

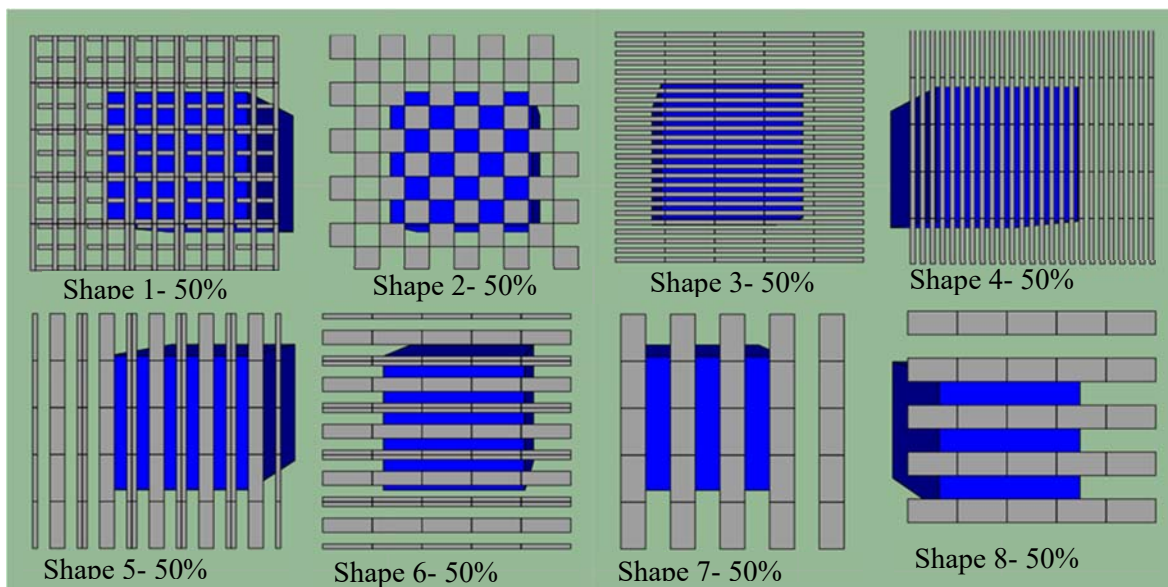


Figure 8.29: Eight different shade mesh geometry with similar 50% shading coefficient

IES was used to simulate eight different geometries of shading mesh through the SunCast simulation to predict the solar radiation on the test room roof. Figure 8.30 shows all geometries with shade mesh.

8.6.9 Direct Solar Radiation (Roof of Test Room)

IES SunCast was used to calculate solar radiation upon the test roof; after the simulation run was completed, a colour grid was used to categorise the amount of solar radiation on the roof of the test room, measured in kWh/m². The colour chart on the left hand side represents the solar radiation value on the surface, and each grid is measured to the legend colour and divided by the total grid number of 144 units (Figure 8.30).

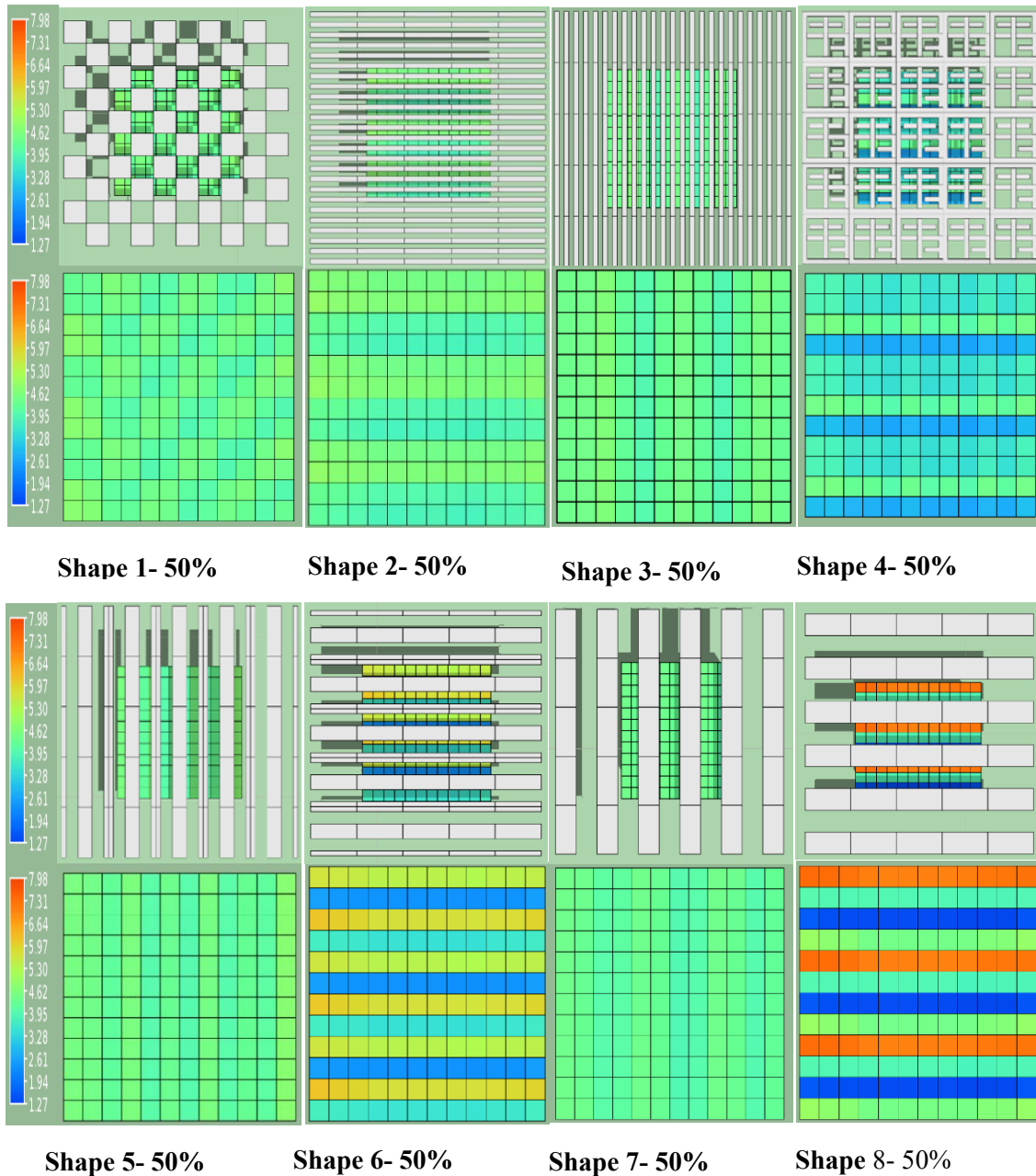


Figure 8.30: Eight different shade mesh geometries, with 50% shading coefficient. Each image represents single solar roof radiation with and without external shade

The eight geometries have different shapes but similar physical characteristics, such as shading coefficient and mesh thickness. The solar radiation on the top for all geometries was similar to the shading coefficient of 50% for all geometries.

Table 8.6: Eight shapes of solar roof radiation calculated manually in colour charts

Geometry	Shape 1	Shape 2	Shape 3	Shape 4	Shape 5	Shape 6	Shape 7	Shape 8
Solar radiation kW /m ²	4.125	4.11	4.15	4.12	4.10	4.16	4.16	4.11

The maximum solar radiation was 4.16 kW/m^2 and the minimum 4.10 kW/m^2 for shapes 6 and 5, respectively (Table 8.6). Overall, the results show that shading mesh geometry has a limited impact on DSR.

8.6.9.1 Dry Bulb Temperature (Inside Test Room)

Dry bulb temperature was predicted for the hypothetical test room with eight different shading mesh geometries, both with shading mesh, for 2nd July 2017 and the base case. The aim of this simulation was to investigate the impact of the shade mesh geometry on the test room's dry bulb temperature. Figure 8.31 shows that the dry bulb temperature for the test room had similar shading mesh geometry, while the ambient temperature was lower than the test room both with and without the shade mesh (Figure 8.31).

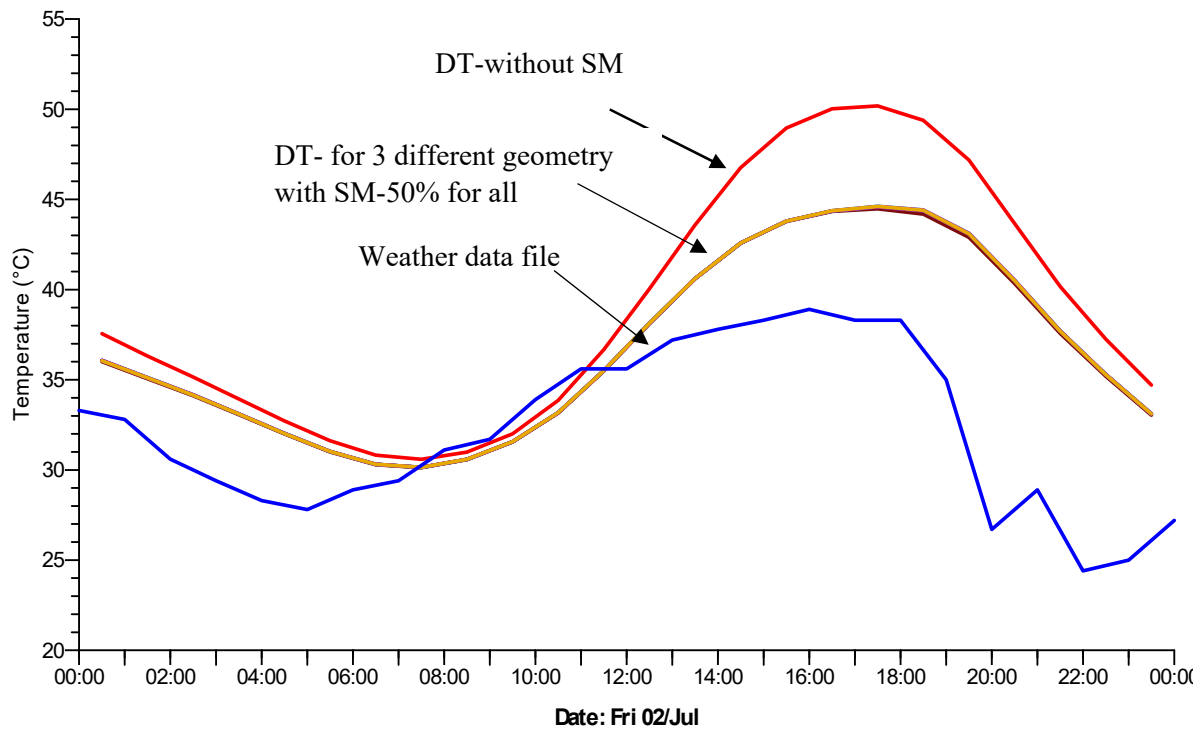


Figure 8.31: Ambient dry bulb and dry bulb temperature for the test room with three geometry shading meshes and 50% shading coefficient for all, compared with the test room without shading mesh

The maximum dry bulb temperature was 50.1°C without shading mesh and the maximum dry bulb temperature with shading mesh was 44.45°C for the test room. The impact of the shading mesh on the inside dry bulb temperature during day time was significantly more than at night time. The dry bulb temperature differences at 16:00 was 5.55 K, and 0.8 K at 7:30 am for day and night time, respectfully (Figure 8.31).

Figure 8.32 shows the impact of the shading mesh on the indoor dry bulb air temperature, which corresponds to the hypothesis that the shading mesh geometry does not have an impact on the air temperature and solar radiation in the test room. However, the shading mesh does affect the inside test room dry bulb temperature significantly when the simulation results are compared between the test room with and without shading mesh.

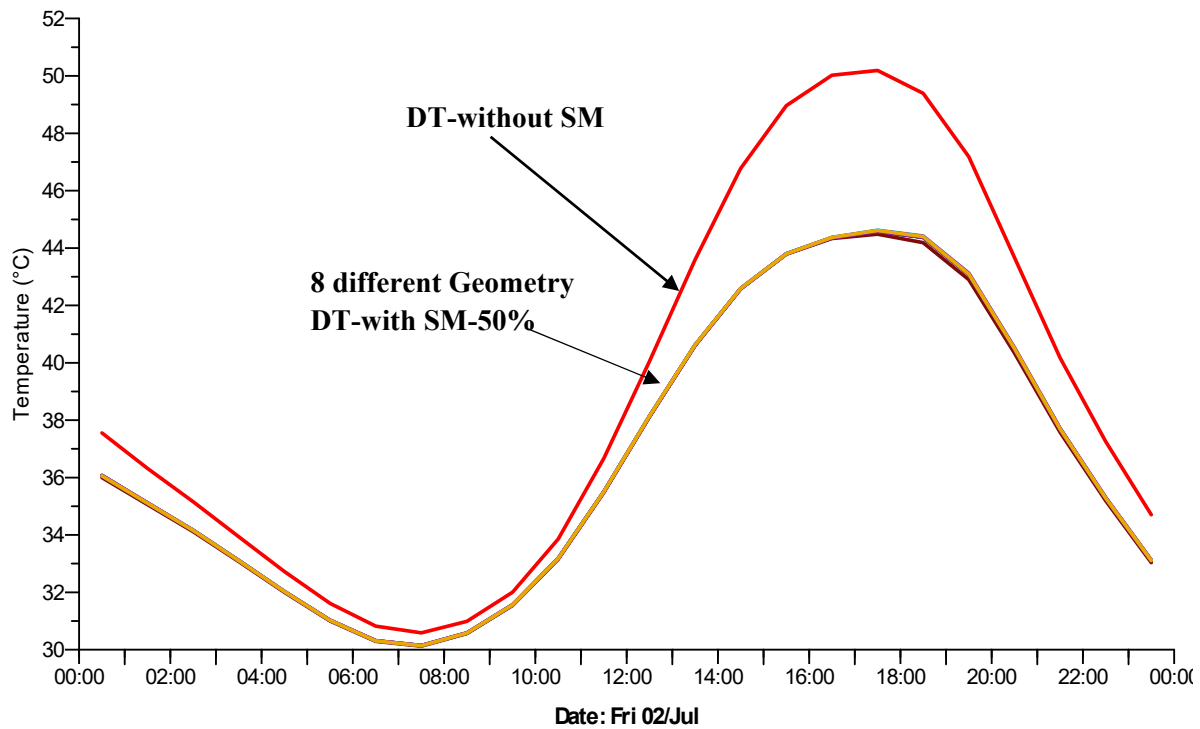


Figure 8.32: Dry bulb air temperature for the test room with three geometries of shading mesh and 50% shading coefficient for all, compared with the test room without shading mesh

8.7 Model Validation

Validation of the IES model can be achieved by *in situ* measurements, but for safety reasons this form of validation was not possible in Kurdistan. To test the validity of the IES models, another simulation package was employed. This study used two different simulation programs, IES and HTB2, to validate the base case model. In the last section, the IES model was discussed; in this section, the HTB 2 model will be explained and compared, and the model's results presented.

8.7.1 HTB 2 Model

The HTB 2 simulation program can be used in Sketch up.¹⁷ It can predict the solar radiation falling on the surfaces and heating and cooling energy demand. In addition, it can test the energy performance of any shape or form, the impact of terrain, and the effect of building surroundings and shading devices. Moreover, the model manipulates direct, normal direct and diffuse solar radiation to calculate the amount of solar radiation falling on external surfaces. The HTB2 model considers orientation, the tilt of external surfaces, surface transparency, and the surrounding site through building shading masks. The shading mask divides the sky dome above the external surface into 324 blocks measured by 10 by 10 degrees (Figure 8.33).

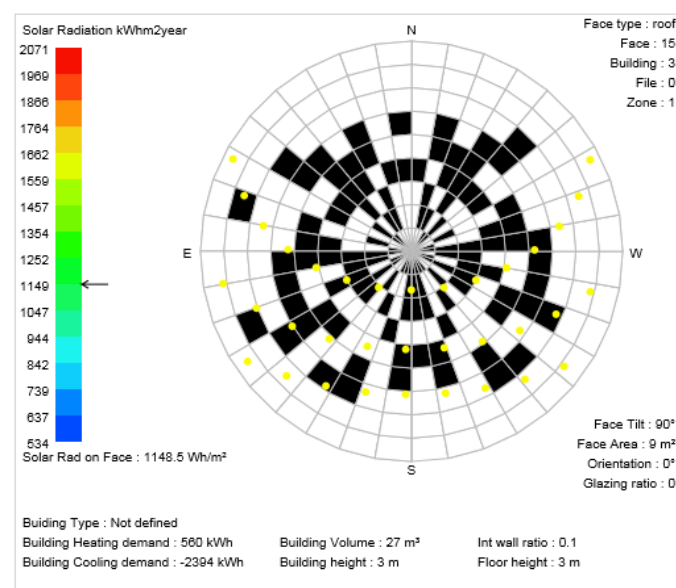


Figure 8.33: Shading mask represented as a sky dome divided into 324 blocks 10 by 10 degrees, the black areas represent obscured, and white areas clear sky

The HTB2 Building Energy Model (BEM) uses Sketch-up to simulate a large group of buildings in an urban context with various input files about the building and microclimate environment surround the site (Huang, Jones et al. 2017). The input data describe the building layout, construction system, HVAC systems, weather data file, topography features of the site, and the Sketch-up plugin is used to calculate solar radiation on external surfaces (Jones, Lannon et al. 2013). The model results were generated with an Excel file and included the model outputs and a surface solar radiation map.

¹⁷ Sketchup is a 3D modelling software which used for creating and editing 2D and 3D models.

The model working with a Vir Vir¹⁸ plugin for Sketch-Up was developed by the Architecture School, Cardiff University. HTB2 is an advanced numerical model which has been developed, tested and validated extensively IEA Annex1, IEA task 12, IEA BESTEST (Yao, Luo et al. 2011). The HTB2 model is highly flexible and easy to modify, so it is well suited for use in the field of energy and sustainable building design. Vir Vir Plugin and HTB2 can be linked and used as a dynamic thermal simulation for single or multiple buildings in an urban scale model. The model has the ability to model shadow from other buildings. Through this model, complex objects and forms can be modelled with the assistance of Sketch-Up. For shading mesh, IES needs a long running time to simulate 24 hours, but HTB2 can simulate much faster.

8.7.2 The IES and HTB2 Model Process

In this section, both IES SunCast and HTB2 model results were compared to validate the performance of the shading mesh model. The aim of this validation was to support the hypothesis that shade mesh segments can be simplified by crude objects without limitation on shading coefficient performance. To quantify the amount of solar radiation which falls onto roof surfaces, a hypothetical test room was modelled by manipulating two building energy simulation programs. The input data needed to describe building variables was similar for both models, such as location and orientation, dimensions, external shading geometry, shading coefficient, and the weather data file.

Three shapes were modelled as a shade mesh and the output results of the hypothetical test 3m room were compared. Solar radiation was measured over the roof surfaces of these test rooms for one year.

8.7.2.1 IES model simulation

SunCast simulation was used to predict fallen solar radiation on roof surfaces. Three different shapes of shading mesh were compared with the test room, which had no external shading (Figure 8.34). Solar radiation was measured using IES modelling with a high resolution grid applied over the roof surface. The grid size was 0.25m², and the roof surfaces were 9m², giving a 144 grid. The solar radiation was estimated for each grid square, to simulate the whole roof.

¹⁸ VirVil : it is a SketchUp extension and uses as an energy simulation tool. It is usable, simple, accessible, and flexible. This plugin is links the 3D design tool (SketchUp) to a Dynamic simulation model HTB2.

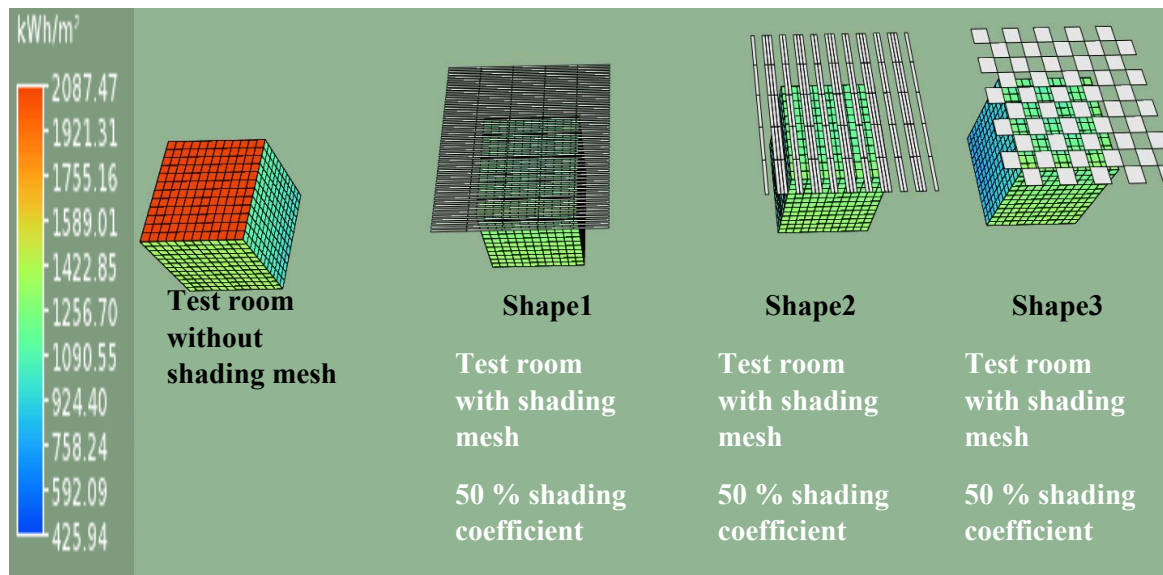


Figure 8.34: Shading mesh laid over the hypothetical test room in three shapes. Shading coefficient is similar for all shapes

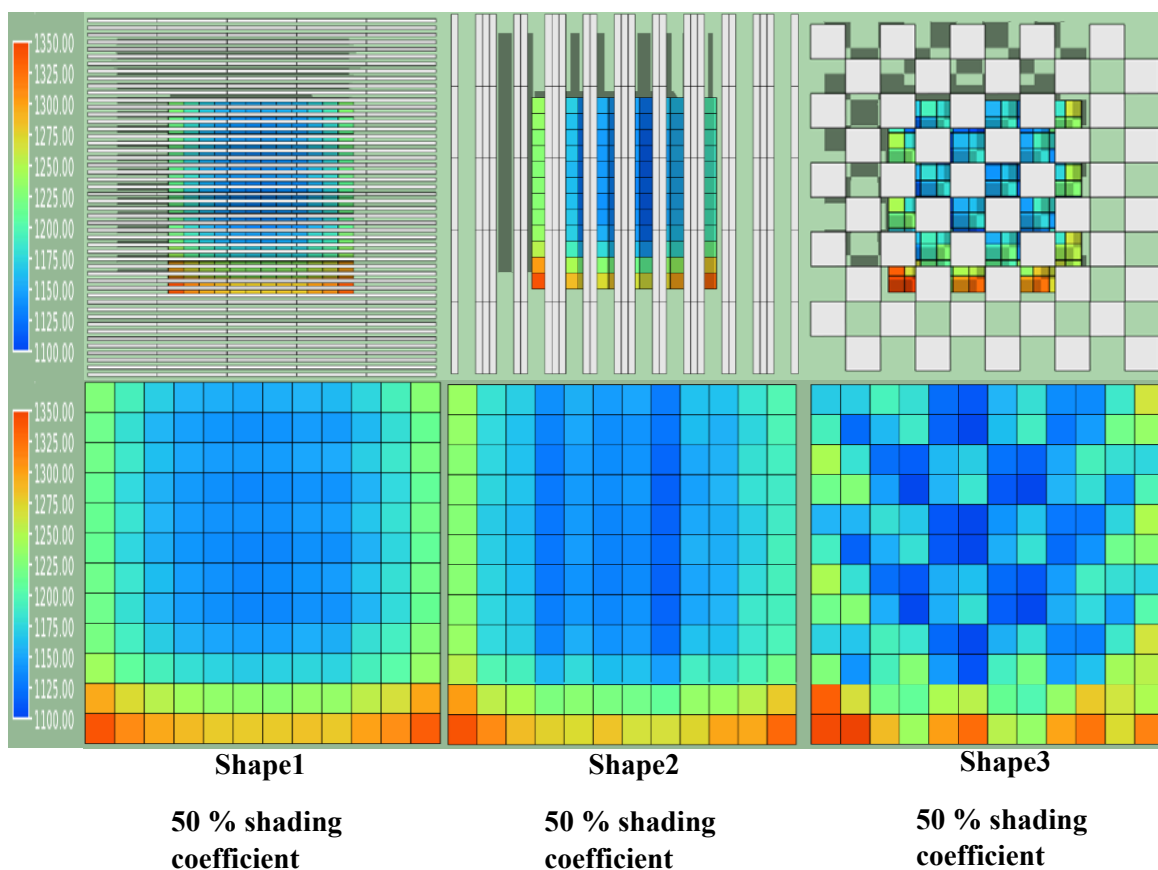
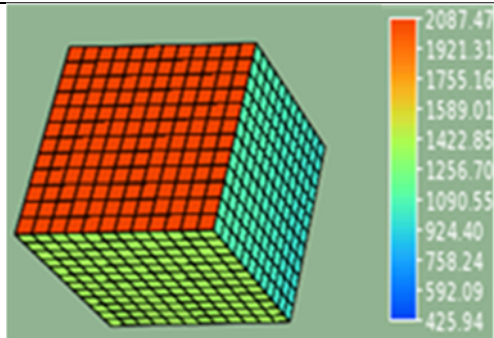
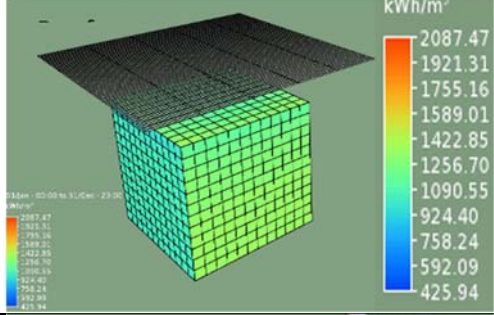
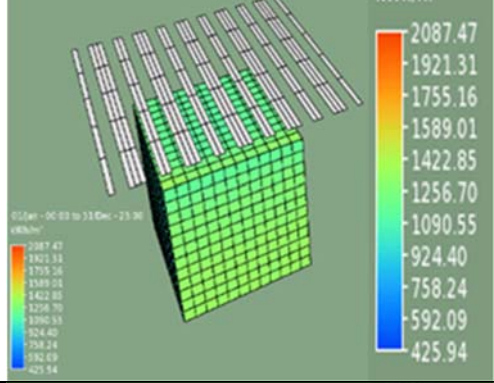
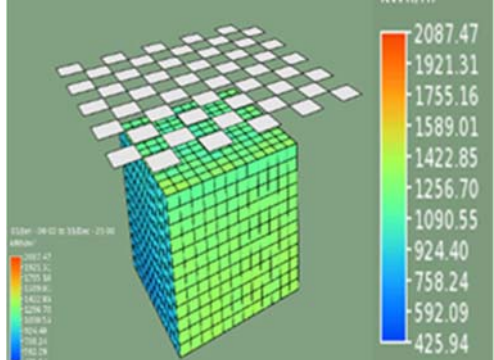


Figure 8.35: IES model for the test room with three different shading meshes

The results show that the values of direct solar radiation on roof surfaces were similar, but with different colour patterns, as shown in Figure 8.35. These colour patterns were calculated using the method described in Section 7.7.2.

Table 8.7: IES model outputs showing the effect of shading mesh on annual direct solar radiation on floor surfaces

Model type	Annual solar radiation on roof surfaces kW/m ²	IES model
Test room without shading mesh	2087.47 kW/m ²	
Shape 1, and 50 % shading coefficient	1178 kW/m ²	
Shape 2 and 50 % shading coefficient	1206 kW/m ²	
Shape 3 and 50 % shading coefficient	1157 kW/m ²	

The maximum annual solar radiation on the roof was recorded for the test room without shading mesh. For the three shapes, the annual solar radiation had small differences at 1,178, 1,206, and 1,157 kW/m² for shapes 1, 2 and 3, respectively. The three shading mesh

geometries were different in shape but had similar physical characteristics, such as shading coefficient and mesh thickness. The solar radiation on the top of all these was similar, as the shading coefficient was 50% for all geometries (Table 7). Overall, the results show that changing shading mesh geometry had a limited impact on direct solar radiation, although the shading mesh had a significant impact on fallen solar radiation on the roof surfaces when the test room was compared with and without shading mesh.

8.7.3 HTB2 model and Sketch-up model simulation

As previously discussed, the building simulation model HTB2 is a widely used simulation program in research and practical projects as a tool to predict the impact of form and shape on energy performance. In this study, it was used to quantify solar radiation over roof surfaces. The Sketch-up 3D program was used to build the model and run the HTB2 model, as shown in Figure 8.36.

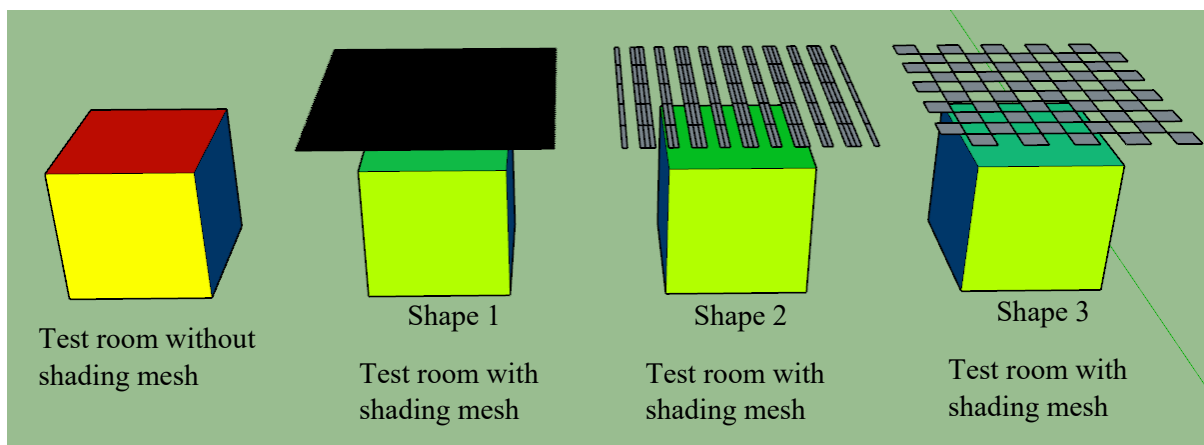
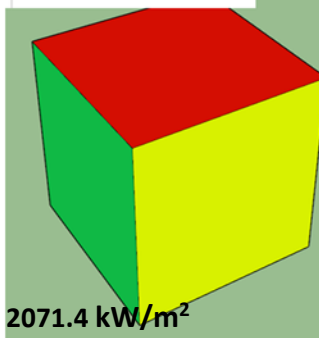
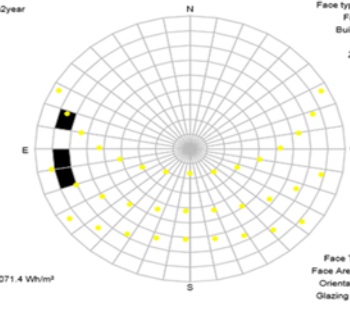
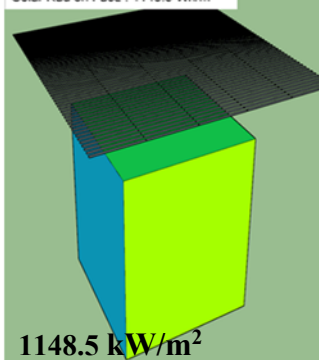
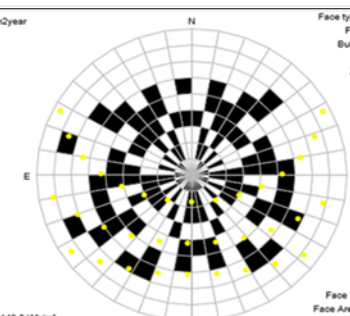
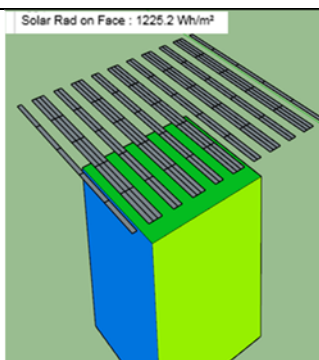
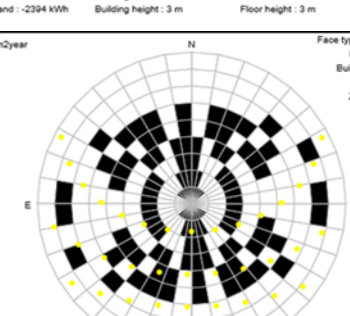
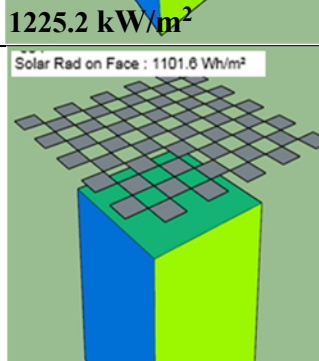
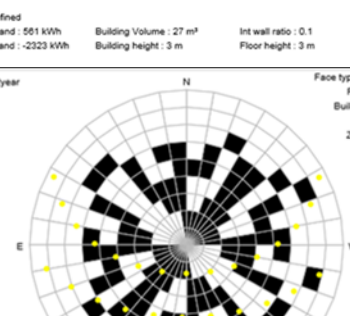


Figure 8.36: Sketch-up model used to run and design mesh objects. Three shapes of shade mesh were applied over a similar hypothetical test room. Input data and shading coefficient were similar for all objects

HTB 2 was used to model the test room without the shading mesh and the test room with three shapes of shading mesh. The three shading meshes had different shapes, but were similar in physical characteristics such as shading coefficient and mesh thickness. The direct solar radiation was measured using the HTB2 model through building shading masks. The shading mask divides the sky dome above the external surface to 324 blocks measured in 10 by 10 degrees (Table 8.7). The test room shading mask was generated for all scenarios; one without the shading mesh and three with. In this simulation, the test room size and shape, orientation, building materials, face area of the internal wall ratio, and face tilt were fixed. The results were presented in two ways, with a colour chart and shading mask of the sky dome (Table 8.7).

Table 8.8: HTB 2 model outputs showing the effect of the shading mesh on annual DSR on floor surfaces

Model type	Annual solar radiation on roof surfaces kW/m ² HTB 2 model
Test room without shading mesh	<p>Solar Rad on Face : 2071.4 Wh/m²</p>  <p>2071.4 kW/m²</p> <p>Solar Radiation kWh/m2year</p>  <p>Face type : roof Face : 21 Building : 4 File : 0 Zone : 1</p> <p>Face Tilt : 90° Face Area : 9 m² Orientation : 0° Glazing ratio : 0</p> <p>Building Type : Not defined Building Heating demand : 527 kWh Building Cooling demand : -2676 kWh</p> <p>Building Volume : 27 m³ Building height : 3 m</p> <p>Int wall ratio : 0.1 Floor height : 3 m</p>
Shape 1, and 50 % shading coefficient	<p>Solar Rad on Face : 1148.5 Wh/m²</p>  <p>1148.5 kW/m²</p> <p>Solar Radiation kWh/m2year</p>  <p>Face type : roof Face : 15 Building : 3 File : 0 Zone : 1</p> <p>Face Tilt : 90° Face Area : 9 m² Orientation : 0° Glazing ratio : 0</p> <p>Building Type : Not defined Building Heating demand : 560 kWh Building Cooling demand : -2394 kWh</p> <p>Building Volume : 27 m³ Building height : 3 m</p> <p>Int wall ratio : 0.1 Floor height : 3 m</p>
Shape 2 and 50 % shading coefficient	<p>Solar Rad on Face : 1225.2 Wh/m²</p>  <p>1225.2 kW/m²</p> <p>Solar Radiation kWh/m2year</p>  <p>Face type : roof Face : 8 Building : 2 File : 0 Zone : 1</p> <p>Face Tilt : 90° Face Area : 9 m² Orientation : 0° Glazing ratio : 0</p> <p>Building Type : Not defined Building Heating demand : 561 kWh Building Cooling demand : -2323 kWh</p> <p>Building Volume : 27 m³ Building height : 3 m</p> <p>Int wall ratio : 0.1 Floor height : 3 m</p>
Shape 3 and 50 % shading coefficient	<p>Solar Rad on Face : 1101.6 Wh/m²</p>  <p>1101.8 kW/m²</p> <p>Solar Radiation kWh/m2year</p>  <p>Face type : roof Face : 2 Building : 1 File : 0 Zone : 1</p> <p>Face Tilt : 90° Face Area : 9 m² Orientation : 0° Glazing ratio : 0</p> <p>Building Type : Not defined Building Heating demand : 543 kWh Building Cooling demand : -2519 kWh</p> <p>Building Volume : 27 m³ Building height : 3 m</p> <p>Int wall ratio : 0.1 Floor height : 3 m</p>

The results show that the DSR values on the roof surfaces were similar for the different shapes, as shown in Table 8. The maximum annual solar radiation on the roof was recorded for the test room without the shading mesh as 2017.4 kW /m², while for the three shapes there were small differences of 1,148, 1,225, and 1,101 kW /m² for Shapes 1, 2 and 3, respectively. The HTB 2 simulation shows that the three shading mesh patterns differed over the shading mask, but the solar radiation on the top of all the test rooms had a similar shading coefficient of 50% for all scenarios (Table 8.8).

Overall, the results show that changing shading mesh shapes had a limited impact on roof surface solar radiation, but the shading mesh had a significant impact on solar radiation on the roof surfaces when compared to the unshaded roof.

8.7.3 Comparison of the IES and HTB2 Models

The IES and HTB2 simulated test rooms with similar input data, which included physical characteristics and weather data file. The IES and HTB2 models were employed to calculate direct solar radiation on the roof surface of the test rooms with and without shading mesh, as shown in Section 7.7.2. The IES and HTB2 models take different approaches to calculating solar radiation on roof surfaces. The results from both simulations are shown in Table 8.9.

Table 8.9: IES and HTB 2 simulation output for fallen DSR on the roof surfaces

Model type –Test Room	IES kW/m ²	HTB2 kW/m ²	% differences
Without shading mesh	2087.47	2071.4	1 %
With shading mesh Shape 1	1178	1149	2.5 %
With shading mesh Shape 2	1206	1225	1.6 %
With shading mesh Shape 3	1157	1102	4.8 %

The results show that there are small differences between the two models' outputs. The maximum difference is 4.8% and the minimum 1% for the test rooms with shade mesh 3 and without shading mesh, respectively (Table 8.9). Overall, there are small differences between the roof surface solar radiation calculated by IES and HTB2. This gives confidence that the IES model can be used as a simulation tool to the calculate shade mesh effect on the roof surfaces.

8.8 Building Scale Model

This section of the study focuses on the research aim to reduce the indoor air temperature in housing projects using architecture design strategies. These strategies will be modelled using IES through a

continuous process of testing on a typical house to produce a productive strategy, which may (help) to reduce the dry bulb temperature of indoor air temperature and hence reduce the cooling load. The last chapter showed that using a shading mesh significantly reduced the impact of direct solar radiation (DSR) on the roofs and indoor dry bulb temperature in the test room (base case scenario).

The aim of this section is to investigate the impact of the shading mesh on indoor dry bulb temperature (DT) for typical houses in Erbil. In addition, a series of scenarios were proposed to investigate the impact of shading mesh and architectural design on DT. The shading mesh is used to cover a typical house to explore the influence of shading on the DT of the housing unit, while architecture design scenarios were combined with the shading mesh to increase the reduction of DT. The first part of this section is about the comparison of the test room and a typical house unit regarding DT. The typical house and test room were covered by the shading mesh and indoor DT was calculated for both scenarios with and without the shading mesh. The second part of this chapter is about the testing of a typical house with two different shading coefficients, 50% and 100%. In addition, these houses are compared with a similar house without a shading mesh to investigate the impact of the shading coefficient on indoor DT. The third part is on the direct comparison of the DT for typical houses in two configurations: single (detached) and attached houses (terraced). The final part of this section is on housing block simulation, throughout which different housing block arrangements and orientations were compared.

A typical house is built on a plot area of 200 m² with two floors, a small garden at and a parking space for a car at the front. The ground floor normally contains a reception room, kitchen, living room, two bedrooms and a bathroom; while the first floor has two bedrooms and a bathroom.

This type of house is normally constructed with hollow concrete blocks 400 x 200x 200 mm (walls) and 200mm thick of reinforced concrete for roofs.

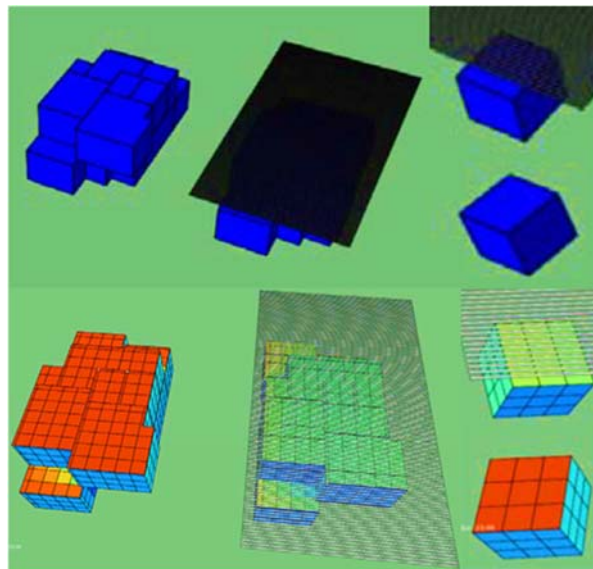


Figure 8.37: Test room and house with and without shade mesh

8.8.1 Typical House¹⁹ With and Without Shade Mesh

The shading mesh was modelled and validated in the last section and the results show that the shading mesh had a significant impact on the DSR that falls on the building's roof. This simulation test room and typical house were compared with and without shading mesh. Figure 8.37 shows the test room and typical house modelled using IES. This simulation is the first set of a long series of simulations investigating the impact of shading mesh on housing units in the summer time to reduce DT and cooling energy consumption.

Figure 8.38 shows the DT for the test room with and without shading mesh, which reduced

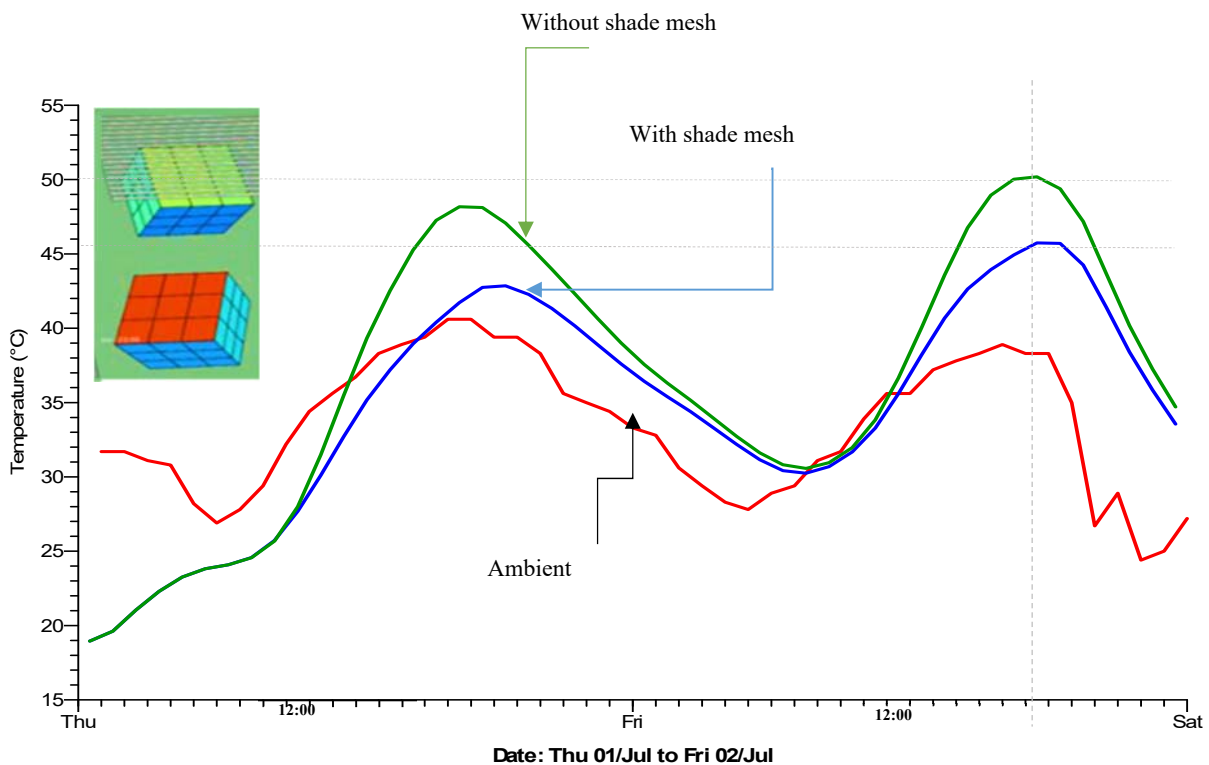


Figure 8.38: IES model for test room, showing DT for the test room with and without shading

the DT from 50°C to 46°C at 18:00. The test room's maximum air temperature was shifted every hour by employing the shading mesh. This means that the shading mesh has an impact on the absorption and emission of the thermal energy in the test room during the day and night time. To reflect this effect on the housing unit, the study proposed a set of simulations on a Erbil typical house.

The second set of simulations compared a typical house unit without openings (doors and windows) similar to the test room in terms of shading mesh and building materials. The

¹⁹ The typical house is the type used in this study for the simulations. Most housing projects are shown in Chapter 4, with housing plots 10 x 20 m. In this study, we used a housing plot of 200 m² for the simulation process to represent a housing unit in Erbil, because most houses have similar types of plot and design details.

typical house in this simulation had 600 mm insulating materials for ground and exterior walls, and 100 mm concrete tiles for the roof. The shade mesh was at a height of 8 m, and the typical house had two floors of a height of 3.2 m. The distance between the second floor to the shading mesh was 1.6 m. The aim of this simulation was to understand the heat gain through the roof and the impact of shading when the typical house was fully covered by the

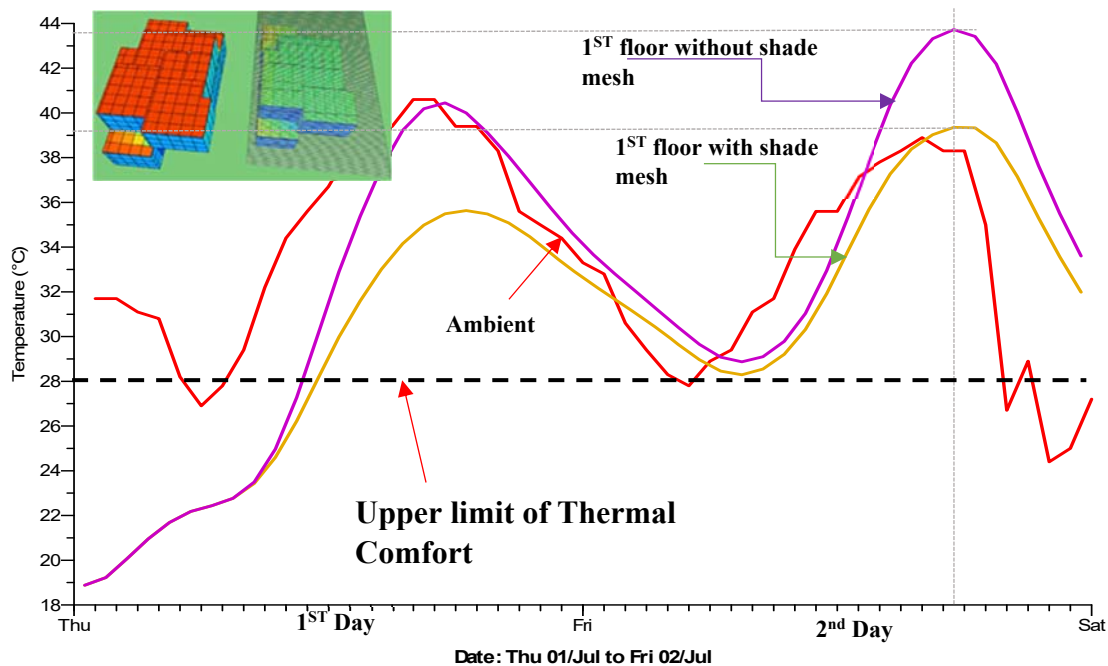


Figure 8.39: DT for the prototype house with and without shading mesh

shading mesh (Figure 8.39).

The simulation measured DT for the first floor of a typical house with and without shading mesh over two days, but only the second day was considered as the model produces inaccurate output for the first 24 hours (Figure 8.39). The maximum DT was 43.6°C and 39°C for both the second floors without and with shading mesh, respectively. The simulation showed that the shading mesh had a significant impact on DT in the prototype house (without any openings).

The thermal comfort maximum level is 28°C (de Dear et al, 1997), the greater the gap between predicted air temperature and the comfort temperature, the greater the need for some artificial intervention to bring this down to acceptable levels. In typical house case with and without opening as showed in figure no 8.39, the artificial intervention needed for both day and night time to reach comfort level. This demand increases gradually from midnight to afternoon when the DT reach 43.6°C.

The next step of the study changed the typical house in terms of construction materials and external openings (doors and windows). The walls, floor and ground materials used in this simulation set can be found in Appendix G.

8.8.2 Typical house models with and without openings

This set of simulations tested a typical house with openings (windows and doors) constructed of similar local materials used in Erbil. The simulation compared three types of houses with three different material properties (Table 8.10).

Table 8.10: Prototype house scenarios with and without shading mesh

Scenario	Wall materials	Ground floor materials	Roof material	Exterior openings	Shading coefficient
Typical house (Type 1)	Isolated material ²⁰	Isolated material	10 cm concrete	Without opening	Without shading mesh
Typical house with Local materials (Type 2)	Hollow concrete blocks	Local floor ²¹	Local roof	Without opening	Without shading mesh
Typical house with Local materials (Type 3)	Hollow concrete blocks	Local floor	Local roof	With opening	Without shading mesh

In these simulations, the following scenarios were tested:

1. Typical house with isolated material (Type1) and typical house with local materials (Type 2)
2. Comparison of models with and without exterior openings (doors and windows) (Type 1, Type 2 and Type 3).
- 3.

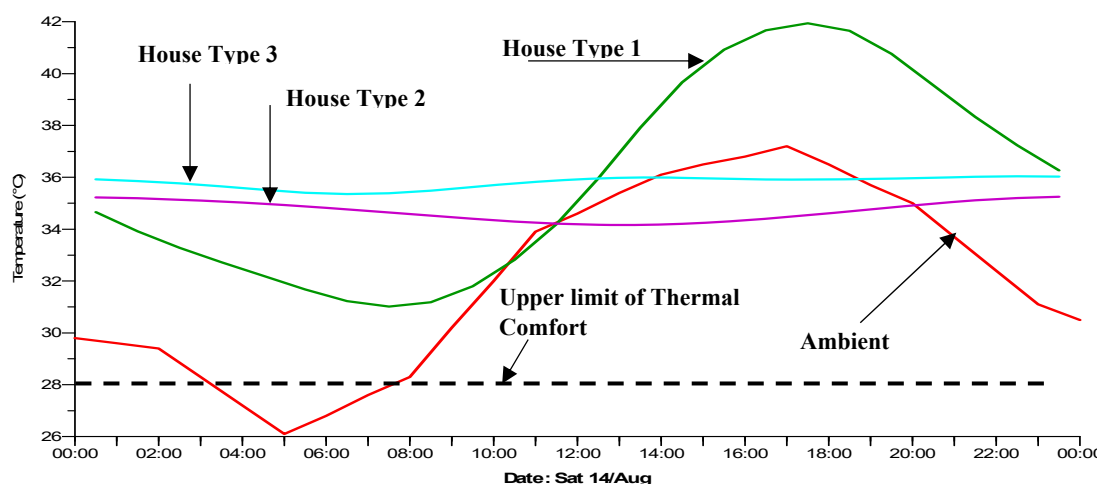


Figure 8.40: Comparison between first floor test houses without shade mesh. Local materials and isolated materials, with and without openings

²⁰ Isolated materials refers to the similar materials used in the test room. 600 mm isolated materials for ground and exterior walls and 100 mm for concrete tiles for the roof.

²¹ Local floor and local roof can be found in Appendix G.

Figure 8.40. shows the comparison simulation of the first floor DT for the three types of typical houses and ambient DT. The results show that house type 1 follows similar patterns of ambient temperature with a one hour shift, as explained in Section 7.6.1. After adding construction materials to the typical house (ground, walls and floors), the thermal performance of the typical house dramatically changed. The typical house (type 2 and type 3) thermal performance does not closely follow the ambient temperature (Figure 8.40). The maximum difference in DT recorded was 11 K for the typical house (type 1) and the minimum ΔT was 0.9 K and 0.5 K for typical house types 2 and type 3, respectively. The maximum air temperature for the typical house (type 3) was 36.0°C and the minimum DT is 35.8°C, while the maximum DT for the typical house (type 1) was 42°C and the minimum DT was 26°C. This shows how local building materials influenced the typical house types 2 and 3 more than the adding openings to the typical house type 3 (Figure 8.40).

Developing the previous results, the next set of simulations compared a typical house (type 3) with and without shade mesh. The aim of this test was to examine the typical house models with and without shade mesh. The DT for the first floor compared the typical house (type 3) with and without shading mesh, as shown in Figure 8.40. The typical house had closed openings 24 hours to completely prevent natural ventilation.

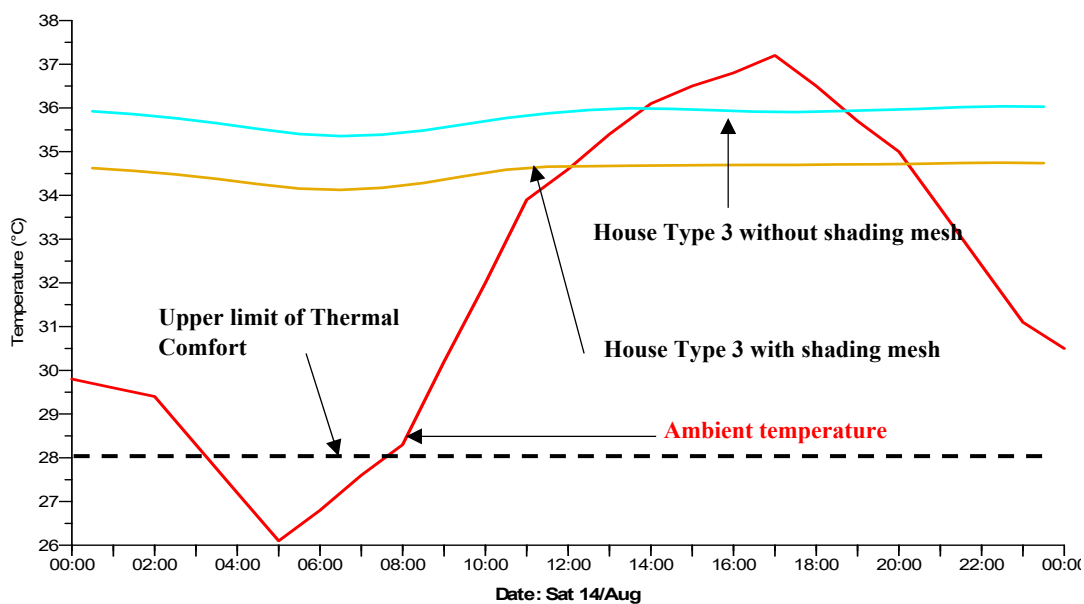


Figure 8.41: Comparison of first floor typical house (Type 3), with and without shade mesh

The results show that the shading mesh reduced overall indoor DT for the typical house with shading mesh during both day and night. Overall, the shading mesh with a shading coefficient 50% reduced the indoor DT by 1.5 k.

8.8.3 Typical house with Different Shading Coefficient Ratio 50, and 100%

This set of simulations tests a typical house (type 3) without shading mesh and with mesh that has shading coefficients of 50% and 100% (Figure 8.41). This simulation investigated the impact of the shading coefficient on the indoor DT for a typical house. The results show that the house without shading mesh had a higher DT compared to houses with shading mesh. The three cases do not closely follow the ambient air temperature pattern during day and night time (Figure 8.42). Moreover, the DT for the three typical houses followed a similar pattern with different DT values. The maximum DT temperature was 36°C recorded for the typical house without shading mesh, while the minimum DT was 33.5°C recorded for the typical house with shading mesh, which had a 100% shading coefficient (Figure 8.42).

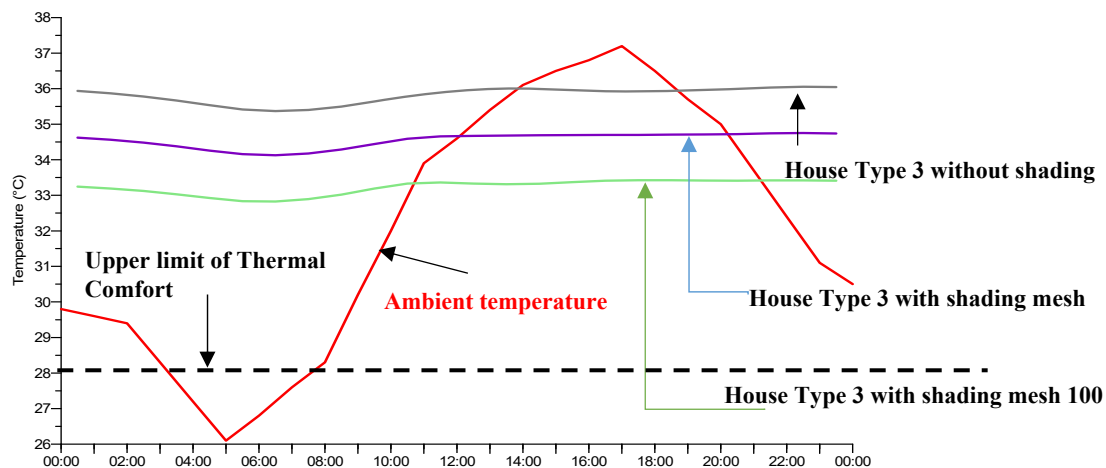


Figure 8.42: Comparison of 1st floor typical house with shade mesh and 50% and 100% shading coefficient.

Increasing the shading coefficient reduced the indoor DT for a typical house, as the house without shading mesh (0% shading coefficient) recorded the maximum air temperature, while the DT was lower for the typical house with 50% and 100% shading coefficient. The maximum difference in DT was 2.6 K and 1.5 K when a typical house without shading mesh

as compared with a typical house with 50% and 100% shading mesh, respectively (Figure 8.42). Overall, the results show that adding the shading mesh over the typical house can reduce the DT, and this reduction depends on the shading coefficient. The shading mesh reduces the amount of DSR during the day and this leads to a reduction in the indoor DT. The thermal mass has a significant impact on indoor DT for all cases. The building absorbs heat during day time and cannot cool down at night, as the ambient temperature drops during night time (Figure 8.42). For more investigation, the next section explains more strategies regarding this issue.

8.9 Single and attached typical house models

In this simulation, typical houses were simulated with the Erbil weather data file for summer 2017. The aim of simulation is to compare single and attached typical houses (Figure 8.43). The typical house has both ground and first floors. The simulation investigated the points below:

1. The difference between DT for single and attached typical houses, unshaded and shaded.
2. Comparison of the DT between floors (ground and first) for both single and attached houses.

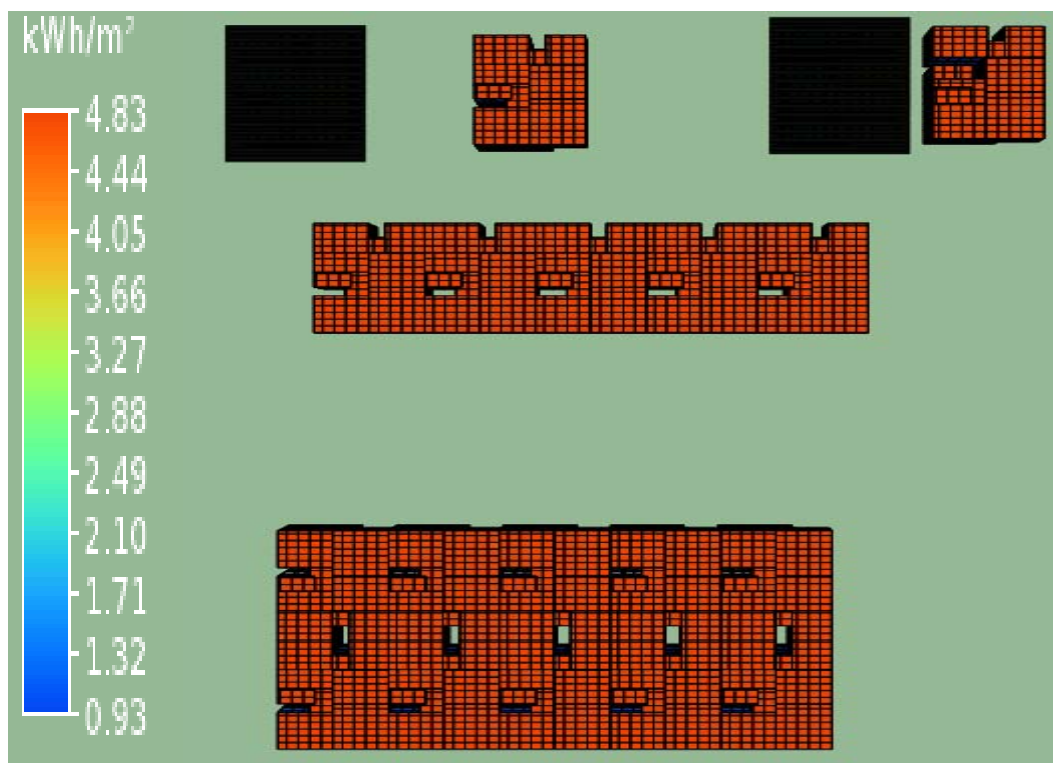


Figure 8.43: Single and attached typical houses

8.9.1 Single and attached house

In this scenario, a typical house was simulated with local Erbil materials (Appendix G), which include ground floors, internal and external walls, internal ceiling and roofs. The first set of simulations compared the first floor of a typical house to determine the impact of attached houses to the DT of the detached house. Three types of houses were compared in this simulation: a single house without a shading mesh, a single house with a shading mesh and an attached house with a shading mesh (Figure 8.44).

The results show that the attached houses had a lower DT compared to the single house (detached). The maximum air temperature recorded for the ambient air temperature was 44.0°C, while the maximum indoor DT recorded for the single house without shading mesh was 36.7°C and the minimum DT for the attached typical house was 34.0°C with shading mesh (Figure 8.44).

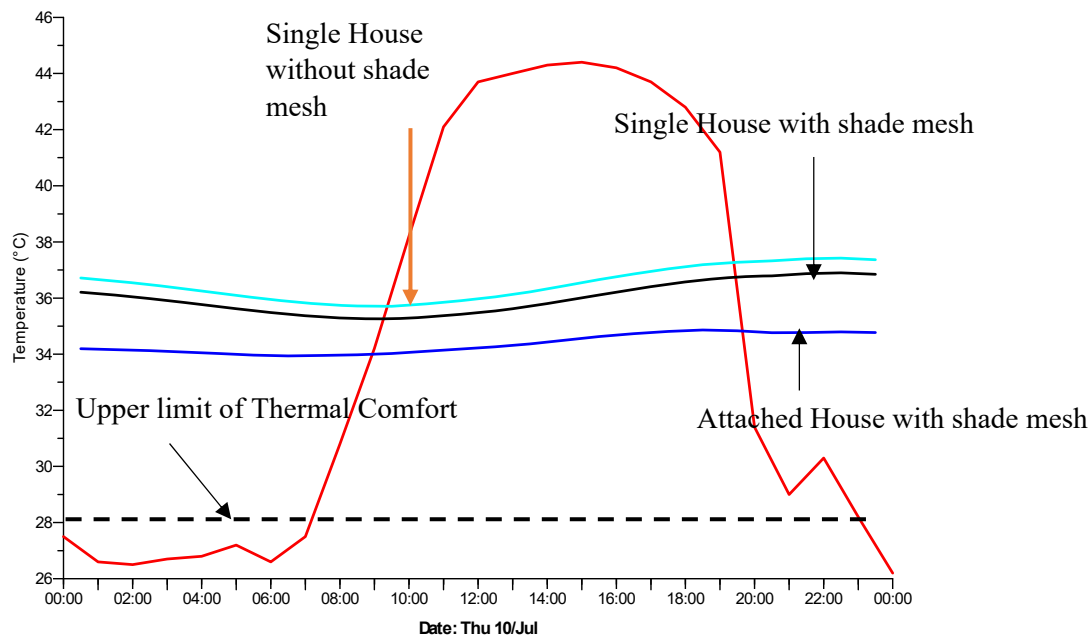


Figure 8.44: Comparison between the first floor test houses: single and attached typical houses

In addition, the shading mesh and attached house combined reduced the indoor DT for the typical house by 2.2 K. The difference in DT between the typical single house with and

without the shading mesh was 0.9 K, while the difference in DT between the attached and detached typical house was 1.7 K. When modelling the attached house the boundary between adjacent houses is treated as adiabatic, whilst for the single house is exposed to the external elements on all sides, hence it would be expected that a single house would perform worse than the attached house. This means that the heat gain of the attached houses is less than single houses, and this type of housing is more useful for hot dry climate cities such as Erbil (Figure 8.43).

8.9.2 Ground and first floor for single and attached typical house

In this simulation, the ground and first floor of a typical house were compared with shading coefficient 50%. The typical house had similar building construction materials, as shown in Section 7.9.2. The simulation first compared the ground and first floors of a typical house for five days as shown in Figure 8.45. The results show that the ground floor recorded a lower DT compared to the first floor. The ΔT was at minimum value late evening and gradually increased to reach a peak at noon, with a maximum ΔT of 2 K (Figure 8.45).

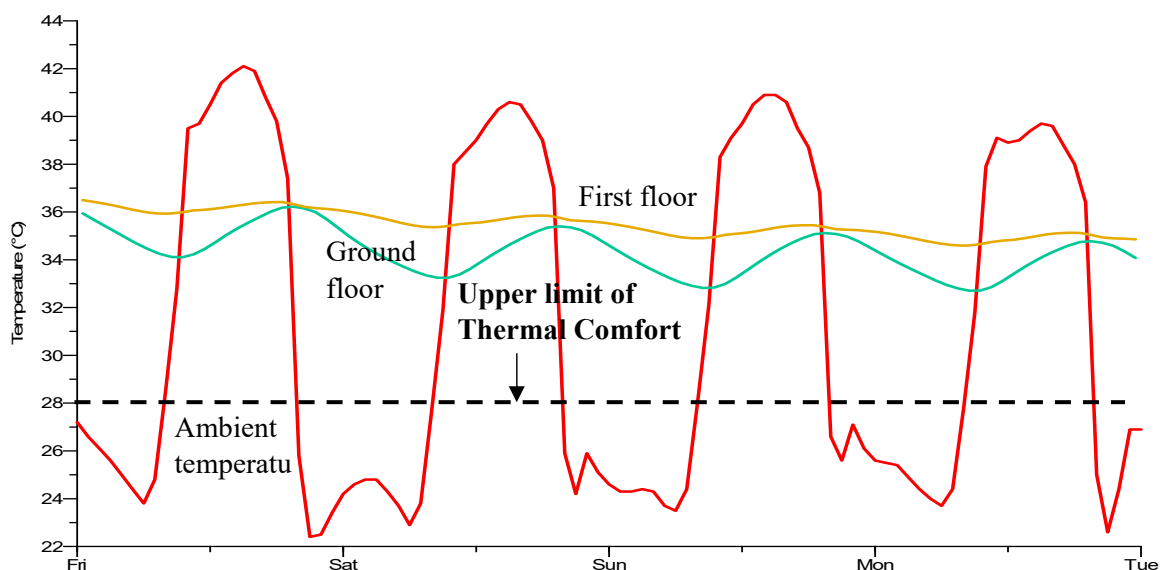


Figure 8.45: Comparison between the attached house on the ground and first floors for the first five days of August

The second simulation set compared the ground and first floor of the attached and detached typical houses with and without shading mesh (Figure 8.45). The shading mesh used in this set of simulations had a shading coefficient of 100% because it has more impact on DT, as shown in Section 7.7.6. The results show that the first floor of the attached and detached houses recorded higher DT compared to the ground floor of the typical

house with and without shading mesh (Figure 8.45). The maximum DT was 36.5 °C and 34.5 °C for the first floor of the single and attached houses without shading mesh, respectively, while the minimum DT was 33.8 °C and 32.2 °C for the ground floor typical house with and without shading mesh, respectively (Figure 8.46). Overall, the shading mesh and attached house reduced the DT of the typical house, and the cooler ground floor was more influenced by these strategies. For this reason, the ground floor of a typical house in Erbil has the most important spaces, such as kitchen, living room, guest room and two beds. The family spends 90% of summer time on the ground floor, because the energy that they use for cooling the ground floor is less than for cooling the first floor. The maximum difference in DT for the ground floor with mesh and first floor without shading mesh was 3.1 K (Figure 8.46). This section of the

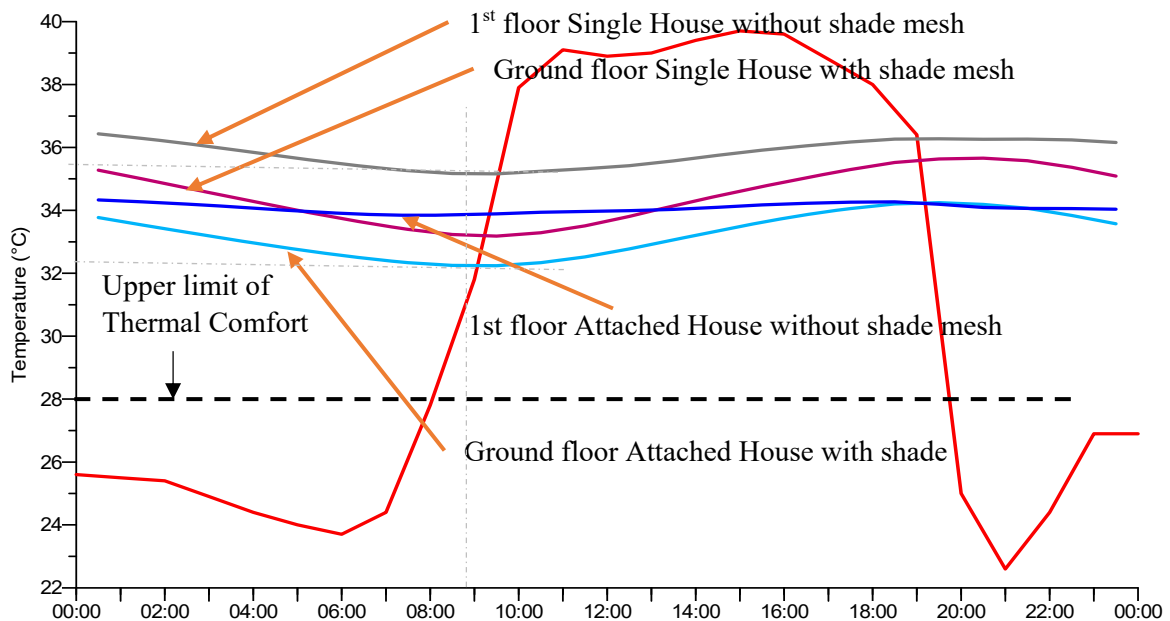


Figure 8.46: Compare between attached and single house Ground and first floor with and without shading mesh.

study shows that shading mesh has a significant impact on indoor DT in the test room (with isolated materials) and the house without openings. Adding openings and local building materials similar to typical houses in Erbil reduced the significant impact of the shading mesh. In addition, the housing blocks were more influenced by orientation and external wall area than the shading mesh.

8.10 Application of Ventilation Strategies'

So far the introduction of a shading mesh has only a limited impact on the internal dry bulb air temperature, with thermal mass being much more effective. With the house shaded by the mesh, the daytime solar radiation gains are reduced but the losses to the clear sky are also reduced and this negates the impact of the overall performance of the shading mesh. However, the houses simulated with in this chapter only had Infiltration as the ventilation setting and did not model the impact of Purpose Ventilation strategies. The final part of this chapter will investigate the impact of ventilation strategies' on the indoor dry bulb air temperature.

Three ventilation scenarios were simulated using the typical design type 1 and North-South orientation. The openings of the typical house were modelled in a way which monitored opening times, as explained next. The first scenario opened the openings for 24 hours a day (24 h open profile), while the second scenario closed the openings for 24 hours (24 h closed profile), and the last scenario opened the openings during the night time and closed them during the day time (night-time open profile). The aim of this simulation was to investigate the impact of opening time profiles on DT using IES-VE.

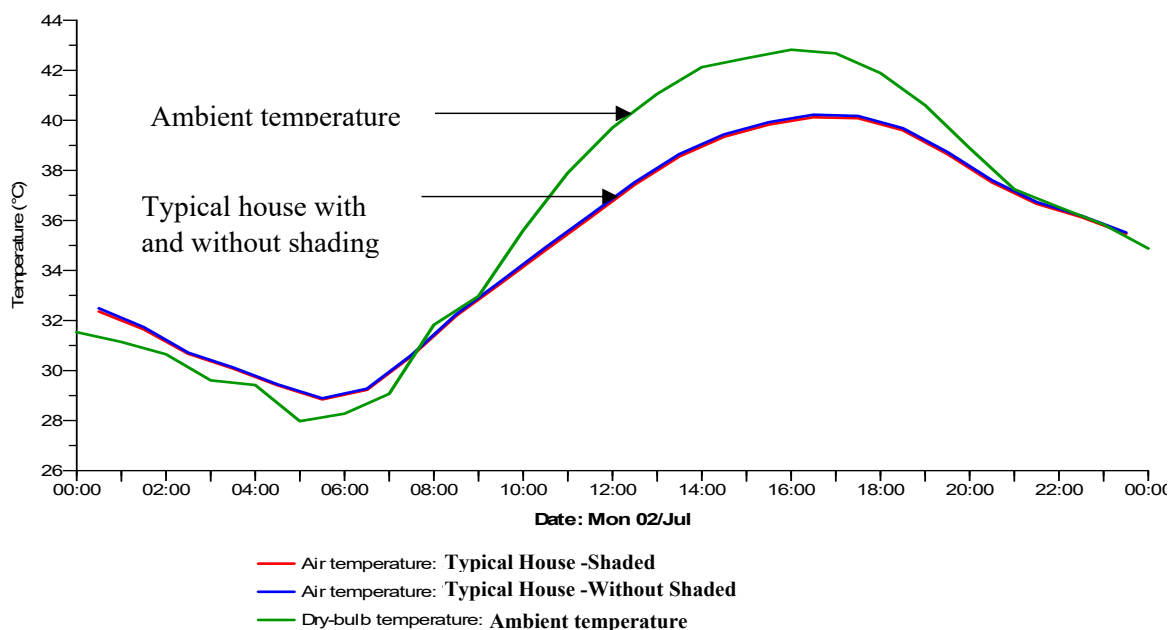


Figure 8.47: Typical house design scenario with and without shading mesh with 24 hour opened profile

8.10.1 Window open profile (24 hours opened)

In this simulation, the typical house openings were simulated as open for 24 hours by incorporating a 24 hour open profile to all the openings using MacroFlo²² into the IES model. This allows the house openings to be open during both daytime and night time and the typical house is naturally ventilated

²² "Simulate air flow driven by wind pressure and buoyancy forces using a fast multi-zone thermo-fluid solver" (www.iesve.com).

for 100% of the day. The typical house was modelled with and without shading mesh for the summer months, but only 24 hours of the results were presented. The results show that overall DT follows the weather data file graph with a one hour shift, as shown in Figure 8.48. The maximum DT was recorded at 17:00 with 40.1°C and the minimum DT was 28.9°C at 05:30 (Figure 8.47).

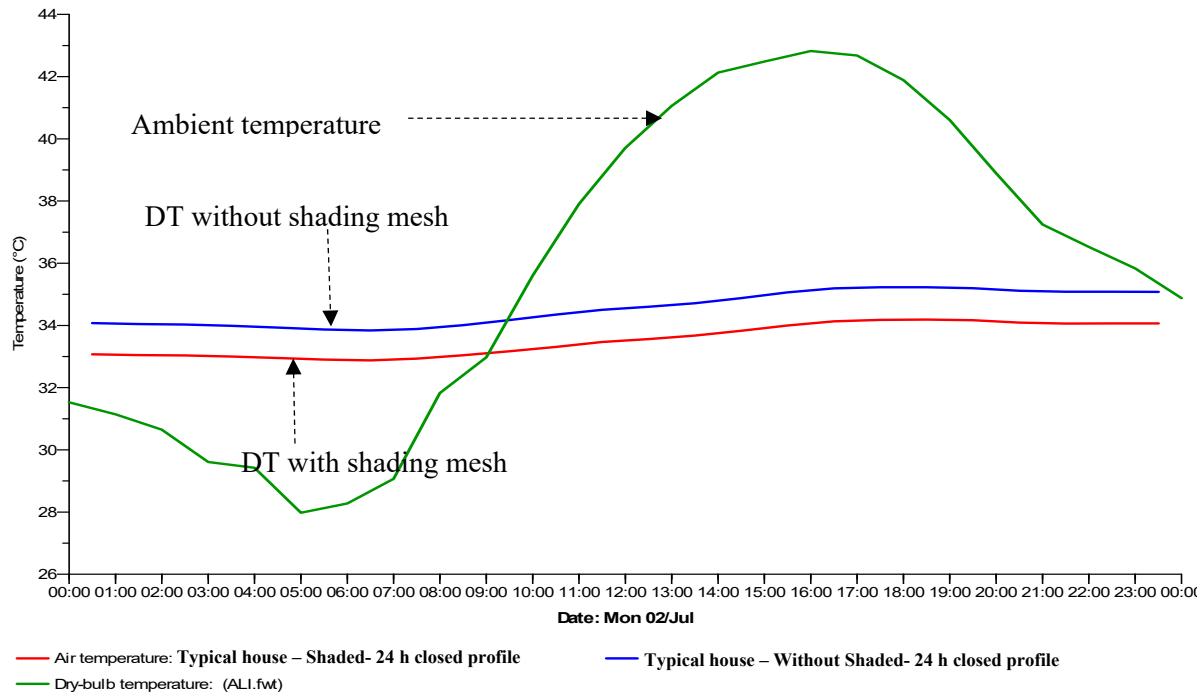


Figure 8.48: DT for the typical house and without shading mesh with 24 hour closed profile

With the windows open for 24 hours the indoor temperature follows the profile of the ambient temperature but modified by the buildings thermal mass, which reduces the peak day time indoor temperature and increases minimum night time indoor temperature. The results show that shading mesh has a limited impact on DT when a typical house is set with an open window profile for 24 hours a day (Figure 8.48).

8.10.2 Windows open profile (24 hours closed)

In this simulation, the openings are set to close for 24 hours using the typical house design with and without shading mesh. The simulation was run for the summer months, but only 24 hours are presented (Figure 8.50). The shading mesh has a shading coefficient of 50%, as explained in Chapter 7. The results show that the maximum and minimum DT are 35.2°C and 32.8°C for the house with and without shading mesh, respectively. When the opening is set to be closed 24 hours, the indoor environment is trapped and not directly influenced by Purpose Ventilation. In addition, the building envelope heats up, and transmits the heat energy slowly into the internal surfaces of the

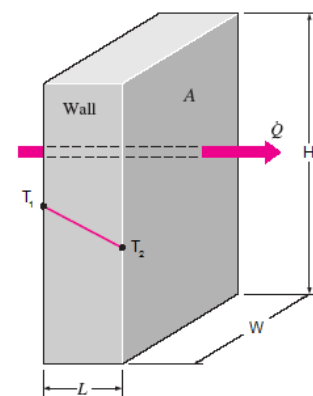


Figure 8.49: Heat transfer through the external walls

building by conductivity during the daytime and the process is reversed during the night time (**Error! Reference source not found.**).

$$Q = KA \frac{T_1 - T_2}{L}$$

Q = Heat Steady State Transfer, T_1 External wall temperature T_2

= Inside wall temperature

K = Thermal Conductivity (W/mK), A wall area (m^2) and L wall thickness (m)

The DT difference recorded similar values for the house with and without shading mesh with a difference of 1.1 K. This simulation shows that the indoor DT does not follow the ambient temperature profile over 24 hours, but instead remains relatively constant in the range of 34°C to 35.1°C. The overall results show that DT is reduced significantly compared to the first scenario, 24 hour opening.

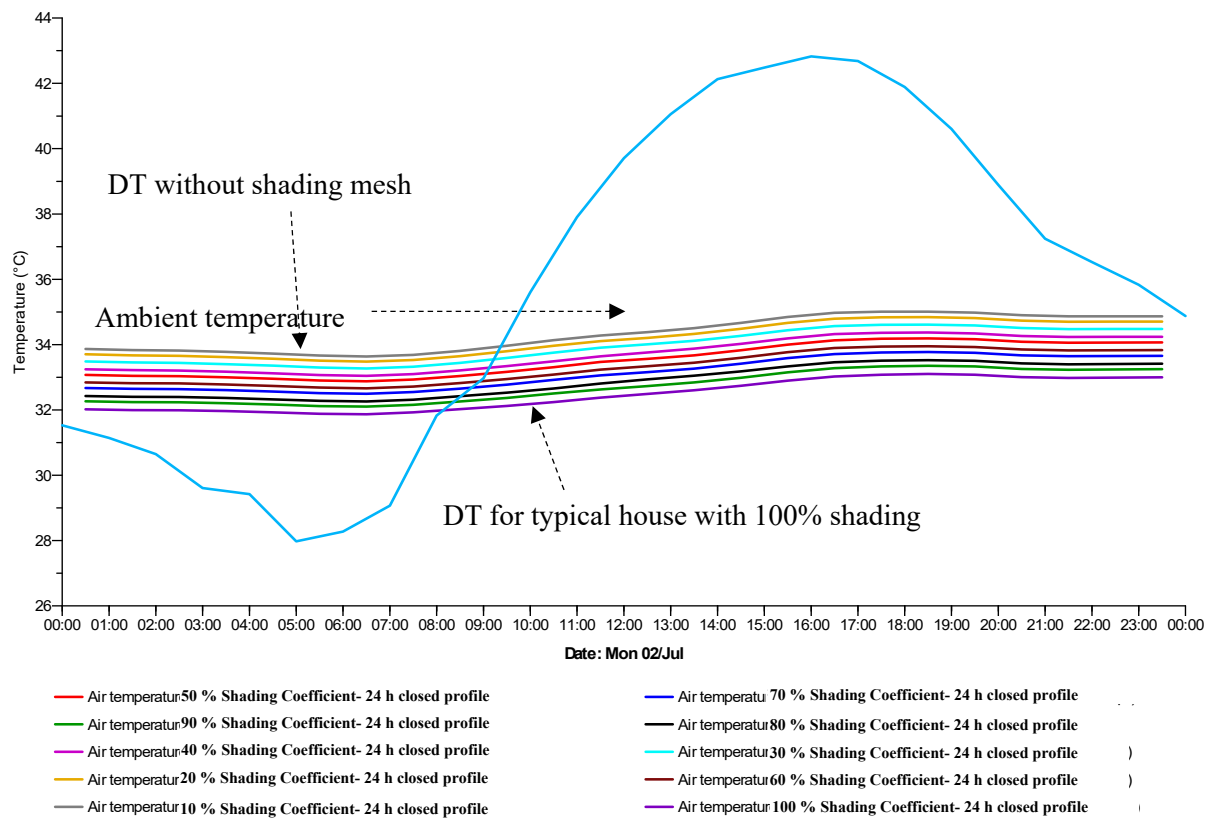


Figure 8.50: DT for the typical house with shading mesh 10% to 100% shading coefficient.

The typical house with a 24 hour closed profile was simulated with ten different shading coefficients (10% to 100%), as shown in **Error! Reference source not found.**. The results show that changing the shading coefficient has a significant impact on DT. The maximum DT for the typical house was 35.2°C for 10% shading, and was 33.0°C with 100% shading coefficient. The indoor DT for the

typical house decreases with increased shading coefficient during day and night-time. The DT is reduced by 0.2 °C or 20% when the shading coefficient is increased by 10% (Figure 8.51).

The difference in DT temperature for the typical house in this scenario is 2.1 K. This means the shading mesh with 100% shading coefficient can reduce the DT for the typical house by 2.1 °C during the day and night (Figure 8.51).

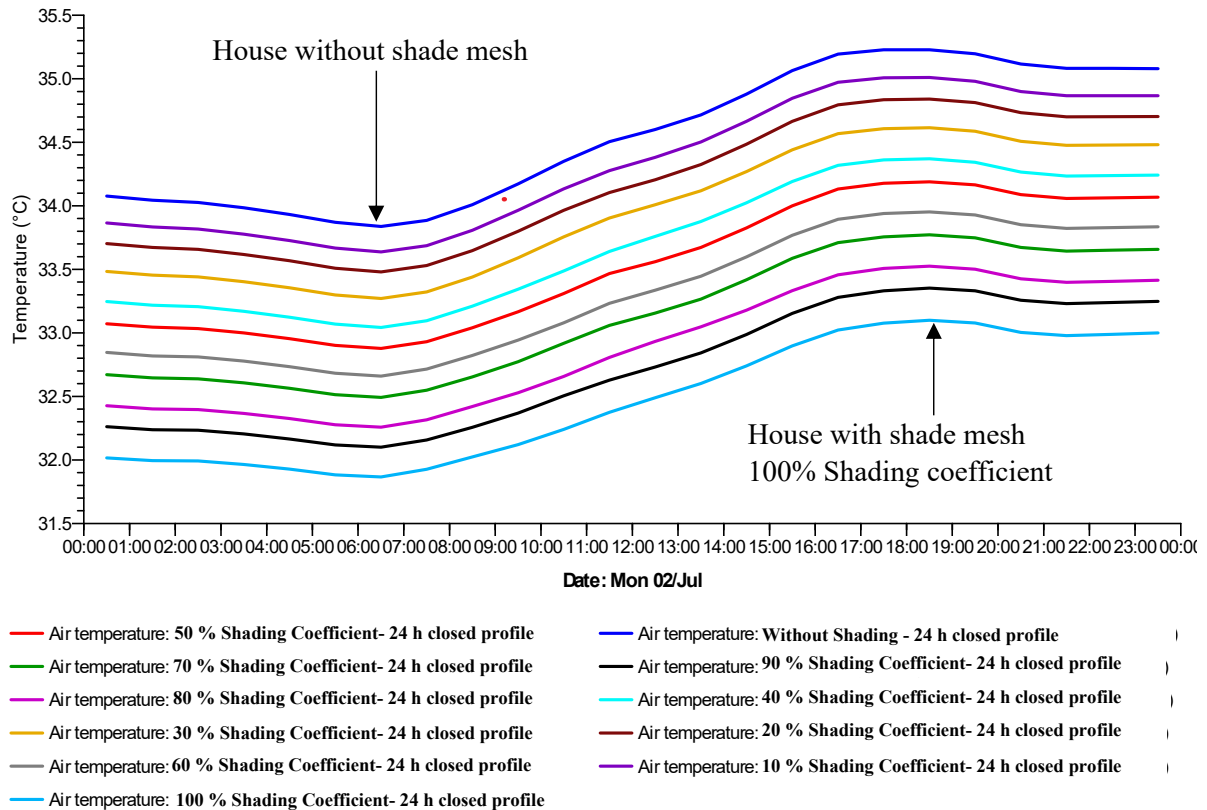


Figure 8.51: Typical house DT with ten shading coefficients (10% to 100%) with 24 hour closed profile

The overall results from this simulation show that the addition of the shading mesh reduces DT for the typical house and this reduction happens only during the day, while during the night the typical house recorded higher DT compared to ambient temperature (Figure 8.51).

8.10.3 Window open profile (night time opening)

MacroFlo was used with IES-VE to model the openings, which were set to be closed during the daytime from 05:30 to 21:00 and then open during the night time, for the typical house design with and without shading mesh. The simulation was run for the summer months, but only 24 hours are presented. The shading mesh has 50% shading coefficient in the first simulation, and 10–100%

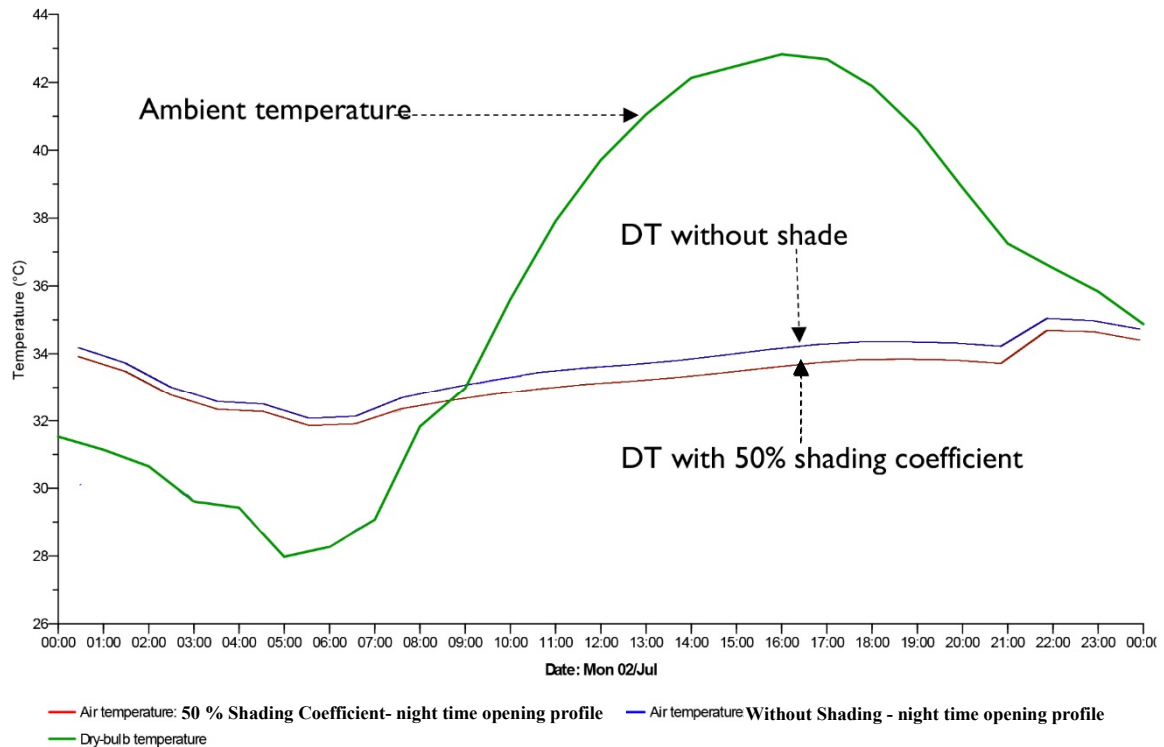


Figure 8.52: Typical house DT with and without shading mesh with night time opening profile

shading coefficients were simulated in the second.

In the first simulation, both shading mesh and opening profile were used to reduce indoor DT for the typical house during the day and night. The results show that DT for the typical house is significantly reduced during the day, and it follows a similar profile as the ambient temperature during the night. The maximum DT for the shaded typical house during the day time was 32.2°C compared to 42.2°C for the ambient temperature Figure 8.52.

The shading mesh has an impact on DT during the day time and this reduces during the night time. The difference in DT between the typical house with 50% shading coefficient and without shading mesh during the day is 0.8 K, while this reduces to 0.1 K during the night time. To reduce indoor DT further, the typical house was simulated with ten different shading coefficients, starting from 10–100% (Figure 8.51). The maximum differences between shading mesh 10–100% happens during the day time at 18:00 was 1.0 K, while the minimum difference in DT happens at midnight with 0.5 K (Figure 8.52).

8.10.4 Comparison of all three scenarios

The simulation results show that the three opening profiles and shading meshes with different shading coefficients have different effects on the DT during the day and night time. The first scenario with the

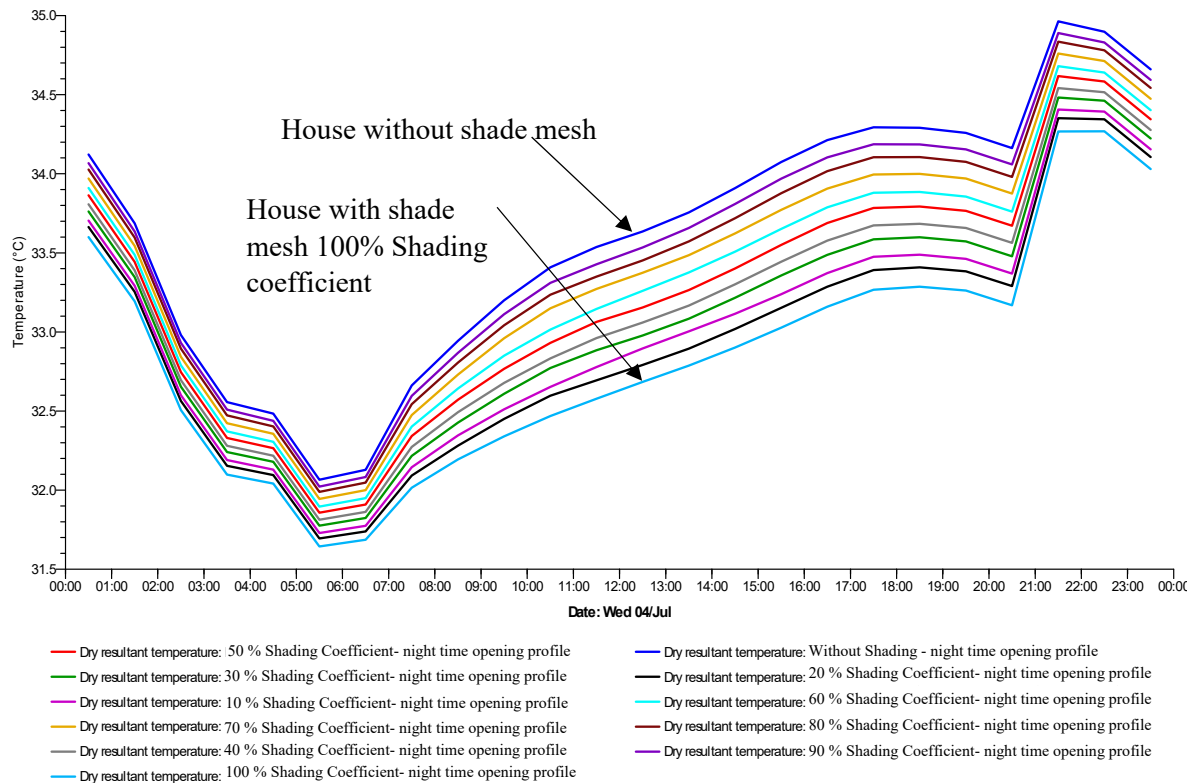


Figure 8.53: Typical house DT with night time opening profile and ten different shading coefficients (10–100%)

24 hours opening profile and various shading coefficients has a limited impact on indoor DT for the typical house. The DT profile for all cases follows ambient temperature during day and night and the typical house recorded similar DT with and without shading mesh (Figure 8.47). The second scenario shows that when the opening profile is closed for 24 hours, the DT for the typical house is significantly below the ambient temperature during the day but higher than ambient temperature during the night (Figure 8.49). The DT for a typical house can be reduced further in this scenario when the shading coefficient is increased. Figure 8.51 shows that DT can be reduced by 0.2 °C when the shading coefficient is increased by 10%. Therefore, the maximum reduction by adding shading mesh with a coefficient of 100% over the typical house is 2.1 °C (Figure 8.51). The third scenario simulated a typical house with a profile adapted from the first and second scenarios, which leads to a reduced indoor DT for the typical house both day and night. The opening profile was set to close during the day and opened during the night (21:00 to 05:30). The result of the third simulation shows that the DT is significantly reduced during daytime and follows a similar profile to the ambient temperature during the night time (Figure 8.52). In addition, the shading coefficient has an impact on the indoor DT for the typical house. The impact of the shading mesh to reduce DT is more during the daytime

than night-time. Figure 8.53 shows that increasing the shading coefficient by 10% achieves a maximum DT reduction of 0.1 °C. During the night the shading mesh and shading coefficient has a limited impact. Figure 8.54 shows all three opening profile scenarios with and without shading mesh and the range of ten shading coefficients from 10% to 100%. The results show that DT for the indoor typical house can be reduced through two different strategies: Firstly, adjusting the opening profile, and adding shading mesh with different shading coefficients. These two factors have different impacts on the reduction of indoor DT. The effectiveness of the factors depends on the presence or absence of the other. The maximum DT for the typical house without shading was 41.1 °C, 35.1 °C and 29.8 °C for scenarios 1, 2 and 3, respectively, while the minimum DT for typical house without shading mesh was 28.8 °C, 33.0 °C and 28.3 °C for scenarios 1, 2 and 3, respectively. The maximum DT reductions compared to ambient temperature are 1.4 K, 7.4 K and 12.7 K for the first, second and third scenario,

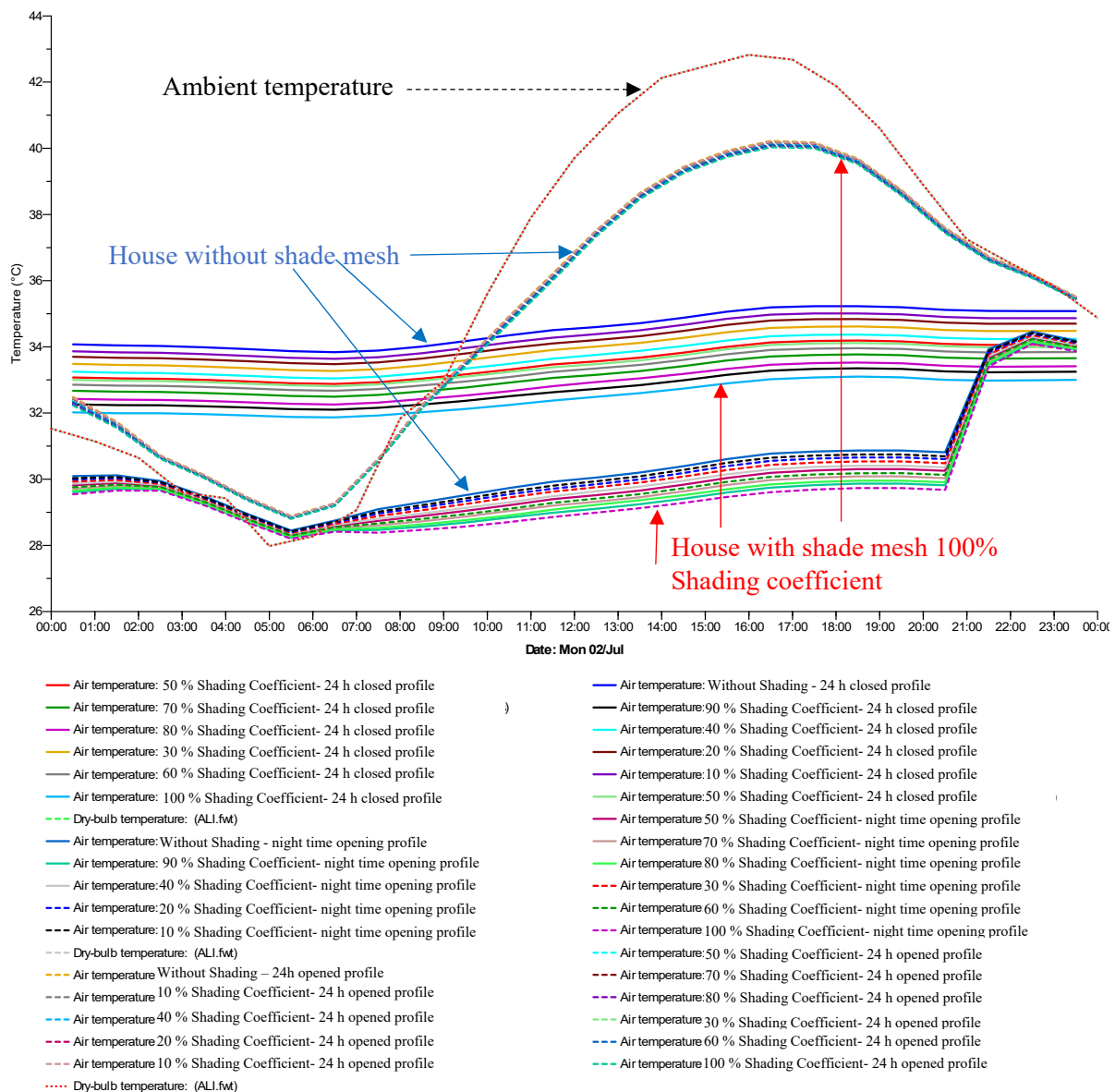


Figure 8.54: Dry bulb temperature for typical house with three opening profiles and 10 different shading coefficients (10% to 100%).

respectively (Figure 8.54).

This analysis shows the impact of night time cooling on the dry bulb air temperature, during the day time the windows are closed, inhibiting the flow of warm air into the typical house and restricting the increase in DT. At 21:00 the windows are open, there is a rapid increase in the DT for the first hour after opening as warmer ambient air enters the house but as the temperature of the ambient air falls, the DT follows, reaching a minimum at dawn. The typical house is now cooled to its minimum dry bulb temperature. Once the windows are close, the DT rises throughout the day, but as night time cooling has taken place, this rise in temperature starts at a lower value resulting in lower DT overall. The addition of the shading mesh, with a porosity of 50% lowers the DT further but the maximum decrease is only 0.8 K.

8.11 Conclusion

This chapter was divided into four sections and aimed to employ IES-VE as a research tool to model the shading mesh and estimate the indoor dry bulb temperature with and without a shading mesh. The first section concerned the IES-VE model inputs and outputs data. The main input data for this model is the weather data file, which has a significant impact on simulation outputs. This section of the chapter compared three different sources (IES, ENVI-met and measured data sets) of weather data (WD) to justify the appropriate set of data for IES-VE model. The IES-VE WD file produced an inaccurate result, and ENVI-met WD, although not perfect, was more accurate than the IES-VE model WD. However, the measured WD file was the most accurate and for this reason it is acceptable to use the measure WD rather than ENVI-met and IES-VE WD.

The second section concerned the shading mesh modelling and the validation process. Shading mesh is used externally to reduce the intensity of solar radiation. This happens because shading mesh reflects and absorbs solar radiation. It can be applied horizontally (shading devices) and vertically (shading screens). The literature shows that shading mesh has been modelled in agricultural studies (practical studies) and architecture and building physics studies (CFD simulation programs). In both groups of studies, the process of modelling shading mesh was problematic because of the shading element scale. Therefore, this study proposed a hypothetical method of simplifying the shading mesh. The model tested shading coefficient (porosity), geometry, and the scale of the shading mesh (Figure 8.12).

The second part of section two concerned the validation of the shading mesh model. In this process, the study employed two simulation programs: IES-VE and HTB2 with similar input data. The aim of this validation was to support the hypothesis that shading mesh segments can be simplified by crude objects without limitation on its performance (Section 8.7). Solar radiation was measured over the roof surface of the test room for one year. The results showed that there are minor differences between the two models' outputs, with a maximum difference of 4.8% and minimum of 1% (IES-VE and HTB2). Therefore, the IES-VE model can be used as a research tool to calculate the shading mesh effect on the roof surface.

The third section concerned the modelling the prototype housing units and analysing their thermal performance using IES-VE. The shading mesh has a significant impact on indoor DT in the test room (with isolated materials) and without openings (Section 8.8.1). While the shading mesh has a limited impact on indoor DT when openings and local building materials

were added to the typical house model (Figure 8.42). This part of the study concludes by investigating the impact of modelling a single house compared to a terrace of houses and the dry bulb temperature recorded at ground floor and first floor levels. The shaded terraced house recorded a lower DT than the single shaded house and for both house types the first floor DT was higher than the ground floor DT. The terrace house is shielded by the adjacent properties and the first floor DT is directly subjected to solar gains through the roof, whilst the ground floor is shielded by the first floor. The results show that maximum difference in DT for the ground floor with mesh and first floor without shading mesh was 3.1 K (Figure 8.46).

All previous modelling had the ventilation set to infiltration only, the windows being closed and air entering and leaving through gaps in the construction. The fourth section of simulations investigated the role Purpose ventilation would have on the DT of the typical house. Purpose ventilation allows air to enter via open windows, and to prevent over heating night time ventilation is a recommended strategy. When this strategy was implemented there was a significant reduction in the DT as the cooler night time air entered the house and cooled the building fabric, during the day the windows were closed and shaded by the mesh which reduced the daytime temperature rise. The impact of the shading mesh at 50% porosity was small in comparison to night time cooling but did lower the DT.

Chapter 9 Discussion

9.1 Introduction

In Erbil, Iraq, the housing shortage was a problem from the 1980s onwards (Chilmeran et al., 2006). To overcome this housing shortage, two solutions were developed.

The first solution was led by the Kurdistan Government. Here a Grid-iron street morphology was adopted within the radial master plan of the city (Akram et al., 2015). The Grid-iron could be aligned either North-South, East-West or in a radial form dictated by the urban plan. Basic infrastructure was provided, including roads, open spaces, schools, policing, petrol stations and health care. The housing plots ranged in size between 200m² and 350m². However, the building of the individual housing units was the responsibility of the plot owner; with the municipalities controlling the height of the development and the set-back from the pavement edge (Sabr, 2014). No guidance, legislation or building codes were employed in the housing design.

The second solution used private companies to develop and build the housing (Costantini, 2013). Again, a Grid-iron morphology was used but each development had various alignments with no consistent pattern emerging. These private companies built housing in a range of styles that were only consistent in the individual developments. The infrastructure provided was more comprehensive than that of the government solution, with developments having their own water treatment plants and power stations.

The main similarity in both government and private projects was the lack of (or very limited) environmental approach (or consideration of local micro-climate) during the design and construction process, at both an urban and building scale.

To address these issues, this thesis investigated the impact of urban form and shading on the local, urban micro-climate and the influence micro-climates have on the indoor air temperature of typical dwellings in Erbil.

9.2 Climate Modelling

In terms of climate, the micro-climate experienced by a building will dictate how the building performs thermally. So being able to predict the micro-climate of a built-up area is essential. ENVI-met is one tool that will allow the prediction of the behaviour of a relatively small section of an urban development, whether it be a canyon, square or park (Bruse et al., 2008). Any mathematical model of a real phenomenon can never model that phenomenon at the molecular level, as the computational complexity would swamp the process and the model would ‘never’ produce an answer. ENVI-met is a mathematical model and is subject to a series of scale and practical assumptions. So, the output of ENVI-met should always be treated with a degree of scepticism and should never be accepted as the ‘answer’. However, it does provide a researcher with a tool to investigate the urban micro-climate and is useful in making comparative observations.

9.2.1 Validation of ENVI-met

The research undertook a validation exercise, for two urban locations, comparing the predicted temperatures to the measured temperatures. In the original research plan, it was envisaged that the researcher would visit Erbil and conduct a series of weather observations within the urban area. However, the security situation in Kurdistan deteriorated and this visit was not possible. Therefore, the weather data had to be sourced remotely. The easiest data to obtain was from the Airport, sited to the North West of the city centre. The difficulty with this data is that the Airport is in an open area away from any urban development and so is not representative of the weather the city experiences. More appropriate weather data was eventually sourced from the Ministry of Agriculture: one weather station was located close to the city centre, adjacent to a high-density urban area with a traditional (organic) morphology; the second weather station was located to the South of the city centre. Originally this second station was in open countryside but the modern urban expansion of Erbil had encroached upon it. The urban development at this second site was in the modern Grid iron morphology. For both locations an urban physical model was created in ENVI-met, replicating the urban morphology of the sites and included the location of the weather stations. Two techniques were used to validate the modelled data against the measured data. The first technique correlated the modelled (predicted) air temperature against the measured (observed) air temperature. The second technique used a statistical method proposed by Willmott (1982) to predict the systematic errors, the unsystematic errors and an agreement index between the

predicted and observed temperatures. Initial results showed a slight under-estimation during daylight hours and over estimation at night-time. Chow (2012) made the same observations. Better agreement was achieved when the comparisons were made using data from the daylight hours only. Therefore, the validation exercise showed that during daylight hours reasonable agreement could be achieved whilst, during the hours of darkness, less reasonable agreement could be achieved. This would seem to reflect how ENVI-met models predict heat loss to a clear night-time sky and the heat storage of individual buildings (Chow, 2012). Notwithstanding this issue, the validation exercise showed that ENVI-met could be used to model the urban micro-climate.

9.2.2 Performance of Grid Iron versus Traditional (Organic) Morphologies

One of the early modelling exercises, after initial validation, was to compare a Grid-iron morphology with a Traditional (organic) morphology. Six locations in both morphologies were selected and at all locations the Traditional morphology yielded lower air temperatures than the Grid-iron morphology. This agreed with conventional wisdom for designing cities in hot dry climates, where narrow streets provide shading, which reduces the air temperature, as reported by Taleb (2012) and Johansson (2012). However, these narrow streets prevent motor traffic from accessing individual buildings and the Grid-iron morphology is now the defacto modern form of urban development. The exception to this is Masdar City in Abu Dhabi, where a Traditional urban morphology has been used but has a planned, though not fully implemented, and underground ‘Personal Rapid Transit’ system to enable movement around the city (Griffiths et al., 2020). The cost of this system is high and the oil rich state of Abu Dhabi is struggling to implement it fully. Therefore, in less wealthy regions the Grid-iron morphology is used, despite the Traditional form providing a better thermal solution.

9.2.3 The Effect of Wind Direction on the Urban Grid

As the Grid-iron morphology was now the established urban form of Erbil, the next series of simulations investigated a proposed urban development to the South of the city. The study investigated the impact of the prevailing wind direction on the urban grid. Higher wind speeds in the urban grid would promote natural ventilation that could be used to modify the thermal environment within buildings. Three wind directions were used in the model, two parallel to the orthogonal grid and one at 45° to the grid. The proposed urban development was aligned on a North-South, East-West grid, so the wind directions corresponded to the

prevailing wind direction from the South West, aligned with the street grid canyons, and from the South West, at 45° to the canyons.

For wind directions parallel to the North-South, East-West axes, wind speeds were high in the parallel axes but low in the perpendicular axes. When the wind direction was at 45° to the grid, wind speeds in both axes were similar. These wind speeds were lower than the wind speeds predicted when the wind flowed parallel to the axis but higher than the corresponding wind speeds in the perpendicular axis. Overall, the 45° wind directions (from the South West) gave a better distribution of air flow through the grid. This agrees with the expectation that, when the wind flows parallel to an axis there is no pressure gradient to push the air down the perpendicular axis. At the intersections, there will be some flow down the perpendicular axis as the street canyon's wind experiences a temporary widening of the flow channel. But the air will then be drawn back down the next parallel street canyon. Away from the intersection the perpendicular axis will experience lower air flow, hence lower wind speeds.

When the wind direction is at 45° to the grid, neither axis is preferred; The air flows down the axes evenly but, because the air is flowing down two canyons, its speed is reduced, as predicted by ENVI-met.

When looking at the air temperatures in the canyons, the differences with wind direction were minor. However, when a canyon was aligned to the wind direction (180° and 270°) the canyons air temperature was close to the boundary air temperature as the higher wind speeds pushed the warm air at the boundary along the canyon. When the wind direction was not aligned with the canyon (225°), only the canyons close to the boundary on the lower right-hand side of the urban block experienced higher air temperatures. This implies that buildings on the side exposed to the prevailing wind need either are not temperature dependant or would require additional cooling.

9.2.4 Interventions in the Urban Grid

The next series of simulations explored urban design interventions that may increase wind speeds or reduce air temperature in the urban canyons. The energy that is used for cooling in the summer can be reduced by means of reducing the air temperature around buildings and increasing the wind speed. The conventional assumption is that a one degree drop in air

temperature results in a 10% reduction in cooling load (Akbari, 2005). Three interventions were proposed: (1) adding additional open green areas; (2) increasing the East-West canyons from 12 metres to 20 metres, and (3) adding additional green areas between housing blocks. The urban developments were divided into three zones but in only Zone One were the interventions applied. This enabled the observation of the impact of the interventions on the neighbouring zones.

However, none of the interventions had a significant impact on air temperature or wind speeds within the modified zone or on the adjacent zones. These interventions can be seen as steps exaggerating the Grid-iron morphology by widening the grid spaces between housing blocks whereas the first simulation showed that an organic street pattern of canyons with a high H/W ratio was an advantage in terms of air temperature (see section 6.2), though would lead to wind speeds being reduced.

9.2.5 Natural Shading

The design challenge is to achieve the shading provided by the organic morphology whilst keeping the Grid-iron morphology as recommended by Johansson (2006). In a hot dry climate shade either by vegetation or a manmade device is an obvious choice, as they would provide the shade achieved by the organic morphology but still allow relatively unimpeded wind flow and traffic movement.

The open areas in one zone were simulated with and without trees, i.e. with and without shading (see section 6.7). What the simulations showed was that for the open areas, the introduction of trees to provide shade reduced wind speed, as the trees partially obstruct air flow as reported by Kang, et al. (2017), but this has a minor impact on air temperatures. Air temperatures for open areas without trees recorded lower values compared to the open areas with trees; this was a result of lower wind speeds not flushing out the spaces as effectively as the higher wind speeds in the unobstructed open areas.

Shading a space with trees will have an impact on the radiant exchange in the space in two ways: Firstly, by reducing the solar gain and secondly, by reducing the radiant loss to the sky. As the reduction in solar gain is greater than the reduction in the radiant loss to the sky, the sensation is that the shaded space is cooler. A metric to measure this shading effect is the Mean Radiant Temperature (MRT), (Li et al., 2016).

With ENVI-met predicting the MRT for the open areas with and without trees, a significant reduction occurred between sunrise and sunset for the shaded areas (see section 6.8.3). During the remainder of the day the MRT was similar for shaded and unshaded spaces. The only caveat to express here is that during the validation studies there was a concern with the accuracy of ENVI-met to account for the radiant losses to the clear sky. Therefore, the magnitude of MRT may be overestimated but the difference between shaded and unshaded values stands.

9.2.6 Manmade Shading

In a hot dry climate, shading by trees is difficult because:

- (1) There are low water resources for irrigation
- (2) Trees suitable for arid regions, provide insufficient shade, (Zhao et al., 2018)
- (3) Trees cannot be modified to provide more shade or be removed in response to weather conditions
- (4) Trees reduce wind speeds near buildings, (Kang et al., 2017; Chew and Norford 2019)

Having shown that shading open areas with trees impacts on the MRT significantly, the next step was to introduce an artificial shading system. The system chosen was a wire shading mesh. This type of shading is robust and would, by adjusting the mesh porosity, allow sufficient day light to pass through. The shading mesh performed in a similar manner to the tree shading, having little impact on air temperature, a slight impact on wind speed and a significant impact on MRT, (Kim et al., 2012; Gupta and Tiwari, 2016).

9.3 Building Shading

The next step of the research was to investigate the use of shading over buildings rather than open spaces, with the intention of reducing the solar gain to the exterior of housing in Erbil. ENVI-met has shown that unsurprisingly, shading significantly reduces solar gain.

The main difficulty in using a building energy model to simulate the impact of shading was the modelling of the shading mesh itself. To investigate the impact of shading, a test room was modelled. The room was a three-metre cube with five faces of the cube insulated with 600mm of insulation and the sixth face was a concrete slab covered with concrete tiles. The concrete slab and tiles were to be the roof of the cube, with the walls and floor insulated to

provide an approximate adiabatic boundary. Natural ventilation by infiltration only was allowed into the cube. The shading mesh extended one metre from the sides of the test room, forming a top hat to the room (See Section 8.5).

The building energy model used was IES-VE and within the model there was a routine called Suncast for the modelling of solar isolation studies and shading. To model the shading mesh, the effect of scale of the mesh was first investigated. The wire mesh is made from threads 1.6mm in diameter and to model at that dimension creates a large computational model which is resource intensive. Therefore, the first questions to ask are, at what scale the mesh can be modelled?, and what is the impact of changing the scale?

Eight thread sizes were used, starting with 500mm thread through to the actual size of 1.6 mm. All meshes had a porosity of 50%. The first impact observed was on simulation runtime, the relatively crude mesh of 500mm threads completing the simulation in two minutes, whilst the fine threads of 1.6mm took over 23 hours (See Table 8.2).

The amount of radiation striking the roof through the mesh, per day, showed very little variation with mesh size, the coarse 500mm mesh recording a value of 4.38 kWh/m²/day, whilst the finest mesh recorded 4.28 kWh/m²/day, a difference of 2.3% between the fine and coarse meshes.

The dry bulb air temperature inside the test room was modelled. The maximum divergence of temperature occurred at 18:00, approximately the time of sunset and the end of direct solar gain. The coarse mesh recorded a dry bulb air temperature of 44.38°C and the fine mesh 43.9° C, a difference of 0.48K. This amounts to an error of 1% between the fine and coarse mesh. Therefore, in terms of modelling the shading mesh, the difference between the coarse and fine meshes was relatively slight and the main gain was a seven hundredfold difference in the runtime between the mesh sizes.

For the test room, the impact the shading mesh had on the dry bulb air temperature, between shaded and unshaded scenarios at 18:00, was a reduction of the dry bulb temperature by 5°C. This indicates that the application of a shading mesh would be beneficial in reducing indoor air temperature and thus reducing the amount of cooling required to achieve thermal comfort.

Having established that shading mesh has an impact on the dry bulb temperature in the test room, the next stage of the research investigated the impact of changing the porosity of the mesh. When the porosity was changed by 10% either side of the 50% value, the dry bulb temperature increased as the porosity decreased, and the opposite was observed when the porosity was increased. A second series of simulations was performed, where the porosity of the mesh was increased from 50% to 100% in 10% stages. Not surprisingly, as the porosity increased, the solar gain decreased, and the predicted dry bulb temperature also decreased.

However, as the porosity increased, the time of the peak dry bulb temperature was delayed. For the unshaded roof, the peak dry bulb temperature occurred at approximately 16:00, whilst for the fully-shaded roof, the peak occurred at approximately 20:00, a four-hour delay. This is due to the thermal mass of the test room's roof. The thermal mass of the roof is fixed, and as the porosity increases, less energy is available to heat the roof, so the roof heats up less and more slowly. This then displaces and reduces the peak dry bulb temperature. For the 50% porosity, the displacement of the peak is approximately two hours when compared to the unshaded scenario.

9.4 Shading Mesh Model Validation

Having performed these simulations on this simple test room, the next question to ask is how valid were the results? Ideally, the model should be validated against measured data but this was beyond the resources available. Therefore, to validate the model a second independent simulation package was employed to model the mesh. The simulation package chosen was HTB2, developed by the Architecture School of Cardiff University, which has been tested and validated extensively, (Yau et al., 2011).

The two simulation methods were used on the cube test room, with and without shading mesh for three shape scenarios. All scenarios having the same shading coefficient of 50% transparency. By using two independent simulation packages to predict the same metric, if the two packages yield similar answers, there is greater confidence that the answers predicted are reasonable.

The results show that there was only a small difference between the two simulation methods: the maximum difference was 4.8% and the minimum 1.0%. Overall, these are small differences and give confidence that the strategy used to model the mesh was appropriate.

9.5 Building Simulation.

So far the simulations have been based on the test room, with its walls and floor heavily insulated; clearly this is not typical of house design in Erbil. The next stage of the research simulated the impact of shading mesh on a typical house using local materials. Three variants of a typical house were modelled: one with heavily insulated wall and floor as per the test room; one without openings (windows and doors); and one with openings, with the latter two having typical roof, walls and floor constructions of vernacular materials. They were first simulated without shading mesh. The typical houses with thermal mass performed in a similar manner, but differed greatly from the house with low thermal mass. The low thermal mass house can be considered as a lightweight construction with thermal mass only in the roof while the other two typical houses have far greater thermal mass in the walls, floor and roof. When the dry bulb air temperatures are predicted, the lightweight house clearly follows the ambient external temperature's diurnal cycle, of approximately 31°C minimum temperature and approximately 42°C maximum temperature, a diurnal range of 11K. The typical house with openings had a much flatter diurnal cycle ranging only 0.5K around 36°C and the typical house without openings had a similar diurnal temperature range but operated around 35°C. This highlights the importance of thermal mass as a moderator of indoor temperature in a hot dry climate. Thermal mass reduces the maximum indoor dry bulb temperature by 6K. When the typical house was simulated with shading mesh with a porosity of 50%, the same diurnal cycle was observed to drop by 1.7 or 1.5 K.

In Chapter Four, two solutions were identified to overcome the housing shortage in Erbil. The private solution produced housing that was mostly detached single houses. These corresponded to the houses modelled in the thesis. The government solution was to provide serviced plots, but not to build the housing. The building of individual housing units was the responsibility of the plot owner; with only building height and set-back from the pavement edge controlled (Sabr, 2014). This results in a terrace of houses each filling the width of the plot. The typical house was then modelled as a terrace, with similar houses attached either side. The attached house had a lower predicted dry bulb temperature, as the properties either side reduced the heat gains.

During the summer months, the first floor of a two-storey house is often left unused and the family occupies the cooler ground floor. This mimics the half basement being used during the summer in traditional designs. In hot dry climates the designation of rooms is more fluid, a living room can become a bedroom and vice versa. The dry bulb temperatures of the first floor and ground floor of a single and terraced house, shaded and unshaded, were modelled. The results show that the first floor was warmer than the ground floor. The coolest conditions being on the ground floor of the shaded terrace house; this reinforces the observation made of how two-story houses are being used during the summer. However, the introduction of a shading mesh has only a limited impact on the internal dry bulb air temperature, with thermal mass being much more effective. With the house shaded by the mesh, the daytime solar radiation gains are reduced, but the losses to the clear night-time sky are also reduced and this negates the impact of the overall performance of the shading mesh. This was a disappointing result, as the promise of the test room was not replicated in a typical house.

All previous modelling had the ventilation set to infiltration only, the windows being closed and air entering and leaving through gaps in the construction. This was done to ensure consistency between the various simulations. In reality, window openings would be used to aid ventilation and in particular to promote night-time cooling. Therefore, a final series of simulations was undertaken to investigate the role purpose ventilation would have on the DT of the typical house. Purpose ventilation allows air to enter via open windows, and to prevent overheating night-time ventilation is a recommended strategy. When this strategy was implemented there was a significant reduction in the DT as the cooler night-time air entered the house and cooled the building fabric, during the day the windows were closed and shaded by the mesh which reduced the daytime temperature rise.

This final series of simulations does point the way forward in terms of the role of shading mesh to shade housing in a hot dry climate. Clearly, the mesh limits daytime solar gain, but also limits night-time radiant exchange to the clear night-time sky. By allowing night-time ventilation the building fabric can be cooled, restoring the effect of night-time radiant losses.

The advantage of the shading mesh is that glazing areas can be increased (giving the opportunity for greater ventilation rates) whilst preventing daytime solar gain. This gives greater flexibility in designing facades in hot dry climates. The traditional approach of small openings can be amended to have larger openings without loss of performance; perhaps correcting recent departures from the traditional approach as described in Chapter 4.

Chapter 10: Conclusions

10.1 Aim of the research

The main aim of this research was to investigate the impact of the urban form and shading, on the urban microclimate and indoor dry bulb temperature. To achieve this aim, the following steps are needed:

- 1) Establishing the extent of building regulation and control of recent urban developments of Erbil.
- 2) Understanding Erbil's local climate and investigation of the methodologies that could be employed to alter the urban climate of the grid iron morphology.
- 3) Modelling the thermal performance of dwelling designs in a hot dry climate in these modified urban climates.

Table 10.1 reiterates the research structure of the thesis and Table 10.2 repeats the research aims, objectives and research questions.

Table 10.1: Research phases structure

Research Phase	Phase Concept
Phase 1	Literature and preliminary studies
Phase 2	Urban planning and regulations of Erbil Urban design process. Government and Private housing projects
Phase 3	Urban Microclimate modelling ENVI-met-Validation-Mitigation-Shading mesh
Phase 4	Building Simulation modelling-IES-VE-Shading mesh model-Validation HTB2- Mitigation, shading mesh, interior design, ventilation and façade opening area

Table 10.2 Research aims, objectives and research questions

Phase 1: Literature and preliminary studies	
1.0 This phase aims to identify the gap in knowledge in microclimate and building energy studies	
Objective	
1.1 To understand the climate of Erbil	
1.2 To understand the urban development of Erbil	
1.3 Review tools to model urban microclimate	
1.4 Review tools to model individual building	
Phase 2: Urban planning and regulation of Erbil	
This phase aims to a detailed understanding of the regulatory framework that currently underpins the urban development of Erbil (urban planning and regulations of Erbil)	
Objective	Research question
To understand the urban development process Erbil city	2.1 How is urban planning and development in Erbil executed?
To understand the regulatory framework of the current urban development of Erbil	
Phase 3: Urban Microclimate modelling	
This phase aims to understanding Erbil’s local climate and investigation of the methodologies that could be employed to alter the urban climate of the grid iron morphology	
Objective	Research question
To understand the urban microclimate of Erbil	3.1 How can urban microclimate be modelled and validated?
To model and validate the urban microclimate of Erbil	
To modify the urban microclimate of local urban area	3.2 What is the impact of urban design interventions on urban microclimate (air temperature, wind speed and MRT)?
To understand the impact of shading on urban microclimate	
Phase 4: Building Simulation modelling	
Modelling the thermal performance of a typical house in a hot dry climate in these modified urban climates	

Objective	Research question
To understand the impact of shading mesh on typical dwellings performance.	4.1 Does IES-VE simulate shading mesh and how can the proposed model be validated?
To understand how the impact of shading mesh, thermal mass and ventilation on air temperature, to allow greater freedom in design	4.2 How does the shading mesh and the dwelling design work together to reduce the indoor air temperature.

10.2 Conclusion

Urban design and building regulations have an important impact on the local microclimate and consequently energy consumption of buildings. The residential sector in Iraq generally and Kurdistan especially are considered the most important sector in terms of energy consumption. Kurdistan residential sector consumes more than 50% of total energy compared to 9% for industry, 12% commerce, 12% government, and 13% agriculture (Morad and Ismail 2017). The aim of this study is to reduce the energy consumption in residential morphologies through modifying the outdoor urban microclimate in a hot dry climate and allowing the designer to exploit this microclimate.

10.2.1 Part one: urban planning, urban design process and regulatory frame work of Erbil

The aim of this part of the study is to understand the current urban planning development process in the city. From the establishment of the Kurdish state in 1991, the urban planning of Erbil was directed from Baghdad (i.e. it was centralised). For example, Bashara city in the south, Baghdad in the centre, and Erbil in the north of Iraq used the same building designs principles and requirements, even though they are located in different environmental and cultural zones. This centralised planning led to a transformation of urban morphology developments from traditional (organic) to grid-iron (modern), without any consideration of the local identity and environmental features of the city.

The current urban planning designs in Erbil are mainly influenced by Western urban design approaches (grid-iron) without any consideration of the local architecture identity. The alignment of grid-iron morphology has been driven by geometry rather than local urban microclimate needs.

As Erbil experiences rapid urban expansion, the absence of government environmental regulations and guidance has led to an urban fabric exposed to a harsh climate, especially during the summer months. **This answers the research question 2.1 “How is urban planning and development in Erbil executed”.**

The residential urban projects from 2006–2014 do not represent the city’s architecture, but are employed to cover high housing demands. They vary in quality depending on the cost and their architecture styles do not correspond to the local identity. In addition, these developments have generated various forms of buildings without any urban interconnection between the city and new developments. This independency of developments has created chaos and miscommunication between the old and modern parts of the city.

10.3 Climate modelling and modifying the local urban microclimate

This part of the study aims to modify the local urban microclimate by manipulating urban morphology. The local microclimate condition within an urban area is influenced by the form of buildings, open spaces, and vegetation, which lead to complex interaction between the urban elements. Moreover, it is difficult to analyse and predict an urban microclimate without in-site measurements. Therefore, the present study depends on a meteorological data from an inside urban area and validation process for actual morphologies using ENVI-met, a numerical climate model. The Central Weather Data station (CWD), which is located near Erbil citadel, was employed to model the urban microclimate for the first case study with high urban density. The Southern Weather Data station (SWD) was employed to model the urban microclimate for the second case study with medium to low urban density.

The model was run more than 24 hours, but only the first 24h were used due to the limitations of the software. The result was validated by two methods; firstly, by direct comparison between modelled and measured air temperature in a qualitative approach; secondly, the study used the Willimott methodology which depends on the Index of Agreement (d) between modelled and measured data, a quantitative approach. The validation process for Erbil microclimate simulations involved both overestimation and underestimation of modelled data compared to observed data. The validation results show good agreement during the day time and less agreement during night time. These discrepancies might be associated with model limitations and systematic or unsystematic errors. In general, the model shows a “good agreement” between predicted and measured air temperature during daytime. Thus, the validation of this study for different urban developments in Erbil was

considered sufficient. **This answers the research question 3.1 on finding and validating a model for the urban microclimate of Erbil.**

Urbanisation and new developments have had a significant impact on the urban microclimate of the city. To understand the urban microclimate of Erbil, a numerical analysis of two different urban morphologies was undertaken, predicting urban air temperatures and wind speeds. Traditional and grid-iron urban morphologies were modelled using ENVI-met. The results show that traditional urban morphology had lower external air temperatures than the grid-iron morphology. The results also show that the air temperature for modern grid-iron morphology is higher than traditional organic morphology in both the east-west and north-south street canyons, with a maximum air temperature of 41.40°C and 38.54°C, respectively. This happens because the tradition morphology was originally designed to adapt to the hot dry climate environment, while grid-iron morphology was designed to adapt to development needs, such as housing demands, the modern transportation system, and current infrastructure systems.

Although the traditional morphology recorded a significant reduction in air temperature compared to grid-iron morphology, the presented study relied on modern morphology. This is because traditional morphology is incompatible with modern society and transportation networks. One of the important climatic features of traditional morphology is narrow canyons of less than 2m, and this will not function in modern society which uses private cars for most individual journeys. For these reasons, the modified grid-iron morphology is considered a practical solution for any development in a city.¹ Consequently, the new design scenarios proposed in this study to modify local microclimate will be through vegetation, arrangement of open greenery spaces, and shading strategies.

This phase concerns modifying the urban microclimate through manipulating the grid-iron morphology. The study proposed three urban interventions: adding more open spaces; increasing the east-west canyon widths with the extra open spaces; and, in setting open spaces within the urban blocks with the extra green spaces (see Section 5.16). To modify the urban microclimate of grid-iron morphology sufficiently, a few climatic options can be applied. For instance, maximise wind speed, and minimise air temperature and solar gain.

¹ Masdar City in Abu Dhabi is an exception, where an organic form can be used but requires infrastructure beyond those available to Erbil.

It is important to mention here that it is very difficult to reduce urban air temperature without water evaporation. However, there are limited water resources in most hot, dry cities, and in Erbil city especially, because it is located in a landlocked region. Thus, other strategies may be more useful, such as maximising wind speed to flush out the canyons and urban areas.

To maximise wind speed, the study found that rotating the canyon direction by 45° on the prevailing wind direction of Erbil city was beneficial. The study concluded that when the canyons are in parallel with wind direction, they recorded higher values, but this had a negative impact for perpendicular canyons, which recorded very low values. Therefore, the results show that rotating the canyons 45° from the wind direction distributes the wind better in both directions. In Erbil, the prevailing wind direction is from the SW, so a north-south, east-west grid is appropriate.

Although this method improves the wind speed distribution, the air temperature was only slightly reduced because the wind speed is very low in the urban areas (see Section 5.5.3). The average wind speed in high density urban areas is 0.55 m/s, which is considered very low. Thus, any improvement in wind speed will not reduce the urban air temperature significantly. Because of the geographical position of Erbil and the urban surface roughness the wind speeds in the urban areas are low, various interventions were modelled to increase wind speeds but these had very little impact. The most promising was a significant increase in the open spaces around the urban blocks; however, it was not possible to increase wind speeds just to reduce the impact the urban form has on the wind speed.

In the previous section, urban interventions had very little impact on air temperature and wind speed. However, it was observed that Mean Radiant Temperature (MRT) changed dependent on canyon air temperature. For north-south canyons, there was a very small change in MRT but for the east-west canyons there were significant reductions in the MRT. This shows the value of shading in a hot dry climate.

As shading was observed to be important. Open spaces were covered (shaded) by trees for research purposes, and air temperature, wind speed and Mean Radiant Temperature (MRT) were measured for these shaded open spaces. The results show a significant reduction in MRT, and a limited impact on air temperature and wind speed. In addition, air temperature in open spaces without trees recorded similar or slightly lower than open spaces that were fully covered with trees. This is because there is lower wind speed in open spaces fully covered by trees, as the trees reduce wind speed. The design scenarios showed that any changes in urban

zones, by mean of shading and orientation, have a limited impact on outdoor air temperature and wind speeds, while shading strategy has a significant impact on Mean Radiant Temperature (MRT).

To control and improve local urban microclimate, it is important to propose a new design product that meets comfortable needs. The research simulations demonstrate that shading is one of the most important strategies to manipulate the urban microclimate of hot, dry climate cities. Shading strategy in open spaces and canyons can be observed in the traditional and modern urban areas, and helps to reduce the impact of direct solar radiation, which causes an uncomfortable environment for occupants. The traditional urban morphology used this principle by minimising the width of canyons to avoid direct solar radiation during day time. In addition, shading elements were used vertically in the openings and windows, such as the shanshol and small openings.

During day time, shading has a positive role to play in traditional design, but narrow canyons and small opening elements are negative during night-time. This is because during the day time the building stores thermal mass heat energy, and starts to release this energy after sunset. The wind speeds are very low in narrow canyons and because there are small openings, the hot air will be trapped inside buildings and urban areas. This study used shading mesh with grid-iron morphology as an active strategy for urban planning in Erbil. The shading mesh shields the urban areas from direct solar radiation during day time and the wider canyons facing the correct direction to the prevailing wind help to flush out the thermal energy by ventilation during night time. In addition, the study concluded that using a shading mesh significantly reduces Mean radiant Temperature (MRT) and slightly reduces wind speed and air temperature.

Shading in urban areas helps to improve urban local microclimate through following points. Firstly, it reduces the impact of direct solar radiation that enters into the urban spaces; secondly, it reduces the thermal load on buildings, which leads to improved thermal comfort; finally, it decreases the cooling load in summer. **This answers the research question 3.2 on determining the impact of urban design interventions on urban microclimate air temperature, wind speed and MRT.**

10.4 Building Simulation modelling

After using the shading mesh on an urban scale and significantly reducing MRT, the questions are raised on what happens if the whole building is shaded by the mesh, and how is the indoor air temperature influenced by covering the typical house with shading mesh. To answer these questions, the study had to model very small elements of the shading mesh to simulate the effect of shading mesh. This part of the study takes advantage of the urban climate manipulation, which was described in Section 10.3, and aims to modify the typical house design to reduce the cooling load during summer time. To model a single building, the study used IES-VE, as described in Chapter 2 (Section 2.19). The shading mesh and single building simulations associated with the modelling process difficulties are as described in Section 10.4.1.

10.4.1 Modelling shading mesh

The aim of this section is to model and validate the shading mesh used to modify the microclimate through reducing direct solar radiation over the building. The preparation of the modelling of a single building using IES-VE had various types of complications, such as the correct weather data file set to use, and how to model the shading mesh. The study firstly compared and modelled three sources of weather data sets to determine the most representative local urban microclimate data. The analysis showed that measured data from the Central Weather Station was the most valuable data to be used as input data for building simulation using IES-VE.

The second difficulty was associated with modelling the shading mesh because of the computer's capability, and the need for a very long time to simulate such a small object (see Section 8.4). Because the shading mesh is dimensionally small and the computer cannot model on that scale and the Simulation Run Time will be relatively long (See Section 8.6.1 and Table 8.3). Therefore, the study employed an approximation or simplification method to model the shading mesh. The steps for modelling the shading mesh are described in detail in Chapter 8, Section 8.5.

To model the shading, a novel method was employed called the Hypothetical Approach, which tested the model's capability of simulating a shading mesh in terms of scale, properties and geometry. To validate the approach, the simulation compared the output of another dependable model. The study compared the solar radiation density on the roof surfaces and good agreement was obtained using IES and HTB2 models. **These results answer the**

research question 4.1 of modelling and validating the shading mesh successfully. The model was also used as a research tool to investigate the impact of shading on building indoor air temperature. The first set of simulations was on a Base Case Scenario to explore the thermal performance of the shading mesh. The limitation of this model was that only the roof allowed energy flow, whilst the remaining surfaces, wall and ground floor were adiabatic (Chapter 8, section 8.3).

10.4.2 Design a Base Case Scenario (BCS)

This study proposed a simple box with adiabatic surfaces, except for the roof. The specific building materials and dimension details of modelling the BCS are described in Section 8.5.5 and Table 8.2. The shading mesh was used to cover the roof of BCS and the results were encouraging compared to BCS without shading mesh. The results showed that the indoor Dry Bulb Air Temperature (DT°) of BCS is significantly improved (decreased) when BCS is covered by shading mesh. The ΔDT° for BCS with and without shading mesh was 5 K at 18:00. In addition, the general performance of BCS with shading mesh was enhanced during day and night time because the shading mesh dramatically eliminated the impact solar radiation effect on indoor environment (see Section 8.6 Table 8.5). The study also examined the impact of shading coefficient on indoor DT and found that shading mesh coefficient had a direct relationship with DT. The study found that increasing shading mesh coefficient reduces the direct solar radiation on the roof and decreases DT of the test room (see Section 8.6.3.1). This result answers part of the research question 4.2 of thermal impact of shading mesh on BCS. This process of simulation was the first step to model and improve the residential houses in Erbil. Thus, a typical house was consequently modelled using IES-VE.

10.4.3 Model a typical house with IES-VE

This section of the study aimed to reduce dry bulb temperature in housing projects using architecture design strategies. The shading mesh is used to cover a typical house to explore the influence of shading on DT° . The typical house covered by shading mesh and DT measured for both scenarios with and without shading mesh. The results show that the impact of shading mesh on DT much reduced, because of the extra thermal mass and energy transfer through the other elements of the typical house. The study showed that shading mesh with 50% transparency can reduce the indoor DT by 1.5 k compared to unshaded case (see Section 8.7.2, Figure 8.41). In addition, there are other factors that can contribute to the reduction of

indoor DT, such as attached houses instead of single houses and increasing the shading coefficient from 50% to 100% (see Sections 8.1.7 and 8.03).

As already discussed in the previous chapter a reduction of 1.5 K of the dry bulb temperature by shading a typical house was disappointing compared to the reduction in the external mean radiant temperature. When night time ventilation was introduced, the ability to cool the typical house during this time had a significant impact on the dry bulb temperature, bringing the daytime dry bulb temperature close to the comfort level of 28 °C. This will have the potential to reduce comfort cooling significantly if introduced. The difference between unshaded and shaded scenarios' produced a difference of 0.8 K, again not a great change.

The final piece of analysis looked at the impact of façade opening areas on the predicted dry bulb temperature. What was shown is that by using shading mesh a modern house with 7 times the glazing as a traditional house performed comparably to the traditional house. This illustrates the benefit of shading, in that it allows a greater freedom of façade design without incurring excessive heat gains. This answers research question 4.4 on how the openings and openable areas of typical house facades impact on the indoor air temperature.

The study concludes that a combination of two strategies has the greatest impact on indoor DT in a hot, dry climate region. For example, instead of using the building fabric to reduce the direct solar gain during day time, this study employed the shading mesh to limited solar gain. Night-time cooling reduces the thermal load during night time (night-time cooling strategy).

Employing a holistic approach provides the best results, and allows the designer greater freedom on how the façade and interior design is organised. The advantage of the shading mesh is it allows the designer to move away from the traditional response of designing in a hot, dry climate, i.e. small façade openings, keeping high thermal mass using local materials, and allowing greater openings in the façade to promote ventilation.

The study partly confirmed some ideas originally used in terms of how to design in hot, dry climate (traditional houses), because these strategies have been ignored and not implemented in the current urban fabric of Erbil (modern houses). One important strategy is to reduce solar gain by means of shading. The shading mesh allows retrofitting and can correct mistakes made in the past. The study shows that shading mesh alone is not the complete answer for the hot, dry climate house design and it must be a part of shading provision and fenestration strategy for night-time ventilation and the provision of thermal mass.

The study found that applying one strategy cannot reduce the indoor air temperature of a building, but it can answer some environmental needs. The shading mesh is important because:

1. It gives the designer more freedom in terms of façade design, and night-time ventilation strategy can be successfully implemented.
2. Shading mesh can be used retrospectively to retrofit the existing developments to make them perform better thermally.

Coupling these strategies not only reduces the impact of microclimate on single building cooling energy consumption, but provides more freedom for the designer to design the façade opening without increasing solar gain.

The study found night-time cooling is the most effective strategy and having larger areas of opening to provide more night-time cooling is essential. This strategy cannot be implemented alone, because the large area openings in the façade are associated with solar gain during day time. For this reason, using shading mesh you can have these areas without paying the penalty during the day of excessive solar gain. The shading mesh allows the manipulation of the façade, which allows more night-time ventilation strategies and this combination takes advantage during the day and night-time to lower indoor air temperature in general. This is answer the research question 4.2 ‘**How does the shading mesh and the dwelling design work together to reduce the indoor air temperature**’.

Although shading mesh is translated from the principle of one of the most important strategies for traditional building styles in a hot, dry climate (shading), applying it over the buildings has some advantages and drawbacks. The advantages have been widely explained, and the drawbacks can be described as non-environmental features.

The drawbacks of adding the shade mesh are associated with culture and identity in terms of contradicting the local architecture style of housing units in Erbil. In addition, although shade mesh reduces direct solar radiation in summer, it needs to be removed during winter time. For these reasons, extensive researches are needed in future on the design and technique of applying shading mesh over buildings and open urban spaces. These researches should include; adapting the shading mesh with local architecture identity and construction techniques of Kurdistan, and for precise period of time during a year.

In addition, and from the traditional identity stand point (already ignored in the city's modern developments), the shading mesh might be an inappropriate idea because it will mean a new style of construction that is completely different from the traditional forms of construction in the city. However, it is enormously difficult to go back to designing traditional house morphology and leave behind the new way of transportation which already exists (cars) and air condition. People will not accept a return to an organic form unless the expensive Masdar approach is employed. Even if it conflicts with cultural identity, it can be used as a sufficient solution when coupled with other strategies to reduce the indoor air temperature and energy consumption for existing and new housing developments. These new and existing housing developments represent more than 90% of city areas, so any environmental solution must be resilient and flexible for existing and future building developments.

10.5 Contributions to knowledge

1. Determine the process of urban and residential project designs in Erbil

The process of urban housing design (UHD) in Erbil is not a new topic, but it has witnessed a dramatic change because of the socio-politics of the city. After 2003, Erbil experienced a rapid residential expansion as a result of continuous housing shortage for 33 years. This research has drawn an outline of the UHD process after the new investment law was established in 2006. The literature concluded that this process is not clearly described from an environmental point of view. Therefore, this study used local municipalities' documents, informal interviews, and case studies to analyse and determine the UHD process. This process is significantly important to eliminate the current limitations of housing projects, such as creating a sustainable building environment, and reflecting on local architecture and identity in these types of projects.

2. The impact of shading mesh on a hot/dry urban microclimate

Shading mesh has been studied in empirical research for a small outdoor area (6 m x 3 m x 3 m) or for an indoor test room (2.4 m x 2.4 x 2m) (Shashua-Bar, Pearlmutter et al. 2009). In the present study, shading mesh was simulated using CFD model ENV-met.4. This includes simulating the open urban spaces with shading mesh using single walls features in ENVI-met, as described in Chapter 5. This model generated a series of proposed design scenarios and tested them on a larger scale (urban scale). The model was then used to measure the urban microclimate elements and generate a weather data file for the modified urban microclimate. In addition, the new weather data file was used as input data for the individual building scale simulation process in the second part of this study.

The modelling is important to quantify the impact of shading mesh on local urban microclimate elements.² In addition, it determined which elements of the urban microclimate can be significantly reduced and which elements are difficult to modify.

3. Use a novel methodology to simulate and validate shading mesh using IES-VE and HTB2

The shading mesh modelling comprised four stages, as shown in Figure 10.1. The process of modelling was associated with difficulties, such as long computer running time when actual

² Urban Microclimate elements are air temperature, wind speed and mean radiant temperature of canyons and open spaces.

scale shading mesh was applied (see Chapter 8). Based on literature and practical studies, we proposed a base case model scenario (see Chapter 8). Stage three of the simplification model included different levels of modelling for the shading mesh. This included eight different scales, shapes, and shading coefficients for shading mesh. The method measures the direct solar radiation that falling on base the case model roof. Moreover, the model was validated by comparing two the model's results IES-VE and HTB2 (Figure 10.1).

4. Use a shading mesh model to optimise the impact of shading coefficient on indoor air temperature.

The study modelled and validated the shading mesh over an individual housing unit as shown (Figure 10.1). To optimise the impact of shading mesh, ten shading coefficients from 10–100% were used to cover the typical house model. The results show that shading has an impact on indoor air temperature and shading coefficient has a linear relationship with the reduction of indoor air temperature.

The contribution to the knowledge in terms of modelling is being able to model a shading device relatively crudely (large scale) and still quite effective as it's shown in chapter 8. And in terms of Building Simulation Modelling it does not makes any difference (Thermal performance).

Applying the shading mesh over the buildings has an impact on the radiation that fallen on the surfaces. But it make a limited impact when we have a heavy weight building (high thermal mass) with small openings.

Applying the shading mesh over the buildings gives us a greater freedom to organise the building's façade. Firstly, it corrects the mistakes of the past and secondly, it allows for larger areas of glazing to provide more ventilation in modern buildings.

5. Environmental possibilities the research highlights

Erbil's traditional urban morphology and housing units designed to adapted to the local urban microclimate. This adaptation strategy fundamentally depends on protecting the indoor climate from direct solar radiation (solar gain). However, the strategy is associated with some drawbacks during night time, such as a low ventilation rate during night time because of small façade openings. To regenerate this strategy and employ it to be suited to modern housing style (large openings), this research coupled between shading mesh (to reduce solar gain) during day time with an optimised openings profile during night time (to increase

cooling ventilation. This provides more freedom for designers to design façade openings without increasing solar gain.

10.6 Personal reflections and limitations of the study

The first part of the study was an overview of residential development of Erbil, from an urban designers' point of view. The research undertaken was limited to the design considerations and the social and economic aspects were outside the scope of this study. With hindsight too much time was devoted to this part of the study, covering semi-structured interviews, analysis of Government documents and searching for and comparing Government and private residential projects. This was undertaken to overcome the lack of information concerning the expansion of the city. The initial write up of this work comprised of nearly 200 pages and had to be condensed considerably to be accommodated in to this thesis. It would have been more efficient to have conducted a limited number of semi-structured interviews and the residential case studies to understand the urban designers' perspective. This would have been a much more efficient use of time, but at the start of the research this was not realised.

The next stage of the study considered the numerical modelling of the urban microclimate. I had no experience of using numerical models, as my background was in construction and building design. I found this work complex and difficult to control. The amount of instruction on using ENVI-met was limited and I had to proceed by trial and error. I was only able to achieve the study by contacting other researchers using the software and through their advice I was able to advance. From this I gained confidence in using a new technique and the methodology needed to master this technique.

ENVI-met was used to investigate environmental factors that had an influence on the climate in a city, in a hot dry region. Considerable amount of research time was used in building and testing the climate models and understanding how dependant ENVI-met was on the weather data input file. The model had a simplified air flow and heat exchange function, with the modelling of the night time radiation loss to the night sky identified as a short coming. It was not possible to run the model for an extended period of time to achieve stability, as all that happened was a build-up of energy in the model causing it to heat up over the modelling period and no stable solution was obtained.

The ENVI-met model was useful in indicating the most effective alignment of the street grid to the prevailing wind direction in summer. However, as the prevailing wind speeds were low during the summer months, the urban design modifications (canyon direction, increasing canyon width and green areas had little impact on the microclimate. When natural shading by vegetation was introduced, an impact on the solar gain was observed and this did reduce the mean radiant temperature. In a hot dry climate, with limited water resources to support natural vegetation, using man-made shading meshes achieved similar effects.

As shading is so important in a hot dry region, it would have been more efficient in time and effort not to have undertaken the urban design microclimate mitigation modelling, but to have concentrated on shading of open spaces and buildings from the start.

During the research, Kurdistan was threatened by invasion from ISIS, this disrupted the research by not permitting site visits. It was envisaged that weather data would have been measured as part of this research. And data collected on the impact of shading mesh on open spaces and buildings. Hence the study is purely theoretical.

The next stage of the research used IES to thermally model a typical house in Erbil. This phase of the research started by using a simple cube, with 5 sides heavily insulated to create an almost adiabatic boundary, with the sixth side modelled as a typical flat roof construction. When modelling this test room the impact of shading mesh was significant, however when modelling progressed to the typical house the impact of the shading mesh was frankly disappointing. Further analysis of the results revealed that the thermal mass of the building played a more major role in controlling indoor temperatures. The shading mesh was reducing the solar gain during the day time but restricting the night time radiation losses to the clear night sky. The shading mesh had little impact on the external air temperature as demonstrated in the microclimate modelling.

Additional modelling, allowing air flow through the fenestration, demonstrated that night time cooling was very important, as it cooled the building fabric overnight and then restricted the warming up of the house during the daytime. In essence the research demonstrated that the traditional design approach in a hot dry climate was the most appropriate approach. Which at one level is reassuring but in terms of research effort somewhat disappointing.

However, there is an advantage in using the shading mesh, the shading provided, limits the solar gain during the day time and allows the designer to incorporate large openings in the façade without a significant heat gain. These larger openings, during the night time do provide enhanced night time cooling, resulting in lower overall internal air temperatures. This aspect of the research does merit further development.

From this stage of the research I have gained valuable experience in building simulation modelling and an understanding of a holistic approach to building design that I will carry forward into practice.

10.6.1 Limitations

1. The principle phenomena modelled by ENVI-met were air temperature, wind speed and mean radiant temperature; other factors such as air pollution and noise control were outside the scope of this study.
2. It was only possible, with the computing resources available; to model a relatively small portion of the urban fabric and this meant that the boundary conditions had too great an influence on the internal urban microclimate.
3. Purely a theoretical exercise, a part from weather data no measurement where made on site.
4. No work was undertaken to understand the social acceptance of shading mesh.
5. No simulations were performed outside the summer peak temperature period to gauge the performance of the shading mesh.
6. No practical work was done on the methods of installation of the mesh or how dust and debris would affect its performance.

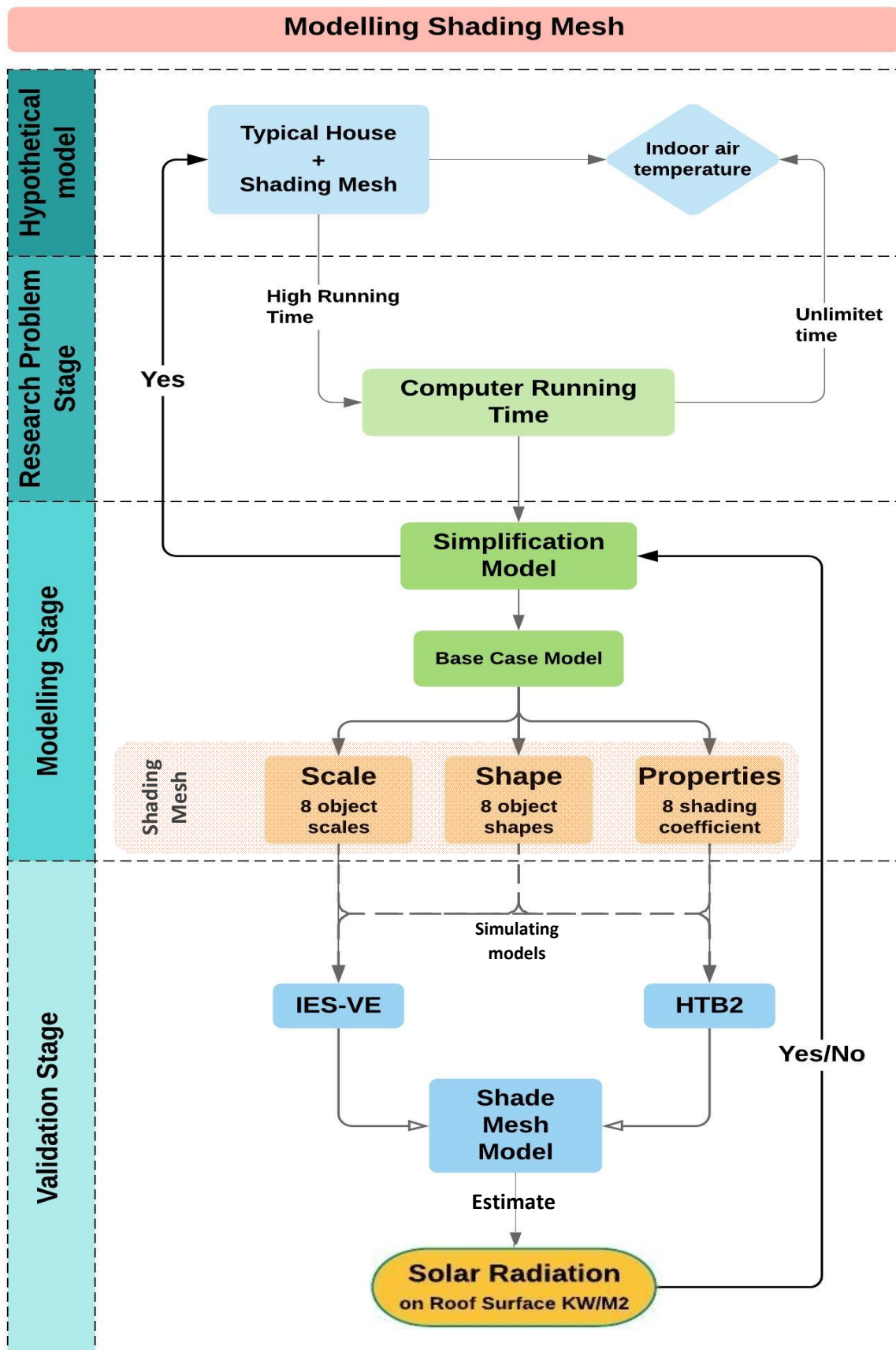


Figure 10.1: Novel methodology to simulate and validate shading mesh using IES and HTB2

10.7 The study recommendations:

1. Rotate the canyon direction by 45° from the prevailing wind directions.
2. Shading mesh with 50% shading coefficient can improve the outdoor thermal comfort for open spaces (crayons and open spaces) and provide sufficient day light.
3. North-south direction is the most appropriate for housing blocks in terms of sufficient solar radiation and wind speed.
4. Attached housing blocks perform better thermally than detached houses.
5. Shading mesh and night-time ventilation work together to reduce the impact of day and night thermal heat gain.
6. Shading mesh can be used to cover urban open spaces and individual housing unit. This reduce the impact of direct solar radiation and increase thermal comfort level for pedestrian.
7. Increase opening openable ratio during night time and closed during day time. This allow to prevent the hot air to enter during day time and allow cooling ventilation to enter during night time.

10.8 Future work

Environmental analysis and measurements of the local urban microclimate show that open spaces and individual buildings can perform better thermally with shading meshes. This environment enhancement represents the theoretical background of shading mesh application in urban and housing units, while the construction and design of this shading mesh could be performed in another study. Moreover, shading mesh may contradict the local architecture and city identity because other buildings are not covered with shading mesh. Therefore, adding new architecture features for environmental purposes needs design work to reflect the local identity of the city and adapt it to the modern style of urban housing projects. These design works should cover local construction techniques and possible removal of shading mesh during winter. In addition, the cost effectiveness of adding shading mesh over both open spaces and housing units needs to be investigated. This includes the amount of energy which can be saved from shading compared to its cost and installation.

References

- Abbas, A. (2017). Erbil Citadel Revitalization and the Presence of Its Emergence History.
- Abdel-Ghany, A. and I. Al-Helal (2011). "Analysis of solar radiation transfer: A method to estimate the porosity of a plastic shading net." *Energy Conversion and Management* 52(3): 1755-1762.
- Abdel-Ghany, A. and I. Al-Helal (2012). "Modeling approach for determining equivalent optical constants of plastic shading nets under solar radiation conditions." *Advances in Materials Science and Engineering* 2012.
- Abdulkareem, S. (2012). *The Adaptation of Vernacular Design Strategies for Contemporary Building Design in Kurdistan*. Texas Tech University, Texas Tech University. Master: 257.
- Abu Hamad - Interviews & Success Stories - interview with Invest in Group, 2014. Available at: <https://investingroup.org/interview/134/rasheed-abu-hamad-trillium-holding/> [Accessed 05 September 2019]
- Ahmed, M. A.-G., et al. (2014). "On the Emissivity and Absorptivity of Plastic Shading Nets under Natural Conditions." *Advances in Mechanical Engineering* 7(1): 165605.
- Ai, Z. T. and C. M. Mak (2015). "From street canyon microclimate to indoor environmental quality in naturally ventilated urban buildings: Issues and possibilities for improvement." *Building and Environment* 94: 489-503.
- Akbari, H., et al. (2001). "Cool surfaces and shade trees to reduce energy use and improve air quality in urban areas." *Solar Energy* 70(3): 295-310. doi:[http://dx.doi.org/10.1016/S0038-092X\(00\)00089-X](http://dx.doi.org/10.1016/S0038-092X(00)00089-X).
- Akbari, H. (2005). "Energy Saving Potentials and Air Quality Benefits of Urban Heat Island Mitigation." Lawrence Berkeley National Lab (2005)
- Akram, O. K., et al. (2015). "The important values of architectural Baghdadi heritage." *Advances in Environmental Biology* 9(24): 46-53.
- Akram, O. K., et al. (2015). "The Significant of Urban Form of Erbil City, Iraq."
- Akram, O. K., et al. (2016). "The Cultural Significant of Erbil City: Case of Traditional Kurdistan Houses." *International Journal of Engineering Technology, Management and Applied Sciences* 4(2): 102-106.
- Al Amoodi, A. and E. Azar (2018). "Impact of Human Actions on Building Energy Performance: A Case Study in the United Arab Emirates (UAE)." *Sustainability* 10(5): 1404.
- Al-Azzawi, S. (1996). "Daily impact of climate on the pattern of urban family life: Indigenous courtyard houses of Baghdad regions of the hot-dry climates Part I: Daily shifts or daily movements in summer." *Renewable Energy* 8(1-4): 289-294.
- Alexander, D. K., et al. (2005). *The simulation of glazing systems in the dynamic thermal model HTB2*. Proceedings of the Ninth International IBPSA Conference, Montréal, QC, Canada.
- Alhagla, K., et al. (2019). "Optimizing windows for enhancing daylighting performance and energy saving." *Alexandria Engineering Journal*.
- Al-Hashimi, F. W. (2016). *The hidden face of Erbil: change and persistence in the urban core*, Nottingham Trent University.

- Al-Hashimi, F. W. (2016). The hidden face of Erbil: change and persistence in the urban core, Nottingham Trent University.
- Al-Hashimi, F. W. and S. Bandyopadhyay (2015). "The Persistent Element in the Old Urban Fabric, Erbil Bazar Area." *Journal of Strategic Innovation and Sustainability* 10(2): 48.
- Al-Homoud, M. S. (2001). "Computer-aided building energy analysis techniques." *Building and Environment* 36(4): 421-433.
- Ali-Toudert, F. and H. Mayer (2006). "Numerical study on the effects of aspect ratio and orientation of an urban street canyon on outdoor thermal comfort in hot and dry climate." *Building and Environment* 41(2): 94-108.
- Ali-Toudert, F. and H. Mayer (2006). "Numerical study on the effects of aspect ratio and orientation of an urban street canyon on outdoor thermal comfort in hot and dry climate." *Building and Environment* 41(2): 94-108.
- Ali-Toudert, F. and H. Mayer (2007). "Effects of asymmetry, galleries, overhanging façades and vegetation on thermal comfort in urban street canyons." *Solar Energy* 81(6): 742-754.
- Ali-Toudert, F. and H. Mayer (2007). "Thermal comfort in an east–west oriented street canyon in Freiburg (Germany) under hot summer conditions." *Theoretical and Applied Climatology* 87(1-4): 223-237.
- Al-Jameel, A. H., et al. (2012). "Spatial configuration of Erbil Citadel."
- Alkmuhtar, A. (2016). "Transformation of place identity; a case of heritage and conflict in Iraq." *International Planning History Society Proceedings* 17(3).
- Allegrini, J., et al. (2015). "A review of modelling approaches and tools for the simulation of district-scale energy systems." *Renewable and Sustainable Energy Reviews* 52: 1391-1404.
- Al-Mudaris, S.B., 2003. The Residential Pattern in Arbil City: An Analytical Study in Urban Geography. M.Sc., Salahaddin University.
- Al-Shwani, S. Y. B. (2011). "Influence of modernity versus continuity of Architectural identity on house facade in Erbil city, Iraq." *Sanis Malaysia*.
- Alznafer, B. M. (2014). The impact of neighbourhood geometries on outdoor thermal comfort and energy consumption from urban dwellings: a case study of the Riyadh city, the kingdom of Saudi Arabia, Cardiff University.
- Amin, R. M. and S. S. M. Al-Din (2019). "Evaluation of the Sustainable Aspects In Housing Sector To Overcome Housing Stress In Northern Iraq." *International Journal of Contemporary Urban Affairs* 3(1): 67-81.
- Ammar, C., Kamran Rakib (2006). "Municipal Strengthening and Training in Erbil." *UN-HABITAT Iraq, Urban and Land Management in Iraq*: 41.
- Andersson, N. (2010). Properties of thermal screens used for energy saving in greenhouses. In *International Conference on Agricultural Engineering-AgEng*.
- Andreou, E. (2013). "Thermal comfort in outdoor spaces and urban canyon microclimate." *Renewable Energy* 55: 182-188.

- Andreou, E. (2014). "The effect of urban layout, street geometry and orientation on shading conditions in urban canyons in the Mediterranean." *Renewable Energy* 63: 587-596.
- Andreou, E. and K. Axarli (2012). "Investigation of urban canyon microclimate in traditional and contemporary environment. Experimental investigation and parametric analysis." *Renewable Energy* 43: 354-363.
- Attia, S., et al. (2009). "Architect friendly": A comparison of ten different building performance simulation tools. Proceedings of 11th International Building Performance Simulation Association Conference and Exhibition, International Building Performance Simulation Association (IBPSA).
- Ayoob Khaleel, I. and N. Ibrahim (2010). "Urban planning for small and medium cities in kurdistan region-iraq." *International Journal of Engineering Science and Technology* 2(12): 7070-7077.
- Ayyash, A. B. (2015). Sustainability in vernacular architecture of Iraq and its applicability in modern residential buildings in Iraq region.
- Bahar, Y., et al. (2013). "A thermal simulation tool for building and its interoperability through the building information modeling (BIM) platform." *Buildings* 3(2): 380-398.
- Baiz, W. H. and S. J. Fathulla (2016). "Urban Courtyard Housing Form as a Response to Human Need, Culture and Environment in Hot Climate Regions: Baghdad as a Case Study." *Int. J. Eng. Res. Appl.* 6(9): 10-19.
- Bakarman, M. A. and J. D. Chang (2015). "The Influence of Height/width Ratio on Urban Heat Island in Hot-arid Climates." *Procedia Engineering* 118: 101-108.
- Bakarman, M. A. and J. D. Chang (2015). "The influence of height/width ratio on urban heat island in hot-arid climates." *Procedia Engineering* 118: 101-108.
- Baker, L. A., et al. (2002). "Urbanization and warming of Phoenix (Arizona, USA): Impacts, feedbacks and mitigation." *Urban ecosystems* 6(3): 183-203.
- Ballarini, I., et al. (2019). "Transformation of an office building into a nearly zero energy building (nZEB): Implications for thermal and visual comfort and energy performance." *Energies* 12(5): 895.
- Balslev, Y. J., et al. (2015). "Climatic and thermal comfort analysis of the Tel-Aviv Geddes Plan: A historical perspective." *Building and Environment* 93, Part 2: 302-318.
- Balslev, Y. J., et al. (2015). "Climatic and thermal comfort analysis of the Tel-Aviv Geddes Plan: A historical perspective." *Building and Environment* 93: 302-318.
- Bazjanac, V. (2008). IFC BIM-based methodology for semi-automated building energy performance simulation, Lawrence Berkeley National Lab.(LBNL), Berkeley, CA (United States).
- Blocken, B. (2014). "50 years of computational wind engineering: past, present and future." *Journal of Wind Engineering and Industrial Aerodynamics* 129: 69-102.
- Blocken, B. (2015). "Computational Fluid Dynamics for urban physics: Importance, scales, possibilities, limitations and ten tips and tricks towards accurate and reliable simulations." *Building and Environment* 91: 219-245.
- Board, A. B. C. (2011). National Construction Code: Building Code of Australia Class 1 and Class 10 Buildings, ABCB.

Bokaie, M., M. K. Zarkesh, P. D. Arasteh and A. Hosseini (2016). "Assessment of Urban Heat Island based on the relationship between land surface temperature and Land Use/Land Cover in Tehran." *Sustainable Cities and Society* 23: 94-104.

Bonan, G. B. (2000). "The microclimates of a suburban Colorado (USA) landscape and implications for planning and design." *Landscape and Urban Planning* 49(3-4): 97-114.

Bornberg, R., et al. (2006). "Traditional versus a global, international style: Aarbil, Iraq." Retrieved on October 7: 2013.

Bornberg, R., et al. (2006). "Traditional versus a global, international style: Aarbil, Iraq." Retrieved on October 7: 2013.

Bourbia, F. and F. Boucheriba (2010). "Impact of street design on urban microclimate for semi-arid climate (Constantine)." *Renewable Energy* 35(2): 343-347.

Bourbia, F. and H. Awbi (2004). "Building cluster and shading in urban canyon for hot dry climate: Part 1: Air and surface temperature measurements." *Renewable Energy* 29(2): 249-262.

Bourbia, F. and H. B. Awbi (2004). "Building cluster and shading in urban canyon for hot dry climate:

Bourikas, L., et al. (2016). "Transforming typical hourly simulation weather data files to represent urban locations by using a 3D urban unit representation with micro-climate simulations." *Future Cities and Environment* 2(1): 7.

Brazel, A. and J. Martin (1997). "Town planning, architecture and building." *Applied Climatology. Principles and Practice*. Routledge, London: 175-186.

Bruse, M. (2004). "ENVI-met 3.0: updated model overview." University of Bochum. Retrieved from: [www. envi-met. com](http://www.envi-met.com).

Calcerano, F. and L. Martinelli (2016). "Numerical optimisation through dynamic simulation of the position of trees around a stand-alone building to reduce cooling energy consumption." *Energy and Buildings* 112: 234-243.

Caldas L. G., and Norford, L. K., (2002) A design optimization tool based on a genetic algorithm, *Automation in Construction*. 11 no. 2 (2002) 173-184.

Carlson, T., et al. (1977). "Potential application of satellite temperature measurements in the analysis of land use over urban areas." *Bulletin of the American Meteorological Society*: 1301-1303.

Castellano, S., et al. (2006). The influence of construction parameters on radiometric performances of agricultural nets. III International Symposium on Models for Plant Growth, Environmental Control and Farm Management in Protected Cultivation 718.

Castellano, S., et al. (2008). "Plastic nets in agriculture: a general review of types and applications. applied engineering in agriculture."

Charabi, Y. and A. Bakhit (2011). "Assessment of the canopy urban heat island of a coastal arid tropical city: The case of Muscat, Oman." *Atmospheric Research* 101(1-2): 215-227.

Chatzidimitriou, A. and S. Yannas (2015). "Microclimate development in open urban spaces: The influence of form and materials." *Energy and Buildings* 108: 156-174.

- Chen, L. and E. Ng (2012). "Outdoor thermal comfort and outdoor activities: A review of research in the past decade." *Cities* 29(2): 118-125.
- Cheung, P. K. and C. Y. Jim (2018). "Comparing the cooling effects of a tree and a concrete shelter using PET and UTCI." *Building and Environment* 130: 49-61.
- Chew, L. W. and L. K. Norford (2019). "Pedestrian-level wind speed enhancement with void decks in three-dimensional urban street canyons." *Building and Environment* 155: 399-407.
- Chi, D. A., et al. (2017). "Design optimisation of perforated solar façades in order to balance daylighting with thermal performance." *Building and Environment* 125(Supplement C): 383-400.
- Chow, W. T. L. and A. J. Brazel (2012). "Assessing xeriscaping as a sustainable heat island mitigation approach for a desert city." *Building and Environment* 47: 170-181.
- Cimmino, M., et al. (2017). "Composite solar façades and wind generators with tensegrity architecture." *Composites Part B: Engineering* 115: 275-281.
- Coban, S. (2013). "Turkey's 'War and Peace': The Kurdish Question and the Media." *Critique* 41(3): 445-457.
- Coccolo, S., et al. (2016). Integration of outdoor human comfort in a building energy simulation database using CityGML Energy Ade. Expanding Boundaries-Systems Thinking in the Built Environment-Proceedings of the Sustainable Built Environment (SBE) Regional Conference Zurich 2016, vdf Hochschulverlag AG ETH Zurich.
- Compagnon, R. (2004). "Solar and daylight availability in the urban fabric." *Energy and Buildings* 36(4): 321-328.
- Costantini, I. (2013). "Statebuilding and Foreign Direct Investment: The Case of Post-2003 Iraq." *International Peacekeeping* 20(3): 263-279.
- Crawley, D. B., et al. (2008). "Contrasting the capabilities of building energy performance simulation programs." *Building and Environment* 43(4): 661-673.
- Creswell, J. W. (2013). *Research design: Qualitative, quantitative, and mixed methods approaches*, Sage publications.
- Dalman, M. (2012). Influences of wind and humidity on thermal comfort of urban canyons in Bandar Abbas, Iran. 7th Windsor Conference: The Changing Context of Comfort in an Unpredictable World 2012.
- Dar (2016). "planning, design, management and consultancy ".
- Díaz-Pérez, J. C. (2013). "Bell pepper (*Capsicum annum* L.) crop as affected by shade level: Microenvironment, plant growth, leaf gas exchange, and leaf mineral nutrient concentration." *HortScience* 48(2): 175-182.
- Din, E. (2008). "6946. 2008. Building Components and building elements—Thermal resistance and thermal transmittance—Calculation method (ISO 6946: 2007); German version EN ISO 6946: 2007." German Institute for Standardization.
- Dong, B., et al. (2007). A comparative study of the IFC and gbXML informational infrastructures for data exchange in computational design support environments. Tenth International IBPSA Conference.

- Duarte, D. H. S., et al. (2015). "The impact of vegetation on urban microclimate to counterbalance built density in a subtropical changing climate." *Urban Climate* 14, Part 2: 224-239.
- Edussuriya, P., et al. (2011). "Urban morphology and air quality in dense residential environments in Hong Kong. Part I: District-level analysis." *Atmospheric Environment* 45(27): 4789-4803.
- EPA (2009). Heat Island Effect. US.
- Erell, E., et al. (2012). *Urban microclimate: designing the spaces between buildings*, Routledge.
- Gao, H., et al. (2019). "Building information modelling based building energy modelling: A review." *Applied Energy* 238: 320-343.
- Ghaffarianhoseini, A., et al. (2019). "Analyzing the thermal comfort conditions of outdoor spaces in a university campus in Kuala Lumpur, Malaysia." *Science of the total environment*.
- Golany, G. S. (1996). "Urban design morphology and thermal performance." *Atmospheric Environment* 30(3): 455-465
- Gómez, F., et al. (2001). "Green zones, bioclimatics studies and human comfort in the future development of urban planning." *Landscape and Urban Planning* 55(3): 151-161.
- González, J. and F. Fiorito (2015). "Daylight design of office buildings: Optimisation of external solar shadings by using combined simulation methods." *Buildings* 5(2): 560-580.
- González, J. and F. Fiorito (2015). "Daylight design of office buildings: Optimisation of external solar shadings by using combined simulation methods." *Buildings* 5(2): 560-580.
- Griffiths S and Sovacool B (2020). "Rethinking the Future Low-carbon City: Carbon Neutrality, Green design, and Sustainability Tensions in Making of Masdar City", *Energy Research and Social Science* Volume 62, 2020
- Grimmond, C. and T. R. Oke (1995). "Comparison of heat fluxes from summertime observations in the suburbs of four North American cities." *Journal of Applied Meteorology* 34(4): 873-889.
- Gupta, N. and G. N. Tiwari (2016). "Review of passive heating/cooling systems of buildings." *Energy Science & Engineering* 4(5): 305-333.
- Haashemi, S., et al. (2016). "Seasonal variations of the surface urban heat island in a semi-arid city." *Remote Sensing* 8(4): 352.
- Hameed, H. (2017). "Estimating the effect of urban growth on annual runoff volume using GIS in the Erbil sub-basin of the Kurdistan Region of Iraq." *Hydrology* 4(1): 12.
- Haywood, J. and M. Schulz (2007). "Causes of the reduction in uncertainty in the anthropogenic radiative forcing of climate between IPCC (2001) and IPCC (2007)." *Geophysical Research Letters* 34(20).
- Hedquist, B. C. and A. J. Brazel (2014). "Seasonal variability of temperatures and outdoor human comfort in Phoenix, Arizona, USA." *Building and Environment* 72: 377-388.
- Hedquist, B. C. and A. J. Brazel (2014). "Seasonal variability of temperatures and outdoor human comfort in Phoenix, Arizona, U.S.A." *Building and Environment* 72: 377-388.

- Hemming, S., et al. (2008). Numerical model to estimate the radiometric performance of net covered structures. Conference proceedings CD AgEng2008 Agricultural and Biosystems Engineering for a Sustainable World, Crete, Greece.
- Herbert, J. M., et al. (1998). "Modelling the thermal climate in city canyons." *Environmental modelling & software* 13(3-4): 267-277.
- House-Peters, L. A. and H. Chang (2011). "Modeling the impact of land use and climate change on neighbourhood-scale evaporation and night-time cooling: A surface energy balance approach." *Landscape and Urban Planning* 103(2): 139-155.
- Hsieh, C.-M., et al. (2016). "A simplified assessment of how tree allocation, wind environment, and shading affect human comfort." *Urban Forestry & Urban Greening* 18: 126-137.
- Huang, J., et al. (2017). "An integrated model for urban microclimate and building energy in high-density cities for early stage design."
- Husami, M. S. (2007). *Energy Crisis Kurdistan And The Impact of Renewable Energy*. Department of Mechanical Engineering. United Kingdom, University of Strathclyde. Master: 141.
- Huttner, S. (2012). "Further development and application of the 3D microclimate simulation ENVI-met." Mainz University, Germany.
- Huttner, S., et al. (2008). Using ENVI-met to simulate the impact of global warming on the microclimate in central European cities. 5th Japanese-German Meeting on Urban Climatology.
- Huttner, S., et al. (2008). Using ENVI-met to simulate the impact of global warming on the microclimate in central European cities. 5th Japanese-German Meeting on Urban Climatology.
- Ibrahim, G. R. F. (2013). *Urban Expansion Monitoring in Erbil City. Utilizing Remote Sensing tools in the Kurdistan Region. Development and society*. UK, Sheffield Hallam University. Master of Science in Geographic Information Systems (GIS): 70.
- Ibrahim, R. I., S. A. Mushatat and M. G. Abdelmonem (2015). "Erbil." *Cities* 49: 14-25.
- Izady, M. (2015). *The Kurds: a concise history and fact book*, Taylor & Francis.
- Jeong, D., et al. (2015). Validation of ENVI-met PMV values by in-situ measurements. ICUC9-9th International Conference on Urban Climate Jointly with 12th Symposium on the Urban Environment Validation.
- Johansson, E. (2006). "Influence of urban geometry on outdoor thermal comfort in a hot dry climate: A study in Fez, Morocco." *Building and Environment* 41(10): 1326-1338.
- Jones, P. J., et al. (2013). "Intensive building energy simulation at early design stage."
- Judkoff, R., et al. (2008). *Methodology for validating building energy analysis simulations*, National Renewable Energy Lab.(NREL), Golden, CO (United States).
- Kadaverugu, R., et al. (2019). "High Resolution Urban Air Quality Modeling by Coupling CFD and Mesoscale Models: a Review." *Asia-Pacific Journal of Atmospheric Sciences*: 1-18.
- Kanda, M. (2007). "Progress in urban meteorology: A review." *Journal of the Meteorological Society of Japan*. Ser. II 85: 363-383.

- Kang, G., et al. (2017). "Development of a computational fluid dynamics model with tree drag parameterizations: Application to pedestrian wind comfort in an urban area." *Building and Environment* 124: 209-218.
- Kaptan, M. V. (2019). "Climate-responsive design strategy for Erbil city." *Archnet-IJAR: International Journal of Architectural Research*.
- Karamata, B. and M. Andersen (2014). *Concept, Design and Performance of a Shape Variable Mashrabiya as a Shading and Daylighting System for Arid Climates*. 30th PLEA Conference- sustainable habitat for developing societies, cept University Ahmedabad.
- Khayat, M. "Uncontrolled Urban Growth in Kurdistan."
- Kim, D.-W. and C.-S. Park (2011). "Difficulties and limitations in performance simulation of a double skin façade with EnergyPlus." *Energy and Buildings* 43(12): 3635-3645.
- Kim, G., et al. (2012). "Comparative advantage of an exterior shading device in thermal performance for residential buildings." *Energy and Buildings* 46: 105-111.
- Kirimtat, A., et al. (2016). "Review of simulation modeling for shading devices in buildings." *Renewable and Sustainable Energy Reviews* 53: 23-49.
- Kong, F., et al. (2016). "Energy saving potential of fragmented green spaces due to their temperature regulating ecosystem services in the summer." *Applied Energy* 183: 1428-1440.
- KRG (2013). *Erbil City Centre; draft master plan*
- Krüger, E. L. (2015). "Urban heat island and indoor comfort effects in social housing dwellings." *Landscape and Urban Planning* 134: 147-156.
- Krüger, E., et al. (2017). "Calibration of the physiological equivalent temperature index for three different climatic regions." *International journal of biometeorology* 61(7): 1323-1336.
- Krüger, E. L., et al. (2011). "Impact of urban geometry on outdoor thermal comfort and air quality from field measurements in Curitiba, Brazil." *Building and Environment* 46(3): 621-634.
- Kubilay, A., et al. (2018). "Coupling of physical phenomena in urban microclimate: A model integrating air flow, wind-driven rain, radiation and transport in building materials." *Urban Climate* 24: 398-418.
- Kumar, R. and S. Kaushik (2005). "Performance evaluation of green roof and shading for thermal protection of buildings." *Building and Environment* 40(11): 1505-1511.
- Kwarteng, A. Y. and C. Small (2005). "Comparative analysis of thermal environments in New York City and Kuwait City." *Proceedings of the Remote Sensing of Urban Areas, Tempe, AZ, USA*: 14-16.
- Lazzarini, M., et al. (2013). "Temperature-land cover interactions: The inversion of urban heat island phenomenon in desert city areas." *Remote Sensing of Environment* 130: 136-152.
- Lee, H., H. Mayer and W. Kuttler (2019). "To what extent does the air flow initialisation of the ENVI-met model affect human heat stress simulated in a common street canyon?" *International Journal of Biometeorology* 63(1): 73-81.
- Li, L., et al. (2016). "Performance evaluation of building integrated solar thermal shading system: Building energy consumption and daylight provision." *Energy and Buildings* 113: 189-201.

- Liang, H., et al. (2018). Study on Evaluation and Control Method for Thermal Environment of a Residential Site Planning Based on CTTC Model. 2018 International Conference on Mechanical, Electrical, Electronic Engineering & Science (MEEES 2018), Atlantis Press.
- Lin, T.-P., et al. (2010). "Shading effect on long-term outdoor thermal comfort." *Building and Environment* 45(1): 213-221.
- Lomas, K. J. (1996). "The UK applicability study: an evaluation of thermal simulation programs for passive solar house design." *Building and Environment* 31(3): 197-206.
- Lomas, K. J. and H. Eppel (1992). "Sensitivity analysis techniques for building thermal simulation programs." *Energy and Buildings* 19(1): 21-44.
- Maile, T., et al. (2007). "Building energy performance simulation tools-a life-cycle and interoperable perspective." Centre for Integrated Facility Engineering (CIFE) Working Paper 107: 1-49.
- Maile, T., et al. (2010). "Formalizing approximations, assumptions, and simplifications to document limitations in building energy performance simulation." CIFE WP126 Stanford University.
- Martinelli, L., et al. (2015). "Assessment of the influence of daily shadings pattern on human thermal MassCity. (2019). "Arbil MassCity." Retrieved 05 September 2019, from www.masscityiraq.com.
- Matson, M., et al. (1978). "Satellite detection of urban heat islands." *Monthly Weather Review* 106(12): 1725-1734.
- McIlmail, T. P. (1994). "No-Fly Zones: The Imposition and Enforcement of Air Exclusion Regimes over Bosnia and Iraq." *LoY. LA Int'l & Comp. LJ* 17: 35.
- Meho, L. I. (1997). *The Kurds and Kurdistan: A selective and annotated bibliography*, ABC-CLIO.
- Meteoblue (2016). "Weather archive Erbil." From https://www.meteoblue.com/en/weather/forecast/week/kirkuk_iraq_94787. comfort and attendance in Rome during summer period." *Building and Environment* 92: 30-38.
- Middel, A., et al. (2012). "Land cover, climate, and the summer surface energy balance in Phoenix, AZ, and Portland, OR." *International Journal of Climatology* 32(13): 2020-2032.
- Middel, A., et al. (2015). "Urban forestry and cool roofs: Assessment of heat mitigation strategies in Phoenix residential neighbourhoods." *Urban Forestry & Urban Greening* 14(1): 178-186.
- Mills, G. (1997). "An urban canopy-layer climate model." *Theoretical and Applied Climatology* 57(3): 229-244.
- Mills, G. Urban climatology: history, status and prospects. *Urban Clim* 2014; 10: 479–89.
- Mirrahimi, S., et al. (2016). "The effect of building envelope on the thermal comfort and energy saving for high-rise buildings in hot-humid climate." *Renewable and Sustainable Energy Reviews* 53: 1508-1519.
- Mohajerani, A., et al. (2017). "The urban heat island effect, its causes, and mitigation, with reference to the thermal properties of asphalt concrete." *Journal of environmental management* 197: 522-538
- Montávez, J. P., et al. (2000). "A study of the urban heat island of Granada." *International Journal of Climatology* 20(8): 899-911.

- Moonen, P., et al. (2012). "Urban Physics: Effect of the micro-climate on comfort, health and energy demand." *Frontiers of Architectural Research* 1(3): 197-228.
- Morad, D. H. and S. K. Ismail (2017). "A Comparative Study Between the Climate Response Strategies and Thermal Comfort of a Traditional and Contemporary Houses in KRG: Erbil." *Kurdistan Journal of Applied Research* 2(3): 320-329.
- Morris, C. J. G., et al. (2001). "Quantification of the influences of wind and cloud on the nocturnal urban heat island of a large city." *Journal of Applied Meteorology* 40(2): 169-182.
- Mortada, H. (2003). *Traditional Islamic principles of built environment*, Routledge.
- Mostafavi, N., et al. (2015). "Envelope retrofit analysis using eQUEST, IESVE Revit Plug-in and Green Building Studio: a university dormitory case study." *International Journal of Sustainable Energy* 34(9): 594-613.
- Naboni, E., et al. (2018). *Outdoor comfort simulation of complex architectural designs: a review of simulation tools from the designer perspective*.
- Nagy, G. (2006). "Strengthening the Capacity of the Housing Sector in Iraq." *Housing Finance International* 20(4): 3.
- Naqshbandi, A. M. A. K. S. (2016). "IMPACT OF THE CITY STREETS ON CITY TEMPERATURES STREETS OF ERBIL CITY AS A CASE STUDY." *two hundred years of urban methodology in the heart of Florence* 11.
- Nastaran, S. (2013). "Street Design and Urban Microclimate: Analysing the Effects of Street Geometry and Orientation on Airflow and Solar Access in Urban Canyons." *Journal of Clean Energy Technologies* 1(1): 52-56.
- Nichol, J. E. (1996). "High-resolution surface temperature patterns related to urban morphology in a tropical city: A satellite-based study." *Journal of Applied Meteorology* 35(1): 135-146.
- Nooraddin, H. (2012). "Architectural Identity in an Era of Change." *Developing Country Studies* 2(10): 81-96.
- Oke, T. R. (1973). "City size and the urban heat island." *Atmospheric Environment* (1967) 7(8): 769-779.
- Oke, T. R. (1976). "The distinction between canopy and boundary-layer urban heat islands." *Atmosphere* 14(4): 268-277.
- Oke, T. R. (1987). *Boundary layer climates*. London New York, London New York: Methuen.
- Oke, T. R. (2002). *Boundary layer climates*, Routledge.
- Okeil, A. (2010). "A holistic approach to energy efficient building forms." *Energy and Buildings* 42(9): 1437-1444.
- O'Leary, B., et al. (2006). *The future of Kurdistan in Iraq*, University of Pennsylvania Press.
- Omidfar, A. (2015). *Performance evaluation of complex facades using various shading systems with ornamental patterns*. IES Annual Conference. Indianapolis, USA.

- Omidfar, A., et al. (2014). Performance-based design of a self-standing building skin; A methodology to integrate structural and daylight performance in a form exploration process. Proceedings of IASS Annual Symposia, International Association for Shell and Spatial Structures (IASS).
- Parow, S. (2017). Italian City Mede in Kurdistan. R. TV. Erbil, Rudaw.
- Pearlmutter, D. and S. Rosenfeld (2008). "Performance analysis of a simple roof cooling system with irrigated soil and two shading alternatives." *Energy and Buildings* 40(5): 855-864.
- Pearlmutter, D., et al. (1999). "Microclimatic analysis of "compact" urban canyons in an arid zone." *Atmospheric Environment* 33(24-25): 4143-4150.
- Pentz, M. (1988). Handling experimental data. Milton Keynes, [England]
Philadelphia, Milton Keynes, England Philadelphia : Open University Press.
- Pisello, A. L., V. L. Castaldo, T. Poli and F. Cotana (2014). "Simulating the Thermal-Energy Performance of Buildings at the Urban Scale: Evaluation of Inter-Building Effects in Different Urban Configurations." *Journal of Urban Technology* 21(1): 3-20.
- Price, J. C. (1979). "Assessment of the urban heat island effect through the use of satellite data." *Monthly Weather Review* 107(11): 1554-1557.
- Radhi, H. (2009). "A comparison of the accuracy of building energy analysis in Bahrain using data from different weather periods." *Renewable Energy* 34(3): 869-875.
- Radhi, H., F. Fikry and S. Sharples (2013). "Impacts of urbanisation on the thermal behaviour of new built up environments: A scoping study of the urban heat island in Bahrain." *Landscape and Urban Planning* 113: 47-61.
- Rao, P. K. (1972). "Remote sensing of urban" heat islands" from an environmental satellite." *Bulletin of the American Meteorological Society* 53(7): 647-648.
- Rasul, A., et al. (2017). "A review on remote sensing of urban heat and cool islands." *Land* 6(2): 38.
- Rasul, A., H. Balzter and C. Smith (2015). "Spatial variation of the daytime Surface Urban Cool Island during the dry season in Erbil, Iraqi Kurdistan, from Landsat 8." *Urban Climate* 14, Part 2: 176-186.
- Rasul, A., H. Balzter and C. Smith (2016). "Diurnal and Seasonal Variation of Surface Urban Cool and Heat Islands in the Semi-Arid City of Erbil, Iraq." *Climate* 4(3): 42.
- Ratti, C., et al. (2005). "Energy consumption and urban texture." *Energy and Buildings* 37(7): 762-776.
- Rijal, H. B., P. Tuohy, M. A. Humphreys, J. F. Nicol, A. Samuel and J. Clarke (2007). "Using results from field surveys to predict the effect of open windows on thermal comfort and energy use in buildings." *Energy and buildings* 39(7): 823-836.
- Rizwan, A. M., et al. (2008). "A review on the generation, determination and mitigation of Urban Heat Island." *Journal of Environmental Sciences* 20(1): 120-128.
- Ruksana, A. (2014). A study on micro-climate of URBAN CANYON and its impact on surrounding urban area.

- Sabr, C. (2016). *Urban Form and Regulations: A Morphological Analysis of Erbil City*, University of Sheffield.
- Santamouris, M. (2014). "Cooling the cities—a review of reflective and green roof mitigation technologies to fight heat island and improve comfort in urban environments." *Solar Energy* 103: 682-703.
- Santos, L. G. R., et al. (2018). "Evaluating approaches for district-wide energy model calibration considering the Urban Heat Island effect." *Applied Energy* 215: 31-40.
- Scherer, D., et al. (1999). "Improved concepts and methods in analysis and evaluation of the urban climate for optimizing urban planning processes." *Atmospheric Environment* 33(24-25): 4185-419
- Shahidan, M. F., et al. (2012). "An evaluation of outdoor and building environment cooling achieved through combination modification of trees with ground materials." *Building and Environment* 58: 245-257.
- Sharmin, T. and K. Steemers (2019). *Impact of urban geometry on indoor air temperature and cooling energy consumption in traditional and formal urban environments*, Ecohouse Initiative Ltd.
- Sharmin, T., et al. (2019). "Outdoor thermal comfort and summer PET range: A field study in tropical city Dhaka." *Energy and Buildings*.
- Shashua-Bar, L. and M. E. Hoffman (2000). "Vegetation as a climatic component in the design of an urban street: An empirical model for predicting the cooling effect of urban green areas with trees." *Energy and Buildings* 31(3): 221-235.
- Shashua-Bar, L. and M. E. Hoffman (2002). "The Green CTTC model for predicting the air temperature in small urban wooded sites." *Building and Environment* 37(12): 1279-1288.
- Shashua-Bar, L., et al. (2009). "The cooling efficiency of urban landscape strategies in a hot dry climate." *Landscape and Urban Planning* 92(3-4): 179-186.
- Sherif, A. El-Zafarany and R. Arafa, *External perforated window Solar Screens: The effect of screen depth and perforation ratio on energy performance in extreme desert environments*, *Energy and Buildings*. 2012 (2012) 1-10.
- Skelhorn, C. P., et al. (2016). "Urban greening and the UHI: Seasonal trade-offs in heating and cooling energy consumption in Manchester, UK." *Urban Climate*.
- Solomon, S. (2007). *Climate change 2007-the physical science basis: Working group I contribution to the fourth assessment report of the IPCC*, Cambridge University Press.
- Taha, A. (2017). "Analysis of developmental role of Non-Governmental Organisations in Iraqi Kurdistan and its impact on long term socio-economic and political stability." *Ethik und Wirtschaft: Wissenschaftliche Schriftenreihe* 7: 27.
- Takebayashi, H. and M. Moriyama (2009). "Study on the urban heat island mitigation effect achieved by converting to grass-covered parking." *Solar Energy* 83(8): 1211-1223.
- Taleb, D. and B. Abu-Hijleh (2013). "Urban heat islands: Potential effect of organic and structured urban configurations on temperature variations in Dubai, UAE." *Renewable Energy* 50: 747-762.
- Thomas, M. J. T. (2006). "Inside outside: A relationship that moves me!".

- Toparlar, Y., et al. (2017). "A review on the CFD analysis of urban microclimate." *Renewable and Sustainable Energy Reviews* 80: 1613-1640.
- Tran, H., et al. (2006). "Assessment with satellite data of the urban heat island effects in Asian mega cities." *International journal of applied Earth observation and Geoinformation* 8(1): 34-48.
- Tsoka, S., A. Tsikaloudaki and T. Theodosiou (2018). "Analysing the ENVI-met microclimate model's performance and assessing cool materials and urban vegetation applications—A review." *Sustainable cities and society* 43: 55-76.
- UNESCO (2009). *World Heritage Cultural Landscape: A handbook for conservation and management*.
- Unger, J. (2004). "Intra-urban relationship between surface geometry and urban heat island: review and new approach." *Climate research* 27(3): 253-264.
- Upreti, R., et al. (2017). "Radiative shading effect of urban trees on cooling the regional built environment." *Urban Forestry & Urban Greening* 26: 18-24.
- Van Esch, M. M. E., et al. (2012). "The effects of urban and building design parameters on solar access to the urban canyon and the potential for direct passive solar heating strategies." *Energy and Buildings* 47: 189-200.
- Waldron, D., et al. (2013). "Embodied energy and operational energy: Case studies comparing different urban layouts."
- Walter, E. and J. H. Kämpf (2015). A verification of CitySim results using the BESTEST and monitored consumption values. *Proceedings of the 2nd Building Simulation Applications conference*, Bozen-Bolzano University Press.
- Weng, Q., et al. (2004). "Estimation of land surface temperature–vegetation abundance relationship for urban heat island studies." *Remote sensing of Environment* 89(4): 467-483.
- Willmott, C. J. (1982). "Some comments on the evaluation of model performance." *Bulletin of the American Meteorological Society* 63(11): 1309-1313.
- Wong, N. H., et al. (2011). "Evaluation of the impact of the surrounding urban morphology on building energy consumption." *Solar Energy* 85(1): 57-71.
- Yang, W., et al. (2013). "Thermal comfort in outdoor urban spaces in Singapore." *Building and Environment* 59: 426-435.
- Yang, X. and Y. Li (2015). "The impact of building density and building height heterogeneity on average urban albedo and street surface temperature." *Building and Environment* 90: 146-156.
- Yang, X., et al. (2012). "An integrated simulation method for building energy performance assessment in urban environments." *Energy and Buildings* 54: 243-251.
- Yang, Y., et al. (2019). "The “plant evaluation model” for the assessment of the impact of vegetation on outdoor microclimate in the urban environment." *Building and Environment*.
- Yao, R., et al. (2011). "A simplified mathematical model for urban microclimate simulation." *Building and Environment* 46(1): 253-265.

Yezioro, A., et al. (2008). "An applied artificial intelligence approach towards assessing building performance simulation tools." *Energy and Buildings* 40(4): 612-620.

Zhao, C., et al. (2011). "Urban planning indicators, morphology and climate indicators: A case study for a north-south transect of Beijing, China." *Building and Environment* 46(5): 1174-1183.

Zhao, Q., et al. (2018). "Impact of tree locations and arrangements on outdoor microclimates and human thermal comfort in an urban residential environment." *Urban Forestry & Urban Greening* 32: 81-91.

A fieldwork plan for July 2017

1. What are the current planning guidance and construction codes in the city of Erbil, what are the problems that effect current urban planning in the region generally and Erbil city specifically?

Research Places	Issues	Fieldwork Activities		
		Semi-structure interview	Government Documentation	Photographs, plans and design works
Municipalities	<ul style="list-style-type: none"> - Municipality requirements for urban design permission (Codes, standards, laws, and personal decisions) - Process of Approving urban design projects. - Responsibility of design control if there wear any. - Building and renovation guideline for urban planning and housing projects. - Environmental requirements of current urban design projects. - What are the current problems associate with urban panning in your municipality - Current and future plan. 			
Architecture offices	<ul style="list-style-type: none"> - Design Process - Standard and Guidelines - Quality control - Design approval - Design products if any (urban or housing) projects. - Current problems associate with design works and local authorities approval - Design specialists <ol style="list-style-type: none"> a. Planners b. Architects c. Engineers 			

Department of Urban planning of Erbil	<ul style="list-style-type: none"> - Role of department in term of design new urban projects. - General Requirement for any urban project and housing projects. - Responsibility of the department and what are the other department that connect to their works. - Any project from 2003 to now. - Lf any, where.... 			
Master plan of Erbil published in 2006 to 2030	<ul style="list-style-type: none"> - Summary of master plan - Who and how they implement the master plan - Requirement of the master plan in both urban scale and building projects - Who take the responsibility of implementation of master plan - Any projects or out come from this masterplan 			
Ministry of municipality and truism	<ul style="list-style-type: none"> - Role of Ministry of municipality in planning and urban design projects. - Ministry requirements for urban projects - Any projects after 2003 and so far - Current and future plan of ministry in term of: <ol style="list-style-type: none"> a. Social b. Economic c. Politics d. Educations and heath e. Infrastructure 			
Department of investment	<ul style="list-style-type: none"> - What are the requirements of urban and housing projects approval? - Role and responsibility of investment department. - Law of investment and implement that law - Quality control and follow-up over the urban projects. - Any environmental requirements associated with housing projects. 			

2. What are the problems that associate with urban Rapid expansion of Erbil city

Themes	Issues	Fieldwork Activities		
		Semi-structure interview	Government Documentation	Photographs, plans and design works
History and process of developing urban design after 2003	<ul style="list-style-type: none"> - Factors and fundamental aspects that associated with rapid expansion in the city after 2003, 2006, 2009, 2012' 2014, and now: - Socially - Economically - Politically 			
Municipalities	<ul style="list-style-type: none"> - How the municipalities deal with rapid expansion in the city? - What are their action towards current urban expansion and future developments? 			
Architecture offices	<ul style="list-style-type: none"> - What are benefits and problems that associate with rapid expansion of city in your point of view? - Did the design project requirements updated with urban growth in the city? - What is the reaction towards new projects if any? 			

Department of Urban planning of Erbil	<ul style="list-style-type: none"> - Why the city face rapid expansion? - When the expansion start and how the department faced that problem? - Who is take the responsibility of rapid expansion? - What is the current and future action for the department to solve this problem? 			
Master plan of Erbil published in 2006 to 2030	<ul style="list-style-type: none"> - How the master plan implemented? - Any update on master plan - What is the problems that associate with accelerate or delay implementation master plan? - 			

Themes of qualitative approach in this study

1. Rapid expansion (socio-economic, geopolitics, migration)
2. Kurdish identity (Iraqi system, lack of regulations and experienced)
3. Urban design (local company and designers, regulations)
4. Master plan of city (without any environmental considerations)

Sample of Interviews

Interview with: Architect from Senior Architect (DA)

Interviewee job title: Manager of Design in Erbil's Investment Department

Date: 15/07/2017

Location: Erbil City, Iraq Kurdistan Region, Investment Department Building, Interviewer: Ali Salih (AL)

Time of interview period: 2 hours

Language: Kurdish Sorani, translated by the researcher

Erbil Urban Development

Al: What do you use as standards for urban design?

DA: We have a book of investment rules in Kurdistan, but nobody works with that. The work here is just temperamental (variable). For example, every manager has their own strategy to follow. In addition, every architect has their understanding of what a rule is or how to follow the law of investment. For this reason, in design we do not have any standards or specific requirements; we design and do not know what we are doing – it might work or not with our environment.

At the time (From 2009 to 2014), that we were attracting investors (locals and foreigners) to come and invest in Kurdistan, our aim was just to let them in with their money. We give companies privileges as well as encouragement to invest in Kurdistan in general and Erbil especially.

The investment law has many advantages for new investors as below:

1. Ten-year tax free period
2. Five-year tax free period for importing any equipment for construction
3. Free land for the construction of any project
4. Provision of basic infrastructure needs to projects, such as roads, electricity and water.

After 2008 and the geopolitical problems in other parts of Iraq, most internal and foreign companies invested in the capital city of Kurdistan (Erbil). A group of architects and engineers suggested that the new projects were designed to follow our instructions and local climate materials to encourage the local identity and traditional architecture. The ideas were a few concepts and a proposal framework to reorganise housing projects. This proposal reflected the traditional and local environment by using:

1. Local materials for construction

2. Cultural and traditional architecture elements in the design process
3. Design products adapted to the local environment.

In 2008, the investment process was at the beginning in the Kurdistan region, and we did not have the power to force investors to follow our rules, but, in contrast, we encouraged them to invest, with some limited requirements.

On one hand, politics played a massive role in changing the requirements and had more power than the designers. This led to a change in our proposal on fundamental requirements. On the other hand, there were other problems related to housing projects. The new projects were having problems such as wastewater recycling and sewage systems.

For design requirements, we depend on the Iraqi Urban Planning Standards Manual. In addition, we depend on notes from our site engineers to update the design requirements to avoid repetitive site problems. In addition, many projects have no building insulation or other building material, which may reduce the construction cost.

Al: After 2006, following the law of investment, when did the housing projects actively begin to be constructed?

Da: In 2011 and 2012, many investment companies and the Urban Planning Department worked on this.

In 2007, the first project was undertaken in a collaboration between the government and the investment company. The owner of a housing unit paid 50% of the cost and the other 50% was paid by the government.

As a site plan, which is the first step of the design proposal, the designers did not use any environmental standards or sustainable principles in their designs. Housing project site plans are normally designed without consideration for orientation, and there is no difference between the north and south facing housing units in terms of design.

The Investment Department did not have any environmental requirements, but after five years of housing project investment, the Ministry of the Environment published new requirements for green areas in housing projects site as 25–30% of total area. This new rule applies to future projects, while old projects did not have the requirement for the green area ratio to total project area.

Al: The investment projects started in Kurdistan after 2006. How was the situation or working environment in 2007 and at the beginning of the construction stage?

Da: The lack of construction experience was not the only problem, but the investors only attempted to reduce the building costs to increase profits. The first stage of housing project design did not reach an acceptable level (low quality), because the projects were designed by architects who had recently graduated or in some cases the projects were designed by architecture students.

In addition, the follow up team in the Investment Department was comprised of only two architects, and they could not control the checking and reviewing process of all the investment projects, including other investment sectors such as health, tourism, and industrial projects.

Moreover, the duty of our team (investment department architects) was not just to review the designs, but supervise the construction process as well.

Al: What are the stages or the process of housing project permission (licencing)?

The process starts with design and ends with a project licence to construct as below:

a. Site Plan:

1. Checking and reviewing the proposal site plan in term of services, green area, open spaces, public spaces and land use in general
2. The ratio of building areas compared to open spaces, plot area, buildings area, roads and canyons
3. Planning requirements: this review includes schools, health centres, petrol stations and shops, and distance to housing unit.

b. Building and Housing designs

1. Reviewing the housing unit's design, in terms of location of plots, building areas to open area.
2. Service buildings design. The design proposal is reviewed in detail.

After that, we send the design proposal to the urban planning department for acceptance of design concepts and comparison with Iraq's urban planning requirements.

Al: What is your role and responsibility as an investment department architect in the process of constructing housing projects?

Da: We have huge responsibility for all project stages. Firstly, we review and accept the design proposal and secondly we review the construction stage. However, I cannot control the projects because of the points below:

1. Limited experience at the time of project starting
2. Limited control over the projects, as I need more staff
3. We do not have any standards and requirements to assess project quality, so we depend on our limited experience and personal point of view
4. In some cases, two architects in the Investment Department have different views about one design proposal. The decisions are based on personal points of view due to the lack of any requirements and standards. In addition, we depend on personal experience.
5. The only requirement that we have is green area average to be 30% of the total project area, without any additional detailed information regarding designs.

AI: What did you understand from the law of investment and has the law been updated?

The law was widely updated, and the changes include:

1. Increasing staff levels from two architects to 50 from different backgrounds: architects, and civil, mechanical and electrical engineers. The new staff work on assessing new projects design and the construction process
2. The supervision of design projects moved from individual architects to the Architectural Bureau in 2012. This consultation office works to help both investors and government. The new investment projects' design is supervised by both investment department engineers and the Architectural Bureau. Each submits weekly and monthly reports on the construction process

The update in the law happened when the government was unable to control and manage the quality of the investment projects and construction processes. In addition, the consultation office faced problems with the financial strength of the investment companies. Consultation offices continue with their roles to develop both designs and the construction process of housing projects in Kurdistan generally and Erbil City specifically.

AI: Does the Investment Department have the power to stop projects?

Exceeding a plan's design might normally happen in the implementation process, such as changing land usage in order to build more housing units in open areas and reduce green spaces. For example, a project designed for 300 housing units might be changed to 500 units. However, so far, we do not have the power to enforce investors to use specific building materials, but there are some projects where they build with high quality materials.

The purpose of using low quality materials is to decrease construction costs and increase profits. In some cases, the companies sell the housing units at double the construction cost. We investigated housing unit construction costs and found that using high quality materials would change the profit rate to 30%, but the investment companies would not accept the proposal.

From the beginning, environmental requirements have not applied, but some environmental materials have been used to build luxury villas, not to achieve a requirement, but to increase the quality of the housing unit in order to increase the profits.

Up to now, there are no environmental requirements on housing projects.

HOUSING CONSTRUCTION TERMES AND CONDITION (Building licensing) for Government projects.

1. The house should build with street alignment and not build on other space (undersigned spaces) under any circumstances.
2. The front setback line is 2.5 meter and 1.2 meter from side for corner plots in old neighbourhoods. While in new neighbourhood the front setback is 4 meter and 1.5 meter from each side.
3. The total height should not exceed 8.65 for two bedrooms house. This type of house should contain internal staircase for final house floor.
4. The Hight should be not exceed 10.2 meter for house with three floors (three levels): ground floor for car parking and two floors. This type of house should not have internal stair case for third roof. The height of ground floor should not exceed 2.6 meter from the walkway level. In addition, this floor should be used for residential purposes (as a part of house) not commercial (Small shops or minimarkets).
5. For multi-level house (car park in ground level, and the Kitchen on the first level) the height of ground level should not exceed 2.8 meter from the walk way level.
6. The final approval for house construction (building license) will be gain after casting concrete for final roof (second floor or roof of stair case). In addition, the house should have fence before final approval.
7. Building and construction materials should not cast or prepared on street (in the plot boundary).
8. The house owner ship should inform the local municipality for the bellow dates:
 - a. Foundation reinforcement before casting concrete.
 - b. Ground floor wall contraction for multi-layer house only.
 - c. Starting the First-floor construction.
 - d. Starting the Second-floor construction.
 - e. Final floor reinforcement (internal stair case)
9. Not informing the local municipality for above dates, the house ownership will be charged even if the house does not have construction problems.
10. The houseowner ship and Architect (designer) will be responsible for any construction problems during or after building house.
11. Add information board size 40* 60 cm at site contain information about; plot area, No of building approval, and plot registration number and starting date.
12. Commit to clean street adjacent neighbourhood and throw debris in designed places outside the city.
13. The black colour waterproof is not allowed to apply as a painting for adjacent walls. And the floor tiles should grinded in the factory before used.
14. The house ownership is responsible for any irregularities on above points.
15. For above points 11, 12, and 13, the house ownership should deposit 500,000 ID (£ 400).
16. Drilling a water well (for irrigation) on the pavement and planting three trees at front of house.
17. If the house is larger than 150 m², the construction process needs approval from Department of Environment¹.

¹ Department of Environment approval: The house needs septic tank for swage for toilets only.

حکومهتی هه‌ریمی کوردستانی عێراق

رئاسه مجلس الوزراء
وزارة البلديات و السياحة
مديرية البلدية الرابعة
قسم التصميم



Ministry of Municipality
Directory of municipality Four
Planning Department

سه‌ڕۆكابه‌تی نه‌جۆمه‌نی وه‌زیران
وه‌زاره‌تی شه‌اره‌وانی و كه‌شك و گوزار
به‌ریوه‌به‌رایه‌تی شه‌اره‌وانی (چوار)
به‌شی نه‌خشه‌دانان

به‌روان / / 201

ژماره

نه‌تکیتی داواي ژيڤيدان بو دروست کردنی ژوڤ (.....) شه‌راوان کردنی خانوو (زياده خانوو)

ره‌زامه‌ندی به‌ره‌مه‌نی نه‌ ژيڤيدانم بو دروست کردنی (.....) نه‌سه‌ر پارچه زه‌وی ژماره (.....)

به‌یستی نه‌م ژانیاڕیانه‌ی خواره‌وه دهم كه پابه‌ندی هه‌موو ژيڤيدانه‌ی نه‌م وه به پێچه‌وانه‌وه به‌ر په‌رسايم له هه‌موو كه‌م و كه‌شك.

ئاوي خاوم داوا (.....) ناوێشان (.....)

ژماره‌ی ته‌له‌فون (.....) به‌روان / / 201 واژوو

ژانیاڕی سه‌بارته به ته‌قسیم دوو :

1. چهند خانوو دروست ده‌كات له‌سه‌ر نه‌م زه‌وی یه ؟ رووبه‌ری پارچه زه‌وی

2. چهند خانووی ته‌قسیم دوو هه‌یه له‌م بۆكه ؟ ا - هه‌یه ب - ژماره ج - نه‌ی یه

3. ژماره‌ی دهرچووله به‌ریوه‌به‌رایه‌تی شه‌اره‌وانی (.....) بۆیه‌ریوه‌به‌رایه‌تی تۆمارگه‌ی خانووبه‌ری یه‌كه‌م و دووهم

له ريكه‌وت

5. ژماره‌ی هاتوو له به‌ریوه‌به‌رایه‌تی تۆمارگه‌ی خانووبه‌ری یه‌كه‌م و دووهم بۆ به‌ریوه‌به‌رایه‌تی شه‌اره‌وانی (.....)

وه له ريكه‌وت

6. وه‌لامی به‌ریوه‌به‌رایه‌تی تۆمارگه‌ی خانووبه‌ری یه‌كه‌م و دووهم له‌گه‌ل به‌ریوه‌به‌رایه‌تی دادنوسی هه‌ولێر

ا - هه‌یه ب - نه‌ی یه پ - نه‌ی یه

7. ره‌زامه‌ندی سه‌رووكی به‌ش , ره‌زامه‌ندی به‌ریوه‌به‌رایه‌تی شه‌اره‌وانی

مه‌رجه‌گانی دروست کردنی خانوو -1

1 - پابه‌ند بوون به هه‌لی راست کردنه‌وه‌ی شه‌قام وه ناییت جیڤیلراو (مه‌تروكه) به هه‌ج شۆبه‌یه‌ك په‌كاربه‌ی نه‌گه‌ر نه‌یکریوه .

2 - به جی هیشته‌ی (2.5) م له رووی پێشه‌وه‌ی خانوو وه به جی هیشته‌ی (1.25) م له لای ته‌نیشت نه‌گه‌ر هاتوو خانووه‌كه رووكن بیت . (4) م له رووی پێشه‌وه له گه‌رگه نوێه‌كان وه له رووی ته‌نیشتی به جی هیشته‌ی 1.5 م

3 - نه‌گه‌ر خانوو (2) نه‌م بوو یان دوو نه‌م و به‌یتونه بوو ناییت به‌ری له (8.65) م زیاتر بیت وه ناییت هادرمه له دهره‌وه دروست بکات.

4 - نه‌گه‌ر خانووه‌گه‌راج و (2) نه‌م بوو ناییت به‌ری له (10.20) م زیاتر بیت وه ناییت به‌یتونه دروست بکات . ده‌ییت به‌ری نه‌می گه‌راج له (2.60) م زیاتر نه‌بیت له ناستی شۆسته وه ته‌نها به مه‌به‌ستی نیشته‌جی په‌کاردیت ناكریته دوكان .

5- خانووی ژێر مه‌ته‌بخ نه‌گه‌ر هادرمه‌ی له دهره‌وه بیت ده‌ییت به‌ری نه‌می سه‌ر زه‌وی 2.8 م زیاتر نه‌بیت.

6- مۆله‌تی كۆتایی پێده‌دریت له كاتی سه‌ب کردنی سه‌قشی نه‌می دووهم یان به‌یتونه , وه ده‌ییت سیاج دروست كرابیت.

7- ناییت گیراوی كۆنكریت وگه‌چ له سه‌ر قه‌ر یگیریته وه .

8- ده‌ییت خاوم مۆلك سه‌ره‌نانه‌مان ده‌كات بۆ چشكه‌ن نه‌م كاته‌نه‌دا وه‌خۆی به‌ر په‌سه‌ له نه‌هاتن - ا . دانانی شیش له بێن بادلۆ .

ب . دیواری نه‌می زه‌وی نه‌گه‌ر گه‌راجی هه‌بیت . ج . دیواری نه‌می یه‌كه‌م . د . دیواری نه‌می دووهم . ه . شیش په‌ستنی سه‌قشی به‌یتونه

9- نه‌گه‌ر هاتوو خاوم مۆلك له كاتی چشكه‌ن سه‌ردانی شه‌اره‌وانی نه‌كرد وه نه‌گه‌ر كێشه‌ی نه‌بوو له‌ها شه‌رامه ده‌كریت .

10- خاوم مۆلك و نه‌ندانیاڕی سه‌ره‌په‌رشتیا به‌ر په‌رسیان له هه‌ر كه‌م و كه‌شك به‌ییت له كاتی یاخود داوی دروست کردنی خانوو وه ده‌ییت ناماده بێن به‌رامبه‌ر

هه‌ر كاره‌انه‌وه‌یه‌كی یاسایی

خزمه‌تگوزاری/به‌شی () /:

- 12- پابه‌ند پوون په پاک و خاوينی ددورو بهری شه‌قام وه فرزندانی پاشماوه بؤ شونښی دیاری کراو (زېلخاندی کانی قرژاله) .
- 13- به‌کاره‌ننای هلیکوپتری رهنګ رښ (قه‌دغه‌یه) وه ده‌بیت کاشی له کارګه جه‌لایه کراپیت نینجا به‌کارپیت پؤ خانوو .
- 14- خاوه‌ن مولک به‌رپرسه له ه‌ر س‌ه‌رپیچیه‌ک که لږم خالان‌دی س‌ه‌ره‌وه باس کراون .
- 15- له کاشی پابه‌ند نه‌پوون په خالنه‌کاشی (11 , 12 , 13) رازیم ب‌ری بارمته (تأمینات) نه‌ګه‌ریت‌م‌وه به‌ری 500,000 دینار .
- 16- لینه‌دان‌ی ب‌یر له‌س‌ر شؤسته وه چان‌دن‌ی (3) دار له پیش خانوو .
- 17 - نه‌ګه‌ر روویه‌ری زه‌وی له 2م150 زیاتر بوو پ‌ن‌ویسته ر‌ه‌زانه‌ندی به‌ری‌وه‌به‌رایه‌تی ژینگه ودرېګریت .

په‌لین نامه‌ی خاوه‌ن داوا :-

من هاوولاتی نیشته‌چی خاوه‌ن مولکی
په‌لین د‌د‌م پابه‌ندیم به‌م خالان‌دی باسکراوه وه به‌ پیچ‌ه‌وان‌ه‌وه به‌رپرس‌یار د‌ه‌یم .
ناسنامه ناو‌ن‌شان واژوو

په‌لین نامه‌ی نه‌ندان‌زیاری س‌ه‌رپه‌رشت‌یار :- نه‌ګه‌ر روویه‌ری زه‌وی له 2م300 که‌م‌تر بوو

نه‌ګه‌ر روویه‌ری له 2م300 زیاتر بوو ده‌بیت له‌لایه‌ن نووسینه‌ګی راو‌ن‌ژګاری نه‌ ن‌جام پ‌ریت

من نه‌ندان‌زیار پ‌س‌و‌ری په‌لین د‌د‌م به‌رپرس‌یار د‌ه‌یم له س‌ه‌رپه‌رشت‌کردن‌ی دروست کردن‌ی خانووی
ژماره له رووی (structure) انشان . ژ ناسنامه ناو‌ن‌شان واژوو

په‌شی ژم‌یریاری :-

و‌ه‌رگرت‌نی بارمته به‌ری (500000) پ‌ن‌ن‌ج س‌د ه‌زار دینار به‌ پ‌سو‌وله‌ی ژماره له
له‌ګه‌ل و‌ه‌رگرت‌نی ک‌ری ی پ‌شک‌ن‌ینی به‌ پ‌سو‌وله‌ی ژماره له
واژووی ه‌رم‌انه‌ری ژم‌یریاری ناو
ت‌ی‌ب‌ینی :- نه‌ګه‌ر ها‌ت‌وو پ‌شک‌ن‌ینه‌که‌ی مان‌یک زیاتر به‌س‌ر ت‌ی‌به‌ر ب‌یت له‌وا ک‌ری پ‌شک‌ن‌ین دو‌ویاره ده‌بیت‌ه‌وه .
له‌ګه‌ل و‌ه‌رگرت‌نی ک‌ری ی پ‌شک‌ن‌ینی به‌ پ‌سو‌وله‌ی ژماره له
واژووی ه‌رم‌انه‌ری ژم‌یریاری ناو

لایه‌ن‌ګری به‌ره‌لست نه‌کردن‌ی ه‌رم‌ان‌ګه‌کاشی په‌یوه‌ندی دار :-

تکایه لایه‌ن‌ګری بؤ دروست کردن‌ی ب‌ک‌ریت به‌ پی‌ی له‌و زان‌یارانه‌ی س‌ه‌ره‌وه نه‌وه‌ی په‌یوه‌ندی به‌ ل‌یوم‌وه ه‌ه‌بیت په‌ پی‌ی
ر‌ن‌ما‌یه‌کان .

- ه‌رم‌ان‌ګه‌ی باج‌ی خانوویه‌ره :-

- ه‌رم‌ان‌ګه‌ی ناو :-

- ه‌رم‌ان‌ګه‌ی ژینگه : نه‌ګه‌ر روویه‌ری زه‌وی له 2م150 زیاتر بوو

خزمه تگوزاری/ بهشی () //:

ریمان پنداوه تاودکو شیش (حدید التسلیح) له بڼاغه دادونیت

له گه ل ریزم

پشکینی بڼاغه

کشانده له شقاسی سهرکی..... کشانده له شقاسی لاوکی..... نه خشه..... جینیرا.....

تییینی:

.....
.....
.....

رووپو

خزمه تگوزاری/ بهشی () //:

ریمان پنداوه تاودکو دیواری گهراج دروست دمکات به بهرزی (.....) م بیت وه ناییت داری نه جاری به ستیت

له گه ل ریزم

پشکینی گهراج یان ژیرزمین

کشانده له شقاسی سهرکی..... م کشانده له شقاسی لاوکی..... م نه خشه..... بهرزی..... م

تییینی:

.....
.....
.....

رووپو

خزمه تگوزاری/ بهشی () //:

ریمان پنداوه تاودکو نهومی یه گم دروست دمکات به بهرزی (.....) م وه ناییت داری نه جاری به ستیت

له گه ل ریزم

پشکینی نهومی یه گم

کشانده له شقاسی سهرکی..... م کشانده له شقاسی لاوکی..... م نه خشه..... بهرزی..... م

تییینی:

.....
.....
.....

رووپو

خزمه تگوزاری/ بهشی () //:

ریمان پنداوه تاودکو نهومی دووم دروست دمکات به بهرزی (.....) م وه ناییت داری نه جاری به ستیت

له گه ل ریزم

پشکینی نهومی دووم

کشانده له شقاسی سهرکی..... م کشانده له شقاسی لاوکی..... م نه خشه..... بهرزی..... م

تییینی:

.....
.....
.....

رووپو

1 - پابه نه بوون به هلواسینی ژماره و بهرواری رینیدان و مؤله ت وه ژماره ی پارچه زوی یه گه له سهر بوردنیک که پیدانه که ی (40*60) سم که متر نه بیت.

رېمان پىداۋە تاۋىكو شېشى بەيتونە دەپەستىت .

لەڭگەل رېزىم

پىشكىنى شېشى بەستى بەيتونە

بەرزى م

پەسەندى يە نەخىر

بە پىنى نەخشە پەسەندە بەلى

سىياچ درووستا كراۋە تىيىنى:

روۋپىيو

خىشە ي پىكەتە ۋ روۋپەرى بىنا :-

ۋ	ناۋى نۆۋم	روۋپەرى بىنا (م2)	كشائەۋە نە شەقامى سەرمكى	كشائەۋە نە پشەۋە و تەنىشتى
1	گەراج/ئىزىمىن			
2	زەۋى			
3	يەكەم			
4	دوۋىم			
5	بەيتونە			
	شۈرە			
	پەردەسىرە			
	كۆى گىشتى			

تىيىنى :-

ناۋى تىيىنەرى خىشە بەروار ۋاژۋو

سەرىك بەش ۋاژۋو

بەشى ژىمىرپارى :-

ۋەرىگىرتى پەرى (.....) دىنار لەپەرى مۇلەتى بىنا و شۈستە بە پىسولەى ژمارە لە لەڭگەل ۋەرىگىرتى پاردى قىر بە پىسولەى ژمارە لە ناۋى ھەرمابەرى ژىمىرپارى ۋاژۋو

لەم ۋۇرە پىۋىستە لەم ھاۋپىچانەى لەڭگەلدا بىت :- 1. ۋىنەى تۇمار لەڭگەل چەسپاندى سئور (سورة قيد مع تىبىت حدود) . 2. نەخشەى پەسندىكراۋ (خرىطە مصادقة) كە دىبىت (plan+elevation+section+section for foundation) لەڭگەلدا بىت. 3. پىسولەى بارمەتە و پىسولەى كرىى پىشكىن (وصل تامىنات و وصل اجور كشف) . 4. بەلىن نامەى تايىبەت (نەڭەر ھەپو) . 5. نووسراۋى تايىبەت (نەڭەر ھەپو) .

ناۋى خاۋەن مولك : ژمارەى پارچە زەۋى بەروارى رىيىدان

1.1 Microclimate measurements equipment and sensors

Microclimate measurements in all three locations were obtained for three summer months. The measurements used a high quality data loggers and sensors to measure the local microclimate. CR 1000 data-logger used for North and Central station, while CR 800 data-logger used in South station. Data-logger in each location connected with numerous sensors and equipment as below:

1. Solar radiation sensor LT 200 X.
2. Temperature and relative humidity sensor HMP 50.
3. Barometric pressure sensor CS106.
4. Wind speed and direction sensor 05106.
5. Rain gauge sensor TR-525M.
6. Soil temperature sensor 108 Temperature Probe.

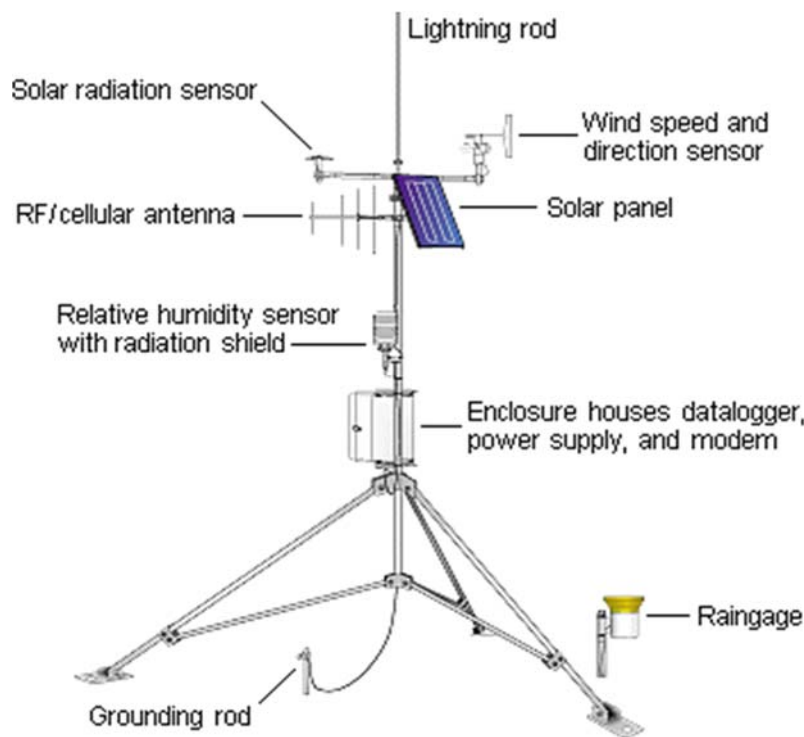


Figure1: .Microclimate weather data tower. Sensors and data logger installed in the site.

For this data collection CR1000 *Campbell scientific* data logger was used. The station basically installation in the site with tower as it is shown in Figure.1. All three stations are located in different urban areas that not effect by local traffic. Campbell weather station is research automatic weather station (AWS) use high meteorological sensors instrumentation. The sensors and instruments proven its field measurement reliability through accuracy measurements that's suitable for any metrological application. This type of weather station is used around the world and have been used in toughest environments such as freezing polar, and arid deserts.

In North and Central locations the data logger were programmed to start recorded data from 00:00 am to 23:00, so 24 hours a day. The sensors sets to save data each 15 mints in one Excel file including all seven microclimate variables. Each station had 6 different remote sensor and solar panel system to save energy. The sensors connect to Enclosure Campbell (Figure.1), which is include

1. CR1000 data logger.
2. Biometric pressure sensor.
3. Radio to send the data back to station.
4. Power battery.

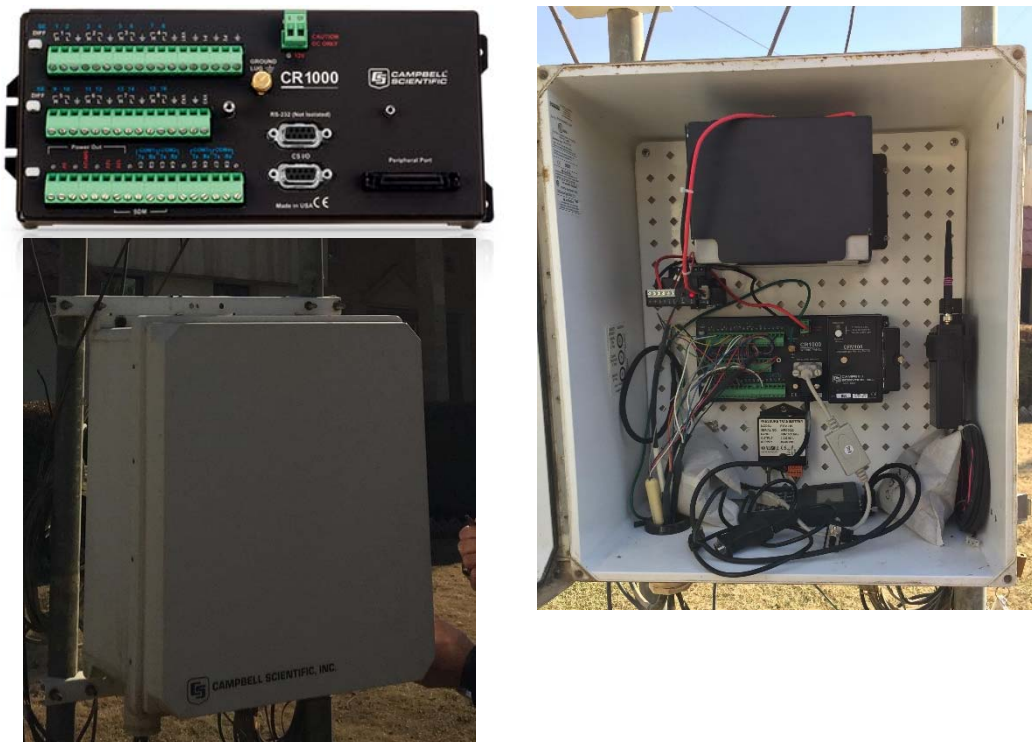


Figure 2: Enclosure Campbell showing how all sensors connect with CR1000 data logger.
Source: Erbil weather stations department-KRG.

Generally different sensors and instruments used to collect precise and accurate microclimate factors. Each sensor will be explain in the section below in term of accuracy and reliability.

1.2 Solar radiation sensor LT 200 X

Used for measured both, flux density KW/m^2 , and total flux MJ/m^2 . Its high quality silicon sensor that measured global solar radiation in outdoor environment. With sensitivity $75 \mu\text{A}$ per $1,000 \text{ W/ m}^2$ with error estimated as $\pm 3\%$ typical within $\pm 60^\circ$ angle of incidence (Campbell 2017).

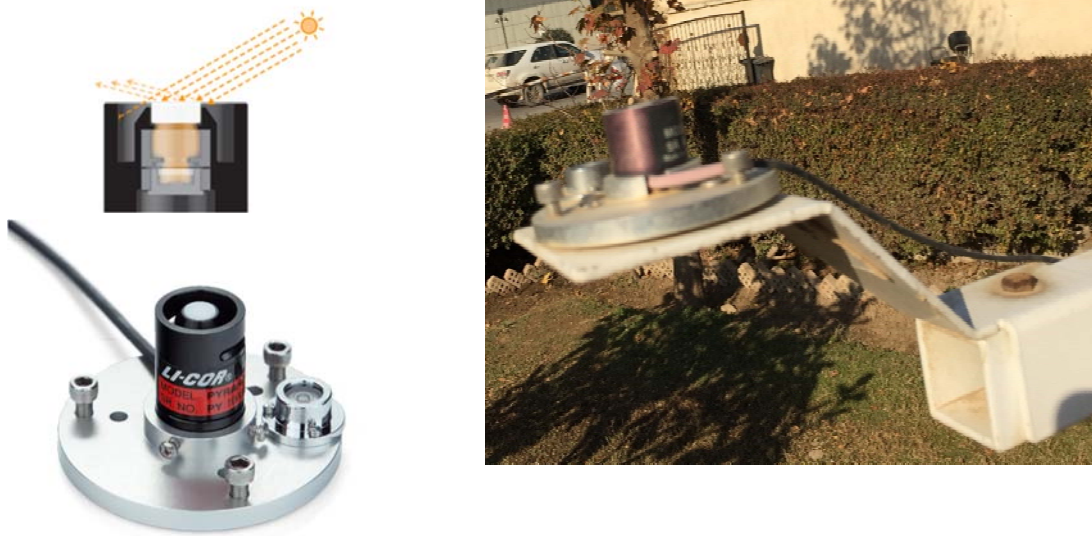


Figure 3: .shows solar radiation sensor LT 200 X. Silicon photovoltaic detector mounted in a cosine-corrected head.

1.3 Temperature and relative humidity sensor HMP 50

Temperature sensor range -40°C to $+60^\circ\text{C}$ with accuracy shown below. While, humidity sensor with range of 0 to 98% non-condensing and accuracy $\pm 3\%$ RH (0 to 90% Relative Humidity). The sensor should be inside solar radiation shield in the field (Campbell 2017).

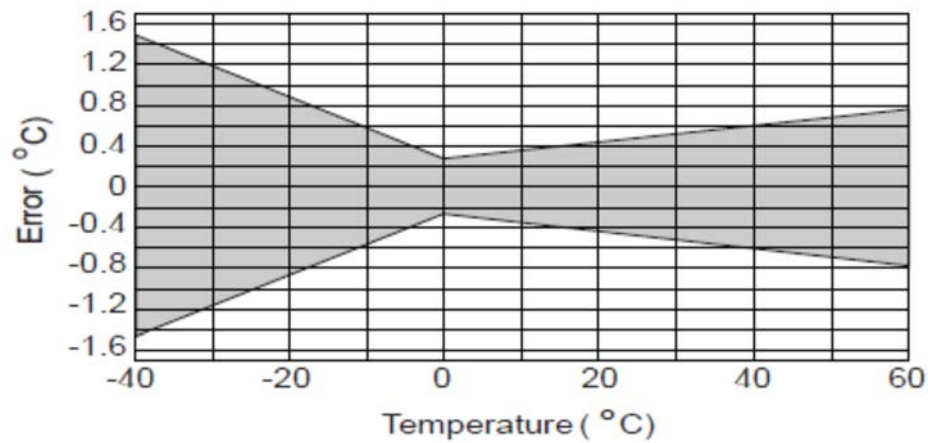


Figure 4: .shows Air temperature sensor accuracy. Temperature Measurement Range: -40°C to +60°C, Temperature Output Signal range: 0 to 1.0 VDC.(CampbellScientific 2017)

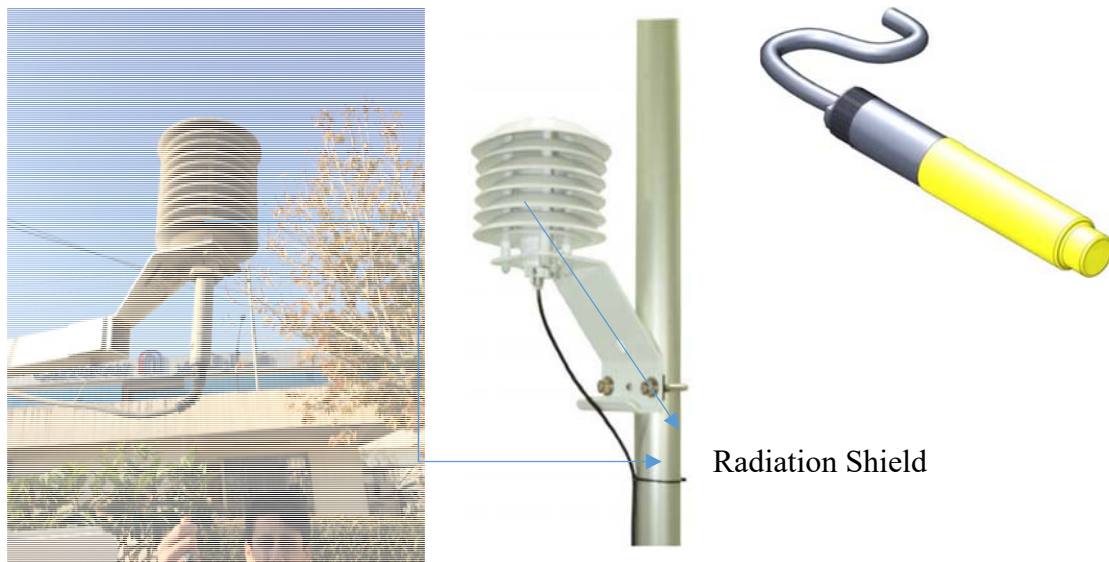


Figure5: shows HMP50 Temperature and Relative Humidity Probe.(CampbellScientific 2017)

1.4 Barometric pressure sensor CS106

The range of this sensor is 600 to 1060 mb connected with data logger and working in a temperature (-40°C to + 60°C) with total accuracy \pm mb @ -20°C to + 45°C. The reliability of this sensor \pm mb @ 20 °C (CampbellScientific 2017).



Figure6:.. Shows Barometric pressure sensor CS106.(CampbellScientific 2017)

1.5 Wind speed and direction sensor 05106

This sensor is design for marine application with light weight, strong instrument to measure wind speed and direction in the same time. The working range temperature of this sensor is -50°C to $+50^{\circ}\text{C}$ with range between 0 to 100 m/s, accuracy ± 0.3 m/s or 1 % of reading and resolution (0.0980 m/s). The sensor were installed on the top of tower in 2 m high. The direction of wind with mechanical range between 0 to 360° , and accuracy $\pm 3^{\circ}$ (CampbellScientific 2017).



Figure7: .shows Wind speed and direction sensor 05106.(CampbellScientific 2017)

1.6 Rain gauge sensor TR-525M

This sensor is a tipping – bucket rain gage measuring rainfall from 0.1mm to 24.5cm. The tipping sensor connect with data logger to record any rain fall into the gage (CampbellScientific 2017).

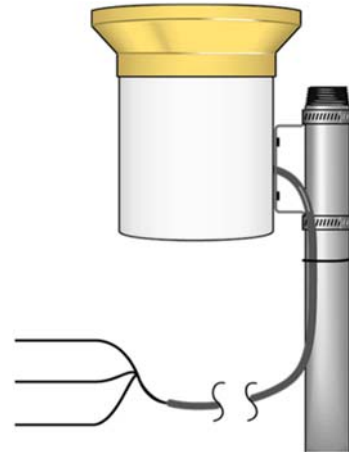


Figure8: .shows Rain gauge sensor TR-525M.(CampbellScientific 2017)

1.7 Soil temperature sensor 108 Temperature Probe.

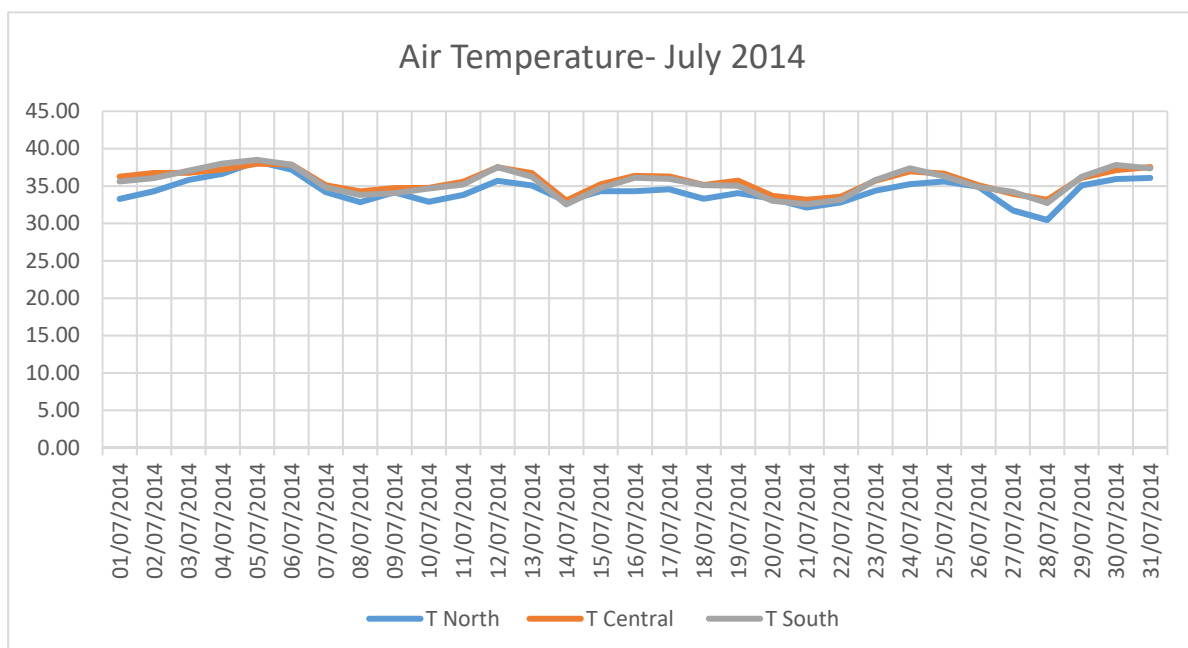
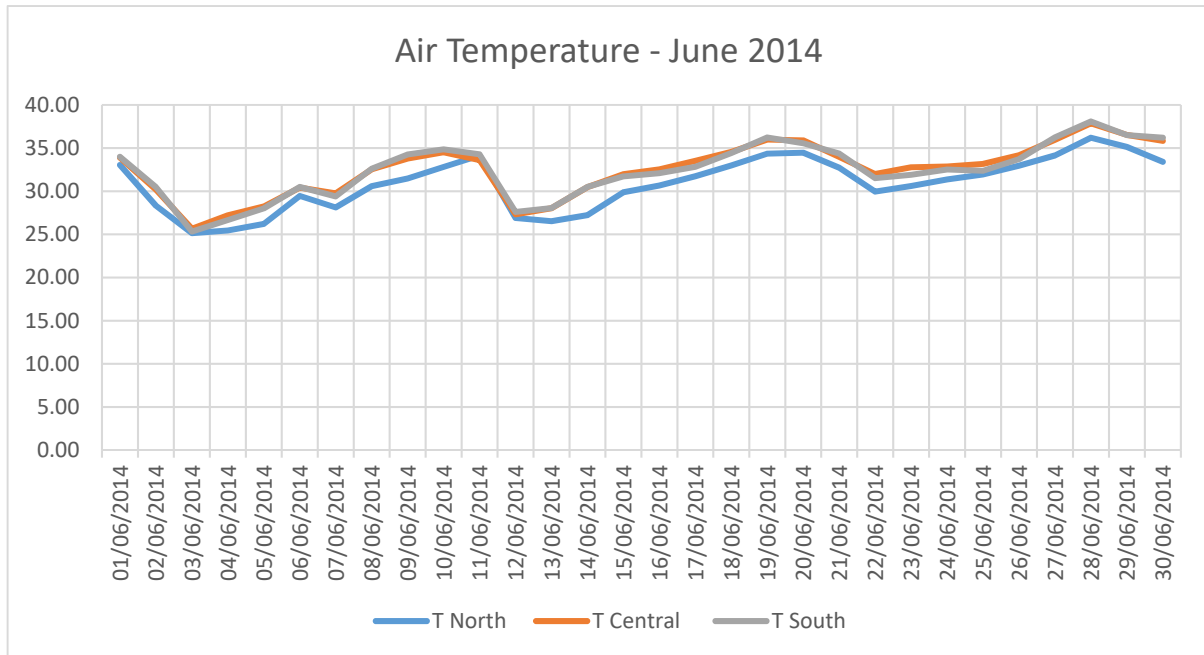
This sensor used to measure soil temperature between 25 cm to 50 cm underground. The sensor design to measure air temperature, soil and water, but in this station it is used for measuring soil temperature only. The probe range is between -35 °C to +50 °C with accuracy $\leq \pm 0.01^\circ\text{C}$ to $\pm 0.5^\circ\text{C}$, over measurement range(CampbellScientific 2017).

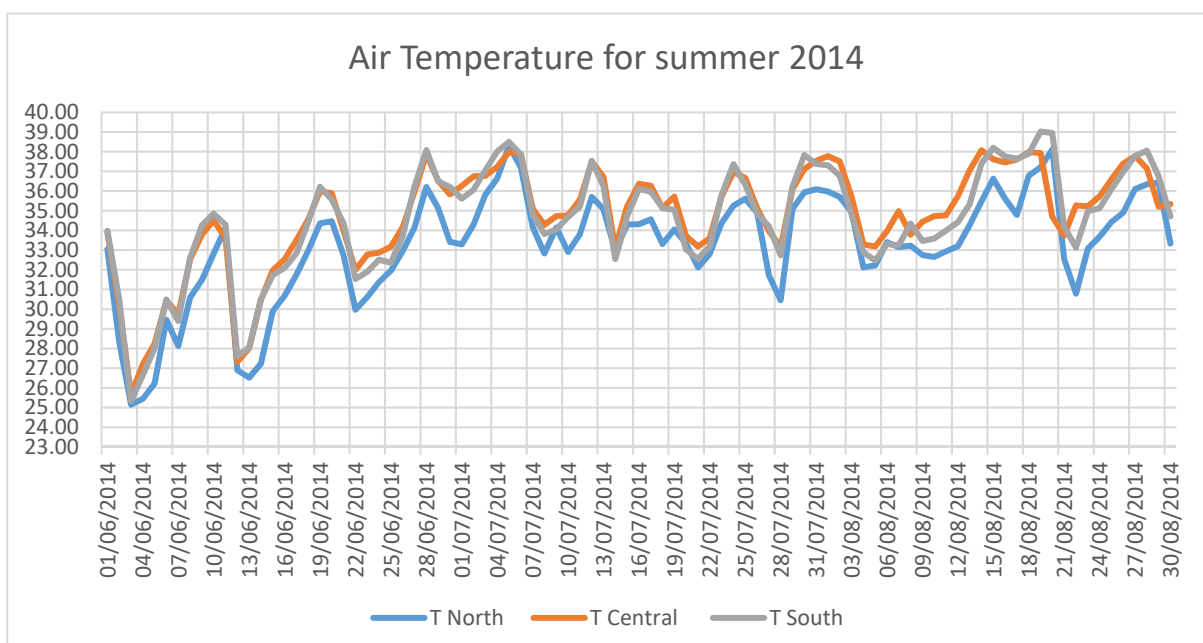
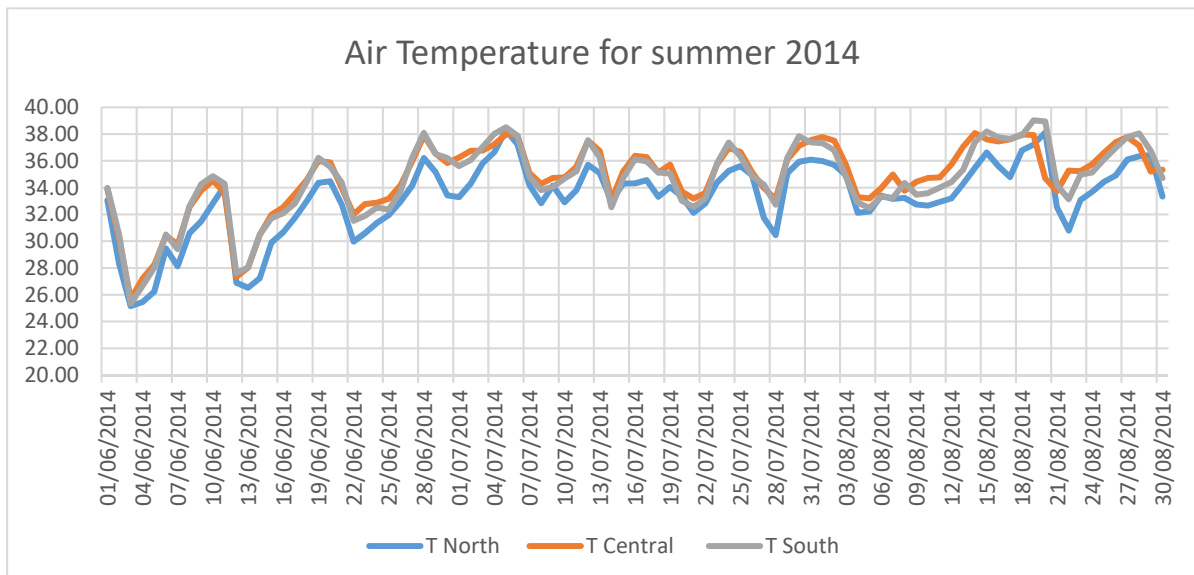
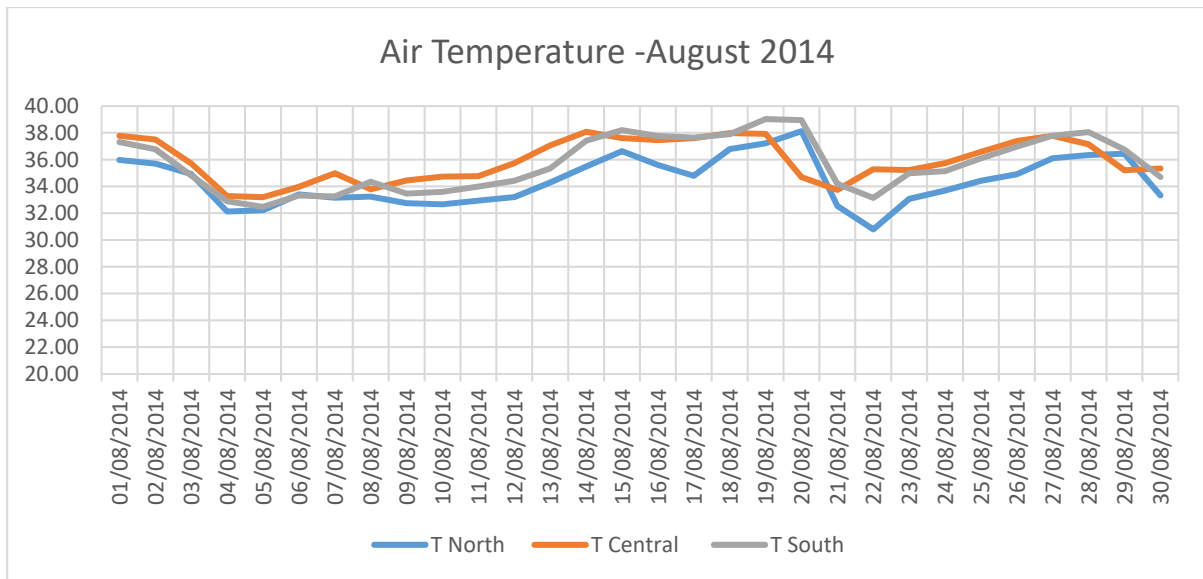


Figure9:..shows Soil temperature sensor 108 Temperature Probe. (CampbellScientific 2017)

Weather data for all stations North, Central and South for summer months:

1. Air Temperature
 - a. June 2014
 - b. July 2014
 - c. August 2014



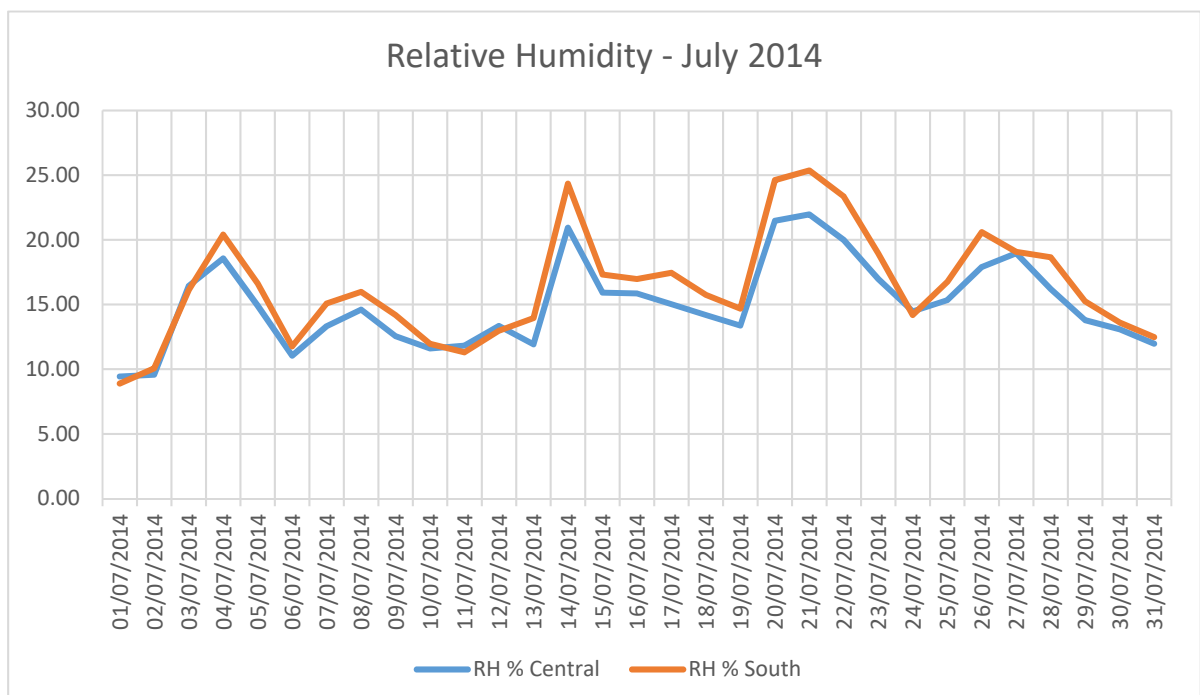
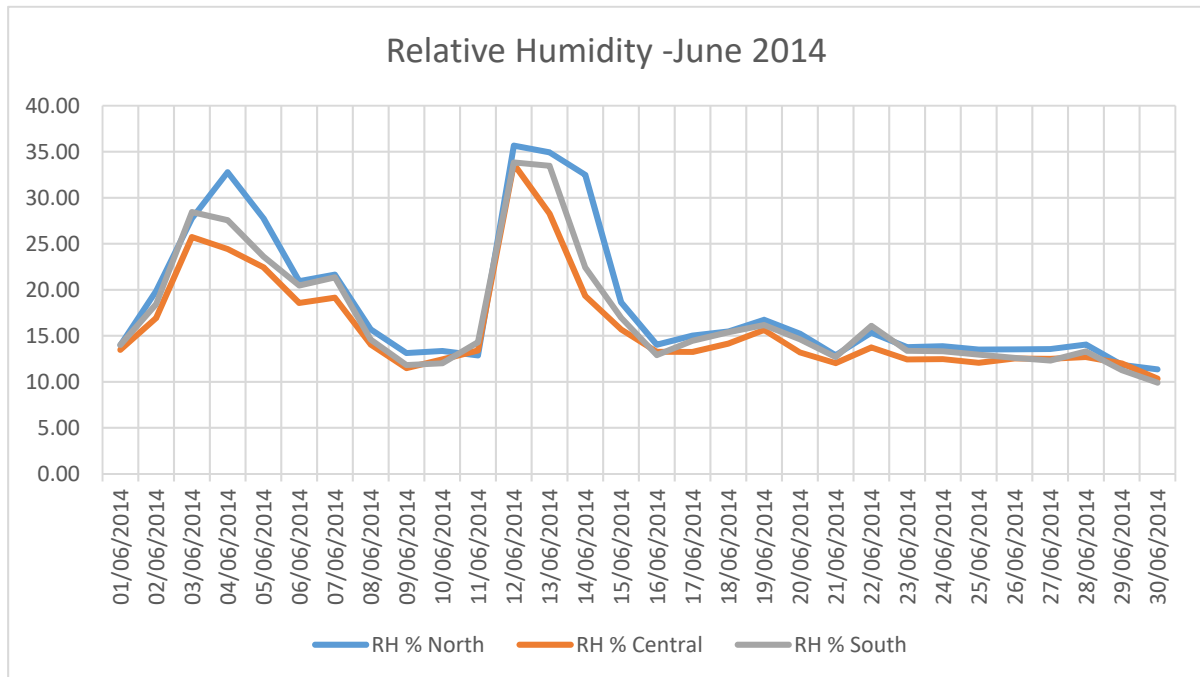


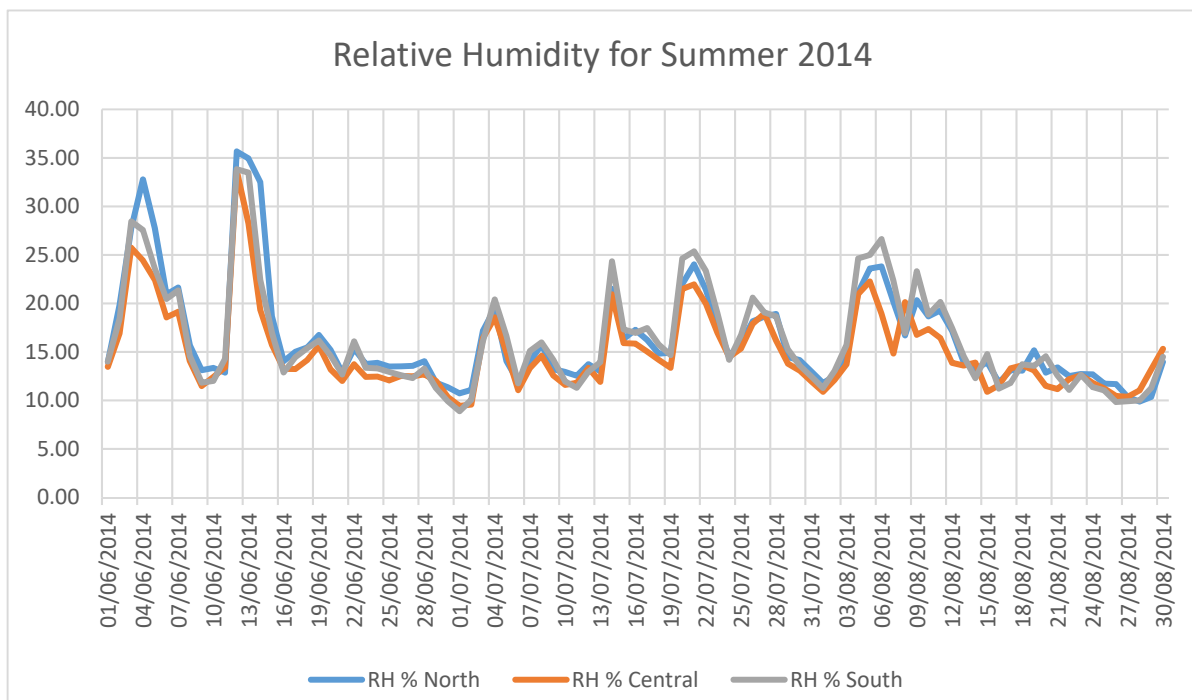
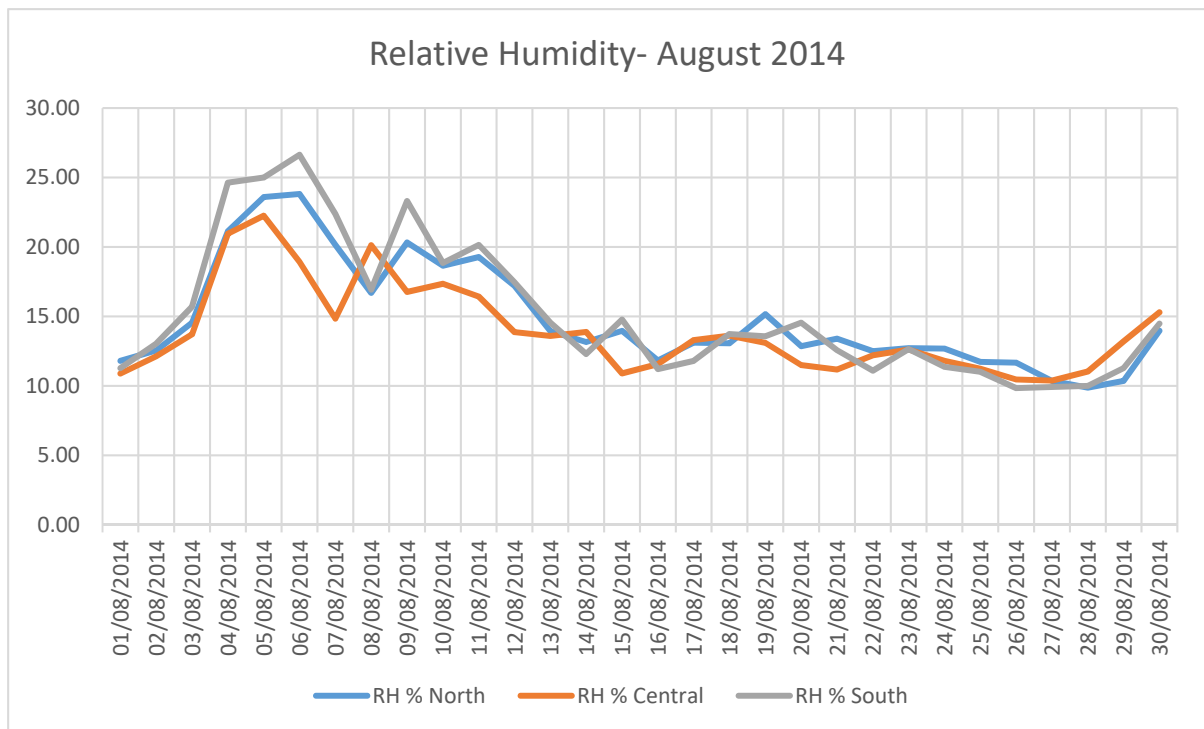
2. Relative Humidity

d. June 2014

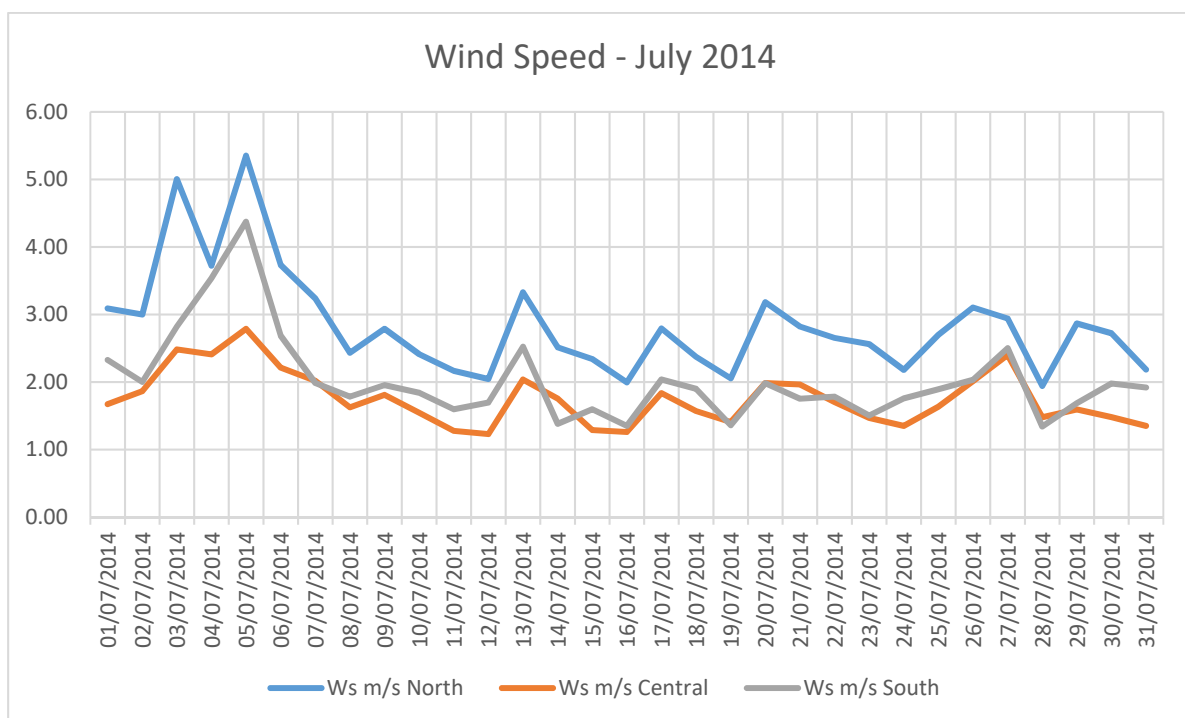
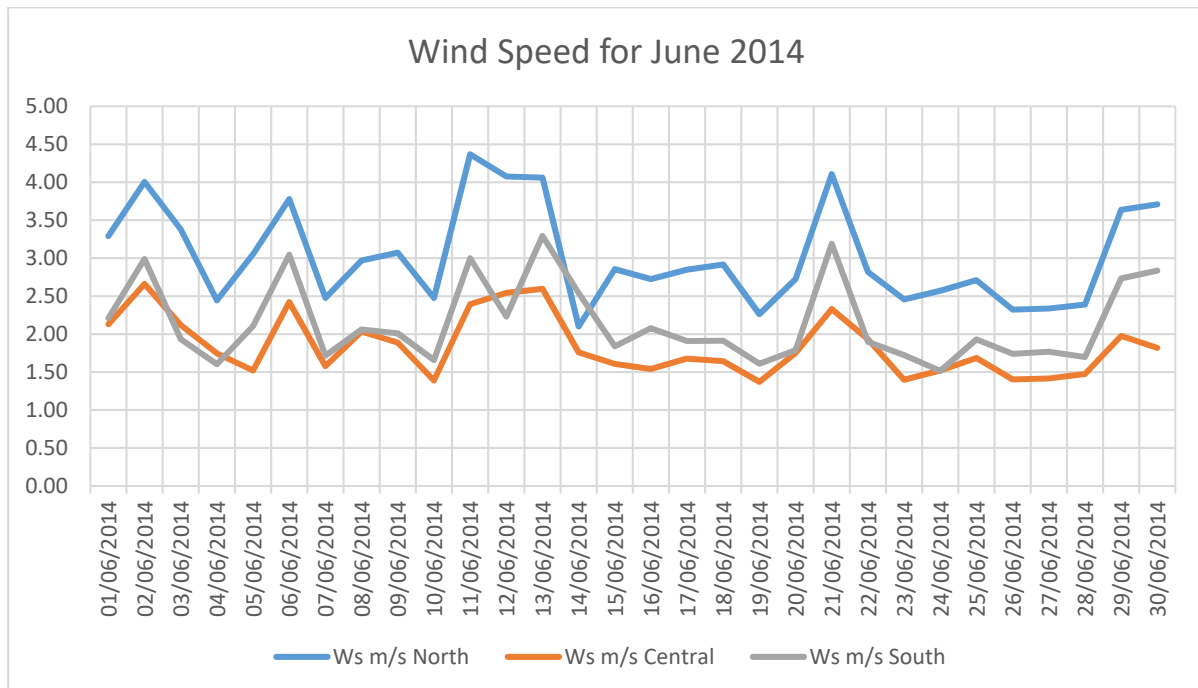
e. July 2014

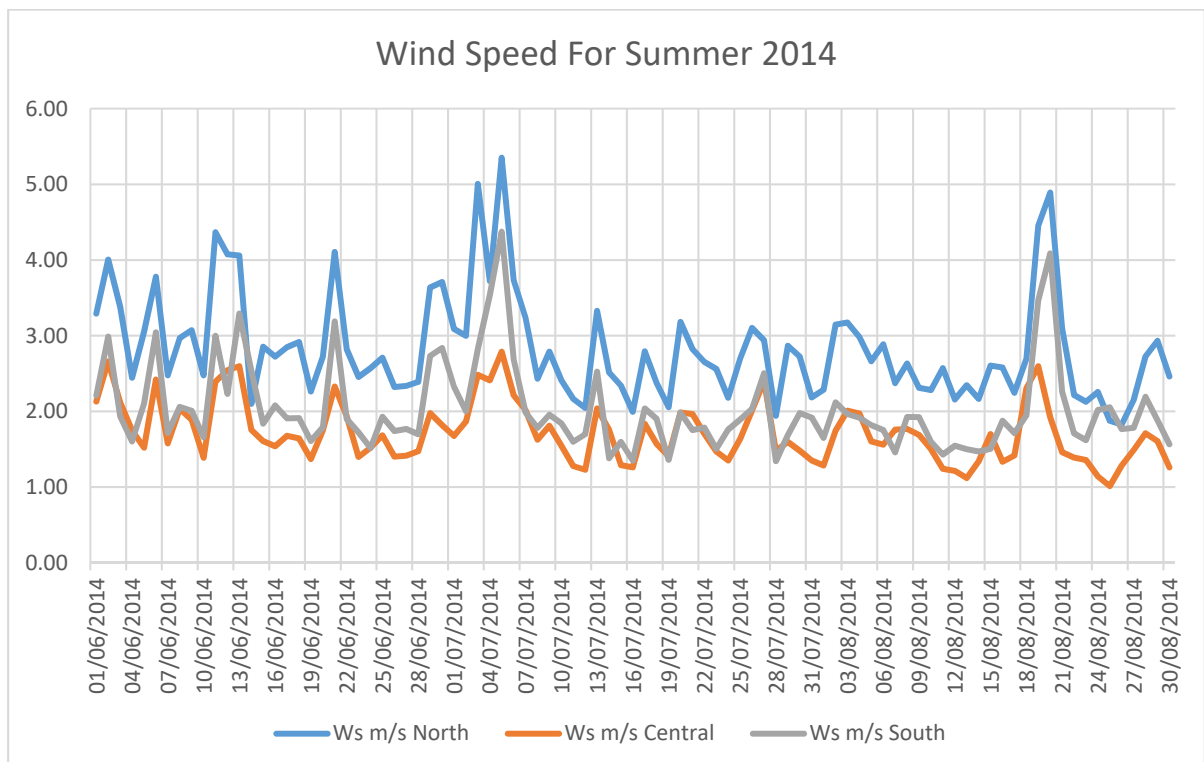
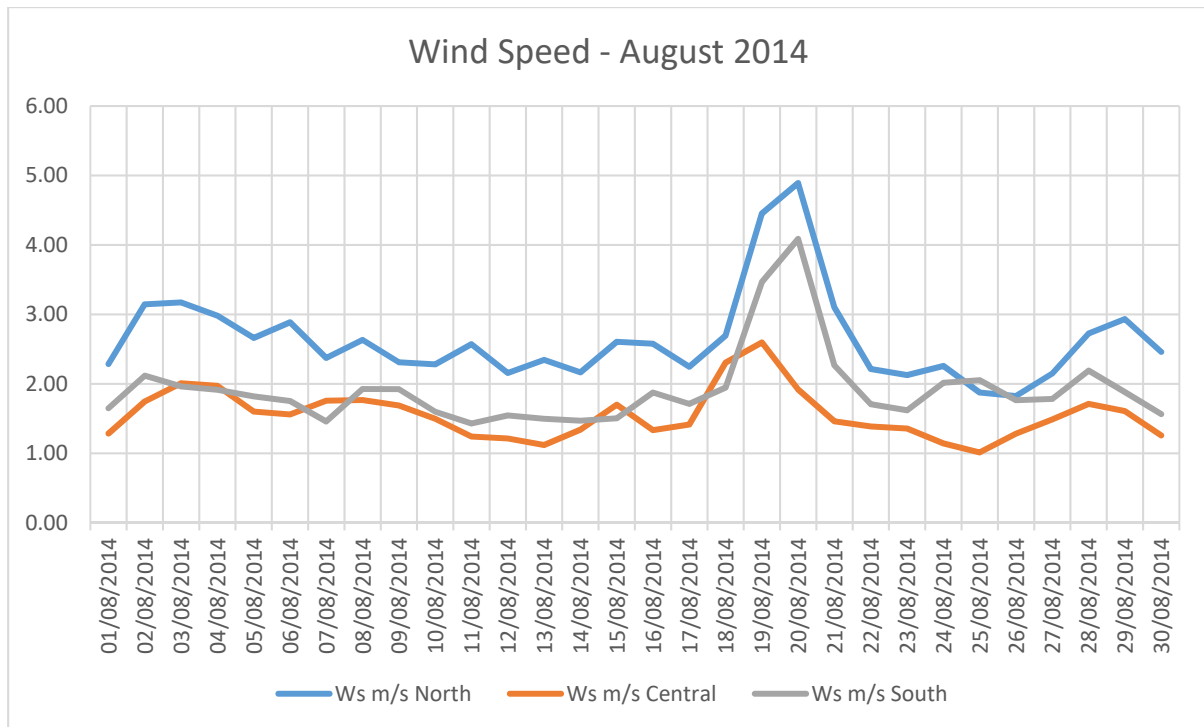
f. August 2014

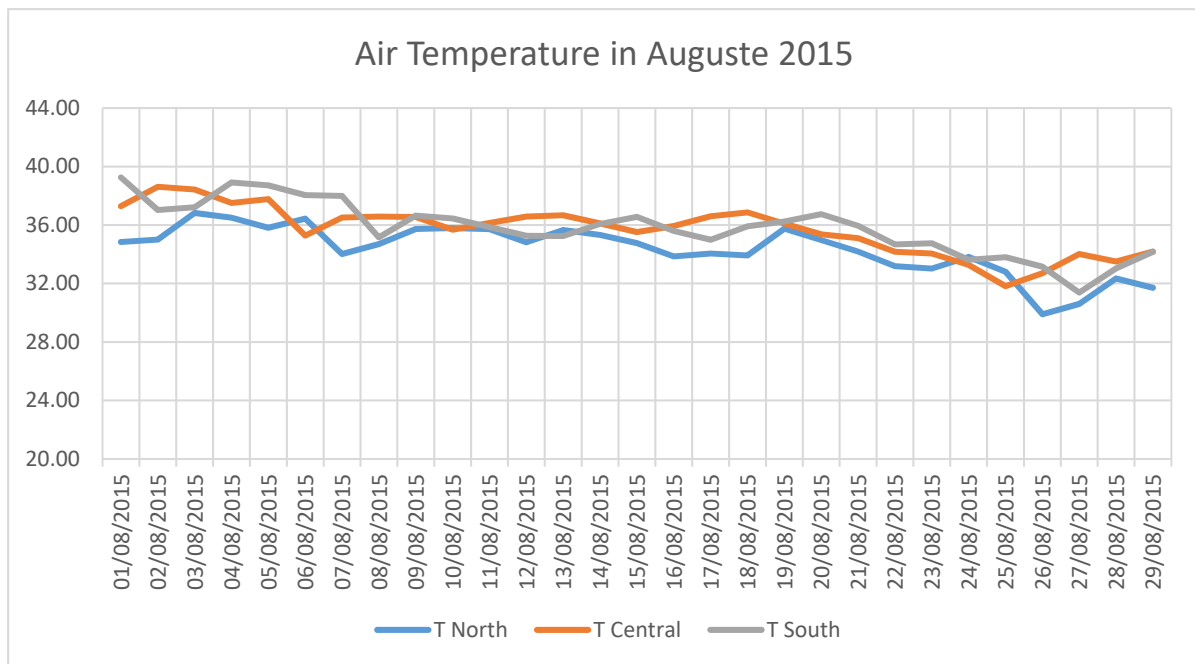




3. Wind Speed
 - g. June 2014
 - h. July 2014
 - i. August 2014

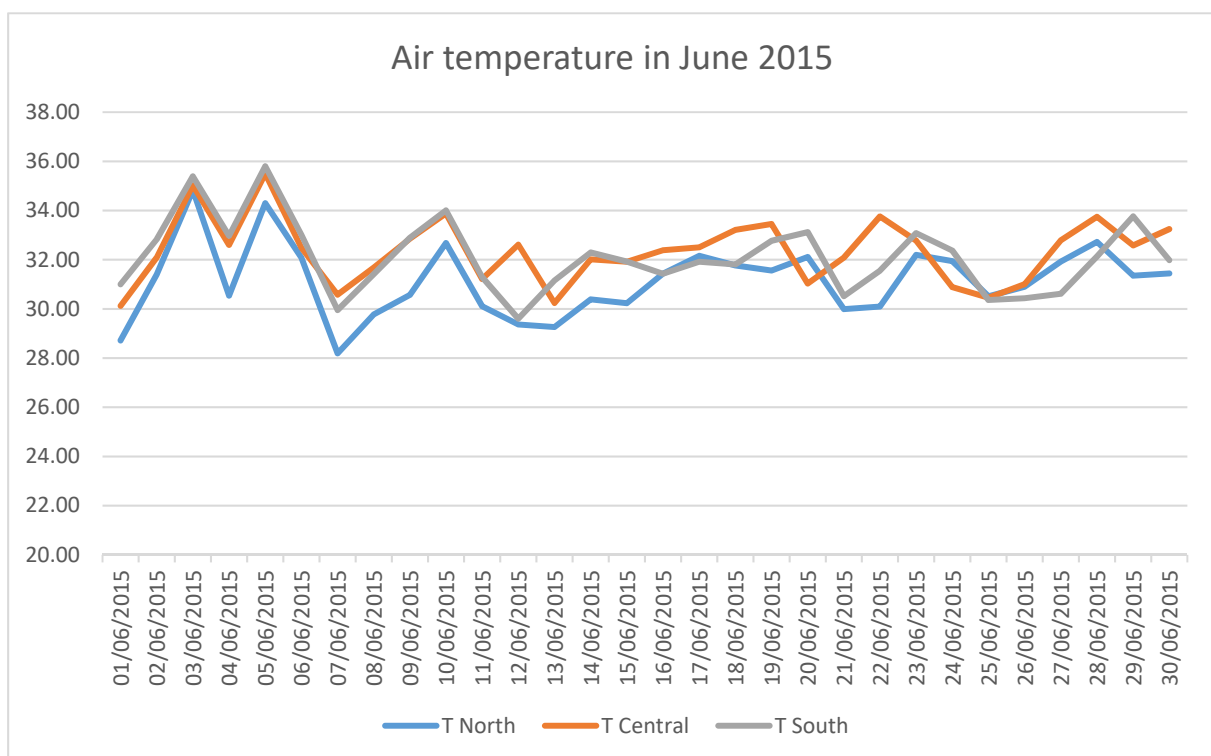


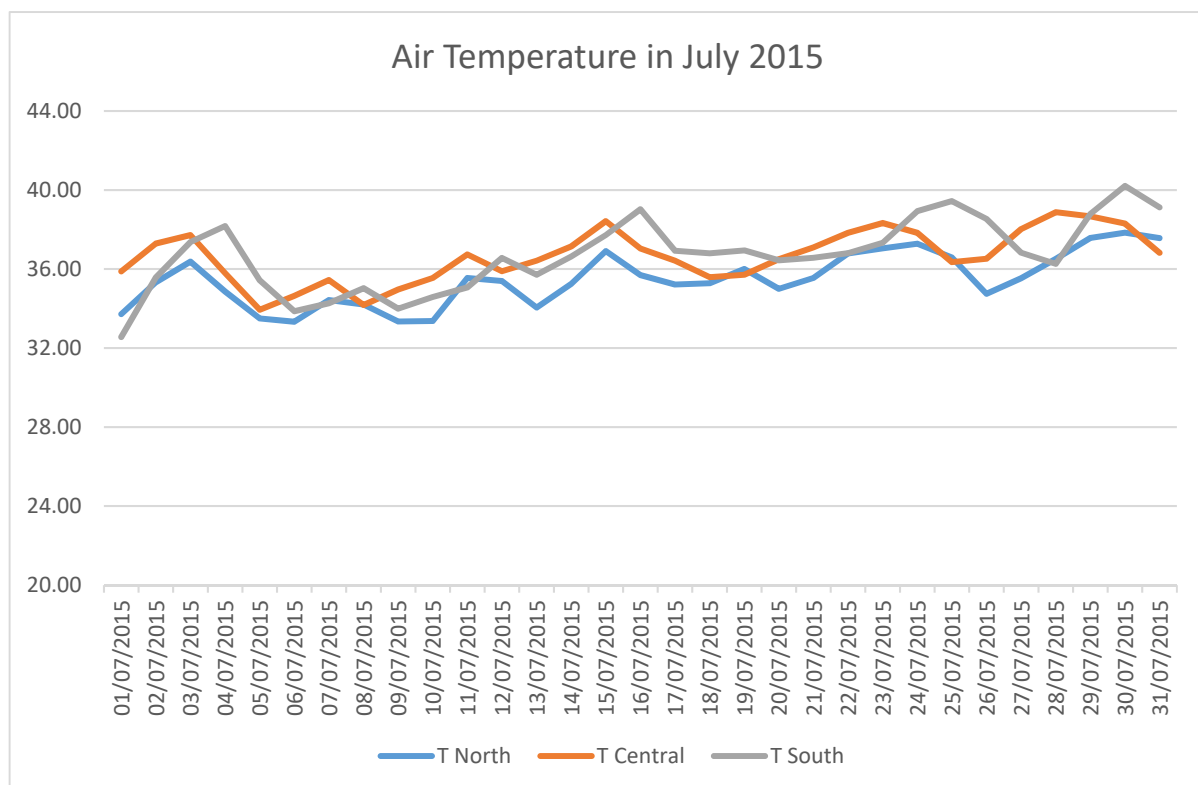
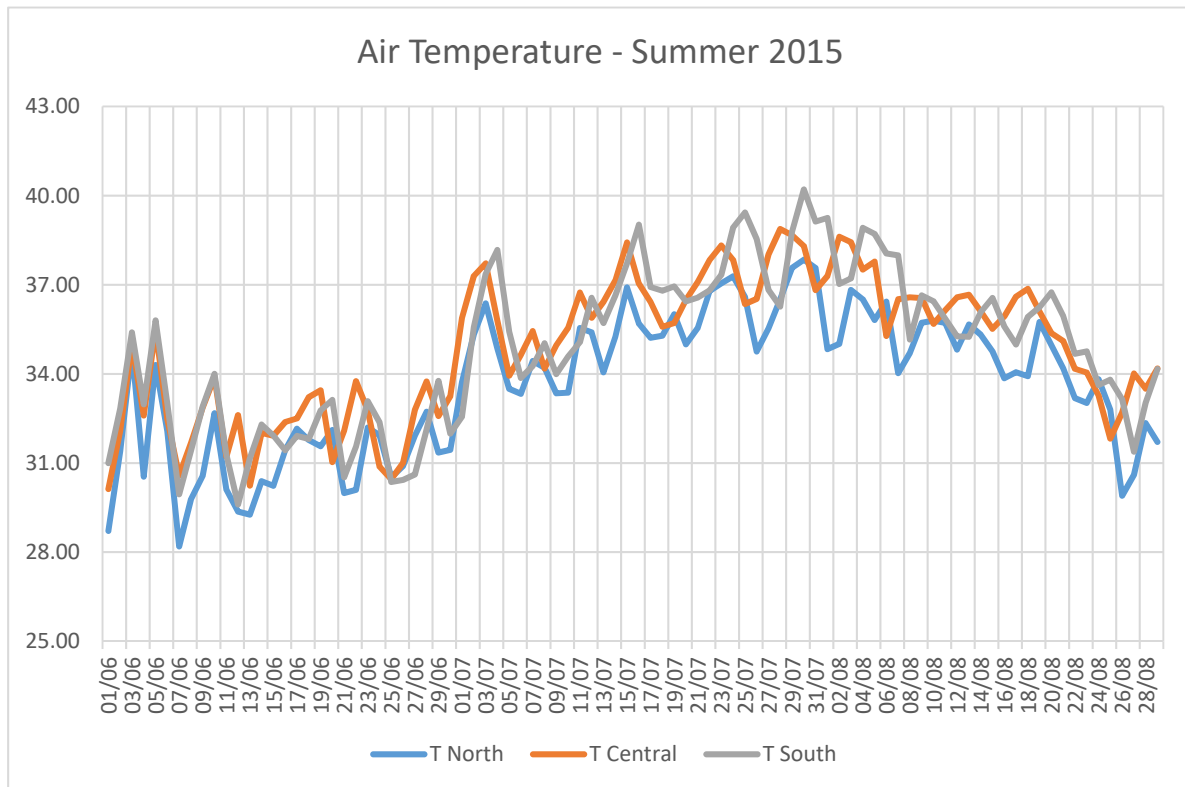


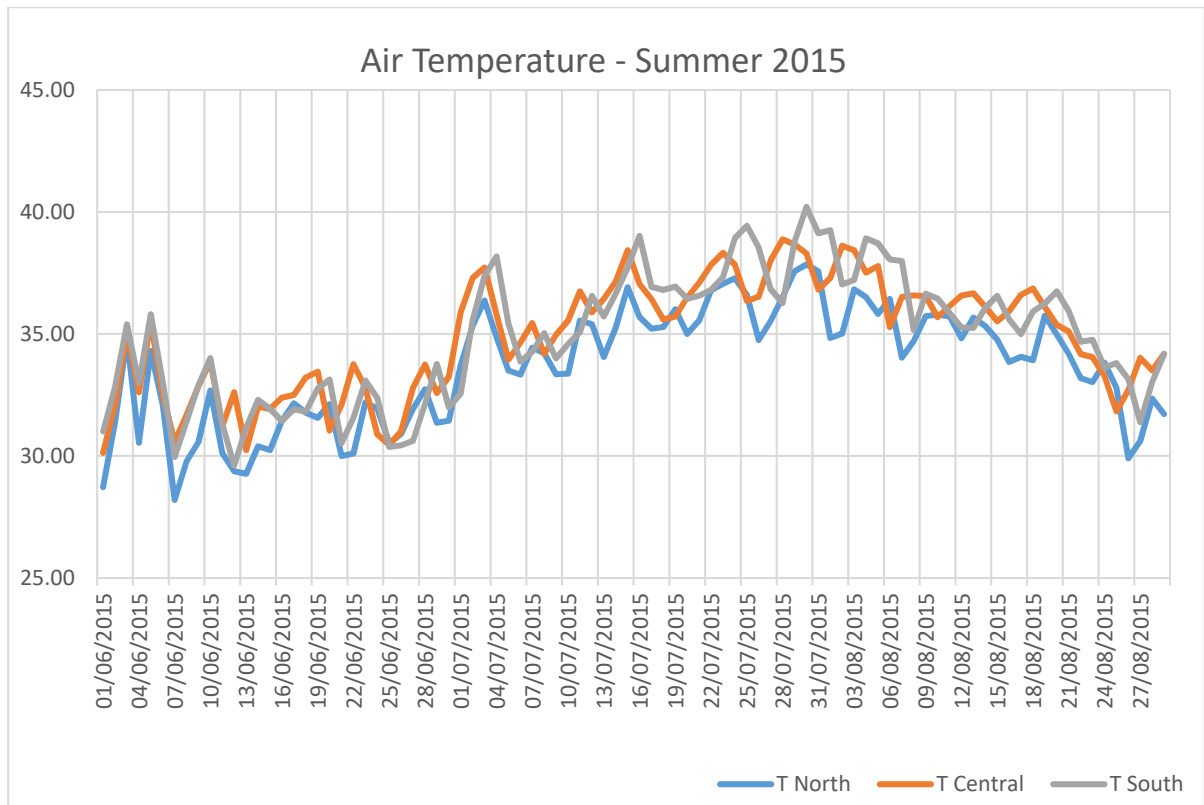


Weather data for all stations North, Central and South for summer months:

4. Air Temperature
 - j. June 2015
 - k. July 2015
 - l. August 2015





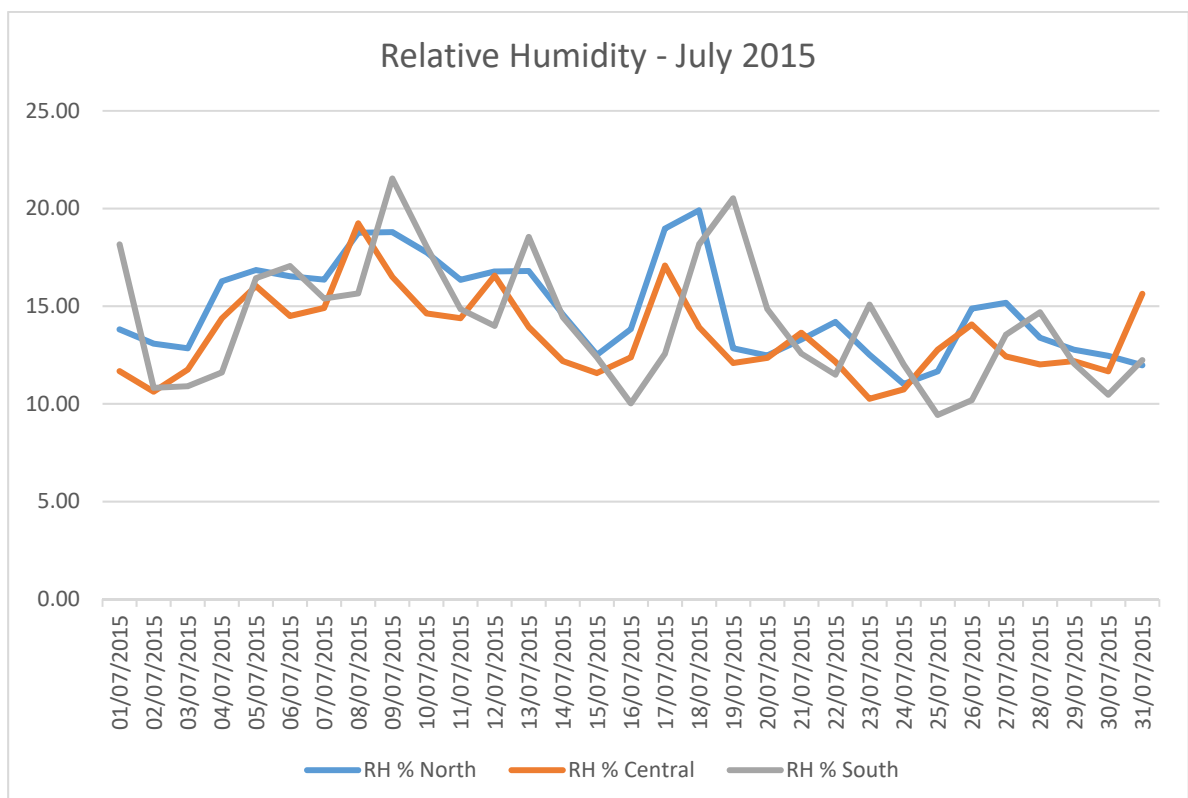
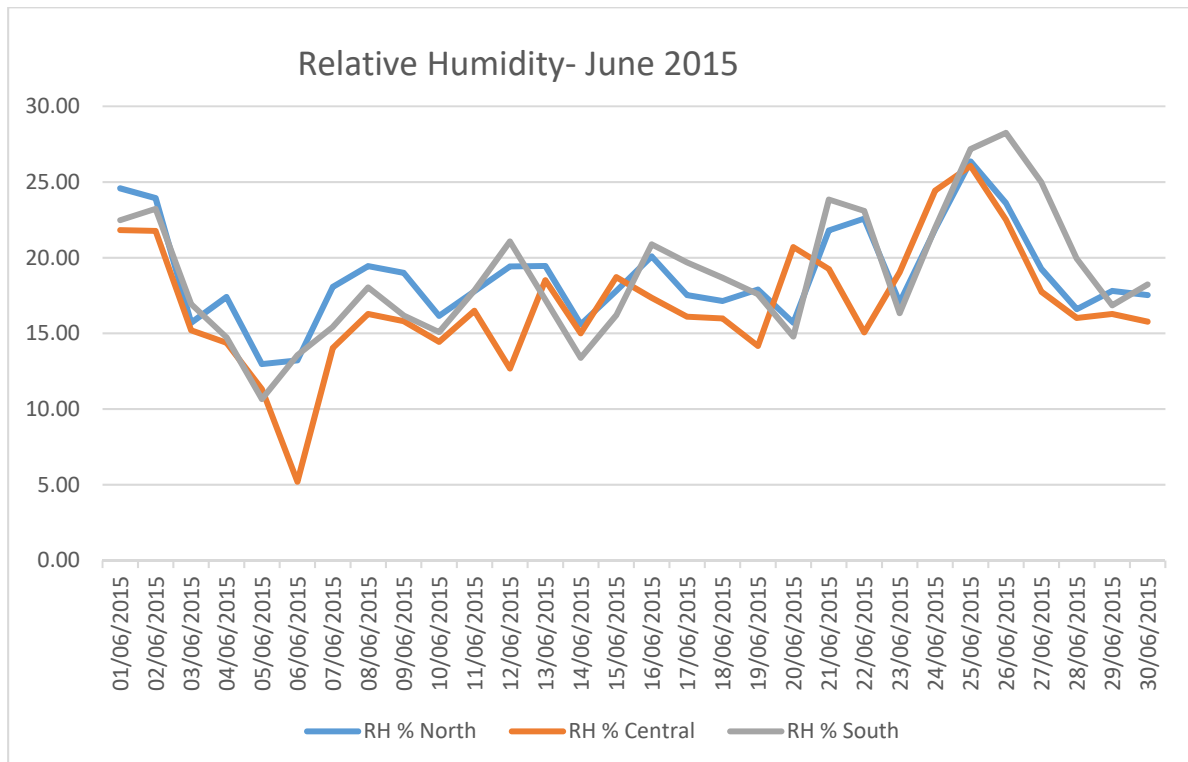


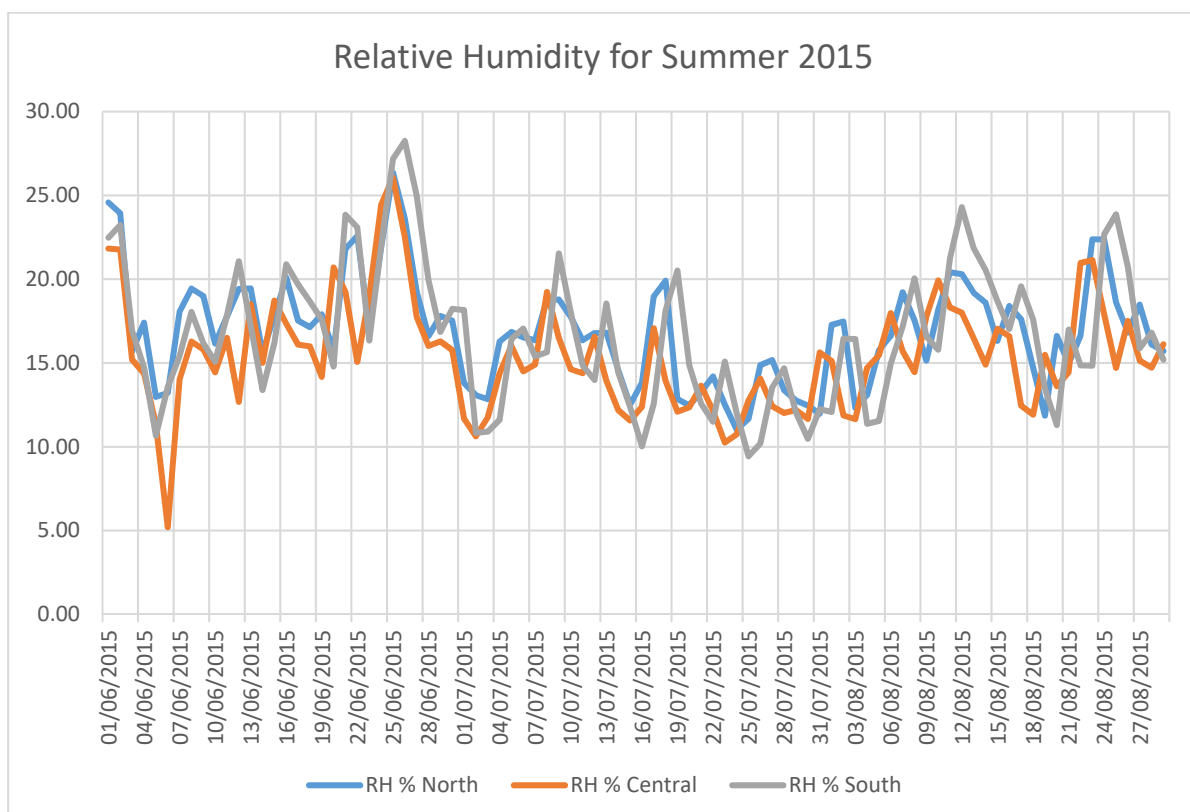
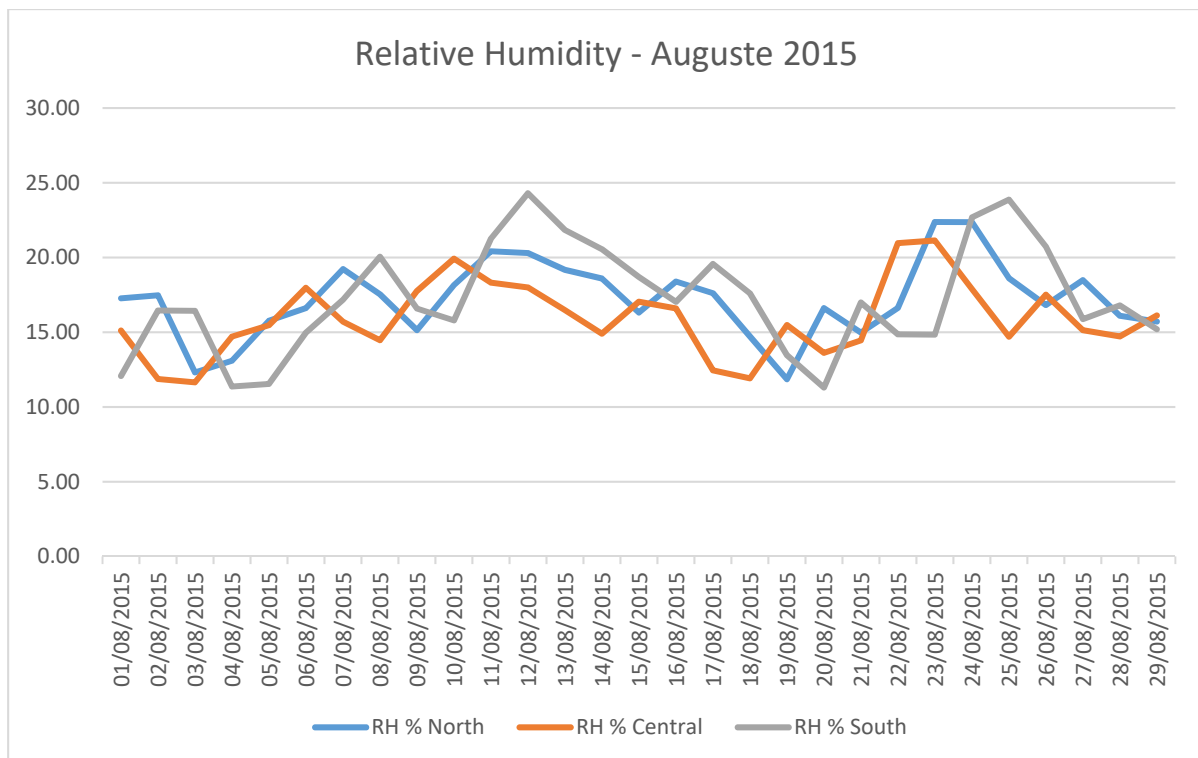
5. Relative Humidity

m. June 2015

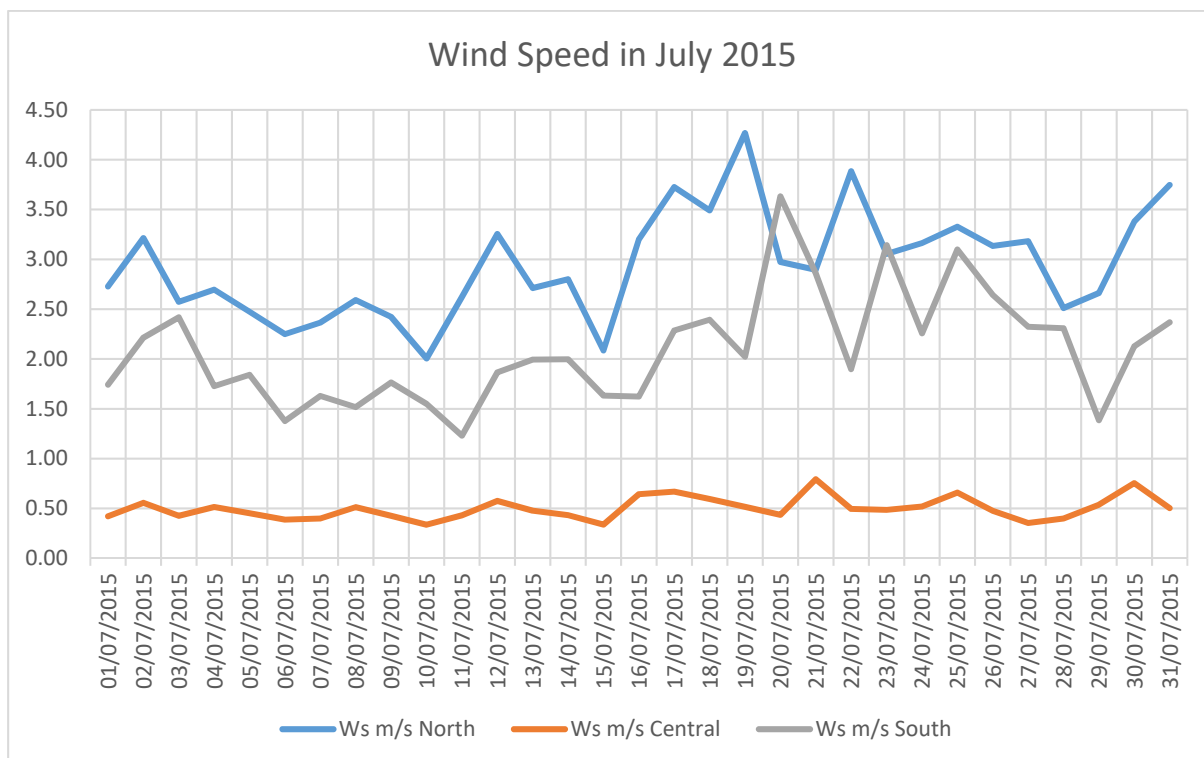
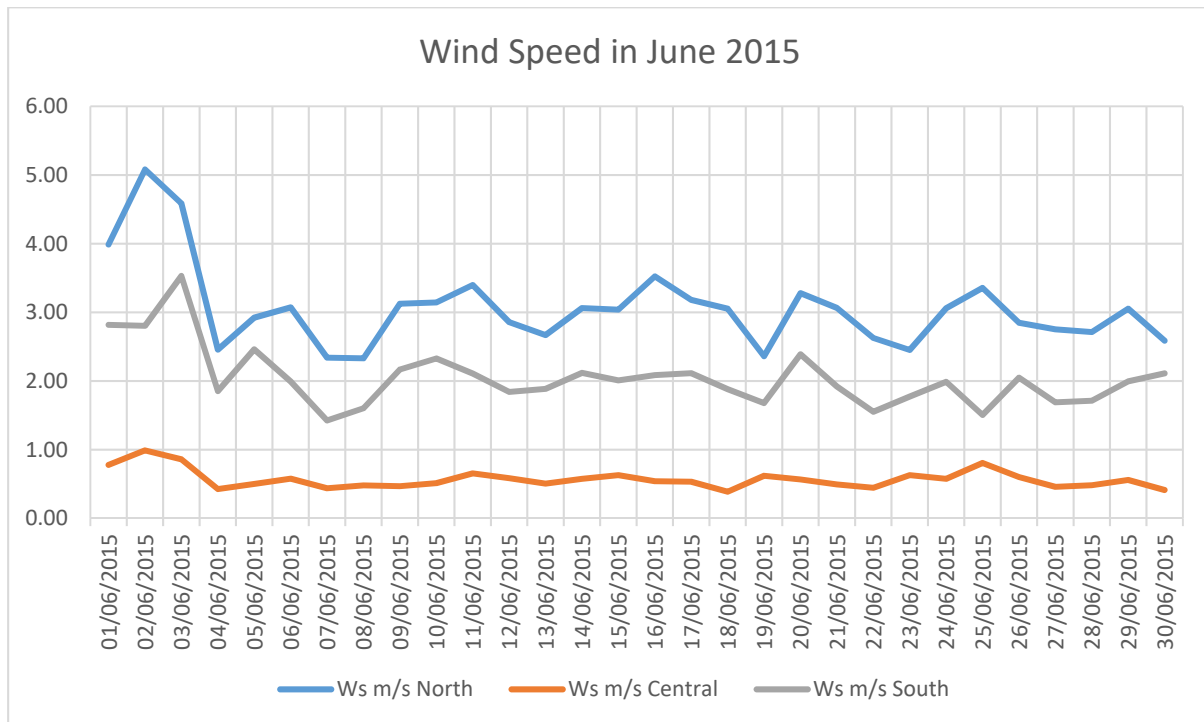
n. July 2015

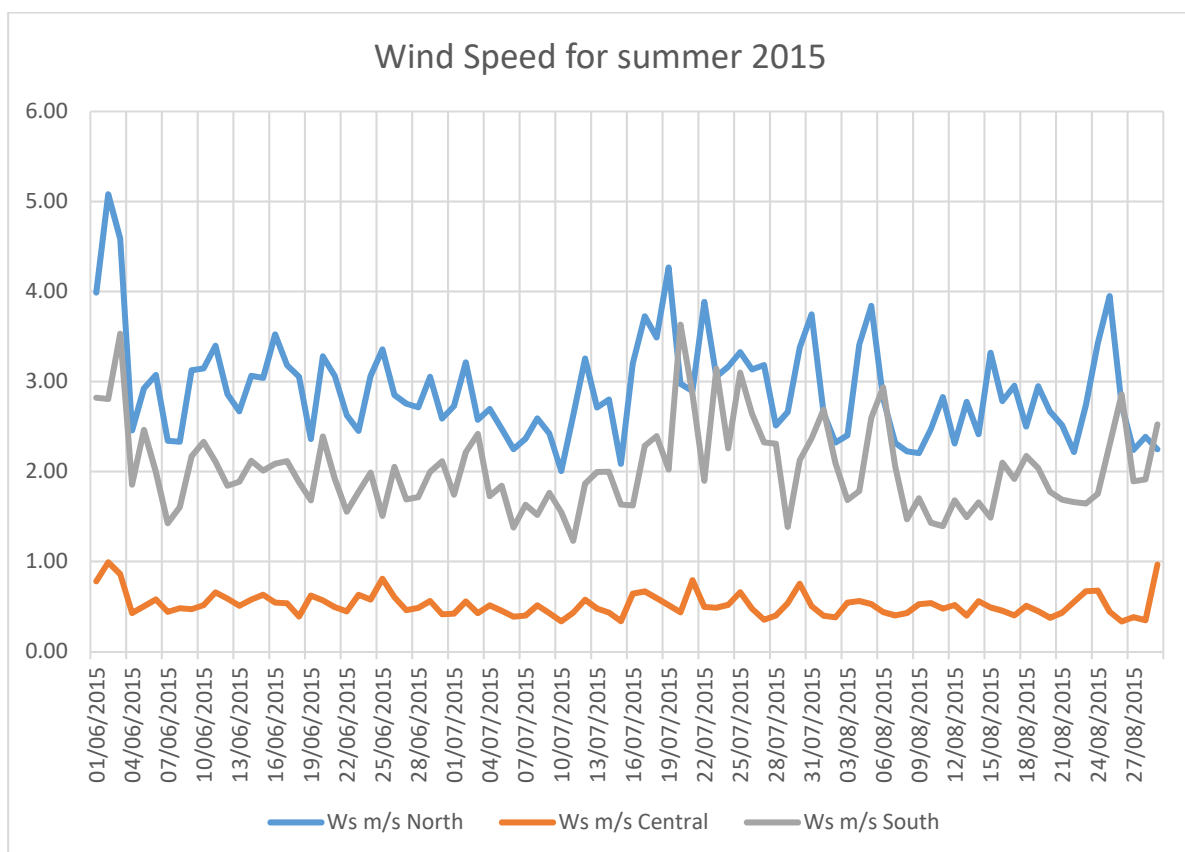
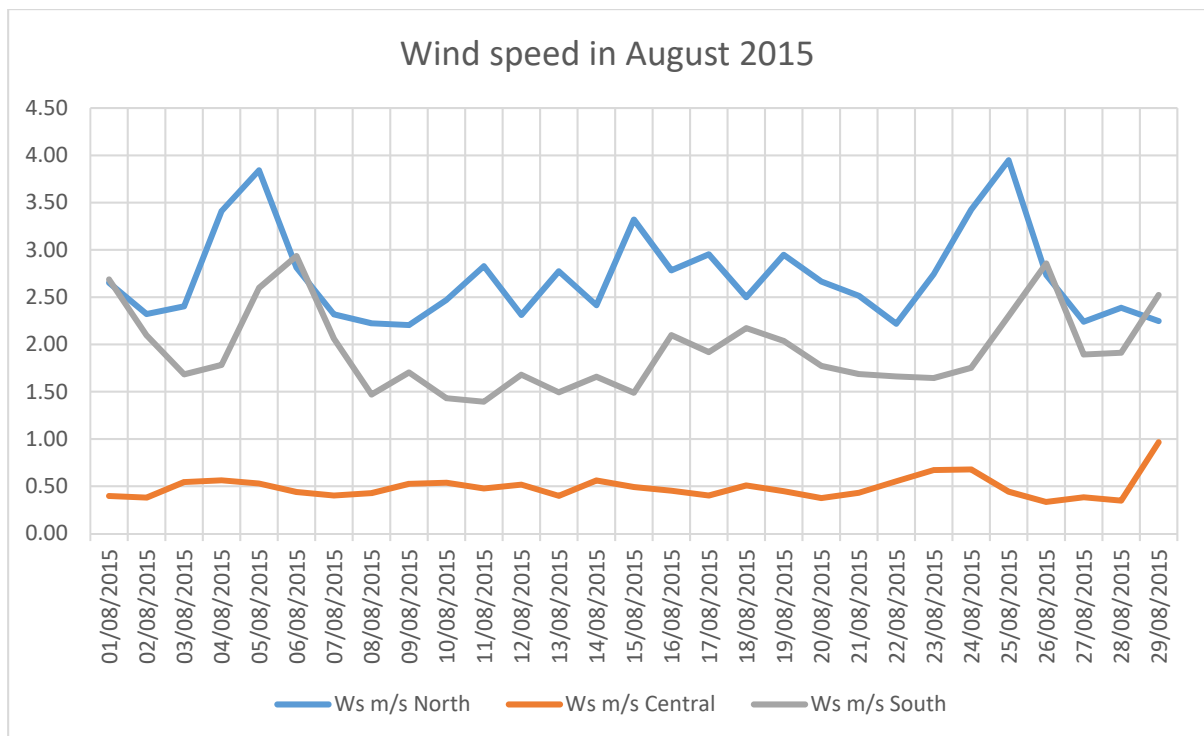
o. August 2015





6. Wind Speed
 p. June 2015
 q. July 2015
 r. August 2015





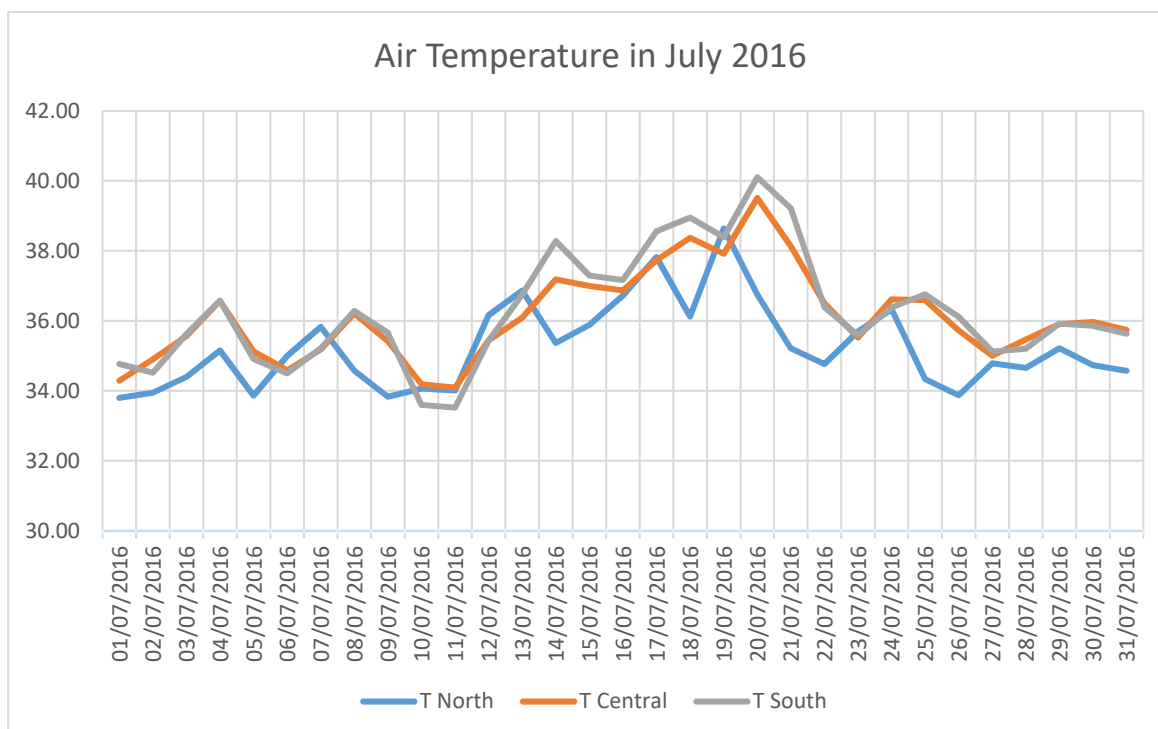
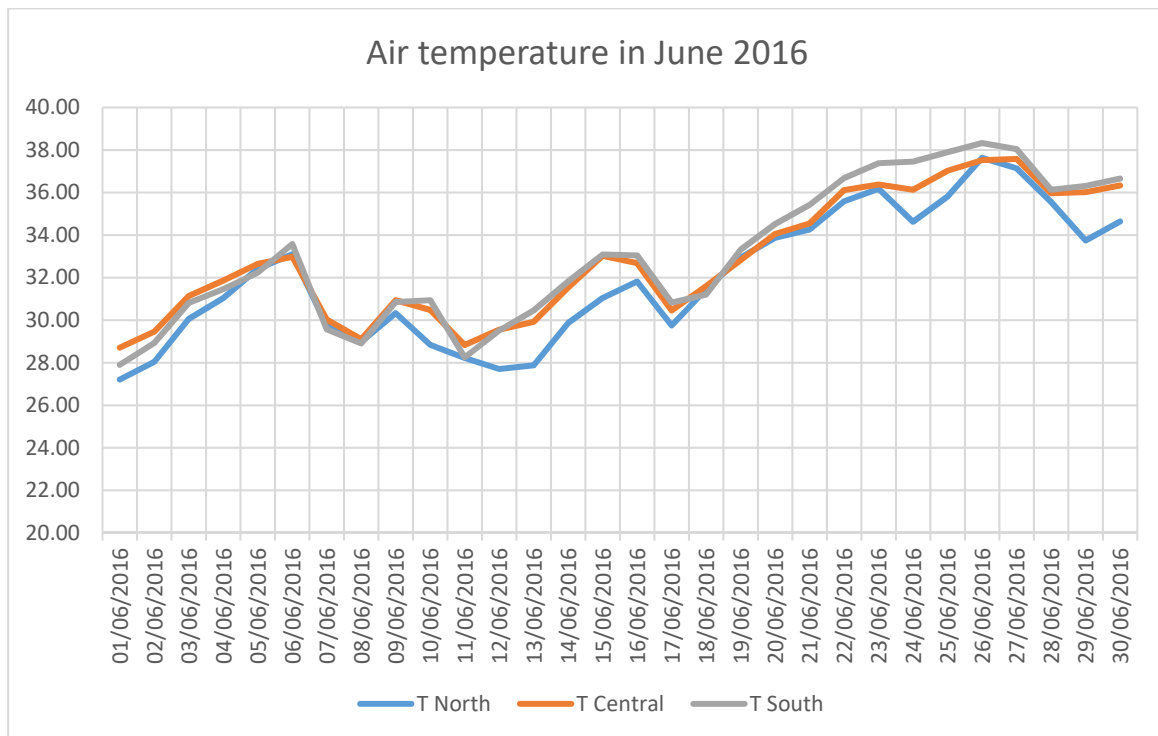
Weather data for all stations North, Central and South for summer months:

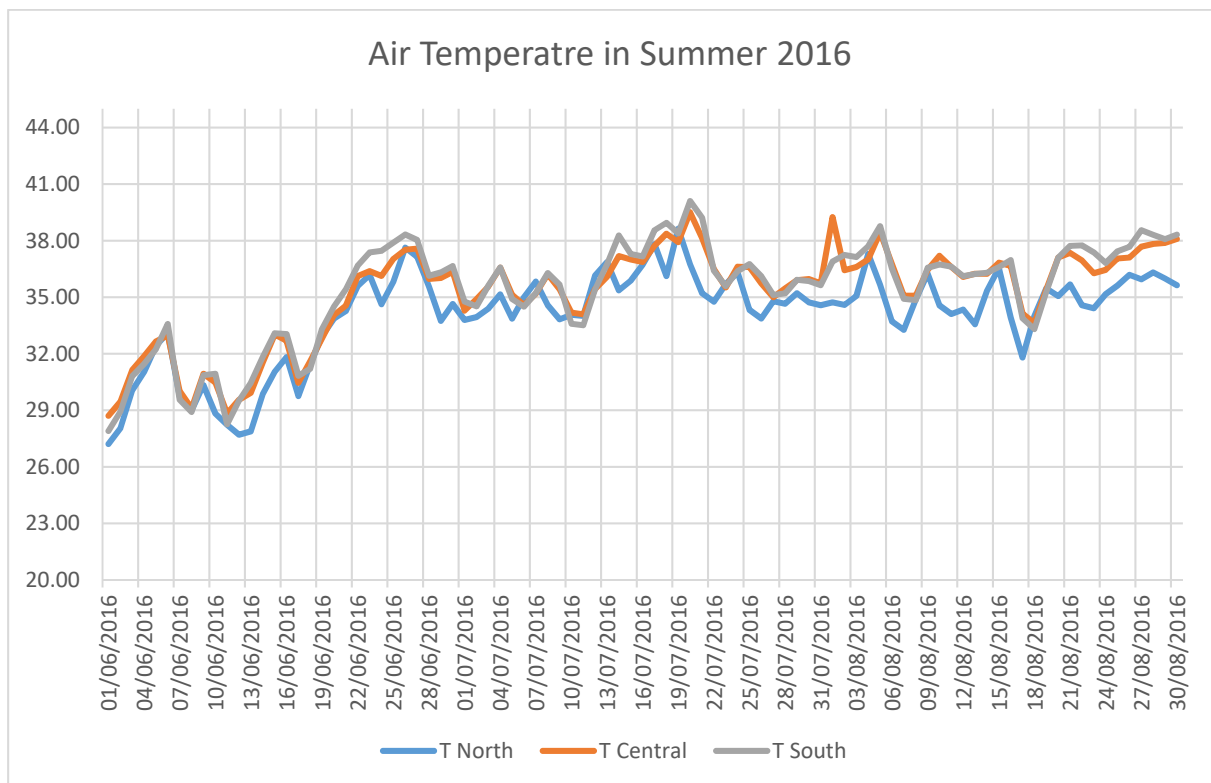
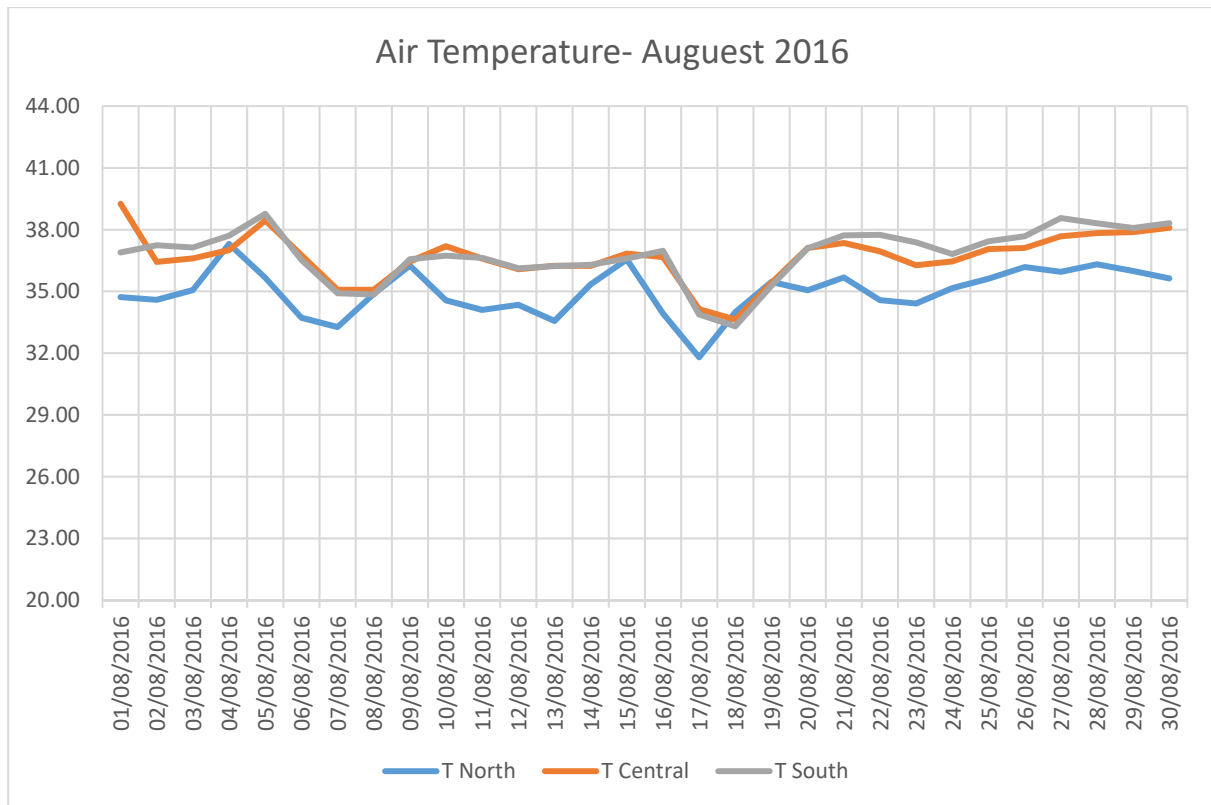
7. Air Temperature

s. June 2016

t. July 2016

u. August 2016



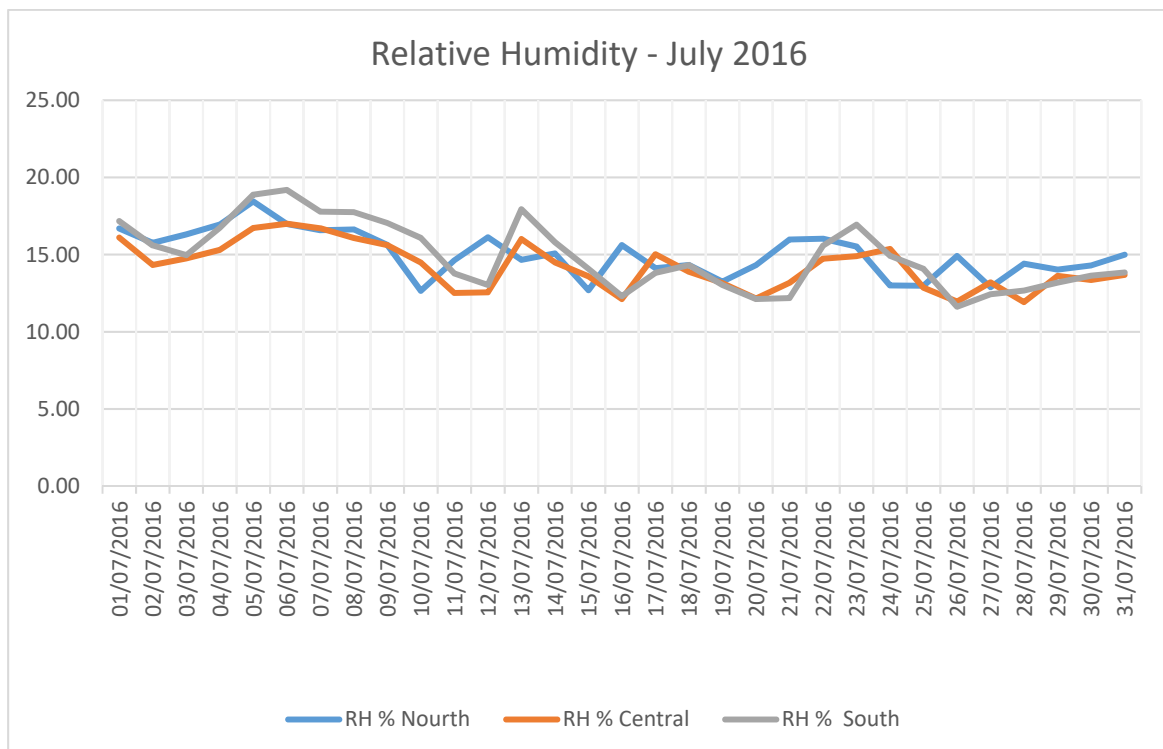
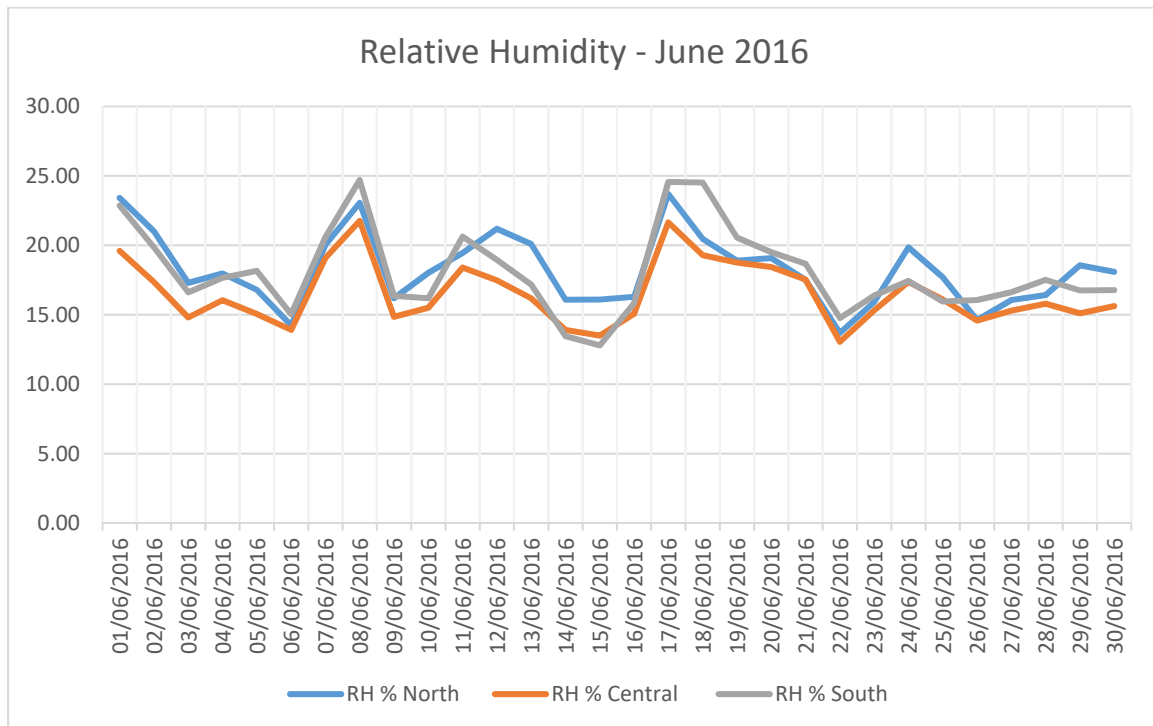


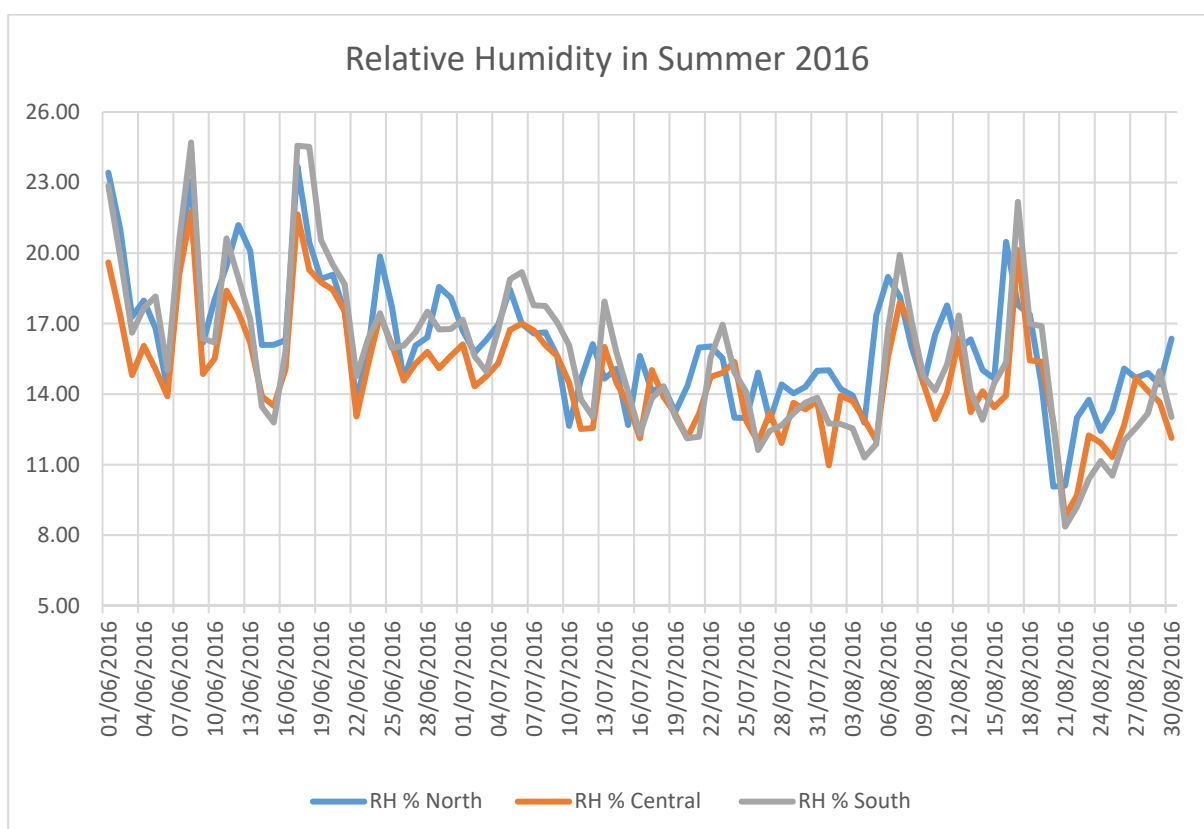
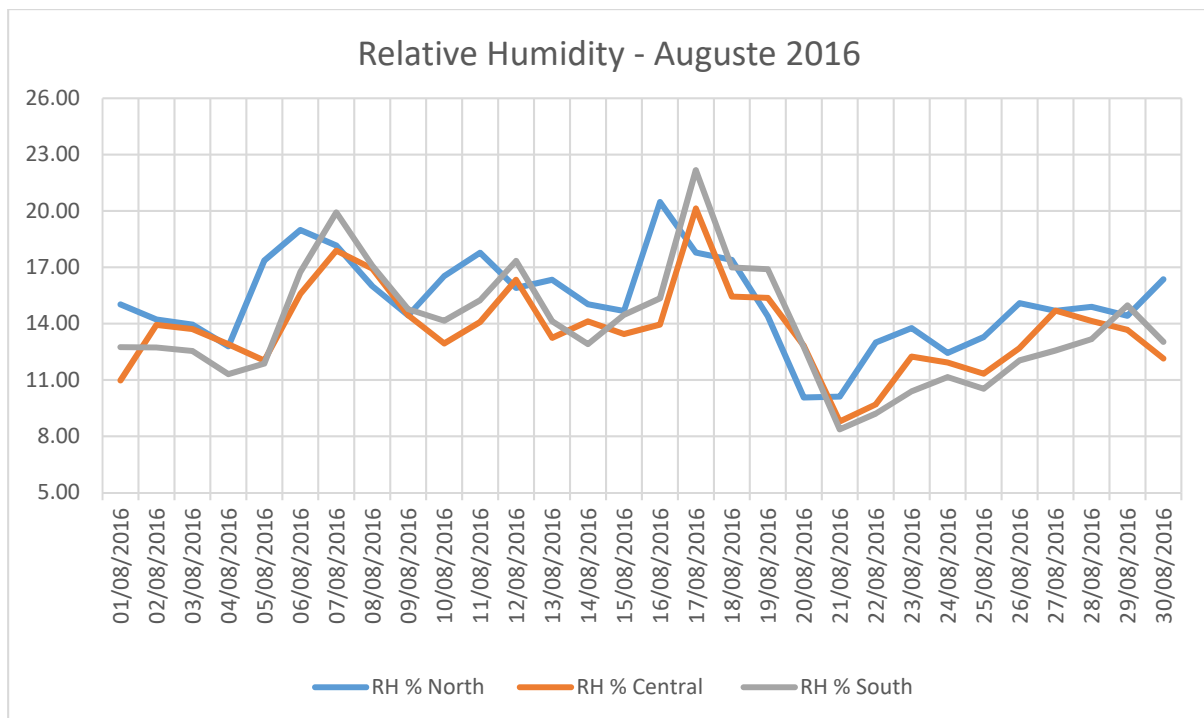
8. Relative Humidity

v. June 2016

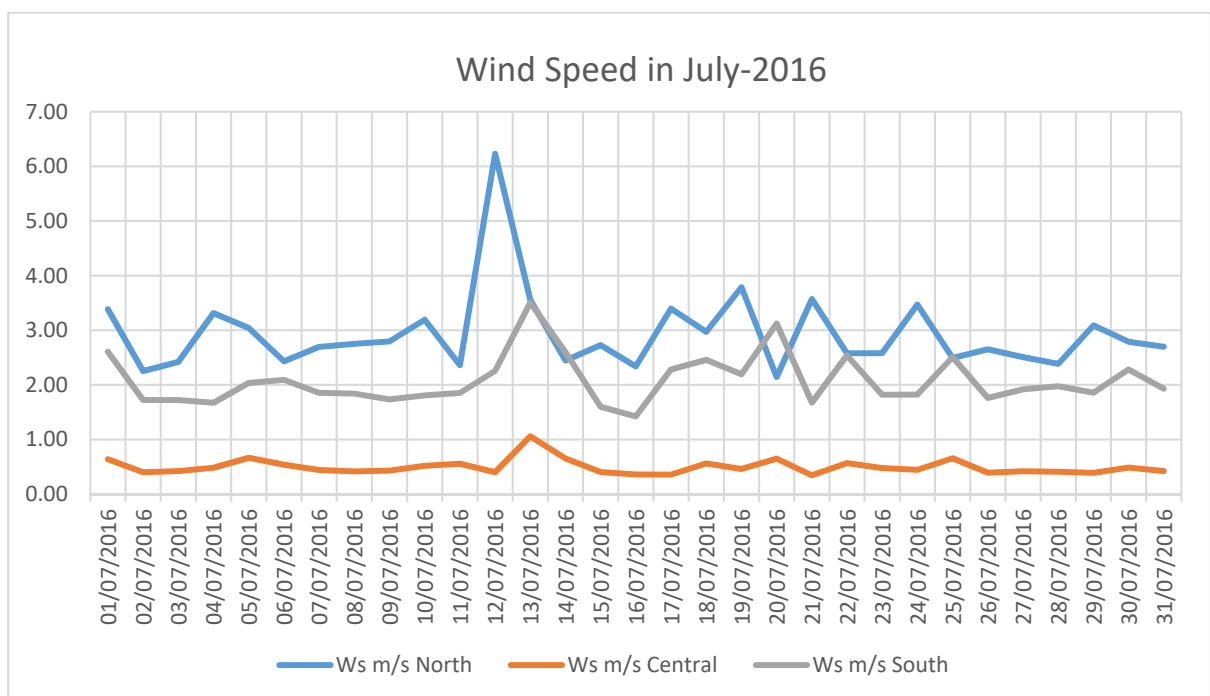
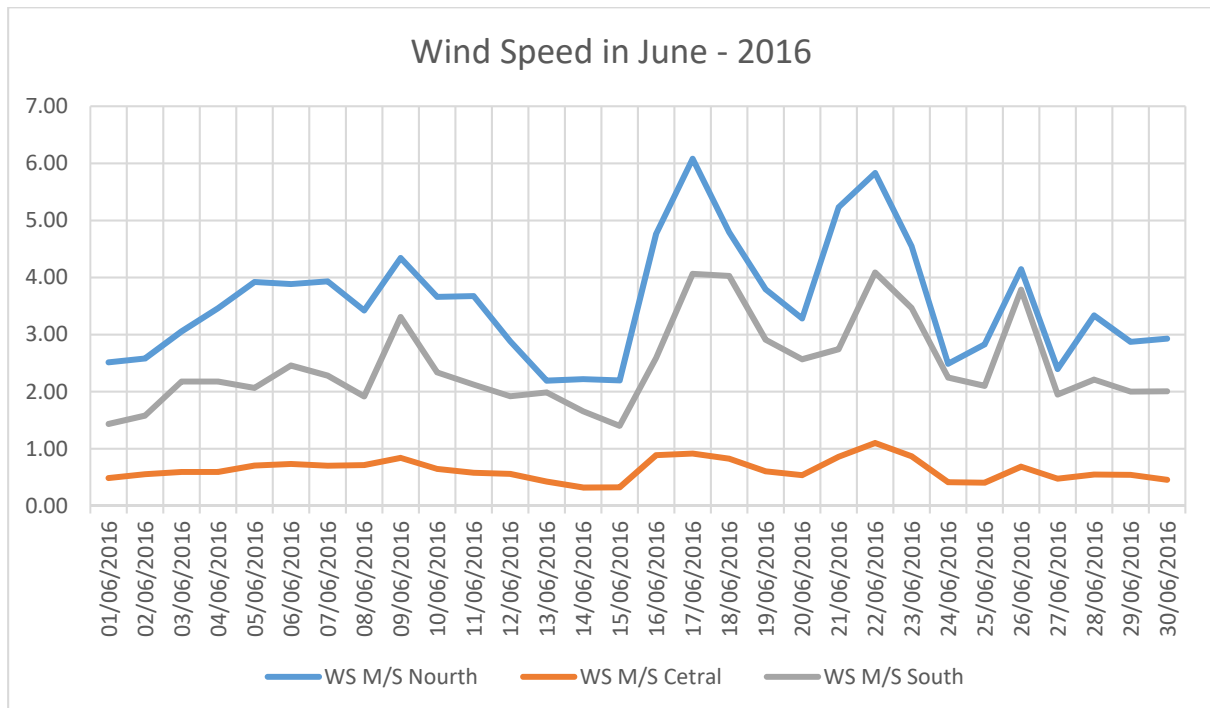
w. July 2016

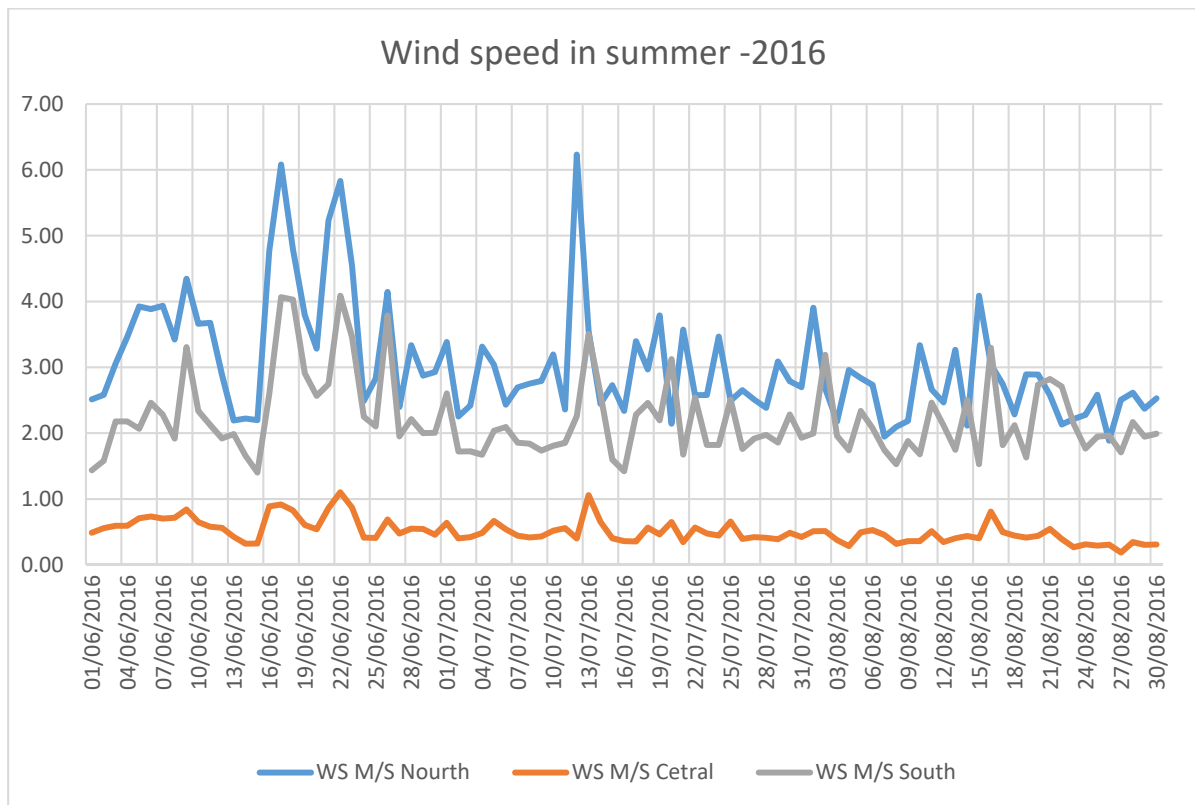
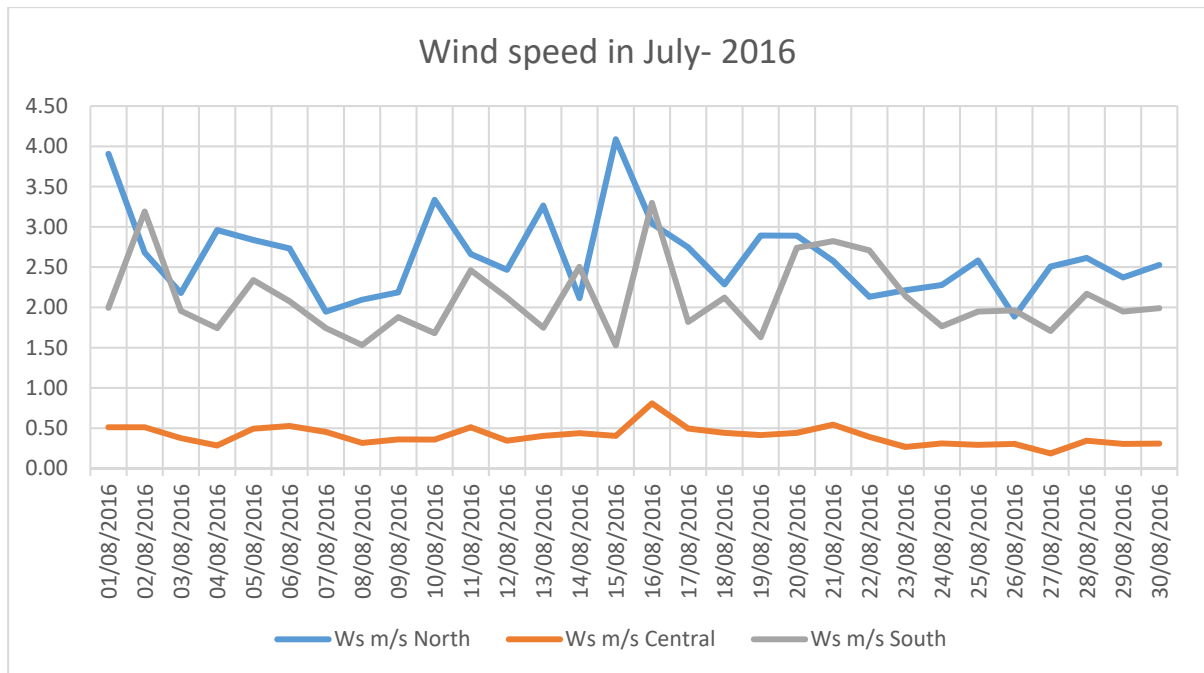
x. August 2016





9. Wind Speed
 y. June 2016
 z. July 2016
 aa. August 2016





1.1 Introduction and Case study of microclimate model

This case study is located in southern part of Erbil city with (36.2063° N, 44.0089° E), Figure.1. The area of study is (1200m x 900m) which, contains three type of buildings: commercial, residential, and public services buildings. The study will concern on residential areas as a main target, open spaces and green areas. The streets have 12m widths between residential blocks, while 15m widths for main roads.

The Case study area is consider as a modern urban development. The urban area was designed by local architectures and planners of Erbil Governor district. The design is based on poor urban planning guidelines that was issued in Baghdad in 1967, which divided the area into a grid of individual blocks and each block into a range of 200m² plots arrangements. Street alignment is North-South, East-west without any concern of climatic and environmental approaches. This study will address two issues: first analysis the urban microclimate of this part of city, and secondly, apply number of modification to improve the urban microclimate using ENVI-met model.

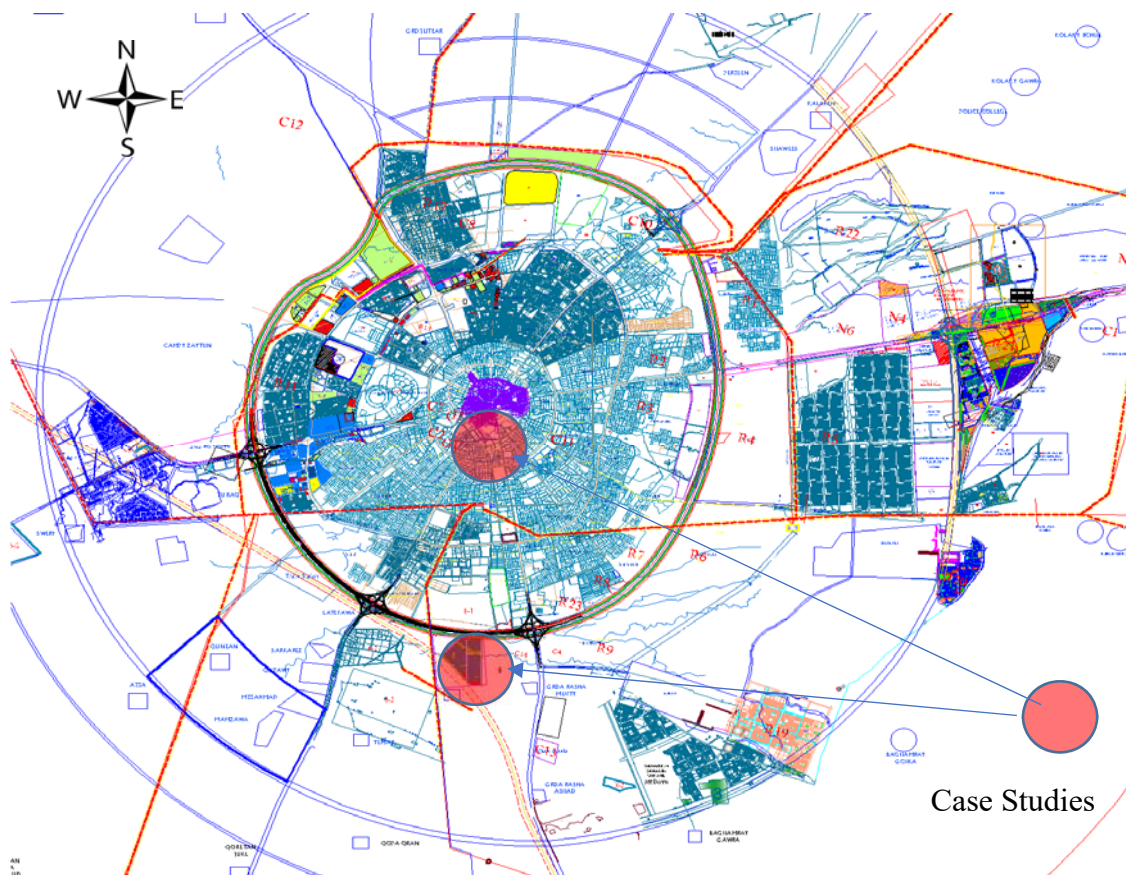


Figure 2: Case study in Erbil city with the study area to the south of the city centre.



Figure 1: Case study area to the south of the city centre.

1.2 The urban plan development of Erbil have problems as below:

- Urban development in Erbil city does not follow local and international guide-lines precisely in term of housing requirement (Ayoob Khaleel and Ibrahim 2010).
- Proposed plan of urban development in Erbil city do not take into account local environmental climate, while it is purely depend on geometry design rather than environmental and sustainable principles (Bornberg, Tayfor et al. 2006).
- The modern design of urban area in the city follows a grid-iron pattern with North-south and East-West direction, which is proposed by Polservice, consultants from Poland in 1977 (PADCO 2006). Polservice proposed five housing typology established in some Iraqi cities.
 1. Type one: in historic core – Organic, indigenous. With density 500-1000 person/ ha and low quality housing.
 2. Type two: planned areas- small irregular plots. With density 500 person/ ha
 3. Type three: planned areas- regular plots. With density 40-80 person/ha
 4. Type four: multi-story housing.
 5. Type five: temporary housing-transitional areas, short residence periods, and low quality infrastructure (PADCO 2006).
- In Case study2 urban area there were an old reviver bed and when they design urban area the reviver not consider as an element during the design, but as an organic element.

1.3 Weather data of Erbil city

Ideally, we would like to collect data and measure the climatic factors within the particular region that we proposed to model, but for variety reasons, security and safety purposes we could not able to access the location, but we have access to three weather stations that cover North, Central, and south of city. Simi-structure interview made with Architects planners.

The quality of data and locality in urban context of Erbil

Weather data stations locations surrounded by various urban areas densities. North and South Station surrounded by lower urban density population compared to city Central Weather Station, which is located in high urban population area. The reliability of data can be seen through a minor difference of data in all three stations, but the South Station data came with systematic error related to day-night timing and was corrected.

Micrometeorological stations positions represent most of the urban microclimate of city. The aim of this data collection is to understand and observe real microclimate data of urban areas of Erbil city. In addition, the data will be used as input for the simulation model and validation phase later.

Weather data stations were originally installed by a US Company originally using modern sensors and data loggers. Temperature, Wind speed, Relative Humidity, Air Pressure, Rainfall, and Specific Humidity and Soil Temperature were measured. The measurement interval uses every 15 mints for June and July 2013, 2014, 2015, and 2016.

These data come with package of microclimate measurements in urban area for summer and winter as in Table 1.1. June and July is peak time of summer when air temperature up to 44 °C. This research qualitatively and quantitatively depend on urban meteorological urban Data for both simulation and validation stage.

Table 1.1.shows the weather data package.

TOA 5	CR1 000	CR 10 00	288 9	CR10 00.Std .06	CPU:ER RAS002. CR1	8149	MIN _15										
TIME STA MP	RE CO RD	ID	Pro gra m	Batt_ Volt_ Min	AirTC	AirT C_M ax	AirT C_M in	R H	BP_ mb ar	WS_ ms_ Avg	ws_g ust_ Max	ws_g ust_ T Mx	Wi nd Dir	Slrk W_ Avg	Slr MJ_ Tot	SoilT1 0_C_A vg	Rain_ mm_ Tot
TS	RN			Volts	Deg C	Deg C	Deg C	%	Mill ibar s	meters/second			Deg rees	kW/ m ²	MJ/ m ²	Deg C	mm
		Smp	Smp	Min	Smp	Max	Min	Smp	Smp	Avg	Max	TMx	Smp	Avg	Tot	Avg	Tot

Finally, the data will use as a guide to propose new design scenarios that modify both air temperature and air speed in urban area for hot dry climate city. For that reasons the section will interpreted three climate elements of Erbil city generally and compare between all three stations. For the three weather stations, 3 weather measurements will be presented.

1. Air temperature.
2. Relative humidity.
3. Wind speed.

1.4 Methods and instruments for data collection

Three locations used in this study are Aynkawa in the North, Komary is 2km distant from city Centre and Zhyan district in South of city (Figure 2).

Central station is surrounded by urban residential neighbourhoods. The urban area crossed by main street 40m, from North – South direction and divides the area into two main parts, residential urban areas on the East side of street, while commercial and city stadium on the West hand side. The position of the North weather station is located in urban area from three directions with two story floor building.

While, main road with 40m width, two directions 12m each and three walk ways 6m each. Surrounding urban area with high population density, while the west side of urban area with commonly with medium population density.

In general, urban area with two story residential building has one viewing to the front yard. The street walk ways contains some trees with green area to provide shade in summer and some trees for each individual house.

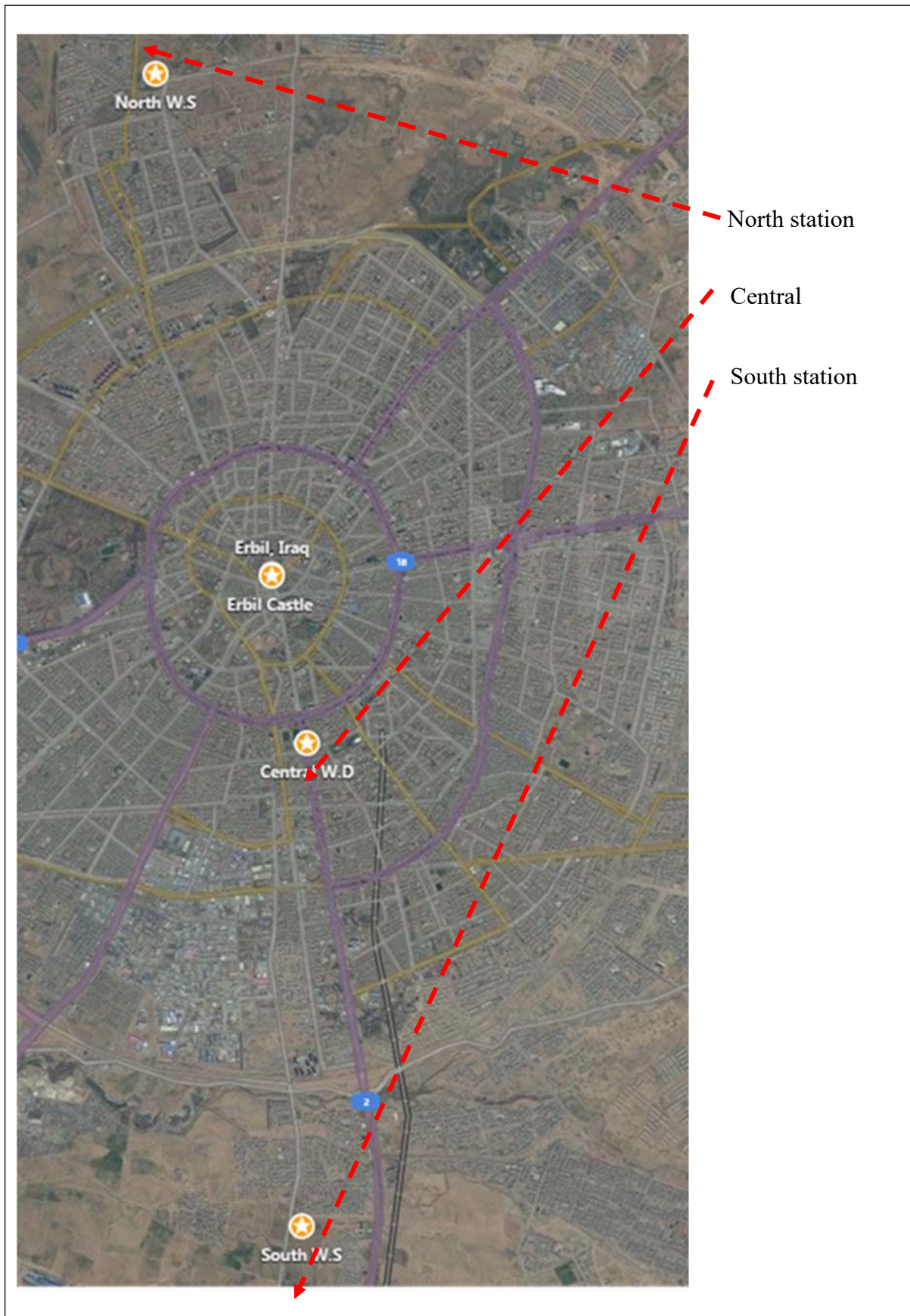


Figure 3. Site plan of Erbil City, showing the locations of three weather stations.




<p>A- North station:</p> <p>Location: 36.243790, 43.994587,</p> <p>Low urban dense area</p>	
<p>B- Central Station</p> <p>Location: 36.171898, 44.014500</p> <p>High dense urban area</p>	
<p>C- South Station:</p> <p>Location: 36.119961, 44.013763</p> <p>Medium dense urban area</p>	

Figure 4. Measurement portions within urban areas. A = Low urban density, B= High urban density and position C= Medium urban density. Source: <https://www.bing.com/maps?FORM=Z9LH3>.

1. Roof of first floor (Erbil houses)

Description: ID:

Performance:

U-value: W/m²·K Thickness: mm Thermal mass Cm: kJ/(m²·K)

Total R-value: m²·K/W Mass: kg/m² Mediumweight

Surfaces

Outside Emissivity: Resistance (m²·K/W): ☒ Default Solar Absorptance:

Inside Emissivity: Resistance (m²·K/W): ☒ Default Solar Absorptance:

Construction Layers (Outside To Inside)

Material	Thickness mm	Conductivity W/(m·K)	Density kg/m ³	Specific Heat Capacity J/(kg·K)	Resistance m ² ·K/W	Vapour Resistivity GN·s/(kg·m)	Category
[CT] CONCRETE TILES	80.0	1.1000	2100.0	837.0	0.0727	500.000	Tiles
[SLCL] LONDON CLAY	150.0	1.4100	1900.0	1000.0	0.1064	250.000	Sands, Stones and Soils
[STD_CC2] Reinforced Concrete	150.0	2.3000	2300.0	1000.0	0.0652	-	Concretes
[PPL] PERLITE PLASTERING	30.0	0.0800	400.0	837.0	0.3750	25.000	Plaster

2. Ground floor of Erbil houses

Description: ID:

Performance:

U-value: W/m²·K Thickness: mm Thermal mass Cm: kJ/(m²·K)

Total R-value: m²·K/W Mass: kg/m² Lightweight

Surfaces

Outside Emissivity: Resistance (m²·K/W): ☒ Default Solar Absorptance:

Inside Emissivity: Resistance (m²·K/W): ☒ Default Solar Absorptance:

Construction Layers (Outside To Inside)

Material	Thickness mm	Conductivity W/(m·K)	Density kg/m ³	Specific Heat Capacity J/(kg·K)	Resistance m ² ·K/W	Vapour Resistivity GN·s/(kg·m)	Category
[CYT] CLAY TILE	20.0	0.8400	1900.0	800.0	0.0238	200.000	Tiles
[BASESC11] SCREED	100.0	0.4100	1200.0	840.0	0.2439	50.000	Screeds & Renders
[CCD1] CAST CONCRETE (DENSE)	100.0	1.4000	2100.0	840.0	0.0714	650.000	Concretes
[TB] TILE BEDDING	200.0	1.4000	2100.0	650.0	0.1429	45.000	Gravels, Beddings, etc.

3. Walls of Erbil houses

Description: ID:

Performance:

U-value: W/m²·K Thickness: mm Thermal mass Cm: kJ/(m²·K)

Total R-value: m²·K/W Mass: kg/m² Lightweight

Surfaces

Outside Emissivity: Resistance (m²·K/W): ☒ Default Solar Absorptance:

Inside Emissivity: Resistance (m²·K/W): ☒ Default Solar Absorptance:

Construction Layers (Outside To Inside)

Material	Thickness mm	Conductivity W/(m·K)	Density kg/m ³	Specific Heat Capacity J/(kg·K)	Resistance m ² ·K/W	Vapour Resistivity GN·s/(kg·m)	Category
[BASESC01] BASESC01REED	30.0	0.4100	1200.0	840.0	0.0732	50.000	Screeds & Renders
[CPAV] CONCRETE PAVIOUR	200.0	0.9600	2000.0	840.0	0.2083	45.000	Brick & Blockwork
[PPL] PERLITE PLASTERING	30.0	0.0800	400.0	837.0	0.3750	25.000	Plaster

NO	Interview Code	Names	Gender	Position	Place	Type of meeting
1	AHM101-II	Architect	Male	Head of Architecture office	Erbil Governorate	Semi-structure interview
2	AMM102-II	Architect	Male	Manager	Department of Urban planning of Erbil	General discussion
3	AMH103-II	Architect	Male	Head of Housing approval Department	Municipality Department Erbil No 4	Semi-Structure interview
4	AMD104-II	Architect	Male	Design Leader of planning office	Ministry of Municipalities and Tourism	Semi-Structure interview
5	AMM105-II	Architecture	Male	Manager of Buffer zone (Erbil)	General Director of planning and follow-up. Ministry of municipality and Tourism	General discussion about buffer zone.
6	AFM106-II	Architecture	Female	Manager of GIS centre (Erbil)	Erbil Governorate	Collecting maps and GIS information
7	AFU107-IV	Architect	Female	Urban Services Designer	Head of Municipalities of Erbil	Semi-Structure interview
8	AFU108-III	Architect	Female	Urban Services Designer	Head of Municipalities of Erbil	Semi-Structure interview
9	AFS109-III	Architect	Female	Senior Architect at Approval department	Head of Municipalities of Erbil	Semi-Structure interview
10	AFU110-III	Architect	Male	Urban Designer	Head of Municipalities of Erbil	Semi-Structure interview
11	AMA111-III	Architect	Male	Architect in Investment of Kurdistan Department	Investment of Kurdistan Department	Semi-Structure interview
12	AMH112-III	Architect	Male	Head of Design Department	Head of Municipalities of Erbil	Semi-Structure interview
13	AMT113-III	Architect	Male	The Manager of Design Department	Head of Municipalities of Erbil	Semi-Structure interview
14	SST114-III	Senior Architect	Male	The Manager of Design	Investment of Kurdistan Department	Semi-Structure interview
15	SMU115-III	Senior Architect	Male	Urban Designer	City council	Semi-Structure interview

Coding system in this study: First digit refers to the name of interviewee (A for Architect and S for Senior Architect). Second digit shows the gender of interviewee (M for Male and F for Female). The number of interviews appears in the three digit displays in code, which is from 101 to 115. The last part of the code system shows the phase of data collection (II and III).

Simulation context:

Envi-met used to simulate the environmental factors of Erbil residential blocks. Three wind directions used to produce data from four scenarios of grid-iron morphology. The simulation is based on exist residential block for Erbil city, the dimensions of site plan are 520m length and 480m width.

Two main variables were simulated; wind direction and canyon width. Firstly, three wind direction are proposed (180°, 225°, and 270°). The wind simulated over four types of canyon width (10m, 15m with plot area of 200m², 15m with plot area 150m² and 20m). The simulation is for 12 hours of 26/ June 2016. The aim of this report is to find the relationship between wind direction and canyon width of attached residential blocks.

wind direction	180°	225°	270°
Canyon widths	10 m		
	15 m (type a) ¹		
	15 m (type b) ²		
	20 m		

Table1.1 shows the simulation types, three wind direction with four scenario morphology types.

15 m (type a)¹ means the canyon is 15m width and 200m² is the plot area.

15 m (type b)² means the canyon is 15m width and 150m² is the plot area.

The simulation runs with similar input data to concentrate on two variables; wind direction and canyon width. Each wind direction applied over four urban morphologies at the similar times and locations (equivalent environment). The output data is measured in the medial of canyon at 1.8m high. Envi-met program used to observe wind speed, air temperature and mean radiate temperature for each scenarios as below:

1. First scenario: when canyon width is 10m, and plot area 200m²
2. Second scenario: when canyon width is 15m, and plot area 200m²
3. Third scenario : when canyon width is 15m, and plot area 150m²
4. Fourth scenario : when canyon width is 20m, and plot area 200m²

Scenarios	Plot area	Canyon width	Wind Direction from the North	Environmental Variables	Simulation date and time duration
First scenario	200m ²	10m	180°, 255°, & 270°	T°,RH,MRT,AS	12 hour 23-06-2016
Second scenario	200m ²	15m	180°, 255°, & 270°	T°,RH,MRT,AS	12 hour 23-06-2016
Third scenario	150m ²	15m	180°, 255°, & 270°	T°,RH,MRT,AS	12 hour 23-06-2016
Fourth scenario	200m ²	20m	180°, 255°, & 270°	T°,RH,MRT,AS	12 hour 23-06-2016

The first scenario

Introduction:

The first scenario is to simulate blocks in a residential area with plot area of 200m², and 10m canyon's width. The site contain residential blocks, attached houses and each block have 26 houses unit. Two floor building with 6 meter high for each unit. The houses are open in front only, while attached from other direction with other unites.

This simulation input data for 26 of June 2016 as below:

1. Air temperature, minimum 309F and maximum 314F.
2. Air speed, 4.5m/s
3. Relative humidity, minimum 11%, and maximum 27%.
4. Wind direction (first scenario) 180°.

The simulation period is 12 hours from 7:00 am to 7:00 pm. three types of wind direction is applied 180°, 225°, and 270°.

Wind direction	180° from the North	225° from the North	270° from the North
Canyon with	10m & 200m ² plot area.	10m & 200m ² plot area.	10m & 200m ² plot area.

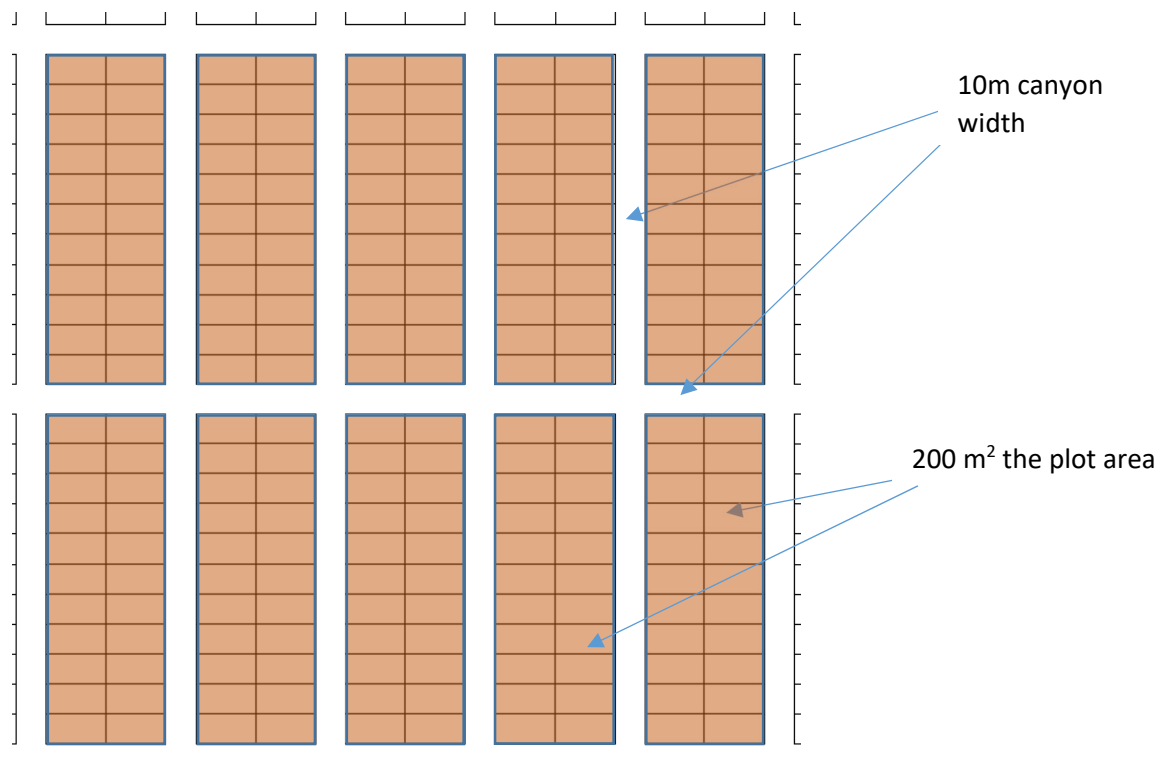
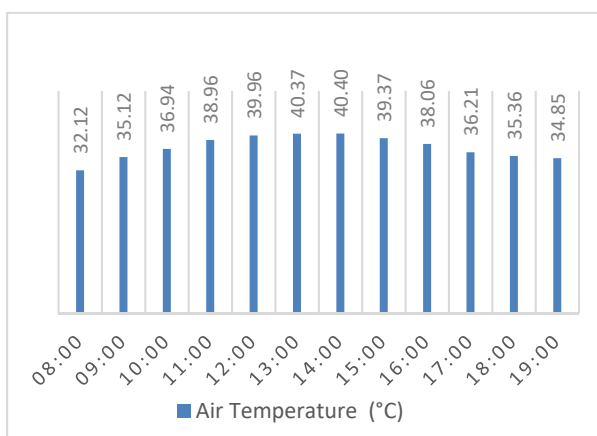


Fig 1.1, shows the residential blocks of first scenario, 200 m² the plot area, and 10m canyon width.

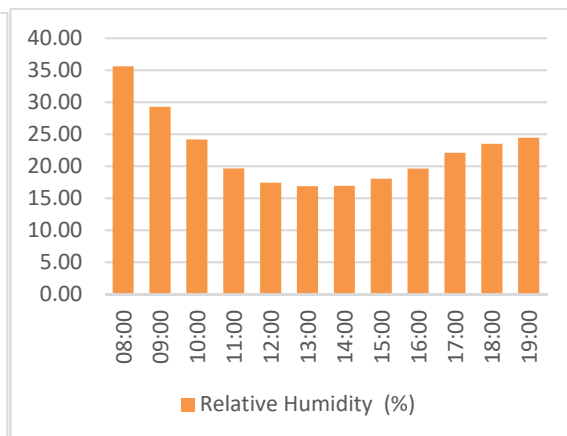
1. When the wind direction is **180°** from the North.

Variables	Air temperature	Relative humidity	Mean radiant temperature	Wind speed
Time				
9:00	35.12	29.28	61.78	3.39
12:00	39.96	17.43	75.01	3.36
15:00	39.37	18.04	45.58	3.33
18:00	35.36	23.50	28.68	3.29
Average	37.45	22.06	52.76	3.34
Max	39.96	29.28	75.01	3.39
Min	35.12	17.43	28.68	3.29

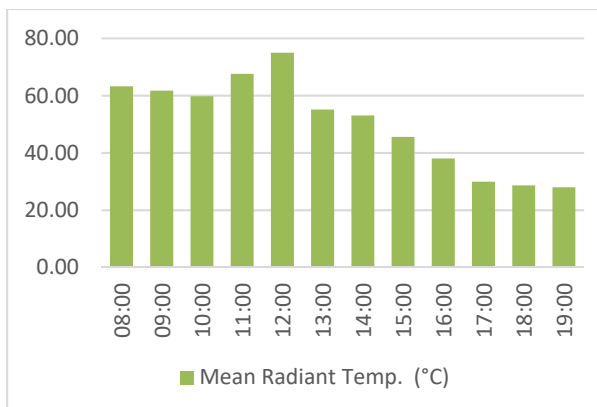
Table 1.1, shows three different time of measurements, air temperature, relative humidity, mean radiant temperature and wind speed for first case with wind direction 180°.



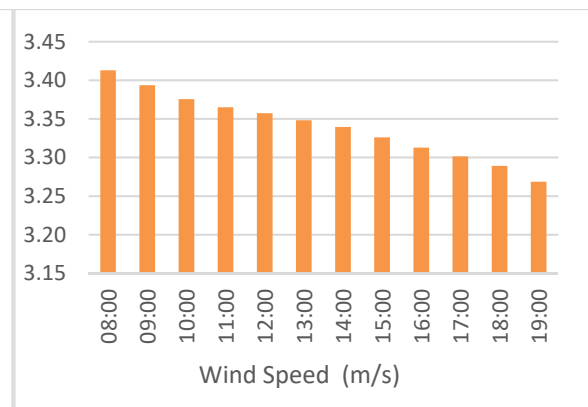
Graph 1.1, shows different time of air temperature measurements with wind direction of 180°.



Graph 1.2, shows different time of Relative humidity measurements with wind direction of 180°.



Graph 1.3, shows different time of Mean Radiant air temperature measurements with wind direction of 180°.



Graph 1.4, shows different time of wind speed with wind direction of 180°.

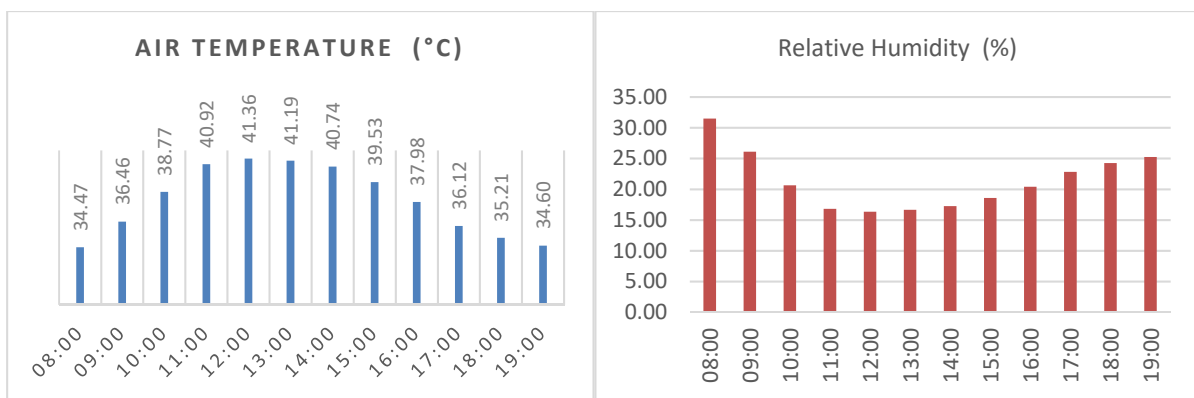
From the graphs above, the maximum air temperature is recorded at 14:00 with 40.40 C°, with lowest relative humidity 16.91 %, and 53.07C° for mean radiant temperature. The wind speed is gradually decrease with time from 3.45 m/s at 8:00am to 3.27 at 19:00.

The average of air temperature during the day time is 37.45C°, 22.06 % for Relative humidity, 52.76 C° is the mean radiant air temperature and 3.34 m/s is the average of wind speed

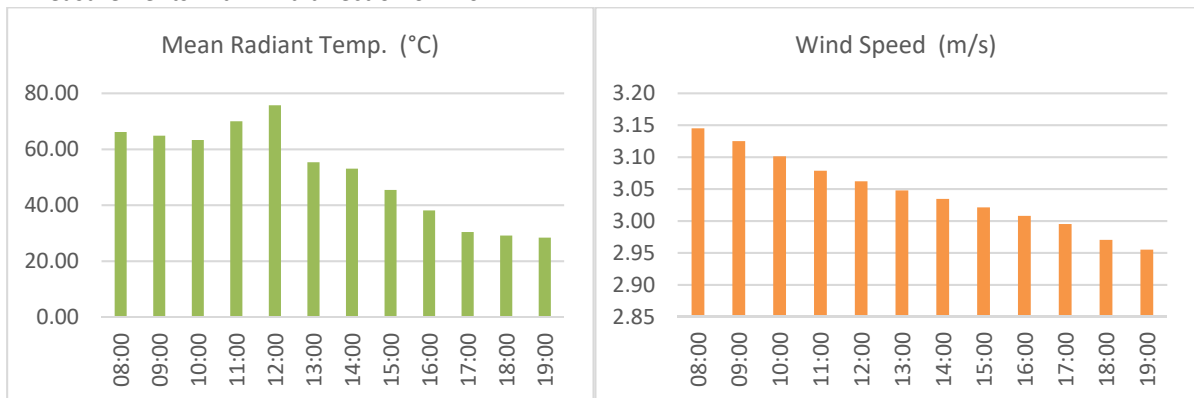
2. When the wind direction is **225°** from the North.

Variables	Air temperature	Relative humidity	Mean radiant temperature	Wind speed
Time				
9:00	36.46	26.09	64.81	3.13
12:00	41.36	16.34	75.69	3.06
15:00	39.53	18.58	45.46	3.02
18:00	35.21	24.26	29.15	2.97
Average	38.14	21.32	53.78	3.04
Max	41.36	26.09	75.69	3.13
Min	35.21	16.34	29.15	2.97

Table 2.1, shows three different time of measurements, air temperature, relative humidity, mean radiant temperature and wind speed for first case with wind direction 270°.



Graph 2.2, shows different time of air temperature measurements with wind direction of 270°.

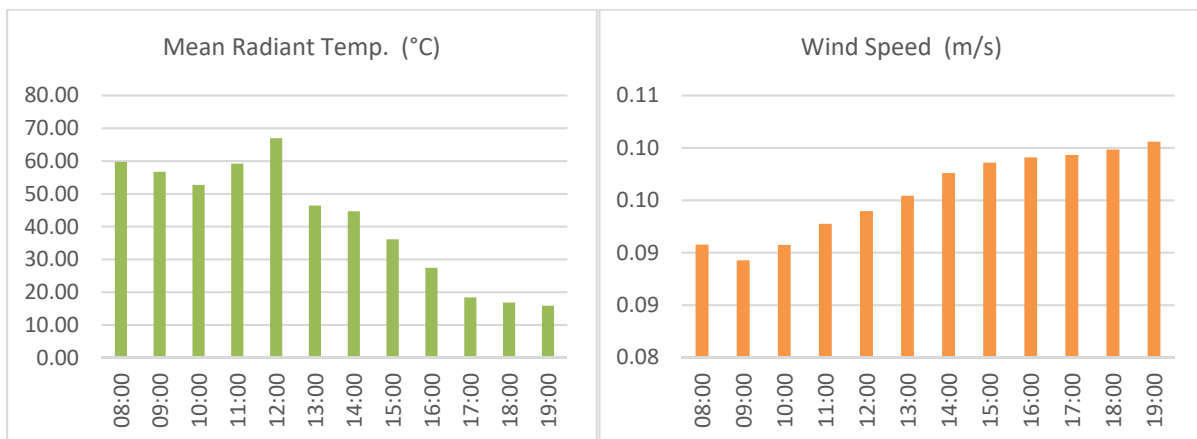
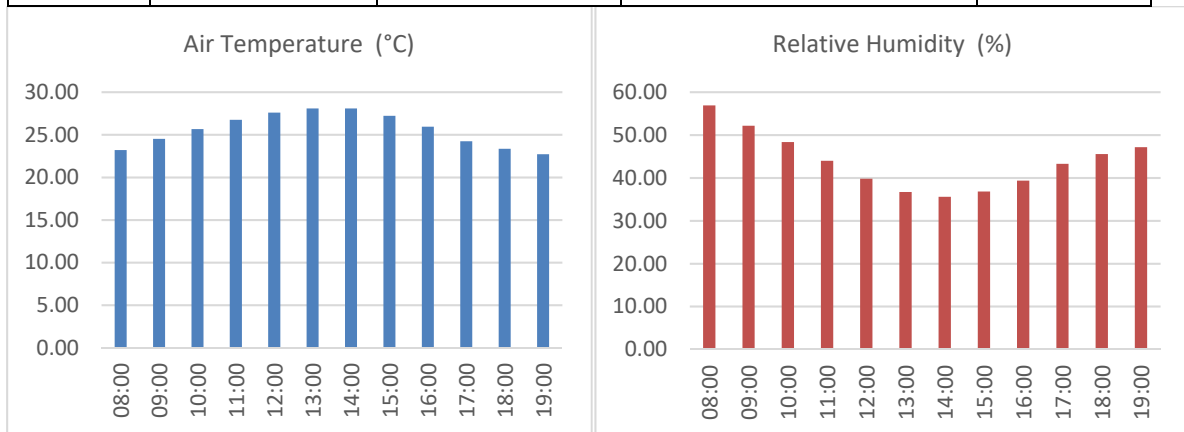


From the graphs above the maximum air temperature is 41.39 C° at 12:00 noon, with 16.34 % for relative humidity, and maximum mean radiant air temperature 75.60 C°. While, the wind speed is decrease during day times, which is start 3.15 m/s at 8:00 to 2.96 m/s at 19:00pm.

The average of air temperature during the day time is 38.14C°, 21.32 % for Relative humidity, 53.78 C° is the mean radiant air temperature and 3.04 m/s is the average of wind speed.

1. When the wind direction is **270°** from the North.

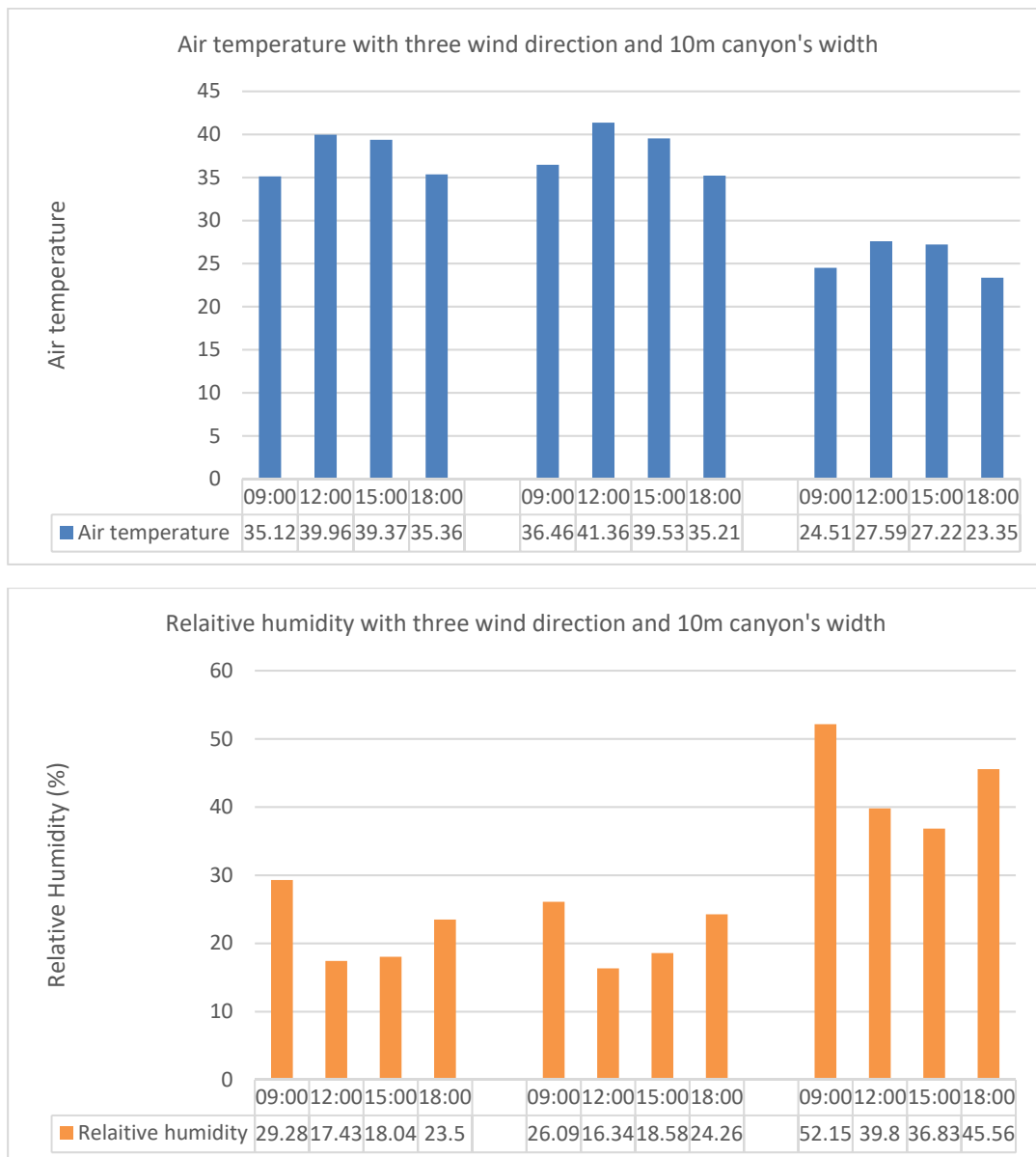
Variables	Air temperature	Relative humidity	Mean radiant temperature	Wind speed
Time				
9:00	32.70	35.20	62.20	0.09
12:00	38.80	18.59	75.44	0.09
15:00	38.73	18.76	46.56	0.10
18:00	35.17	23.89	28.95	0.10
Average	36.35	24.11	53.29	0.09
Max	38.80	35.20	75.44	0.10
Min	32.70	18.59	28.95	0.09



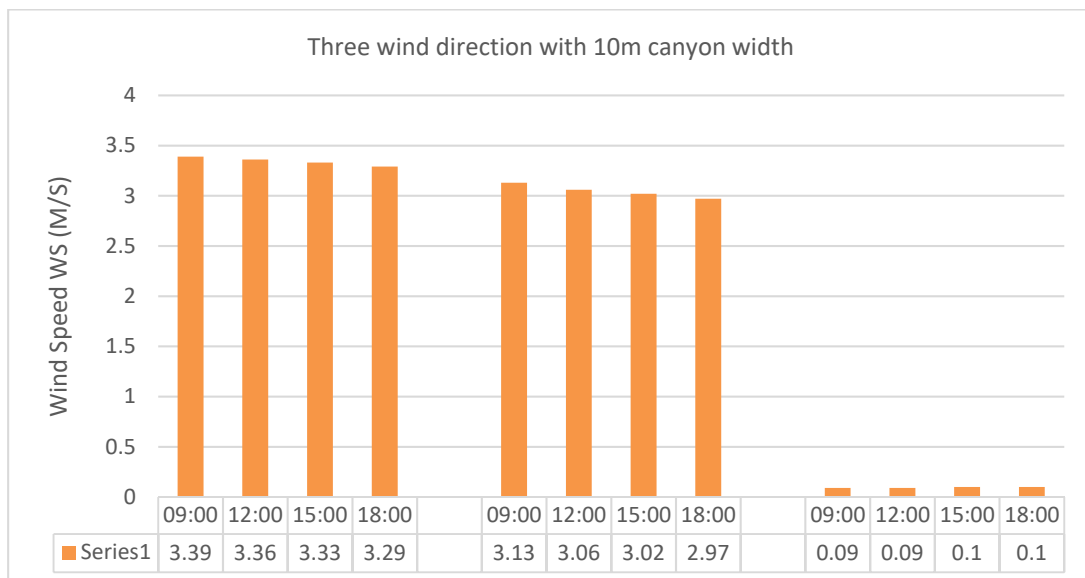
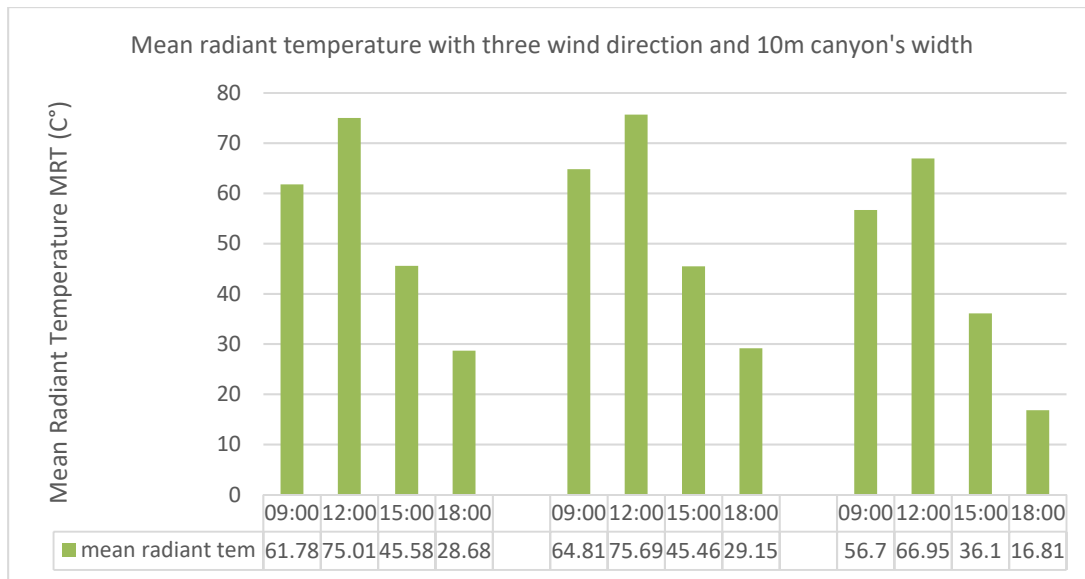
From the graphs above the maximum air temperature is 41.39 C° at 12:00 noon, with 16.34 % for relative humidity, and maximum mean radiant air temperature 75.60 C°. While, the wind speed is decrease during day times, which is start with 3.15 m/s at 8:00 to 2.96 m/s at 19:00pm.

The average of air temperature during the day time is 38.14C°, 21.32 % for Relative humidity, 53.78 C° is the mean radiant air temperature and 3.04 m/s is the average of wind speed.

1.3 Compare between three types of wind direction (180°, 225°, and 270°) over 10m canyon width in three similar Environment during 12 hour (7:00am to 7:00 pm).



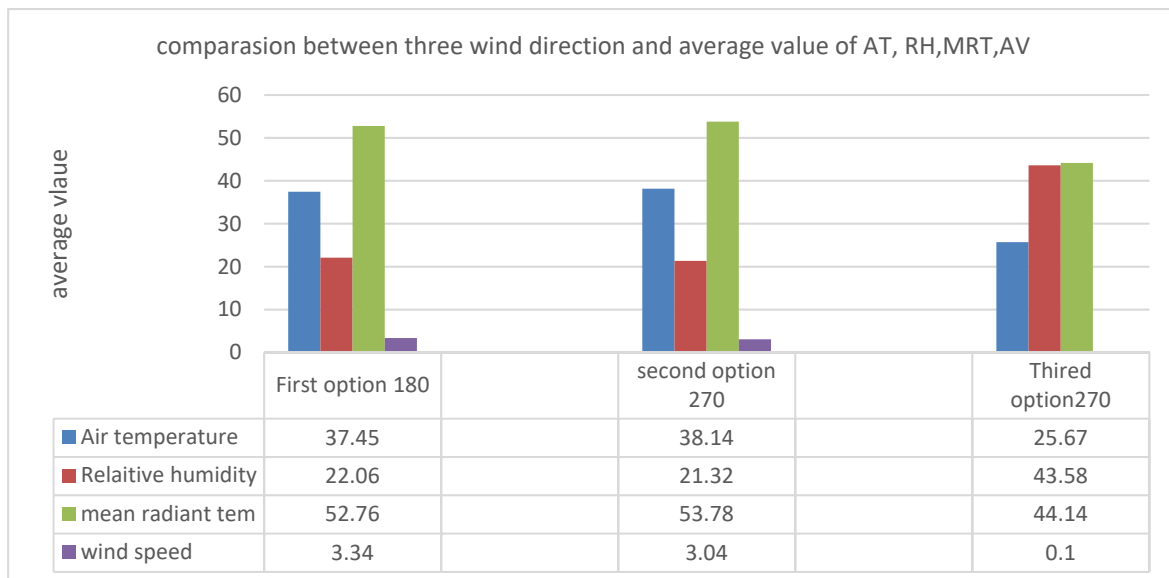
The two graph above shows air temperature and relative humidity for all three different wind directions (180°, 225°, 270°). The variables measured at four times during day times, the maximum air temperature (AT) for first case with wind direction (180°) is 39.96C° with minimum relative humidity (RH) 17.43% , while the maximum AT for second case with wind direction 225° is 41.36 C° with minimum RH 16.34%. In addition the Third case with wind direction 270°, record the lower air temperature and relative humidity during day time AT is 27.59C° and RH is 38.8%. The residential block with 10m width with 270° wind direction perform better than first and second cases 180° and 225° wind direction.



The two graph above shows Mean radiant temperature (MRT) and Wind speed during day time with three different wind direction (180°, 225°, 270°) which applied over similar residential block with 10m canyon width. The maximum MRT°C was 75.69°C recorded with wind direction 270° at 12:00 noon. While the minimum was 16.81 C° with 270° wind direction at 18:00. In addition, the maximum wind speed was 3.39 m/s at 9:00 for first case when wind direction is 180°. However, the air temperature and mean radiant temperature recorded minimum values for third case when wind direction is 270°, but the wind speed is very low during day time.

From above the second case when the wind direction is 225° from the North perform better than first and third cases 180° and 270° scenario.

1.4 Compare between three types of wind direction (180°, 225°, and 270°) over 10m canyon width in three parallel Environment during 12 hour (7:00am to 7:00 pm). The comparison include all variables in an average values with all three wind directions. The table shows all values with all scenarios of wind directions.



This graph shows the average of all variables during 12 hours with three wind directions 180°, 225°, and 270°.

The comparison shows that third case when wind direction is 270° record lower values for Air temperature, mean radiant temperature and wind speed with highest value of relative humidity.

1.5 The Envi-met simulation outputs:

In this section the study shows, four figures for each wind direction. Each figure represent one factor at specific time with specific wind direction. The study based on three wind direction (180° , 225° , and 270° from the north), and four environmental factors (Air temperature TC° , Relative humidity RH%, Mean Radiant temperature $MRT(C^\circ)$, and Wind speed WS (m/s). The study will used three different canyons width to test those environment factors.

Wind Direction			Environmental factors				Time of measurement				Canyon width			
180°	225°	270°	$T^\circ C$	RH %	$MRT^\circ C$	WS m/s	9:00	12:00	15:00	18:00	10m (200m ²)	15m (200m ²)	15m (150m ²)	20m (200m ²)
•			•	•	•	•	•	•	•	•			•	
	•		•	•	•	•	•	•	•	•			•	
		•	•	•	•	•	•	•	•	•			•	

1.1- Air temperature from 7:00am to 7:00pm for morphology 10m canyon width, and 180° wind direction from the North.

- a- Air temperature at 9:00 am
- b- Air temperature at 12:00 noon
- c- Air temperature at 15:00 pm
- d- Air temperature at 18:00 am

1.2- Relative Humidity from 7:00 am to 7:00pm for morphology 10m canyon width and 180° wind direction from the North.

- a- Relative Humidity at 9:00 am
- b- Relative Humidity at 12:00 noon
- c- Relative Humidity at 15:00 pm
- d- Relative Humidity at 18:00 am

1.3- Mean Radiant temperature from 7:00 am to 7:00pm for morphology 10m canyon width and 180° wind direction from the North.

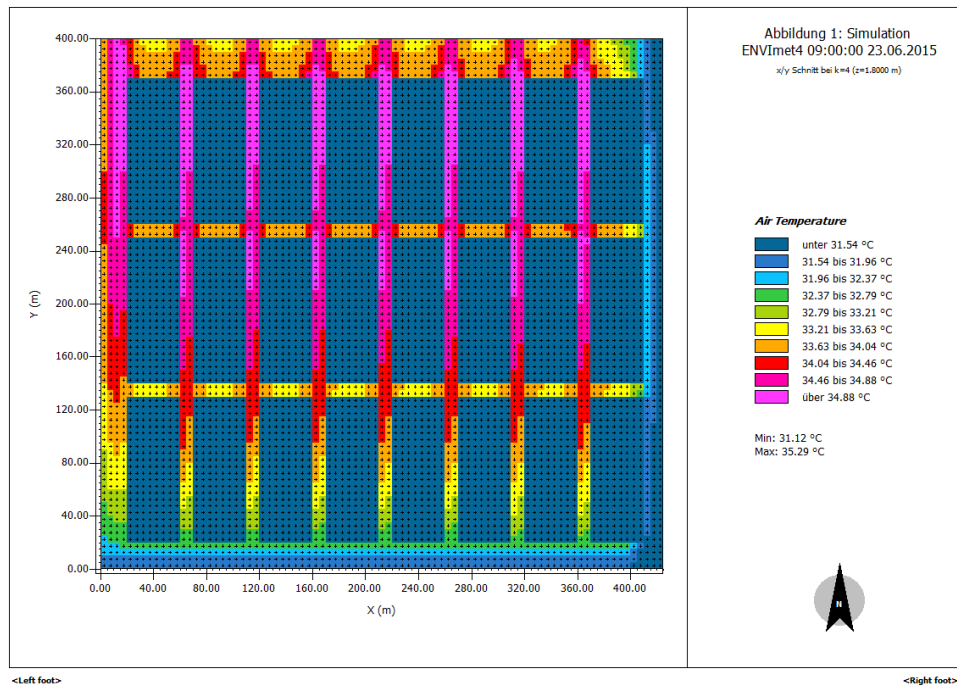
- a- Relative Humidity at 9:00 am
- b- Relative Humidity at 12:00 noon
- c- Relative Humidity at 15:00 pm
- d- Relative Humidity at 18:00 am

1.4- Wind speed from 7:00 am to 7:00pm for morphology 10m canyon width and 225° wind direction from the North.

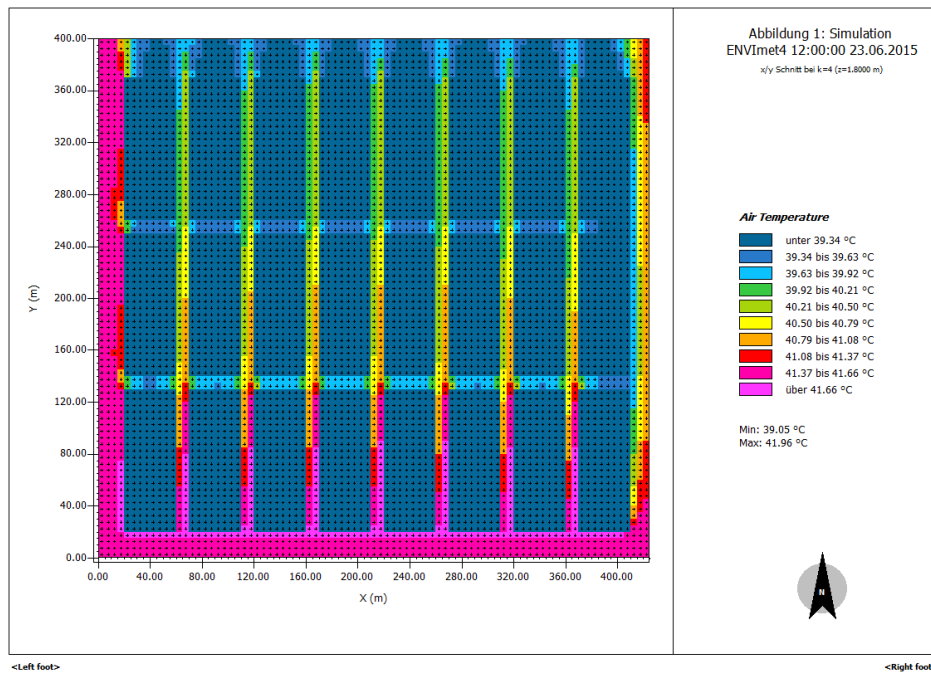
- a- Relative Humidity at 9:00 am
- b- Relative Humidity at 12:00 noon
- c- Relative Humidity at 15:00 pm
- d- Relative Humidity at 18:00 am

- a. Air temperature from 7:00am to 7:00pm for morphology 10m canyon width, and 180° wind direction from the North.

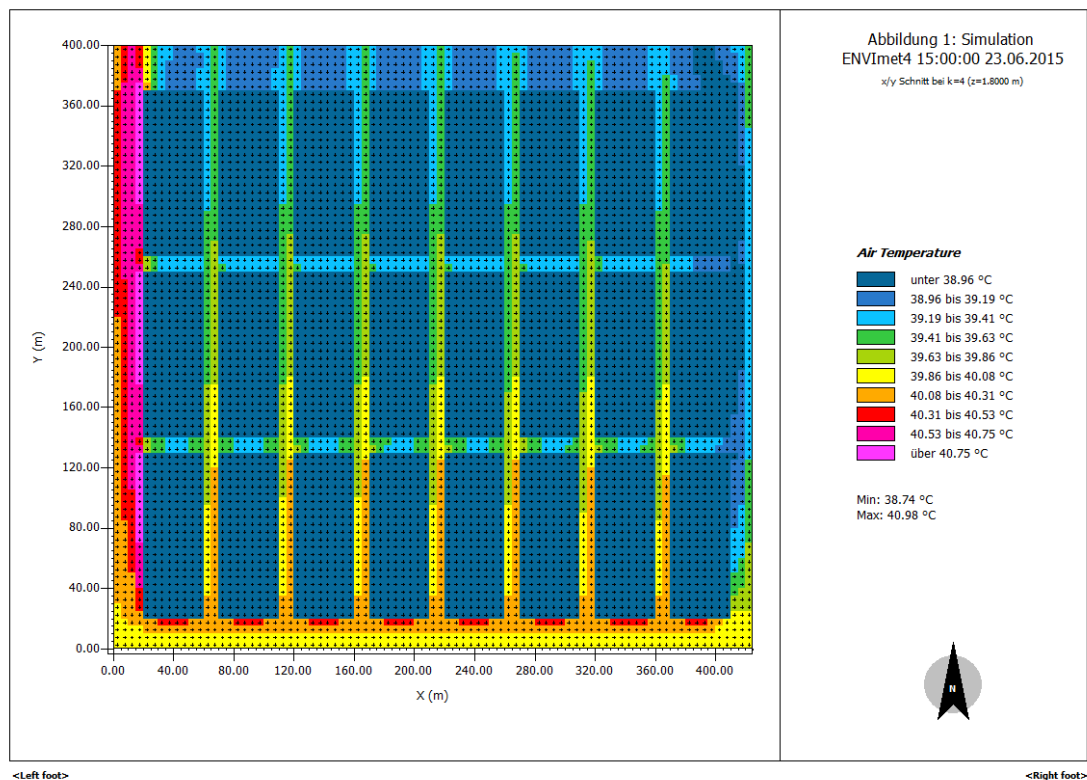
Wind Direction			Environmental factors				Time of measurement				Canyon width			
180°	225°	270°	T C°	RH %	MRT C°	WS m/s	9:00	12:00	15:00	18:00	10m (200m ²)	15m (200m ²)	15m (150m ²)	15m (200m ²)
●			●				●	●	●	●	●			



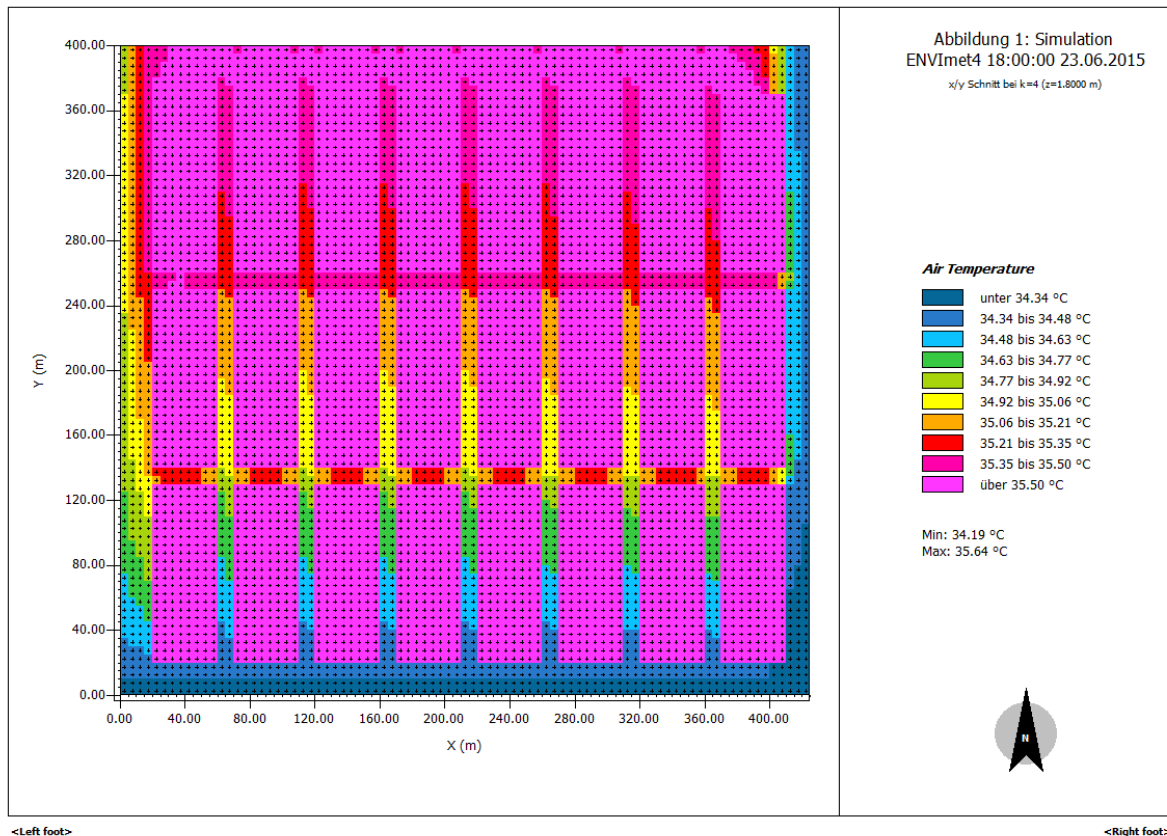
The graph above show the simulation of air temperature over residential block with 10m canyon's width and wind direction 180° from the North. Air temperature at the morning mainly trapped in the long canyons as a result of heat lost from heat lost during night time. The air temperature is higher in the deep canyons compare with short canyons. The maximum air temperature is 31.12°C and the maximum is 35.29°C. However the most canyons of the site is with air temperature above 34.5 °C towards north and south canyons, while north and south canyons recorded lower air temperature.



The graph above show the simulation of air temperature over residential block with 10m canyon's width and wind direction 180° from the North. The air temperature recorded high values for first groups of blocks from the south sides of site, while recorded minimum values from the north and east parts. Mainly the short canyons are lower air temperature than long canyons although the wind direction is parallel with long canyons.



The graph above show the simulation of air temperature over residential block with 10m canyon's width and wind direction 180° from the North. The air temperature recorded high values for first groups of blocks from the south sides of site, while recorded minimum values from the north and east parts. Mainly the short canyons are lower air temperature than long canyons although the wind direction is parallel with long canyons.

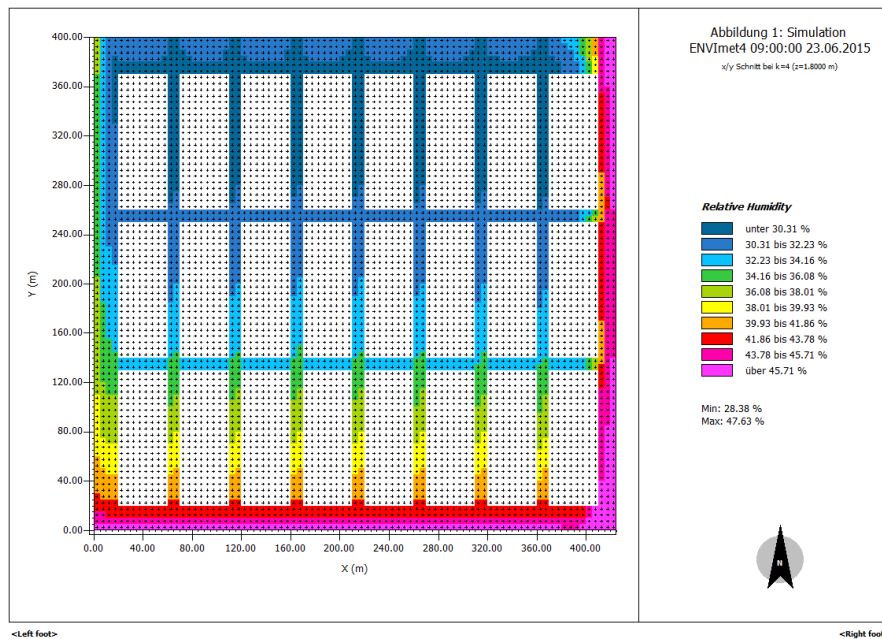


The graph above show the simulation of air temperature over residential block with 10m canyon's width and wind direction 180° from the North. The air temperature recorded high values for final groups of blocks from the North sides of site, while recorded minimum values from the south and east parts. Mainly the deep canyons are higher air temperature than shallow canyons from south part from the site. The air temperature increased gradually from 34.19C° from south part of site to 34.19 C° for north part.

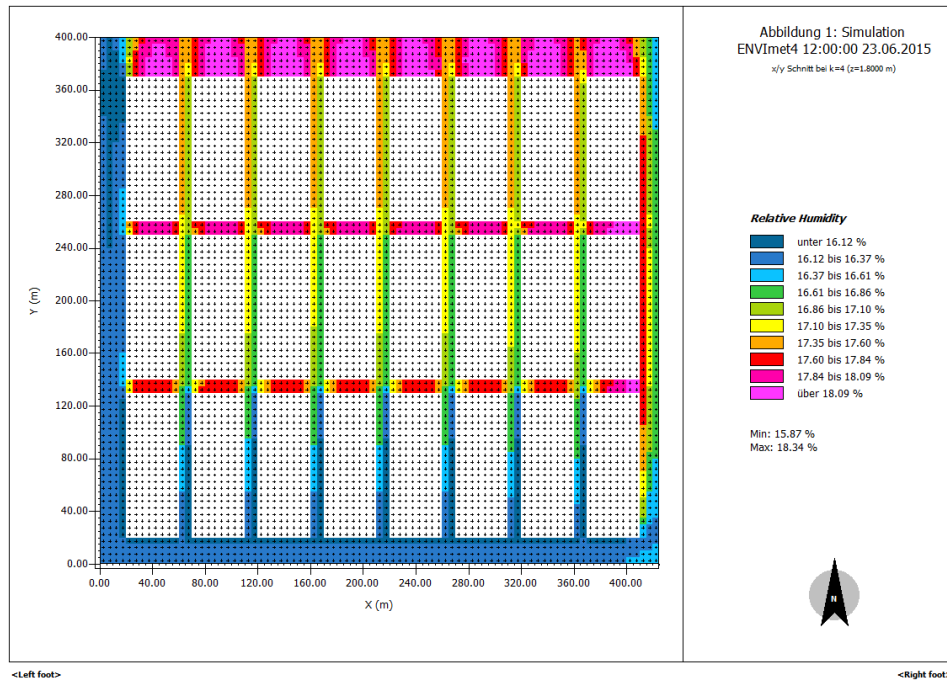
In comparison with other three times of simulations the air temperature is on its maximum rate at 12:00 noon with 41.96C° and lower rate at 9:00 29.34C°.

1.2 Relative Humidity from 7:00 am to 7:00pm for morphology 10m canyon width and 225° wind direction from the North.

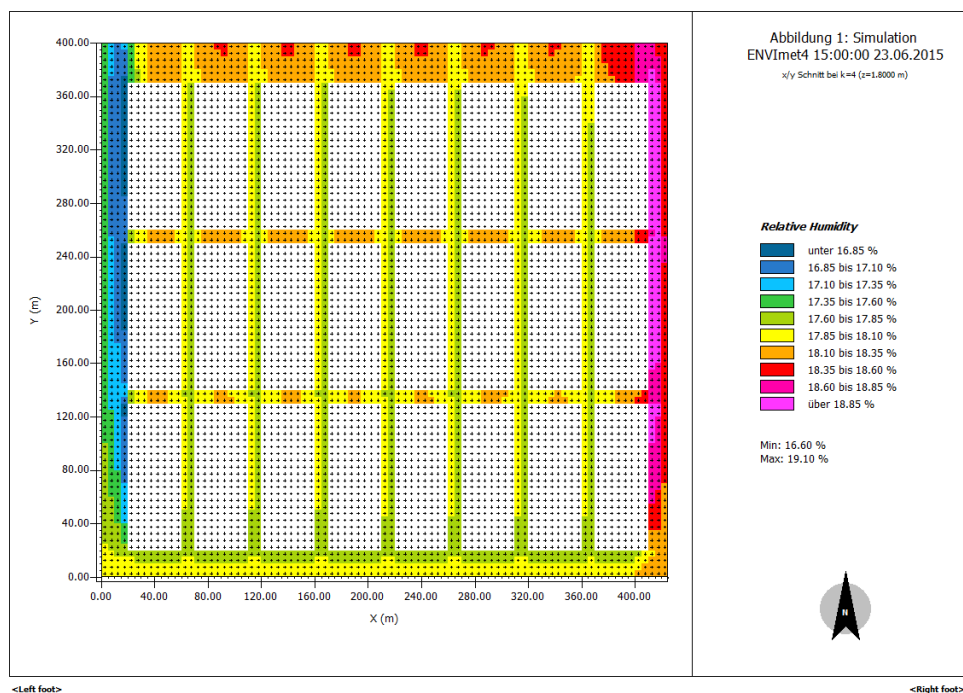
Wind Direction			Environmental factors				Time of measurement				Canyon width			
180°	225°	270°	T C°	RH %	MRT C°	WS m/s	9:00	12:00	15:00	18:00	10m (200m ²)	15m (200m ²)	15m (150m ²)	15m (200m ²)
●				●			●	●	●	●	●			



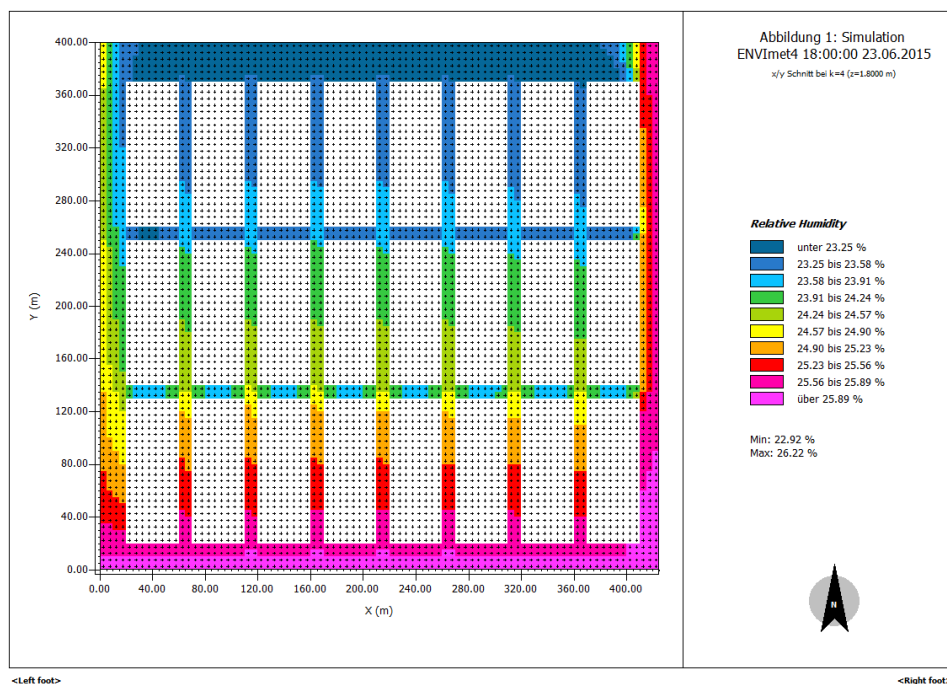
The graph above show the simulation of Relative humidity over residential block with 10m canyon's width and wind direction 180° from the North at 9:00 clock morning. The Relative humidity recorded high values for first groups of blocks from the south sides of site, while recorded minimum values from the north and east parts. Mainly the first group canyons from south part are with higher Relative humidity than medial and last blocks from the north part, although the wind direction is parallel with long canyons. The relative humidity decrease gradually in deeper canyons at the similar rate for both long and short canyons. The maximum value of relative humidity is 47.71%, while the minimum is 28.38%.



The graph above show the simulation of Relative humidity over residential block with 10m canyon's width and wind direction 180° from the North at 12:00 clock. The Relative humidity recorded lower values for first groups of blocks from the south part of site, while recorded higher values from the north and east parts. Mainly the first group canyons from south part are with lower Relative humidity than medial and last blocks from the north part, although the wind direction is parallel with long canyons. The relative humidity increase gradually in deeper canyons by similar rate for both long and short canyons. The maximum value of relative humidity is 19.10%, while the minimum is 18.34%.



The graph above show the simulation of Relative humidity over residential block with 10m canyon's width and wind direction 180° from the North at 15:00 clock. The Relative humidity recorded lower values for first canyon from the west part of site, while recorded higher values from the east parts. Mainly the first group canyons from south part, medial and last blocks from the north part, although the wind direction is parallel with long canyons. The relative humidity is similar value. The maximum value of relative humidity is 19.10%, while the minimum is 18.34%.

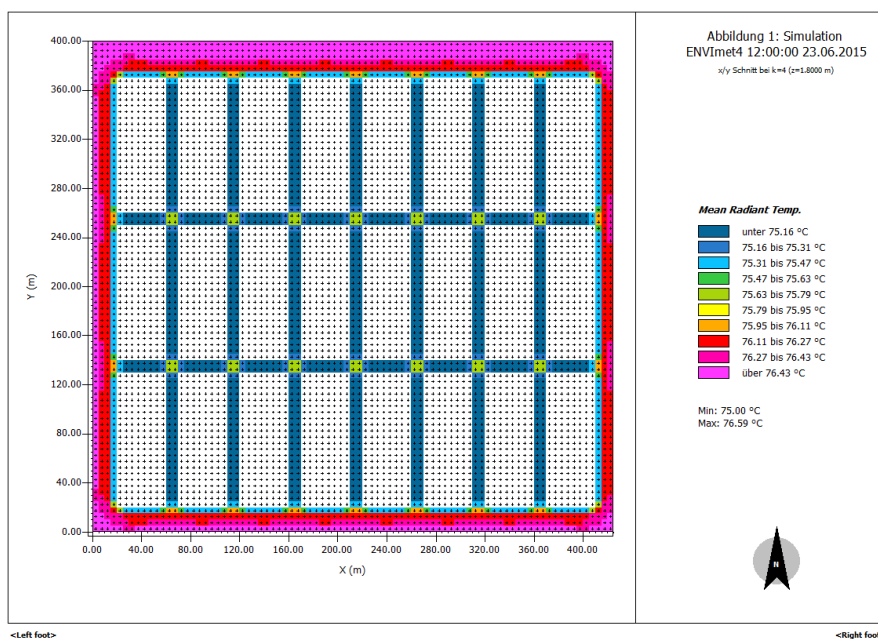
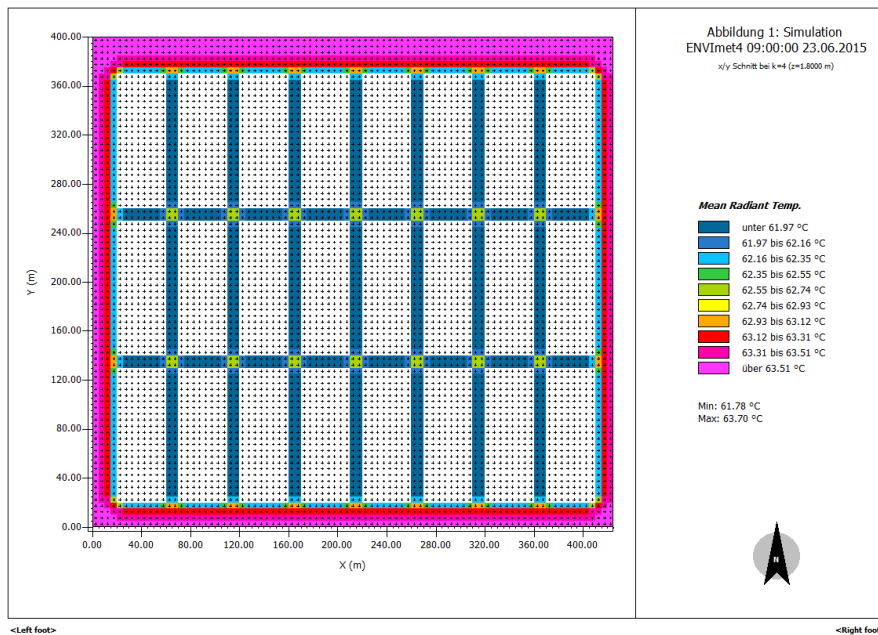


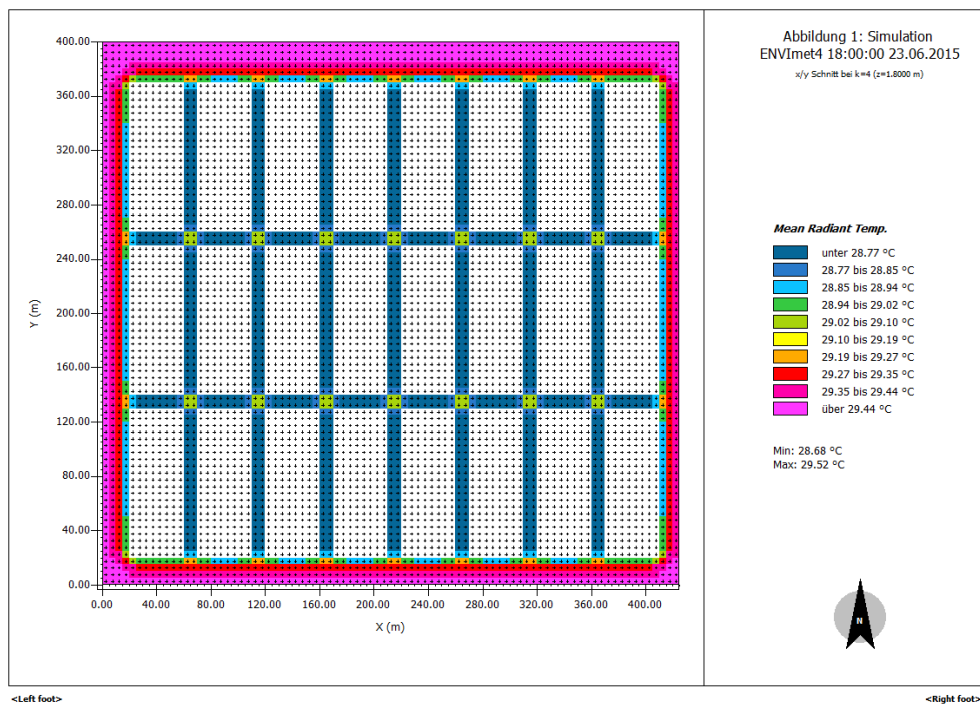
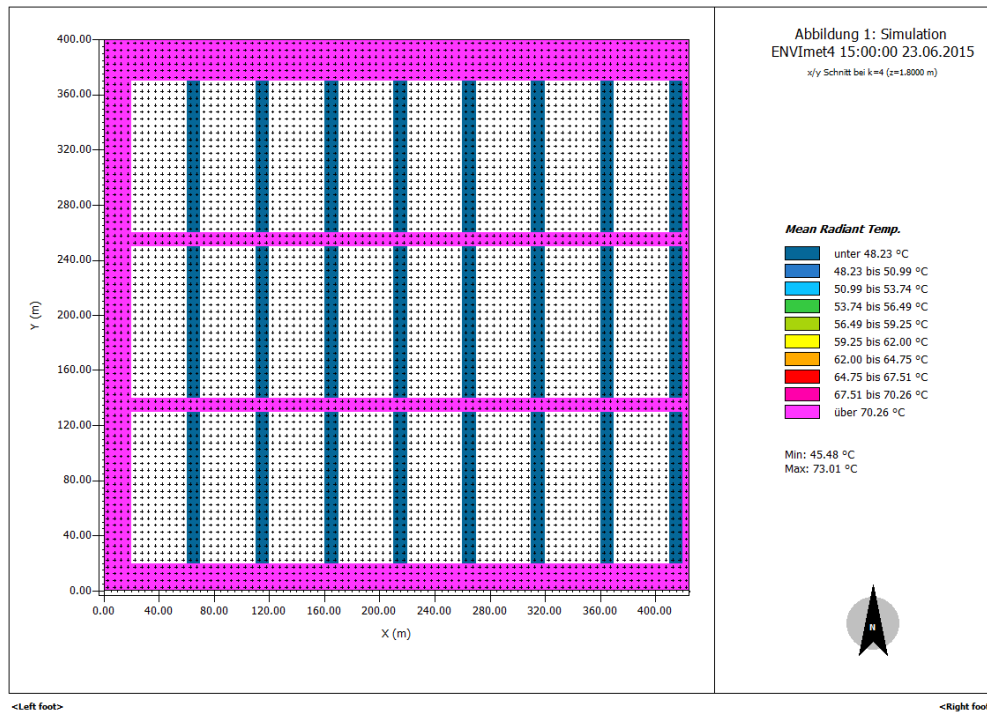
The graph above show the simulation of Relative humidity over residential block with 10m canyon's width and wind direction 180° from the North at 18:00 clock. The Relative humidity recorded higher values for first canyon from the south part of site, while recorded lower values from the north parts. Mainly the first group canyons from north and medial part higher than last blocks from the north part, although the wind direction is parallel with long canyons. The maximum value of relative humidity is 26.22%, while the minimum is 22.95%.

In comparison the four times of measurement, relative humidity is recoded at morning the higher rates and lower values at 12:00 noon. The values mainly not changed by wind direction as much as changed by changing the air temperature.

1.3 Mean Radiant temperature from 7:00 am to 7:00pm for morphology 10m canyon width and 180° wind direction from the North.

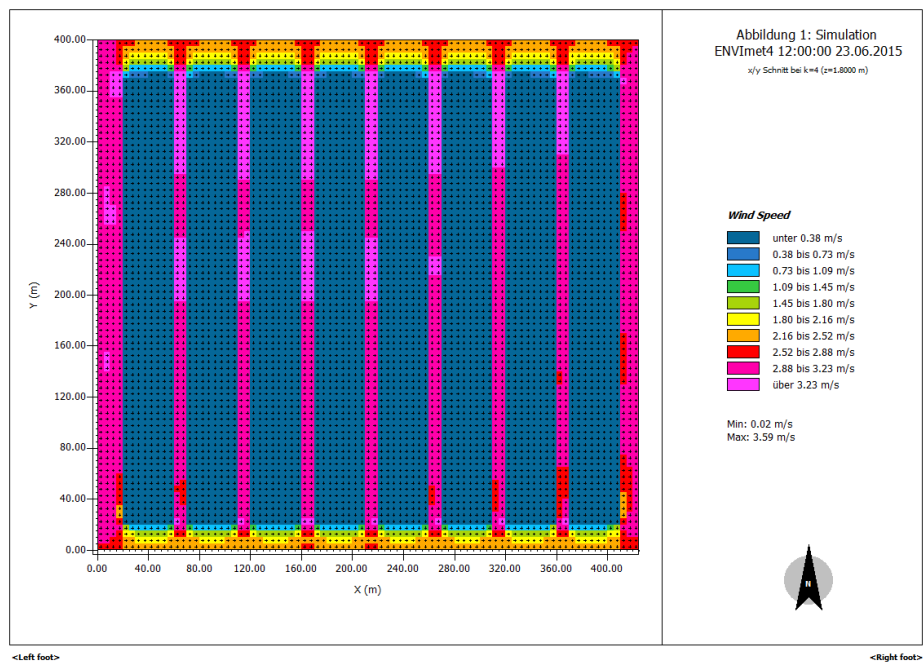
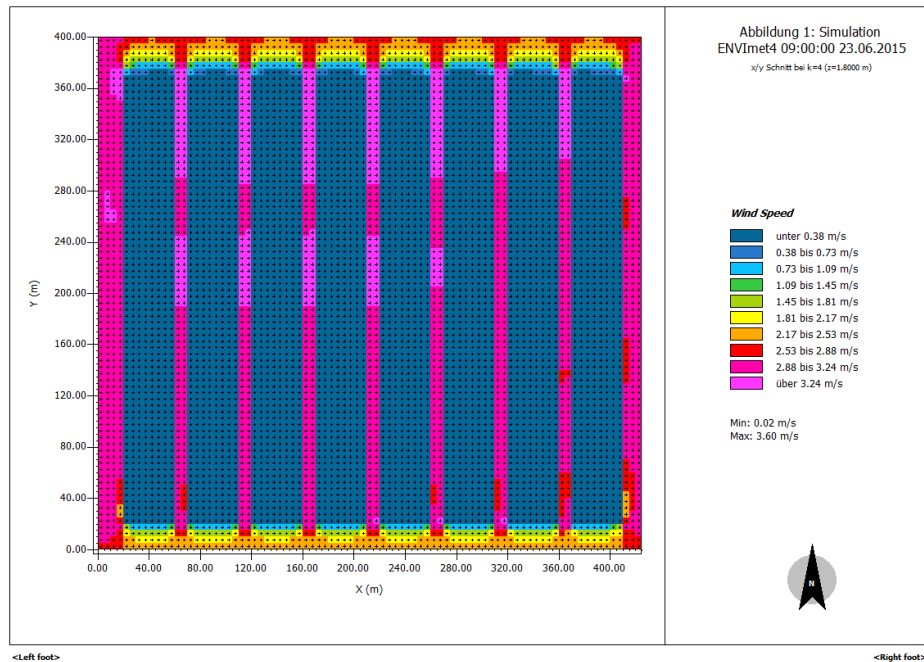
Wind Direction			Environmental factors				Time of measurement				Canyon width			
180°	225°	270°	T C°	RH %	MRT C°	WS m/s	9:00	12:00	15:00	18:00	10m (200m ²)	15m (200m ²)	15m (150m ²)	15m (200m ²)
●					●		●	●	●	●	●			

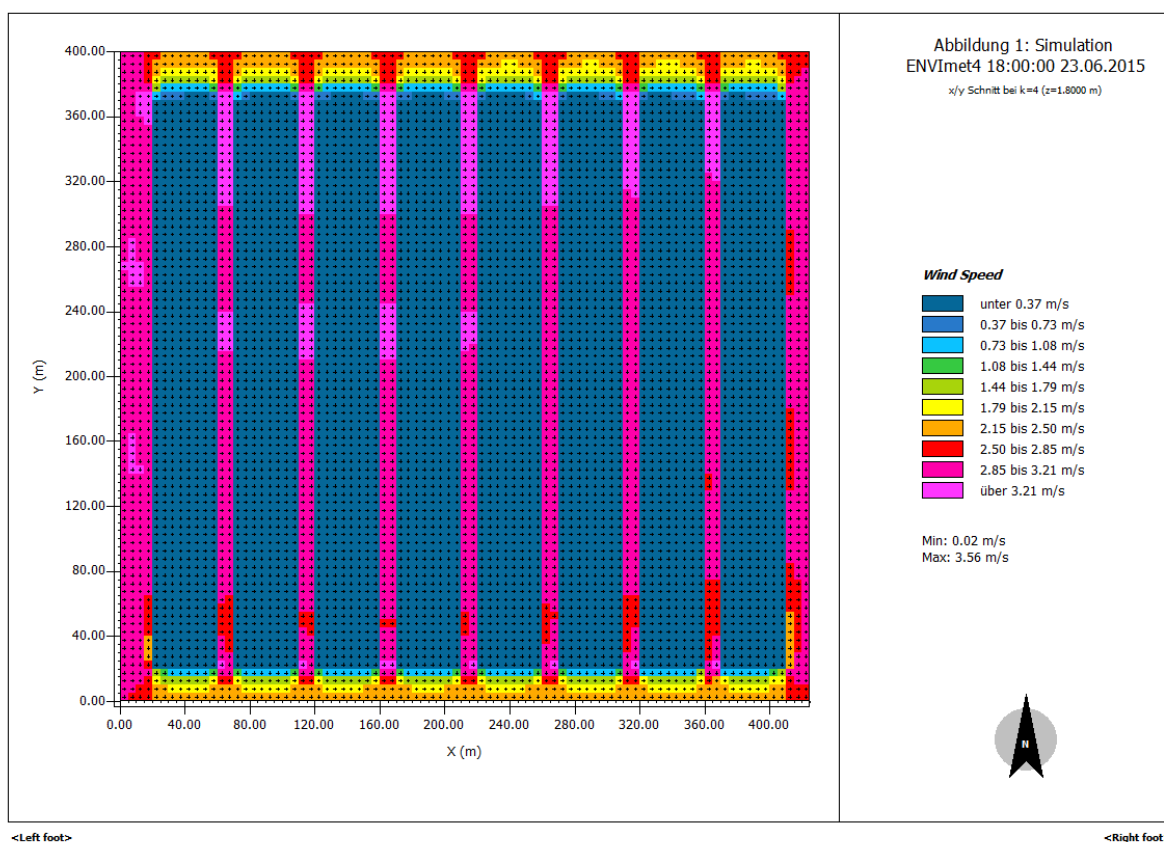
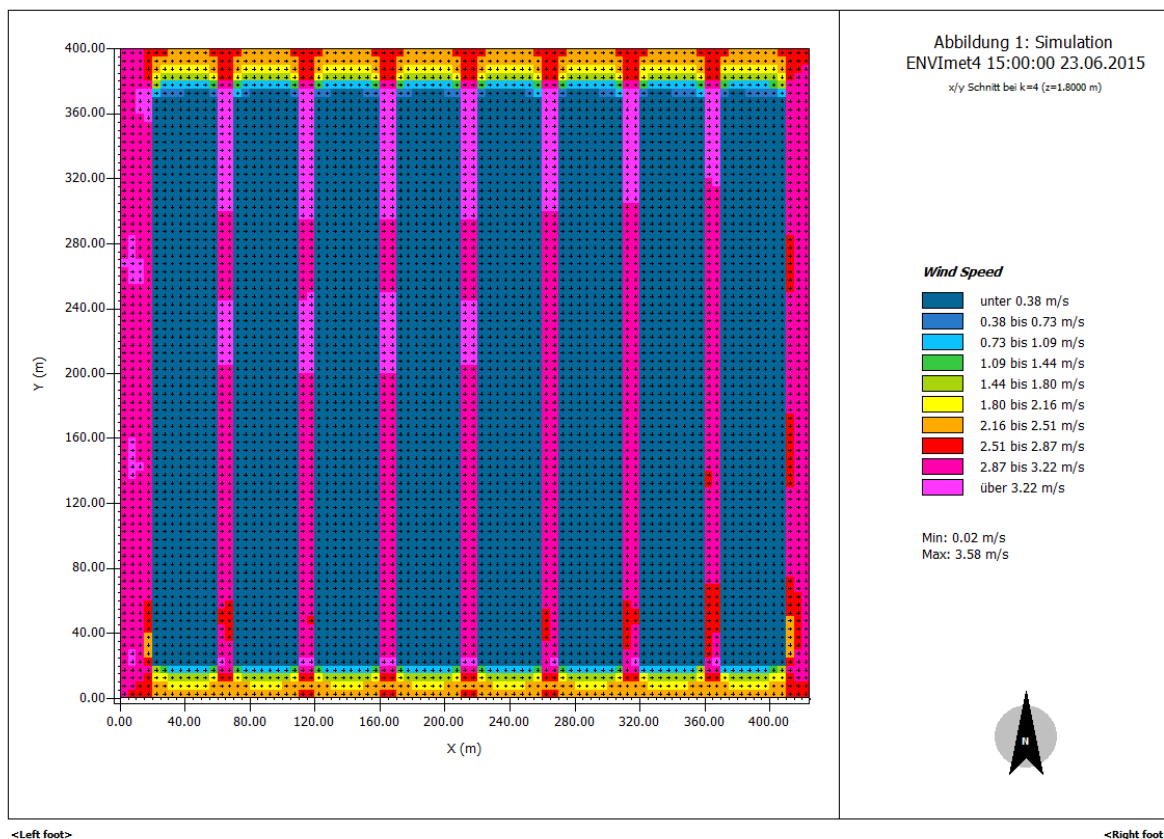




1.5- Wind speed from 7:00 am to 7:00pm for morphology 10m canyon width and 225° wind direction from the North.

Wind Direction			Environmental factors				Time of measurement					Canyon width			
180°	225°	270°	T C°	RH %	MRT C°	WS m/s	9:00	12:00	15:00	18:00		10m (200m²)	15m (200m²)	15m (150m²)	15m (200m²)
●						●	●	●	●	●		●			





The Envi-met simulation outputs:

- 1.6- Air temperature from 7:00am to 7:00pm for morphology 10m canyon width, and 225° wind direction from the North.
 - e- Air temperature at 9:00 am
 - f- Air temperature at 12:00 noon
 - g- Air temperature at 15:00 pm
 - h- Air temperature at 18:00 am

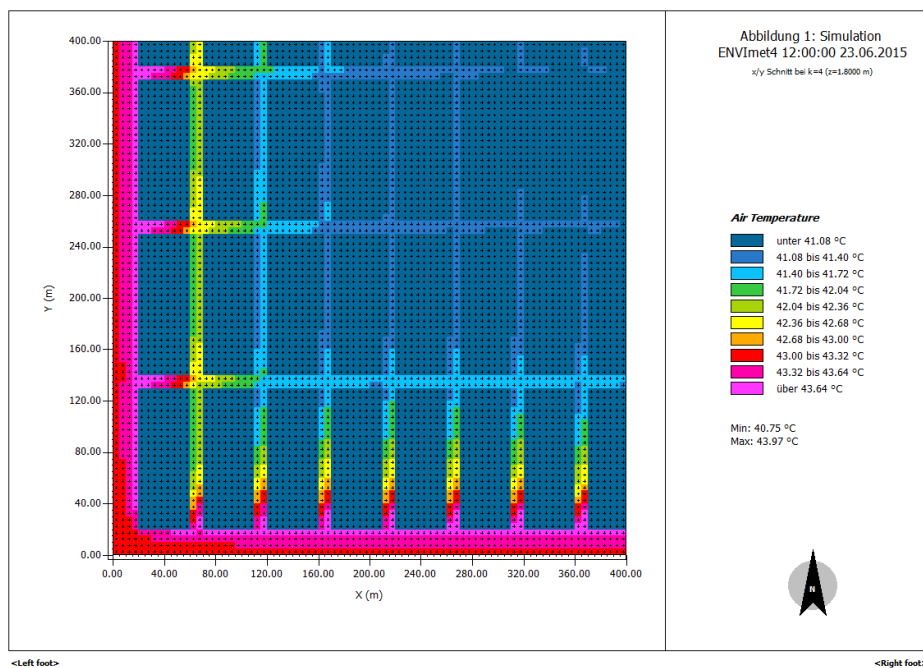
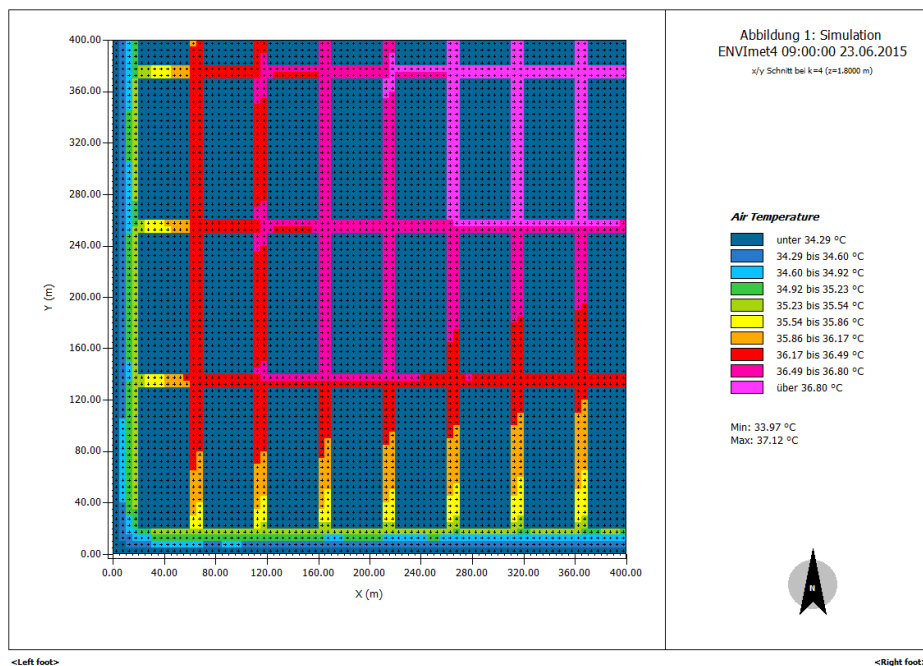
- 1.7- Relative Humidity from 7:00 am to 7:00pm for morphology 10m canyon width and 225° wind direction from the North.
 - e- Relative Humidity at 9:00 am
 - f- Relative Humidity at 12:00 noon
 - g- Relative Humidity at 15:00 pm
 - h- Relative Humidity at 18:00 am

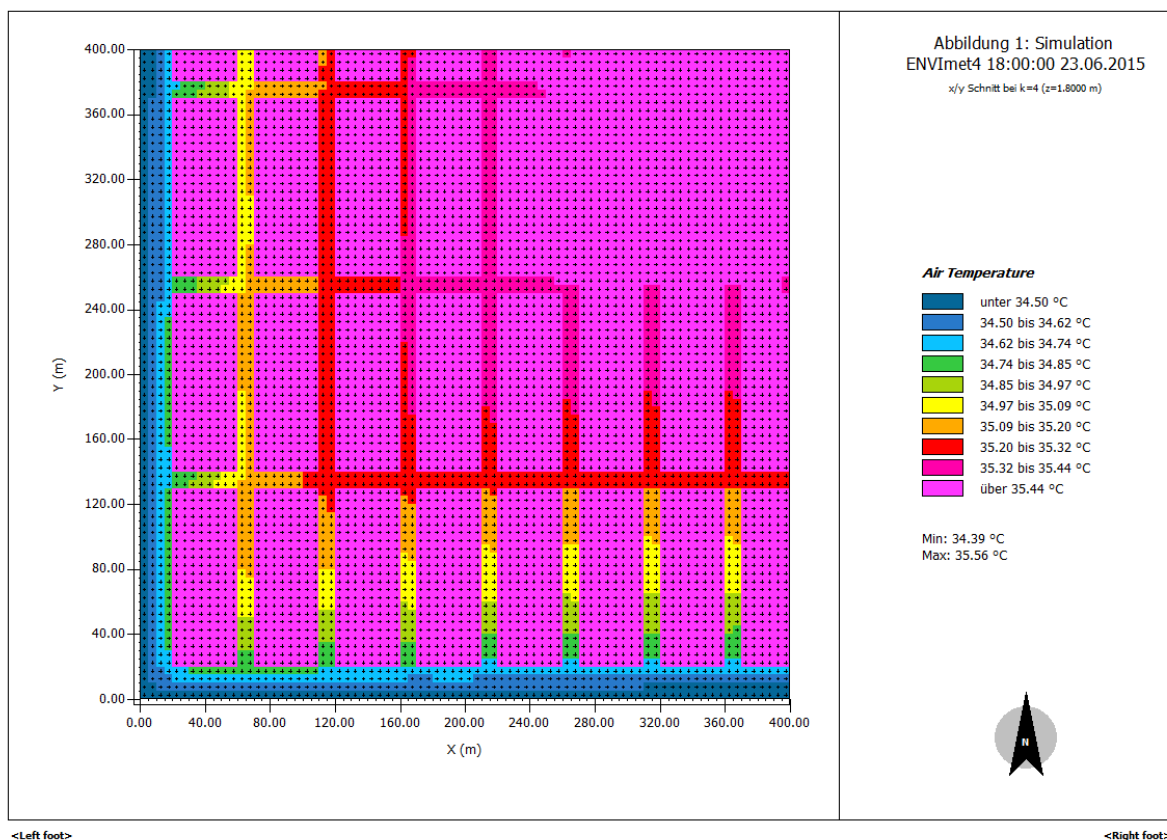
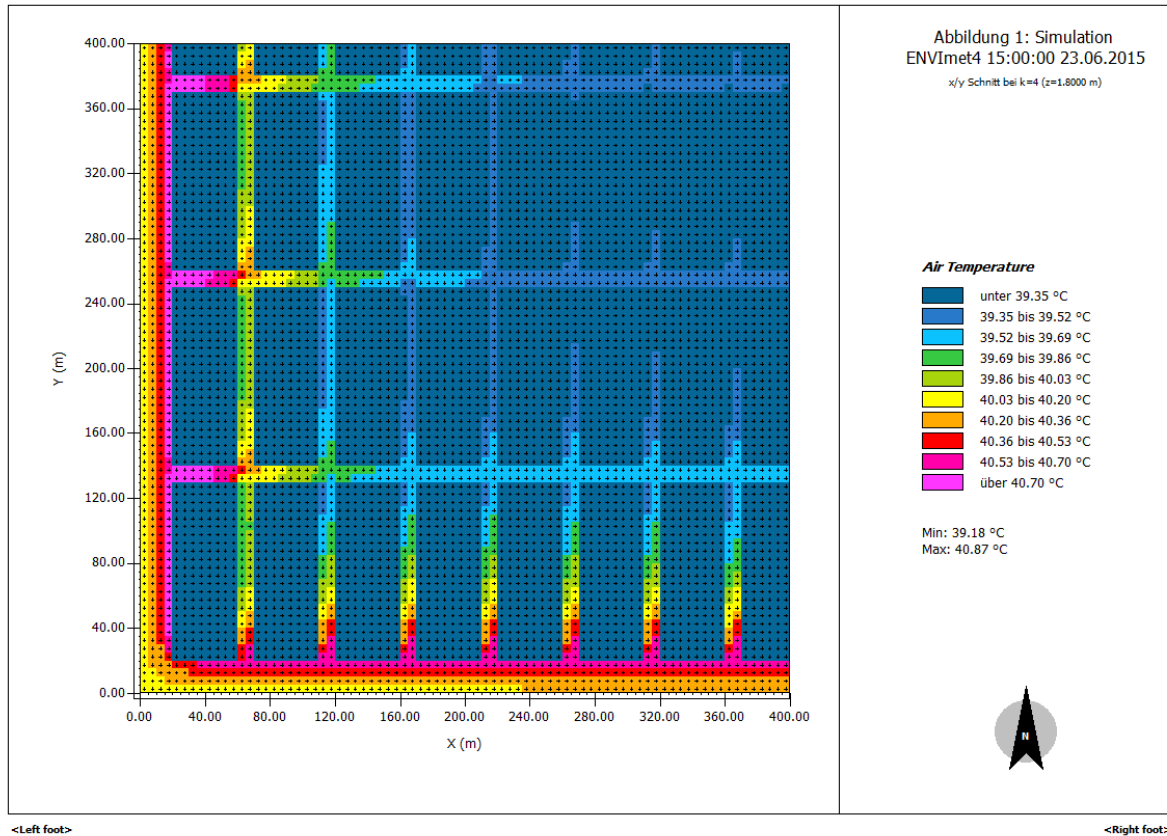
- 1.8- Mean Radiant temperature from 7:00 am to 7:00pm for morphology 10m canyon width and 225° wind direction from the North.
 - e- Relative Humidity at 9:00 am
 - f- Relative Humidity at 12:00 noon
 - g- Relative Humidity at 15:00 pm
 - h- Relative Humidity at 18:00 am

- 1.9- Wind speed from 7:00 am to 7:00pm for morphology 10m canyon width and 255° wind direction from the North.
 - e- Relative Humidity at 9:00 am
 - f- Relative Humidity at 12:00 noon
 - g- Relative Humidity at 15:00 pm
 - h- Relative Humidity at 18:00 pm

1.6 Air temperature from 7:00am to 7:00pm for morphology 10m canyon width, and 225° wind direction from the North.

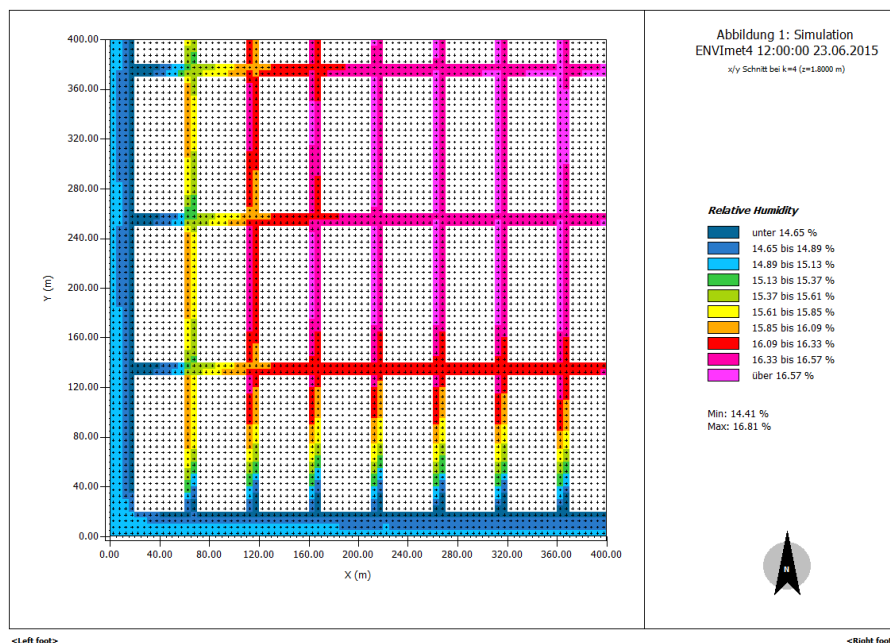
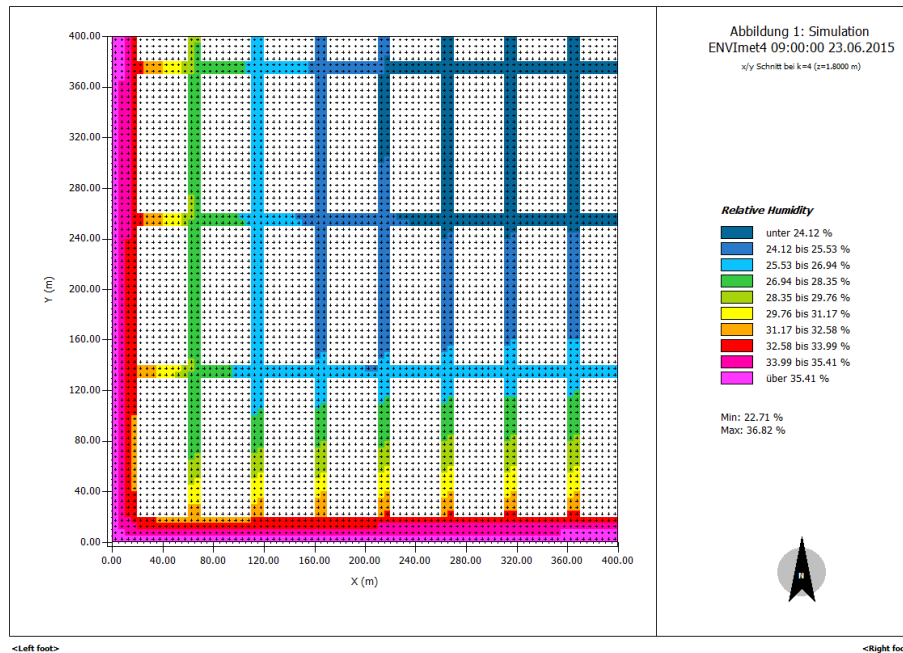
Wind Direction			Environmental factors				Time of measurement				Canyon width			
180°	225°	270°	T °C	RH %	MRT °C	WS m/s	9:00	12:00	15:00	18:00	10m (200m²)	15m (200m²)	15m (150m²)	15m (200m²)
	●		●				●	●	●	●	●			

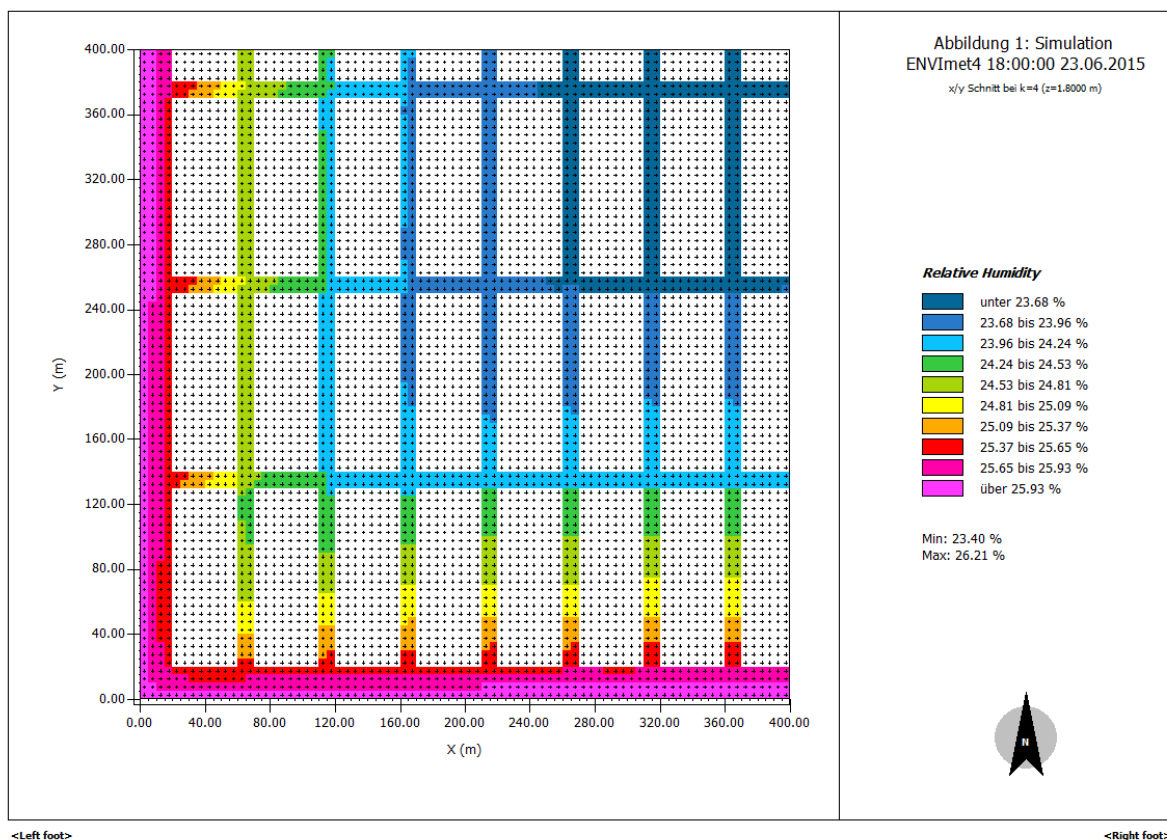
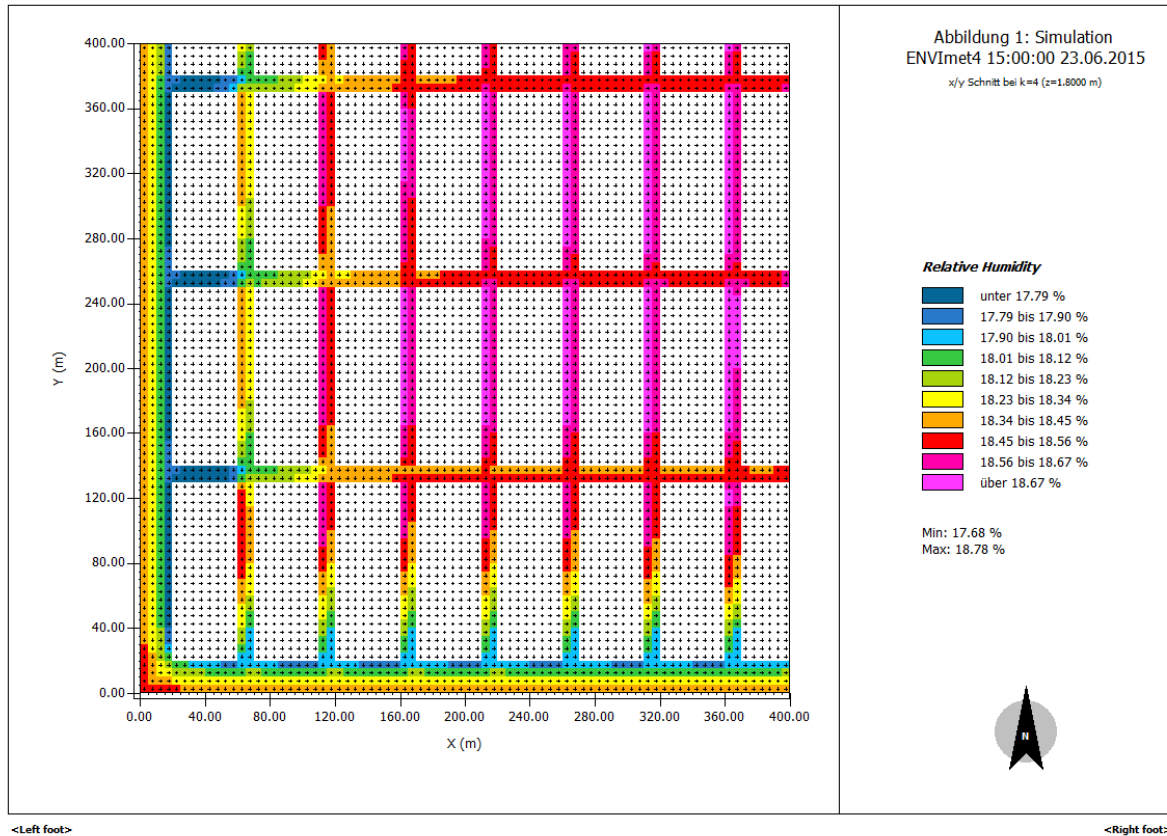




1.4 Relative Humidity from 7:00 am to 7:00pm for morphology 10m canyon width and 225° wind direction from the North.

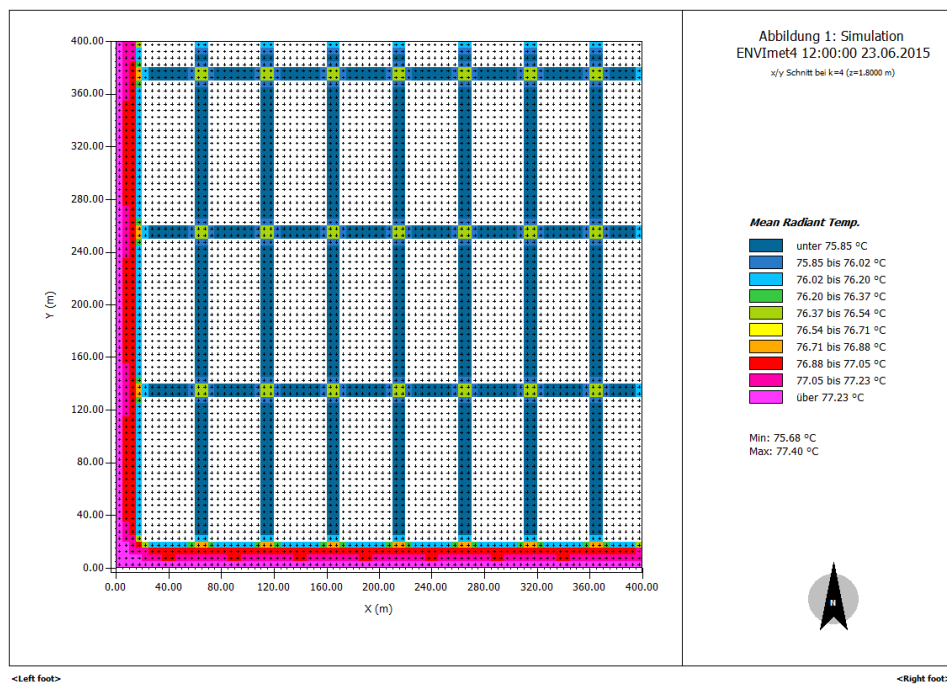
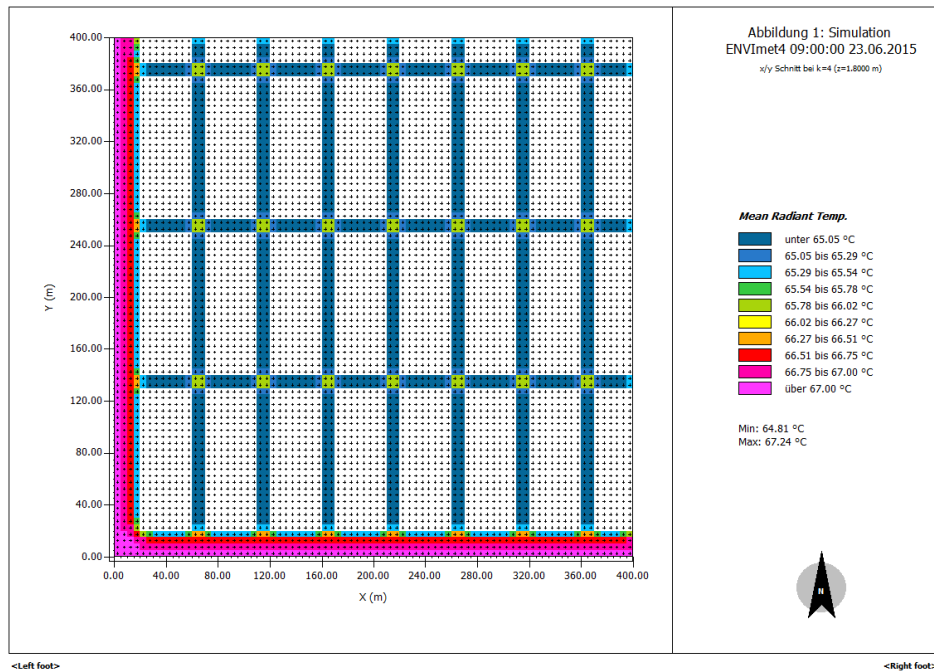
Wind Direction			Environmental factors				Time of measurement				Canyon width			
180°	225°	270°	T C°	RH %	MRT C°	WS m/s	9:00	12:00	15:00	18:00	10m (200m ²)	15m (200m ²)	15m (150m ²)	15m (200m ²)
●			●				●	●	●	●	●			

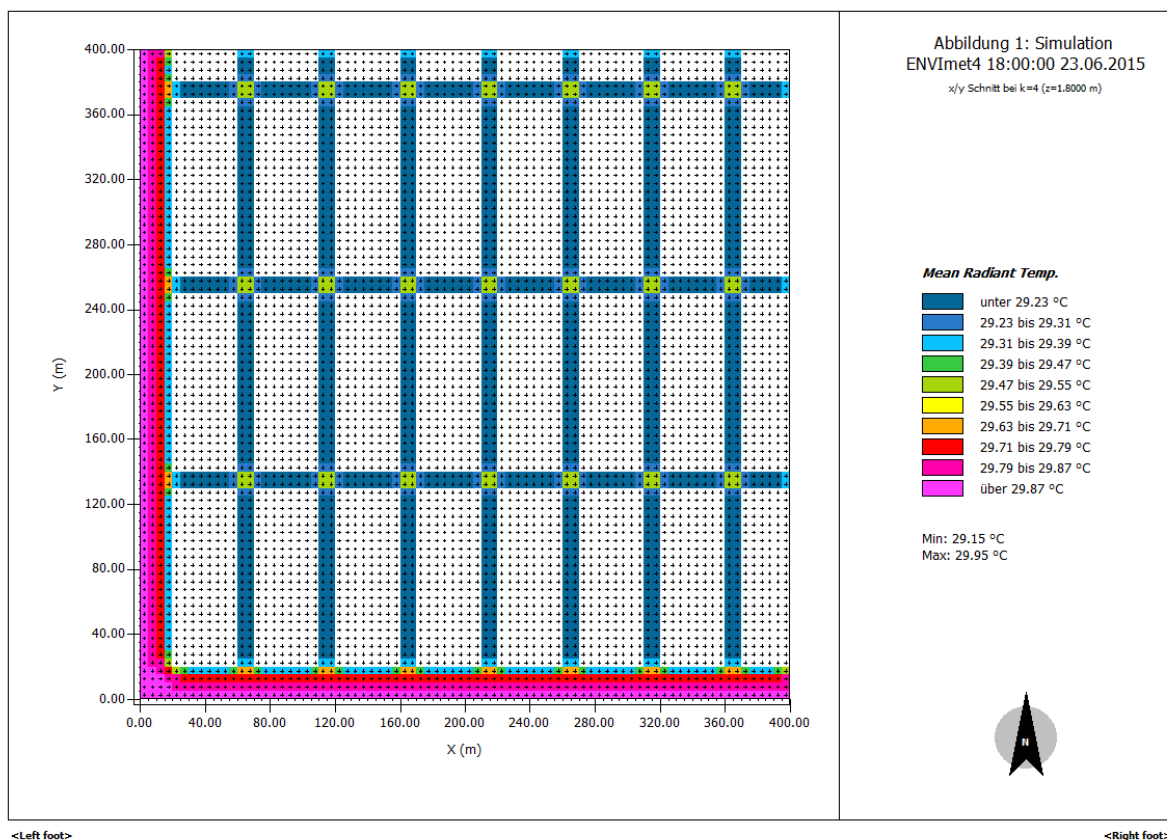
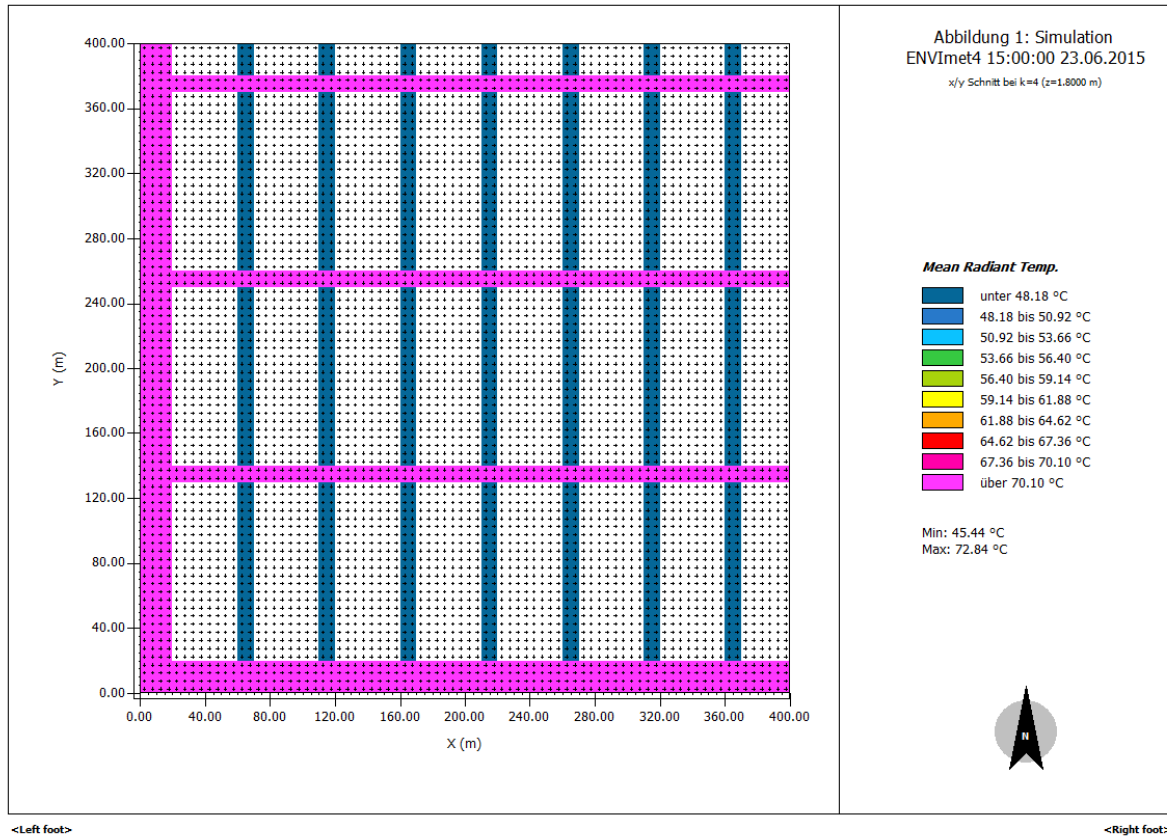




1.5 Mean Radiant temperature from 7:00 am to 7:00pm for morphology 10m canyon width and 225° wind direction from the North.

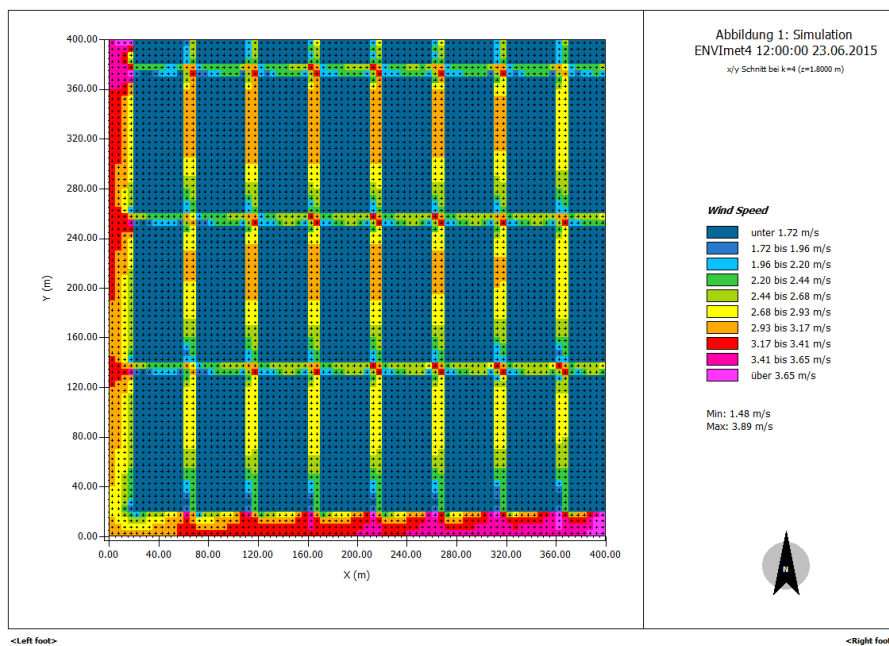
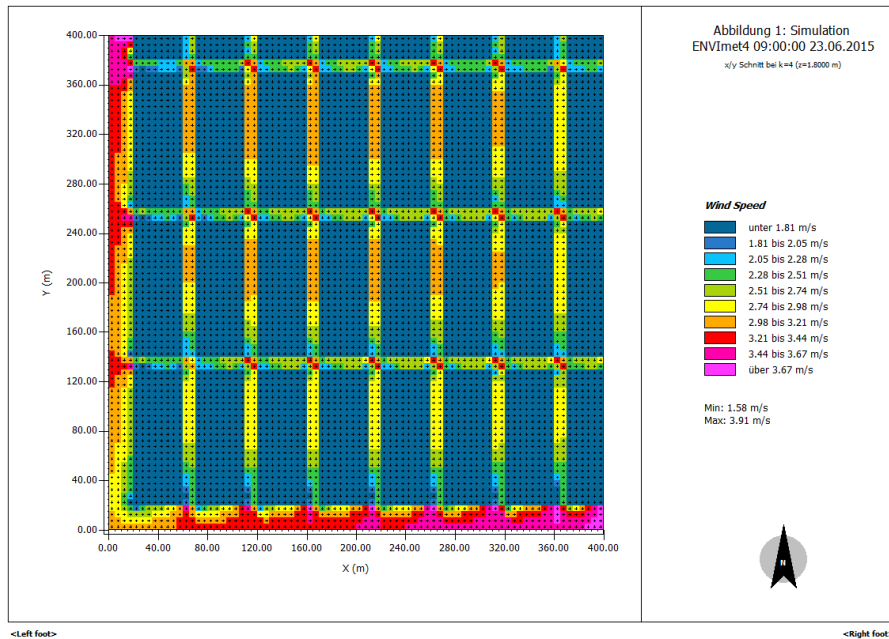
Wind Direction			Environmental factors				Time of measurement				Canyon width			
180°	225°	270°	T °C	RH %	MRT °C	WS m/s	9:00	12:00	15:00	18:00	10m (200m ²)	15m (200m ²)	15m (150m ²)	15m (200m ²)
●			●				●	●	●	●	●			

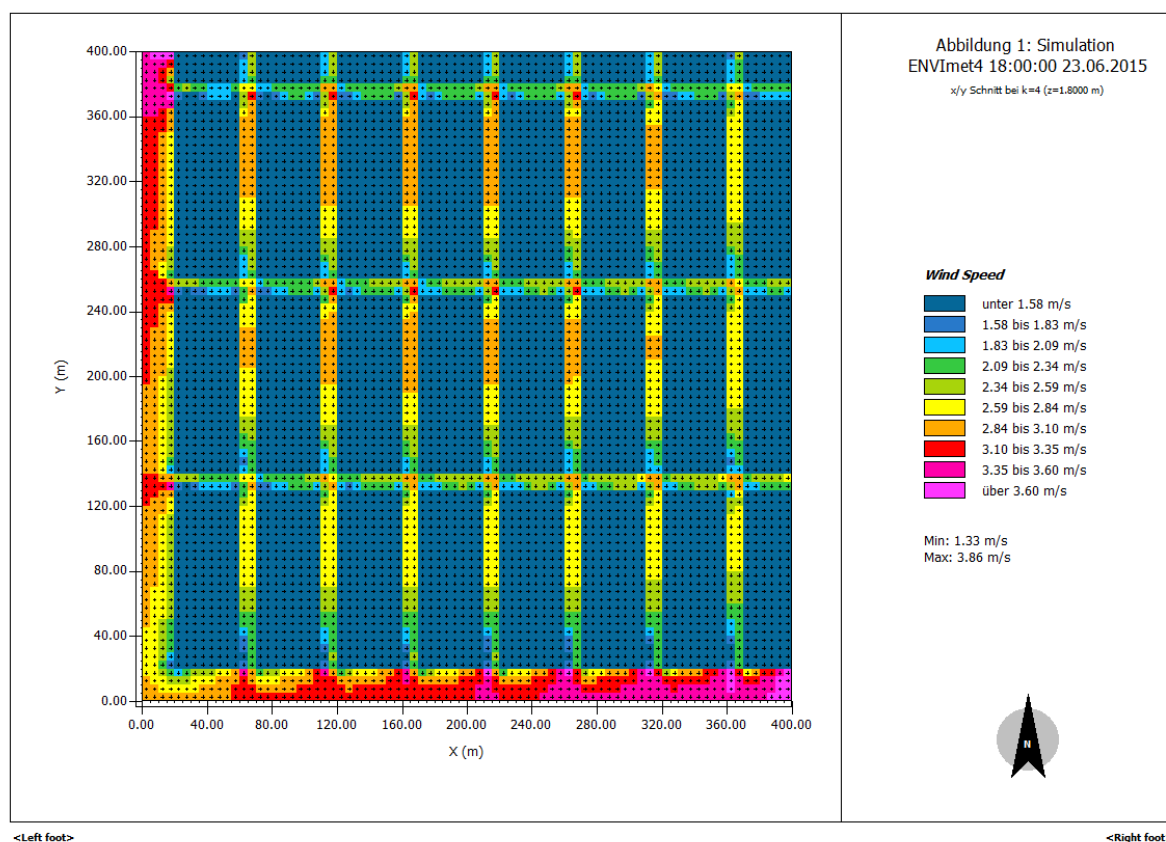
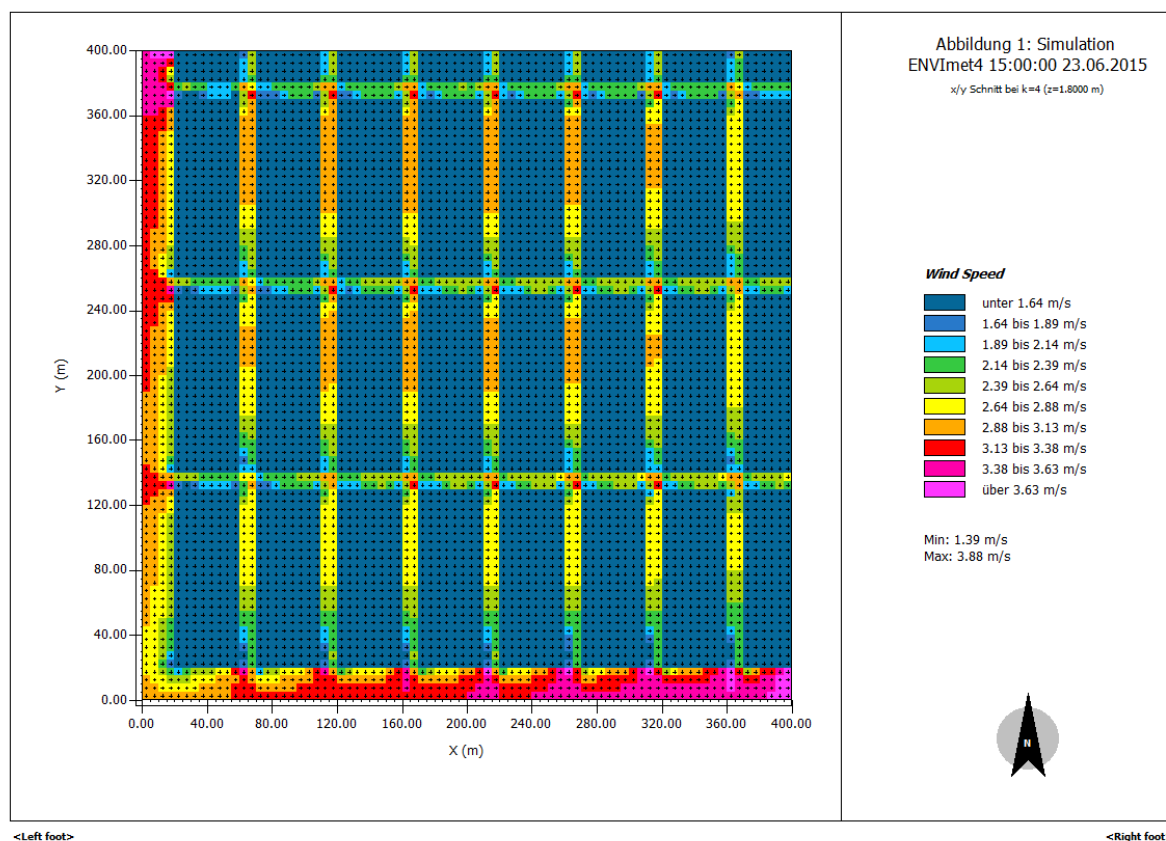




1.6 Wind speed from 7:00 am to 7:00pm for morphology 10m canyon width and 255° wind direction from the North.

Wind Direction			Environmental factors				Time of measurement				Canyon width			
180°	225°	270°	T C°	RH %	MRT C°	WS m/s	9:00	12:00	15:00	18:00	10m (200m ²)	15m (200m ²)	15m (150m ²)	15m (200m ²)
●			●				●	●	●	●	●			





The weather data package

RH	BP_mbar	WS_ms_Avg	WS_gust_Max	WS_gust_TMx	WindDir	SlrkW_Avg	SlrMJ_Tot	SoilT10_C_Avg	Rain_mm_Tot
%	Millibars	meters/second			Degrees	kW/m2	MJ/m2	Deg C	mm
Smp	Smp	Avg	Max	TMx	Smp	Avg	Tot	Avg	Tot

RH: Relative Humidity, Smp; Sample, BP-mbar: Barometric Pressure – millibar, smp: Sample, WS-ms-Avg: Wind Speed – meter / second – Average, WS-gust-Max: Maximum Wind Speed, WS-Gust-TMx : Maximum Wind Speed at maximum air temperature, WindDir: Wind direction, Slrkw-Avg: Solar Irradiance Kilo Watt – Average, kW/m2: Kilo Watt/ square meter, SlrMJ_Tot: Solar Irradiance Mega Jull, SoilT10_C_Avg: Average Soil Temperature (°C), Rain_mm_Tot: Rainfall - Total rain in mm.

TOA5	CR1000	CR1000	2889	CR1000.Std.06	CPU:ERRAS002.CR1	8149	MIN_15
TIMESTAMP	RECORD	ID	Program	Batt_Volt_Min	AirTC	AirTC_Max	AirTC_Min
TS	RN			Volts	Deg C	Deg C	Deg C
		Smp	Smp	Min	Smp	Max	Min